ISSN 0031 - 9465

PHYTOPATHOLOGIA MEDITERRANEA

Plant health and food safety

Volume 59 • No. 1 • April 2020

The international journal of the
Mediterranean Phytopathological Union

FIRENZE UNIVERSITY PRESS

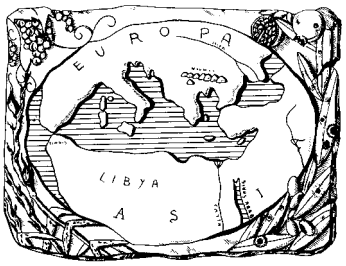

PHYTOPATHOLOGIA MEDITERRANEA

Plant health and food safety

The international journal edited by the Mediterranean Phytopathological Union
founded by A. Ciccarone and G. Goidànich

Phytopathologia Mediterranea is an international journal edited by the Mediterranean Phytopathological Union The journal's mission is the promotion of plant health for Mediterranean crops, climate and regions, safe food production, and the transfer of knowledge on diseases and their sustainable management.

The journal deals with all areas of plant pathology, including epidemiology, disease control, biochemical and physiological aspects, and utilization of molecular technologies. All types of plant pathogens are covered, including fungi, nematodes, protozoa, bacteria, phytoplasmas, viruses, and viroids. Papers on mycotoxins, biological and integrated management of plant diseases, and the use of natural substances in disease and weed control are also strongly encouraged. The journal focuses on pathology of Mediterranean crops grown throughout the world.

The journal includes three issues each year, publishing Reviews, Original research papers, Short notes, New or unusual disease reports, News and opinion, Current topics, Commentaries, and Letters to the Editor.

PHYTOPATHOLOGIA MEDITERRANEA

The international journal of the Mediterranean Phytopathological Union

Volume 59, April, 2020

Firenze University Press

***Phytopathologia Mediterranea*. The international journal of the Mediterranean Phytopathological Union**

Published by
Firenze University Press – University of Florence, Italy
Via Cittadella, 7 - 50144 Florence - Italy
http://www.fupress.com/pm

Direttore Responsabile: **Giuseppe Surico**, University of Florence, Italy

Phytopathologia Mediterranea
The international journal of the
Mediterranean Phytopathological Union

Firenze University Press
www.fupress.com/pm

Obituary

Professor Antonio Graniti, 1926-2019

Professor Antonio Graniti died in Rome, on 11 September 2019.

Antonio Graniti was born in Florence on 9 October 1926. In 1950 he graduated in Agricultural Sciences from the University of Florence, and in 1956 he obtained the Libera Docenza of Plant Pathology, allowing him to teach this discipline in the University. From 1951 to 1966 he worked as Assistente Incaricato of Plant Pathology at the Universities of Sassari and Catania, and then at the University of Bari. In 1967, at the age of 41, he became Chair Professor in Plant Pathology at the University of Bari.

Antonio Graniti was initially trained in mycology and plant pathology, focusing on plant disease problems in agricultural crops in the southern and island regions of Italy. In 1956 he studied in Zurich, Switzerland, with Prof. Ernst Gäumann, who was a leader in development of the toxigenic theory of plant diseases. This began Prof. Graniti's interest in phytotoxins. Under the guidance of his mentor Prof. Antonio Ciccarone, he began to make significant contributions to the knowledge of diseases of olive, grapevine, citrus, almond, cereals and cypress, crops and plants that important in Mediterranean environments.

Prof. Graniti was a leader in the foundation of the Mediterranean Phytopathological Union (MPU) and the MPU journal *Phytopathologia Mediterranea*. He strongly supported the principles that established the MPU, and worked diligently to organize meetings and promote *Phytopathologia Mediterranea*. His work assisted in the establishment/success of the journal and personal interactive knowledge exchange for plant pathology in Mediterranean countries. From 1960 to 1981 he was on the Editorial Board of *Phytopathologia Mediterranea*, and from 1982 to 1992 he served as Co-Editor of the journal with Prof. Antonio Canova. For over 30 years, Prof. Graniti was, therefore, primarily responsible for production of *Phytopathologia Mediterranea*.

Prof. Graniti has held key roles in the University of Bari. He was Director of the Institute of Agricul-

ISSN 0031-9465 (print) | ISSN 1593-2095 (online) | DOI: 10.14601/Phyto-11618

tural Microbiology, the Institute of Plant Pathology, and the Department of Biology and Plant Pathology, and he became Dean of the Faculty of Agriculture. He was appointed to several academies, including the National Academy of Agriculture of Bologna, the Academy of Georgofili of Florence, the Academy of Physiocritics of Siena, the National Academy of Sciences (Academy of the XL) and the Lincei National Academy, the most prestigious Italian Academy. He was a member of the Advisory Committee for Agricultural Sciences of the National Research Council, Rome; a member of the Council of the International Society for Plant Pathology (ISPP), and the ISPP Task Force on Global Food Security. He served as Director of the Experimental Institute for Plant Pathology for the Ministry of Agriculture and Forests, Rome. He was President and Past-President (1992-2002) of the MPU, and he helped with organization of numerous scientific conferences, in Italy and elsewhere. He was the Organizer and Scientific Director of two "Advanced Study Institute" events and an "Advanced Research Workshop" of the NATO's Scientific Division. Prof. Graniti visited many laboratories overseas, and developed an extensive international network of collaborators, colleagues and friends.

During the latter part of Prof. Graniti's career, his research contributions were on physiological aspects of plant diseases. His studies of phytotoxin production, chemistry, roles and mechanism of action were of international renown. His research on fusicoccin from *Fusicoccum amygdali* and on toxins from *Seiridium cardinale* (the cypress bark canker pathogen) were particularly important.

Prof. Graniti made a very significant organizational contribution during the 1960s, when he established the interdisciplinary and inter-institute research initiative on phytotoxins. This included plant pathologists in Bari, biochemists in Rome, organic chemists in Naples and plant physiologists in Milan. This group concentrated first on fusicoccin, and later on many other phytotoxins. This model of research collaboration has since been widely adopted in Italy and elsewhere.

Following retirement Prof. Graniti was appointed Emeritus Professor of Plant Pathology at the University of Bari, and he continued to follow the research of his former students and collaborators. As an Academician of the Lincei, he also returned to his initial passion of mycology. In the last years of his life, he undertook valuable historical investigations that have resulted in key publications. These include *Federico Cesi - a naturalist prince*, a tribute to the founder of the Lincei National Academy, and a book on Giuseppe de Notaris, one of the greatest Italian botanists of the nineteenth century.

Antonio Graniti was a reserved person, who fully respected the prerogatives of his colleagues and friends. He was never a dominating personality, but always present for every need of his students and collaborators. He was a highly cultured person, elegant in manner, witty with strong intellect, and ability to focus on the future of phytopathology. Faithful to the guidance of Antonio Ciccarone, who approached old age with dignity and a lively mind, Prof. Antonio Graniti pursued the nurturing and advancement of knowledge until his death. His leadership and contributions to plant pathology leave a profound legacy.

Giuseppe Surico

Phytopathologia Mediterranea
The international journal of the
Mediterranean Phytopathological Union

Firenze University Press
www.fupress.com/pm

Review

Mycotoxins in maize: mitigation actions, with a chain management approach

Roberta PALUMBO[1], Ana GONÇALVES[2], Athanasios GKRILLAS[3], Antonio LOGRIECO[4], Jean-Lou DORNE[5], Chiara DALL'ASTA[3], Armando VENÂNCIO[2], Paola BATTILANI[1]

[1] *Faculty of Agriculture, Università Cattolica del Sacro Cuore, Via Emilia Parmense 84, 29100 Piacenza, Italy*
[2] *CEB - Centre of Biological Engineering, University of Minho, 4710-057 Braga, Portugal*
[3] *Università degli studi di Parma, Via Università 12, 43121, Parma, Italy*
[4] *National Research Council, Institute of Sciences of Food Production, via Amendola 122/O, 70126, Bari, Italy*
[5] *European Food Safety Authority (EFSA), Via Carlo Magno 1A, 43126, Parma, Italy*
*Corresponding author: paola.battilani@unicatt.it

Summary. Maize is the principal staple food/feed crop exposed to mycotoxins, and the co-occurrence of multiple mycotoxins and their metabolites has been well documented. This review presents the infection cycle, ecology, and plant-pathogen interactions of *Aspergillus* and *Fusarium* species in maize, and current knowledge on maize chain management to mitigate the occurrence of aflatoxins and fumonisins. Preventive actions include at pre-harvest, as part of cropping systems, at harvest, and at post-harvest, through storage, processing, and detoxification to minimize consumer exposure. Preventive actions in the field have been recognized as efficient for reducing the entrance of mycotoxins into production chains. Biological control of *Aspergillus flavus* has been recognized to minimize contamination with aflatoxins. Post-harvest maize grain management is also crucial to complete preventive actions, and has been made mandatory in government food and feed legislation.

Keywords. *Aspergillus*, *Fusarium*, aflatoxins, fumonisins, deoxynivalenol.

OPEN ACCESS

Citation: R. Palumbo, A. Gonçalves, A. Gkrillas, A. Logrieco, J.-L. Dorne, C. Dall'Asta, A. Venâncio, P. Battilani (2020) Mycotoxins in maize: mitigation actions, with a chain management approach. *Phytopathologia Mediterranea* 59(1): 5-28. doi: 10.14601/Phyto-11142

Accepted: November 8, 2019

Published: April 30, 2020

Data Availability Statement: All relevant data are within the paper and its Supporting Information files.

Competing Interests: The Author(s) declare(s) no conflict of interest.

Editor: Dimitrios I. Tsitsigiannis, Agricultural University of Athens, Greece.

INTRODUCTION

Maize is one of the most important cereals produced for human and animal consumption in the European Union (EU), and is grown mainly for grain and forage. More than 80% of maize grain is used for feed, and the rest is used for production of starch and semolina (Eurostat, 2019). In 2017/2018, the EU maize yields reached approx. 65 million tons (European Commission, 2019), approx. 5% of the global maize production. Maize is second to wheat in total EU cereal production (Statista, 2018). Since 2017, the EU has been importing significant volumes of maize, mainly coming from Ukraine, Brazil, and Canada. This is partly due to the increased demand for maize feed (+8%), and significant reductions in the production of barley and other cere-

als for feed consumption (European Commission, 2019). As well, there has been significant reduction in maize growing areas in some European countries, where mycotoxin contamination is a major concern. That is because of the economic losses caused by discarded lots that are non-compliant with legal mycotoxin limits, and the consequent income uncertainty for farmers.

Maize is exposed to mycotoxins, which are secondary metabolites of fungi with toxic effects on humans and animals, and which cause illnesses and also economic losses. Mycotoxin contamination is the major non-tariff trade barrier for agricultural products, which negatively impacts the health and income of small-holder farmers, regional and international trade, and the world economy (Logrieco *et al*., 2018). A range of toxic effects has been associated with exposure to mycotoxins in humans and in many animal species (Eskola *et al*., 2018). Hence, the maximum concentrations of the main class of mycotoxins in agricultural food and feed products, as well as in their commodities, are regulated in Europe, or recommendations are listed for animal consumption (Commission Regulation (EU) 576/2006; Commission Regulation (EU) 1881/2006; Commission Regulation (EU) 574/2011; Commission Recommendations (EU) 165/2013).

One of the major issues in the contamination of maize is infection with *Aspergillus flavus* and *Aspergillus parasiticus,* and the resulting occurrence of aflatoxins (AFs). In addition, the occurrence of aflatoxin B1 (AFB1) in feed can lead to contaminated milk, because the toxin is metabolized to aflatoxin M1 (AFM1) by dairy cattle when fed with contaminated feed, and there is carry-over to dairy products (EFSA, 2004; van der Fels-Klerx and Camenzuli, 2016).

Fusarium species also infect maize and contaminate grains with mycotoxins, which include deoxynivalenol (DON), zearalenone (ZEN), fumonisins (FBs), nivalenol (NIV), T-2 toxin (T2), and HT-2 toxin (HT2). In maize the co-occurrence of AFs and FBs is common (Camardo Leggieri *et al*., 2015). Although there are no data demonstrating significant interaction between these toxins, reports suggest that both additive and synergistic interactions may occur (Torres *et al.,* 2015; Abbès *et al*., 2016; Qian *et al*., 2016). Mycotoxins are very stable compounds and accumulate in maize grain in the field after fungal infections during the crop growing season, with possible post-harvest increases when the environment remains suitable for fungal activity. Main factors affecting maize infection are: environmental conditions, plant susceptibility (depending on crop genetics and health status) as well as insect populations.

Many efforts have been devoted to develop strategies, both at the pre- and post-harvest crop stages, to reduce production and occurrence of these mycotoxins in maize, and their entry into the food and feed chains. The present provides an account of advances since 2000 in strategies to reduce the occurrence of AFs, FBs, and DON across the maize supply chain.

ASPERGILLUS AND *FUSARIUM* SPECIES IN MAIZE

Many of the most relevant mycotoxins in maize are synthesized by two fungal genera: *Aspergillus* and *Fusarium*. *Aspergillus* spp. include all validated AF-producing fungi and most of the known species belong to the *Aspergillus* section *Flavi*, including *A. flavus* and its close relative *A. parasiticus*. *Aspergillus flavus* and *A. parasiticus* are very similar species of the section, sharing 96% DNA similarity of the aflatoxin gene clusters (Cary and Ehrlich, 2006). These species can be distinguished from one another using morphological and physiological characteristics, but *A. flavus* commonly only produces B series AFs, while *A. parasiticus* can produce both B and G series AFs. Non-aflatoxigenic strains also naturally occur in both species (Smith and Moss, 1985). *Aspergillus flavus* almost exclusively occurs in maize (Giorni *et al.,* 2007).

The most frequently isolated *Fusarium* species from maize are *F. verticillioides*, *F. proliferatum*, *F. graminearum*, and *F. subglutinans* (Leslie and Logrieco, 2014). These cause two different types of ear rot: (i) Fusarium ear rot or pink ear rot is caused primarily by members of the *Liseola* section, including *F. verticillioides*, *F. proliferatum* and *F. subglutinans*, now preferably referred to as the *Gibberella fujikuroi* species complex (GFsc); and (ii) *Gibberella* ear rot or red ear rot which is caused by species of the *Discolor* section, with *F. graminearum* being the prevalent species. *Fusarium verticillioides* and *F. proliferatum* can synthesize large amounts of FBs. Other species can be involved in the pathogenesis of maize ear rot, including *F. culmorum* and *F. equiseti* (Logrieco *et al.,* 2002). These two fungi produce trichothecenes (DON and NIV) and ZEN. Studies reporting the presence of *F. sporotrichioides* and *F. langhsethiae* in maize are scarce (Görtz *et al.,* 2008), but these two species have been shown to produce T2 and HT2, and their roles in maize contamination with these two mycotoxins needs to be clarified. Recently, a new mycotoxin-producing species of *Fusarium*, *F. temperatum*, has been reported in Europe and South America by different authors. This species is morphologically similar and phylogenetically close to *F. subglutinans*, and has been reported as a producer of FBs, beauvericin (BEA), fusaproliferin (FUS) and moniliformin (MON) (Scauflaire *et al.,* 2012; Fumero *et al.,* 2016).

Infection cycle of Aspergillus *and* Fusarium *species on maize*

Maize is susceptible to mycotoxin-producing fungi from flowering, at growth stage BBCH63 (male: beginning of pollen-shedding; female: when tips of stigmata are visible), and fungus infection efficacy is optimized at BBCH67 (female: stigmata drying) (Battilani *et al.,* 2003; Battilani *et al.,* 2013). *Aspergillus* and *Fusarium* species commonly reproduce by asexual spores (Battilani *et al.,* 2013). The conidia of *Aspergillus* are dispersed mainly by air movement (Battilani *et al.,* 2003). *Fusarium* species produce macroconidia which, for *F. graminearum,* are typically dispersed by splashing rain, and for the GFsc, also by air movement (Shaner, 2003; Paul *et al.,* 2004; Manstretta and Rossi, 2015; Manstretta and Rossi, 2016). Conidia in crop debris are considered the main sources of infection, and they enter host plants through natural openings or wounds (Cotten and Munkvold, 1998). Sexual reproduction is possible for Fusaria, and the relevance of this depends on the species and the crop location, while for *A. flavus* sexual reproduction has been demonstrated in the laboratory, and some evidence suggests that it could occur in nature although not yet observed (Horn *et al.,* 2009; Horn *et al.,* 2016).

Systemic development of *Fusarium* species from maize seeds and roots to the stalks and to cobs can also contribute to kernel infection, but the role of systemic infections remains to be confirmed (Munkvold *et al.,* 1997; Murillo-Williams and Munkvold, 2008). Systemic infection by *Aspergillus* has never been considered.

Beside silk and systemic infection, insect-assisted infections by mycotoxigenic fungi have also been identified as important pathway for maize ear infections by *Aspergillus* and *Fusarium* species. Insects can be vectors of inoculum and host entry can be assisted by larvae feeding on kernels (Munkvold and Carlton, 1997). *Lepidoptera* typically have the greatest impacts on mycotoxin-producing fungi in maize. Much attention has been given to the interactions between *Lepidoptera*, including the European corn borer (ECB; *Ostrinia nubilalis*), and *F. verticillioides* infections (Blandino *et al.,* 2015; Drakulic *et al.,* 2017). ECB is the main maize pest in Central and Southern Europe, and this insect has been shown to promote *F. verticillioides* and *F. proliferatum* infections in maize grains and consequent FB contamination, in temperate areas (Blandino *et al.,* 2015). The incidence of the western flower thrips (*Frankliniella occidentalis*) on maize ears has also been correlated with the presence of *F. verticillioides* (Parsons and Munkvold, 2012). Further evidence also indicates that kernel injury attributed to the western bean cutworm (WBC; *Striocosta albicosta*) can lead to increased levels of *F. verticillioides* and subsequent increased levels of FBs in maize (Parker *et al.,* 2017).

Ecology

Every fungal species has unique ecological requirements, and optimum conditions for fungal growth are not always those that are most appropriate to mycotoxin biosynthesis (Figures 1 and 2). Therefore, it is difficult to identify common ecological trends across different fungal species. Nevertheless, *A. flavus* is well adapted to warm and dry weather conditions (Giorni *et al.,* 2016). In contrast, the optimum conditions for the development of *F. verticillioides* include warm temperature (T) and moderate rainfall. Mild T and high rainfall during maize grain maturation are best for infections by *F. graminearum* (Bhatnagar *et al.,* 2014). T, relative humid-

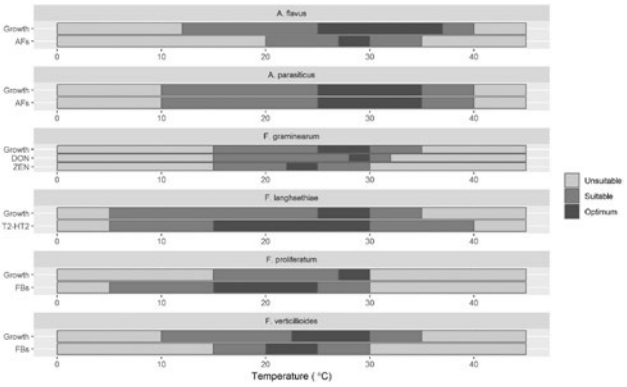

Figure 1. Temperatures (°C) required for fungal growth and mycotoxin production for *Aspergillus* and *Fusarium* species isolated from maize.

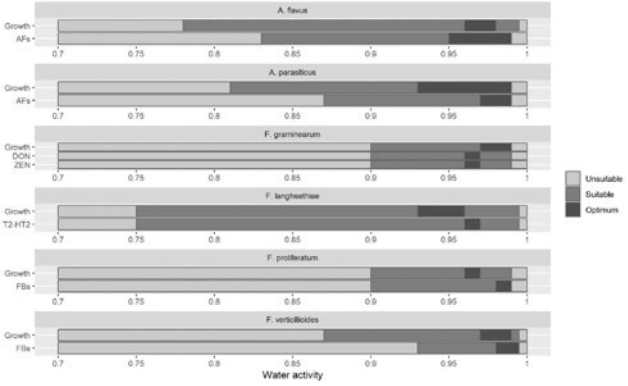

Figure 2. Water activity (a_w) required for fungal growth and mycotoxin production for same of the most relevant *Aspergillus* and *Fusarium* species isolated from maize.

ity (RH), and, above all, grain water activity (a_w) are the most important ecological factors influencing fungal colonization of maize grain substrates (Giorni *et al.,* 2011; Lazzaro *et al.,* 2012; Battilani *et al.,* 2016).

In vitro trials have indicated that the optimum a_w for growth of *A. flavus* is in the range of 0.96 to 0.98 at 25°C, 0.98 at 30°C, and 0.96 at 37°C (Pitt and Miscamble, 1995). In the field, *A. flavus* can grow in maize grain at a_w as low as 0.73 (8–12 % moisture content), and produce AFs down at a_w = 0.85 (17–19% moisture) (Giorni *et al.,* 2011; Battilani *et al.,* 2013; Battilani *et al.,* 2016). *In vivo* trials also shown that AFB1 is positively correlated with a_w when $a_w \geq 0.95$, confirming the *in vitro* data, and is negatively correlated when $a_w < 0.95$ (Giorni *et al.,* 2016). Therefore, a_w of 0.95 is proposed as a threshold, at which AF production increases rapidly. The influence of abiotic stresses on *A. flavus* infection is complicated by the co-existence of different fungal species in maize kernels during the crop growing season. Previous *in vitro* studies considered the competition between *F. verticillioides* and *A. flavus* (Giorni *et al.,* 2014). Dominance of one species over the other was demonstrated only under extreme conditions, while mutual antagonism was more common (Giorni *et al.,* 2016).

Growth of *F. verticillioides* occurs within a wide range of T, with an optimum T range of 22.5 to 27.5°C and a minimum a_w = 0.87. The optimum T and a_w reported for inducing FB production are from 20 to 25°C and 0.95 to 0.99 a_w, while no production was observed at 10°C and $a_w \leq 0.93$ (Medina *et al.,* 2013). *Fusarium temperatum* strains reached maximum growth rate at T values greater than 22°C and the least growth was at 15°C and 0.95 a_w, and these strains produced maximum amounts (1000 μg g^{-1}) of fumonisin B1 (FB1) at 0.98 a_w and 15°C (Fumero *et al.,* 2016). *Fusarium graminearum* grew over a wide range of T and moisture conditions, with the optimum growth at approx. 25°C and a_w = 0.977-0.995. The influence of incubation T (15, 20, 28, or 32°C) and a_w (0.96, 0.97, or 0.98) on the production on DON by *F. graminearum* on maize kernels was studied by Llorens *et al.* (2004). They demonstrated that a_w in the range considered did not significantly affect trichothecene synthesis, while T affected DON production with the optimum T being 28°C.

Plant-pathogen interactions

Differences in chemical composition of maize kernels during each growing season and related plant physiology, can be variedly associated with fungal colonization and mycotoxin contamination (Luo *et al.,* 2008; Luo *et al.,* 2011).

The dynamics of a_w in grains during the growing season determines the competitiveness of *A. flavus* against other co-occurring ear rot fungi (Giorni *et al.,* 2011). The ability of *A. flavus* and other ear rot fungi such as *F. verticillioides* to utilize carbon sources at different T and a_w conditions could also influence the dynamics of AF contamination (Giorni *et al.,* 2016). Other factors, such as crop growth stage, physiology, active plant defenses, and grain composition, are also likely to influence the dynamics of AF production during grain ripening (Ojiambo *et al.,* 2018). The rate of drying of the ripening kernels critically affects their contamination with AFs and FBs (Medina *et al.,* 2013). The most significant increase in FB production and accumulation occurs after the dent stage. This stage is also characterized by acidification and maximum levels of amylopectin content; both of which enhance FB synthesis (Picot *et al.,* 2011).

Lipid composition of maize kernels also affects fungal infection and toxin accumulation by *Aspergillus* and *Fusarium* species (Dall'Asta *et al.,* 2012; Dall'Asta *et al.,* 2015; Battilani *et al.,* 2018). Plant and fungal oxylipins play crucial roles in cross-talk between the pathogens and their host (Scala *et al.,* 2013; Ludovici *et al.,* 2014; Battilani *et al.,* 2018).

OCCURRENCE OF MULTIPLE MYCOTOXINS

A survey by Streit *et al.,* (2013) indicated that, on a global scale, 84% of maize was contaminated with at least one mycotoxin, and 46% was co-contaminated with multiple mycotoxins. The natural co-occurrence of mycotoxins produced by different fungi in maize and maize products has been reported, and most surveys have focused on the major mycotoxins AFs, FBs, ZEN, and trichothecenes (mainly DON) (Smith *et al.,* 2016; Ingenbleek *et al.*, 2019). Only a few studies have specified the percentage of the co-contaminated samples. Common co-occurrence of AFs + FBs, FBs + DON, and FBs + DON + ZEN has been reported (ranging from 25% to 40%). More details of the main reported mycotoxin combinations are summarized in Table 1.

Apart from the occurrence of parent forms, modified mycotoxins have been frequently reported to co-occur in cereals, including maize (Rasmussen *et al.,* 2012; Nakagawa *et al.,* 2013; Kovalsky *et al.,* 2016). Glucosides of DON, ZEN, and other minor trichothecenes have been frequently described. Mycotoxin modification in wheat is part of the biotransformation machinery expressed by host plants in response to pathogen attacks (Berthiller *et al.,* 2009a). However, toxin biotransformation has been little investi-

Table 1. Co-occurrence of mycotoxins in maize and derived products.

Mycotoxin	Commodity	Observation	References
AFs; FBs	Maize	95.6% of samples with AFB1 and FBs (FB1+FB2)	Camardo Leggieri *et al.* (2015)
FBs; DON	Maize products	High co-occurrence of fb1, fb2 and don strong evidence of co-occurrence of fb1 and fb2	Cano-Sancho *et al.* (2012)
	Maize and maize products	38% of samples with fbs and don	Kirincic *et al.* (2015)
	Maize	25% of samples with don+fb1	Zachariasova *et al.* (2014)
FBs; BEA	Maize	97% of samples with fb1 and fb2 10% of samples with ota 17% of samples with bea 15% of samples with bea, fb1 and fb2 3% of samples with bea and ota	Jurjevic *et al.* (2002)
FBs; ZEN	Maize	40% of samples with fb1 and zen	Domijan *et al.* (2005)
FBs; DON; ZEN; OTA	Maize and maize products	57% of samples with co-occurring mycotoxins 38% of samples with fbs, don and zen	Kirincic *et al.* (2015)
	Maize	40% of samples with fb1, zen and ota 6% of samples with fb1, fb2 and ota	Domijan *et al.* (2005)
DON; DON derivates	Maize	High occurrence of don and don3g	Desmarchelier and Seefelder (2011)
	Maize and maize products	High co-occurrence of don, 3-adon, 15-adon and don3g	De Boevre *et al.* (2012)
	Maize	Consistent co-occurrence of don and don3g in all tested samples	Berthiller *et al.* (2009b)
	Maize	50% of sample with don + its acetylated and/or glycosylated derivates	Zachariasova *et al.*(2014)
DON; BEA	Maize	38% of sample with don and bea	Zachariasova *et al.* (2014)
DON; ZEN	Maize and maize products	25% of samples with don and zen	Kirincic *et al.* (2015)
	Maize	26% of sample with don and zen	Zachariasova *et al.* (2014)
DON; T2-HT2	Maize and maize products	High co-occurrence of don and ht2	Cano-Sancho *et al.*(2012)
DON;NIV; T2-HT2	Maize	Relatively high content of niv, higher than for don for same samples	Rasmussen *et al.* (2012)

Abbreviations: AFs = aflatoxins, FBs = fumonisins, FB1 = fumonisin B1, FB2 = fumonisin B2, DON = deoxynivalenol, DON3G = deoxynivalenol-3-glucoside, 3-ADON = 3-acetyl-deoxynivalenol, 15 ADON = 15-acetyl-deoxynivalenol, BEA = beauvericin, ZEN = zearalenone, T2 = T-2 toxin, HT2 = HT-2 toxin, NIV = nivalenol, OTA = ochratoxin A.

gated in maize. Occurrence of modified FBs in maize has been reported (Bryła *et al.,* 2013a; Dall'Asta and Battilani, 2016), and conjugation of FBs with fatty acids (oleic and linoleic acids) through the formation of ester bonds has been described (Bartók *et al.,* 2010; Bartók *et al.,* 2013; Falavigna *et al.,* 2016). Recent evidence strongly supports the hypothesis that fatty acid esters of FB1 are produced by *F. verticillioides* using fatty acids from the substrate (Falavigna *et al.,* 2016). These compounds are formed by the fungus in a substrate concentration-dependent manner (Falavigna *et al.,* 2016), and they may undergo cleavage in the gastrointestinal tracts of mammals.

FBs can also occur as non-covalently bound forms, also known as "hidden fumonisins", now referred to as modified mycotoxins (Rychlik *et al.,* 2014). Several studies have demonstrated the complexation of FBs with maize macro-constituents, the main one being starch (Dall'Asta *et al.,* 2009; Dall'Asta *et al.,* 2010; Dall'Asta *et al.,* 2012; Bryła *et al.,* 2015). This complexity may significantly affect the quantification of FBs under routine conditions, requiring additional hydrolysis steps under alkaline conditions. The amounts of modified FBs are closely related to environmental factors and chemical composition of maize, and may significantly contribute to the overall amount of FBs occurring in each sample. The ratio between free and total FBs has been reported at between 0.4 to 0.7, depending on yearly variations and host hybrid examined (Dall'Asta *et al.,* 2012; Bryła *et*

al., 2015; Giorni *et al.,* 2015). Dry milling of maize also increased free FBs in bran by 69% and total FBs partitioning in fractions by 46%, while free FBs decreased in flour by 28% and total FBs partitioning in fractions by 20% (Bryła *et al.,* 2015). Total release of this fraction under digestive conditions has been considered by the European Food Safety Authority. The contribution of modified FBs to overall FB exposure in animals, using an additional factor of 1.6 with respect to the free FB contents has been proposed. This factor has been extrapolated from several studies and a broad database (n = 316) (Dall'Asta *et al.,* 2010; Dall'Asta *et al.,* 2012; Bryła *et al.,* 2013b; Bryła *et al.,* 2014; Bryła *et al.,* 2015; Oliveira *et al.,* 2015).

In contrast to *Fusarium* mycotoxins, no modification of AFs in maize has yet been reported.

FIELD PREVENTION STRATEGIES FOR MAIZE MYCOTOXINS

Several research efforts have defined good agricultural practices (GAPs) to apply during pre-harvest stages, including: (i) farming systems, (ii) host resistance and hybrid selection, (iii) soil management, crop residues and crop rotations, (iv) irrigation, (v) pest and disease control, and (vi) biological control agents (BCAs) (Blandino *et al.,* 2009a; Blandino *et al.,* 2009b; Battilani *et al.,* 2012).

Farming systems

Little information is available on fungal incidence in organic *versus* conventional farming of maize. Lazzaro *et al.* (2015) demonstrated that *Fusarium* incidence was different between farming systems in Italian maize (20% in conventional production and 35% for organic production). However, *Aspergillus* incidence was not linked to the farming system but to weather conditions. Mycotoxin occurrence was not considered by Lazzaro *et al.,* (2015).

The most relevant agricultural factors that should be considered essential for integrated programmes to reduce *Aspergillus* and *Fusarium* toxins are outlined below, and are summarized in Supplementary Table S1.

Host resistance and hybrid selection

Comprehensive knowledge of plant defense mechanisms may help to identify kernel resistance mechanisms, and assist the development of targeted and innovative approaches for breeding resistant crops (Alberts *et al.,* 2016). Plant breeding has been used as a tool to develop maize varieties resistant to abiotic and biotic stresses (Cary *et al.,* 2011; Lanubile *et al.,* 2011; Brown *et al.,* 2013; Farfan *et al.,* 2015; Lanubile *et al.,* 2017). These efforts have resulted in a number of germplasm releases. However, no maize hybrids were found to be completely resistant to fungal infection and/or mycotoxin contamination, because of the need to select for multiple traits and associated genes that contribute collectively to plant resistance. Resistance mechanisms are interconnected processes involving many gene products and transcriptional regulators, as well as host interactions with environmental factors, particularly, drought stress and high T (Jiang *et al.,* 2011). The molecular mechanisms underlying maize resistance have yet to be determined. Research has been devoted to understanding kernel resistant mechanisms at the transcriptional level, and to identify stress and/or defense related genes induced during *A. flavus* infection in maize (Chen, *et al.,* 2001; Chen *et al.,* 2015). Microarray or proteomic studies have led to the discovery of many genes involved in maize resistance including several resistance-related quantitative trait loci (QTLs) (Kelley *et al.,* 2012; Brown *et al.,* 2013). Comparisons between the resistant and susceptible lines indicate differences in gene expression networks (Luo *et al.,* 2011). Several research outputs are available on plant-pathogen interactions and host resistance; these are promising starting points for future developments, but clear suggestions regarding hybrid selection, considered the best prevention tool, is not feasible.

Soil management, crop residues and crop rotation

Crop rotation and tillage are recommended practices to reduce inoculum of fungi on overwintering crop residues. Studies on the effects of these practices in maize show variable results, depending on the nature of the pathogen, the geographical location and the combinations with other strategies (Leslie and Logrieco, 2014). Under conditions of high T and low a_w, *A. flavus* becomes the dominant fungal species in the soil and produces abundant inoculum (Horn, 2003). *Fusarium* inoculum is always copious in crop residue in soil, irrespective of environmental conditions. Therefore, soil tillage is commonly considered to reduce inoculum availability. The effects of crop rotation are likely to be negligible, however, in areas with high prevalence of maize, because of long-distance air dispersal of *A. flavus* and *GF*sc (Munkvold, 2014).

Baliukoniene *et al.,* (2011) demonstrated that *F. verticillioides*, *F. proliferatum* and *F. subglutinans* survive

for at least 630 d in maize stalk residues left on the soil surface or buried up to 30 cm deep. Under conventional tillage, the soil was contaminated with 7.0 ± 0.5 $\log_{10}$ CFU g^{-1} of fungal spores belonging to 17 genera of fungi. They identified *Fusarium* from 80% soil samples from conventional tillage. In contrast, the soil under no-tillage was contaminated with 13.5 ± 12.5 $\log_{10}$ CFU g^{-1} fungal spores. There is evidence that crop rotation has greater impacts on *F. graminearum* and *F. culmorum* and relative mycotoxins, especially DON and ZEN, rather than FB- and AF-producing fungi (Munkvold, 2014). This is consistent with splash dispersal of their inoculum. Besides affecting fungal population growth, soil conditions also influence plant root development. Crops with poorly developed root systems are more susceptible to water and nutritional stresses, and consequently, are more susceptible to *Aspergillus* and *GF*sc infections. Adequate soil drainage to avoid drought stress, especially in clay soils, and adapting tillage strategies to soil conditions (Arino *et al.,* 2009; Blandino *et al.,* 2009a) may reduce fungal activity. Furthermore, crop rotation is applied to control maize pests. This practice is recommended in maize to reduce larval populations of western corn rootworm *(Diabrotica virgifera)* (Munkvold, 2014).

Irrigation

Maize has low tolerance to drought-stress, which is considered to be the most crucial factor promoting mycotoxin contamination, in addition to causing significant yield losses. Limited water availability predisposes plants to AF contamination (Battilani *et al.,* 2008; Abbas *et al.,* 2012; Torelli *et al.,* 2012; Damianidis *et al.,* 2018). For *A. flavus* infection, water stress is particularly critical during silk emergence and kernel ripening, so it is recommended to irrigate according to water needs taking into account also the evapo-transpiration precipitation (water balance). For geographical areas where water can be limiting, maize hybrids tolerant to water stress, in addition to early sowing, should be considered.

Data on FBs are less well defined compared with that for AFs. A field study by Arino *et al.* (2009) showed that drought stress during early maize reproductive growth was associated with increased risk for grain contamination with FBs due to *F. verticillioides*. However, the type of irrigation (flood or sprinkler) did not affect FB levels. Although the contribution of water stress to FB contamination is controversial, irrigation according to water needs to avoid drought stress to plants is still recommended, but avoiding excessive and prolonged irrigation close to the stage of milk ripening growth stage is important, as this could enhance FB accumulation (Blandino *et al.,* 2009a; Munkvold, 2014). Increases of DON concentration of up to 3.5 to 5-fold, caused by *F. graminearum,* were also documented by Oldenburg and Schittenhelm (2012) in kernels derived from limited watered plots compared to well-watered plots.

Pest and disease control

Several measures are applied against maize pests, including crop rotation, insecticides, fungicides and other chemical treatments, the use of resistant maize hybrids and biological control agents (BCAs), as well as monitoring and forecasting.

The use of insecticides reduces risk of mycotoxin contamination associated with insects (Folcher *et al.,* 2009). The links between insecticide use (mainly pyrethroids) for the control of ECB and reduction of FB contamination have frequently been described (Blandino *et al.,* 2009a; Blandino *et al.,* 2009b; Blandino *et al.,* 2009c; Folcher *et al.,* 2009; Mazzoni *et al.,* 2011; Folcher *et al.,* 2012). Studies of beneficial effects of combined use of insecticides and fungicides have provided equivocal results. Folcher *et al.* (2009) demonstrated no synergy between deltamethrin and tebuconazole. Efficacy for reducing FBs was 89.96% reduction from the insecticide treatment and 89.97% from insecticide + fungicide. Mazzoni *et al.,* (2011) demonstrated benefit from the combination deltamethrin + tebuconazole in reducing FB contamination, whereas no modification in AF content was observed after treatments. Content of FB1 decreased by 35% in plots treated with tebuconazole and by 56% with tebucoazole + deltamethrin.

Biological control agents (BCAs)

Several pre-harvest biological control systems have been developed for maize against *Aspergillus* spp. and *Fusarium* spp. These have used a variety of potential biocontrol agents (BCAs), including fungal and bacterial strains or atoxigenic fungal strains, as summarized in Table 2. Many microorganisms have been tested, but only *Trichoderma harzianum* (Nayaka *et al.*, 2010) and *Clonostachys rosea* (Luongo *et al.,* 2005; Xue *et al.*, 2014; Samsudin *et al.*, 2017) have been studied under field conditions, and only atoxigenic *A. flavus* strains have been applied on large scale.

Biological control of pathogenic *A. flavus* has been based on the use of atoxigenic isolates of this fungus, which act through competitive exclusion of AF-producers in the environment, and during crop tissue infection (Cotty and Bayman, 1993). The efficacy

Table 2. Current information on reduction of mycotoxin-producing *Aspergillus* spp. and *Fusarium* spp., and mycotoxins production by bio-control microorganisms *in vitro*, *in planta*, and in field trials in maize.

BCA(s)	Target fungal species	Type of assay	References
Pre-harvest			
Atoxigenic *A.flavus* strains	*A. flavus*	*In vitro* and in field	Cotty and Bayman (1993); Cotty (2006); Mauro *et al.* (2015); Bandyopadhyay *et al.*(2016); Mauro *et al.* (2018)
Trichoderma harzianum	*A. flavus*	In greenhouse and in field	Sivparsad and Laing (2016)
Streptomyces spp.	*A. flavus*	*In vitro*	Verheecke *et al.* (2016)
Bacillus megaterium	*A. flavus*	*In vitro*	Kong *et al.* (2014)
Bacillus subtilis (CW14)	*Aspergillus spp., Penicillium spp.*	*In vitro*	Shi *et al.* (2014)
Saccharomyces cerevisiae	*A. parasiticus*	*In vitro*	Armando *et al.* (2012)
Clonostachys rosea, Gram negative bacterium (BCA5)	*F. verticillioides*	*In vitro*	Samsudin *et al.* (2017)
Atoxigenic *F. equiseti, Clonostachys rosea, Epicoccum nigrum, Idriella bolleyi, Trichoderma harzianum, Trichoderma viride*	*F. culmorum* *F. graminearum* *F. proliferatum* *F. verticillioides*	In field	Luongo *et al.* (2005)
Epicoccum nigrum	*F. graminearum*	*In vitro* and *in planta*	Abdallah *et al.* (2018)
Bacillus mojavensis (RRC101)	*F. verticillioides*	*In vitro*	Blacutt *et al.* (2016)
Bacillus spp., *Pseudomonas* spp. *Paenibacillus* spp.	*F. verticillioides*	*In planta*	Figueroa-López *et al.* (2016)
Trichoderma harzianum	*F. verticillioides*	*In vitro*, in greehouse and in field	Nayaka *et al.* (2010)
Clonostachys rosea	*F. graminearum*	In field	Xue *et al.* (2014)
Trichoderma asperellum	*F. graminearum*	*In vitro* and *in planta*	Yaqian *et al.* (2016)
Post-harvest			
Pichia anomala	*A. flavus*	*In vitro*	Tayel *et al.* (2013); Hua *et al.* (2014)
Lactobacillus plantarum	*A. flavus*	*In vitro*	Ahlberg *et al.* (2017)
Debaryomyces hansenii, BCS003	*Aspergillus* spp., *F. proliferatum, F. subglutinans*	*In vitro*	Medina-Cordova *et al.* (2016)
Lactobacillus plantarum MYS6	*F. proliferatum*	*In vitro*	Deepthi *et al.* (2016)
Lactobacillus delbrueckii, L. acidophilus, L. sakei, Pediococcus acidilactici, Enterococcus faecalis	*F. proliferatum*	*In vitro*	Khalil *et al.* (2013)

of this technique has been validated for control of AF contamination in maize. Two bio-pesticides with atoxigenic *A. flavus* active ingredients are registered for use on maize crops in the USA (Cotty, 2006), and several are available in the sub-Saharan Africa, grouped under AFLASAFE mark (Bandyopadhyay *et al.,* 2016). Atoxigenic *A. flavus* communities that are endemic to Italy have been identified, and their efficacy for reducing AF contamination by AF-producers has been demonstrated. One strain (MUCL 54911) displayed the greatest efficacy against several AF-producers (Mauro *et al.,* 2015), and was selected as the active ingredient in AF-X1, now under consideration for registration in Europe (Mauro *et al.,* 2018). To maximize efficacy for preventing aflatoxin contamination, the product should be adapted to the target crop and environment (Cotty, 2006), and the product should also be applied at the 5th leaf crop growth stage (Mauro *et al.,* 2015).

Far less field-based information is available on the effects of BCAs on FB-producing *Fusarium* spp. Results

of bio-assays conducted under controlled conditions have demonstrated moderate suppression of toxigenic *F. verticillioides* and *F. proliferatum* strains using non-pathogenic *Fusarium* strains, including *F. equiseti* (Luongo *et al.,* 2005). Samsudin *et al*., (2017) studied the effects of two BCAs, a fungus (*C. rosea*) and a gram-negative bacterium (BCA5), on growth rates of *F. verticillioides* (FV1), the relative expression of the FUM1 gene and FB1 production. The fungal antagonist reduced FB1 contamination on maize cobs by >70% at 25°C, and almost 60% at 30°C regardless of the maize ripening stage. For the bacterial antagonist, however, FB1 levels on maize cobs were significantly decreased only in some temperature/a_w treatments (25° C and a_w=0.976-0.958; 30° C and a_w=0.976).

Abdallah *et al.,* (2018) demonstrated the capacity of two endophytic fungi (*Epicoccum nigrum* and *Sardoria fimicola*) to reduce ZEN amounts in maize under *in vitro* and *in planta* conditions. *Epicoccum nigrum* consistently reduced amounts of DON and 15-ADON. Some microorganisms have also been studied *in vitro* for their ability to inhibit spoiling *Aspergillus* spp. and *Fusarium* spp. species in maize feed and food products, and for use as natural post-harvest preserving agents (Table 2).

GRAIN HARVESTING AND DRYING

Late harvesting has major impacts on the levels of mycotoxins in maize grain, possibly due to high grain moisture levels and greater periods for fungal growth and toxin production (Munkvold, 2014). *Apergillus flavus* efficiently produces AFs when maize grain moisture content is less er than 28%. In this context, high T (>25°C) and a_w less than 0.95 have been suggested as thresholds above which AF accumulates rapidly (Giorni *et al.,* 2016). To reduce AF contamination, therefore, harvesting in hot and dry years should be carried out while avoiding very low moisture contents in maize grain, and limiting the time available for rapid growth of *A. flavus* and rapid synthesis of AFs. A working compromise for farmers would be to harvest at 22-24% grain moisture, but not at less than 20%.

Detrimental effects of a late harvesting are also confirmed in *Fusarium* spp. A study conducted on maize silage in Switzerland demonstrated that samples with high DON contents often came from fields harvested after September (Eckard *et al.,* 2011).

Moisture content of maize grain at harvest is commonly not low enough to guarantee safe storage, so the grain must be dried before storage commences (Bullerman and Bianchini, 2014). Drying is performed using heated air dryers. Many technologies, and different Ts and time combinations, can be applied for artificial drying of cereals. Treatments at 70°C for 24 h have been shown to be the more effective for reducing the incidence and extent of fungal populations, than greater T and shorter exposure time (95°C for 9 h) (Giorni *et al.,* 2015). Grain should also be dried to less than 14% moisture content to be stored safely, with rapid reduction of moisture content during the first 24 h post-harvest. A final moisture content <13% is suggested when *A. flavus* is present (Channaiah and Maier, 2014).

POST-HARVEST GRAIN MANAGEMENT TO MINIMIZE RISKS OF MYCOTOXIN CONTAMINATION

Grain cleaning and grading

Pest attacks, harvesting and subsequent handling of maize grain can generate broken kernels, as well as contamination from soil and foreign materials which may be sources of mycotoxin contamination. Several physical processes are used for automated grain cleaning and grading (e.g. sieving, flotation, density segregation). Maize cleaning is commonly applied to remove powder and small kernel pieces, commonly the portions with the greatest mycotoxin contamination. Grading gained increased interest for improving grain lots to comply with legislated standards for processed products. Originally, grain grading machines were based on particle weight and size and used centrifugation and flotation in air flows. Contemporary grading machines are mainly based on optical sensors. Grading using UV light illumination for AF reduction is widely used, although mycotoxins can accumulate without visible symptoms and so pose limits to the use of optical sorting techniques (Karlovsky *et al.,* 2016).

Studies on the effectiveness of gain cleaning/grading processes have produced equivocal results, possibly due to the different initial levels of contamination of the raw materials tested (Pietri *et al.,* 2009), and because of differences between mycotoxins. Intact kernels were shown to contain approx. 10 times less FBs than broken maize kernels (Murphy *et al.,* 1993), and removal of broken kernels and other impurities from unprocessed maize reduced DON and ZEN by around 70–80 % (Trenholm *et al.,* 1991). For FB, however, contrasting results have been published. The cleaning step did not affect FB concentration from unprocessed and cleaned maize grain with low contamination (Generotti *et al.,* 2015), while a decrease of 45% was in medium-high contaminated grain (Fandohan *et al.,* 2005). Removal of fine material (approx. 10% by weight) in maize grain has been shown to reduce AF levels by 84% (Hu *et al.,* 2017).

Grain storage

After drying and cleaning, maize grain is placed in silos, for short or long periods, where it is prone to toxigenic fungal contamination and subsequent mycotoxin production, if conductive conditions occur. Air temperature, relative humidity and kernel moisture content have been identified as major storage factors influencing fungal activity and grain quality. Moderate T, kernel moisture less than 14% and dry environment have been demonstrated to limit *A. flavus* growth and subsequent AF contamination in stored maize (Giorni *et al.,* 2008). Monitoring of T and moisture has been suggested for early detection of fungal growth (Mason and Woloshuk, 2010), and this can be done using manual grain inspection for spoilage by moulds and other quality parameters, and measuring grain T. Both approaches, however, have inherent limitations: human sensory detection could be influenced by subjectivity errors caused by individual biases. Cables used to monitor T inside bulk grain bins detect changes only when spoiling grain mass is large enough to raise the T, and these changes must happen close to the sensors. Recent studies have examined the use of CO_2 production as an early indicator of levels of AFs (Garcia-Cela *et al.,* 2019) or FBs (Mylona *et al.,* 2012) in stored maize, and in other cereals (Mylona *et al.,* 2011; Martín Castaño *et al.,* 2017). These studies have shown CO_2 production and trends in the respiration rates, measured by Gas Chromatographic (GC) equipment, can be used as 'storability risk indices' to predict overall quality changes in stored grain.

Hermetic storage in silo bags is an alternative method to mitigate variations of environmental parameters and prevent fungal activity. No variations in AFs, FBs, DON, and OTA or in fungal contamination was observed in silo bags when dynamics of fungi and related mycotoxins were examined during maize storage (Gregori *et al.,* 2013).

Natural compounds with fungicidal or fungistatic activity may be useful for preventing fungal growth in stored maize (Bullerman and Bianchini, 2014; Caceres *et al.,* 2016). Different categories of plant-based compounds with bioactivity against a wide range of fungi have been identified as alternative agents, including antioxidants (Coma *et al.,* 2011; Azaiez *et al.,* 2013; De Lucca *et al.,* 2013; Thippeswamy *et al.,* 2013; Tracz *et al.,* 2016), phenolic compounds (Ferrochio *et al.,* 2013; Thippeswamy *et al.,* 2015), and essential oils (Da Gloria *et al.,* 2010; Matasyoh *et al.,* 2011; Elsamra *et al.,* 2012; Garcia *et al.,* 2012; Koc and Kara, 2014; Sahab *et al.,* 2014; Abhishek *et al.,* 2015; Kalagatur *et al.,* 2015; Liang *et al.,* 2015; Achugbu *et al.,* 2016; Kosegarten *et al.,* 2017; Sawai*et al.,* 2017) (see Supplementary Table S2). It is difficult to draw general conclusions from available information, due to the diversity of variables considered, including the fungal species and the types of compounds tested. Results have mostly been from small scale experiments, and efficacy in maize storage trials remains to be tested and confirmed. Some general conclusions can be drawn, but results remain to confirmed in practical situations. Most studies have tested effects of particular compounds on fungal growth, whereas few have reported effects on mycotoxin reduction. The reported inhibition rates on AFs (Thippeswamy *et al.,* 2013; Liang *et al.,* 2015; Tracz *et al.,* 2016) and on FBs (Coma *et al.,* 2011; Elsamra *et al.,* 2012; Thippeswamy *et al.,* 2015) ranged from 30 to 100%. Eugenol (4-allyl-2-methoxyphenol) has been frequently reported as the active ingredient in the majority of the tested essential oils (eugenol concentration 34.7–78.4 %), highlighting the promise for this compound to reduce *Aspergilli* and *Fusaria* toxin production (Sahab *et al.,* 2014; Kalagatur *et al.,* 2015; Sawai *et al.,* 2017).

Grain processing

Food and feed processing can have affect initial content of mycotoxins in raw materials and these processes are here discussed individually.

Milling of maize grain does not destroy mycotoxins, but this process leads to redistribution of mycotoxins among mill fractions. Distribution of *Aspergillus* and *Fusarium* toxins in maize products after dry-milling has been investigated in several studies, showing similar patterns of distribution. Mycotoxin contaminations increase, compared to unprocessed maize grain, in bran, germ and fractions intended for animal feed (Coradi *et al.,* 2016), whereas they decrease in flaking grits and flour which are mainly destined to human consumption (Bullerman and Bianchini, 2014; Savi *et al.,* 2016). The distribution of *Fusarium* toxins (FBs, ZEN and DON) in dry-milled maize products has been assessed, and these results indicate that average mycotoxin content in meals and grits was reduced by 65-88% compared to the unprocessed grain (Reyneri *et al.,* 2004). A significant decrease (40%) in FB content from unprocessed maize to cornmeal semolina has also been demonstrated, whereas a significant increase in FB content has been found in middlings, commonly intended for feed production (Generotti *et al.,* 2015). In wet-milling, mycotoxins may be dissolved in the steep water and further redistributed. Forty to 50% of AFs were moved from corn grain into steep water during wet milling, where 28–38% of these mycotoxins remained in the fiber fraction, 11–17% in the gluten fraction, 6–11% in

the germ, and only 1% in starch (Karlovsky *et al.,* 2016; Vanara *et al.,* 2018).

Thermal processing. Most mycotoxins are heat stable, but varying degrees of destruction can be achieved with the application of different time/T combinations. AFs have high decomposition Ts ranging from 237°C to 306°C, but all heat treatments (boiling, roasting, baking or steaming) have been reported to reduce foodstuff contamination (Jalili, 2015). Boiling maize grits reduced AF levels by 28%, while frying the boiled grits gave total reduction of 34–53% (Bullerman and Bianchini, 2014). Also, FBs are moderately stable compounds in high T, as a significant decrease in these compounds only occurs above 150–200°C, where thermal processing such as baking, frying, roasting or extruding are applied (Humpf and Voss, 2004; Mohanlall *et al.,* 2013). Bread baking has been shown to reduce concentrations of free FBs by 30–32% and concentrations of modified FBs by 10–19%. The differences in reduction of modified FBs were explained by the presence of proteins or starch capable of stabilizing the mycotoxins during baking (Bryła *et al.,* 2014). The effects of bread making on DON, T-2 and HT-2 toxin stability in naturally contaminated flour samples have been studied in wheat, but no data are available for maize derived products (Stadler *et al.,* 2018). Increases of DON after bread making have been reported, whereas the conjugated form as glucoside derivative DON3G (deoxynivalenol-3-glucoside) was reduced by approx. 50% after baking (Monaci *et al.,* 2013). In contrast, only 7.2% degradation of DON was recorded after baking at 100–250°C for 180 min (Numanoglu *et al.,* 2012).

Decreases in FB contents after thermal processing could be ascribed to the masking phenomena, as well as possible modifications of mycotoxin structure through interactions with other food components leading to the formation of conjugates (Falavigna *et al.,* 2012). Free and total FBs have also been shown to increase after heated drying, especially at 70°C for 24 h exposure. This evidence suggests possible retrogradation of starch, after heating, particularly for amylose, was closely related to modifications in detectable FBs (Giorni *et al.,* 2015).

Flaking and extrusion processes, obtained with high pressure and heating, have been recently reviewed (Jackson *et al.,* 2012; Bullerman and Bianchini, 2014). Several reports showed that FBs decreased after cornflake processing. About 60 to 70% of the initial amounts of FB1 and FB2 were lost during entire cycle of cornflake processing, with less than 30% losses occurring during the intermediate extrusion-cooking step (De Girolamo *et al.,* 2001). During extrusion cooking, the product is forced through metal tubes by rotating screws and is subjected to high T, high pressure, and severe shear. Extrusion usually causes decreases in mycotoxin concentrations. However, the effects on mycotoxin levels is probably influenced by the screw speed and T. Stability of FB1 in corn grits was affected by the extrusion parameters: up to 50% reduction in FB1 was measured when the grits were extruded at 160°C (Jackson *et al.,* 2012). The effects of extrusion on AF levels was also influenced by the presence or absence of additives, moisture content and T. Extrusion alone reduced AF content by 50–80%, and with addition of ammonia, either as hydroxide (0.7-1.0%) or as bicarbonate (0.4%), the decreases in AF levels were greater than 95% (Jalili, 2015). Inclusion of sugar also altered the stability of FBs during extrusion processing (Castelo *et al.,* 2006). This was also the case for DON for which extrusion decomposed DON, which was more susceptible to extrusion than AFB1 (Cazzaniga *et al.,* 2001).

Traditional nixtamalization production of tortillas, the process of cooking in alkaline solution, is reduced initial total AFs by 60-65% and FBs by 80% (Schaarschmidt *et al.,* 2019). This was through physical removal during steeping and washing, and by degradation after application of elevated pH and high T. However, the reductions varied depending on cooking time T, steeping time, and initial toxin concentration in maize grain (Mendez-Albores *et al.,* 2014). The impacts of different nixtamalization processes on AF and FB concentrations was reviewed by Schaarschmidt *et al.* (2019). Besides reduction in the free parent forms, nixtamalization can also cause modification, and/or binding or release of matrix-associated mycotoxins, but their toxicity has yet to be evaluated (De Girolamo *et al.,* 2016).

Detoxification

Preventive actions are not effective for fully avoiding mycotoxin contamination, so detoxification methods may still be necessary to recover contaminated commodities. These include the use of physical processes, or chemical and biological additives. The efficacy of these processes in reducing AFB1 was reviewed by Rushing *et al.,* (2019). They reported a reduction range of AFB1 between 51 and 100% after thermal treatment at Ts between 150 and 200°C, and exposure times between 20 and 200 min. However, none of the reviewed studies were conducted on maize matrices, but were on other cereals (rice and wheat). Gbashi *et al.* (2019) examined decontamination effects of heating on maize flour, and demonstrated that AFs (AFB1, AFB2, AFG1) were completely degraded at 217°C for 35 min. Heat treatment is a low cost and simple approach for mitigating the presence of mycotoxins. However, thermal stability of mycotox-

ins requires the use of high Ts and long exposure times, which result in a significant impacts on grain quality factors.

Effects of UV or gamma irradiation have been reported in maize for AFB1 (Markov *et al.,* 2015) and FBs (Mansur *et al.*, 2014). Reductions of AFB1 by radiation were reported to range between 60 and 90% (Markov *et al.,* 2015).

Chemical treatments have included acidification, ammonization and ozonation, the latter has shown a decontamination rate of AFB1 in maize of 88% (Luo *et al.,* 2014).

Microbial degradation of mycotoxins in less-toxic products has been examined. These biological treatments include inoculation with *Bacillus* (Oluwafemi *et al.,* 2010; Noah Badr *et al.,* 2017) or yeast species (Verheecke *et al.,* 2016), and botanical extracts or enzymes from different biological sources (Karlovsky *et al.,* 2016), with reported reductions in mycotoxins of 60-100%. However, all the described methods are remain experimental, and have yet to be considered as practical management strategies for mycotoxin detoxification.

MODELLING, AND EFFECTS OF CLIMATE CHANGE

Mechanistic models, using weather data as inputs, can predict mycotoxin contamination during the maize growing season and at harvest. They provide valuable support to crop management in a whole food chain view aimed at minimizing mycotoxin contamination. Mechanistic models are available for the prediction of AF and FB occurrence in maize crops, based on actual weather data (Battilani *et al.,* 2003; Maiorano *et al.,* 2009; Battilani *et al.,* 2013), but have not been developed for DON contamination. The impacts of cropping systems are yet to be included in these models. The models could be adapted for the post-harvest periods, but this has yet to be considered. Instead, risk maps have been drawn using historical meteorological data inputs to characterize the most common contamination in relevant geographic areas (Battilani and Camardo Leggieri, 2015).

Apart from seasonal prediction and risk maps, the interest in predictive models for mycotoxins contamination in crops is increasing to take account of climate change. At a global level, climate change is expected to have significant impacts on plant biogeography and fungal populations, with consequences on mycotoxin patterns, as confirmed with predictive approaches (Battilani *et al.,* 2016; van der Fels-Klerx *et al.,* 2016), and by field surveys in Europe (Piva *et al.,* 2006; Dobolyi *et al.,* 2013; Levic *et al.,* 2013). Uncertainties in climate conditions and extreme events have been stressed, and also described as crucial at farm levels (Camardo Leggieri *et al.,* 2019), increasing the emerging risk of co-occurring mycotoxins. Predictive models have therefore become important, to address uncertainties and highlight risk conditions on a geographic basis. Predictive models are likely to be important tools in chain management for mycotoxin reduction as support for farmers, extension services and stakeholders. These willrationalize pre- and post-harvest crop and product management, and provide tools to policy makers for relevant strategic decisions.

CONCLUSIONS

This review has addressed *Aspergillus* and *Fusarium* species in maize, and provided an account of available strategies to mitigate the occurrence of AFs, FBs and DON in maize. Mycotoxin contamination with more than one congener, including modified mycotoxin forms, is an issue that needs further investigation, particularly regarding the consequences for human and animal health. A large body of literature exists on fungal growth and mycotoxin production, and on factors impacting plant-pathogen interactions. Research efforts to support the development of mycotoxin prevention strategies have resulted in sound mitigation methods, mainly at pre-harvest stages (Figure 3). Nevertheless, removal of mycotoxin contamination in maize cannot yet be foreseen, and further efforts are needed to increase the production of maize with mycotoxins below safe levels set by scientific advisory bodies. Key research areas that need further attention include:

- Management of maize genetic resistance, with particular focus on effectiveness towards all mycotoxin producing fungi;
- Increased understanding of plant-pathogen interactions and plant defense mechanisms, including the role of mycotoxins in maize-fungi cross-talk;
- Extension of biocontrol to Fusaria and pest control as sustainable approaches for mycotoxin mitigation;
- Improvement of the performance of predictive models, including investigating the impacts of cropping systems and of co-occurring fungi on model predictions;
- Prediction of future scenarios of mycotoxin occurrence as supporting tools for decision makers;
- Further development of alternative biological tools to be applied post-harvest, to improve safe storage or detoxification of contaminated grain and complete sustainable management of the maize value chain.

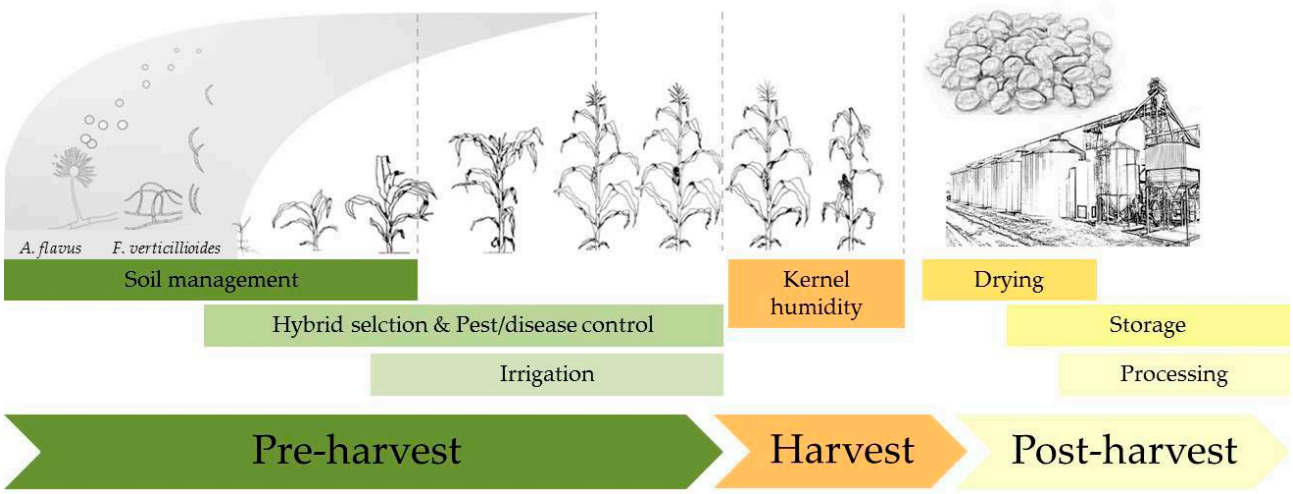

Figure 3. Crucial action in pre- and post-harvest management of maize to minimize mycotoxin contamination by *Aspergillus flavus* and *Fusarium vertcillioides*. Crop phenology is based on the BBCH scale edited by the Federal Biological Research Centre for Agriculture and Forestry.

Harmonized methodologies for human and animal health risk assessment have been recently developed (EFSA, 2019). Such methodologies need to be applied to multiple mycotoxins, using available co-occurrence data and comparative toxicity metrics, to investigate the potential impacts on human and animal health of multiple mycotoxins, in a range of crops including maize.

ACKNOWLEDGMENTS

This review was prepared as part of MYCHIF EFSA project (GP/EFSA/AFSCO/2016/01). Roberta Palumbo carried out this work within the PhD school Agrisystem of Università Cattolica del Sacro Cuore, Italy. This study was supported by the Portuguese Foundation for Science and Technology (FCT) under the scope of the strategic funding of UID/BIO/04469 unit and COMPETE 2020 (POCI-01-0145-FEDER-006684) and BioTecNorte operation (NORTE-01-0145-FEDER-000004) funded by the European Regional Development Fund under the scope of Norte2020 - Programa Operacional Regional do Norte. This paper was critically reviewed in collaboration with MycoKey project (Horizon 2020, Grant Agreement No. 678781).

AUTHOR CONTRIBUTIONS

R. Palumbo: literature review, paper writing. A. Gonçalves: literature review. A. Gkrillas: literature review. A. Logrieco: paper revision. J. L. Dorne: paper revision. C. Dall'Asta: paper writing and revision. A. Venâncio: conception and design, paper revision. P. Battilani: paper conception and design, paper coordination, revision, and final approval. All authors provided critical feedback and helped to shape the manuscript.

LITERATURE CITED

Abbas H.K., Mascagni H.J., Jr. Bruns H.A., Shier W.T., 2012. Effect of planting density, irrigation regimes, and maize hybrids with varying ear size on yield, and aflatoxin and fumonisin contamination levels. *American Journal of Plant Sciences* 3: 1341–1354. DOI:10.4236/ajps.2012.310162

Abbès S., Salah-Abbès J.B., Jebali R., Younes R.B., Oueslati R., 2016. Interaction of aflatoxin B1 and fumonisin B1 in mice causes immunotoxicity and oxidative stress: Possible protective role using lactic acid bacteria. *Journal of Immunotoxicology* 13: 46–54. DOI:10.3109/1547691X.2014.997905

Abdallah M.F., De Boevre M., Landschoot S., De Saeger S., Haesaert G., Audenaert K., 2018. Fungal Endophytes Control *Fusarium graminearum* and Reduce Trichothecenes and Zearalenone in Maize. *Toxins* 10: 493. DOI:10.3390/toxins10120493

Abhishek R.U., Thippeswamy S., Manjunath K., Mohana D.C., 2015. Antifungal and antimycotoxigenic potency of *Solanum torvum* Swartz. leaf extract: isolation and identification of compound active against myco-

toxigenic strains of *Aspergillus flavus* and *Fusarium verticillioides*. *Journal of Applied Microbiology* 119: 1624–1636. DOI:10.1111/jam.12956

Achugbu A.N., Amadi J.E., Ilodibia C.V., Ikegbunam M.N., 2016. Effects of *Garcinia kola* and *Azadirachta indica* seeds in the inhibition of *Aspergillus flavus* and *Aspergillus parasiticus* isolated from *Zea mays* L. Awka, Nigeria. *American Journal of Plant Sciences* 7: 1555–1563. DOI:10.4236/ajps.2016.711147

Ahlberg S., Joutsjoki V., Korhonen H., Laurikkala S., Varmanen P., 2017. *Aspergillus flavus* growth inhibition by Lactobacillus strains isolated from traditional fermented Kenyan milk and maize products. *Archives of microbiology* 199: 457–464. DOI:10.1007/s00203–016-1316-3

Alberts J.F., van Zyl W.H., Gelderblom W.C.A., 2016. Biologically based methods for control of fumonisin-producing *Fusarium* species and reduction of the fumonisins. *Frontiers in Microbiology* 7: 548. DOI:10.3389/fmicb.2016.00548

Arino A., Herrera M., Juan T., Estopanan G., Carraminana J.J., Rota C., Herrera A., 2009. Influence of agricultural practices on the contamination of maize by fumonisin mycotoxins. *Journal of Food Protection* 72: 898–902.

Armando M.R., Dogi C.A., Rosa C.A.R., Dalcero A.M., Cavaglieri L.R., 2012. *Saccharomyces cerevisiae* strains and the reduction of *Aspergillus parasiticus* growth and aflatoxin B1 production at different interacting environmental conditions, *in vitro*. *Food Additives and Contaminants* 29: 1443–1449. DOI:10.1080/19440049.2012.698655

Azaiez I., Meca G., Manyes L., Fernandez-Franzon M., 2013. Antifungal activity of gaseous allyl, benzyl and phenyl isothiocyanate in vitro and their use for fumonisins reduction in bread. *Food Control* 32: 428–434. DOI:10.1016/j.foodcont.2013.01.020

Baliukoniene V., Bakutis B., Januskeviciene G., Miseikiene R., 2011. Fungal contamination and *Fusarium* mycotoxins in cereals grown in different tillage systems. *Journal of Animal and Feed Sciences* 20: 637–647. DOI:10.22358/jafs/66222/2011

Bandyopadhyay R., Ortega-Beltran A., Akande A., Mutegi C., Atehnkeng J., Kaptoge L., Cotty P.J., 2016. Biological control of aflatoxins in Africa: current status and potential challenges in the face of climate change. *World Mycotoxin Journal* 9: 771–789. DOI:10.3920/WMJ2016.2130

Bartók T., Szécsi Á., Juhász K., Bartók M., Mesterházy Á., 2013. ESI-MS and MS/MS identification of the first ceramide analogues of fumonisin B1 mycotoxin from a *Fusarium verticillioides* culture following RP-HPLC separation. *Food Additives and Contaminants- Part A Chemistry, Analysis, Control, Exposure and Risk Assessment* 30: 1651–1659. DOI:10.1080/19440049.2013.809626

Battilani P., Rossi V., Pietri A., 2003. Modelling *Fusarium verticillioides* infection and fumonisin synthesis in maize ears. *Aspects of applied biology* 1: 91–100.

Battilani P., Barbano C., Piva G., 2008. Aflatoxin B1 contamination in maize related to the aridity index in North Italy. *World Mycotoxin Journal* 1: 449–456.

Battilani P., Camardo Leggieri M., 2015. Predictive modelling of aflatoxin contamination to support maize chain management. *World Mycotoxin Journal* 8: 161–170. DOI:10.3920/WMJ2014.1740

Battilani P., Rossi V., Giorni P., Pietri A., Gualla A., van der Fels-Klerx H.J., Brera C., 2012. Modelling, predicting and mapping the emergence of aflatoxins in cereals in the EU due to climate change. *EFSA Supporting Publication 2012* 9: 172. DOI:10.2903/sp.efsa.2012.EN-223

Battilani P., Camardo Leggieri M., Rossi V., Giorni P., 2013. AFLA-maize, a mechanistic model for *Aspergillus flavus* infection and aflatoxin B1 contamination in maize. *Computers and Electronics in Agriculture* 94: 38–46. DOI:10.1016/j.compag.2013.03.005

Battilani P., Toscano P., Van der Fels-Klerx H.J., Moretti A., Camardo Leggieri M., Brera C., … Robinson T., 2016. Aflatoxin B1 contamination in maize in Europe increases due to climate change. *Scientific Reports* 6: 24328. DOI:10.1038/srep24328

Battilani P., Lanubile A., Scala V., Reverberi M., Gregori R., Falavigna C., … Kolomiets M.V., 2018. Oxylipins from both pathogen and host antagonize ja-mediated defense via the 9-lipoxygenase pathway in *Fusarium verticillioides* infection of maize. *Molecular Plant Pathology* 19: 2162–2176. DOI:10.1111/mpp.12690

Berthiller F., Schuhmacher R., Adam G., Krska R., 2009a. Formation, determination and significance of masked and other conjugated mycotoxins. *Analytical and Bioanalytical Chemistry* 395: 1243–1252. DOI:10.1007/s00216–009-2874-x

Berthiller F., Dall'asta C., Corradini R., Marchelli R., Sulyok M., Krska R., … Schuhmacher R., 2009b. Occurrence of deoxynivalenol and its 3-β-D-glucoside in wheat and maize. *Food Additives and Contaminants* 26: 507–511. DOI:10.1080/02652030802555668

Bhatnagar D., Payne G., Klich M., Leslie J.F., 2014. Identification of toxigenic *Aspergillus* and *Fusarium* species in the maize grain chain. In: *Mycotoxin Reduction in Grain Chains* (J. F. Leslie, A. F. Logrieco, eds), Wiley Blackwell: Iowa USA, 11–25.

Blacutt A.A., Mitchell T.R., Bacon C.W., Gold S.E., 2016. *Bacillus mojavensis* RRC101 lipopeptides provoke physiological and metabolic changes during antagonism against *Fusarium verticillioides*. *Molecular Plant Microbe Interactions* 29: 713–723. DOI:10.1094/mpmi-05–16-0093-r

Blandino M., Reyneri A., Colombari G., Pietri A., 2009a. Comparison of integrated field programmes for the reduction of fumonisin contamination in maize kernels. *Field Crops Research* 111: 284–289. DOI:10.1016/j.fcr.2009.01.004

Blandino M., Reyneri A., Vanara F., Tamietti G., Pietri A., 2009b. Influence of agricultural practices on Fusarium infection, fumonisin and deoxynivalenol contamination of maize kernels. *World Mycotoxin Journal* 2: 409–418. DOI:10.3920/WMJ2008.1098

Blandino M., Peila A., Reyneri A., 2009c. Timing clorpirifos + cypermethrin and indoxacarb applications to control European corn borer damage and fumonisin contamination in maize kernels. *Journal of the Science of Food and Agriculture* 90: 521–529. DOI:10.1002/jsfa.3850

Blandino M., Scarpino V., Vanara F., Sulyok M., Krska R., Reyneri A., 2015. Role of the European corn borer (*Ostrinia nubilalis*) on contamination of maize with 13 Fusarium mycotoxins. *Food Additives & Contaminants* 32: 533–543. DOI:10.1080/19440049.2014.966158

Brown R. L., Menkir A., Chen Z.Y., Bhatnagar D., Yu J., Yao H., Cleveland T.E., 2013. Breeding aflatoxin-resistant maize lines using recent advances in technologies - a review. *Food Additives & Contaminants* 30: 1382–1391. DOI:10.1080/19440049.2013.812808

Bryła M., Roszko M., Szymczyk K., Jędrzejczak R., Obiedziński M., Sękul J., 2013a. Fumonisins in plant-origin food and fodder-a review. *Food Additives and Contaminants- Part A Chemistry, Analysis, Control, Exposure and Risk Assessment* 30: 1626–1640. DOI:10.1080/19440049.2013.809624

Bryła M., Jezdrzejczak R., Roszko M., Szymczyk K., Obiedzinski M. W., Sekul J., Rzepkowska M., 2013b. Application of molecularly imprinted polymers to determine B1,B 2, and B3 fumonisins in cereal products. *Journal of Separation Science* 36: 578–584. DOI:10.1002/jssc.201200753

Bryła M., Roszko M., Szymczyk K., Jędrzejczak R., Słowik E., Obiedzinski M.W., 2014. Effect of baking on reduction of free and hidden fumonisins in gluten-free bread. *Journal of Agricultural and Food Chemistry* 62: 10341–10347. DOI:10.1021/jf504077m

Bryła M., Szymczyk K., Jedrzejczak R., Obiedzinski M. W., 2015. Free and hidden fumonisins in various fractions of maize dry milled under model conditions. *LWT-Food Science and Technology* 64: 171–176. DOI:org/10.1016/j.lwt.2015.05.048

Bullerman L.B., Bianchini A., 2014. Good food-processing techniques: Stability of mycotoxins in processed maize-based foods. In: *Mycotoxin Reduction in Grain Chains* (J. F. Leslie, A. F. Logrieco, eds), Wiley Blackwell: Ames, Iowa 50010, USA, 978–971.

Caceres I., El Khoury R., Medina Á., Lippi Y., Naylies C., Atoui A., … Puel O., 2016. Deciphering the anti-aflatoxinogenic properties of eugenol using a large-scale q-PCR approach. *Toxins* 8: 123. DOI:10.3390/toxins8050123

Camardo Leggieri M., Lanubile A., Dall'Asta A., Pietri A., Battilani P., 2019. The impact of seasonal weather variation on mycotoxins: maize crop in 2014 in northern Italy as a case study. *World Mycotoxin Journal* in press. DOI:10.3920/WMJ2019.2475

Camardo Leggieri M., Bertuzzi T., Pietri A., Battilani P., 2015. Mycotoxin occurrence in Italian maize produced in 2009–2011 and focus on the role of crop related factors. *Phytopathologia Mediterranea* 53: 459–469. DOI:10.14601/Phytopathol_Mediterr-14632

Cano-Sancho G., Ramos A.J., Marín S., Sanchis V., 2012. Presence and co-occurrence of aflatoxins, deoxynivalenol, fumonisins and zearalenone in gluten-free and ethnic foods. *Food Control* 26: 282–286. DOI:10.1016/j.foodcont.2012.01.052

Cary J.W., Ehrlich K.C., 2006. Aflatoxigenicity in *Aspergillus*: molecular genetics, phylogenetic relationships and evolutionary implications. *Mycopathologia* 162: 167–177. DOI:10.1007/s11046–006-0051-8

Cary J.W., Rajasekaran K., Brown R.L., Luo M., Chen Z. Y., Bhatnagar D., 2011. Developing resistance to aflatoxin in maize and cottonseed. *Toxins* 3: 678–696. DOI:10.3390/toxins3060678

Castelo M., Katta K., Sumner S., Milford A., Bullerman L., 2006. Extrusion cooking reduces recoverability of Fumonisin B1 from extruded corn grits. *Journal of Food Science* 63: 696–698. DOI:10.1111/j.1365–2621.1998.tb15815.x

Cazzaniga D., Basílico J.C., González R.J., Torres R.L., de Greef D.M., 2001. Mycotoxins inactivation by extrusion cooking of corn flour. *Letters in Applied Microbiology* 33. DOI:10.1046/j.1472–765x.2001.00968.x

Chen Z.Y., Brown R.L., Cleveland T.E., Damann K.E., Russin J. S., 2001. Comparison of constitutive and inducible maize kernel proteins of genotypes resistant or susceptible to aflatoxin production. *Journal of Food Protection* 64: 1785–1792. DOI:10.4315/0362–028X-64.11.1785

Chen Z.Y., Rajasekaran K., Brown R.L., Sayler R.J., Bhatnagar D., 2015. Discovery and confirmation of genes/

proteins associated with maize aflatoxin resistance. *World Mycotoxin Journal* 8: 211–224. DOI:10.3920/wmj2014.1732

Coma V., Portes E., Gardrat C., Richard-Forget F., Castellan A., 2011. In vitro inhibitory effect of tetrahydrocurcuminoids on *Fusarium proliferatum* growth and fumonisin B1 biosynthesis. *Food Additives & Contaminants* 28: 218–225. DOI:10.1080/19440049.2010.540721

Coradi P.C., Maier D.E., Channaiah L.H., Campabadal C., 2016. Effects of the processing on the distribution of aflatoxin and fumonisin levels in corn fractions and feeds. *Journal of Food Process Engineering* 39: 215–225. DOI:10.1111/jfpe.12212

Cotten T.K., Munkvold G.P., 1998. Survival of *Fusarium moniliforme, F. proliferatum,* and *F. subglutinans* in maize stalk residue. *Phytopathology* 88: 550–555.

Cotty P.J., Bayman P., 1993. Competitive exclusion of atoxigenic strain of *Aspergillus flavus* by an atoxigenic strain. *Phytopathology* 83: 1283–1287. DOI: 10.1094/Phyto-83–1283

Cotty P.J., 2006. Biocompetitive exclusión of toxigenic fungi. In: *The mycotoxin factbook: food and feed topics* (D. Barug, D. Bhatnagar, H. P. van Egmond, J. W. van der Kamp, W. A. van Osenbruggen, & A. Visconti, eds), Wageningen Academic Marijkeweg 22, 6709 PG Wageningen, The Netherlands, 179–192.

Da Gloria E.M., Mengai B., Steffen Almeida G., Cuccovia Mazotti N.C., Tadeu dos Santos Dias C., Moreira e Moreira R., … Calori Domingues M.A. (2010). *Effect of essential oils from Eucalyptus on the growth of aflatoxigenic species.* Paper presented at the 10th International Working Conference on Stored Product Protection, Brazil.

Dall'Asta C., Mangia M., Berthiller F., Molinelli A., Sulyok M., Schuhmacher R., … Marchelli R., 2009. Difficulties in fumonisin determination: The issue of hidden fumonisins. *Analytical and Bioanalytical Chemistry* 395: 1335–1345. DOI:10.1007/s00216–009-2933-3

Dall'Asta C., Falavigna C., Galaverna G., Dossena A., Marchelli R., 2010. In vitro digestion assay for determination of hidden fumonisins in maize. *Journal of Agricultural and Food Chemistry* 58: 12042–12047. DOI:10.1021/jf103799q

Dall'Asta C., Falavigna C., Galaverna G., Battilani P., 2012. Role of maize hybrids and their chemical composition in Fusarium infection and fumonisin production. *Journal of Agricultural and Food Chemistry* 60: 0021–8561. DOI:10.1021/jf300250z

Dall'Asta C., Giorni P., Cirlini M., Reverberi M., Gregori R., Ludovici M., Scala V., 2015. Maize lipids play a pivotal role in the fumonisin accumulation. *World Mycotoxin Journal* 8: 87–97. DOI:10.3920/wmj2014.1754

Dall'Asta C., Battilani P., 2016. Fumonisins and their modified forms, a matter of concern in future scenario? *World Mycotoxin Journal* 9: 727–739. DOI:10.3920/WMJ2016.2058

Damianidis D., Ortizb B.V., Windhamc G.L., Bowend K.L., Hoogenboome G., Scullyf B.T., … Williamsc W. P., 2018. Evaluating a generic drought index as a predictive tool for aflatoxin contamination of corn: From plot to regional level. *Crop Protection* 113: 64–74. DOI:10.1016/j.cropro.2018.07.013

De Boevre M., Di Mavungu D.J., Landschoot S., Audenaert K., Eeckhout M., Maene P., … De Saeger S., 2012. Natural occurrence of mycotoxins and their masked forms in food and feed products. *World Mycotoxin Journal* 5: 207–219. DOI:10.3920/WMJ2012.1410

De Girolamo A., Solfrizzo M., Visconti A., 2001. Effect of processing on fumonisin concentration in corn flakes. *Food Protection Trends* 64: 701–705.

De Girolamo A., Lattanzio V.M.T., Schena R., Visconti A., Pascale M., 2016. Effect of alkaline cooking of maize on the content of fumonisins B1 and B2 and their hydrolysed forms. *Food Chemistry* 192: 1083–1089. DOI:10.1016/j.foodchem.2015.07.059

De Lucca A.J., Carter-Wientjes C.H., Boue S.M., Lovisa M.P., Bhatnagar D., 2013. Inhibition of bacterial and filamentous fungal growth in high moisture, nonsterile corn with intermittent pumping of trans-2-hexenal vapor. *Journal of Food Science* 78: 1029–1035. DOI:10.1111/1750–3841.12151

Deepthi B.V., Rao K. P., Chennapa G., Sreenivasa M.Y., Naik M.K., Chandrashekara K.T., 2016. Antifungal attributes of *Lactobacillus plantarum* MYS6 against fumonisin producing *Fusarium proliferatum* associated with poultry feeds. *PLoS One* 11: 1932–6203. DOI:10.1371/journal.pone.0155122

Desmarchelier A., Seefelder W., 2011. Survey of deoxynivalenol and deoxynivalenol-3-glucoside in cereal-based products by liquid chromatography electrospray ionization tandem mass spectrometry. *World Mycotoxin Journal* 4: 29–35. DOI:10.3920/WMJ2010.1236

Dobolyi C., Sebok F., Varga J., Kocsube S., Szigeti G., Baranyi N., … Kukolya J., 2013. Occurrence of aflatoxin producing *Aspergillus flavus* isolates in maize kernel in Hungary. *Acta Alimentaria* 42: 451–459. DOI:10.1556/AAlim.42.2013.3.18

Domijan A.M., Peraica M., Cvjetkovij B., Turcin S., Jurjevic Z., Ivic D., 2005. Mould contamination and co-

occurrence of mycotoxins in maize grain in Croatia. *Acta Pharmaceutica* 55: 349–356.

Drakulic J., Ray R.V., Bruce T.J.A., 2017. Direct and host-mediated interactions between Fusarium pathogens and herbivorous arthropods in cereals. *Plant Pathology* 66: 3-13. DOI:I 10.1111/ppa.12546

Eckard S., Wettstein F.E., Forrer H.R., Vogelgsang S., 2011. Incidence of *Fusarium* species and mycotoxins in silage maize. *Toxins* 3: 949–967. DOI:10.3390/toxins3080949

EFSA. 2004. Opinion of the Scientific Panel on Contaminants in the Food Chain on a request from the Commission related to Aflatoxin B1 as undesirable substance in animal feed. *EFSA Journal* 39: 1-27.

EFSA., More S. J., Bampidis V., Benford D., Bennekou S. H., Bragard C., … Hogstrand C., 2019. Guidance on harmonised methodologies for human health, animal health and ecological risk assessment of combined exposure to multiple chemicals. *EFSA Journal EFSA Journal* 17: 5634–5677. DOI: 10.2903/j.efsa.2019.5634

Elsamra I.A., Shama S.M., Hamza A.S., Youssef N.H., Youssef M.S., Alabd S.M., 2012. Effect of some mould inhibitors and herbal plants on mycotoxins production by *Aspergillus flavus* and *Fusarium verticilloides in vitro* and in stored corn grains. *Archives of Phytopathology and Plant Protection* 45: 1861–1878. DOI:10.1080/03235408.2012.713799

Eskola M., Altieri A., Galobart J., 2018. Overview of the activities of the European Food Safety Authority on mycotoxins in food and feed. *World Mycotoxin Journal* 11: 277–289. DOI:10.3920/WMJ2017.2270

European Commission, 2006a. Regulation (576/2006) on the presence of deoxynivalenol, zearalenone, ochratoxin A, T-2 and HT-2 and fumonisins in products intended for animal feeding. *Official Journal of the European Union* 229: 7-9.

European Commission, 2006b. Regulation (1881/2006) setting maximum levels for certain contaminants in foodstuffs. *Official Journal of the European Union* 364: 4-24.

European Commission, 2011. Regulation (574/2011) amending Annex I to Directive 2002/32/EC of the European Parliament and of the Council as regards maximum levels for nitrite, melamine, *Ambrosia* spp. and carry-over of certain coccidiostats and histomonostats and consolidating Annexes I and II thereto. *Official Journal of the European Union* 159: 7-23.

European Commission, 2013. Recommendations (165/2013) on the presence of T-2 and HT-2 toxin in cereals and cereal products. *Official Journal of the European Union* 91: 12–15.

European Commission, 2019. Short-term outlook for EU agricultural markets in 2018 and 2019. Retrieved from https://ec.europa.eu/agriculture/markets-and-prices/short-term-outlook_en

Eurostat, 2019. Agriculture, forestry and fishery statistical book. Retrieved from https://ec.europa.eu/eurostat/statistics-explained/index.php?title=Agricultural_production_-_crops

Falavigna C., Cirlini M., Galaverna G., Dall'Asta C., 2012. Masked fumonisin in processed food: co-occurrence of hiddend and bound forms and stability under digestive conditions. *World Mycotoxin Journal* 5: 325–334. DOI:10.3920/WMJ2012.1403

Falavigna C., Lazzaro I., Galaverna G., Dall'Asta C., Battilani P., 2016. Oleoyl and linoleoyl esters of fumonisin B1 are differently produced by *Fusarium verticillioides* on maize and rice based media. *International Journal of Food Microbiology* 217. DOI:10.1016/j.ijfoodmicro.2015.10.013

Fandohan P., Zoumenou D., Hounhouigan D.J., Marasas W.F.O., Wingfield M.J., Hell K., 2005. Fate of aflatoxins and fumonisins during the processing of maize into food products in Benin. *International Journal of Food Microbiology* 98: 249–259. DOI:10.1016/j.ijfoodmicro.2004.07.007

Farfan I.D.B., De La Fuente G.N., Murray S.C., Isakeit T., Huang P.C., Warburton M., Kolomiets M., 2015. Genome wide association study for drought, aflatoxin resistance, and important agronomic traits of maize hybrids in the sub-tropics. *PLoS ONE* 10: 1932–6203. DOI:10.1371/journal.pone.0117737

Ferrochio L., Cendoya E., Farnochi M.C., Massad W., Ramirez M.L., 2013. Evaluation of ability of ferulic acid to control growth and fumonisin production of *Fusarium verticillioides* and *Fusarium proliferatum* on maize based media. *International Journal of Food Microbiology* 167: 215–220. DOI:10.1016/j.ijfoodmicro.2013.09.005

Figueroa-López A.M., Cordero-Ramírez J.D., Martínez-Álvarez J.C., López-Meyer M., Lizárraga-Sánchez G.J., Félix-Gastélum R., Maldonado-Mendoza I.E., 2016. Rhizospheric bacteria of maize with potential for biocontrol of *Fusarium verticillioides*. *SpringerPlus* 5: 330. DOI:10.1186/s40064–016-1780-x

Folcher L., Marc J., Weissenberger A., Gérault F., Eychenne N., Délos M., Regnault-Roger C., 2009. Comparative activity of agrochemical treatments on mycotoxin levels with regard to corn borers and Fusarium mycoflora in maize (*Zea mays L.*) fields. *Crop Protection* 28: 302–308. DOI:10.1016/j.cropro.2008.11.007

Folcher L., Weissenberger A., Delos M., 2012. Quantitative relationships between *Ostrinia nubilalis* activity and deoxynivalenol contamination in French maize.

International Journal of Pest Management 58: 302–309. DOI:10.1080/09670874.2012.679641

Fumero M.V., Sulyok M., Chulze S., 2016. Ecophysiology of *Fusarium temperatum* isolated from maize in Argentina. *Food Additives and Contaminants - Part A Chemistry, Analysis, Control, Exposure and Risk Assessment* 33: 147–156. DOI:10.1080/19440049.2015.1107917

Garcia-Cela E., Kiaitsi E., Sulyok M., Krska R., Medina A., Petit Damico I., Magan N., 2019. Influence of storage environment on maize grain: CO2 production, dry matter losses and aflatoxins contamination. *Food Additives and Contaminants*. DOI:10.1080/19440049.2018.1556403

Garcia D., Ramos A., Sanchis V., Marin S., 2012. Effect of *Equisetum arvense* and *Stevia rebaudiana* extracts on growth and mycotoxin production by *Aspergillus flavus* and *Fusarium verticillioides* in maize seeds as affected by water activity. *International Journal of Food Microbiology* 153: 1-2. DOI:10.1016/j.ijfoodmicro.2011.10.010

Gbashi S., Madala N. E., De Saeger S., De Boevre M., Njobeh P. B., 2019. Numerical optimization of temperature-time degradation of multiple mycotoxins. *Food and Chemical Toxicology* 125: 289–304. DOI:10.1016/j.fct.2019.01.009

Generotti S., Cirlini M., Dall'Asta C., Suman M., 2015. Influence of the industrial process from caryopsis to cornmeal semolina on levels of fumonisins and their masked forms. *Food Control* 48: 170–174. DOI:10.1016/j.foodcont.2014.06.003

Giorni P., Magan N., Pietri A., Bertuzzi T., Battilani P., 2007. Studies on *Aspergillus* section *Flavi* isolated from maize in northern Italy. *International Journal of Food Microbiology* 113: 330–338. DOI:10.1016/j.ijfoodmicro.2006.09.007

Giorni P., Magan N., Pietri A., Battilani P., 2011. Growth and aflatoxin production of an Italian strain of *Aspergillus flavus*: influence of ecological factors and nutritional substrates. *World Mycotoxin Journal* 4: 425–432. DOI:10.3920/wmj2011.1300

Giorni P., Formenti S., Bertuzzi T., Magan N., Battilani P., 2014. Influence of water activity and anti-fungal compounds on development and competitiveness of *Fusarium verticillioides*. *Phytopathologia Mediterranea* 53: 459–469.

Giorni P., Dall'Asta C., Gregori R., Cirlini M., Galaverna G., Battilani P., 2015. Starch and thermal treatment, important factors in changing detectable fumonisins in maize post-harvest. *Journal of Cereal Science* 61: 78–85. DOI:10.1016/j.jcs.2014.10.006

Giorni P., Bertuzzi T., Battilani P., 2016. Aflatoxin in maize, a multifaceted answer of *Aspergillus flavus* governed by weather, host-plant and competitor fungi. *Journal of Cereal Science* 70: 256–262. DOI:10.1016/j.jcs.2016.07.004

Görtz A., Oerke E. C., Steiner U., Dehne H. W. (2008, 6-10 May 2007). *Incidence and Control of Fusarium Ear Rot of Maize*. Paper presented at the Modern fungicides and antifungal compounds V: 15th International Reinhardsbrunn Symposium, Friedrichroda Germany.

Gregori R., Meriggi P., Pietri A., Formenti S., Baccarini G., Battilani P., 2013. Dynamics of fungi and related mycotoxins during cereal storage in silo bags. *Food Control* 30: 280–287. DOI:10.1016/j.foodcont.2012.06.033

Horn B. W., 2003. Ecology and population biology of aflatoxigenic fungi in soil. *Journal of Toxicology* 22: 351–379. DOI:10.1081/TXR-120024098

Horn B. W., Moore G. G., Carbone I., 2009. Sexual reproduction in *Aspergillus flavus*. *Mycologia* 101: 423–429. DOI:10.3852/09–011

Horn B. W., Gell R. M., Singh R., Sorensen R. B., Carbone I., 2016. Sexual reproduction in *Aspergillus flavus* sclerotia: acquisition of novel alleles from soil populations and uniparental mitochondrial inheritance. *PLoS One* 11: 1. DOI:10.5061/dryad.sk35h

Hu S., Stroshine R. L., Ileleji K., 2017. Differences in kernel shape, size, and density between healthy kernels and mold discolored kernels and their relationship to reduction in aflatoxin levels in a sample of shelled corn. *Applied Engineering in Agriculture* 33: 421–431.

Hua S. T., Beck J. J., Sarreal S. B. L., Gee W., 2014. The major volatile compound 2-phenylethanol from the biocontrol yeast, *Pichia anomala*, inhibits growth and expression of aflatoxin biosynthetic genes of *Aspergillus flavus*. *Mycotoxin Research* 30: 71–78. DOI:10.1007/s12550–014-0189-z

Humpf H. U., Voss K. A., 2004. Effect of thermal food processing on the chemical structure and toxicity of fumonisin mycotoxins. *Molecular Nutrition and Food Research* 48: 255–269.

Ingenbleek L., Sulyok M., Adegboye A., Hossou S. E., Koné A. Z., Oyedele A. D., … Krska R., 2019. Regional Sub-Saharan Africa total diet study in Benin, Cameroon, Mali and Nigeria reveals the presence of 164 mycotoxins and other secondary metabolites in foods. *Toxins* 11: 54. DOI: 10.3390/toxins11010054

Jackson L. S., Jackson L. S., Voss K. A., Ryu D., 2012. Effects of different extrusion conditions on the chemical and toxicological fate of fumonisin B-1 in maize: a short review. *World Mycotoxin Journal* 5: 251–260. DOI:I 10.3920/wmj2012.1431

Jalili M., 2015. A Review on Aflatoxins Reduction in Food. *Iranian Journal of Health, Safety and Environment* 3: 445–459.

Jiang T., Zhou B., Luo M., Abbas Hamed K., Kemerait R., Lee Robert D., Guo B., 2011. Expression analysis of stress-related genes in kernels of different maize (*Zea mays L.*) inbred lines with different resistance to aflatoxin contamination. *Toxins* 3: 538–550. DOI:10.3390/toxins3060538

Jurjevic Z., Solfrizzo M., Cvjetkovic B., De Girolamo A., Visconti A., 2002. Occurrence of beauvericin in corn from Croatia. *Food Technology and Biotechnology* 40: 91–94.

Kalagatur N. K., Mudili V., Siddaiah C., Gupta V. K., Natarajan G., Sreepathi M. H., … Putcha V. L. R., 2015. Antagonistic activity of *Ocimum sanctum* L. essential oil on growth and zearalenone production by *Fusarium graminearum* in maize grains. *Frontiers in Microbiology* 6: 1664–1302. DOI:10.3389/fmicb.2015.00892

Karlovsky P., Suman M., Berthiller F., De Meester J., Eisenbrand G., Perrin I., … Dussort P., 2016. Impact of food processing and detoxification treatments on mycotoxin contamination. *Mycotoxin Research* 32: 179–205. DOI:I 10.1007/s12550–016-0257-7

Kelley R. Y., Williams W. P., Mylroie J. E., Boykin D. L., Harper J. W., Windham G. L., Xueyan S., 2012. Identification of maize genes associated with host plant resistance or susceptibility to *Aspergillus flavus* infection and aflatoxin accumulation. *PLoS One* 7: 1932–6203. DOI:10.1371/journal.pone.0036892

Khalil A., Abdellatef A. A., Abou-Gabal A. E., Khaled A. E., Elfaramawy A. M., 2013. Lactic acid bacteria as antimycotic and antimycotoxins agents against toxigenic *Fusarium* species associated to maize grains stored in Egyptian markets. *Journal of Pure and Applied Microbiology* 7: 93–105.

Kirincic S., Skrjanc B., Kos N., Kozolc B., Pirnat N., Tavcar-Kalcher G., 2015. Mycotoxins in cereals and cereal products in Slovenia - Official control of foods in the years 2008–2012. *Food Control* 50: 157–165.

Koc F., Kara S., 2014. Environmental factors affecting efficacy of some essential oils and potassium sorbate to control growth of *Aspergillus flavus, Aspergillus parasiticus* on wheat and maize grains. *Journal of Agricultural Science and Technology* 16: 1325–1334.

Kong Q., Chi C., Yu J., Shan S., Li Q., Li Q., … Bennett J. W., 2014. The inhibitory effect of *Bacillus megaterium* on aflatoxin and cyclopiazonic acid biosynthetic pathway gene expression in *Aspergillus flavus*. *Applied microbiology and biotechnology* 98: 5161–5172. DOI:10.1007/s00253–014-5632-8

Kosegarten C. E., Ramirez-Corona N., Mani-Lopez E., Palou E., Lopez-Malo A., 2017. Description of *Aspergillus flavus* growth under the influence of different factors (water activity, incubation temperature, protein and fat concentration, pH, and cinnamon essential oil concentration) by kinetic, probability of growth, and time-to-detection models. *International Journal of Food Microbiology* 240: 115–123. DOI:10.1016/j.ijfoodmicro.2016.04.024

Kovalsky P., Kos G., Nährer K., Schwab C., Jenkins T., Schatzmayr G., … Krska R., 2016. Co-Occurrence of regulated, masked and emerging mycotoxins and secondary metabolites in finished feed and maize-An extensive survey. *Toxins* 8: 363.

Lanubile A., Pasini L., Lo Pinto M., Battilani P., Prandini A., Marocco A., 2011. Evaluation of broad spectrum sources of resistance to *Fusarium verticillioides* and advanced maize breeding lines. *World Mycotoxin Journal* 4: 43–51. DOI:10.3920/WMJ2010.1206

Lanubile A., Maschietto V., Borrelli V. M., Stagnati L., Logrieco A. F., Marocco A., 2017. Molecular Basis of Resistance to Fusarium Ear Rot in Maize. *Frontiers in Plant Science* 8: 1774. DOI:10.3389/fpls.2017.01774

Lazzaro I., Susca A., Mule G., Ritieni A., Ferracane R., Marocco A., Battilani P., 2012. Effects of temperature and water activity on FUM2 and FUM21 gene expression and fumonisin B production in *Fusarium verticillioides*. *European Journal of Plant Pathology* 134: 685–695. DOI:10.1007/s10658–012-0045-y

Lazzaro I., Moretti A., Giorni P., Brera C., Battilani P., 2015. Organic vs conventional farming: Differences in infection by mycotoxin-producing fungi on maize and wheat in Northern and Central Italy. *Crop Protection* 72: 22–30. DOI:10.1016/j.cropro.2015.03.001

Leslie J.F., Logrieco A.F., 2014. *Mycotoxin Reduction in Grain Chains*. Wiley Blackwell, Ames, Iowa, USA, 352 pp.

Levic J., Gosic-Dondo S., Ivanovic D., Stankovic S., Krnjaja V., Bocarov-Stancic A., Stepanic A., 2013. An outbreak of *Aspergillus* species in response to environmental conditions in Serbia. *Pestic Phytomed* 28: 167–179. DOI:10.2298/PIF1303167L

Liang D., Xing F., Selvaraj J., Liu X., Wang L., Hua H., … Liu Y., 2015. Inhibitory effect of cinnamaldehyde, citral, and eugenol on aflatoxin biosynthetic gene expression and aflatoxin B1 biosynthesis in *Aspergillus flavus*. *Journal of Food Science* 80: 2917–2923. DOI:10.1111/1750–3841.13144

Llorens A., Mateo R., Hinojo M. J., Valle-Algarra F. M., Jimenez M., 2004. Influence of environmental factors on the biosynthesis of type B trichothecenes by isolates of *Fusarium* spp. from Spanish crops. *International Journal of Food Microbiology* 94: 43–54.

Logrieco A., Mulè G., Moretti A., Bottalico A., 2002. Toxigenic *Fusarium* species and mycotoxins associated with maize ear rot in Europe. *European Journal of Plant Pathology* 108: 597–609. DOI:10.1023/A:1020679029993

Logrieco A., Miller J. D., Eskola M., Krska R., Ayalew A., Bandyopadhyay R., … J.F. L., 2018. The Mycotox Charter: increasing awareness of, and concerted action for, minimizing mycotoxin exposure worldwide. *Toxins* 10: 1-17. DOI:10.3390/toxins10040149

Ludovici M., Ialongo C., Reverberi M., Beccaccioli M., Scarpari M., Scala V., 2014. Quantitative profiling of oxylipins through comprehensive LC-MS/MS analysis of *Fusarium verticillioides* and maize kernels. *Food Additives & Contaminants, Part A: Chemistry, Analysis, Control, Exposure & Risk Assessment* 31: 2026–2033. DOI:10.1080/19440049.2014.968810

Luo M., Liu J., Lee R. D., Guo B. Z., 2008. Characterization of gene expression profiles in developing kernels of maize (*Zea mays*) inbred Tex6. *Plant Breeding* 127: 569–578. DOI:10.1111/j.1439–0523.2008.01538.x

Luo M., Brown R. L., Chen Z. Y., Menkir A., Yu J., Bhatnagar D., 2011. Transcriptional profiles uncover *Aspergillus flavus*-induced resistance in maize kernels. *Toxins* 3: 766–786. DOI:10.3390/toxins3070766

Luo X., Wang R., Wang L., Li Y., Wang Y., Chen Z., 2014. Detoxification of aflatoxin in corn flour by ozone. *Journal of the Science of Food and Agriculture* 94: 2253–2258. DOI:10.1002/jsfa.6550

Luongo L., Galli M., Corazza L., Meekes E., Haas L., Plas L. C., 2005. Potential of fungal antagonists for bio-control of *Fusarium* spp. in wheat and maize through competition in crop debris. *Biocontrol Science and Technology* 15: 229–242. DOI:10.1080/09583150400016852

Maiorano A., Reyneri A., Sacco D., Magni A., Ramponi C., 2009. A dynamic risk assessment model (FUMAgrain) of fumonisin synthesis by *Fusarium verticillioides* in maize grain in Italy. *Crop Protection* 28: 243–256.

Manstretta V., Rossi V., 2015. Effects of weather variables on ascospore discharge from *Fusarium graminearum* perithecia. *PLoS One* 10: 1932–6203. DOI:10.1371/journal.pone.0138860

Manstretta V., Rossi V., 2016. Effects of temperature and moisture on development of *Fusarium graminearum* perithecia in maize stalk residues. *Applied and Environmental Microbiology* 82: 184–191. DOI:10.1128/aem.02436–15

Mansur A. R., Yu C. C., Oh D. H., 2014. Efficiency of gamma irradiation to inactivate growth and fumonisin production of *Fusarium moniliforme* on corn grains. *Journal of Microbiology and Biotechnology* 24: 209–216.

Markov K., Mihaljević B., Domijan A. M., Pleadin J., Delaš F., Frece J., 2015. Inactivation of aflatoxigenic fungi and the reduction of aflatoxin B-1 *in vitro* and *in situ* using gamma irradiation. *Food Control* 54: 79–85. DOI:10.1016/j.foodcont.2015.01.036

Martín Castaño S., Medina A., Magan N., 2017. Impact of storage environment on respiration, dry matter losses and fumonisin B1 contamination of stored paddy and brown rice. *World Mycotoxin Journal* 10: 319–326. DOI:10.3920/WMJ2017.2237

Mason L. J., Woloshuk C. P., 2010. Maximize grain quality and profits using S.L.A.M. Retrieved from http://extension.entm.perdue.edu/grainlab/content/pdf/ID-207.pdf

Matasyoh J. C., Wagara I. N., Nakavuma J. L., Kiburai A. M., 2011. Chemical composition of *Cymbopogon citratus* essential oil and its effect on mycotoxigenic *Aspergillus* species. *African Journal of Food Science* 5: 138–142.

Mauro A., Battilani P., Cotty P. J., 2015. Atoxigenic *Aspergillus flavus* endemic to Italy for biocontrol of aflatoxins in maize. *BioControl* 60: 125–134. DOI:10.1007/s10526–014-9624-5

Mauro A., Garcia-Cela E., Pietri A., Cotty P. J., Battilani P., 2018. Biological control products for aflatoxin prevention in Italy: Commercial field evaluation of atoxigenic *Aspergillus flavus* active ingredients. *Toxins* 10. DOI:10.3390/toxins10010030

Mazzoni E., Scandolara A., Giorni P., Pietri A., Battilani P., 2011. Field control of Fusarium ear rot, *Ostrinia nubilalis* (Hubner), and fumonisins in maize kernels. *Pest Management Science* 67: 458–465. DOI:10.1002/ps.2084. Epub 2011 Jan 6

Medina-Cordova N., Lopez-Aguilar R., Ascencio F., Castellanos T., Campa-Cordova A. I., Angulo C., 2016. Biocontrol activity of the marine yeast *Debaryomyces hansenii* against phytopathogenic fungi and its ability to inhibit mycotoxins production in maize grain (*Zea mays L.*). *Biological Control* 97: 70–79. DOI:10.1016/j.biocontrol.2016.03.006

Medina A., Magan N., Schmidt-Heydt M., Geisen R., Cardenas-Chavez D. L., Parra R., 2013. Integrating toxin gene expression, growth and fumonisin B-1 and B-2 production by a strain of *Fusarium verticillioides* under different environmental factors. *Journal Of The Royal Society Interface* 10: 1742–5689. DOI:10.1098/rsif.2013.0320

Mendez-Albores A., Cardenas-Rodriguez Denisse A., Vazquez-Duran A., 2014. Efficacy of microwave-heating during alkaline processing of fumonisin-con-

taminated maize. *Iranian journal of public health* 43: 147–155.

Mohanlall R., Odhav B., Mohanlall V., 2013. The effect of thermal processing on fumonisin B1(FB1) levels in maize-based foods. *African Journal of Food Science* 7: 45–50.

Monaci L., De Angelis E., Pascale M., Visconti A., 2013. Effect of bread making on the levels of deoxynivalenol, T-2 and HT-2 toxins and their conjugated forms. *Tecnica Molitoria* 64: 974–982.

Munkvold G. P., Carlton W. M., 1997. Influence of inoculation method on systemic *Fusarium moniliforme* infection of maize plants grown from infected seeds. *Plant Disease* 81: 211–216.

Munkvold G. P., McGee D. C., Carlton W. M., 1997. Importance of different pathways for maize kernel infection by *Fusarium moniliforme*. *Phytopathology* 2: 209.

Munkvold G. P., 2014. Crop management practices to minimize the risk of mycotoxins contamination in temperate-zone maize. In: *Mycotoxin Reduction in Grain Chains* (J. F. Leslie, A. F. Logrieco, eds), Wiley Blackwell, Ames, Iowa, USA, 2083–2085.

Murillo-Williams A and Munkvold GP, 2008. Systemic infection by *Fusarium verticillioides* in maize plants grown under three temperature regimes. *Plant Disease* 92:1695–1700. DOI:10.1094/PDIS-92–12-1695

Murphy P. A., Rice L. G., Ross P. F., 1993. Fumonisin-B1, fumonisin B2,and fumonisin B3 content of Iowa,Wisconsin, and Illinois corn and corn screenings. *Journal of Agricultural and Food Chemistry* 41: 263–266. DOI:10.1021/jf00026a024

Mylona K., Magan N., 2011. *Fusarium langsethiae*: storage environment influences dry matter losses and T2 and HT-2 toxin contamination of oats. *Journal of Stored Products Research* 47: 321–327. DOI: 10.1016/j.jspr.2011.05.002

Mylona K., Sulyok M., Magan N., 2012. Relationship between environmental factors, dry matter loss and mycotoxin levels in stored wheat and maize infected with Fusarium species. *Food Additives & Contaminants* 29: 1118–1128. DOI: 10.1080/19440049.2012.672340

Nakagawa H., Sakamoto S., Sago Y., Kushiro M., Nagashima H., 2013. Detection of masked mycotoxins derived from type A trichothecenes in corn by high-resolution LC-Orbitrap mass spectrometer. *Food Additives & Contaminants: Part A* 30: 1407–1414. DOI:10.1080/19440049.2013.790087

Nayaka S. C., Niranjana S. R., Shankar A., Raj S. N., Reddy M. S., Prakash H. S., Mortensen C. N., 2010. Seed biopriming with novel strain of *Trichoderma harzianum* for the control of toxigenic *Fusarium verticillioides* and fumonisins in maize. *Archives of Phytopathology and Plant Protection* 1: 265–284. DOI:10.1080/03235400701803879

Noah Badr A., Amra H. A., Youssef M. M., Logrieco A. F., 2017. Ability of *Bacillus Amyloliquefaciens* isolated from corn on mycotoxins degradation. *Research Journal of Pharmaceutical, Biological and Chemical Sciences* 8: 1994–2004.

Numanoglu E., Gökmen V., Uygun U., Koksel H., 2012. Thermal degradation of deoxynivalenol during maize bread baking. *Food Additives & Contaminants* 29: 423–430. DOI:10.1080/19440049.2011.644812

Ojiambo P., Battilani P., Cary J., Bluhm B., Carbone I., 2018. Cultural and genetic approaches to manage aflatoxin contamination: recent insights provide opportunities for improved control. *Phytopathology* 108: 1024–1037. DOI:10.1094/PHYTO-04–18-0134-RVW

Oldenburg E., Schittenhelm S., 2012. Effect of plant water deficit on the deoxynivalenol concentration in Fusarium-infected maize kernels. *Mycotoxin Research* 28: 229. DOI:10.1007/s12550–012-0136-9

Oliveira M. S., Diel A. C. L., Rauber R. H., Fontoura F. P., Mallmann A., Dilkin P., Mallmann C. A., 2015. Free and hidden fumonisins in Brazilian raw maize samples. *Food Control* 53: 217–221. DOI:10.1016/j.foodcont.2014.12.038

Oluwafemi F., Kumar M., Bandyopadhyay R., Ogunbanwo T., Ayanwande K. B., 2010. Bio-detoxification of aflatoxin B1 in artificially contaminated maize grains using lactic acid bacteria. *Toxin Reviews* 29: 3-4. DOI: 10.3109/15569543.2010.512556

Parker N. S., Anderson N. R., Richmond D. S., Long E. Y., Wise K. A., Krupke C. H., 2017. Larval western bean cutworm feeding damage encourages the development of Gibberella ear rot on field corn. *Pest Management Science* 73: 546–553. DOI:I 10.1002/ps.4313

Parsons M. W., Munkvold G. P., 2012. Effects of planting date and environmental factors on fusarium ear rot symptoms and fumonisin B1 accumulation in maize grown in six North American locations. *Plant Pathology* 61: 1130–1142.

Paul P. A., El-Allaf S. M., Lipps P. E., Madden L. V., 2004. Rain splash dispersal of *Gibberella zeae* within wheat canopies in Ohio. *Phytopathology* 94: 1342.

Picot A., Barreau C., Pinson-Gadais L., Piraux F., Caron D., Lannou C., Richard-Forget F., 2011. The dent stage of maize kernels is the most conducive for fumonisin biosynthesis under field conditions. *Applied and Environmental Microbiology* 77: 8382–8390. DOI:10.1128/aem.05216–11

Pietri A., Zanetti M., Bertuzzi T., 2009. Distribution of aflatoxins and fumonisins in dry-milled maize fractions. *Food Additives & Contaminants* Part A, 26: 372–380. DOI:10.1080/02652030802441513

Pitt J. I., Miscamble B. F., 1995. Water relations of *Aspergillus flavus* and closely related species. *Journal of Food Protection* 58: 86–90.

Piva G., Battilani P., Pietri A., 2006. Emerging issues in Southern Europe: aflatoxins in Italy. In: *The mycotoxin factbook* (D. Barug, D. Bhatnagar, H. P. van Egmong, J. W. van der Kamp, W. A. van Osenbruggen, & A. Visconti, eds), Wageningen Academic Publisher: The Netherlands, 139–153.

Qian G., Tang L., Lin S., Xue K. S., Mitchell N. J., Su J., … Wang J. S., 2016. Sequential dietary exposure to aflatoxin B1 and fumonisin B1 in F344 rats increases liver preneoplastic changes indicative of a synergistic interaction. *Food and Chemical Toxicology* 95: 188–195. DOI:10.1016/j.fct.2016.07.017

Rasmussen P. H., Nielsen K. F., Ghorbani F., Spliid N. H., Nielsen G. C., Jørgensen L. N., 2012. Occurrence of different trichothecenes and deoxynivalenol-3-β-D-glucoside in naturally and artificially contaminated Danish cereal grains and whole maize plants. *Mycotoxin Research* 28: 181–190. DOI:10.1007/s12550–012-0133-z

Reyneri A., Vanara F., Peila U., Bertetto L., 2004. The distribution of mycotoxins (*Fusarium* toxins) in products and byproducts of the industrial processing of maize. *Tecnica Molitoria* 55: 957–966.

Rushing B. R., Selimb M. I., 2019. Aflatoxin B1: A review on metabolism, toxicity, occurrence in food, occupational exposure, and detoxification methods. *Food and Chemical Toxicology* 124: 81–100. DOI:10.1016/j.fct.2018.11.047

Rychlik M., Humpf H.U., Marko D., Danicke S., Mally A., Berthiller F.H. Lorenz N., 2014. Proposal of a comprehensive definition of modified and other forms of mycotoxins including "masked" mycotoxins. *Mycotoxin Research* 30:197–205. DOI: 10.1007/s12550–014-0203-5

Sahab A. F., Aly S., Hathout A. S., Ziedan E. H., Sabry B. A., 2014. Application of some plant essential oils to control *Fusarium* isolates associated with freshly harvested maize in Egypt. *Journal of Essential Oil Bearing Plants* 17: 1146–1155. DOI:10.1080/097206 0x.2014.891447

Samsudin N. P. I., Rodriguez A., Medina A., Magan N., 2017. Efficacy of fungal and bacterial antagonists for controlling growth, FUM1 gene expression and fumonisin B1 production by *Fusarium verticillioides* on maize cobs of different ripening stages. *International Journal of Food Microbiology* 246: 72–79. DOI:10.1016/j.ijfoodmicro.2017.02.004

Savi G. D., Piacentini K. C., Marchi D., Scussel V. M., 2016. Fumonisins B-1 and B-2 in the corn-milling process and corn-based products, and evaluation of estimated daily intake. *Food Additives & Contaminants* 33: 339–345. DOI:10.1080/19440049.2015.1124459

Sawai B., Poonsuk P., Supalak S., 2017. Evaluation of antifungal activity of essential oils against aflatoxigenic *Aspergillus flavus* and their allelopathic activity from fumigation to protect maize seeds during storage. *Industrial Crops and Products* 97: 558–566. DOI:10.1016/j.indcrop.2017.01.005

Scala V., Bello C., Fabbri A. A., Fanelli C., Reverberi M., Camera E., Battilani P., 2013. *Fusarium verticillioides* and maize interaction in vitro: Relationship between oxylipin cross-talk and fumonisin synthesis. *World Mycotoxin Journal* 6: 343–351. DOI:10.3920/wmj2013.1527

Scauflaire J., Gourgue M., Callebaut A., Munaut F., 2012. *Fusarium temperatum* a mycotoxin-producing pathogen of maize. *European Journal of Plant Pathology* 133: 911–922. DOI:10.1007/s10658–012-9958-8

Schaarschmidt S., Fauhl-Hassek C., 2019. Mycotoxins during the processes of nixtamalization and tortilla production. *Toxins* 11: 227. DOI: 10.3390/toxins11040227

Shaner G., 2003. Epidemiology of Fusarium head blight of small grain cereals in North America. In: *Fusarium Head Blight of Wheat and Barley* (K. J. Leonard, W. Bushnell, eds),(1st ed.), APS Press, St Paul Minnesota US, 84–119.

Shi L., Liang Z., Li J., Hao J., Xu Y., Huang K., … Xu W., 2014. Ochratoxin A biocontrol and biodegradation by *Bacillus subtilis* CW 14. *Journal of the Science of Food and Agriculture* 94: 1879–1885. DOI:10.1002/jsfa.6507

Sivparsad B. J., Laing M. D., 2016. Pre-harvest silk treatment with *Trichoderma harzianum* reduces aflatoxin contamination in sweetcorn. *Journal of Plant Diseases and Protection* 123: 285–293. DOI:10.1007/s41348–016-0037-9

Smith J. E., Moss M. O., 1985. *Mycotoxins: Formation, Analysis and Significance* (J. W. Sons, ed.), Chichester-New York-Brisbane-Toronto-Singapore, pp.

Smith M. C., Madec S., Coton E., Hymery H., 2016. Natural co-occurrence of mycotoxins in foods and feeds and their *in vitro* combined toxicological effects. *Toxins* 8: 94. DOI:10.3390/toxins8040094

Stadler D., Lambertini F., Bueschl C., Wiesenberger G., Hametner C., Schwartz-Zimmermann H., … Krska

R., 2018. Untargeted LC-MS based ^{13}C labelling provides a full mass balance of deoxynivalenol and its degradation products formed during baking of crackers, biscuits and bread. *Food Chemistry*. DOI: 10.1016/j.foodchem.2018.11.150

Statista, 2018. European Union-28: maize production volume forecast 2015–2027. Retrieved from https://www.statista.com/statistics/614393/maize-production-volume-european-union-28/

Streit E., Naehrer K., Rodriguesc I., Schatzmayr G., 2013. Mycotoxin occurrence in feed and feed raw materials worldwide: long-term analysis with special focus on Europe and Asia. *Journal of the Science of Food and Agriculture* 93: 2892–2899. DOI:10.1002/jsfa.6225

Tayel A. A., El-Tras W. F., Moussa S. H., El-Agamy M. A., 2013. Antifungal action of *Pichia anomala* against aflatoxigenic *Aspergillus flavus* and its application as a feed supplement. *Journal of the Science of Food and Agriculture* 93: 3259–3263. DOI:10.1002/jsfa.6169

Thippeswamy S., Mohana D. C., Abhishek R. U., Manjunath K., 2013. Efficacy of bioactive compounds isolated from *Albizia amara* and *Albizia saman* as source of antifungal and antiaflatoxigenic agents. *Journal of Consumer Protection and Food Safety* 8: 297–305. DOI:10.1007/s00003–013-0839-7

Thippeswamy S., Abhishek R. U., Manjunath K., Raveesha K., Mohana D. C., 2015. Antifumonisin efficacy of 2-Hydroxy-4-Methoxybenzaldehyde isolated from *Decalepis hamiltonii*. *International Journal of Food Properties* 18: 2002–2008. DOI:10.1080/10942912.2014.960930

Torelli E., Firrao G., Bianchi G., Saccardo F., Locci R., 2012. The influence of local factors on the prediction of fumonisin contamination in maize. *Journal of the Science of Food and Agriculture* 92: 1808–1814. DOI:10.1002/jsfa.5551

Torres O., Matute J., Gelineau-van Waes J., Maddox J. R., Gregory S. G., Ashley-Koch A. E., … Riley R. T., 2015. Human health implications from co-exposure to aflatoxins and fumonisins in maize based foods in Latin America: Guatemala as a case study. *World Mycotoxin Journal* 8: 143–159. DOI:10.3920/WMJ2014.1736

Tracz B. L., Bordin K., Nazareth T., Costa L. B., Freitas M., Renata E., … Luciano F. B., 2016. Assessment of allyl isothiocyanate as a fumigant to avoid mycotoxin production during corn storage. *LWT Food Science and Technology* 75: 692–696. DOI:10.1016/j.lwt.2016.10.030

Trenholm H. L., Charmley L. L., Prelusky D. B., Warner R. M., 1991. Two physical methods for the decontamination of four cereals contaminated with deoxynivalenol and zearalenone *Journal of Agricultural and Food Chemistry* 39: 356–360. DOI:10.1021/jf00002a026

van der Fels-Klerx H. J., Camenzuli L., 2016. Effects of milk yield, feed composition, and feed contamination with aflatoxin B1 on the aflatoxin M1 concentration in dairy cows' milk investigated using Monte Carlo simulation modelling. *Toxins* 8: 290. DOI:10.3390/toxins8100290

van der Fels-Klerx H. J., Liu C., Battilani P., 2016. Modelling climate change impacts on mycotoxin contamination. *World Mycotoxin Journal* 9: 717–726. DOI:10.3920/WMJ2016.2066

Vanara F., Scarpino V., Blandino M., 2018. Fumonisin distribution in maize dry-milling products and by-products: impact of two industrial degermination systems. *Toxins* 10: 357. DOI:10.3390/toxins10090357

Verheecke C., Liboz T., Anson P., Zhu Y., Mathieu F., 2016. *Streptomyces- Aspergillus flavus* interactions: impact on aflatoxin B accumulation. *Food Additives and Contaminants* 32: 572–576. DOI:10.1080/19440049.2014.1003336

Xue A. G., Chen Y. H., Sant'anna S. M. R., Voldeng H. D., Fedak G., Savard M. E., … Harman G. E., 2014. Efficacy of CLO-1 biofungicide in suppressing perithecial production by *Gibberella zeae* on crop residues. *Canadian Journal of Plant Pathology* 36: 161–169. DOI:10.1080/07060661.2014.881920

Yaqian L., RuiYan S., Jia Y., Saravanakumar K., Jie C., 2016. Antagonistic and biocontrol potential of *Trichoderma asperellum* ZJSX5003 against the maize stalk rot pathogen *Fusarium graminearum*. *Indian Journal of Microbiology* 56: 318–327. DOI:10.1007/s12088–016-0581-9

Zachariasova M., Dzuman Z., Veprikova Z., Hajkova K., Jiru M., Vaclavikova M., … Hajslova J., 2014. Occurrence of multiple mycotoxins in European feeding stuffs, assessment of dietary intake by farm animals. *Animal Feed Science and Technology* 193: 124–140. DOI:10.1016/j.anifeedsci.2014.02.007

Phytopathologia Mediterranea
The international journal of the
Mediterranean Phytopathological Union

Firenze University Press
www.fupress.com/pm

Review

Current knowledge on Grapevine Trunk Diseases with complex etiology: a systemic approach

Marion CLAVERIE[1,*], Martin NOTARO[1], Florence FONTAINE[2], Jacques WERY[3]

[1] *Institut Français de la Vigne et du Vin, Institut Rhodanien, 84100 Orange, France*
[2] *Structure Fédérative de Recherche (SFR) Condorcet-FR CNRS 3417, Université de Reims Champagne-Ardenne, Unité de Recherche Résistance Induite et Bioprotection des Plantes EA 4707, BP 1039, (Cedex 2), F-51687 Reims, France*
[3] *SYSTEM Montpellier SupAgro, Inra, Cirad, IAMM-CIHEAM, Université Montpellier, France*
*Corresponding author: marion.claverie@vignevin.com

Summary. Among all causes of grapevine decline, Grapevine Trunk Diseases (GTDs) are major concerns for grape growers. This paper reviews knowledge and proposes hypotheses on two major GTDs, esca and Botryosphaeria dieback, and assembles a conceptual model. The objective was to collect information into a sequence, from grapevine nursery propagation processes, through foliar symptom expression, to plant death in mature vineyards. Pathogen infection and colonization steps in woody vine tissues, and the hypotheses that have been formulated to explain the outburst of foliar symptoms, are reported and discussed. Factors that could aggravate or repress GTD symptoms and incidence expansion are also addressed. Vine physiology and pathology together could expand understanding of these diseases. Knowledge and hypotheses that need validation are summarized, and a conceptual model is proposed to explain the occurrence of symptoms and the influencing factors. The model could be useful to cope with the complexity of GTDs, and as a starting point for research to unravel knowledge gaps and suggest new disease management strategies.

Keywords. Esca, Botryosphaeria dieback, foliar symptoms, impacts, hypotheses, conceptual model.

OPEN ACCESS

Citation: M. Claverie, M. Notaro, F. Fontaine, J. Wery (2020) Current knowledge on Grapevine Trunk Diseases with complex etiology: a systemic approach. *Phytopathologia Mediterranea* 59(1): 29-53. doi: 10.14601/Phyto-11150

Accepted: February, 18, 2020

Published: April 30, 2020

Data Availability Statement: All relevant data are within the paper and its Supporting Information files.

Competing Interests: The Author(s) declare(s) no conflict of interest.

Editor: Hanns-Heinz Kassemeyer, Staatliches Weinbauinstitut Freiburg, Germany.

INTRODUCTION

Grapevine Trunk Diseases (GTDs) are caused by several fungi belonging to nine different families (Mondello *et al.*, 2018). These pathogens cause wood discolouration and necroses, different foliar symptoms, yield damage, and subsequent death of shoots, canes, spurs and whole grapevines (Bertsch *et al.*, 2013; Gramaje *et al.*, 2018; Guérin-Dubrana *et al.*, 2019). GTDs are major causes of grapevine decline, especially in European countries. These diseases can be divided into different syndromes, depending on symptoms,

the families of pathogens involved (often related to geographical areas), environmental factors and vine age. Major GTDs on adult vines include esca, Botryosphaeria dieback, and Eutypa dieback. On young vines, main GTDs are Black foot disease, Petri disease or diebacks due to Botryosphaeriaceae, *Verticillium* or *Fusarium* (Mugnai *et al.*, 1999; Surico, 2009; Larignon, 2016; Gramaje *et al.*, 2018).

Wood inhabiting fungi and their related necrosis in the trunks and arms of vines are considered to be the agents associated with the different foliar symptom expressions, but in some GTDs, there is no clear evidence of their role in symptoms expression. All the associated pathogens have been proven to provoke wood symptoms when inoculated to grapevine wood (Mugnai *et al.*, 1999; Larignon *et al.*, 2009a; Bertsch *et al.*, 2013), but Koch's postulates have not always been completed to reproduce foliar symptoms. Foliar symptoms of Eutypa dieback (stunted shoots, witch's brooms) have been fully reproduced on young or mature vines after wood inoculation with *Eutypa lata* (Sosnowski *et al.*, 2007), those of esca and Botryosphaeria dieback have not. Only two papers (Sparapano *et al.*, 2001; Feliciano *et al.*, 2004) have reported reproducing foliar symptoms on mature vines, in 20 years of research, and the etiology of these diseases has not been completely elucidated (Mondello *et al.*, 2018).

Grapevine decline is a major problem for French grape growers and winemakers. In 2016, a National Plan against Vine Decline (Plan National Dépérissement du Vignoble; PNDV) has given special attention to the issue, and has helped to determine the causes, and propose sustainable solutions for growers, to counteract decline. Decline can be described as abnormal reduction in vineyard productivity and longevity, related to multiple causes (biotic and abiotic factors). GTDs are one of these causes. Although long-recognized (Chiarappa, 2000; Surico, 2009; Larignon, 2016), GTD incidence is increasing in France since the 2000s and has reached an annual average of 13% (Grosman and Doublet, 2012; Bruez *et al.*, 2013). In Europe, GTD incidence could be similar, with reports fluctuating from 1.8 to 10.5% in Spain and from 8 to 19% in Italy. Incidence of these diseases has reached 60 to 80% in some old vineyards in Tuscany, Apulia and Sicily. Outside Europe, 30% of old vineyards in Argentina are affected, and considerable economic losses due to GTDs have been reported in the United States of America, Australia and New Zealand (De La Fuente *et al.*, 2016).

The present review aims to provide increased understanding of the etiology of "tiger stripe" foliar symptoms (FS) and apoplexy, two damaging symptoms frequently found in France and Europe on mature grapevines. The apoplexy form involves sudden vine death while tiger stripe symptoms are a milder form, with interveinal discolourations and necrosis on leaf blades, affecting all or part of vine foliage (Mugnai *et al.*, 1999; Lecomte *et al.*, 2012). FS can lead, for the more severe form, to complete leaf wilting and leaf fall. Grape bunches may also be affected, either directly or indirectly, leading to berry shriveling, and yield and quality losses (Calzarano *et al.*, 2004; Fontaine *et al.*, 2016; Claverie *et al.*, 2017), as well as drying up of canes, spurs and eventually whole plants (Mondello *et al.*, 2018; Guérin-Dubrana *et al.*, 2019).

On adult vines, tiger stripes and apoplexy are associated with esca and to some extent, in France, and for tiger stripes, to Botryosphaeria dieback although this association has been controversial (Dubos *et al.*, 2001; Surico *et al.*, 2006; Úrbez-Torres, 2011; Lecomte *et al.*, 2012). Esca has been assumed to be a complex of diseases, with symptoms associated to Grapevine Leaf Stripe Disease (GLSD) and esca proper (Surico, 2009). In this review, the terms esca and Botryosphaeria dieback are used to refer to the diseases potentially responsible of tiger-stripe like symptoms or apoplexy. Because Eutypa dieback symptoms are better understood, and although this disease also affects grapevine productivity, it is not within the scope of this review.

FS are associated with a complex of fungi whose roles and associations are not always clear, and these may be altogether present in a single vine and influenced by genotypic and environmental factors. Fungi can be wood-inhabiting but the detrimental symptoms they cause for growers occur in the foliage at some distance from the infections. FS may be absent for many years although necroses and cankers are present in vine trunks as latent infections, and then can fluctuate from year to year (Calzarano *et al.*, 2018). For these reasons, esca and Botryosphaeria dieback are regarded as complex diseases (Mondello *et al.*, 2018). Understanding the host/pathogen/environment triangle is critical to explain the occurrence of FS (Fischer and Peighami-Ashnaei, 2019).

Because of the complexities of these diseases, a systemic approach to understand their etiologies has been taken, focusing on fungi and on vine physiology and related factors to explain the emergence of disease symptoms. This approach consisted of reviewing knowledge on esca and Botryosphaeria dieback to present a sequence of events from young grafted plants to the death of mature vines, using conceptual modelling (Lamanda *et al.*, 2012). This approach has two differences from a traditional review. First, it is set to provide a global overview of the syndrome indicating the

interactions between many factors. For this reason, the approach fails to provide a detailed exploration of individual aspects, but relies on existing reviews by specialists. Secondly, in addition to existing data on these diseases, we have attempted to fill knowledge gaps, making assumptions supported either by published research (e.g. agronomy and physiology) on grapevine subjects other than GTDs, or from forest decline and forest pathology disciplines. A significant principle for conceptual modelling that we have used is 'parsimony', which begins at the general level and moves to the specific. Complexity is added only if necessary in response to assumptions (Lamanda *et al.*, 2012). The conceptual model was submitted to an expert group to challenge the hypotheses developed.

This review is organized in two parts: the first presents the hypothetical sequence of events leading to FS and vine death, and the second discusses the major influencing factors that are likely to aggravate or repress this sequence. Figures supporting each part are also presented to summarize the hypothetical sequence of events and the different interference drivers.

FROM PLANTATION TO SYMPTOM EMERGENCE AND GRAPEVINE DEATH, THE KEY STEPS

Step 1: Infection

To contaminate vine tissues, it is assumed that GTD fungi need fresh wounds as entry points, as few pathogens colonize hosts without entry points, because of host protection layers such as periderm and rhytidome (Pearce, 1996). Each successful infection initially occurs with the simultaneous occurrence of outer inoculum and a wound, although it is unclear whether some fungi can enter through uninjured tissues (Feliciano and Gubler, 2001) or infections could initiate from endophytic propagules after being triggered by some environmental changes, as occurs in forest trees (Baum *et al.*, 2003). The term 'outer inoculum' can be defined as the air-borne or soil-borne propagation forms of GTD fungi (spores or mycelium) that can remain on the surface or in the vicinity of the vine or wood debris, or on alternative hosts in the field or during nursery processes. In contrast, 'inner inoculum' characterizes GTD fungi that have penetrated and developed within grapevine tissues.

Outer inoculum

Phaeomoniella chlamydospora (Pch), *Phaeoacremonium minimum* (Pmi) and *Fomitiporia mediterranea* (Fmed) are the three fungi commonly associated with the esca complex, but *Eutypa lata* (El), which causes Eutypa dieback and several Botryosphaeriaceae species (e.g. *Diplodia seriata* (Ds) and *Neofusicoccum parvum* (Np)) are also frequently retrieved from the wood of vines showing FS.

The life cycles of these pathogens have been thoroughly documented. Larignon and Gramaje (2015) presented a review which compiled for each fungus its mode of dissemination, infection points, favourable climatic conditions and period of wound susceptibility, depending on the region of the world. Spore release is commonly associated with a rain event, but the best periods for inoculum dissemination can differ between fungi. In France Pch spreads throughout the year, and infections occur mainly in winter through pruning wounds (Larignon *et al.*, 2009a; Larignon and Gramaje, 2015), whereas Pmi is mostly present during the vegetative host period and infections on pruning wounds occur mostly after grapevine budburst. Both of these fungi can also enter vines through green stems during spring (Davy *et al.*, 2011). Infections by Botryosphaeriaceae are reported to occur following rain events, but during periods from mostly winter to throughout the year, depending on the region (Úrbez-Torres, 2011). Some Botryosphaeriaceae species can penetrate vines through pruning wounds, especially after bud bleeding, but some can also enter through wounds on green stems in spring and summer (Molot *et al.*, 2006; Reis *et al.*, 2019).

Infection is also probably influenced by the intrinsic abilities of each fungus, and their modes of wood colonization. An hypothesis formulated for esca was that the fungi act in sequence, where colonization is initiated by pioneer fungi, as occurs for forest trees (Shigo, 1979; Boddy and Rayner, 1983; Pearce, 1996). Pioneer fungi could survive greater amounts of phenolics and other antimicrobial compounds than decay fungi. Decay fungi start acting on host tissues when pioneer fungi have sufficiently "detoxified" the plant tissues. For esca, the hypothesis was that Pch and Pmi colonize first, and then Fmed can invade (Larignon and Dubos, 1997; Mugnai *et al.*, 1999). Valtaud *et al.* (2009) also reported that Pch and Pmi have specific life traits, enzymatic ones in particular, leading them to hypothesize that Pch could be more specialized in toxin production (naphtalenones, phenolics, polysaccharides) and Pmi more efficient at degrading and colonizing tissues. Another hypothesis (Mugnai *et al.*, 1999) was that these fungi, included the basidiomycete fungus Fmed, can interact but can also act as primary pathogens, as shown by experimental data (Sparapano *et al.*, 2001; Surico, 2009).

Despite information on pathogen life cycles, there is little literature on the diversity and amounts of the outer inoculum in vineyards, and on variability between neighbouring plots, or between regions. Knowing this would be important to indicate if outer inoculum is a limiting factor, and vineyard or region specificities of different Botryosphaeriaceae and Pch/Pmi/Fmed compositions in the outer inoculum. However, there is a lack of validated monitoring methods to measure these effects, at least in Europe.

Wounding

Grapevine is a liana that is pruned every year, in winter. On an adult vine, this results in many wounds between the 1-year-old wood (canes as lignified shoots) and 2-year, 3-year or older wood (spurs, arms, trunk). Grosclaude (1993) demonstrated the double impact of pruning a fruit tree: first, connection between the woody tissues and the atmosphere, characterized by drying and embolizing vessels and the development of callose or gel deposits; and second, the aspiration of air and particles (including spores) inside the wood to, generally, a few centimeters depth.

While other wound types (cracks or wounds caused by biotic or abiotic factors) can also play roles, winter pruning wounds are thought to be the major entry points for GTD fungi. Considerable research has been carried out on the susceptibility of pruning wounds to pathogen infections. This differs depending on the fungus, pruning date (early or late in winter) and climatic conditions, and consequently the year and geographical region (Larignon, 2011; Larignon and Gramaje, 2015; Mondello *et al.*, 2019). Wounds generally stay susceptible for several weeks and up to 4 months (Gramaje *et al.*, 2018). Pruning type and "quality" can also have indirect consequence on GTDs, as these factors create specific wood necroses and decay in the perennial host organs (see below).

Grafting and production processes in grapevine nurseries as well can result in wounding that has been shown to provide infection points for GTD fungi. This has been largely documented during the last decade, and outlined by Gramaje and Armengol (2011) and Gramaje *et al.* (2018). When a ready-to-sell nursery plant is dissected, most of the GTD fungi can be detected (Vigues *et al.*, 2007; Larignon *et al.*, 2009b; Gramaje and Armengol, 2011; Spagnolo *et al.*, 2011). In France, Pch and Botryosphaeriaceae are the major fungi isolated from plants, Pmi is less frequently isolated, and Fmed or El have never been detected. These fungi have been shown to be present on rootstock and scion canes before grafting, but with much lower frequency than on ready-to-sell plants. This suggests that some steps in the nursery processes (rehydrating, grafting, callusing and in nursery fields) are key infection steps that increase the presence of GTD fungi. This has been shown to be the case in different countries (Aroca *et al.*, 2010; Vigues *et al.*, 2012; Vigues *et al.*, 2013; Gramaje and Di Marco, 2015; Gramaje *et al.*, 2018).

It would be important to determine the respective contributions of the initial infections in nurseries from year-to-year accumulation of infections in vineyards to the sanitary status of mature vines.

Yobregat *et al.* (2018) showed that plants initially free of GTD fungi at planting (from green grafting techniques) are repeatedly infected from in-field infections, and show the same amounts of inner inoculum as traditionally-produced plants within 3 years after planting. This suggests that the contribution of outer inoculum to the wood infections can be important in some cases. This also highlights the importance of protecting the wounds from field infections (Mondello *et al.*, 2018), although this is difficult, time-consuming and expensive (Bertsch *et al.*, 2013; Mondello *et al.*, 2019).

Another related question is the contribution of wounds during the first years of grapevine life (from planting year up to 2- to 5-year-old plants), compared to wounds made during later decades in older vines. In young vines, pruning wounds (and possibly desuckering wounds as well) provide dead wood and access for fungi directly to the cores of the future trunks and arms.

These two points are important, in order to determine the respective contributions of nursery procedures, management of young vineyards and further repeated infections on the sanitary status of mature vines.

Step 2: Colonization/defence; host/pathogen relationships

Once GTD fungi have infected the woody tissues, the colonization phases by fungal communities begin, and these induce the formation of discoloured and decayed host wood. This step leads to accumulation of potential inner inoculum of GTD pathogens, and restricts vine living and functional wood.

Tree defence concepts

Literature on forest tree pathology gives a key contribution. At basic process levels, knowledge from trees can be used as a basis for assumptions of vineyard functioning (Lamanda *et al.*, 2012). Reaction zones in trees are created after infections, at the interface of injured and functional wood, and these zones restrict the path-

ogens to particular woody zones. The *reaction zone* concept, and more generally the defence mechanisms that develop after infection to limit the pathogen colonization, have been well-documented and conceptualized in forest trees (Shain, 1971; Boddy and Rayner, 1983; Pearce, 1996, 2000). To simplify, we here use the *reaction zone* concept to describe the place where active vine defences and mechanisms of fungal colonization are observed. Progression of this reaction zone and subsequent degradation of tissues are assumed to be due to alterations of micro-environments, or to the microfloral evolution and dynamics. Resistance mechanisms can also interfere, as reported by the CODIT model (Shigo, 1979). This considers four types of barriers ("walls") that restrict pathogen progression. These "walls" are related to wood anatomy (parenchyma rays, *wall 3*, and annual rings, *wall 2*), or to active vine responses to pathogenic fungi. *Wall 1* is the synthesis of gums and phenolics in the host vessels to longitudinally restrict the fungus, and *wall 4* is reinforcement of the cambium zone, so that growth of functional wood rings can occur ahead of the infections. Pearce (1996) presented a detailed review of the different concepts in forest trees, and this has been also discussed in relation to esca of grapevine (Mugnai *et al*., 1999).

Characteristics of GTDs-associated fungi

Fungi associated with GTDs show different abilities to colonize wood that can be categorized into wood degrading ability, defence compounds or ability to counteract the production of grapevine metabolites. Active compounds synthesized by fungi and grapevines have been intensively studied, benefitting from the recent progress in molecular techniques used to characterize fungi and their biosynthesis pathways or interactions. GTD fungi have different enzymatic abilities for degradation of lignin, pectin or starch.

Mature xylem vessels of grapevines are dead cells, composed of cellulose surrounded by hemicellulose and lignin, and pectic compounds, conferring mechanical resistance. These walls have different layers (from the outside to the inside of cell): middle lamella then primary and secondary walls each showing different composition of lignin, cellulose, hemicellulose and pectin. This level of detail is important for understanding the pathogen colonizing processes, since the intrinsic enzymatic abilities of each fungus differ and could assist with developing a multi-dimensional model of grapevine wood degradation. Full characterization of fungus modes of action exists for forest trees, and was outlined by Schwarze and Baum (2000).

The GTD pathogens Pch and Pmi show poor lignolytic activity but strong abilities to degrade starch (Mugnai *et al*., 1999). Pch mainly occurs in host vessels (Larignon and Dubos, 1997; Troccoli *et al*., 2001; Cottral *et al*., 2004; Valtaud *et al*., 2009; Fleurat-Lessard *et al*., 2010; Mutawila *et al*., 2011; Pierron, 2015) and is unable to degrade secondary walls, but can digest membranes and thus progress into xylem vessels, potentially in the presence of tyloses and gum. Pch is also unable to pass through annual rings (Larignon, 2004). Pmi has been less extensively studied; it is found mainly in the fibers (Valtaud *et al*., 2009; Pierron, 2015) where it can degrade secondary walls (Fleurat-Lessard *et al*., 2014), as well as El. Both of these fungi can be characterized as soft rot agents (Larignon *et al*., 2009a; Pouzoulet, 2012) whereas Pch would rather be like a blue stain fungus (Larignon, 1990; Larignon *et al*., 2009a). The mode of action of Botryosphaeriaceae is poorly documented, although Gómez *et al*. (2016) showed lignolytic activity in an uncharacterized species of Botryosphaeriaceae retrieved from vineyard surveys. Some research still in progress will probably provide more information about Botryosphaeriaceae fungi and their action in GTDs. Fmed is a basidiomycete considered as a white rot (decay) fungus, with high lignolytic activity and ability to completely degrade woody tissues (Mugnai *et al*., 1999).

In addition to predicting the architecture of wood necrosis, increased knowledge on fungus modes of action and on trophic relationship in host tissues could assist prediction of impacts of the fungi on grapevine carbon (C) metabolism (Oliva *et al*., 2014). Depending on the trophic interactions between host and fungi (including biotrophs, necrotrophs, vascular pathogens or a mix of these) the impact on C metabolism may come from direct consumption by the fungus, such as enhanced costs for defences or for repair, negative impacts on photosynthesis or hydraulic failure. Knowledge on GTD fungi has not determined their trophic modes of action, even where their non-biotrophic nature can be postulated. Knowing this could give clues for unravelling the mechanisms underlying pathogen colonization and their impacts on the grapevine decline.

Multiple conditions determining wood colonization

Apart from the scheme of one-way progression of fungi presented above, the host/pathogens relationships found in the reaction zones could be multiple dialogues between vines and fungi, fungi and fungi (species and strains), fungi and associated microflora (fungi and bacteria), and the whole is likely to be modulated by environmental conditions.

Three drivers can, theoretically, determine the extent of wood colonization by fungi:

- *Relationships within trunk microbiota*. Predominance of one pathogen over another, co-action of two micro-organisms or of two strains: microbiota can be considered as complex networks where microbes interact with each other, with the environment determining specific conditions that can be more or less conducive to pathogenicity (Brader *et al.*, 2017). For GTDs, the grapevine wood microbiota is particularly rich (Hofstetter *et al.*, 2012; Bruez, 2013; Pinto *et al.*, 2014), and several studies suggest that interactions inside the community of GTD fungi, as well as vine physiology and the environment, can strongly affect the behaviour of each fungus alone (Bruno and Sparapano, 2006a; Oliveira *et al.*, 2009). Bruez *et al.* (2014) showed that microflora composition inside visually healthy trunk tissues varies during the year. This composition also evolves in time and with plant tissues. Diversity of the microflora is greater on young vines (Rey *et al.*, 2011; Hofstetter *et al.*, 2012; Bruez, 2013) and in visually healthy tissues rather that in decayed tissues.
- *Structural or micro-environmental conditions in trunks*. Although cell walls are mainly used as substrates for fungus nutrition, some fungi can likely have specific nutritional requirements (Pearce, 1996). Soluble compounds in parenchyma or in sap can also influence the progression of fungi. These compounds include amino acids (Magnin-Robert *et al.*, 2014), soluble sugars (Spagnolo *et al.*, 2014a) or ions (e.g. iron (Di Marco *et al.*, 2001; Osti and Di Marco, 2010). Temperature (Sosnowski *et al.*, 2011; Landi *et al.*, 2012; Pontini *et al.*, 2014) and pH (Surico *et al.*, 2001; Valtaud *et al.*, 2009) have also been shown to be important factors determining wood colonization by fungi. In addition, the micro-environmental theory (Boddy and Rayner, 1983), developed for forest trees, is also pertinent considering. This assumes that the water content of woody tissues close to the host/pathogen reaction zones can alone explain fungus progression inside tree trunks, as fungi follow the dehydrated and oxygen rich zones that occur along the reaction zones close to wounds.
- *Active vine defences*. Living xylem of grapevine, like other woody perennials, is composed of dead (vessels, fibers) and living cells (paratracheal and ray parenchyma cells), the whole xylem being submitted to reaction zones and CODIT walls of compartmentalization following infection and colonization by wood pathogens. Reaction zones are regions of active host responses where active compounds are released to slow the progression of pathogens (Pearce, 1996), thanks to the living cells they host and that co-exist in the vicinity of dead cells. The first active defence is tylosis formation inside the vessels. Tyloses are outgrowths of membranes of neighbouring parenchyma cells, inside each vessel through the pits, and are generally reinforced by gels or gums. This first defence response to the presence of a pathogen slows longitudinal progression (del Rio *et al.*, 2001; Troccoli *et al.*, 2001; Larignon, 2010; Pierron, 2015; Gómez *et al.*, 2016). Among the defences commonly observed in forest trees (Pearce, 1996; Yadeta and Thomma, 2013; Smith, 2015), lignin or suberin deposits reinforce cell walls in the injured zones. Tannins or other phenolics (e.g. phytoalexins and 'pathogenesis related' (PR) proteins synthesized around zones exposed to slow radial infection), trap some fungus enzymes or prevent sporulation. Similar compounds have also been detected in GTDs (del Río *et al.*, 2004; Rolshausen *et al.*, 2008; Bertsch *et al.*, 2013; Pouzoulet *et al.*, 2013; Fontaine *et al.*, 2016). Responses to GTD fungi are thought to occur due to PAMP-triggered immunity (PTI). Phytoalexins, compounds from the phenylpropanoid pathway such as resveratrol or viniferin, are found in greater amounts in tissues after infection by GTD fungi (Amalfitano *et al.,* 2000; del Rio *et al.*, 2001; Bruno and Sparapano, 2006b; Martin *et al.*, 2009; Spagnolo *et al.*, 2014b). Phytoalexins could inhibit fungal growth and colonization, as well as block some metabolites produced by the fungi during infection, or interfere in oxido-reduction reactions (Gómez *et al.*, 2016). In addition to the active defence processes implemented by vines, the anatomy of the wood could also be important. Density of parenchyma rays and arrangement in space, could contribute to increased active responses to infection (Pearce, 1996). The diameter of vessels (Pouzoulet *et al.*, 2014) could also be a factor (see below).

Necrotic decayed and discoloured wood, and their consequences

The ongoing host-pathogen process ends with the formation of discoloured and decayed zones in the wood. In grapevine, these "necroses" are observed in the wood cylinders on any adult plant, even in the absence of FS (Maher *et al.*, 2012; Spagnolo *et al.*, 2012; Bruez *et al.*, 2014). But these decayed wood zones vary between plants, in terms of aspect (such as black spotting, brown-red wood, sectorial necrosis, white rot), volume, and location in the trunks and arms. Shape and

colour of necroses can be associated with specific fungi which may be isolated from them (Larignon and Dubos, 1997; Mugnai *et al.*, 1999; Calzarano and di Marco, 2007; Kuntzmann *et al.*, 2010; Maher *et al.*, 2012). These necroses are often spatially associated with pruning wounds (Galet, 1977; Larignon and Dubos, 1997; Mugnai *et al.*, 1999). This suggests that these areas could be entry points and the altered tissues of the desiccation cones could be more likely to be colonized by fungi, although this has not been proven. In some forest trees, it has been shown that discolouration developing from wounds extends more rapidly in an axial than a radial or tangential direction (Deflorio *et al.*, 2007), and that the pith has a role in the extent of decay from a branch to a trunk. In grapevine, the role of the pith in disseminating fungi has also been questioned (Feliciano and Gubler, 2001; van Niekerk *et al.*, 2011).

Volume of necrosis in vine trunks and arms probably decreases downwards from their tops (Mugnai *et al.*, 1999). This is consistent with the fact that the upper trunks (where the Guyot pruning type has been used) and the arms (for cordon and "gobelet" pruning types) host most pruning wounds, compared to the lower trunks and the grafting points supporting fewer wounds established during the first years of vine life.

Necroses are thus double sources of risk for GTDs. Firstly, they host inner inoculum that is likely to further disseminate inside the trunks and arms, and secondly, they reduce functional sapwood and storage capacity of the trunks. However, not all of necrosis types are likely to impede hydraulic conductivity of grapevines. This probably depends on necrosis localization with respect to the functional sapwood. Ascent of the xylem flux can rely on several annual rings of wood although only the last rings are thought to be functional. The older rings are naturally occluded by tyloses (Fournioux and Adrian, 2011), which is analogous to the heartwood of forest trees. We can thus postulate that necroses affecting the external rings play greater roles on the reduction of the xylem sap flow than the more central stem rings.

This raises questions of the impacts of nonfunctional wood associated with GTDs on conductivity, that need to be documented. It would be useful to assess whether GTD fungi and wood necroses actually impact sap conductivity, and how. In that case, exploring alterations of photosynthesis and carbon metabolism would also be required. Increasing knowledge of xylem functional structure in grapevine, and the possible existence of distinct pathways of xylem sap from roots to leaves, would also be very useful to indicate why FS are sometimes expressed on few shoots or on entire vine canopies. These points are being addressed in several recently commenced research initiatives.

Step 3: Outburst of tiger stripe-like foliar symptoms

Tiger stripe-like FS have been well-described by many authors. Notwithstanding, the so called "tiger stripes" (i.e. interveinal drying or discoloured zones) show a range of variability (Lecomte *et al.*, 2012), depending on cultivar or the age of the symptoms.

Because tiger stripe-like FS appear irregularly on vines that also have perennial necroses and inner pathogen inoculum, additional factors besides pathogens and their induced wood necroses need to be considered to explain symptom occurrence. As GTD pathogens have never been retrieved from host leaves, these factors must be remotely inducible from where they act.

Some studies have been dedicated to characterizing the physiological disturbance that occurs on symptomatic leaves showing esca disease or Botryosphaeria dieback, or on asymptomatic leaves from symptomatic canes, and prior to the outburst of FS (Petit *et al.*, 2006; Christen *et al.*, 2007; Andreini *et al.*, 2009; Letousey *et al.*, 2010; Valtaud *et al.*, 2011). This has been reviewed by Wagschal *et al.* (2008) and Fontaine *et al.* (2016). Symptomatic leaves show low rates of photosynthesis induced by stomatal closure, impairment of photosynthetic apparatus, and alteration of chlorophyll pigments. These modifications have also been observed on visually healthy leaves of symptomatic grapevine canes, but not on asymptomatic canes.

Apart from GLSD symptoms on leaves, the "brown stripe" needs to be considered, which was found on 95% of symptomatic vines by Lecomte *et al.* (2012). This symptom on a vine is a longitudinal stripe of variable width and a few millimetres thick, affecting the young xylem (visible after removing the bark), directly connected to the shoot affected by FS and extending down the arms and trunk, and sometimes reaching the roots. The stripe appearance is first yellow or orange and then ages to brown. Histological observations showed that the colour is due to vessel occlusion and filling with tyloses and gums (Dubos *et al.*, 2001; Larignon, 2010). The brown stripe is not necessarily located close to necrotic tissues or wounds, but severity of FS are related to the width of the stripe (Lecomte *et al.*, 2012). As Botryosphaeriaceae species are frequently retrieved from these brown stripes (Dubos *et al.*, 2001; Kuntzmann *et al.*, 2010), some French authors have considered the symptom to be typical of Botryosphaeria dieback. Lecomte *et al.* (2012), however, reported data showing that the wood brown stripe was generic of esca disease.

Two hypotheses can account for the outburst of tiger stripe-like FS, based on the reports of Galet (1977), Mugnai *et al.* (1999), Lecomte *et al.* (2005), Surico *et al.* (2006), Pouzoulet *et al.* (2014), and Gómez *et al.* (2016). These are: (i) the action of GTD fungus-associated phytotoxic compounds, which disseminate and reach the foliage; and (ii) disturbance of sap flow to the leaves on given xylem pathways altered by fungi. These hypotheses are here respectively termed the "toxins" and the "hydraulic dysfunction" hypotheses.

A third hypothesis has recently emerged, which suggests that FS could be due to annual infections by some fungi through pruning or green wounds. The pathogens then progress into the annual shoots, directly causing local FS (Larignon, 2017). More research is required to develop this hypothesis.

The "toxins" hypothesis

In the "toxins" hypothesis, tiger stripe-like FS would be provoked by the phytotoxic action of one or several metabolites produced by one or several fungi. The metabolites would be released in the vine sap flow to move up to the leaves. The metabolites could affect leaf functioning following their production (or over-production) by the fungi, or because of a lack of capacity of the host to detoxify them. The inciting factors could be a change in micro-environment conditions eliciting toxin production, or a progression of the fungi across reaction zones to infect previously healthy and functional parts of the wood, or an ineffective cellular response of the leaf tissues to the entering toxins.

Considerable research has been reported examining the hypothesis of secondary metabolites and their potential phytotoxic activity on leaves (Sparapano *et al.*, 2000; Abou-Mansour *et al.*, 2004; Martos *et al.*, 2008; Wagschal *et al.*, 2008; Andolfi *et al.*, 2011; Abou-Mansour *et al.*, 2015). These studies have been encouraged by the similarity of symptoms resulting when the toxins or fungus culture extracts have been re-injected into vine leaves or shoots, compared to GTD symptoms observed in the field. Some of these toxins have also been retrieved in xylem sap or leaves (Bruno and Sparapano, 2006c; Andolfi *et al.*, 2011).

Visual leaf stripe symptoms may appear after the onset of foliar lesions (Fontaine *et al.*, 2016; Magnin-Robert *et al.*, 2017), which suggests that the visual symptoms may not be directly caused by the toxin(s) but could be a consequence of an oxidative burst triggered by the toxin(s) up to the leaves (Calzarano and Di Marco, 2018). Foliar applications of a mixture containing calcium, reported to limit plant oxidative stress (Calzarano *et al.*, 2014), reduce incidence of GLSD foliar symptoms (Calzarano *et al.*, 2014; Calzarano and Di Marco, 2018), supporting this hypothesis.

Several questions remain. It is not known if one or potentially all of these compounds cause symptoms. The threshold concentrations inducing toxicity have not been determined. The interactions with factors determining leaf susceptibility, and the modes of access to sap flow also remain to be outlined.

Fmed alone has sometimes been assumed to be responsible of tiger stripe-like FS (Lafon, 1921), as suggested by positive results from the "curetage" (trunk cleaning) method for reducing FS occurrence (Thibault, 2015; Yobregat and Abidon, 2019; Cholet *et al.*, 2019). This method involves removal of all the spongy white rot off the wood of affected plants, using a small chainsaw trimmer, regardless of the discoloured wood that could remain. As the positive effect of "curetage" has been confirmed in different vineyards, the method could be useful for investigating the role of Fmed in symptom appearance, even even if an effect of "curetage" on reducing inner inoculum, or triggering vine defences, cannot be excluded to explain symptom reduction (Mondello *et al.*, 2019).

The "hydraulic dysfunction" hypothesis

This hypothesis assumes that typical tiger stripe-like symptoms could be due to impairment of the sap flow to the leaves. Following a progression of the fungi to an apparently functional part of the wood, the associated volume of vessels would no longer be able to drive the sap, whether because of a reaction of the vine occluding vessels, the occurrence of "cavitation" phenomena, or because of both. Cavitation is caused by air bubbles that form and coalesce inside the vessels, leading to embolism (Tyree and Sperry, 1989; Cochard, 2006). This can occur when the ratio between transpiration and xylem flow is too great. It generally occurs at the junctions where resistance to the flow is greatest, particularly in petioles and roots (Lovisolo *et al.*, 2008; Zufferey *et al.*, 2011). The same explanation was used by Yadeta and Thomma (2013) to explain the symptoms caused by some vascular pathogens in forest trees.

Unlike the "toxins" hypothesis, where tiger stripe-like symptoms are observed after toxin injection into healthy detached leaves, the "hydraulic dysfunction" hypothesis shows no similarity with tiger stripe-like FS. Tiger-stripe symptoms are not visually or physiologically similar to typical grapevine symptoms of edaphic water stress (Christen *et al.*, 2007; Andreini *et al.*, 2009; Letousey *et al.*, 2010; Fontaine *et al.*, 2016; Reis *et al.*,

2016). FS can show similarities with symptoms of *folletage* described by Branas (1974), or to some senescence symptoms in autumn.

The impact of wood necrosis or the presence of wood inhabiting fungi on vine hydraulics have not been intensively studied, except for Pch infections on young plants (Edwards *et al.*, 2007; Fischer and Kassemeyer, 2012) or some measurements of resistance to sap flow (Andreini *et al.*, 2009). Recent research (Bortolami *et al.*, 2019) has advanced this area, and is likely to open new research on the hydraulic dysfunction hypothesis.

Compatibility of the hypotheses with major characteristics of tiger stripe-like FS

Tiger stripe-like symptoms can affect whole or parts of plant canopies. With the cordon spur pruning type, the smallest affected unit is the spur, while with Guyot pruning, it is the cane. The explanation could be that xylem of the vine may be sectored, so that a particular part of the xylem is driving sap from a particular part of roots to a particular part of shoots (Shani *et al.*, 1993). Whatever the explanation, severity of canopy FS probably reflects the number or the extent of xylem vessels which are transporting toxin(s), or which express xylem flow dysfunction.

FS can show different expressions (colours, severity on one leaf, severity on each shoot, with or without leaf abscission). These symptoms could be explained by the nature and the concentration of the toxic compounds in the leaves, which may be related to the types of GTD fungi, and to the intensity of hydraulic disruption, or by a combined action of both. The type and status of leaf tissue showing symptoms could also be involved, depending on cultivar, tissue, age, physiological or nutritional status, or developmental stage. In case of the toxins hypothesis, the volume of foliage that receives the toxic compounds (acting as a dilution factor) should also be considered.

In France, tiger stripe-like FS begin after flowering (sometimes late in July for some regions/cultivars). This could be correlated, as for the toxins hypothesis, to vine phenological stage. Flowering is a period of active growth; inflorescences and young grapes become significant sinks for carbon (Lebon *et al.*, 2008). This can result in poor defences capacities, thereby allowing fungi to overstep reaction zones or vine defences. According to the xylem dysfunction hypothesis, this could correspond to the first intense flush of climatic transpiration demand, contributing to impairment of the xylem.

The two hypotheses also explain fluctuations of FS from year to year. Conditions for production, release and distribution of toxins may be fulfilled in one year but not in that following, due to variation in plant defence responses, microbiota and/or environmental status. Xylem function could also be greater in one growing season than in the next. Increased radial growth of new xylem, reduced progression of fungi in healthy ring of wood, or reduced climatic demand could all affect xylem function.

Step 4: Apoplectic events

Apoplexy is the longest-known symptom attributable to esca (Larignon, 2016), and is probably the most striking. It involves complete wilting of grapevine canopies, leaves and stems within a few days, generally leading to the death of affected vines (Mugnai *et al.*, 1999). Apoplexy occurs most frequently during hot days in July and August each year following rainy events. Old vines are more prone than younger ones (Surico *et al.*, 2006), although apoplexy symptoms have also been noted recently on young vines (Larignon, 2016). When the trunks of affected plants are sectioned longitudinally, they generally show large amounts of decayed and discoloured wood (Maher *et al.*, 2012), with "spongy" material (due to Fmed decay). Hypothesis most frequently proposed is that the abrupt symptom development results from collapse of entire vine hydraulic system, because of decay and critically poor xylem function. These conditions are detrimental to sap flow when associated with intense climatic demand. Apoplexy is a nonspecific symptom which can occur with several other problems or diseases, including the ultimate stages of decline due to *Grapevine fanleaf virus* or Syrah decline, 'folletage' symptoms, or to mechanical trunk injuries.

Step 5: Vine death

Apart from the consequence of apoplexy, death of vines that previously expressed FS is poorly described in the literature. Guérin-Dubrana *et al.* (2012) showed that vine death is associated with GLSD, because affected plants die if FS have occurred at least once in the last 4 previous years. More recently, Calzarano *et al.* (2018) showed that the percentage of mortality was higher for vines showing severe symptoms at the first appearance.

Vine death can occur progressively as plant canes, arms or spurs die. Lecomte *et al.* (2014) mention the death of canes and spurs as indicators of GTDs, in addition to FS. In several countries, death of spurs is also typical of Botryosphaeria dieback (van Niekerk *et al.*, 2006; Úrbez-Torres, 2011). Claverie *et al.* (2017) observed that FS lead to variable death of spurs, from 0 to 96%,

depending on the FS severity, year, vine cultivar and the vineyard.

Vines can also decline, reducing growth and yield before dying. Petit *et al.* (2006) showed that tiger stripe-like FS lead to reduced reserve restoration in the canes. Andreini *et al.* (2013) observed bud break delay on vines that were esca symptomatic the year before, with reduced growth rates in the early season being a consequence of less reserve replenishment the previous year (McArtney and Ferree, 1999; Duchêne *et al.*, 2003). Claverie *et al.* (2017) also observed delayed spring growth and yield reduction for vines that had shown FS the previous year. These results indicate that FS can alter vine growth parameters, at least the year following the appearance of FS. The extent to which lost 'vigour' contributes to decline and death of vines is yet to be assessed.

A given rate of plant mortality in a vineyard could result from the cumulative effects of apoplexy, death of individual canes and spurs, and decline. As a consequence, FS occurrence and plant mortality in a vineyard are only partially correlated, so information on both is needed to describe particular GTD status.

THE ROLE OF "SOIL-CLIMATE-MANAGEMENT" SYSTEMS, MICROBIOTA AND PLANT MATERIAL AS GTD INFLUENCING FACTORS

Once the process is sequenced, the factors that may influence the GTDs can be integrated. We have been discussing the relationships of these with each component of the model: wounds, outer and inner inoculum, plant defences and sap conductivity. These factors can be in different categories, including host genotype, climate and soil, microbiota, vine physiology and cropping practices.

Influence of vine physiology

FS and wood symptoms of esca and Botryosphaeria dieback directly impact on vine physiology by reducing the volume of functional tissues for photosynthesis and carbohydrate storage. Beside these direct effects on vine structure, the host-pathogen relationship could also have consequences for grapevine physiology. Expression of active responses to infection at the plant/pathogen interface, as for release of active defence compounds in wood reaction zones, or detoxification of toxins in leaves, implies that plant defence is a substantial expense for carbon assimilates (Pearce, 1996; Berger *et al.*, 2007; Bolton, 2009). This has been conceptualized on plants other than grapevine, especially for pathogens that attack the source organs (leaves) (Berger *et al.*, 2007) and also extensively studied for forest trees and wood pathogens. This assumes trade-offs of tree resources between growth and defences. Optimizing the plant defence pool requires consideration of source/sink relationships at the whole plant level (amount of sources production, competition between sinks). At that point, plant pathology interferes with plant physiology.

Origin and costs of defences

Little information is available on the influence of GTDs on the amount of carbon allocated for plant defences (Bertsch *et al.*, 2013), and on the origin of the carbon used for defences: either C storage or recently produced photoassimilates, either local storage (in trunks) or distant storage (in roots).

Forest pathology has explored this more deeply, although there is no conclusive consensus. Creation of reaction zones is considered as an investment for host trees, as evidenced by the increased amount of carbon compounds (and derivatives) in the reaction zones, which are surrounded by zones where these compounds are depleted (Christiansen *et al.*, 1987; Viiri *et al.*, 2001; Guérard *et al.*, 2007).

For GTDs, reduced starch is also observed in parenchyma tissues close to the wood infected by fungi (Larignon, 1990; Mugnai *et al.*, 1999; Rudelle *et al.*, 2005; Fontaine *et al.*, 2016) for Eutypa dieback and esca. This indicates that the starch has been used for host defence responses, although direct metabolization of starch by the fungi cannot be excluded.

Some forest tree studies have shown that sources for carbon used for induced defences are primarily from local storage, and if they are required, photosynthates from the leaves translocate to the infection sites (Guérard *et al.*, 2007; Goodsman *et al.*, 2013). Similarly, trees with depleted C storage show increased susceptibility to some pathogens (Wargo, 1996).

These results underline the possible role of C storage, that, beside ensuring good renewal of the vegetation each spring, may be important in pathogen attack. Reserve allocation in grapevine is commonly assumed to be passively restored every year, from C excess that is unused for growth of shoots and fruit. Recent studies on trees have reported that, in some cases (tapping of rubber trees or after wounding and attack by pathogens), C storage could be an active sink (Silpi *et al.*, 2007; Chantuma *et al.*, 2009; Goodsman *et al.*, 2013). Identifying energy expensive C sinks for plant defences suggests the need for study of allocation and partitioning of C within vines infected by GTD pathogens.

Competition between sinks

Different models account for allocation of carbon among organs in plants (Lacointe, 2000), and models based on source/sink relationships are the most commonly referred to in grapevine. Traditional source/sink relationships in grapevine, such as those summarized by Champagnol (1984), assume that the compounds produced by the source organs are allocated to the sinks with priority levels depending on the phenological stages of vine development. Photoassimilates are first used locally by leaves, for respiration and growth, and are then exported to the other sinks depending on their sink strength. Sinks are, firstly, shoot apices, then young berries during their active growth, and then berries and perennial organs (trunks and roots) after cessation of shoot growth. Additional research on grapevine has also reported and assessed C partitioning patterns among organs (Castelan Estrada, 2001; Bates *et al.*, 2002; Grechi *et al.*, 2007).

Defences against pathogens are generally not explicitly mentioned as sinks, with these responses being commonly aggregated by physiologists with respiration and maintenance costs. In forest trees, it has been demonstrated that following a pathogen attack, the infected host organs become important sinks for C, either for wood (Goodsman *et al.*, 2013) or for infected leaves (that were previously source organs) (Berger *et al.*, 2007). Berger *et al.* (2007) reported that sink strength can be indicated from cell wall invertase activity. In grapevine canes inoculated with Pmi (lignified internodes), upregulation of a gene coding for a cell wall invertase has been recorded soon (48 h) after infection (Pierron, 2015).

As "sink strength" varies during each year, the C allocation to defence responses can show different seasonal trends. In forest trees, development of reaction zones is considered to be a dynamic process that can be overcome by pathogens and re-built (Schwarze and Baum, 2000). Host trunks therefore exhibit alternate phases of breakout and new compartmentalization (Christiansen *et al.*, 1987; Pearce, 1996). This dynamic process can be explained by successive greater and lesser amounts of C allocated to the maintenance of reaction zones. For GTDs, seasonality is also suggested by the variation of host susceptibility depending on phenological stage: Spagnolo *et al.* (2014a and 2017) observed that flowering was the most susceptible stage to inoculations by two Botryosphaeriaceae species, compared to the earlier Baggiolini stage G (ten leaves separated) and veraison. They suggested a shift in C allocation rules at flowering that led to reduced C dedicated to defences. Similarly, tiger stripe-like FS can appear several times on each plant between June and September (Claverie, 2015). The extent to which these successive FS outbursts are due to different amounts of C allocation to defence, in combination with variations in microbiota ecology or microenvironmental conditions, remains to be studied.

Sources are regulated by stress

Sources are also influenced by environmental stresses, such as drought or nitrogen shortage, in nonlinear ways described by McDowell (2011) and Christiansen *et al.* (1987). Conceptual models exist to display the effects of resource availability on whole plant metabolism, especially the allocation between primary and secondary metabolisms (for review see Stamp (2003)). Free of water or nitrogen stress, assimilates are dedicated to growth (primary metabolism), resulting in small amounts for defences. When resource availability reduces, growth slows before photosynthesis (Pellegrino *et al.*, 2006), and excess C is allocated to secondary metabolites such as phenolics. Under prolonged drought, photosynthesis is altered so less C is available for defences. This is why drought is frequently considered as a predisposing factor for forest tree declines (Desprez-Loustau *et al.*, 2006; Piou *et al.*, 2006), even where it is unclear whether drought acts on defences allocation or on tissues composition and attractiveness for pathogens.

This model is consistent with some observations of grapevine (van Niekerk *et al.*, 2011; Amponsah *et al.*, 2014) and other plants (Schoeneweiss, 1981), showing that, following stem inoculations by Botryosphaeriaceae, the lengths of the wood lesions are increased when predisposed by drought. It is also well-known that tiger stripe-like FS are favoured in fertile soils and vigorous host growth situations (Destrac-Irvine *et al.*, 2007). This apparent contradiction with the previous observations can be explained in that those vineyards show intensive growth and production, which can be deleterious to the secondary metabolism, including defence. In this case, shoot apex and leaf sink strength would be too significant to leave enough C for defence mechanisms. This is only one possible explanation. Others could be that wood composition is more favourable for nutrition of one or several fungi (Calzarano *et al.*, 2009), or for toxin production (related to FS emergence). Large numbers of shoots and canes pruned in winter could also act as many entry points for the fungi or sources of dead wood. Combined with low overall defences, this may lead to insufficiently protected reaction zones, as hypothesized for forest trees during severe attacks by bark beetles (Christiansen *et al.*, 1987).

These two examples of possible nonlinear stress effects on source/sink relationships emphasize the

importance of first, identification of which stress factor promotes either wood necrosis, FS outburst or both, as reviewed by Songy *et al.* (2019), and second, to specify drought or vigour intensities or consequences on grapevines, in order to give objective determination of the amounts of stress on vine C metabolism. The specific reactions and interactions to stress of all GTD pathogens of the complex must also be considered.

Combining the ecological defence/growth approach (as characterized in trees) and physiological source/sink allocation rules between organs would be of great importance for GTDs and even for grapevine pathology. It could help assess respective defence, biomass production and reserve replenishment costs and propose cultural practices to define trade-offs between the three factors.

Management and environmental factors related to vine physiology

Grapevine physiology (especially C production and allocations) is determined by the environment, genotype, and crop management practices. Climate (temperature, light, rainfall) is a key factor in vegetative growth, bunch development and phenology, and, therefore, C allocation. Climate and soil also influence water and nitrogen availability, and the water and nitrogen stresses that regulate photosynthesis and carbohydrate production in leaves. Since cropping practices such as irrigation, fertilization, weed control (competition for nitrogen and water) and planting density (competition with neighbouring vines) affect water and nitrogen resources, they also affect vine physiology. Vine rootstock is also important, because of effects on root development and uptake capacity, and effects on scion vigour. Cropping practices, such as de-budding or green harvesting, may influence the sinks (e.g numbers of bunches), and numbers of wounds (see below). Other practices affecting the C sources could also be involved, including the vine training system, vegetation topping or trimming, and defoliation.

Additional study of grapevine involving physiology or agronomy could improve knowledge of effects of cropping practices on vine C and nitrogen balance.

Factors influencing the wounds. Numbers and size of wounds are assumed to be important mainly as probable entry points for pathogens. However, wounds could also affect infection success depending on pruning characteristics.

The effects of pruning on production of dead wood, and on the effectiveness of fungus inoculations have been intensively studied in forest trees (Dujesiefken and Stobbe, 2002; Eisner *et al.*, 2002), and to a lesser extent in fruit trees (Grosclaude, 1993) and grapevine (Cholet *et al.*, 2017). The influencing pruning parameters are branch diameter (compared to that of trunks), angle of branch insertion on trunks which affects pith continuity, and cut angle, especially with respect to collars. On grapevine, old reports noted similar relationships between pruning parameters (number, size and localization of the pruning wounds, and association with cane collars) and production of "desiccated wood" beneath wounds (Lafon, 1921). More recently, studies have focused on good pruning practices, which protect the wood from discolouration and decay, and thus maintain more functional sap flows (Dal *et al.*, 2008; Lecomte *et al.*, 2011; Simonit *et al.*, 2012; Anonymous, 2013; Delorme, 2015).

In grapevine, the next step will be to define pruning characteristics (number, size, disposition of wounds) that impact inner inoculum and conductivity and hydraulics of host plants. This could help unravel the causes of FS outburst, along with the 'xylem dysfunction' hypothesis; but also confirm if resulting dead wood or non-functional vessels are more susceptible to fungal penetration and colonization than sound tissues.

An indirect consequence of wounding effects is indicated by observations from unpruned or minimally pruned grapevines, as well as from mechanical hedging. With these two pruning methods, wounds are mainly localized on young branches, and less at the interface with old wood. Consequently, these pruning methods are expected to give less dead wood and trunk and arm necroses (Lecomte *et al.*, 2015; Travadon *et al.*, 2016). Recent studies suggest that there is less impact of esca and Botryosphaeria dieback on FS and mortality when these pruning methods are used (Dumot, 2019; Lecomte *et al.*, 2019) but these effects require further confirmation.

To reduce the number of wounds produced in winter**,** de-budding in spring is likely to have negative influence on GTD infections, as described by Morvan *et al.* (2012). They observed that elimination of excessive shoots in early spring reduced FS occurrence, possibly because this reduces cane number and subsequent wounding that occurs with winter pruning. Further research is required in different situations to confirm these observations.

Climate and soil. As most GTD fungi utilize airborne inoculum, the role of soil on fungus life cycles has not been closely investigated. The hypothesis requires further investigation for fungi such as Pch and Pmi (Larignon and Gramaje, 2015). The role of the soil has been considered indirectly, through impacts on grapevine physiology, and especially on vine vigor. The soil

parameters to be considered are numerous. They especially relate to soil structure, texture and depth, and to fertility (organic matter, microbial status, mycorrhiza). Recent studies on GTDs have emphasized the role of soilborne micro-organisms in plant defence induction, including effects of endophytic rhizobacteria or fungus biocontrol agents (Di Marco and Osti, 2007; Spagnolo *et al*., 2015; Yacoub *et al*., 2016).

Climate can influence several steps of GTD development, including conservation and dissemination of outer inoculum, and colonization inside host wood (Fischer and Peighami-Ashnaei, 2019). These aspects as influenced by heat and drought stress, have been reviewed by Songy *et al.* (2019), particularly the dual effects of both these stresses, and emphasizing the variable consequences when one or a complex of fungi is considered. Growth of fungi has temperature optima, as reported by many authors for Botryosphaeriaceae (van Niekerk *et al*., 2006; Úrbez-Torres *et al*., 2014), Pch and Pmi (Valtaud *et al*., 2009; Pontini *et al*., 2014) and El (Sosnowski *et al*., 2011).

Climate may also influence the composition and evolution of the whole microbiota. Bruez *et al.* (2014) observed evolution of microbiota composition inside healthy grapevine trunk wood during each year. For apoplexy and tiger stripe-like FS outburst, climate affects transpiration flow, which is consistent with both hypotheses (but possibly greater for xylem dysfunction, although possibly also for triggering toxin production (Pontini *et al*., 2014)).

Several studies have focused on relationships between temperature, rain and FS. Most indicate occurrence of FS is positively correlated to years with high rainfall in spring and summer (Surico *et al*., 2000; Marchi *et al*., 2006; Larignon, 2009; Andreini *et al*., 2014; Calzarano *et al*., 2018). This association requires further elucidation with gradual assessment, to answer to the following questions: do rainy events act on vine carbon and nitrogen balance and on host defences and host/pathogen relationships? Does climate affect temperature and moisture content of trunks favouring colonization by fungi or evolution of internal trunk microbiota? Does it act on soil water content and induce high levels of transpiration and sap flow?

Genotypic factors. No *Vitis* species used as rootstocks and no grapevine (*Vitis vinifera*) cultivars are known to be resistant to GTDs (Bertsch *et al*., 2013). Genetically controlled abilities to counteract GTDs are most likely tolerance based on combination of host life traits (Péros, 1995).

In grafted vines, the effects of rootstocks on GTDs is indirect, acting through vigour conferred to scions and rootstock rooting capacity. On rootstock mother grapevines, that are pruned each year, discolouration and decay are observed on trunks (Liminana *et al*., 2009). But when these genotypes are used as rootstocks, they show fewer lesions than the scions (Mugnai *et al*., 1999). This is probably due to reduced recurrent wounding when they are located belowground (after grafting and planting) than to less intrinsic susceptibility, since rootstocks have no greater tolerance when inoculated with GTD fungi (Billones-Baaijens *et al*., 2014; Guan *et al*., 2016). When rootstocks are compared in field trials for ability to develop FS, they show variable performance (Eskalen *et al*., 2001; Marchi, 2001; Morvan *et al*., 2011; Andreini *et al*., 2014; Murolo and Romanazzi, 2014; Laveau *et al*., 2015; Dumot, 2019). These results suggest the indirect influences of rootstocks on GTD development through one or several effects on grapevine physiology.

The influence of the host cultivar can be in three actions: (i) direct action on the colonization by fungi; (ii) direct action on the outburst of FS; and (iii) indirect action through grapevine physiology at any stage, from pruning wounds and infections, to hydraulic conductivity, fruit production and leaf/shoot ratio. This is suggested by the different susceptibility rankings of cultivars, based on their FS expression or on their responses to infection (e.g. extent of wood discolouration). Multi-faceted tolerance is also suggested by the combined results of tiger stripe-like FS rate, recurrence, and mortality rates for different cultivars. Cabernet Sauvignon had high rates and recurrence of FS but low mortality, while Chardonnay had high rate of mortality but low amounts of FS (Andreini *et al*., 2014). This has also been observed for Grenache compared with Cabernet Sauvignon (Claverie, unpublished). This suggests an uncoupling between the causes underlying FS and mortality.

Some distinct factors associated with tolerance to GTDs have been identified. Cultivars show different capacities for production of defence compounds, with more and more rapidly produced defence compounds detected in tolerant than in susceptible genotypes (Martin *et al*., 2009; Lambert *et al*., 2013; Spagnolo *et al*., 2014b). Different wood compositions (e.g lignin) may affect constitutive defence levels. The sizes of xylem vessels could also affect tolerance to GTDs, as it may be more energy expensive to occlude large vessels than small ones (CODIT *wall 1*). Large vessels could also be more prone to cavitation (Pouzoulet *et al*., 2014). Compared to rootstock or cultivar, the impact of cultivar clones on expression of esca or Botryosphaeria dieback have been less documented (Chevrier, 2013; Murolo and Romanazzi, 2014; Moret *et al*., 2019). Results suggest that if a clone effect on GTD expression can be observed at the vineyard scale, no stable effect can be generalized at

a more global scale, across different seasons or with different changing rootstocks.

Microbiota. Antagonist microorganisms can impact other microbes by competing for niches or nutrients, interfering with toxins or secreting toxic compounds (Compant *et al*., 2013). They can also stimulate grapevine defences (particularly systemic defences) or enhance host resistance to stress (Mondello *et al*., 2018).

Several reports highlight absence of correlations of fungal composition between symptomatic and asymptomatic wood (Bruez, 2013; Elena *et al*., 2019). This can be explained by the multiple conditions and steps that are necessary to trigger FS (e.g particular plant physiological status, or amounts of decayed and discoloured wood required before FS appear). Another explanation may be the dynamic evolution of the vine microbiota (in a time span as little as a year) compared to the generally long-lasting process (several years) from infection and colonization to FS emergence.

Nevertheless, the action of antagonistic microorganisms on the populations of fungi associated with GTDs can be assumed. High amounts of GTD fungi and *Trichoderma* have been found in visually clear wood of 50-year-old asymptomatic vines, suggesting a microbial balance that may contribute to maintaining the healthy status of these vines (Bruez *et al*., 2016). It has also been suggested that such a balance between plant host, environment and microbiota could trigger pathogenicity from non-pathogenic endophytes (Úrbez-Torres, 2011), thus emphasizing on the importance of the host-pathogen-environment triangle (Fischer and Peighami-Ashnaei, 2019), or even adding it a fourth component, resulting in the pathobiome concept (Brader *et al*., 2017).

Mondello *et al*. (2018) reported that 40 bacteria or fungi have been studied as potential biocontrol agents for GTDs. These agents can interfere at different stages in the disease conceptual model. These could affect microbial balance inside grapevine trunks, but also as pruning wound protectants (both in nurseries and vineyards) or defence stimulators (e.g. using *Pythium oligandrum*; Yacoub *et al*., 2016). With the increasing demand for environmentally acceptable disease control agents, and the development of molecular technologies to accelerate their selection and assess their efficacy, investigations on exploiting the biocontrol potential of microbiota are important.

Another influencing factor to mention in the scope of microbiota is: if a lot of work has been done to select efficient active ingredients against GTDs associated fungi (Mondello *et al*., 2018), the chemical control against annual grapevine diseases and pests has also proven to impact the whole grapevine microbiota (Pinto *et al*., 2014) without being able to know in which way they influence this complex system.

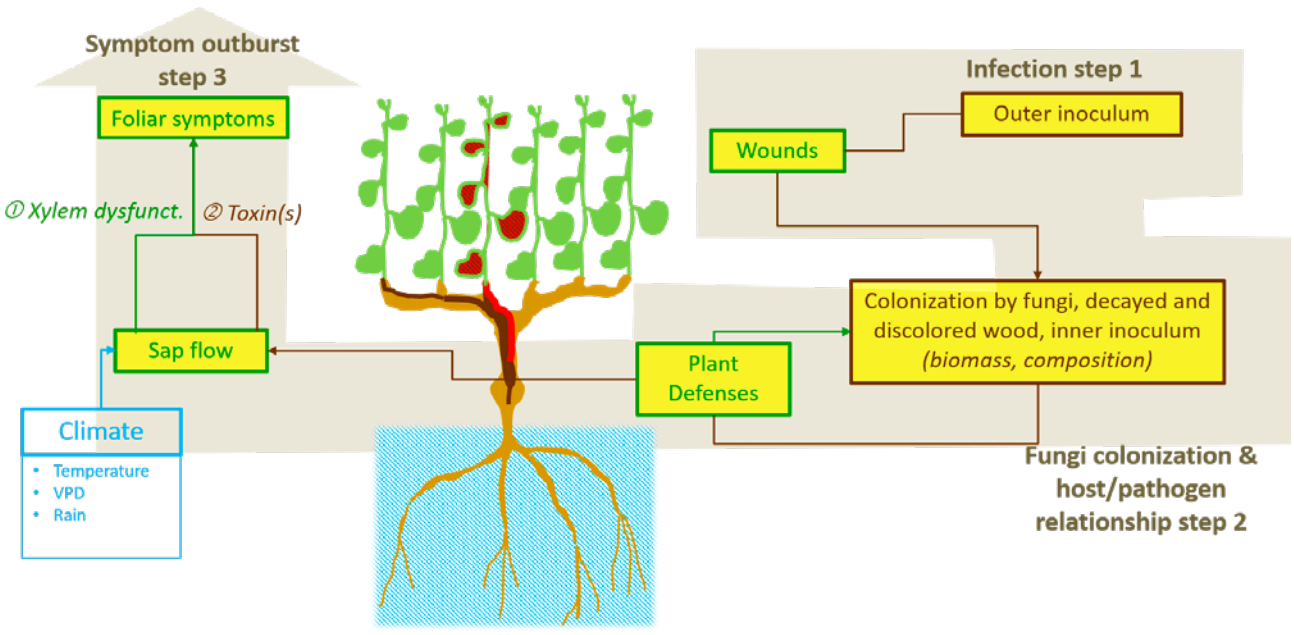

Figure 1. Hypothetical sequence of events leading to grapevine foliar symptom outburst. The process can be divided into three steps that can unfold over several years or occur several times each year and on different parts of each vine. The sequence ends with production of dead, discoloured wood (necrosis) on perennial structures as well as foliar symptoms, leading to grape quantity or quality losses, and to death of parts of, or entire, vines. VPD = vapor pressure deficit.

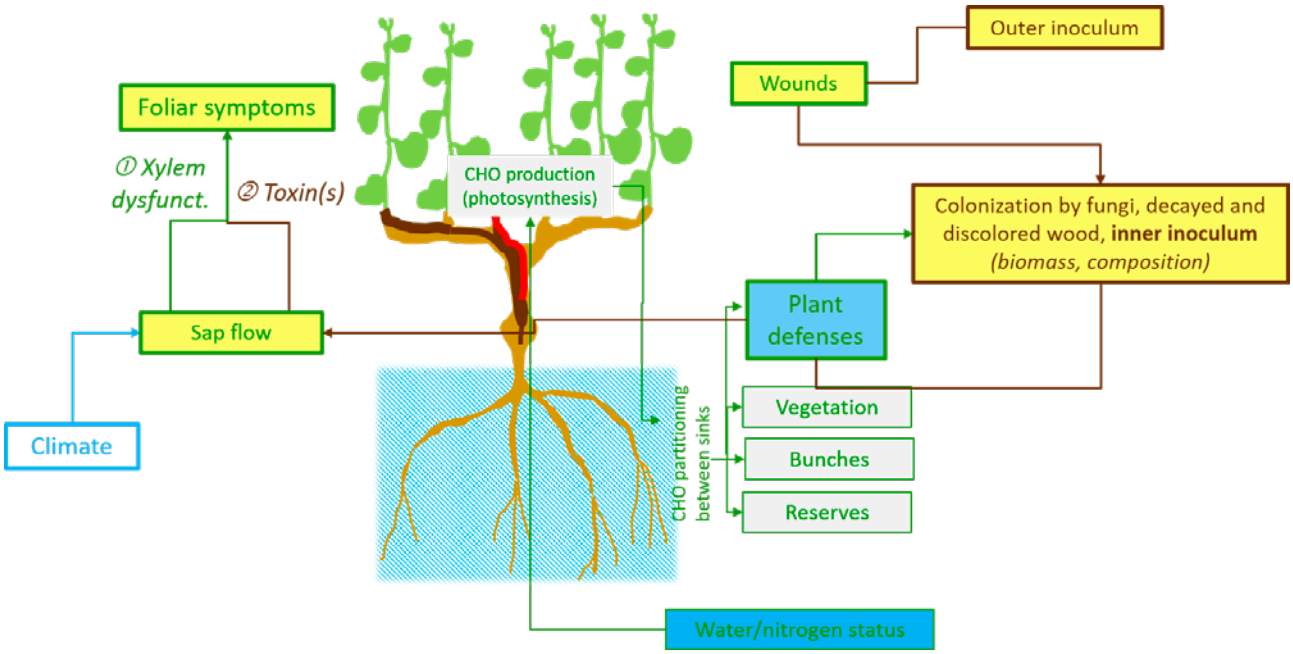

Figure 2. Investment in defences at the host/pathogen interface and probable implication of whole plant physiology: when pathology meets physiology. If foliar and wood symptoms cause direct losses for grapevine functioning, defence allocation will also be a probable expensive investment for affected vines, at the host/pathogen interfaces. This expense could be considered as a sink for C assimilates, like shoot growth, grape production or reserve replenishment. The role of trunk reserves (starch and derivatives) in supplying energy for local defences in the wood is possible, but still to be investigated. Implication of vine balance in optimizing defence allocation would be an interesting direction for future research. CHO = Carbon, Hydrogen, Oxygen (C assimilates)

CONCLUSIONS AND PERSPECTIVE

This review aimed to integrate, with a systemic approach, the hypothetical or demonstrated processes, dysfunctions and stages explaining the occurrence of FS and death of grapevines affected by esca and Botryosphaeria dieback. Available literature on these diseases has been reviewed, as well as other relevant topics on grapevine and on forest trees. The main hypotheses currently proposed by researchers and advisors for these diseases has been summarized. Building a sequence of steps in the progression of GTDs helped to develop assumptions to elucidate their complex etiology, and brought knowledge from several disciplines into a broad perspective.

A conceptual model is proposed, based on Figures 1, 2 and 3. Figure 1 summarizes the three distinct steps that lead to tiger stripe-like FS, Figure 2 presents the possible connections of GTDs with vine physiology at the host/pathogen interface, and Figure 3 summarizes the major factors contributing to slow down or acceleration of the processes added on a prior "baseline". This system is a grapevine-microbiota association within a set of environmental factors according to specific conditions. These conditions can be either positive for the pathogenic fungi, or deleterious to host grapevines. They can lead to the progression of the fungi in host wood, inducing various amounts of dead or non-functional wood, and be sources of inner inoculum for further colonization. Both can culminate in expression of FS, either through direct phytotoxic effects or indirect disruption of the sap conductive systems. This unfavourable situation for grapevines causes yield and quality losses, and death of parts of, or entire, vine wood structures (branches or trunks), mainly through direct FS impact. Some indirect drawbacks can also occur, through alteration of grapevine physiological functioning, including photosynthesis efficiency, potential reserve replenishment, enhanced costs for defences or modifications in source/sink relationships. Together, these trigger the negative grapevine decline process.

From the knowledge integrated in this review, we propose a sequence of events taking place to explain FS outburst. Since this analysis remains "qualitative", it is not possible to "rank" the importance of the events for the probability or rapidity of FS occurrence. The respective contributions of infection, colonization, host defences and FS outburst putative causes to avoidance or reduction of FS and mortality are unable to be assessed. Nevertheless, this knowledge is necessary before test-

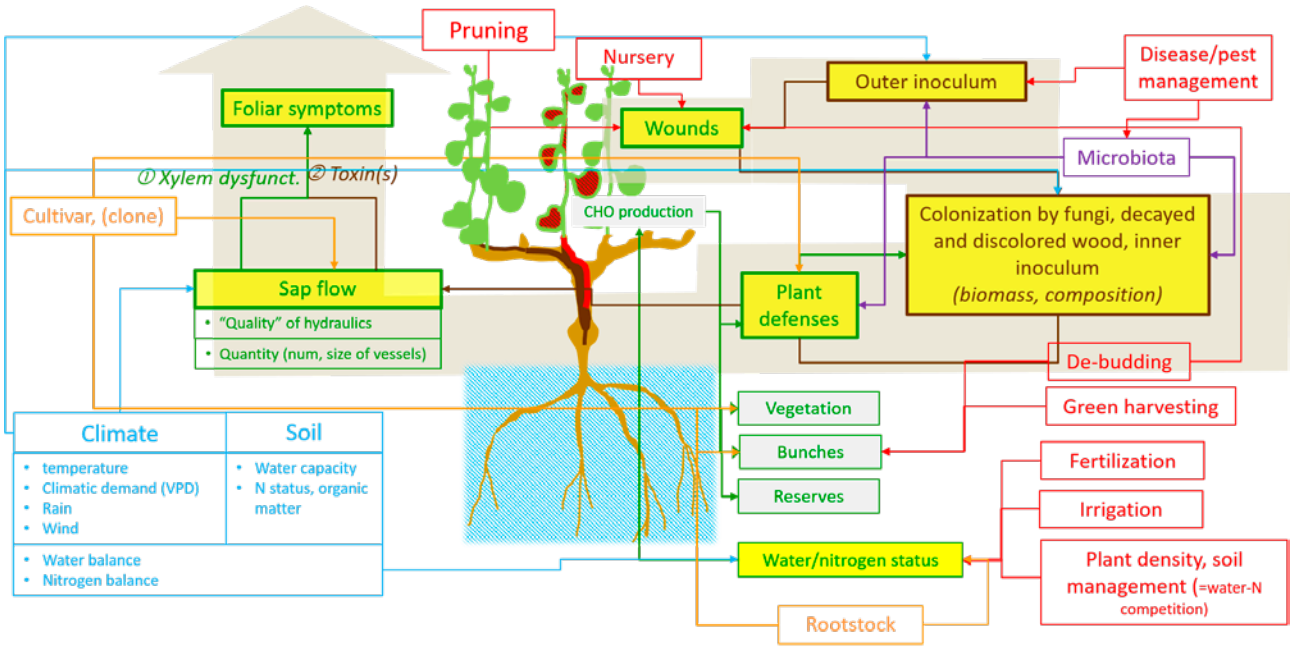

Figure 3. Conceptual model of GTDs based on the hypothetical sequence of events and adding major drivers of the system. GTD-associated fungi are part of the microbiota and account for outer and inner inoculum. They enter vines through wounds, at many possible stages during the vine lifetimes, co-existing and interacting at the reaction zones. Because they are wood inhabiting fungi that alter wood (where storage and sap flow take place), because defences are needed, and because FS can alter vine physiology, global source/sink relationships need to be considered as indirect drivers in this approach. Grapevine/fungi relationships are modulated by microbiota and environmental conditions during each growing season and during vine lifetimes. These multiple combinations result in occasional outbursts of foliar symptoms contributing to vine decline and death. The modulating factors belong to different categories: relations inside the microbiota (indicate in purple), climate and soil (blue), scion and rootstock genotypes (orange), cultural practices (red), that impact wound production and infection or grapevine physiology. A single factor can impact different parts of the sequence, aggravating the complexity. This conceptual model needs to be validated. N = Nitrogen, VPD = vapor pressure deficit, CHO = Carbon, Hydrogen, Oxygen (C assimilates).

ing solutions to avoid or limit GTDs. Would it be more relevant to improve defence mechanisms or to reduce the amount of infection points to limit FS occurrence? Would it be sufficient to associate a tolerant cultivar with few pruning wounds to control GTDs in most climates of the world? Are pathogenic fungi the most influential factors in the model, or is vine physiology, generated by combinations of unfavourable cropping practices, more important? How efficient would it be to fulfill requirements to maintain particular favourable equilibria of vine microbiota? How will the system evolve in the context of ongoing global climate change? Some of these questions could be addressed by research in factorial vineyard experiments and long-term monitoring, which is probably difficult establish. As vine growers are subject to technical and economic constraints, they are unlikely to explore and implement all possible approaches to GTD management. Knowledge upon these methods will be crucial for profitable grapevine production.

As the proposed conceptual model attempts to identify each step in FS development, approach could also be used to build a diagnostic tool in real situations, for example to suggest the GTD weakness points for a given vineyard, or to elaborate vineyard monitoring systems leading to low FS and damage. For that, it will be important to have practical indicators and tools describing the system status. This could include a real-time indicator of grapevine defence status, a practical tool to assess qualitative and quantitative outer inoculum patterns in a vineyard, a marker of grapevine hydraulic efficiency, and a non-destructive indicator of the amount of decayed or non-functional wood in vine trunks.

ACKNOWLEDGEMENTS

The authors thank gratefully the experts interviewed who shared their vision, submitted literature or gave opinions on the approach outlined in this review. These people include: J.P. Goutouly, UMR EGFV, INRA Bordeaux ; J.P. Péros, UMR AGAP, INRA Supagro Montpellier ; P. Lecomte, UMR SAVE, INRA Bordeaux ; L. Gué-

rin-Dubrana, UMR SAVE, INRA Bordeaux ; C. Bertsch, Université de Haute-Alsace ; F. Fontaine, A. Spagnolo, Université de Reims Champagne-Ardenne ; P. Larignon, IFV ; Patrice Rey, UMR SAVE, INRA Bordeaux ; J.C. Domec, Bordeaux Sciences Agro ; V. Dumot, Station Viticole du BNIC ; M. Barthe, CIVB ; L. Le Cunff et C. Moisy, IFV ; O. Jacquet, Chambre d'agriculture de Vaucluse ; G. Delorme, Chambre d'agriculture du Jura ; M. Badier, Chambre d'agriculture du Loir-et-Cher ; F. Dal, SICAVAC ; J.C. Payan, IFV ; G. Morvan, C. Grosjean, Chambre d'agriculture de l'Yonne et Chambre Régionale de Bourgogne ; B. Broquedis, Chambre d'agriculture du Gard ; H. Cochard, A. Lacointe, UMR PIAF, INRA Clermont-Ferrand ; J.Y. Cahurel, IFV; M. Coarer, IFV.

We also thank the experts solicited for overviews during the COST meeting in Cognac in June 2015: S. di Marco, CNR IBE, Bologna, Italy ; M. Sosnowski, SARDI, Australia; J.R. Urbez Torres, Pacific Agri-Food Research Center, British Columbia, Canada ; C. Rego, Instituto Superior de Agronomia, Lisboa, Portugal; D. Ezra, Volcani center, Bet-Dagan, Israël; V. Hoffsteter, Agroscope Changins, Switzerland; J. Armengol, Instituto Agroforestal Mediterráneo, Valencia, Spain; E. Karaffa, Z. Bihari, Institute of Food Science, University of Debrecen, Hungary.

The authors also acknowledge the V1303 CASDAR project and its leader C. Chevrier for supporting this study, and the *CASDAR* and the *Ministère de l'Alimentation, de l'Agriculture et de la Forêt* for funding.

LITERATURE CITED

Abou-Mansour E., Couché E., Tabacchi R., 2004. Do fungal naphthalenones have a role in the development of esca symptoms? *Phytopathologia Mediterranea* 43: 75–82.

Abou-Mansour E., Débieux J.L., Ramírez-Suero M., Bénard-Gellon M., Magnin-Robert M., … Larignon P., 2015. Phytotoxic metabolites from *Neofusicoccum parvum*, a pathogen of Botryosphaeria dieback of grapevine. *Phytochemistry* 115: 207–215.

Amalfitano C., Evidente A., Surico G., Tegli S., Bertelli E., Mugnai L., 2000. Phenols and stilbene polyphenols in the wood of esca-diseased grapevine. *Phytopathologia Mediterranea* 39: 178–183.

Amponsah N.T., Jones E.E., Ridgway H.J., Jaspers V.M., 2014. Factors affecting *Neofusicoccum luteum* infection and disease progression in grapevines. *Australasian Plant Pathology* 43: 547–556.

Andolfi A., Mugnai L., Luque J., Surico G., Cimmino A., Evidente A., 2011. Phytotoxins produced by fungi associated with grapevine trunk diseases. *Toxins (Basel)* 3: 1569–1605.

Andreini L., Caruso G., Bertolla C., Scalabrelli G., Viti R., Gucci R., 2009. Gas exchange, stem water potential and xylem flux on some grapevine cultivars affected by esca disease. *South African Journal of Enology and Viticulture* 30: 142–147.

Andreini L., Guarino L., Viti R., Scalabrelli G., 2013. Evaluation of the effect of esca disease on bud break in *Vitis vinifera* L.: Possible relationship between cultivars and rootstocks. *Vitis-Journal of Grapevine Research* 52: 33.

Andreini L., Cardelli R., Bartolini S., Scalabrelli G., Viti R., 2014. Esca symptoms appearance in" *Vitis vinifera*" L.: influence of climate, pedo-climatic conditions and rootstock/cultivar combination. *Vitis: Journal of Grapevine Research* 53: 33–38.

Anonymous, 2013. *Manuel des pratiques viticoles contre les maladies du bois*. Sicavac BIVC.

Aroca Á., Gramaje D., Armengol J., García-Jiménez J., Raposo R., 2010. Evaluation of the grapevine nursery propagation process as a source of *Phaeoacremonium* spp. and *Phaeomoniella chlamydospora* and occurrence of trunk disease pathogens in rootstock mother vines in Spain. *European Journal of Plant Pathology* 126: 165–174.

Bates T.R., Dunst R.M., Joy P., 2002. Seasonal dry matter, starch, and nutrient distribution in 'Concord' grapevine roots. *HortScience* 37: 313–316.

Baum S., Sieber T.N., Schwarze F.W., Fink S., 2003. Latent infections of *Fomes fomentarius* in the xylem of European beech (*Fagus sylvatica*). *Mycological Progress* 2: 141–148.

Berger S., Sinha A.K., Roitsch T., 2007. Plant physiology meets phytopathology: plant primary metabolism and plant–pathogen interactions. *Journal of Experimental Botany* 58: 4019–4026.

Bertsch C., Ramírez-Suero M., Magnin-Robert M., Larignon P., Chong J., … Fontaine F., 2013. Grapevine trunk diseases: complex and still poorly understood. *Plant Pathology* 62: 243–265.

Billones-Baaijens R., Jones E.E., Ridgway H.J., Jaspers M.V., 2014. Susceptiblity of common rootstock and scion varieties of grapevines to *Botryosphaeriaceae* species. *Australasian Plant Pathology* 43: 25–31.

Boddy L., Rayner A.D.M., 1983. Origins of decay in living deciduous trees: the role of moisture content and a re-appraisal of the expanded concept of tree decay. *New Phytologist* 94: 623–641.

Bolton M.D., 2009. Primary metabolism and plant defence—fuel for the fire. *Molecular Plant-microbe Interactions* 22: 487–497.

Bortolami G., Gambetta G.A., Delzon S., Lamarque L.J., Pouzoulet J., … Delmas C., 2019. Exploring the Hydraulic Failure Hypothesis of Esca Leaf Symptom Formation. *Plant Physiology* 181: 1163–1174.

Brader G., Compant S., Vescio K., Mitter B., Trognitz F.,… Sessitsch A., 2017. Ecology and genomic insights into plant-pathogenic and plant-nonpathogenic endophytes. *Annual Review of Phytopathology* 55: 61–83.

Branas J., 1974. Folletage. In *Viticulture* (ED. Dehan), Montpellier, 606–611.

Bruez E., 2013. *Etude comparative des communautés fongiques et bactériennes colonisant le bois de ceps de vigne ayant exprimé ou non des symptômes d'esca,* PhD Thesis, University of Bordeaux II, 258 pp.

Bruez E., Lecomte P., Grosman J., Doublet B., Bertsch C., … Rey P., 2013. Overview of grapevine trunk diseases in France in the 2000s. *Phytopathologia Mediterranea* 52: 262–275.

Bruez E., Vallance J., Gerbore J., Lecomte P., Da Costa J. P., … Rey P., 2014. Analyses of the temporal dynamics of fungal communities colonizing the healthy wood tissues of esca leaf-symptomatic and asymptomatic vines. *PLoS One* 9(5).

Bruez E., Baumgartner K., Bastien S., Travadon R., Guérin-Dubrana L., … Rey P., 2016. Various fungal communities colonise the functional wood tissues of old grapevines externally free from grapevine trunk disease symptoms. *Australian Journal of Grape and Wine Research* 22: 288–295.

Bruno G., Sparapano L., 2006a. Effects of three esca-associated fungi on *Vitis vinifera* L.: III. Enzymes produced by the pathogens and their role in fungus-to-plant or in fungus-to-fungus interactions. *Physiological and Molecular Plant Pathology* 69*:* 182–194.

Bruno G., Sparapano L., 2006b. Effects of three esca-associated fungi on *Vitis vinifera* L.: I Characterization of secondary metabolites in culture media and host responses to the pathogens in calli. *Physiological and Molecular Plant Pathology* 69*:* 209–223.

Bruno G., Sparapano L., 2006c. Effects of three esca-associated fungi on *Vitis vinifera* L.: II. Characterization of biomolecules in xylem sap and leaves of healthy and diseased vines. *Physiological and Molecular Plant Pathology* 69: 195–208.

Calzarano F., Di Marco S., 2007. Wood discoloration and decay in grapevines with esca proper and their relationship with foliar symptoms. *Phytopathologia Mediterranea* 46: 96–101.

Calzarano F., Di Marco S., 2018. Further evidence that calcium, magnesium and seaweed mixtures reduce grapevine leaf stripe symptoms and increase grape yields. *Phytopathologia Mediterranea* 57: 459–471.

Calzarano F., Seghetti L., Del Carlo M., Cichelli A., 2004. Effect of esca on the quality of berries, musts and wines. *Phytopathologia Mediterranea* 43: 125–135.

Calzarano F., Amalfitano C., Seghetti L., Cozzolino V., 2009. Nutritional status of vines affected with esca proper. *Phytopathologia Mediterranea* 48: 20–31.

Calzarano F., Di Marco S., D'Agostino V., Schiff S., Mugnai L., 2014. Grapevine leaf stripe disease symptoms (esca complex) are reduced by a nutrients and seaweed mixture. *Phytopathologia Mediterranea* 53: 543–558.

Calzarano F., Osti F., Baranek M., Di Marco S., 2018. Rainfall and temperature influence expression of foliar symptoms of grapevine leaf stripe disease (esca complex) in vineyards. *Phytopathologia Mediterranea* 57: 488–505.

Castelan Estrada M., 2001. *Répartition de la biomasse chez* Vitis vinifera *L.; rendement de conversion du rayonnement solaire global et coûts énergétiques.* PhD Thesis, Paris, Institut national d'agronomie de Paris Grignon, Paris, 132 pp.

Champagnol F., 1984. *Elements de physiologie de la vigne et de viticulture generale*, 351 pp.

Chantuma P., Lacointe A., KasemsapP., Thanisawanyangkura S., Gohet E., ...Thaler P., 2009. Carbohydrate storage in wood and bark of rubber trees submitted to different level of C demand induced by latex tapping. *Tree Physiology* 29: 1021.

Chevrier C., 2013. *Etude de l'impact des choix culturaux des viticulteurs sur le développement des maladies du bois*. Paper presented at the Les maladies du Bois de la Vigne- Réunion du groupe national Maladies du Bois de la Vigne, Angers. 19&20/03/2013, 31–35.

Chiarappa L., 2000. Esca (black measles) of grapevine. An overview. *Phytopathologia Mediterranea* 39: 11–15.

Cholet C., Martignon T., Giudici M., Simonit M., Geny L., 2017. Vigne: pourquoi tailler moins ras aide à freiner l'esca. *Phytoma* 702: 38–41.

Cholet C., Bruez E., Lecomte P., Rey P., Boury T., ... Geny-Denis L., 2019. Intérêt du curetage dans la lutte contre l'esca. *Phytoma* 728: 24–27.

Christen D., Schönmann S., Jermini M., Strasser R.J., Défago G., 2007. Characterization and early detection of grapevine (*Vitis vinifera*) stress responses to esca disease by in situ chlorophyll fluorescence and comparison with drought stress. *Environmental and Experimental Botany* 60: 504–514.

Christiansen E., Waring R.H., Berryman A.A., 1987. Resistance of conifers to bark beetle attack: searching for general relationships. *Forest Ecology and Management* 22: 89–106.

Claverie M., 2015. *Suivi symptômes et fonctionnement du cep*. Paper presented at the Journées Nationales Maladies du Bois, Colmar.

Claverie M., Jouandou N., Jacquet O., Richy D., 2017. Foliar symptoms of GTDs are associated with decline of the vines. *Phytopathologia Mediteranea* 56: 533.

Cochard H., 2006. Cavitation in trees. *Comptes Rendus Physique* 7: 1018–1026.

Compant S., Brader G., Muzammil S., Sessitsch A., Lebrihi A., Mathieu F., 2013. Use of beneficial bacteria and their secondary metabolites to control grapevine pathogen diseases. *BioControl* 58: 435–455.

Cottral E., Pascoe I.G., Edwards J., Jaudzems G., Taylor P.A., 2004. Host–pathogen interaction of *Phaeomoniella chlamydospora*, causal organisms of Petri disease, in grapevine tissue. *Phytopathologia Mediterranea* 43: 150.

Dal F., Bricaud E., Chagnon L., Daulny B., 2008. Relation entre qualite de la taille et deperissement des vignes. Exemple de l'esca. *Le Progrès Agricole et Viticole* 125: 602–608.

Davy A., Larignon P., Vergnes M., Cestaret S., 2011. *Study of the responsiveness of wounds generated during the vegetative period regarding two pioneer esca fungi*. Lacanau, Gironde, France, 3–5 octobre 2011.

De La Fuente M., Fontaine F., Gramaje D., Armengol J., Smart R., … Corio-Costet M.-F., 2016. Grapevine trunk diseases. A review. In OIV (Ed.), *1st edition* (pp. 24). Paris, France: International Organisation of Vine and Wine (OIV).

Deflorio G., Barry K.M., Johnson C., Mohammed C. L., 2007. The influence of wound location on decay extent in plantation-grown *Eucalyptus globulus* and *Eucalyptus nitens*. *Forest Ecology and Management* 242: 353–362.

del Rio J., Gonzalez A., Ortuño A., Botia J.M., Fuster M.D., … Frias V., 2001. Tylose Formation and Changes in Phenolic Compounds of Grape Roots Infected with «*Phaeomoniella chlamydospora*» and «*Phaeoacremonium*» Species. *Phytopathologia Mediterranea* 40: 394–399.

del Río J., Gómez P., Baidez A., Fuster M.D., Ortuno A., Frías V., 2004. Phenolic compounds have a role in the defence mechanism protecting grapevine against the fungi involved in Petri disease. *Phytopathologia Mediterranea* 43: 87–94.

Delorme G., 2015. *Influence du fonctionnement interne du cep sur l'expression des symptômes Esca/BDA*. Paper presented at the Les maladies du Bois de la vigne, Colmar, 17 et 18/11/15, 53–54.

Desprez-Loustau M.-L., Marçais B., Nageleisen L.-M., Piou D., Vannini A., 2006. Interactive effects of drought and pathogens in forest trees. *Annals of Forest Science* 63: 597–612.

Destrac-Irvine A., Goutouly J.P., Laveau C., Guerin-Dubrana L., 2007. L'écophysiologie de la vigne – Mieux comprendre les maladies de dépérissement. *L'Union Girondine des Vins de Bordeaux* 1035: 28–32.

Di Marco S., Osti F., Mazzullo A., Cesari A., 2001. How iron could be involved in esca fungi development. *Phytopathologia Mediterranea* 40: S449–S452.

Di Marco S., Osti F., 2007. Applications of *Trichoderma* to prevent *Phaeomoniella chlamydospora* infections in organic nurseries. *Phytopathologia Mediterranea* 46: 73–83.

Dubos B., Cere L., Larignon P., Fulchic R., 2001. Observation on black dead arm in French vineyards. *Phytopathologia Mediterranea* 40: 336–342.

Duchêne E., Monamy C., Langellier F., Jaegli N., Salber R., … Panigai L., 2003. Effects of the ripening conditions in the vineyard on growth and yield components in the following season. *Journal International des Sciences de la Vigne et du Vin* 37: 103–116.

Dujesiefken D., Stobbe H., 2002. The Hamburg Tree Pruning System–A framework for pruning of individual trees. *Urban Forestry & Urban Greening* 1: 75–82.

Dumot V., 2019. *Effets et limites des pratiques viticoles sur les maladies du bois*. Paper presented at the 4èmes Assises des Vins du Sud-Ouest, 24/01/2019, 61–63.

Edwards J., Pascoe I.G., Salib S., 2007. Impairment of grapevine xylem function by *Phaeomoniella chlamydospora* infection is due to more than physical blockage of vessels with goo. *Phytopathologia Mediterranea* 46: 87–90.

Eisner N.J., Gilman E.F., Grabosky J.C., 2002. Branch morphology impacts compartmentalization of pruning wounds. *Journal of Arboriculture* 28: 99–105.

Elena G., Bruez E., Rey P., Luque J., 2019. Microbiota of grapevine woody tissues with or without esca-foliar symptoms in northeast Spain. *Phytopathologia Mediterranea* 57: 425–438.

Eskalen A., Gubler W.D., Khan A., 2001. Rootstock Susceptibility to «*Phaeomoniella chlamydospora*» and «*Phaeoacremonium*» spp. *Phytopathologia Mediterranea* 40: 433–438.

Feliciano A.J., Gubler W.D., 2001. Histological Investigations on Infection of Grape Roots and Shoots by «*Phaeoacremonium*» spp. *Phytopathologia Mediterranea* 40: 387–393.

Feliciano A.J., Eskalen A., Gubler W.D., 2004. Differential susceptibility of three grapevine cultivars to *Phaeomoniella chlamydospora* in California. *Phytopathologia Mediterranea* 43: 66–69.

Fischer M., Kassemeyer H.H., 2012. Water regime and its possible impact on expression of Esca symptoms in *Vitis vinifera*: growth characters and symptoms in the greenhouse after artificial infection with *Phaeomoniella chlamydospora*. *Vitis-Journal of Grapevine Research* 51: 129.

Fischer M., Peighami-Ashnaei S., 2019. Grapevine, esca complex, and environment: the disease triangle. *Phytopathologia Mediterranea* 58: 17–37.

Fleurat-Lessard P., Luini E., Berjeaud J.M., Roblin G., 2010. Diagnosis of grapevine esca disease by immunological detection of *Phaeomoniella chlamydospora*. *Australian Journal of Grape and Wine Research* 16: 455–463.

Fleurat-Lessard P., Luini E., Berjeaud J.-M., Roblin G., 2014. Immunological detection of *Phaeoacremonium aleophilum*, a fungal pathogen found in esca disease. *European Journal of Plant Pathology* 139: 137–150.

Fontaine F., Pinto C., Vallet J., Clément C., Gomes A.C., Spagnolo A., 2016. The effects of grapevine trunk diseases (GTDs) on vine physiology. *European Journal of Plant Pathology* 144: 707–721.

Fournioux J.C., Adrian M., 2011. *Morphologie et anatomie de la vigne*, Edition Féret, 144 pp.

Galet P., 1977. Apoplexie. In *Les Maladies et les Parasites de la Vigne Tome I. Les Maladies dues à des Végétaux*. Montpellier, France: Imprimerie du Paysan du Midi, 409–430.

Gómez P., Báidez A.G., Ortuño A., Del Río J.A., 2016. Grapevine xylem response to fungi involved in trunk diseases. *Annals of Applied Biology* 169: 116–124.

Goodsman D.W., Lusebrink I., Landhäusser S.M., Erbilgin N., Lieffers V.J., 2013. Variation in carbon availability, defence chemistry and susceptibility to fungal invasion along the stems of mature trees. *New Phytologist* 197: 586–594.

Gramaje D., Armengol J., 2011. Fungal trunk pathogens in the grapevine propagation process: potential inoculum sources, detection, identification, and management strategies. *Plant Disease* 95: 1040–1055.

Gramaje D., Di Marco S., 2015. Identifying practices likely to have impacts on grapevine trunk disease infections: a European nursery survey. *Phytopathologia Mediterranea* 54: 313–324.

Gramaje D., Úrbez-Torres J.R., Sosnowski M. R., 2018. Managing grapevine trunk diseases with respect to etiology and epidemiology: current strategies and future prospects. *Plant Disease* 102: 12–39.

Grechi I., Vivin P., Hilbert G., Milin S., Robert T., Gaudillère J.-P., 2007. Effect of light and nitrogen supply on internal C:N balance and control of root-to-shoot biomass allocation in grapevine. *Environmental and Experimental Botany* 59: 139–149.

Grosclaude C., 1993. Pathologie des blessures mettant à nu le bois chez les végétaux ligneux. *Agronomie* 13: 441–456.

Grosman J., Doublet B., 2012. Maladies du bois de la vigne: synthèse des dispositifs d'observation au vignoble, de l'observatoire 2003–2008 au réseau d'épidémiosurveillance actuel. *Phytoma-La Défense des Végétaux* 651: 31–35.

Guan X., Essakhi S., Laloue H., Nick P., Bertsch C., Chong J., 2016. Mining new resources for grape resistance against *Botryosphaeriaceae*: a focus on *Vitis vinifera* subsp. *sylvestris*. *Plant Pathology* 65: 273–284.

Guérard N., Maillard P., Bréchet C., Lieutier F., Dreyer E., 2007. Do trees use reserve or newly assimilated carbon for their defence reactions? A 13C labeling approach with young Scots pines inoculated with a bark-beetle-associated fungus (*Ophiostoma brunneo ciliatum*). *Annals of Forest Science* 64: 601–608.

Guérin-Dubrana L., Labenne A., Labrousse J.C., Bastien S., Rey P., Gégout-Petit A., 2012. Statistical analysis of grapevine mortality associated with esca or eutypa dieback foliar expression. *Phytopathologia Mediterranea* 52: 276–288.

Guérin-Dubrana L., Fontaine F., Mugnai L., 2019. Grapevine trunk disease in European and Mediterranean vineyards: occurrence, distribution and associated disease-affecting cultural factors *Phytopathologia Mediterranea* 58: 49–71.

Hofstetter V., Buyck B., Croll D., Viret O., Couloux A., Gindro K., 2012. What if esca disease of grapevine were not a fungal disease? *Fungal Diversity* 54: 51–67.

Kuntzmann P., Villaume S., Larignon P., Bertsch C., 2010. Esca, BDA and Eutypiosis: foliar symptoms, trunk lesions and fungi observed in diseased vinestocks in two vineyards in Alsace. *Vitis-Journal of Grapevine Research* 49: 71–76.

Lacointe A., 2000. Carbon allocation among tree organs: a review of basic processes and representation in functional-structural tree models. *Annals of Forest Science* 57: 521–533.

Lafon R., 1921. *Modifications à apporter à la taille de la vigne des Charentes, taille Guyot-Poussart mixte et double: l'apoplexie, traitement préventif (méthode Poussard), traitement curatif*, Roumégous et Déhan, 93 pp.

Lamanda N., Roux S., Delmotte S., Merot A., Rapidel B., … Wery J., 2012. A protocol for the conceptualisation of an agro-ecosystem to guide data acquisition and analysis and expert knowledge integration. *European Journal of Agronomy* 38: 104–116.

Lambert C., Khiook I.L.K., Lucas S., Télef-Micouleau N., Mérillon J.-M., Cluzet S., 2013. A faster and a stronger defence response: one of the key elements in

grapevine explaining its lower level of susceptibility to Esca? *Phytopathology* 103: 1028–1034.

Landi L., Murolo S., Gianfranco R., 2012. Colonization of *Vitis* spp. Wood by sGFP-Transformed *Phaeomoniella chlamydospora*, a Tracheomycotic Fungus Involved in Esca Disease. *Phytopathology* 102: 290–297.

Larignon P., 1990. *Contribution à de l'Esca de la vigne: identification des champignons responsables et étude de leur mode d'action.* PhD Thesis, University of Bordeaux II, Bordeaux, France, 238 pp.

Larignon P., 2004. Réflexions sur l'esca: Ce que l'on sait déjà montre qu'il en reste beaucoup à apprendre: Vigne. *Phytoma-La Défense des Végétaux* 576: 28–31.

Larignon P., 2009. Y a-t-il un lien entre climat et expression du Black Dead Arm?: Identification des facteurs climatiques favorisant l'expression des symptômes. *Phytoma-La Défense des végétaux* 628: 27–29.

Larignon P., 2010. Dépérissement de jeunes plantes: Des symptômes liés au champignon *Neofusicoccum parvum* déjà connu comme lié au black dead arm sur vignes adultes. *Phytoma-La Défense des végétaux* 635: 41–46.

Larignon P., 2011. Vigne, de nouvelles connaissances sur les maladies du bois: Éléments inédits sur la biologie de deux champignons associés, *P. aleophilum* et *D. seriata*. *Phytoma-La Défense des végétaux* 646: 41–44.

Larignon P., 2016. Maladies cryptogamiques du bois de la vigne: symptomatologie et agents pathogènes (Vol. 2ème édition, pp. 168pp). http://vignevin.com.

Larignon P., 2017. Effect of sodium arsenite on the life cycles of the pathogenic agents involved in wood grapevine diseases. *Phytopathologia Mediterranea* 56: 537.

Larignon P., Dubos B., 1997. Fungi associated with esca disease in grapevine. *European Journal of Plant Pathology* 103: 147–157.

Larignon P., Gramaje D., 2015. *Life cycle of pathogens*. Paper presented at the Abstracts of oral and poster presentation given at the first COST Action FA 1303 workshop on Grapevine Trunk Diseases, Cognac, France, 23–24 June 2015, 420–436.

Larignon P., Fontaine F., Farine S., Clément C., Bertsch C., 2009a. Esca et Black Dead Arm: deux acteurs majeurs des maladies du bois chez la Vigne. *Comptes rendus de l'Académie des Sciences- BIOLOGIES* 332: 765–783.

Larignon P., Coarer M., Girardon K., Berud F., Jacquet O., 2009b. Propagation of pioneer fungi associated with esca disease by vegetative material in French grapevine nurseries. *Phytopathologia Mediterranea* 48: 177.

Laveau C., Mary S., Roby J.-P., 2015. *Impact du porte-greffe sur l'expression des symptômes foliaires de l'esca*. Paper presented at the Les maladies du Bois de la Vigne- Réunion du groupe national Maladies du Bois de la Vigne, Colmar, 17&18/11/2015.

Lebon G., Wojnarowiez G., Holzapfel B., Fontaine F., Vaillant-Gaveau N., Clément C., 2008. Sugars and flowering in the grapevine (*Vitis vinifera* L.). *Journal of Experimental Botany* 59: 2565–2578.

Lecomte P., Leyo M., Louvet G., Corio-Costet M.F., Gaudillere J., Blancard D., 2005. Développement des symptômes de Black Dead Arm: un lien avec la rupture des trajets de sève. *Le Progrès agricole et viticole* 122: 307–316.

Lecomte P., Darrieutort G., Laveau C., Louvet G., Goutouly J.P., … Guérin-Dubrana L., 2011. *Impact of biotic and abiotic factors on the development of esca decline disease*. Paper presented at the «Integrated Protection and Production in Viticulture», 171–180.

Lecomte P., Darrieutort G., Liminana J.M., Comont G., Muruamendiaraz A., … Fermaud M., 2012. New insights into esca of grapevine: the development of foliar symptoms and their association with xylem discoloration. *Plant Disease* 96: 924–934.

Lecomte P., Darrieutort G., Liminana J.M., Comont G., Muruamendiaraz A., … Fermaud M., 2014. Spécial Esca de la Vigne. *Phytoma-La Défense des Végétaux, Supplément* 674: 22 p.

Lecomte P., Diarra B., Carbonneau A., Patrice R., Chevrier C., 2019. Esca of grapevine and training practices in France: results of a 10-year survey. *Phytopathologia Mediterranea* 57: 472–487.

Lecomte P., Diarra B., Chevrier C., Carbonneau A., 2015. *Esca of grapevine and training system*. Paper presented at the 19th International Meeting of Viticulture GiESCO, Pech Rouge - Montpellier, 31 May - 5 June 2015, 356–361.

Letousey P., Baillieul F., Perrot G., Rabenoelina F., Boulay M., … Fontaine F., 2010. Early events prior to visual symptoms in the apoplectic form of grapevine esca disease. *Phytopathology* 100: 424–431.

Liminana J.-M., Pacreau G., Boureau F., Menard E., David S., … Dumot V., 2009. Inner necrosis in grapevine rootstock mother plants in the Cognac area (Charentes, France). *Phytopathologia Mediterranea* 48: 92–100.

Lovisolo C., Perrone I., Hartung W., Schubert A., 2008. An abscisic acid-related reduced transpiration promotes gradual embolism repair when grapevines are rehydrated after drought. *New Phytologist* 180: 642–651.

Magnin-Robert M., Spagnolo A., Alayi T.D., Cilindre C., Mercier L., … Fontaine F., 2014. Proteomic insights into changes in grapevine wood in response to esca

proper and apoplexy. *Phytopathologia Mediterranea* 53: 168–187.

Magnin-Robert M., Adrian M., Trouvelot S., Spagnolo A., Jacquens L., … Clément C., 2017. Alterations in grapevine leaf metabolism occur prior to esca apoplexy appearance. *Molecular Plant-Microbe Interactions* 30: 946–959.

Maher N., Piot J., Bastien S., Vallance J., Rey P., Guérin-Dubrana L., 2012. Wood necrosis in esca-affected vines: types, relationships and possible links with foliar symptom expression. *Journal International des Sciences de la Vigne et du Vin* 46: 15–27.

Marchi G., 2001. Susceptibility to esca of various grapevine («*Vitis vinifera*») cultivars grafted on different rootstock in a vineyard in the Province of Siena (Italy). *Phytopathologia Mediterranea* 40: 27–36.

Marchi G., Peduto F., Mugnai L., Di Marco S., Calzarano F., Surico G., 2006. Some observations on the relationship of manifest and hidden esca to rainfall. *Phytopathologia Mediterranea* 45: 117–126.

Martin N., Vesentini D., Rego C., Monteiro S., Oliveira H., Ferreira R. B., 2009. *Phaeomoniella chlamydospora* infection induces changes in phenolic compounds content in *Vitis vinifera*. *Phytopathologia Mediterranea* 48: 101–116.

Martos S., Andolfi A., Luque J., Mugnai L., Surico G., Evidente A., 2008. Production of phytotoxic metabolites by five species of *Botryosphaeriaceae* causing decline on grapevines, with special interest in the species *Neofusicoccum luteum* and *N. parvum*. *European Journal of Plant Pathology* 121: 451–461.

McArtney S.J., Ferree D.C., 1999. Shading effects on dry matter partitioning, remobilization of stored reserves and early season vegetative development of grapevines in the year after treatment. *Journal of the American Society for Horticultural Science* 124: 591–597.

McDowell N.G., 2011. Mechanisms linking drought, hydraulics, carbon metabolism, and vegetation mortality. *Plant Physiology* 155: 1051–1059.

Molot B., Larignon P., Coarer M., 2006. *Black dead arm. De nouvelles pistes*. Paper presented at the Colloque Mondiaviti, Bordeaux, 29–30 novembre 2006, 15–17.

Mondello V., Songy A., Battiston E., Pinto C., Coppin C., … Fontaine F., 2018. Grapevine trunk diseases: a review of fifteen years of trials for their control with chemicals and biocontrol agents. *Plant Disease* 102: 1189–1217.

Mondello V., Larignon P., Armengol J., Kortekamp A., Vaczy K., … Fontaine F., 2019. Management of grapevine trunk diseases: knowledge transfer, current strategies and innovative strategies adopted in Europe. *Phytopathologia Mediterranea* 57: 369–383.

Moret F., Lemaître-Guillier C., Grosjean C., Clément G., Coelho C., … Adrian M., 2019. Clone-Dependent Expression of Esca Disease Revealed by Leaf Metabolite Analysis. *Frontiers in Plant Science* 9: 1–12.

Morvan G., Grosjean C., Petitot P., Dureuil J., 2011. Lettre Maladies du Bois n°2,8 pp.

Morvan G., Grosjean C., Petitot P., Dureuil J., 2012. Vrai/Faux: l'ébourgeonnage favorise t il l'esca? *Lettre Maladies du Bois* 3: 1–2.

Mugnai L., Graniti A., Surico G., 1999. Esca (black measles) and brown wood-streaking: two old and elusive diseases of grapevines. *Plant Disease* 83: 404–418.

Murolo S., Romanazzi G., 2014. Effects of grapevine cultivar, rootstock and clone on esca disease. *Australasian Plant Pathology* 43: 215–221.

Mutawila C., Fourie P.H., Haleen F., Mostert L., 2011. Histo-pathology study of the growth of *Trichoderma harzianum*, *Phaeomoniella chiamydospora* and *Eutypa lata* on grapevine pruning wounds. *Phytopathologia Mediterranea* 50 (Supplement): S46–S60.

Oliva J., Stenlid J., Martínez-Vilalta J., 2014. The effect of fungal pathogens on the water and carbon economy of trees: implications for drought-induced mortality. *New Phytologist* 203: 1028–1035.

Oliveira H., Freitas R., Rego C., Ferreira R.B., 2009. Interactions among grapevine disease-causing fungi. The role of reactive oxygen species. *Phytopathologia Mediterranea* 48: 117–127.

Osti F., Di Marco S., 2010. Iron-dependant, non enzymatic processes promoted by *Phaeomoniella chlamydospora* and *Phaeoacremonium aleophilum*, agents of esca in grapevine. *Physiological and Molecular Plant Pathology* 74: 309–316.

Pearce R.B., 1996. Antimicrobial defences in the wood of living trees. *New Phytologist* 132: 203–233.

Pearce R.B., 2000. Decay development and its restriction in trees. *Journal of Arboriculture* 26: 1–11.

Pellegrino A., Gozé E., Lebon E., Wery J., 2006. A model-based diagnosis tool to evaluate the water stress experienced by grapevine in field sites. *European Journal of Agronomy* 25: 49–59.

Péros J.P., 1995. Sensibilité des cepages à l'eutypiose: le problème du comportement de référence au vignoble. *Progrès Agricole et Viticole* 112: 61–67.

Petit A.N., Vaillant N., Boulay M., Clément C., Fontaine F., 2006. Alteration of photosynthesis in grapevines affected by esca. *Phytopathology* 96: 1060–1066.

Pierron R., 2015. *Esca et vigne: compréhension des mécanismes de défense précoces du bois de la vigne Vitis vinifera L. suite à la maladie, colonisation des champignons in planta et proposition de moyens de lutte*

pour une viticulture durable. PhD Thesis, University of Toulouse, Toulouse, France, 228 pp.

Pinto C., Pinho D., Sousa S., Pinheiro M., Egas C., C. Gomes A., 2014. Unravelling the diversity of grapevine microbiome. *PLoS ONE* 9: e85622.

Piou D., Nageleisen L.M., Desprez-Loustau M.L., Candau J.N., 2006. Les risques sanitaires consécutifs à 2003 à la lumière de la littérature. *RDV techniques* 11: 28–34.

Pontini S., Fleurat-Lessard P., Béré E., Berjeaud J.-M., Roblin G., 2014. Impact of temperature variations on toxic effects of the polypeptides secreted by *Phaeoacremonium aleophilum*. *Physiological and Molecular Plant Pathology* 87: 51–58.

Pouzoulet J., 2012. *Développement d'une méthodologie PCR en temps réel pour la détection et la quantification in planta des principaux champignons pathogènes associés aux maladies du bois de la vigne.* PhD Thesis, University of Toulouse, Toulouse, France, 176 pp.

Pouzoulet J., Jacques A., Besson X., Dayde J., Mailhac N.H., 2013. Histopathological study of response of *Vitis vinifera* cv. Cabernet Sauvignon to bark and wood injury with and without inoculation by *Phaeomoniella chlamydospora*. *Phytopathologia Mediterranea* 52: 313–323.

Pouzoulet J., Pivovaroff A.L., Santiago L.S.,,Rolshausen P.E., 2014. Can vessel dimension explain tolerance toward fungal vascular wilt diseases in woody plants? Lessons from Dutch elm disease and esca disease in grapevine. *Frontiers in Plant Science* 5: 1–11.

Reis P., Alves A., Fontaine F., Lourenço I., Saramago J., Rego C., 2019. Early season symptoms on grapevine stem and inflorescences associated with *Botryosphaeriacea* species. *Phytopathologia Mediterranea* 58: 398-399.

Reis P., Magnin-Robert M., Nascimento T., Spagnolo A., Abou-Mansour E., … Fontaine F., 2016. Reproducing *Botryosphaeria* dieback foliar symptoms in a simple model system. *Plant Disease* 100: 1071–1079.

Rey P., Lecomte P., Guérin-Dubrana L., Corio-Costet M.-F., Fontaine F., … de la Roque B., 2011. Maladies du bois de la vigne situation, enjeux et perspective. *Phytoma-La Défense des Végétaux* 640: 22–26.

Rolshausen P.E., Greve L.C., Labavitch J.M., Mahoney N.E., Molyneux R.J., Gubler W.D., 2008. Pathogenesis of *Eutypa lata* in grapevine: identification of virulence factors and biochemical characterization of cordon dieback. *Phytopathology* 98: 222–229.

Rudelle J., Octave S., Kaid-Harche M., Roblin G., Fleurat-Lessard P., 2005. Structural modifications induced by *Eutypa lata* in the xylem of trunk and canes of *Vitis vinifera*. *Functional Plant Biology* 32: 537–547.

Schoeneweiss D.F., 1981. Infectious diseases of trees associated with water and freezing stress. *Journal of arboriculture* 7: 13–19.

Schwarze F.W.M.R., Baum S., 2000. Mechanisms of reaction zone penetration by decay fungi in wood of beech (*Fagus sylvatica*). *New Phytologist* 146: 129–140.

Shain L., 1971. The response of sapwood of Norway spruce to infection by *Fomes annosus*. *Phytopathology* 61: 301–307.

Shani U., Waisel Y., Eshel A., Xue S., Ziv G., 1993. Responses to salinity of grapevine plants with split root systems. *New Phytologist* 124: 695–701.

Shigo A.L., 1979. Tree decay an expanded concept. United States Department of Agriculture Forest Service. Agriculture information Bulletin number 419 (Avril 1979).

Silpi U., Lacointe A., Kasempsap P., Thanysawanyangkura S., Chantuma P., … Thaler P., 2007. Carbohydrate reserves as a competing sink: evidence from tapping rubber trees. *Tree Physiology* 27: 881–889.

Simonit M., Deledda F., Giudici M., Manfreda L., Ostan M., … Zanutta A., 2012. Potatura ramificata della vite *L'Informatore agrario* 35-46..

Smith K.T., 2015. Compartmentalization, resource allocation, and wood quality. *Current Forestry Reports* 1: 8–15.

Songy A., Fernandez O., Clément C., Larignon P., Fontaine F., 2019. Grapevine trunk diseases under thermal and water stresses. *Planta* 249: 1655–1679.

Sosnowski M.R., Lardner R., Wicks T., Scott E.S., 2007. The influence of grapevine cultivar and isolate of *Eutypa lata* on wood and foliar symptoms. *Plant Disease* 91: 924–931.

Sosnowski M.R., Luque J., Loschiavo A., Martos S., Garcia-Figueres F., … Scott E., 2011. Studies on the effect of water and temperature stress on grapevines inoculated with *Eutypa lata*. *Phytopathologia Mediterranea* 50: 127–138.

Spagnolo A., Marchi G., Peduto F., Phillips A.J., Surico G., 2011. Detection of *Botryosphaeriaceae* species within grapevine woody tissues by nested PCR, with particular emphasis on the *Neofusicoccum parvum*/*N. ribis* complex. *European Journal of Plant Pathology* 129: 485–500.

Spagnolo A., Magnin-Robert M., Alayi T.D., Cilindre C., Mercier L., … Fontaine F., 2012. Physiological changes in green stems of *Vitis vinifera* L. cv. Chardonnay in response to esca proper and apoplexy revealed by proteomic and transcriptomic analyses. *Journal of Proteome Research* 11: 461–475.

Spagnolo A., Larignon P., Magnin-Robert M., Hovasse A., Cilindre C., … Fontaine F., 2014a. Flowering as the

most highly sensitive period of grapevine (*Vitis vinifera* L. cv Mourvèdre) to the *Botryosphaeria* dieback agents *Neofusicoccum parvum* and *Diplodia seriata* infection. *International Journal of Molecular Sciences* 15: 9644–9669.

Spagnolo A., Magnin-Robert M., Alayi T.D., Cilindre C., Schaeffer-Reiss C., … Fontaine F., 2014b. Differential responses of three grapevine cultivars to *Botryosphaeria* dieback. *Phytopathology* 104: 1021–1035.

Spagnolo A., Wu H., Chollet J.F., Clément C., Fontaine F., 2015. *Maladies du bois de la vigne: mise au point d'un modèle simplifié en vue de tester des moyens de lutte*. Paper presented at the Les maladies du Bois de la vigne, Colmar, 17 et 18/11/15, 48.

Spagnolo A., Mondello V., Larignon P., Villaume S., Rabenoelina F., … Fontaine F., 2017. Defence responses in grapevine (cv. Mourvèdre) after inoculation with the *Botryosphaeria* dieback pathogens *Neofusicoccum parvum* and *Diplodia seriata* and their relationship with flowering. *International Journal of Molecular Sciences* 18: 393.

Sparapano L., Bruno G., Graniti A., 2000. Effects on plants of metabolites produced in culture by *Phaeoacremonium chlamydosporum*, *P. aleophilum* and *Fomitiporia punctata*. *Phytopathologia Mediterranea* 39: 169–177.

Sparapano L., Graniti A., Bruno G., 2001. Three-year observation of grapevines cross-inoculated with esca-associated fungi. *Phytopathologia Mediterranea* 40: 376–386.

Stamp N., 2003. Out of the quagmire of plant defence hypotheses. *The Quarterly Review of Biology* 78: 23–55.

Surico G., 2009. Towards a redefinition of the diseases within the esca complex of grapevine. *Phytopathologia Mediterranea* 48: 5–10.

Surico G., Marchi G., Mugnai L., Braccini P., 2000. Epidemiology of esca in some vineyards in Tuscany (Italy). *Phytopathologia Mediterranea* 39: 190–205.

Surico G., Marchi G., Mugnai L., D'Ovidio R., Roberti S., 2001. Pectic Enzymes Production by «*Phaeomoniella chlamydospora*». *Phytopathologia Mediterranea* 40: 407–416.

Surico G., Mugnai L., Marchi G., 2006. Older and more recent observations on esca: a critical overview. *Phytopathologia Mediterranea* 45: 68–86.

Thibault M., 2015. *Le curetage*. Paper presented at the Les maladies du Bois de la Vigne- Réunion du groupe national Maladies du Bois de la Vigne, Colmar, 17–18/11/2015.

Travadon R., Lecomte P., Diarra B., Lawrence D.P., Renault D., … Baumgartner K., 2016. Grapevine pruning systems and cultivars influence the diversity of wood-colonizing fungi. *Fungal Ecology* 24: 82–93.

Troccoli L., Mori B., Surico G., Mugnai L., Calamassi R., 2001. «*Phaeomoniella chlamydospora*»-Grapevine interaction: histochemical reactions to fungal infection. *Phytopathologia Mediterranea* 40: 400–406.

Tyree M.T., Sperry J.S., 1989. Vulnerability of xylem to cavitation and embolism. *Annual Review of Plant Biology* 40: 19–36.

Úrbez-Torres J.R., 2011. The status of *Botryosphaeriaceae* species infecting grapevines. *Phytopathologia Mediterranea* 50 (Supplement): S5–S45.

Úrbez-Torres J.R., Haag P., Bowen P., O'Gorman D.T., 2014. Grapevine trunk diseases in British Columbia: incidence and characterization of the fungal pathogens associated with esca and petri diseases of grapevine. *Plant Disease* 98: 469–482.

Valtaud C., Larignon P., Roblin G., Fleurat-Lessard P., 2009. Developmental and ultrastructural features of *Phaeomoniella chlamydospora* and *Phaeoacremonium aleophilum* in relation to xylem degradation in esca disease of the grapevine. *Journal of Plant Pathology* 91: 37–51.

Valtaud C., Thibault F., Larignon P., Bertsch C., Fleurat-Lessard P., Bourbouloux A., 2011. Systemic damage in leaf metabolism caused by esca infection in grapevines. *Australian Journal of Grape and Wine Research* 17: 101–110.

van Niekerk J., Fourie P.H., Hallenn F., Crous P., 2006. *Botryosphaeria* spp. as grapevine trunk disease pathogens. *Phytopathologia Mediterranea* 45: 43–54.

van Niekerk J., Strever A.E., Du Toit G.P., Halleen F., Fourie P.H., 2011. Influence of water stress on *Botryosphaeriaceae* disease expression in grapevines. *Phytopathologia Mediterranea* 50: 151–165.

Vigues V., Serrano E., Dumas C., Coarer M., Yobregat O., Larignon P., 2007. Les maladies du bois peuvent commencer en pépinières: Contaminations des plants de vignes par les champignons associés aux maladies du bois, une enquête en Midi-Pyrénées. *Phytoma-La Défense des Végétaux* 609: 20–23.

Vigues V., Yobregat O., Mille B., Berud F., Ayme-Sevenier V., … Larignon P., 2012. Maladie du bois, gros plan sur les greffons et porte-greffes en entrée de pépinière. *Phytoma-La Défense des végétaux* 658: 26–28.

Vigues V., Yobregat O., Barthélémy B., Dias F., Coarer M., Philippe L., 2013. Les champignons associés aux Maladies du Bois: identification des étapes à risque en pépinière. In: *Vignevin Sud Ouest* (Ed.), pp. 2.

Viiri H., Niemelä P., Kitunen V., Annila E., 2001. Soluble carbohydrates, radial growth and vigour of fertilized

Norway spruce after inoculation with blue-stain fungus, *Ceratocystis polonica*. *Trees* 15: 327–334.

Wagschal I., Abou-Mansour E., Petit A.N., Clément C., Fontaine F. 2008. Wood diseases of grapevine: a review on eutypa dieback and esca. In: *Plant-Microbe interactions. Research signpost* (Ait-Barka E., Clément C., ed.), 367–391.

Wargo P.M., 1996. Consequences of environmental stress on oak: predisposition to pathogens. *Annals of Forest Science* 53: 359–368.

Yacoub A., Gerbore J., Magnin N., Chambon P., Dufour M.-C., … Rey P., 2016. Ability of *Pythium oligandrum* strains to protect *Vitis vinifera* L., by inducing plant resistance against *Phaeomoniella chlamydospora*, a pathogen involved in Esca, a grapevine trunk disease. *Biological Control* 92: 7–16.

Yadeta K.A., Thomma B.P., 2013. The xylem as battleground for plant hosts and vascular wilt pathogens. *Frontiers in Plant Science* 4: 1–12.

Yobregat O., Larignon P., Mille B., Bloy P., Carcenac D., … Charlot S., 2018. *Etude de la cinétique de contamination de jeunes plants par les champignons responsables des maladies du bois*. Paper presented at the V'innoDAY 2018, Toulouse, France, 11 janvier 2018, 21–25.

Yobregat O., Abidon C., 2019. *Le curetage des souches: résultats récents pour une technique ancienne*. Paper presented at the 4èmes assises des vins du Sud-Ouest, France, 24 janvier 2019, 55–59.

Zufferey V., Cochard H., Ameglio T., Spring J.L., Viret O., 2011. Diurnal cycles of embolism formation and repair in petioles of grapevine (*Vitis vinifera* cv. Chasselas). *Journal of Experimental Botany* 62: 3885–3894.

Phytopathologia Mediterranea
The international journal of the
Mediterranean Phytopathological Union

Firenze University Press
www.fupress.com/pm

Research Paper

Identification of phytoplasma strains associated with witches' broom and yellowing in *Ziziphus jujube* nurseries in Iran

Ghobad BABAEI[1,*], Seyyed Alireza ESMAEILZADEH-HOSSEINI[2], Mahbobeh ZANDIAN[1], Vahid NIKBAKHT[3]

[1] *Plant Protection Research Department, Chaharmahal and Bakhtiari Agricultural and Natural Resources Research and Education Center, AREEO, Shahrekord, Iran*
[2] *Plant Protection Research Departments, Yazd Agricultural and Natural Resources Research and Education Center, AREEO, Yazd, Iran*
[3] *Chaharmahal and Bakhtiari Agricultural Organization, Shahrekord, Iran*
*Corresponding author: ghobad.babaee@gmail.com

Summary. Phytoplasma symptoms, including proliferation, witches' broom, leaf rolling and yellowing, were observed in jujube (*Ziziphus jujube*) nurseries in the East of Iran. Total nucleic acid was extracted from symptomatic and symptomless plants, and was tested for phytoplasma presence using nested PCR. Amplicons of about 1.8 kb (primer pair P1/P7) and 1.25 kb (R16F2n/R16R2) were obtained from all symptomatic plants but not from symptomless plants. Restriction fragment length polymorphism (RFLP) analysis of R16F2n/R2 amplicons using *Kpn*I, *Hae*III, *Rsa*I, *Alu*I, *Hpa*II, *Hha*I, *Taq*I, *Mse*I, *Bfa*I and *Tha*I restriction enzymes showed two RFLP patterns referable to 16SrI and 16SrVI phytoplasma groups. The consensus sequences of *Z. jujube* yellowing and witches' broom of six samples correspond to '*Candidatus* Phytoplasma asteris' and '*Candidatus* Phytoplasma trifolii'-related strains. Two R16F2n/R16R2 16S rDNA sequences representative of each RFLP profile, one each from witches' broom (accession number MK379605) and yellowing (MK379604) host symptoms, were submitted to the GenBank. Phylogenetic analysis confirmed that the phytoplasma strains associated with jujube yellowing clustered within the 16SrI phytoplasma clade, and those associated with witches' broom clustered within the 16SrVI clade. Restriction analysis confirmed that virtual RFLP patterns of the jujube yellowing and witches' broom phytoplasma strains were identical to the reference pattern of 16SrI-B and 16SrVI-A. This is the first report of these phytoplasma strains associations with witches' broom and yellowing in jujube plants.

Keywords. Aster yellows phytoplasma, clover proliferation phytoplasma, jujube.

OPEN ACCESS

Citation: G. Babaei, S.A. Esmaeilzadeh-Hosseini, M. Zandian, V. Nikbakht (2020) Identification of phytoplasma strains associated with witches' broom and yellowing in *Ziziphus jujube* nurseries in Iran. *Phytopathologia Mediterranea* 59(1): 55-61. doi: 10.14601/Phyto-10857

Accepted: December 6, 2019

Published: April 30, 2020

Data Availability Statement: All relevant data are within the paper and its Supporting Information files.

Competing Interests: The Author(s) declare(s) no conflict of interest.

Editor: Assunta Bertaccini, Alma Mater Studiorum, University of Bologna, Italy.

INTRODUCTION

Jujube (*Ziziphus jujube* Mill) is a small shrub or tree with small fruits about in the size of date, that is native to southern and central Asia and is grown in the northeast and central parts of Iran. Jujube has different cultivars, the fruit is used as food, and the plants can be used as a vegetable and for medicinal purposes.

Jujube witches' broom (JWB) was first reported as a graft transmissible disease (Kim, 1965), as phyllody, lack of fruit production and dieback in China (La and Woo, 1980). The disease symptoms included little leaf, phyllody and leaf yellowing, and the disease is a severe production-limiting factor, distributed in all Asian countries including China, Korea and Japan. Yield losses up to of 80% have been reported, and rapid tree death can result (Tsai *et al*., 1988; Lee, 1988; Ohashi *et al*., 1996).

Phytoplasma agents associated with JWB belong to subgroup 16SrV-B, and showed the same 16S ribosomal sequence in China and Korean strains (Zhu *et al*., 1998; Han and Cha, 2002). This phytoplasma had been described as '*Candidatus* Phytoplasma ziziphi' (Jung *et al*., 2003), and it is transmitted by the leafhoppers *Hishimonoides chinensis* and *H. sellatus* (La and Woo, 1980). Jujube trees with symptoms of proliferation, yellowing and witches' broom were reported from *Z. jujube* and *Z. nummularia* in India, and were associated with '*Ca*. P. ziziphi'-related strains (Khan *et al*., 2008). Mixed infections of jujube by two phytoplasmas of groups of 16SrI and 16SrV-B were reported in Korea (Lee *et al*., 2009).

The aim of the present study was to assess the presence of phytoplasmas in diseased jujube, and to identify the phytoplasma strains associated with proliferation, witches' broom and yellowing in jujube nurseries in the Eastern part of Iran. This information was required to plan appropriate disease management strategies.

MATERIALS AND METHODS

Plant sampling

During surveys in 2017 in the Razavi Khorasan Province in eastern Iran, witches' broom, proliferation, leaf rolling and yellowing symptoms (Figure 1) were observed in jujube nursery plants, and 22 symptomatic and four asymptomatic jujube plants were sampled and subjected to molecular analyses for phytoplasma detection and identification.

DNA extraction and nested PCR amplification

Total DNA was extracted from 0.2 g of midrib tissue of fresh leaves from symptomatic and symptomless *Z. jujube* nursery plants, following the procedure described by Li *et al*. (2005). Midrib tissue samples were ground in liquid nitrogen and homogenized in 3M CTAB buffer. After chlorophorm/isoamyl alcohol (24: 1) treatment, the aqueus phase was mixed with 5M NaCl and maintained for 1 h at -20°C. After precipitation by centrigufation, the resulting pellet was washed with 70% etanol, and the final DNA pellet was dissolved in 100 µL of sterilized water. The total DNA extracted from *Prunus persica* yellowing and decline in Iran ('*Ca*. P. omanense'-related strain) (Esmailzadeh Hosseini *et al*., 2017b) was used as positive control. The DNA quality and concentration were estimated by spectrophotometer and agarose gel electrophoresis, and 100 ng of nucleic acids was used for each PCR reaction with universal primer pair P1/P7 (Deng and Hiruki, 1991; Schneider *et al*., 1995) to amplify parts of the rRNA operon. This included the 16S rRNA gene, 16S-23S rRNA spacer region (SR) and the 5' end of the 23S rRNA gene. The amplified products (1 µL) were diluted in 30 µL with sterile deionized water, and 1 µL of the resulting solution was used as template in nested PCR with the primer pair R16F2n/R16R2 (Gundersen and Lee, 1996). The PCR reactions were performed in 50 µL mixtures containing 0.4 µM of each primer, with EmeraldAmp PCR master mix (Takara). The reaction cycled 30 times in a programmable thermocycler (QuantaBiotech), with the following parameters: denaturation for 30 sec at 94°C (2 min in the first round), annealing for 30 sec at 55°C and primer extension for 1 min at 72°C (10 min in the final cycle). The PCR conditions for the nested PCR reaction were the same except that the annealing temperature was 58°C. Five µL of each reaction mixture were analyzed by electrophoresis in a 1% (w/v) agarose gel in TBE 1X buffer and visualized with a UV imaging system (Isogen Life Science) after ethidium bromide staining. The sizes of the PCR products were estimated by comparison with a 100 bp DNA ladder (Biobasic).

Restriction fragment length polymorphism analyses

Restriction fragment length polymorphism (RFLP) analyses of R16F2n/R16R2 amplicons, using *Kpn*I, *Hae*III, *Rsa*I, *Alu*I, *Hpa*II, *Hha*I, *Taq*I, *Mse*I, *Bfa*I and *Tha*I restriction enzymes, were performed according to the instructions of the manufacturer (Thermo). The restriction products were then separated by electrophoresis through an 8% polyacrylamide gel, stained with ethidium bromide and visualized with a UV imaging system (Isogen Life Science). The resulting RFLP patterns were compared with those published for the same 16S rDNA amplicons of other phytoplasmas (Lee *et al*., 1998).

Sequencing and phylogenetic analysis

R16F2n/R16R2 primed PCR products (1.2 kb) from six samples of symptomatic *Z. jujube* plants from nurs-

Figure 1. Phytoplasma disease symptoms on jujube plants: (A) and (B) proliferation and witches' broom, (B) and (C), (D) yellowing, leaf rolling and stunting of an infected plant.

eries in Razavi Khorasan province in eastern Iran were sequenced from both directions. Consensus assembled sequences were compared with deposited sequences in the GeneBank database using BlastN (https://blast.ncbi.nlm.nih.gov/Blast.cgi), and aligned with Bio edit tools. The 1,250 bp of 16S rDNA sequences of the two strains associated with witches' broom and yellowing of *Z. jujube* were aligned using MEGA7 software (Kumar *et al*., 2016), and a phylogenetic tree was constructed using the neighbor-joining method. *Acholeplasma laidlawii* was used as an out group to root the tree. Bootstrapping was performed 1,000 times to estimate branch stability.

Virtual RFLP

Virtual RFLP analysis using *i*PhyClassifier (Zhao *et al*., 2009) was used to confirm subgroup affiliation of phytoplasmas detected in *Z. jujube* plants displaying witches' broom and yellowing. The DNA fragment was digested *in silico* with 17 distinct restriction enzymes: *Alu*I, *Bam*HI, *Bfa*I, *Bst*UI (*Tha*I), *Dra*I, *Eco*RI, *Hae*III, HhaI, *Hin*fI, *Hpa*I, *Hpa*II, *Kpn*I, *Mbo*I (*Sau3A*I), *Mse*I, *Rsa*I, *Ssp*I and *Taq*I.

RESULTS

Symptoms and disease incidence

Diseased *Z. jujube* plants with witches' broom, little leaf, yellowing or leaf roll symptoms in Razavi Khorasan province (Figure 1) were present in 6% of the plants in the jujube nurseries, and 4% of the plants with yellowing and thickening of leaves symptoms.

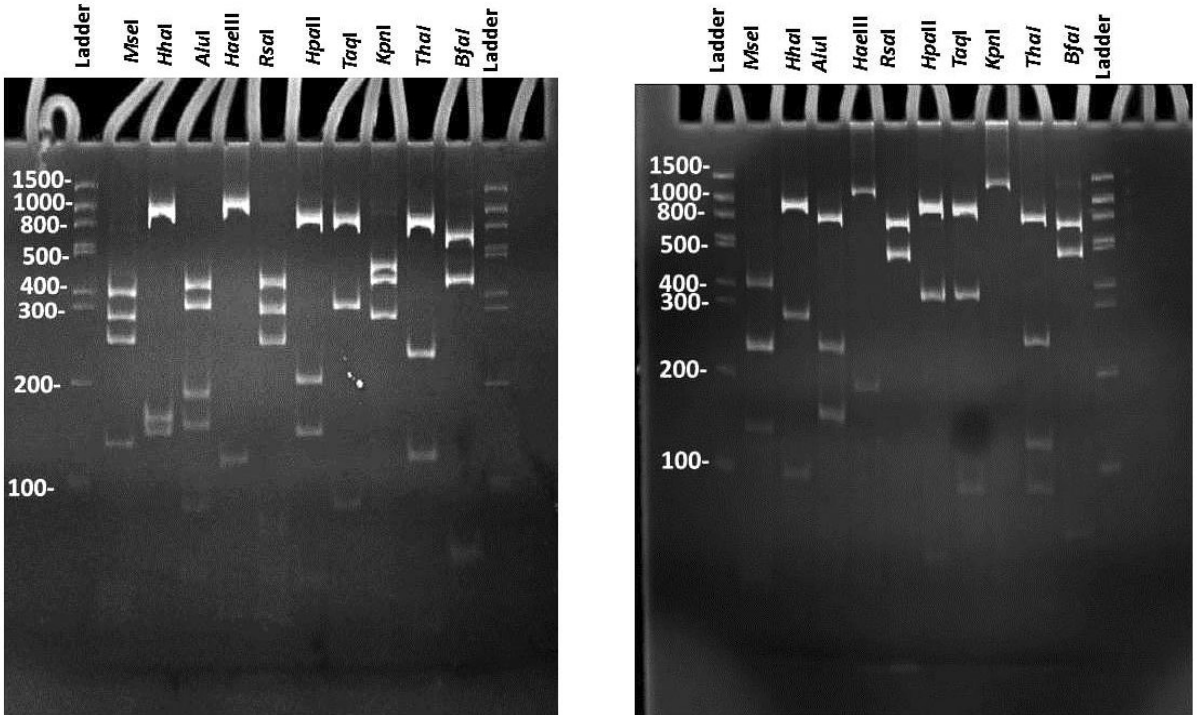

Figure 2. Polyacrylamide gel showing RFLP profiles of 16S rDNA amplified by nested PCR using P1/P7 followed by R16F2n/R16R2 primer pairs from (left) yellowing and (right) witches' broom symptomatic jujube plants. PCR products were digested by the enzymes indicated at the top of the figures; Ladder, 100 bp DNA ladder (Biobasic, Canada).

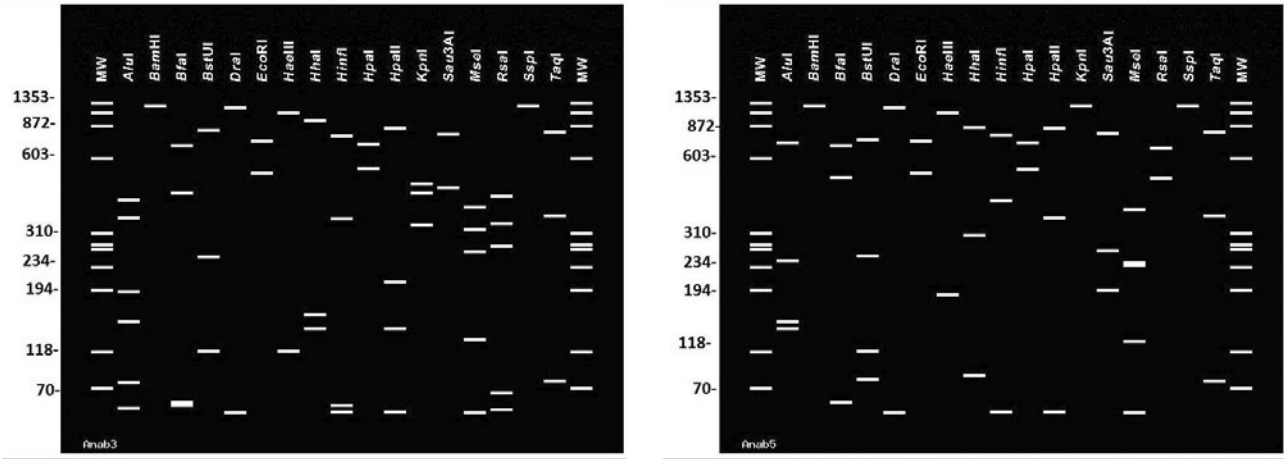

Figure 3. Virtual RFLP generated with program *i*PhyClassifier from *in silico* digestion of the R16F2n/R16R2 fragments of the (left) jujube yellowing (GenBank accession number MK379604) and (right) jujube witches' broom phytoplasma (GenBank accession number MK379605).

PCR-RFLP analyses

P1/P7 faint PCR amplicons of about 1.8 kb and R16F2n/R16R2 nested-PCR amplicons of 1.25 kb, were obtained from all symptomatic *Z. jujube* plants, but not from the symptomless plants. RFLP analysis of R16F2n/R16R2 amplicons using *Kpn*I, *Hae*III, *Rsa*I, *Alu*I, *Hpa*II, *Hha*I, *Taq*I, *Mse*I, *Bfa*I and *Tha*I restriction enzymes showed two RFLP patterns, one identical to those of the 16SrI-B phytoplasma subgroup and the other identical to the 16SrVI-A subgroup (Lee *et al.*, 1998) (Figure 2).

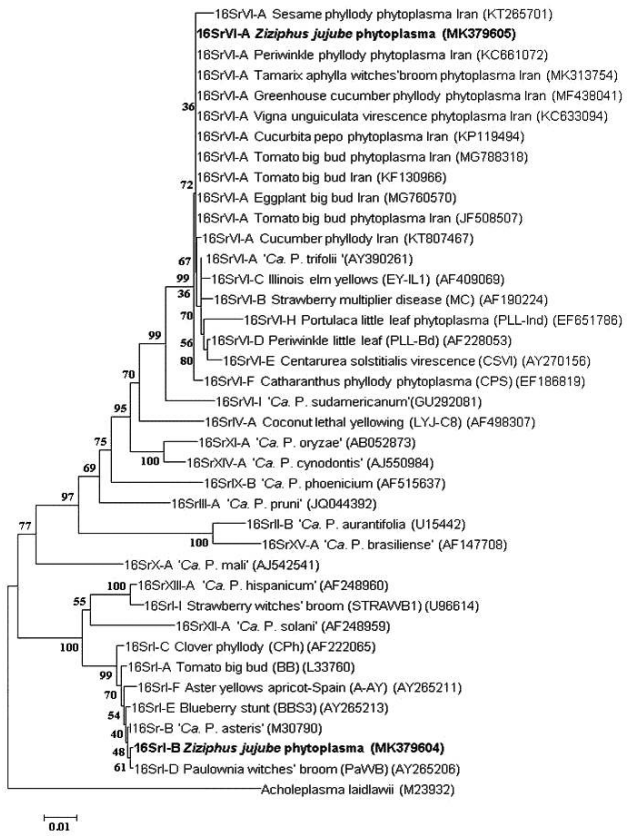

Figure 4. Phylogenetic tree constructed by the Neighbor-Joining method of 16S rRNA gene sequences from 31 phytoplasmas and *Acholeplasma laidlawii*, as the outgroup. The JWB phytoplasmas are indicated in bold font. Numbers at the nodes are bootstrap values based on 1,000 repetitions.

Analysis of nucleotide sequences

The 1.2 kb DNA fragments amplified from six samples of *Z. jujube* and two from yellowing symptoms) had sequence identity with '*Ca.* P. trifolii' related strains (four samples from witches' broom symptoms) and '*Ca.* P. asteris'-related strains (two samples from yellowing symptoms). One R16F2n/R16R2 16S rDNA sequence of each symptom was submitted to GenBank with accession numbers MK379605 and MK379604.

Phylogenetic analysis and virtual RFLP

The restriction analysis indicated that the detected phytoplasma strains were classified in the 16SrI-B and 16SrVI-A subgroups (Figure 3). Similarity coefficient and phylogenetic analyses confirmed that the phytoplasma strain associated with the yellowing symptoms was related to '*Ca.* P. asteris' with 99.7% similarity to the reference strain (GenBank accession number: M30790), while the phytoplasma strain associated with witches' broom symptoms was related to the '*Ca.* P. trifolii' group with 99.8% similarity with the reference strain (GenBank accession number AY390261) (Figure 4).

DISCUSSION

Direct and nested PCR assays using phytoplasma universal primers confirmed the presence of phytoplasmas in jujube plants with witches' broom and yellowing symptoms. RFLP analyses showed that phytoplasma strains associated with JWB belong to the clover proliferation ribosomal group (16SrVI-A), while jujube yellowing phytoplasmas belong to the aster yellows ribosomal group (16SrI-B). However the phytoplasma subgroup 16SrV-B ('*Ca.* P. ziziphi') is the agent associated with JWB disease in different jujube varieties in China, Korea, Japan and India (Ohashi *et al*., 1996; Zhu *et al*., 1998; Fan *et al*., 2008; Khan *et al*., 2008). Phytoplasmas in the 16SrI group have only been reported in jujube trees in Korea in mixed infections with phytoplasmas of group 16SrV (Lee *et al*., 2009). Therefore, the present study is the first demonstration of the presence of these two phytoplasmas in jujube nurseries.

Phytoplasma groups 16SrI and 16SrVI have broad host plant ranges (Lee *et al*., 2004; Hiruki *et al*., 2004), and have also been reported from numerous and different plant hosts in Iran (Babaie *et al*., 2007; Salehi *et al*., 2016; 2018; Asghari Tazehkand *et al*., 2010; Rashidi *et al*., 2010; Esmailzadeh Hosseini *et al*., 2015, 2016, 2017a; Fattahi *et al*., 2016). This indicates that various reservoir host plants besides jujube nurseries are likely to be present.

Planning for phytoplasma disease management requires the identification of phytoplasma subgroups, to better identify the plant reservoirs and the pathways through insect vectors for entry into jujube nurseries. The phytoplasmas in 16SrI-B and 16SrVI-A in Iran are mostly transmitted by leafhopper species including *Circulifer haematoceps*, *Macrosteles* sp. and *Neoaliturus haematoceps* (Salehi *et al*., 2011; 2016). These insects are present in Iran and probably feed on other plant hosts and transmit phytoplasmas from reservoir hosts to jujube plants in nurseries. Selecting distance of nurseries from infected reservoir plants and protecting nursery plants from insect vectors is likely to assist disease management, together with the use of barrier plants or insect proof nets. Jujube cultivars resistant to phytoplasmas have been reported (Liu *et al*., 2006), and further research with Iranian cultivars may identify resistant varieties that can help in the disease management. How-

ever, a certification and sanitation programme for producing healthy plant material is needed in jujube nurseries to prevent transmission of phytoplasma infections to new jujube orchards and to more geographical areas.

ACKNOWLEDGEMENTS

The authors thank CHB Agricultural Organization, and the Chaharmahal and Bakhtiari Agricultural and Natural Resources Research and Education Center, AREEO, Shahrekord, Iran, for supporting this research.

LITERATURE CITED

Asghari Tazehkand S., Hosseini Pour A., Heydarnejad J., Massumi H., Azadvar M., 2010. Identification of phytoplasmas associated with cultivated and ornamental plants in Kerman province, Iran. *Journal of Phytopathology* 158: 713–720.

Babaie G., Khatabi B., Bayat H., Rastgou M., Hosseini A., Salekdeh G.H., 2007. Detection and characterization of phytoplasma infecting ornamental and weed plants in Iran. *Journal of Phytopathology* 155: 368–372.

Deng S., Hiruki C., 1991. Amplification of 16S rRNA genes from culturable and non-culturable mollicutes. *Journal of Microbiological Methods* 14: 53–61.

Esmailzadeh Hosseini S.A., Salehi M., Salehi E., 2015. First report of a 16SrI-B subgroup related phytoplasma associated with *Eruca sativa* phyllody in Iran. *New Disease Reports* 32: 22.

Esmailzadeh Hosseini S.A., Khodakaramian G., Salehi M., Bertaccini A., 2016. First report of 16SrVI-A and 16SrXII-A phytoplasmas associated with alfalfa witches' broom diseases in Iran. *Journal of Plant Pathology* 98: 369.

Esmailzadeh Hosseini S.A., Salehi, M., Babaie, Gh., 2017a. Occurrence and molecular characterization of a 16SrVI-A phytoplasma strain associated with greenhouse cucumber phyllody in Iran. In: *Proceeding of 6th Asian Conference on Plant Pathology*, Jeju, South Korea, 232.

Esmailzadeh Hosseini S.A., Salehi M., Babaie Gh., Mohammadi S., Purmohamadi S., Bertaccini A., 2017b. Occurrence and molecular characterization of a '*Candidatus* Phytoplasma omanense'-related strain associated with *Prunus persica* yellowing and decline in Iran. In: *Proceeding of 6th Asian Conference on Plant Pathology*, Jeju, South Korea, 233.

Fan X.P., Paltrinieri S., Pastore M., Petriccione M., Wang X., … Bertaccini A., 2008. Molecular detection of '*Candidatus* Phytoplasma ziziphi' in different jujube varieties. *Acta Horticulturae* 772: 207–210.

Fattahi M., Salehi M., Sharzehi A., Esmailzadeh Hosseini S.A., 2016. Partial biological and molecular characteristics of a phytoplasma associated with Behshahr (Mazandaran) periwinkle phyllody. *Iranian Journal of Plant Pathology* 52: 135-141.

Gundersen D.E., Lee I-M., 1996. Ultrasensitive detection of phytoplasmas by nested-PCR assays using two universal primer sets. *Phytopathologia Mediterranea* 35: 144-151.

Han S.S., Cha B., 2002. Genetic similarity between jujube witches` broom and mulberry dwarf phytoplasmas transmitted by *Hishimonus sellatus* Uhler. *Korean Journal Plant Pathology* 18: 98-101.

Hiruki C., Wang K., 2004. Clover proliferation phytoplasma: '*Candidatus* Phytoplasma trifolii'. *International Journal of Systematic and Evolutionary Microbiology* 54: 1349-53.

Jung H.Y., Sawayanagi T., Kakizawa S., Nishigawa H., Wei W., … Namba S., 2003. '*Candidatus* phytoplasma ziziphi', a novel phytoplasma taxon associated with jujube witches' broom disease. *International Journal of Systematic and Evolutionary Microbiology* 53: 1037–1041.

Khan M.S., Raj S.K., Snehi S.K., 2008. Natural occurrence of '*Candidatus* Phytoplasma ziziphi' isolates in two species of jujube trees (*Ziziphus* spp.) in India. *Plant Pathology* 57: 1173.

Kim C.J., 1965. Witches' broom of jujube tree (*Zizyphus jujube* Mill. var. inermis Rehd.). Transmission by grafting. *Korean Journal of Microbiology* 3: 1–6.

Kumar S., Stecher G., Tamura K., 2016. MEGA7: Molecular evolutionary genetics analysis version 7.0 for bigger datasets. *Molecular Biology Evolution* 33: 1870-1874.

La Y., Woo K., 1980. Transmission of jujube witches' broom mycoplasma by the leafhopper *Hishimonus sellatus* Uhler. *Journal of Korean Forestry Society* 48: 29–39.

Lee J.T., 1988. Investigation on jujube diseases and their severities of incidence. *Res Rept RDA* (Agri Institutional Cooperation) 31: 155–161.

Lee I-M., Gundersen-Rindal D.E., Davis R.E., Bartoszyk I.M., 1998. Revised classification scheme of phytoplasmas based on RFLP analyses of 16S rRNA and ribosomal protein gene sequences. *International Journal of Systematic and Evolutionary Microbiology* 48: 1153-1169.

Lee I-M., Gundersen-Rindal D.E., Davis R.E., Bottner K.D., Marcone C., Seemüller E., 2004. '*Candidatus* Phytoplasma asteris', a novel phytoplasma taxon

associated with aster yellows and related diseases. *International Journal of Systematic and Evolutionary Microbiology* 54:1037-48.

Lee S., Han S., Cha B., 2009. Mixed infection of 16S rDNA I and V groups of phytoplasma in a single jujube tree. *The Plant Pathology Journal* 25: 21–25.

Li D.K., Huang C.L., Tian J.B., Wang Y.K., Wang Y.Q., 2005. Extraction ways of high quality of DNA from *Z. jujuba* Mil. *Molecular Plant Breeding* 3: 579-583.

Liu M., Zhou J., Zhao J., Wang J., Liu P., … Wang Y. 2006. An excellent new cultivar of chinese jujube with high resistance to jujube witches' broom disease "Xingguang". *Acta Horticulturae Sinica* 33: 687.

Ohashi A., Nohira T., Yamaguchi K., Kusunoki M., Shiomi T., 1996. Jujube (*Zizyphus jujuba*) witches' broom caused by phytoplasma in Gifu prefecture. *Transcripts of Forest Society of Japan* 107: 309–310.

Rashidi M., Ghosta Y., Bahar M., 2010. Molecular identification of a phytoplasma associated with Russian olive witches' broom in Iran. *European Journal of Plant Pathology* 127: 157–159.

Salehi M., Izadpanah K., Siampour M., 2011. Occurrence, molecular characterization and vector transmission of a phytoplasma associated with rapeseed phyllody in Iran. *Journal of Phytopathology* 159: 100-105

Salehi M., Esmailzadeh Hosseini S.A., Salehi E., Bertaccini A., 2016. Genetic diversity and vector transmission of phytoplasmas associated with sesame phyllody in Iran. *Folia Microbiologica* 62: 99–109.

Salehi M., Esmailzadeh Hosseini S.A., Salehi E., 2018. First report of a *'Candidatus* Phytoplasma asteris'-related strain (16SrI-B) associated with *Sonchus oleraceus* (common sowthistle) phyllody disease in Iran. *New Disease Reports* 37: 6.

Schneider B., Seemüller E., Smart C.D., Kirkpatrick B.C., 1995. Phylogenetic classification of plant pathogenic mycoplasma-like organisms or phytoplasmas. In: *Molecular and Diagnostic Procedures in Mycoplasmology* (S.Razin, J.G. Tully, ed.), Academic Press, San Diego, CA, USA, 369-380.

Tsai J.H., Chen X.Y., Shen C.Y., Jin K.X., 1988. Mycoplasmas and fastidious vascular prokaryotes associated with tree disease in China. In: *Tree Mycoplasmas and Mycoplasma Diseases* (C.J. Hiruki, ed.), Alberta Press, Canada, 69–96.

Zhao Y., Wei W., Lee I.-M., Shao J., Suo X., Davis R.E., 2009. Construction of an interactive online phytoplasma classification tool, *i*PhyClassifier, and its application in analysis of the peach X-disease phytoplasma group (16SrIII). *International Journal of Systematic and Evolutionary Microbiology* 59: 2582–2593.

Zhu S.F., Hadidi A., Lee I-M., Gundersen D.E., Zhang C.L., 1998. Characterization of the phytoplasmas associated with cherry lethal yellows and jujube witches' broom disease in China. *Acta Horticulture* 472: 701–707.

Phytopathologia Mediterranea
The international journal of the
Mediterranean Phytopathological Union

Firenze University Press
www.fupress.com/pm

Research Paper

Essential oil from fennel seeds (*Foeniculum vulgare*) reduces Fusarium wilt of tomato (*Solanum lycopersicon*)

Fatma KALLELI[1,2], Ghassen ABID[3], Ibtissem BEN SALEM[4], Naïma BOUGHALLEB-M'HAMDI[4], Mahmoud M'HAMDI[1,2,*]

[1] *Department of Horticultural Sciences and Vegetable Crops, High Institute of Agronomy of Chott Mariem, University of Sousse, 4042 Sousse, Tunisia*
[2] *Horticultural Science Laboratory,National Agronomic Institute of Tunisia. University of Carthage, Tunisia*
[3] *University of Tunis El Manar, Center of Biotechnology of Borj Cedria, Laboratory of Legumes, BP 901, 2050 Hammam-Lif, Tunisia*
[4] *Department of Biological Sciences and Plant Protection, High Institute of Agronomy of Chott Mariem, University of Sousse, UR13AGR03, 4042 Sousse, Tunisia*
* Corresponding author: address: mhamdimahmoud@yahoo.fr

Summary. Natural products have been considered a viable alternatives for managing plant diseases. This study investigated *in vitro* and *in planta* antifungal activity of an essential oil from fennel seeds against *Fusarium oxysporum* f. sp. *lycopersici* (FOL). The essential oil inhibited FOL *in vitro* mycelium growth by up to 83% and sporulation by up to 97%. Protective effects against *Fusarium* wilt were observed *in planta,* especially when the oil was applied curatively at a concentration of 500µl mL^{-1}. The fennel essential oil reduced disease severity from 98% in untreated FOL-inoculated plants to 57% in plants inoculated with FOL and treated with the oil at 8 weeks after of inoculation. GC-MS spectrometry analyses showed that the major chemical components in the essential oil were *trans*-anethole (78%), fenchone (11%), estragole (5%) and limonene (4%). Applications of the essential oil resulted in increased soluble sugars, total phenolic and total flavonoid contents in leaves compared with untreated inoculated (control) plants. The defence-related genes, such as those encoding pathogenesis-related (*SlPR1*) proteins, *SlWRKY*, thaumatin-like protein (*SlTLP*), lipoxygenase (*SlLOX*), ethylene response factor (*SlERF*) and chitinase (*SlChi*), were differentially expressed. This study has indicated that essential oil from fennel seeds has potential as a control agent against *Fusarium* wilt of tomato.

Keywords. Antifungal activity, defence related genes, plant disease, phytochemicals, RT-qPCR.

OPEN ACCESS

Citation: F. Kalleli, G. Abid, I. Ben Salem, N. Boughalleb-M'hamdi, M. M'hamdi (2020) Essential oil from fennel seeds (*Foeniculum vulgare*) reduces Fusarium wilt of tomato (*Solanum lycopersicon*). *Phytopathologia Mediterranea* 59(1): 63-76. doi: 10.14601/Phyto-11143

Accepted: December 13, 2019

Published: April 30, 2020

Data Availability Statement: All relevant data are within the paper and its Supporting Information files.

Competing Interests: The Author(s) declare(s) no conflict of interest.

Editor: Philippe Nicot, Plant Pathology Research Unit INRA, Avignon, France.

INTRODUCTION

Fusarium wilt, caused by *Fusarium oxysporum* f. sp. *lycopersici* (FOL) is one of the most aggressive and destructive soil-borne diseases affecting tomato. FOL infects host roots and colonizes the xylem vessels, causing wilting, stunting and death of plants, and results in significant economic losses

(Salim *et al*., 2016). Integrated management approaches against FOL, such as cultural practices, soil disinfestation, crop rotations, resistant cultivars, and chemical treatments, were reported to be inefficient in reducing the incidence and severity of the disease, due to the production of resistant spores by the pathogen (chlamydospores) and the emergence of new races (Amini and Sidovich, 2010). The use of synthetic fungicides may also lead to adverse effects on human health and the environment, due to their high toxicity, slow degradation and bioaccumulation (Mohammadi and Aminifard 2013). Therefore, development of new "green" technologies for plant disease management based on biostimulant and biocontrol tools, could be reliable for reducing the amount of chemical residues in the environment (Dihazi *et al*., 2011). In plants, infection with microorganisms induces secondary metabolic pathways. The production of secondary metabolites, including antifeedants, phytoanticipins and phytoalexins, enhances plant defence systems (Pino *et al*., 2013). Medicinal and aromatic plants are important rich sources of plant secondary metabolites, which exhibit antifungal activity against numerous phytopathogenic fungi, and may induce systemic acquired resistance processes (Pusztahelyi *et al*., 2015). These bioactive products are biodegradable, sustainable for integrated disease management, and are generally less toxic than synthetic products towards nontarget species.

Essential oils are complex organic substances, biosynthesized through secondary metabolic pathways of plants, which play important roles as signaling molecules in plant defence against bio-aggressors including pest insects, fungi, bacteria and viruses (Rehmana *et al,*. 2016). According to Zake (2016), essential oils from aromatic and medicinal plants exhibited *in vitro* and *in vivo* activity against plant pathogenic fungi, and can be used as bio-fungicide products. Essential oils have been used in various contexts and were proposed as possible tools for safe and sustainable alternative agriculture. This is because they possess various agronomic activities, including antimicrobial, antiviral, antifungal, insecticidal and herbicidal, they have better biodegradability compared to conventional synthetic fungicides (Arshad *et al*., 2014).

Several studies have demonstrated that plant hormones such as salicylic acid (SA), jasmonic acid (JA), and ethylene (ET) could play crucial roles in plant defence signalling (Yang *et al.,* 2012). Several families of defence-response (DR) genes, including plant transcription factors and signalling molecules such as peroxidase, PR1, PR10, chitinase, osmotin, thionin, SAR8.2 and defensin, were shown to be associated with plant responses to diverse biotic stresses (Lee and Hwang, 2005).

Fennel (*Foeniculum vulgare* Mill), belonging to the *Umbelliferae*, is a perennial or annual herbaceous plant that grows in several regions of the world (Ozcan *et al.,* 2006). Roby *et al.* (2013) reported that essential oils from fennel showed different degrees of antimicrobial and antioxidant activities depending on the applied doses. Essential oil from fennel was reported to possess antifungal activity by reducing the mycelium growth and germination of *Sclerotinia sclerotiorum* (Soylu *et al*., 2007). The objectives of the present study were to (i) evaluate the effectiveness of essential oil from local fennel seeds for inhibition of hyphal growth of *Fusarium oxysporum* f. sp. *lycopersici, in vitro*; (ii) reduce the *in planta* severity of *Fusarium* wilt of tomato; and (iii) determine the expression of defence-related genes in tomato**.**

MATERIALS AND METHODS

Plant material

Fully ripened fennel seeds used in this study were collected from cultivated plants from the experimental station of the Higher Agronomic Institute of Chott Mariem, Sousse, Tunisia. Collected seeds were dried at room temperature and stored in polyethylene bags at 4°C until use.

Isolation of essential oil

The essential oil was obtained from fennel seeds by hydro-distillation using a Clevenger apparatus, according to Bettaieb *et al.* (2011). The obtained oil was dried over anhydrous sodium sulphate and stored at 4°C after filtration, until used in tests and analyses.

Identification and quantification of the oil components

Analyses of the essential oil were performed using an Agilent 7890A gas chromatograph (GC) coupled to an Agilent 5972C mass spectroscopy detector with electron impact ionization (70 eV). A HP-5 MS capillary column (30 m × 0.25 mm, coated with 5% phenyl methyl silicone, 95% dimethylpolysiloxane, 0.25 µm film thickness; Agilent Technologies) was used to separate compounds. Components were identified based on the comparison of their mass spectra with Wiley Registry 9th Edition/ NIST 2011 mass spectral library, and from comparison

of their retention indices either with those of authentic compounds or with literature values. Relative percentage amounts of the identified compounds were obtained from the electronic integration of the peak areas without the use of the correction factor.

In vitro *antifungal effects of fennel essential oil*

Fungal culture. Isolate FO14 of *Fusarium oxysporum* f. sp. *lycopersici*, obtained from tomato, was tested for its pathogenicity. The isolate was identified morphologically (using microscopy) according to Leslie and Summerell (2006), and molecularly by sequencing the 18S rDNA using ITS1/ITS4 primers (White *et al*., 1990). The pure culture was maintained on potato dextrose agar (PDA) and stored in glycerol at -20°C until required.

Mycelium growth inhibition. The fennel essential oil was incorporated into molten PDA at desired final concentrations, and well mixed. Different concentrations of essential oil were prepared by dissolving the required amounts in sterile PDA amended with Tween 20 (0.1%, v/v) to obtain the desired concentrations (C0, negative control; C1, 15.6 µL mL^{-1}; C2, 31.3; C3, 62.5; C4, 125; C5, 250 or C6, 500 µL mL^{-1}). The medium was then poured into Petri dishes. After overnight pre-incubation, the centre of each plate was inoculated with a mycelium plug (0.7 mm diam.) from a 5-day-old culture, and the plates were then incubated at 28°C. Mycelium growth was assessed daily by measuring the horizontal and vertical diameters of the colony in each plate, and antifungal activity was assessed 6 d post-inoculation (DPI) according to Soylu *et al*. (2007). For each essential oil concentration treatment, five plates were used. The experiment was conducted twice independently. The percentage of mycelium growth inhibition (MGI) was determined according to the formula:

$$MGI\ (\%) = ((dc-dt)/dc) \times 100;$$

where dc was the diameter of the control (C0) colony, and dt was the diameter of the essential oil treated colony.

Sporulation test. Assessment of sporulation was carried out according to the method of Kanoun *et al*. (2014). Each entire Petri dish (15-d after inoculation) containing the fungus was washed with 10 mL of sterile distilled water to release all the conidia. Subsequently, a pooled conidial suspension was obtained by mixing all five plates (50 mL). The number of conidia (conidia mL^{-1}) for each treatment (three replicates) was counted with a Malassez cell using a light microscope.

In planta *antifungal effects of fennel essential oil*

Fungal inoculum. Inocula of FOL were prepared by culturing the isolate in potato dextrose broth (PDB) amended with streptomycin sulfate, and with agitation at 25 ± 2°C for 5 d. Conidia were counted using a Malassez cell and microscopy, and appropriate dilutions were made to adjust the inoculum to a concentration of 10^6 conidia mL^{-1} with sterile distilled water.

Host plant material, growth conditions and treatments. Five-week-old seedlings of tomato 'Murano' (susceptible to FOL) were transplanted into 20 cm diam. plastic pots (one plant/pot), which were arranged in a randomized complete block design with three replicates per treatment. The seedlings were then grown in a greenhouse at 30/25°C (day/night) and 14 h photoperiod, with relative humidity of 70 ± 10%.

All the tomato seedlings were drench-inoculated with 1 mL of FOL conidium suspension (10^6 mL^{-1}) around the seedling rhizospheres. For a preventive treatment, 50 mL of fennel essential oil at 500 µL mL^{-1} was applied as a soil drench, 1 week before inoculation. The effects of a curative treatment were also evaluated, with an application of the essential oil preparation 2 weeks after inoculation. Plants were irrigated with distilled water served as untreated experimental controls. All combinations of treatments are listed in Table 1 and the experiment was repeated twice.

Table 1. Experimental treatments applied to tomato seedlings.

T1	Plants non inoculated and non-treated.
T2	Plants non-inoculated and treated with fungicide: Tachigaren fungicide was applied by soil drench two weeks after inoculation with FOL at a dose of 0.25 mL/plant.
T3	Plants non-inoculated and treated with essential oil by soil drench application.
T4	Plants were drench-inoculated with 1 mL of conidium suspension of FOL (10^6 conidia. mL^{-1}) around the tomato rhizosphere.
T5	Plants inoculated with FOL and treated with fungicide by soil drench application.
T6	Plants inoculated with FOL and treated with essential oil by soil drench application 1 week before inoculation.
T7	Plants inoculated with FOL and treated with essential oil by soil drench application 2 weeks after inoculation.

Disease severity assessments

The severity of Fusarium wilt was estimated according the scale of Song *et al.* (2004), where: 1 = healthy, no sign of symptoms; 2 = slight symptoms, mainly on lower leaves (about 25% of full scale); 3 = advanced symptoms (≅50%); 4 = extensive symptoms (≅75%); and 5 = entire plant affected (dead plant). Four plants were randomly chosen from each treatment in each experiment (eight in total). Disease severity (%) was calculated from the disease rating using the following formula:

Disease severity (%) = (∑ scale number of infected plants) * 100 / (greatest scale * total number of plants).

The disease severity assessments were carried out 60 d after plant inoculation. Re-isolation of the pathogen was accomplished at the end of the assay to confirm Koch's postulates.

Biochemical analyses

Preparation of tomato leaf extracts. For each treatment, tomato leaves from five plants were collected 3, 5 or 7 weeks after inoculation in the greenhouse experiment. Sample extracts were obtained following Mau *et al.* (2001) with slight modifications. To prepare the extracts, 2.5 g of dry leaf powder was extracted with 25 mL of methanol (60%) solvent. Each mixture was then magnetically stirred for 30 min and the extracts were then kept at 4°C for 24h in darkness. The mixtures were then filtered through a Whatman No. 4 filter paper and evaporated to dryness under vacuum. The extracts thus obtained were stored at 4°C for further use.

Determination of total phenolic contents. The total phenolic content of the tomato leaf extracts was determined using Folin-Ciocalteu reagent, according to Falleh *et al.* (2008). Absorbance was determined against a blank at 760 nm using UV-visible spectroscopy. The content of total phenolic compound in each extract was expressed as mg of gallic acid equivalents per g fresh weight (mg GAE g^{-1} FW) from a calibration curve with gallic acid. All determinations were carried out in triplicate. Gallic acid was used as the reference standard for plotting the calibration curve.

Determination of total flavonoid contents. The total flavonoid content in methanolic extracts of leaves was determined with a colorimetric assay, using a method described by Faudale *et al.* (2008). Briefly, 1 mL of methanolic extract from each sample was mixed with 5 mL of distilled water, followed by addition of 0.3 mL of a 5% (w/v) $NaNO_2$ solution. After 6 min, 0.6 mL of $AlCl_3$ (10% m/v) was added. After 5 min of incubation at room temperature, 2 mL of NaOH (1 M) was added. The final volume was adjusted to 10 mL with the addition of distilled water. The mixture was homogenized and the absorbance was determined at 510 nm. Total flavonoid content was measured using a quercetin calibration curve, and was expressed as mg of quercetin equivalents (QE) per g of dry weight (mg QE g^{-1} FW). All samples were analyzed in three replications.

Determination of soluble sugars. The soluble sugars were estimated using the colorimetric method described by Dubois *et al.* (1956). For each sample, 100 mg of dried leaf material was homogenized with 3 mL of 80% ethanol (v/v) and then mixed with concentrated sulfuric acid and 5% phenol. The mixture was kept for 1 h and then the absorbance at 490 nm was determined with a spectrophotometer. Glucose was used as standard. Contents of soluble sugars were expressed as mg g^{-1} FW. Analyses were carried out in triplicate.

Expression of defence-related genes

RNA isolation and cDNA synthesis. For quantitative real-time PCR, tomato leaf tissues (from treatments T1, T2, T3, T4, T5 and T7) were collected at 0, 6, 12, 24, 48 or 72 h post treatment (HPT). Two hundred milligrams of each sample was ground to a fine powder using liquid nitrogen and transferred into a 2 mL centrifuge tube for total RNA extraction following the protocol described by Chang *et al.* (1993). The quantity and quality of total RNA were assessed on a NanoDrop Spectrophotometer and by electrophoresis in a 1.2% agarose gel. Genomic DNA contamination was removed by treating the samples with 1 µL of DNase I, RNase-free (5 U μL^{-1}) (Biomatik) at 37°C for 30 min. First-strand cDNA was synthesized from 5 µg of total RNA using 200 U Turbo-I reverse transcriptase (Biomatik) according to the manufacturers' instructions.

Quantitative RT-PCR (RT-qPCR) analysis. Gene-specific primer pairs for *SlChi*, *SlERF*, *SlPR1*, *SlLOX*, *SlTLP* and *SlWRKY* genes used in this study were designed using the Primer3 Input (version 0.4.0) software (Rozen and Skaletsky 2000) (http://frodo.wi.mit.edu/primer3/), with default criteria of the software and with amplified products ranging from 80 to 150 bp and Tm approx. 60°C. Actin was used as a control to normalize the samples. The primer sequences are listed in Table 2. RT-qPCR was performed in a 7300 Real-Time PCR System (Applied Biosystems) using the Maxima SYBR Green/ROX qPCR Master Mix (2X) kit (Biomatik). Each 20 µL reaction mix contained 10 µL Maxima SYBR Green/ROX qPCR Master Mix (2X), 1 µL of each primer at 10 µM (Table 2), 6 µL dd H_2O and 2 µL cDNA (50 ng). The reactions were performed in trip-

Table 2. Sequences of the primers used for RT-qPCR analysis.

Gene name	GenBank accession ID	Forward and reverse primer 5'-3'	Amplicon size (bp)
SlChi	U30465	Forward: 5'-ATCGGCACACGATGTCATTA-3' Reverse: 5'-TGAACCGCTGTTACATTCCA -3'	127
SlERF	NM_001247384	Forward: 5'-CCCAATTTCCCGTTACTTCA-3' Reverse: 5'-GCCTTCTCCTTACCCCTCTG-3'	149
SlPR1	NM_001247429	Forward: 5'-ACGTCTTGGTTGTGCTAGGG -3' Reverse: 5'-TCAAAAGCCGGTTGATTTTC -3'	126
SlLOX	XR_183132	Forward: 5'-TGGGATTAAACTGCCAGACC-3' Reverse: 5'-GGCATCGGAAATTTGAGAAA-3'	114
SlWRKY	XM_004232149	Forward: 5'-TCTCGATCTGACCAGGTTCC-3' Reverse: 5'-TTGCCGTCTTCGTTCTCTTT-3'	139
SlTLP	XM_004235762	Forward: 5'-CCATCTTTGCTTCCCACATT-3' Reverse: 5'-ATCGGTTTACCTGCACTTGG-3'	100
SlActin	U60480	Forward: 5'-AGGCACACAGGTGTTATGGT-3' Reverse: 5'-AGCAACTCGAAGCTCATTGT-3'	177

licate for each sample with the following settings: initial denaturation at 95°C for 5 min followed by 40 cycles at 95°C for 30 s and 60°C for 1 min. The specificity of the PCR amplification was verified with a melt curve analysis (from 55°C to 94°C) following the final cycle of the PCR. All reactions were performed in triplicate. The relative expression levels were analyzed using the $2^{-\Delta\Delta CT}$ method, as described by Schmittgen and Livak (2008).

Statistical analyses

Data were subjected to an analysis of variance (ANOVA), and means and standard errors were calculated. All parameters were subjected to a one-way-analysis ($P<0.001$) and compared using Tukey's test at 5% of probability. The statistical analyses were performed using Statistical Package for the Social Sciences software (SPSS; version 20).

RESULTS

Chemical composition of the essential oil

The yield of hydro-distilled essential oil from fennel seeds was found to be 0.54% (w/w). The chemical composition of the oil is given in Table 3. GC-MS analysis 18 compounds in different seed tissues. These compounds were assigned to three classes: phenylpropanoids (83%), oxygenated monoterpenes (11%) and monoterpene hydrocarbons (6%). This oil was characterized by a high content of the *trans*-anethole (78%), L-fenchone (11%), estragole (5%) and limonene (4%).

In vitro *antifungal effects of fennel seed essential oil*

Mycelium growth. The *in vitro* antifungal activity of the essential oil against FOL was recorded 6 DPI (Figure 1). Greatest inhibition of mycelium growth by the oil was at 500 µL mL^{-1}, where mean inhibition was 83%. At 250 µL mL^{-1} the oil also reduced the mycelial growth of FOL by 44%.

Sporulation test. The presence of essential oil in PDA reduced FOL conidium production compared to the experimental controls without essential oil. Conidium production decreased with increasing oil concentrations, and the greatest highest reduction (97%) was recorded at 500 µL mL^{-1} (Figure 2).

In planta *effects of fennel seed essential oil*

Disease severity. As the infections progressed, disease severity increased ($P < 0.05$) for the untreated tomato plants, reaching severity greater than 90%. Disease severity was least for tomato plants treated with fungicides preventively or curatively. Application of the essential oil also provided some protection against Fusarium wilt when the oil was applied curatively (Figure 3). At the end of the assay, Koch's postulates were confirmed by re-isolating FOL from roots, collars and leaves of inoculated plants.

Total phenolic contents of leaves. The total phenolic content in the tomato leaves showed differences depending on treatments (Figure 4). This significantly greater in treatments T2, T3, T4, T5, T6 and T7 compared with T1, at 21, 28 or 35 DPI. Phenolic content was greatest in plants inoculated and treated with essential oil (T6 and

Table 3. Chemical composition of the essential oil extracted from fennel seeds, determined using GC-MS.

Compounds	RI[a]	RI[b]	Identification[c]	Percentage
α-pinene	1032	934	RI, MS	0.43 ± 0.02
Camphene	1086	951	RI, Co-GC	0.10 ± 0.02
Sabinene	1132	975	RI, MS, Co-GC	0.16 ± 0.02
β-pinene	1123	980	RI, Co-GC	0.08 ± 0.02
β-myrcene	1166	991	MS	0.26 ± 0.02
I-phellandrene	1118	980	RI, MS, Co-GC	0.10 ± 0.02
p-cymene	1280	1026	RI, MS, Co-GC	0.09 ± 0.03
Limonene	1206	1030	MS	3.88 ± 0.47
trans-β-ocimene	1266	1050	RI, MS, Co-GC	0.29 ± 0.03
γ-terpinene	1255	1062	RI, MS, Co-GC	0.12 ± 0.03
L-fenchone	1402	1072	RI, MS, Co-GC	10.64 ± 0.03
Camphor	1532	1143	RI, MS, Co-GC	0.25 ± 0.04
Terpinen-4-ol	1611	1178	RI, MS, Co-GC	0.09 ± 0.04
p-anisic aldehyde	1976	1281	RI, MS, Co-GC	0.16 ± 0.05
Cis-anethole	1655	1252	RI, MS	0.25 ± 0.05
Estragole	1688	1196	RI, MS, Co-GC	4.67 ± 0.04
trans-anethole	1654	1297	RI, MS, Co-GC	78.26 ± 0.01
α-fenchyl acetate	1643	1220	RI, MS	0.18 ± 0.04
Class of compounds (%)				
Monoterpene hydrocarbons				5.50
Oxygenated monoterpenes				11.32
Phenylpropanoids				83.18
Total identified				100

Values are means of three replicates ± SD. [a] Retention index on an apolar column (HP-5). [b] Retention index on a polar column (HP-Innowax). [c] RI, identification by retention index relative to C8-C22 n-alkanes on the (HP-Innowax); MS, identification by mass spectrometry; Co-GC, identification by co-injection with authentic compound.

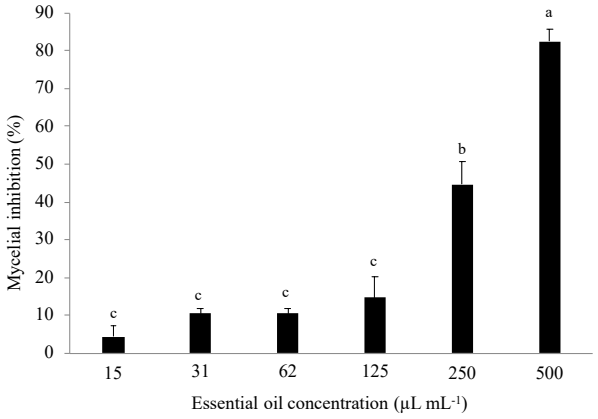

Figure 1. Mean *in vitro* growth reduction (%) of *Fusarium oxysporum* f. sp. *lycopersici* mycelium when exposed to different concentrations of fennel essential oil in PDA medium. Each value represents the mean of three replicates (two Petri plates per replicate). Values accompanied by different letters differ significantly ($P \leq 0.05$) according to Tukey's test.

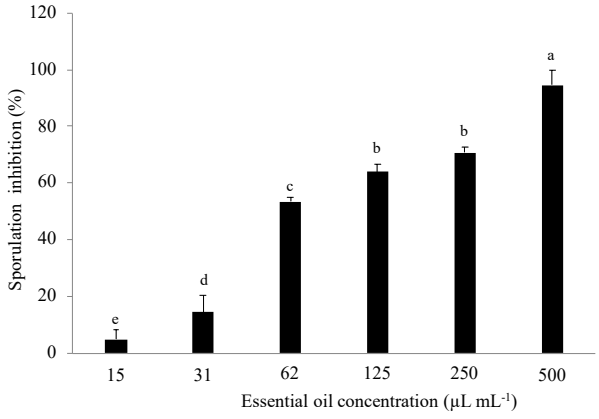

Figure 2. Mean inhibition of *Fusarium oxysporum* f. sp. *lycopersici* sporulation *in vitro* (%) when exposed to different concentrations of fennel essential oil in PDA medium. Each value is the mean of three replicates. Values accompanied by different letters differ significantly ($P \leq 0.05$), according to Tukey's test.

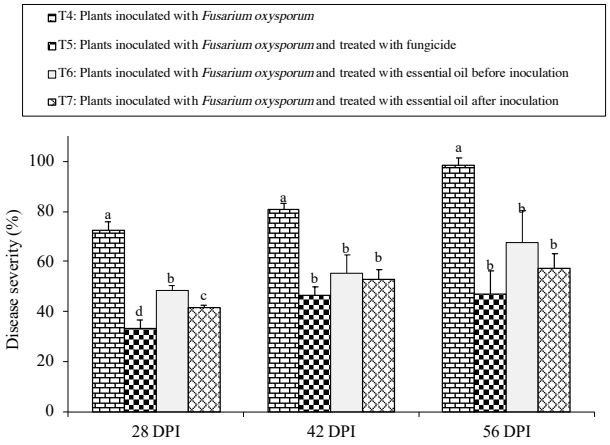

Figure 3. Mean Fusarium wilt severity for non-inoculated, inoculated and treated tomato plants at 28, 42 or 56 d post inoculation (DPI). Each value is the mean of the three replicates, and error bars represent ±SD. Values for each time accompanied by different letters differ significantly ($P \leq 0.05$), according to Tukey's test.

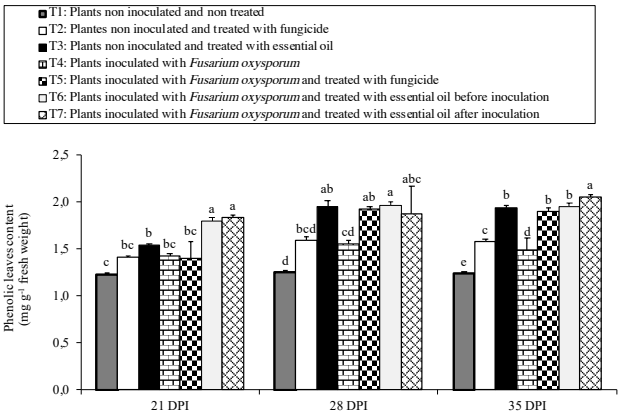

Figure 4. Mean amounts of total phenol in tomato leaf samples, from different treatments of FOL inoculation and essential oil application, at 21, 28 or 35 d post inoculation (DPI). Each value is the mean of the three replicates, and error bars represent ±SD. Values for each time accompanied by different letters differ significantly ($P \leq 0.05$), according to Tukey's test.

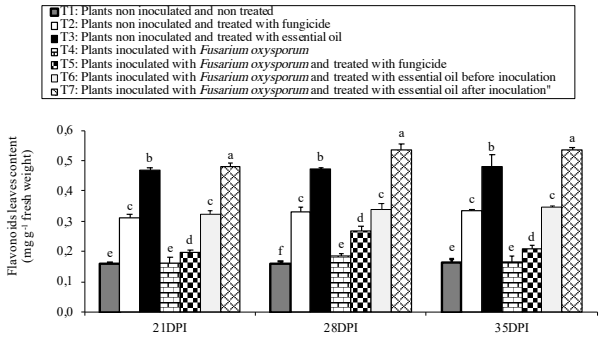

Figure 5. Mean amounts of total flavonoid in tomato leaf samples from different treatments of FOL inoculation and essential oil application, at 21, 28 or 35 d post inoculation (DPI). Each value is the mean of the three replicates, and error bars represent ±SD. Values for each time accompanied by different letters differ significantly ($P \leq 0.05$), according to Tukey's test.

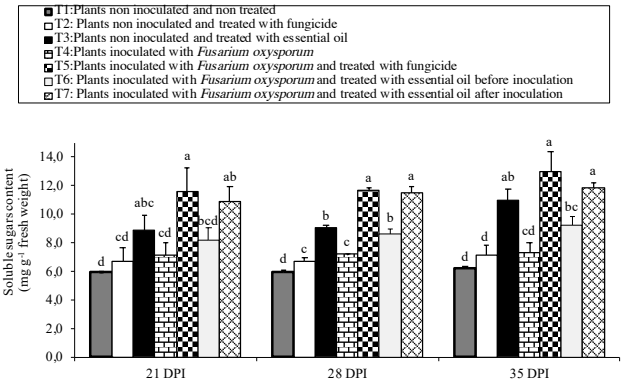

Figure 6. Mean amounts of soluble sugars in tomato leaf samples from different treatments of FOL inoculation and essential oil application, at 21, 28 or 35 d post inoculation (DPI). Each value is the mean of the three replicates, and error bars represent ±SD. Values for each time accompanied by different letters differ significantly ($P \leq 0.05$), according to Tukey's test.

T7), while fungicide did not significantly affect the phenol content in non-infected plants (T2). At 28 or 35 DPI, the least total phenolic contents were observed in non-inoculated and non-oil treated plants (T1). These results indicated that preventive and curative applications of the essential oil could be responsible for the increases of total phenolic contents in tomato leaves infected with FOL.

Total flavonoid contents

Total flavonoid contents (TFC) varied among the treatments (Figure 5). These were significantly greater in T2, T3, T6 and T7 compared to other treatments at 21, 28 or 35 DPI.

Soluble sugars contents

The greatest soluble sugars contents were observed in tomato plants treated with fungicide and in those that received a curative treatment with the essential oil (Figure 6). The least sugars content was in the experimental control plants.

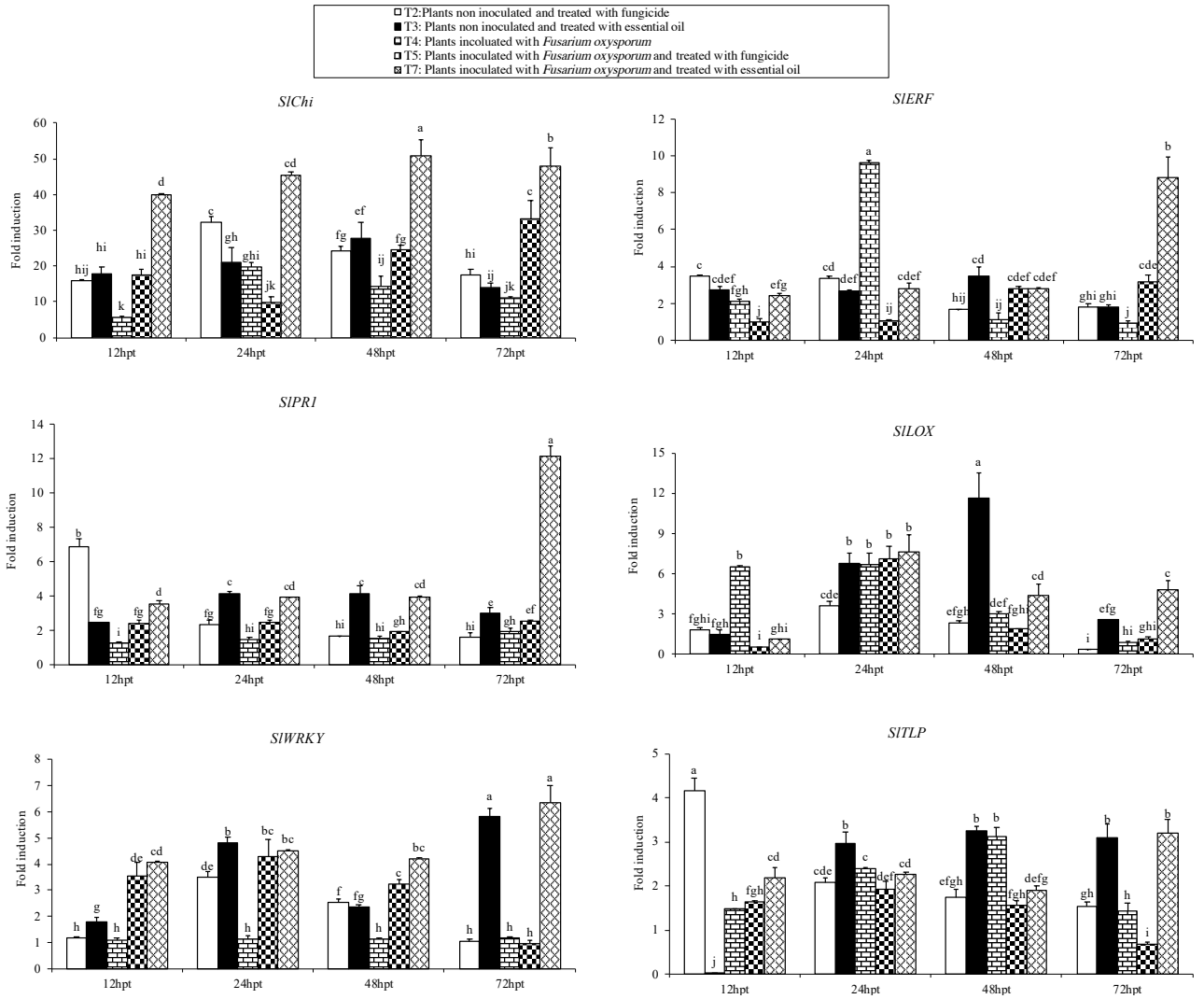

Figure 7. Fold changes in accumulation of the genes *SlChi, SlERF, SlPR1, SlLOX, SlWRKY* and *SlTLP* in tomato leaf samples, for different treatments relative to nil treatment (controls), and at different period (h post treatment; hpt). Values are the means (± SD) of three repeated experiments. Different letters above columns for all sampling stages indicate significant differences ($P \leq 0.05$), according to Tukey's test.

Expression profiles of defence genes in tomato leaf tissues. To confirm whether tomato plant defence mechanisms would be affected by treatments with the essential oil, expression of defence genes, including *SlChi, SlERF, SlPR1, SlLOX, SlWRKY* and *SlTLP* were quantified in leaf tissue at 0, 12, 24, 48 and 72 HPT, using RT-qPCR (Figure 7). Generally, from all treatments, the selected genes were upregulated compared to the experimental control. *SlChi* and *SlWRKY* were highly induced after curative treatment with the essential oil compared to the control. However, after fungicide treatment *SlChi* and *SlWRKY* showed the least expression. *SlERF* displayed high expression after fungicide treatment at 24 HPT, and after curative treatment with the essential oil at 72 HPT. The least expression of *SlERF* was measured in inoculated plants treated with fungicide at 12 and 24 HPT. At 12 HPT, FOL induced a 6.5-fold increase in expression of the *SlLOX* gene compared to the non-inoculated controls (plants treated with water), while no significant upregulation of *SlLOX* expression was observed in plants inoculated and treated with essential oil or fungicide. At 24 HPT, *SlLOX* was similarly induced in all treated plants compared to non-infected plants treated with fungicide. *SlLOX* transcript accumulation was significantly increased at 48 HPT, with respect to the other treatments, for plants treated with the essential oil. In the infected plants treated with the essential oil, *SlLOX* expression at 72 HPT was less than that at the

other time points after treatment. Expression of *SlPR1* decreased from 12 to 72 HPT in the fungicide treated plants, but high expression levels of this gene were measured only at 72 HPT in the inoculated and essential oil treated plants. However, in untreated and FOL-infected plants, levels of *SlPR1* gene transcription remained similar at all time points. The thaumatin-like protein (*SlTLP*) was up-regulated at 24, 48 and 72 HPT in the non-inoculated and essential oil treated plants. *SlTLP* expression was maximum at 12 HPT, followed by decreases at later stages in non-inoculated plants and treated with fungicide. There were no significant *SlTLP* expression differences at 12 or 24 HPT in the FOL inoculated and essential oil treated plants. However, *SlTLP* transcript at 48 and 72 HPT was significantly greater than at the other time points.

DISCUSSION

This study was within the scope of evaluating Tunisian medicinal and aromatic plants for discovery of new bioactive natural products that could be used against fungal diseases such Fusarium wilt of tomato caused by FOL. Based the results obtained, the essential oil from fennel seeds, which was rich in *trans*-anethole, exhibited good antimicrobial activity against FOL, as shown by the results for MGI and disease severity. Other compounds, such as α-pinene, sabinene, camphor, limonene and β-myrcene are present at concentrations usually less than 1%. According to Anwar *et al.* (2009), the major constituents of the fennel seeds essential oil tested were *trans*-anethole (70%), fenchone (10%), estragole (5%) and limonene (5%). Mimica-Dukic *et al.* (2003) also observed that the major compounds identified in the essential oil from fennel seeds were *trans*-anethole (74%, fenchone (11%), estragole (5%), and limonene (3%), which were constituents similar to those determined in the present study. In the Podgorica region of central south Montenegro, the essential oil composition assessed by Damjanović *et al.* (2005) was *trans*-anethole (62%), fenchone (20%), estragole (5%) and limonene (3.%) as the major components. Bernath *et al.* (1996) indicated that anethole (40-70%), fenchone (1-20%) and estragole (2-9%) were the most abundant compounds in fennel seed essential oil. *Trans*-anethole, the dominant component in fennel seeds essential oil, was also found in essential oils from other plants, and has been reported to possess insecticidal, larvicidal, and antimicrobial activities (Zoubiri *et al.*, 2014).

The results of the present study indicated that essential oil from fennel seeds inhibited mycelium growth of FOL *in vitro* at 500 µL mL^{-1}. Inhibition of mycelium growth increased from 5 to 80% with increasing concentration of the essential oil. The essential oil showed significant activity against FOL sporulation. Recently, Bomfim Costa *et al.* (2015) concluded that the essential oil from *Ocimum selloi* and its major constituents (phenylpropanoids) including methyl chavicol, were efficient inhibitors of mycelium growth and conidium germination of *Moniliophthora perniciosa*. Similar results were obtained with essential oil from *Ocimum basilicum* which reduced mycelium growth of *Botrytis fabae* (Oxenahm *et al.*, 2005). In the present study, the essential oil showed antifungal activity against FOL, which could be attributed to the presence of phenylpropanoids such as *trans*-anethole. Huang *et al.* (2010) reported that antifungal activity of the essential oil from *Illicium verum* was attributed to the high content of *trans*-anethole. In contrast, the essential oil from fennel seeds has shown low antifungal activities *in vitro* and *in vivo* against cucumber root and stem rot caused by *Fusarium oxysporum* f. sp. *radicis-cucumerinum* (Soylu and Incekara 2017).

In the present study, the activity of fennel seed essential oil was also investigated *in planta* under greenhouse conditions. Curative and protective treatments with the oil were effective in reducing FOL infection, especially when essential oil was applied after inoculation. The least disease severity was observed at 28 DPI. These data suggest that all treatments exerted their greatest effects on early fungal invasion.

Fennel seed essential oil significantly increased total phenolic content in inoculated and non-inoculated tomato plants (treatments T3, T6 and T7) at 21, 28 or 35 DPI compared to T1, T2, T4 and T5. Similar results were reported by Akladious *et al.* (2015), Rajeswari (2014), Benhamou *et al.* (2000) and Pearce *et al.* (1998). These reports suggested that phenolic compounds may impede pathogen infection by increasing the mechanical strength of host cell walls resulting in the inhibition of pathogen invasion. Flavonoids are the polyphenolic compounds produced by plants for overcoming the oxidative stress in cells (Panche *et al.*, 2016). Our results showed that flavonoid content only increased in plants inoculated and treated with the essential oil (curative treatment) in comparison with either untreated inoculated plants or control plants. The increased content of phenol in tomato plants inoculated and treated with the essential oil may be due to induction of systemic resistance in the host plants (Rajeswari, 2014).

Total soluble sugar contents were increased in all treated plants at all time points (21, 28 or 35 DPI) compared to controls. The greatest level was recorded in

plants inoculated and treated with fungicide, followed by those treated with essential oil (curative treatment). These results are similar to those from other research. Nath *et al.* (2015) indicated that sugars enhanced the oxidative burst at early stages of infection, increasing lignification of host cell walls, stimulating synthesis of flavonoids, phenolics and phytoalexins, which suppress the pectolytic and cellulolytic enzymes that are essential for pathogenesis and induction of PR proteins.

In order to investigate the molecular mechanisms involved in fennel seed essential oil-induced resistance in tomato, the expression of the six defence-related genes, *SlChi, SlERF, SlPR1, SlLOX, SlWRKY*and *SlTLP*, was analyzed in treated tomato at different time points (12, 24, 48 or 72 HPT). After these time periods, the essential oil increased chitinase (*SlChi*) gene expression in infected tomato plants compared to the controls, while much lower levels have often been observed in other treatments. This could be related to the early response of tomato, which counteracts the penetration by FOL mycelium (Banani *et al*., 2018). Ahmed *et al.* (2012) reported that plant chitinases target fungus cell wall components as substrate that limits the invasion and growth of pathogens into their hosts. In sugar beet (Nielsen *et al.,* 1993), wheat (Anguelova *et al.,* 2001) and tomato (Lawrence *et al.,* 2000), high expression and strong induction of chitinase against phytopathogen systems were reported in resistant compared to susceptible varieties. Transgenic tobacco plants over-expressing the bean (*Phaseolus vulgaris*) chitinase gene showed increased resistance to *Rhizoctonia solani* infection and delayed development of disease symptoms (Broglie *et al.,* 1991). Transgenic grapevine plants overexpressing the rice chitinase gene had enhanced resistance against powdery mildew caused by *Uncinula necator* (Yamamoto *et al*., 2000). Early and high expression of *SlChi* in FOL-infected and essential oil treated tomato plants may affect the cell walls of germinating FOL conidia, releasing elicitors leading to the expression of host PR-genes and disease resistance.

The PR1 gene has been frequently used as a marker for salicylic acid-mediated disease resistance (Breen *et al*., 2017). Transgenic plants overexpressing *PR-1* exhibit enhanced resistance to numerous potential phytopathogens, including bacteria and fungi. Overexpression of pepper *PR-1* (*CABPR1*) in tobacco plants enhanced tolerance to *Phytophthora nicotianae*, *Ralstonia solanacearum* and *Pseudomonas syringae* pv. *tabaci* (Sarowar *et al.,* 2005). Transgenic tobacco plants overexpressing *PR*-1 showed increased tolerance to *Peronospora tabacina* and *Phytophthora nicotianae var. parasitica*, by exhibiting reduced disease symptoms (Alexander *et al*., 1993). Accumulation of *PR-1* transcripts was reported in broad bean plants inoculated with *Puccinia striiformis* f. sp. *tritici,* the causal agent of wheat stripe rust (Cheng *et al.,* 2012). In the present study, the greatest expression of *SlPR1* was found at 72 HPT in tomato plants treated with essential oil. We initially suggested that induction of *SlPR1* is characteristic of Systemic Acquired Resistance (SAR) in tomato. Our results for *SlPR1*gene expression in tomato leaves following treatment with the fennel seed essential oil (elicitor) support the hypothesis that induction of the SAR pathway (Bonasera *et al*., 2006) may be responsible for the phenotypic increase in tomato resistance to FOL.

High transcriptional levels of *PR-1*, *PR-2* and *PR-5* genes were reported in transgenic *Arabidopsis* plants expressing *AtWRKY18* or *AtWRKY70* (Li *et al.,* 2004). These data suggested that some *WRKY* genes could play a role in plant immunity and act as activators of fungal elicitor-induced genes (*PRs*) in plants. As for *SlPR1* expression, *SlWRKY* was differentially expressed, and the greatest level of *SlWRKY* was measured in the present study at 72 HPT, in tomato plants inoculated and treated with the essential oil. It is possible to hypothesize that *SlWRKY* might induce the expression of genes containing *W-box* in their promoters, including *SlPR1*. Similar observations were reported by Aamir *et al.* (2018). In root and leaf tissues of tomato infected with FOL, increased expression was found for *SolyWRKY4*, *SolyWRKY33*, *SolyWRKY37* at 24 and 48 HPT.

Based on amino acid composition, structure and biochemical function, PRs can be classified into 17 families. Among them, Thaumatin-like proteins (TLPs) are the products of a large and complex gene family involved in host defence. An lovar and Dermastia (2003) reported that specific TLPs have been shown to protect plants against osmotic stress and pathogen attack. Over-expression of the rice thaumatin-like protein (*Ostlp*) gene in transgenic cassava conferred enhanced tolerance to *Colletotrichum gloeosporioides* (Ojola *et al*., 2018). Transgenic wheat overexpressing *tlp-1* showed reductions in Fusarium head blight severity (Mackintosh *et al.,* 2007). *Brassica oleracea* TLPs (*BoTLP*5, 8 and 12) responded positively after *Pectobacterium carotovorum* subsp. *carotovorum* infection, and Ahmed *et al.* (2013) suggested these TLPs were useful resources for biotic stress resistance. Jiao *et al.* (2018) suggested that a Thaumatin-like protein from banana (*BanTLP*) inhibited *in vitro* conidium germination of *Penicillium expansum*. In the present study, *SlTLP* was differentially expressed after different treatments. This suggests that *SlTLP* may be responsive to FOL attack and that essential oil from fennel seeds may have acted as an elicitor.

Expression of *SlERF* was induced by inoculation with FOL at 24 HPT, and after treatment with the fennel essential oil at 72 HPT in inoculated tomato plants. At

24 and 72 HPT the high expression of *SlERF* could activate the expression of several ethylene-inducible genes, including *PR* genes through binding specifically the *GCC* box sequence of these gene families (Ohme-Takagi and Shinshi 1995). Previous investigations showed that increased expression of Ethylene-responsive element binding factor (ERF) genes in transgenic *Arabidopsis* or tobacco plants induced expression of various PR genes involved in increased resistance to microbial pathogens (Yi *et al.,* 2004; Zuo *et al*., 2007). Overexpression of *ERF1* conferred enhanced resistance to *Botrytis cinerea* and *Fusarium oxysporum* in transgenic *Arabidopsis* lines (Berrocal-Lobo *et al*., 2002).

Porta and Rocha-Sosa (2002) suggested that lipoxygenase (*LOX*) may be responsible for the synthesis of chemical compounds with plant defence signalling functions against biotic stresses. Wilson *et al.* (2001) also found that resistance to fungal pathogens in maize seeds was positively correlated with *LOX* transcript levels. *Botrytis cinerea* strongly induced the expression of *VvLOXC* and *VvLOXO* in *Vigna vinifera* (Podolyan *et al*., 2010). Transcriptome analyses by Wang *et al.* (2016) showed differential expression of several *LOX* genes after *Aspergillus flavus* infection. In the present study, expression of *SlLOX* steadily increased after FOL inoculation at 24 HPI, which suggested that *SlLOX* gene expression is related to the response to FOL infection. The greatest RNA level was observed at 48 HPI in tomato plants treated with the fennel essential oil. Expression patterns of the *SlLOX* gene differed significantly between treatments.

CONCLUSIONS

An essential oil from fennel seeds, applied at a concentration of 500 µL mL^{-1} had antifungal activities against FOL *in vitro* and *in planta* on tomato plants. The expression profile of the genes *SlChi, SlERF, SlPR1, SlLOX, SlWRKY*and *SlTLP* indicated that these genes may play crucial roles in the mechanism of resistance, whereby the essential oil reduced Fusarium wilt in tomato. Although further research is required to validate and fully understand of its mode of action, the essential oil from fennel seeds has promise as a promising biofungicide against FOL.

ACKNOWLEDGEMENTS

We thank the researchers and technicians of the Laboratory of Medicinal and Aromatic Plants (Biotechnology Center of Borj-Cedria-Tunisia) for their assistance in the identification of essential oil compounds by GC/MS analyses.

LITERATURE CITED

Aamir M., Singh V.K., Dubey M.K., Kashyap S.P., Zehra A., Surendra S., 2018. Structural and functional dissection of differentially expressed tomato WRKY transcripts in host defense response against the vascular wilt pathogen (*Fusarium oxysporum* f. sp. *lycopersici*). *PLoS ONE* 13(4), e0193922, doi: 10.1371/journal. pone.0193922

Ahmed N.U., Park J.I., Seo M.S., Kumar T.S., Lee I.H., Nou I.S., 2012. Identification and expression analysis of chitinase genes related to biotic stress resistance in Brassica. *Molecular Biology Reports* 39: 3649–3657.

Ahmed N.U., Park J.I., Jung H.J., Chung M.Y., Cho Y.G., Nou I.S., 2013. Characterization of thaumatin-like gene family and identification of *Pectobacterium carotovorum* subsp. *carotovorum* inducible genes in *Brassica oleracea*. *Plant Breeding and Biotechnology* 1: 111–121.

Akladious S.A., Isaac G.S., Abu-Tahon M.A., 2015. Induction and resistance against *Fusarium* wilt disease of tomato by using sweet basil (*Ocimum basilicum* L) extract. *Canadian Journal of Plant Science* 95: 689–701.

Alexander D., Goodman R.M., Gut-Rella M., Glascock C., Weymann K., Ryals J., 1993. Increased tolerance to two oomycete pathogens in transgenic tobacco expressing pathogenesis-related protein. *Proceedings of the National Academy of Sciences of the United States of America* 90: 7327–7331.

Amini J., Sidovich D.F., 2010. The effects of fungicides on *Fusarium oxysporum* f. sp. *Lycopersici* associated with *Fusarium* wilt of tomato. *Journal of Plant Protection Research* 50:172–178.

An lovar S., Dermastia M., 2003. The comparative analysis of osmotins and osmotin-like PR5 proteins. *Plant Biology* 5: 116–124.

Anguelova M. V., Westhuizen V.D., Pretorius Z.A., 2001. Beta-1,3-glucanase and chitinase activities and the resistance response of wheat to leaf rust. *Journal of Phytopathology* 149: 381–384.

Anwar F., Ali M., Hussain Shahid M., 2009. Antioxidant and antimicrobial activities of essential oil and extracts of fennel (*Foeniculum vulgare* Mill.) seeds from Pakistan. *Flavour and Fragrance Journal* 24: 170–176.

Arshad Z., Hanif M.A., Khan Qadri R.W., Khan M.M., 2014. Role of essential oils in plant diseases protec-

tion: A review. *International Journal of Chemical and Biochemical Sciences* 6: 11–17.

Banani H., Olivieri L., Santoro K., Garibaldi A., Gullino M.L., Spadaro D., 2018. Thyme and savory essential oil efficacy and induction of resistance against *Botrytis cinerea* through priming of defense responses in apple. *Foods* 7, doi: 10.3390/foods7020011

Benhamou N., Gagne S., Quere D.L., Dehbi L., 2000. Bacterial mediated induced resistance in cucumber beneficial effect of the endophytic bacterium *Serratia plymuthica* on the protection against infection by *Pythium ultimum*. *Phytopathology* 90: 45–46.

Bernath J., Nemeth E., Kattaa A., Hethelyi E., 1996. Morphological and chemical evaluation of Fennel (Foeniculum vulgare Mill.) population of different origin. *Journal of Essential Oil Research* 8: 247–253

Berrocal-Lobo M., Molina A., Solano R., 2002. Constitutive expression of ETHYLENE-RESPONSE-FACTOR1 in Arabidopsis confers resistance to several necrotrophic fungi. *Plant Journal* 29: 23–32.

Bettaieb I., Bourgou S., Sriti J., Msaada K., Limam F., Marzouk B., 2011. Essential oils and fatty acids composition of Tunisian and Indian cumin (*Cuminum cyminum* L.) seeds: a comparative study. *Journal of the Science of Food and Agriculture* 91: 2100–2107.

Bomfim Costa L.C., Pereira Pinto J.E.B., Vilela Bertolucci S.K., do Bomfim Costa J.C., Alves P.B., dos Santos Niculau E., 2015. In *vitro* antifungal activity of *Ocimum selloi* essential oil and methylchavicol against phytopathogenic fungi. *Revista Ciência Agronômica* 46: 428–435.

Bonasera J.M., Kim J.F., Beer S.V., 2006. PR genes of apple: identification and expression in response to elicitors and inoculation with *Erwinia amylovora*. *BMC Plant Biology* 6: 23, doi: 10.1186/1471-2229-6-23

Breen S., Williams S.J., Outram M., Kobe B., Solomon P.S., 2017. Emerging insights into the functions of pathogenesis related protein 1. *Trends in Plant Science* 22: 871–879.

Broglie K., Chet I., Holliday M., Cressman R., Biddle P., Broglie R., 1991. Transgenic plants with enhanced resistance to the fungal pathogen *Rhizoctonia solani*. *Science* 254: 1194–1197.

Chang S., Puryear J., Cairney J., 1993. A simple and efficient method for isolating RNA from pine trees. *Plant Molecular Biology Reporter* 11: 113–116.

Cheng Y., Zhang H., Yao J., Wang X., Xu J., Kang Z., 2012. Characterization of non-host resistance in broad bean to the wheat stripe rust pathogen. *BMC Plant Biology* 12: 96.

Damjanović B., Lepojević Z., Živković V., Tolić A., 2005. *Extraction of fennel (Foeniculum vulgare* Mill.) seeds with supercritical CO2: Comparison with hydrodistillation. *Food Chemistry* 92: 143–149.

Dihazi A., Serghini M.A., Jaiti F., Daayf F., Driouich A., El Hadrami I., 2011. Structural and Biochemical Changes in Salicylic-Acid-Treated Date Palm Roots Challenged with *Fusarium oxysporum* f. sp. Albedinis. *Journal of Pathogens* 2011: 9.

Dubois M., Gilles K.A., Hamilton J.K., Rebers P.A., Smith F., 1956. Colorimetric method for determination of sugars and related substances. *Analytical Chemistry* 28: 3506.

Falleh H., Ksouri R., Chaieb K., Karray-Bouraoui N., Trabelsi N., Abdelly C., 2008. Phenolic composition of *Cynara cardunculus* L. organs, and their biological activities. *Comptes rendus Biologies* 331: 372–379.

Faudale M., Viladomat F., Bastida J., Poli F., Codina C., 2008. Antioxidant Activity and Phenolic Composition of Wild, Edible, and Medicinal Fennel from Different Mediterranean Countries. *Journal of Agricultural and Food Chemistry* 56: 1912–1920.

Huang Y., Zhao J., Zhou L., Wang J., Gong Y., Jiang W., 2010. Antifungal Activity of the Essential Oil of *Illicium verum* Fruit and Its Main Component trans-Anethole. *Molecules* 15: 7558–7569.

Jiao W., Li X., Zhao H., Cao J., Jiang W., 2018. Antifungal activity of an abundant Thaumatin-Like Protein from banana against *Penicillium expansum*, and its possible mechanisms of action. *Molecules* 23: 1442. doi: 10.3390/molecules23061442

Kanoun K., Abbouni B., Bénine L., Benmahdi F.Z., Marouf B., 2014. Etude de l'éfficacité de l'extrait ethanolique d'écorces de *Punica Granatum* LINN sur deux souches phytopathogènes: *Ascocyhta rabiei* (PASS.) LABR et *Fusarium oxysporum* F.SP *Radicis lycopersici*. *European Scientific Journal* 10(12): 1857– 7881.

Lawrence C.B., Singh N.P., Qui J., Gardner R.G., Tuzun S., 2000. Constitutive hydrolytic enzymes are associated with polygenic resistance of tomato to *Alternaria solani* and may function as an elicitor release mechanism. *Physiological and Molecular Plant Pathology* 57: 211–220.

Lee S.C., Hwang B.K., 2005. Induction of some defense-related genes and oxidative burst is required for the establishment of systemic acquired resistance in *Capsicum annuum*. *Planta* 221 (6): 790–800.

Leslie J.F., Summerell B.A., 2006. The *Fusarium* laboratory manual. 1st ed. Blackwell Publishing Ltd, Oxford, London. doi: 10.1002/9780470278376.

Li J., Brader G., Palva E.T., 2004. The WRKY70 transcription factor: a node of convergence for jasmonate-mediated and salicylate-mediated signal in plant defense. *The Plant Cell* 16: 319–331.

Mackintosh C.A., Lewis J., Radmer L.E., Shin S., Heinen S.J., Muehlbauer G.J., 2007. Overexpression of defense response genes in transgenic wheat enhances resistance to Fusarium head blight. *Plant Cell Reports* 26: 479–488.

Mau J.L., Chao G.R., Wu K., 2001. Antioxidant properties of methanolic extracts from several ear mushrooms. J. Agric. *Food Chemistry* 49: 5461–5467.

Mimica-Dukic N., Kujundzic S., Sokovic M., Couladis M., 2003. Essential oil composition and antifungal activity of Foeniculum vulgare Mill obtained by different distillation conditions. *Phytotherapy Research* 17: 368–371.

Mohammadi S., Aminifard M.H., 2013. Inhibition of grey mould *in vitro and in vivo* with essential oil of fennel (*Foeniculum vulgare* L.). *Journal of Central European Agriculture* 14(1): 420–431.

Nath K., Solanky K.U., Mahatma M.K., Madhubala Swami R.M., 2015. Role of total soluble sugar, phenols and defense related enzymes in relation to banana fruit rot by *Lasiodiplodia theobromae* [(Path.) Griff. and Maubl.] during ripening. *Journal of Plant Pathology and Microbiology* 6: 299. doi: 10.4172/2157-7471.1000299

Nielsen K.K., Mikkelsen J.D., Dragh K.M., Bojsen K., 1993. An acidic class III chitinase in sugar beet: induction by *Cercospora beticola*, characterization, and expression in transgenic tobacco plants. *Molecular Plant-Microbe Interactions* 6: 495–506.

Ohme-Takagi M., Shinshi H., 1995. Ethylene-inducible DNA binding proteins that interact with an ethylene-responsive element. *The Plant Cell* 7: 173–182.

Ojola P.O., Nyaboga E.N., Njiru P.N., Orinda G., 2018. Overexpression of rice thaumatin-like protein (*Ostlp*) gene in transgenic cassava results in enhanced tolerance to *Colletotrichum gloeosporioides* f. sp. *manihotis*. *Journal of Genetic Engineering and Biotechnology* 16: 125–131.

Oxenahm S.K., Svobodal K.P., Walters D.R., 2005. Antifungal activity of the essential oil of basil (*Ocimum basilicum*). *Journal of Phytopathology* 153: 174–180.

Ozcan M., Chalchat J.C., Arslan D., Ates A., Unver A., 2006. Comparative essential oil composition and antifungal effect of bitter fennel (*Foeniculum vulgare* subsp. *piperitum*) fruit oils obtained during different vegetation. *Journal of Medicinal Food* 9: 552–561.

Panche A.N., Diwan A.D., Chandra S.R., 2016. Flavonoids: an overview. *Journal of Nutritional Science* 5: 1–15.

Pearce G., Marchand P., Griswold J., Lewis N.G., Ryan C.A., 1998. Accumulation of feruloyltyramine and p-coumaryltyramine in tomato leaves in response to wounding. *Phytochemistry* 47: 659–664.

Pino O., Sánchez Y., Rojas M.M., 2013. Plant secondary metabolites as an alternative in pest management. I: Background, research approaches and trends. *Revista de Protección Vegetal* 28 (2): 81–94.

Podolyan A., White J., Jordan B., Winefield C., 2010. Identification of the lipoxygenase gene family from *Vitis vinifera* and biochemical characterisation of two 13-lipoxygenases expressed in grape berries of Sauvignon Blanc. *Functional Plant Biology* 37: 767–784.

Porta H., Rocha-Sosa M., 2002. Plant lipoxygenase. Physiological and molecular features. *Plant Physiology* 130: 15–21.

Pusztahelyi T., Holb I.J., Pócsi I., 2015, Secondary metabolites in fungus-plant interactions. *Frontiers in Plant Science* 6: 573.

Rajeswari P., 2014. Role of phenols and antioxidant enzymes in biocontrol of *Fusarium oxysporum* causing fusarium wilt of *Arachis Hypogeae*. L (groundnut). *International Journal of Agricultural Science and Research* 4: 95–104.

Rehmana R., Hanifa M.A., Mushtaq Z., Al-Sadi A.M., 2016. Biosynthesis of essential oils in aromatic plants: A review. *Food Reviews International* 32: 117–160.

Roby M.H., Sarhana M.A., Selima K.A.H., Khalela K.I., 2013. Antioxidant and antimicrobial activities of essential oil and extracts of fennel (Foeniculum vulgare L.) and chamomile (*Matricaria chamomilla* L.). *Industrial Crops Products* 44: 437–445.

Rozen S., Skaletsky H.J., 2000. Primer3 on the WWW for general users and for biologist Programmers. In *Bioinformatics methods and protocols: methods in molecular biology* (S. Krawetz and S. Misener, ed.), *Humana Press*, Totowa, N.J.; 365–386.

Salim H.A., Salman I.S., Jasim B.N., 2016. IPM Approach for the management of wilt disease caused by *Fusarium oxysporum* f. sp. *lycopersici* on tomato (*Lycopersicon esculentum*). *Journal of Experimental Biology and Agricultural Sciences* 4: 742–747.

Sarowar S., Kim Y.J., Kim E.N., Kim K.D., Hwang B.K., Shin J.S., 2005. Overexpression of a pepper basic pathogenesis-related protein 1 gene in tobacco plants enhances resistance to heavy metal and pathogen stresses. *Plant Cell Reports* 24: 216–224.

Schmittgen T.D., Livak K.J., 2008. Analyzing Real-Time PCR Data by the Comparative CT Method. *Nature Protocols* 3: 1101–1108.

Song W., Zhou L., Yang C., Cao X., Zhang L., Liu X., 2004. Tomato *Fusarium* wilt and its chemical control strategies in a hydroponic system. *Crop Protection* 23: 243–247.

Soylu S., Yigitbas H., Soylu E.M., Kurt S., 2007. Antifungal effects of essential oils from oregano and fennel on Sclerotinia sclerotiorum. *Journal of Applied Microbiology* 103:1021–1030.

Soylu E.M., Incekara R., 2017. Biofungicidal activities of plant essential oils against root and stem rot disease caused by *Fusarium oxysporum* f. sp. *radicis-cucumerinum*. *Journal of Plant Pathology* 99: 437–444.

Wang H., lei Y., Wan L., Yan L., Lv J., Liao B., 2016. Comparative transcript profiling of resistant and susceptible peanut post-harvest seeds in response to aflatoxin production by *Aspergillus flavus*. *BMC Plant Biology* 16: 54.

White T.J., Bruns T., Lee S., Taylor J.W., 1990. Amplification and direct sequencing of fungal ribosomal RNA genes for phylogenetics. In PCR Protocols: A Guide to Methods and Applications Edited by: Innis M.A., D.H. Gelfand, J.J. Sninsky and T.J. White. New York: Academic Press Inc: 315–322.

Wilson R.A., Gardner H.W., Keller N.P., 2001. Cultivar-dependent expression of a maize lipoxygenase responsive to seed infesting fungi. *Molecular Plant-Microbe Interactions* 14: 980–987.

Yamamoto T., Iketani H., Leki H., Nishizawa Y., Notsuka K., Matsuta N., 2000. Transgenic grapevine plants expressing a rice chitinase with enhanced resistance to fungal pathogens. *Plant Cell Reports* 19: 639–646.

Yang D.L., Yao J., Mei C.S., Tong X.H., Zeng L.J., He S.Y., 2012. Plant hormone jasmonate prioritizes defense over growth by interfering with gibberellin signaling cascade. *Proceedings of the National Academy of Sciences of the United States of America* 109: 1192–1200.

Yi S.Y., Kim J.H., Joung Y.H., Lee S., Kim W.T., Choi D., 2004. The pepper transcription factor CaPF1 confers pathogen and freezing tolerance in Arabidopsis. *Plant Physiology* 136: 2862 –2874.

Zake M., 2016. Natural plant products as eco-friendly fungicides for plant diseases control- A review. *The Agriculturists* 14, 134–141.

Zoubiri S., Baaliouamer A., Seba N., Chamouni N., 2014. Chemical composition and larvicidal activity of Algerian Foeniculum vulgare seed essential oil. *Arabian Journal of Chemistry* 7: 480–485.

Zoubiri S., Baaliouamer A., Seba N., Chamoun N., 2014. Chemical composition and larvicidal activity of Algerian Foeniculum vulgare seed essential oil. *Arabian Journal of Chemistry* 7: 480–485.

Zuo K.J., Qin J., Zhao J.Y., Ling H., Zhang L.D., Tang K.X., 2007. Over-expression GbERF2 transcription factor in tobacco enhances brown spots disease resistance by activating expression of downstream genes. *Gene* 391: 80–90.

Phytopathologia Mediterranea
The international journal of the
Mediterranean Phytopathological Union

Firenze University Press
www.fupress.com/pm

Research Paper

Evaluation of different carbon sources for anaerobic soil disinfestation against *Rhizoctonia solani* on lettuce in controlled production systems

Giovanna GILARDI[1,*], Massimo PUGLIESE[1,2], Maria Lodovica GULLINO[1,2], Angelo GARIBALDI[1]

[1] *Centre for Innovation in the Agro-Environmental Sector, AGROINNOVA, University of Torino, Largo Braccini 2, 10095 Grugliasco (TO), Italy*
[2] *Department of Agricultural, Forest and Food Sciences (DISAFA), University of Torino, Largo Braccini 2, 10095 Grugliasco (TO), Italy*
*Corresponding author: giovanna.gilardi@unito.it

Summary. Effects of anaerobic soil disinfestation (ASD) on *Rhizoctonia solani* basal rot of lettuce were assessed considering: two soil types; different C-sources; different temperature regimes; two treatment durations; and two lettuce crop cycles, in the presence of a high disease incidence from artificial infestation with the pathogen. C-source, temperature, and incubation period, and their interaction, affected the efficacy of the ASD treatment for the lettuce–*R. solani* pathosystem, with differences depending on the soil type. *Brassica carinata* pellets, used as a C-source, reduced incidence of Rhizoctonia basal rot in the first crop cycle by 50 to 69% in a peat soil after 3 weeks of treatment at 21°C, and by 52 to 60% after 3 weeks of treatment at 26 or 31°C, compared to the inoculated and untreated experimental controls without anaerobic conditions. The best disease reduction was provided by *B. carinata* pellets applied, under anaerobic conditions, to peat soil (79% efficacy) and a sandy loam soil (100% efficacy) kept at 31°C for 6 weeks. Generally, ASD based on *B. carinata* pellets provided greater disease reduction in the first crop cycle than the second, with the only exception being for results achieved in both soils incubated for 6 weeks at 21, 26 and 31°C. Wild rocket used as a C-source provided the greatest disease reduction (78–83%) on plants grown in peat soil at the first crop cycle after 6 weeks of the ASD treatment at 31°C, while wild rocket provided disease reduction of 29 and 50% when mixed with the sandy-loam soil under the same conditions for 6 weeks. The efficacy of the ASD treatment with compost was improved in the second crop cycle, compared to the first, resulting in the greatest disease reduction (52 and 66% efficacy) reached in the sandy-loam soil incubated for 3 weeks at 21°C, and 63% efficacy in peat soil previously treated for 6 weeks at 26 and 31°C. However, slight reductions in lettuce plant development was generally evident in the first crop cycle, which could be due to differences in efficacy of the tested ASD treatments and to phytotoxicity. The greatest yield from sandy loam soil was obtained for the *B. carinata* pellets and wild rocket at 26 and 31°C in the second cultivation cycle. Partial efficacy of ASD does not justify the adoption of this method against *R. solani* on lettuce under intensive crop systems. However, ASD based on *Brassicaceae* and compost as carbon source applied in a sandy-loam soil may be valuable for reducing *R. solani* incidence, at lower temperatures than those required for soil solarisation or biosolarisation.

Keywords. *Lactuca sativa*, pre-plant treatments, soil-borne pathogens, biological soil disinfestation.

OPEN ACCESS

Citation: G. Gilardi, M. Pugliese, M.L. Gullino, A. Garibaldi (2020) Evaluation of different carbon sources for anaerobic soil disinfestation against *Rhizoctonia solani* on lettuce in controlled production systems. *Phytopathologia Mediterranea* 59(1): 77-96. doi: 10.14601/Phyto-10911

Accepted: December 19, 2019

Published: April 30, 2020

Data Availability Statement: All relevant data are within the paper and its Supporting Information files.

Competing Interests: The Author(s) declare(s) no conflict of interest. The Author Massimo Pugliese declares he has a financial interest (shareholder) in AgriNewTech, the company that provided the compost tested in this research.

Editor: Jean-Michel Savoie, INRA Villenave d'Ornon, France.

INTRODUCTION

Anaerobic soil disinfestation (ASD) is a method based on the anaerobic decomposition of organic matter, and this was developed as a possible alternative to the use of fumigants (Shennan *et al*., 2014). ASD is based on two systems, one developed in the Netherlands, as a biological soil disinfestation (Blok *et al*., 2000), and the other in Japan, as a soil reductive sterilisation process (Shinmura, 2004). This is applied in Japan, the Netherlands, the United States of America, and Argentina, to control of different pathogens and pests under practical conditions (Rosskopf *et al*., 2015; Shrestha *et al*., 2016; Shennan *et al*., 2018).

The ASD process is based on the addition of labile carbon sources to the soil to stimulate microbial growth and respiration, followed by irrigation to fill the water pore spaces, and covering the soil with plastic films, to reduce gas exchange. This then permits diffusion through the soil of by-products of decomposition, as well as reduced soil oxygen (Butler *et al*., 2012a, 2012b; Shennan *et al*., 2014). These treatments establish anaerobic conditions, as the aerobic microorganisms consume the remaining oxygen present in the soil, and the microbial communities shift to facultative and obligate anaerobes (Mazzola *et al*., 2007; Momma *et al*., 2010; Mowlick *et al*., 2012, 2013; Huang *et al*., 2016; Hewavitharana and Mazzola, 2016). After the anaerobic conditions have been maintained for a period, depending on soil temperature and the type of C-source used, the soil is uncovered to allow oxygen to return, stimulating the degradation of the remaining anaerobic decomposition by products (Shennan *et al*., 2014). ASD is effective against soil-borne pathogens and pests through different mechanisms, including production of organic acids via anaerobic decomposition of the added C, production of volatiles (Okazaki and Nose, 1986; Momma *et al*., 2006; Mazzola and Hewavitharana, 2014; Huang *et al*., 2016), and biocontrol activity of fungal and bacterial communities that grow during the process (Momma *et al*., 2010; Mazzola and Manici, 2012; Mowlick *et al*., 2012, 2013; Runia *et al*., 2012, 2014; Butler *et al*., 2014 a, 2014b).

Most studies and practical applications of ASD have dealt with crops such as asparagus, tomato, pepper, eggplant, cucumber, melon, spinach, strawberry, cut flowers and fruit trees (Blok *et al*., 2000; Mazzola *et al*., 2001; Goud *et al*., 2004; Messiha *et al*., 2007; Yossen *et al*., 2008; Lamers *et al*., 2010; Mazzola and Manici, 2012; Butler *et al*., 2012 a, 2012b; Mowilck *et al*., 2013; Hewavitharana and Mazzola, 2016; Serrano-Pérez *et al.,* 2017; Shennan *et al*., 2014, 2018). The C-sources used generally depends on the availability of inexpensive or waste materials in the different locations, and there is variability among countries. Among the tested C-sources, the most common have been: wheat bran (Yossen *et al*., 2008; Momma *et al*., 2010), rice bran (Shennan *et al*., 2010; Strauss and Kluepfel, 2015), ryegrass (Blok *et al*., 2000; Goud *et al*., 2004), molasses (Momma *et al*., 2010, 2013; Butler *et al*., 2012 a), diluted ethanol (Momma *et al*., 2010; Hewavitharana and Mazzola, 2013), green manure (Butler *et al*., 2012b; Mowilck *et al*., 2013; Hewavitharana *et al*., 2014; McCarty *et al*., 2014), composted broiler litter (Hewavitharana *et al*., 2014; Di Gioia *et al*., 2017), and residues of different cover crops. Amendment rates with these materials have varied between 3 to 90 t ha^{-1} (Shrestha *et al*., 2016).

ASD has not yet been practically applied in Italy, and there is still a need to adapt this soil disinfestation method to the cultural and environmental conditions of this country. The choice of effective, cheap and easily available C-sources is of particular importance. Although a number of studies have reported effects of ASD on soil-borne pathogens of many crops, no studies have been carried out on leafy vegetables. These represent an intensive production system in many countries, and are particularly important in Italy, both in open fields and protected systems (Gullino *et al*., 2019). There is no standardised ASD method to determine the best combination for soil-borne pathogen control, and several factors, such as the C-source, the rate of application, the treatment duration, the temperature under the plastic covers or the type of soil, can influence the effectiveness of this disease management method.

Rhizoctonia solani (Kühn), the soil-borne fungus that causes basal rot of a broad range of hosts, is one of the most important pathogens affecting lettuce production in Italy. This pathogen is also important in most countries where lettuce is grown (Blancard *et al*., 2003; Barrière *et al*., 2014; Gullino *et al*., 2019).

The present study aimed to evaluate effects of ASD on the *R. solani*-lettuce pathosystem, under controlled conditions, and considering several factors. These included: i) different carbon sources; ii) different temperature regimes; and iii) two treatment durations. The effects on disease incidence and lettuce fresh weight were evaluated in two soil types considering two crop cycles planted in an ASD-treated soil, and in reference experimental controls with or without anaerobiotic conditions. Results obtained have been compared with those from tolclofos-methyl, the available fungicide for control of *R. solani* basal rot of lettuce.

MATERIALS AND METHODS

Experimental layout

Two trials were carried out at the Agroinnova Centre of Competence of the University of Torino, Grugliasco, under controlled conditions. ASD treatments were applied in four growth chambers and in two greenhouse compartments (64 m^2 each), to test the treatment efficacies against *R. solani*. Different carbon sources, including compost (Comp), *Diplotaxis tenuifolia* green manure (WR) and *Brassica carinata* pellets (BCp), and two types of soil (peat and sandy-loam) were used, at different temperatures (21, 26 or 31°C) and two durations (3 and 6 weeks) as the main experiment factors. The ASD treatments were carried out in plastic containers (capacity, 40 L; dimensions 50 × 40 × 20 cm), soil surface area (2,000 cm^2) using two types of soil: i) a mixture (50:50 v:v) of a sandy loam soil (sand : silt : loam, 68.16 : 10.7 : 21.1; pH 7.9; organic matter 0.94%), and perlite (Perlite Italiana Agrilit 3); ii) a peat substrate (Tecno 2, 70% white peat and 30% clay; pH 6.1–6.5; N 110-190 mg L^{-1}; P_2O_5 140–230 mg L^{-1}; K_2O 170–280 mg L^{-1}, Turco Silvestro terricci). The plastic containers were filled with 30 L of the treated or untreated soil distributed in a layer of 15 cm deep.

At the end of each ASD incubation period carried out in the growth chambers, the treated and untreated soil from each container was redistributed into four 12 L capacity plastic pots and kept in two compartments in a greenhouse at temperatures ranging from 27 to 30°C, and relative humidity (RH) of 70-80 %. The pots were arranged on benches in a completely randomized block design with one pot serving as a replicate, using four replicates per treatment. The experimental design of the trials is illustrated in Figure 1.

ASD treatment simulated under growth chamber conditions, and measurements

The ASD treatments started immediately, under controlled conditions in the growth chambers, after addition of the selected C-sources to the soil, and application of irrigation water at 17.0 L per container for the peat soil, or 7.0 L per container for the sandy loam soil. These irrigation rates were estimated by adding excess water to the respective soils and then allowing water to drain for 24 h, to simulate saturation conditions. The soil was then covered with standard polyethylene (PE) sheets (50 µm thick), immediately after the application of the different carbon sources and water, and the containers were moved to the growth chambers to start the ASD treatments at different temperatures.

The soils were incubated for 3 or 6 weeks at constant temperatures of 21°C (Trials 1 and 2), and at 26 (Trial 1) or 31°C (Trial 2) (Figure 1). These temperatures were selected to simulate typical soil conditions in the Mediterranean area during spring and summer (Tamietti and Garibaldi, 1987). The soil temperatures were monitored using a sensor data logging system (Digital Data Logger EM50; Decagon Devices). Redox potential values were taken manually each day (5 d per week, for 3 or 6 weeks), using an ORP/temp pen style meter (VWR International) at three positions in each container. The temperature and redox sensors were placed at the centre of each container at a depth of 10 cm.

The ORP values of the soil redox potential, expressed in mV, were converted to Eh mV, related to the redox potential of a standard hydrogen electrode, by adding 200 mV (Fiedler *et al*., 2007). To calculate the cumulative soil anaerobic conditions, the absolute values of the difference between each redox value and the critical redox potential (CEh), calculated using the formula: 595 mV – (60 mV × soil pH measured at the end of the ASD treatment), were summed for redox values below CEh. Since the recorded data were the average daily redox potential values, the values obtained were multiplied by 24 h and converted into hourly units (mVh), then summed for each day. The cumulative soil anaerobic conditions (mVh) over the 3 or 6 weeks of the ASD treatments was then obtained (Rabenhorst and Castenson, 2005; Butler *et al*., 2012 a; b).

Artificial infestation with the pathogen

One isolate (code AG2-L) of *R. solani,* obtained from affected lettuce, was used. The isolate was grown on PDA plates for 10 d. Flasks (1 L capacity), containing 300 g of sterilised wheat kernels, were inoculated with 5 mm diam. agar disks from *R. solani* PDA colonies, and were then maintained for 20 d at 23°C. Soils were infested with the pathogen by mixing 0.5 g L^{-1} of the infested kernels, immediately before commencing the ASD treatments, using a total of 15 g of inoculum per container. The same amount of non-infested kernels was used for the non-inoculated experimental controls.

Carbon sources

Four carbon sources, selected among a number of different sources used in preliminary trials, were tested, and these are reported hereafter at selected field doses selected, according to the recommendations by Butler *et al*. (2014b) for moderate soil temperature:

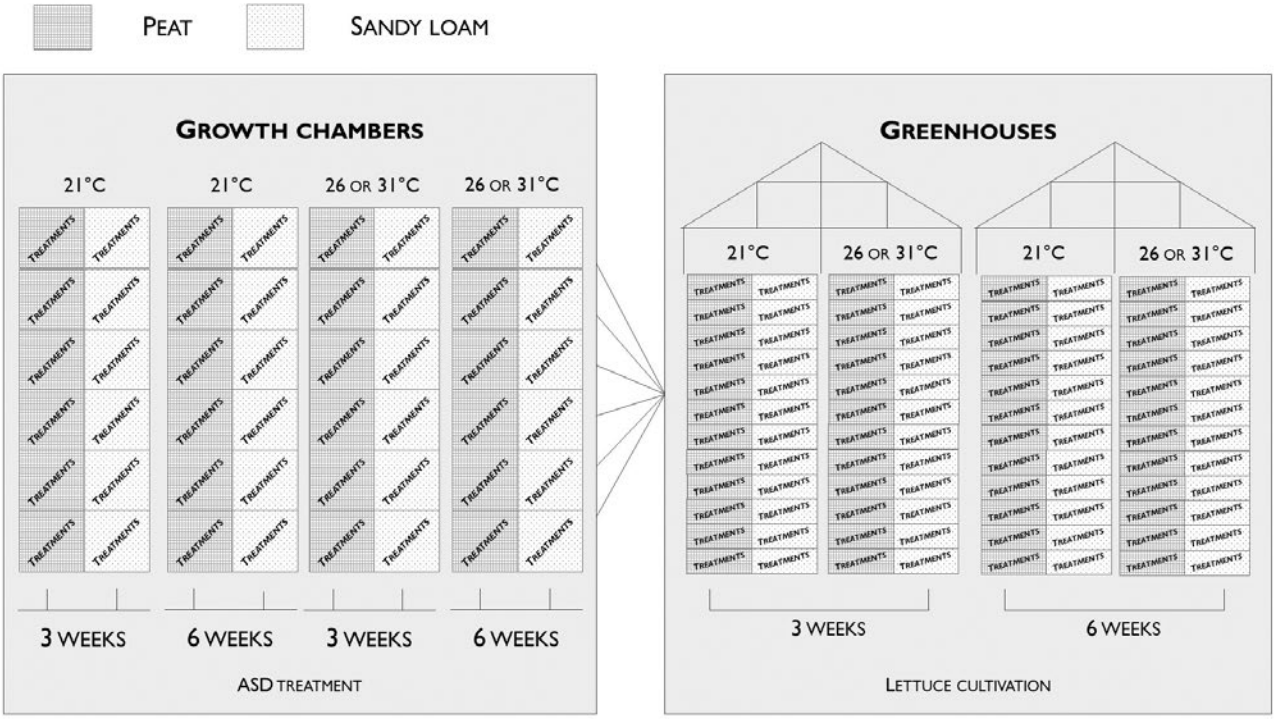

Figure 1. Experimental protocols utilized to assess the effect of anaerobic soil disinfestation (ASD) for the control of *Rhizoctonia solani* on lettuce. Assays were conducted in four growth chambers and in two greenhouse compartments during two trials carried out in peat and sandy-loam soils.

i) WR, wild rocket (*Diplotaxis tenuifolia*, C/N 6.9) applied as a green manure crop, at 10 g L^{-1}, equivalent to 15 t ha^{-1} 15 cm depth, or at 20 g L^{-1}, equivalent to 30 t ha^{-1};

ii) BCp, *Brassica carinata* defatted pellet ('Biofence': C/N 10.96, organic N 6%, P 2.2%, K 2%, organic C 52%: Triumph), mixed into the soil at 10 g L^{-1}, equivalent to 15 t ha^{-1} 15 cm depth;

iii) Comp, compost prepared from green wastes in a dynamic industrial treatment system, and passed through a 20 mm sieve (Ant's Compost V, lot number N-2015, AgriNewTech: C/N 16.5, pH 6.58; total N 0.971%; total C 16%; P_2O_5 0.57%; K_2O 1.35%), mixed into the soil at 10 g L^{-1}, equivalent to 15 t ha^{-1} 15 cm depth.

Diplotaxis tenuifolia, 'Grazia', was sown at 1-1.2 g m^{-2} in plastic pots filled with sterile blonde sphagnum peat, to produce wild rocket green manure. The pots were kept in a greenhouse at 24-26°C for 40–50 d (50% flowering). The plants were harvested, weighed, and cut into 1 to 3 cm pieces and incorporated into the soil, immediately before commencing the ASD treatment.

Experimental control treatments

Tolclofos-methyl TM (Rizolex, BASF Crop Protection, 50% a.i.) was used at 2 g m^{-2} in both trials as a fungicide experimental control, because this compound is effective for management of basal rot of lettuce, caused by *R. solani* (Sneh *et al*., 1996). In Trial 2, the commercial formulation 'Biofence' based on *Brassica carinata* defatted pellets was applied without anaerobic conditions, at the same rate used for the ASD treatment, as reference control (BCp-No anaerobic control).

Two inoculated untreated controls, without any carbon source incorporated into the soil but with differences in the volume of water used, were prepared:

i) a standard untreated control (INT-Standard control): irrigated to field soil capacity;

ii) an INT-Anaerobic control: irrigated to exceed field capacity, to provide reducing conditions.

In the inoculated and non-inoculated untreated controls (INT and NINT) as well as for the BCp-No anaerobic control, water equivalent to the moisture capacity of the peat soil (8.0 L per container) and sandy loam soil (5.0 L per container) was used. Two non-inoculated control pots, which received sterile wheat kernels, under an anaerobic condition (NINT- Anaerobic control) and under a standard condition (NINT-Standard control), were also included.

Both INT and NINT standard and anaerobic controls as well TM and BCp- No anaerobic control were

each covered with a transparent polyethylene film (50 µm thick) for the 3 or 6 weeks time treatments.

Effects of ASD treatment in greenhouse trials

At the end of the ASD treatments carried out in growth chambers, the soil was transferred into 12 L capacity pots and was then aerated for 1 week before planting lettuce 'Elisa' (20 plants per pot). Lettuce seedlings were transplanted 20 to 25 day after sowing into the treated and untreated soil in two subsequent crop cycles.

Fertilizer equivalent to 20 kg ha^{-1} (N 18; P 18; K 18 + 2 MgO, Osmoform) was applied to the soil surfaces at the end of the first cycle in both trials.

Disease incidence (percent dead plants) was evaluated each week by counting the collapsed and dead plants that showed brown, sunken lesions and rotting at the base of the crowns. Dead plants were removed and randomly selected to perform pathogen isolation. The plants were removed from the soil at the end of each cropping cycle in both trials, at the full maturity stage, to evaluate the final Rhizoctonia basal rot incidence, and the fresh weights of all healthy plants were determined.

Data analyses

The experiments were carried out and analysed as two independent trials, at the end of the first and second crop cycles (Tables 1, 2 and 3). Data of mean accumulated soil anaerobic conditions values were subjected to analysis of variance (ANOVA) in the SPSS software, with means separation based Tukey's test ($P \leq 0.05$). Disease incidence *(DI)* and fresh weights (*FW*) of the healthy lettuce plants were subjected to ANOVA using the univariate procedure in the SPSS software 25.0 statistical package. Levene's test was used to test the homogeneity of variances. The *DI* data, expressed as a percentage of affected plants, were arc-sin-transformed to stabilise the variances and normalise their distribution. The effect of each carbon source, temperature, ASD duration (3 or 6 weeks) for two types of soil (peat or sandy-loam), and their interactions for both crop cycles, were evaluated as main factors. When the effects of the tested factors were significant ($P \leq 0.05$) and interactions were observed among the considered factors (Table 3), one-way ANOVA was carried out to evaluate the combined effects of the involved factors on the percent disease incidence and plant fresh weights. The means were separated using Tukey's test ($P \leq 0.05$) when the multiple comparisons of the considered factors were shown to be significantly related.

Table 1. List and dates of the different operations carried out in greenhouse experiments.

Operations	Trial 1	Trial 2
Artificial soil infestation with *Rhizoctonia solani*	17/01/16	31/05/16
Start of the ASD treatments lasting 6 weeks	18/01/16	1/06/16
Start of the ASD treatments lasting 3 weeks	8/02/16	22/06/16
Lettuce transplant (Cycle I)	11/03/16	20/07/16
Disease assessments	4/04/16	10/08/16
Lettuce fresh weights determined (Cycle I)	4/04/16	10/08/16
Lettuce transplant (Cycle II)	8/04/16	11/08/16
Disease assessments	10/5/16	20/09/16
Lettuce fresh weights determined (end of Cycles I and II)	10/05/16	20/09/16

RESULTS

Impacts of the soil treatments on soil parameters

On the basis of the oxidation-reduction potential (ORP), the reduced conditions in the ASD treatments of the peat and sandy-loam soils were generally reached within 4 to 5 d for all the tested temperatures. The lowest cumulative soil anaerobic conditions indicated by the redox potential were observed in the no C source control (INT-Standard control) in the sandy-loam soil at 21°C and 26°C for both 3 and 6 weeks, and in the peat soil at 21°C for 3 weeks, while increased values were observed in the INT- control under anaerobic conditions for 6 weeks at 31°C (85,766 mVh) (Table 2). The greatest levels of cumulative anaerobic conditions were observed in the peat soil treated with WR at 15 g ha^{-1} for 6 weeks at 26°C in Trial 1 (211,935 mVh), and at 30°C for 6 weeks in Trial 2 (180,162 mVh at 15 t ha^{-1} and 184,683 mVh at 30 t ha^{-1}). The ASD based-WR treatment at 15 ha^{-1} in the sandy-loam soil at 31°C (trial 2) provided cumulative anaerobic conditions of 82,788 mVh, and at 30 t ha^{-1}, 119,066 mVh. At 21°C cumulative anaerobic conditions were 43,947 mVh from 15 t ha^{-1} and 72,440 mVh from 30 t ha^{-1}. The cumulative anaerobic conditions calculated for 6 weeks from the ASD based-BCp treatment were different among the trials, and the temperature conditions tested (from 106,054 to 176,736 mVh in the peat soil and from 86,950 to 112,968 mVh in the sandy-loam soil), with significantly lower mVh values for 3 weeks of ASD duration. Three weeks of ASD based-Comp in the peat soil at 21°C provided cumulative anaerobic conditions of the soil between 1,206 and 4,803 mVh and of

Table 2. Average soil pH and the mean cumulative soil redox potential (mVh) indicating anaerobic conditions, for the peat and sandy-loam soils after different soil treatments. Standard errors are indicated.

Carbon source[a], dosage	ASD	Treatment duration (weeks)	Trial 1				Trial 2			
			21°C		26°C		21°C		31°C	
			pH	mVh	pH	mVh	pH	mVh	pH	mVh
Peat soil										
Comp, 15 t ha^{-1}	+	3	6.6	1,206 ± 603 b[c]	6.7	12,532 ± 889 de	6.6	4,803 ± 109 e	6.6	13,667 ± 837 de
BCp, 15 t ha^{-1}	+	3	7.1	41,235 ± 3,405 ab	7.2	34,666 ± 1,987 cd	6.8	27,708 ± 970 c	6.9	50,409 ± 1,705 c
WR, 15 t ha^{-1}	+	3	7.0	25,330 ± 7,491 ab	7.0	33,646 ± 6,014 cd	6.4	30,916 ± 371 c	6.6	30,696 ± 1,242 cd
WR, 30 t ha^{-1}	+	3	- [b]	-	-	- -	6.3	31,373 ± 1,028 c	6.7	47,706 ± 3,148 c
TM, 2 gm^{-2}	-	3	6.6	0 ± 0 b	6.8	0 ± 0 e	6.8	0 ± 0 e	6.8	0 ± 0 e
BCp, 15 t ha^{-1}- No anaerobic control	-	3	-	-	-	- -	6.8	0 ± 0 e	6.9	0 ± 0 e
INT- Anaerobic control	+	3	6.8	650 ± 620 b	6.6	4,811 ± 1,941 e	6.5	1685 ± 822 e	6.5	5,267 ± 382 e
INT- Standard control	-	3	6.4	0 ± 0 b	5.9	0 ± 0 e	6.7	0 ± 0 e	6.7	0 ± 0 e
C, 15 t ha^{-1}	+	6	6.6	25,972 ± 1,482 ab	6.6	46,495 ± 5,078 c	6.6	18,205 ± 1,267 d	6.5	95,550 ± 4,349 b
BCp, 15 t ha^{-1}	+	6	6.9	106,054 ± 4,167 a	7.1	145,895 ± 1,0183 b	6.9	135,800 ± 1,094 a	6.7	176,736 ± 1,094 a
WR, 15 t ha^{-1}	+	6	6.7	89,537 ± 3,866 a	6.9	211,935 ± 8,192 a	6.6	92,639 ± 5,773 b	6.6	180,162 ± 4,002 a
WR, 30 t ha^{-1}	+	6	-	-	-	- -	6.7	101,487 ± 2,181 b	6.5	184,683 ± 7,705 a
TM, 2 gm^{-2}	-	6	6.7	0 ± 0 b	6.6	0 ± 0 e	6.8	0 ± 0 e	6.6	0 ± 0 e
BCp, 15 t ha^{-1}- No anaerobic control	-	6	6.6	0 ± 0 b	6.7	0 ± 0 e	6.9	0 ± 0 e	6.7	0 ± 0 e
INT-Anaerobic control	+	6	6.7	21,770 ± 650 ab	6.5	21,107 ± 1,049 de	6.5	23,949 ± 1,562 cd	6.5	85,766 ± 5,795 b
INT-Standard control	-	6	6.3	0 ± 0 b	6.1	0 ± 0 e	6.7	0 ± 0 e	6.6	0 ± 0 e
Sandy-loam soil										
Comp, 15 t ha^{-1}	+	3	7.8	1,017 ± 709 b	7.3	2,606 ± 1,598 c	7.8	1,914 ± 475 d	7.9	2,805 ± 1,426 c
BCp, 15 t ha^{-1}	+	3	7.4	10,822 ± 4,962 b	7.3	23,579 ± 2,335 bc	7.5	11,315 ± 2,507 cd	7.8	20,403 ± 3,342 c
WR, 15 t ha^{-1}	+	3	7.0	10,980 ± 1,371 b	7.3	22,110 ± 971 bc	7.7	10,937 ± 4,042 cd	7.9	23,491 ± 2,790 c
WR, 30 t ha^{-1}	+	3	-	-		-	7.6	12,474 ± 4,305 cd	7.6	25,470 ± 2,221 c
TM, 2 gm^{-2}	-	3	7.7	0 ± 0 b	7.8	0 ± 0 c	7.1	0 ± 0 d	7.8	0 ± 0 c
BCp, 15 t ha^{-1}- No anaerobic control	-	3	-	-		-	7.8	0 ± 0 d	7.9	0 ± 0 c
INT-Anaerobic control	+	3	7.8	583 ± 333 b	7.8	1,158 ± 657 c	7.9	36 ± 36 d	7.9	1,272 ± 756 c
INT-Standard control	-	3	7.8	0 ± 0 b	7.8	0 ± 0 c	7.9	0 ± 0 d	7.8	0 ± 0 c
Comp, 15 t ha^{-1}	+	6	7.1	8,632 ± 1,495 b	7.1	15,516 ± 4,228 c	7.9	15,485 ± 1,842 cd	7.5	31,817 ± 1,593 bc
BCp, 15 t ha^{-1}	+	6	7.2	86,950 ± 3,994 a	7.0	112,968 ± 5,599 a	7,8	109,688 ± 7,260 a	7.6	88,945 ± 3,893 a
WR, 15 t ha^{-1}	+	6	7.4	78,396 ± 5,631 a	7.2	101,994 ± 4,806 a	7.9	43,947 ± 16,737bc	7.7	82,788 ± 796 ab
WR, 30 t ha^{-1}	+	6		-		-	7.8	72,440 ± 25,320ab	7.7	119,066 ± 13,879 a
TM, 2 gm^{-2}	-	6	8	0 ± 0 b	7.7	0 ± 0 c	7.8	0 ± 0 d	7.8	0 ± 0 c
BCp, 15 t ha^{-1}- No anaerobic control	-	6	8	0 ± 0 b	7.5	0 ± 0 c	7.7	0 ± 0 d	8.0	0 ± 0 c
INT-Anaerobic control	+	6	7.4	353 ± 353 b	7.5	1916 ± 1,057 c	7.9	2,311 ± 643 cd	7.9	2,372 ± 754 c
INT-Standard control	-	6	-	0 ± 0 b	7.7	0 ± 0 c	7.8	0 ± 0 d	7.7	0 ± 0 c

[a] Comp: Compost; BCp: *Brassica carinata* pellet; WR: *Diplotaxis* green manure; TM: Tolclofos methyl; INT-anaerobic control: Inoculated untreated control with anaeorobic conditions; INT-Standard control: Inoculated untreated control without aneorobic conditions.
[b] – indicates not tested.
[c] Means accompanied by the same letter are not significantly different ($P \leq 0.05$), Tukey test.

between 1,017 and 1,914 mVh in the sandy-loam soil. The cumulative anaerobic conditions of the ASD based-Comp were increased in the peat soil at 26°C and 31°C after 3 weeks to, respectively, 12,532 mVh and 13,667 mVh, while the cumulative values in the sandy loam soil after 3 weeks from this treatment at 26°C and 31°C

were, respectively, 2,606 and 2,805 mVh (Table 2). These values were greater in the sandy-loam soil after 6 weeks of ASD application with values between 15,516 mVh at 26°C and 31,817 mVh at 31°C.

The pH values of the soils were similar in both trials immediately after the ASD treatment. The pH increased from 6.4 to 6.7-7.1 after the BCp and WR green manure treatments were used as the C-sources and mixed in the peat soil, and were slightly reduced from 7.8 to 7.5-7.7 after the Brassica carbon sources were applied to the sandy-loam soil, compared to the INT-Standard control (Table 2).

Effects of soil treatments on the pathogen and plant fresh weights

The soil type and crop cycle both significantly ($P < 0.05$) influenced the *DI* and the *FW* in both the trials, and these results are presented separately for the peat soil and sandy-loam soil, as well as for Cycles I and II, in Tables 5A and 5B to Tables 8A and 8B.

Carbon source, temperature and incubation period, and the interactions between temperature × ASD duration (3 or 6 weeks), carbon source × ASD duration, and carbon source × temperature generally influenced ($P < 0.05$) the percentage of lettuce plants affected by *R. solani* (*DI*) and the harvested lettuce plant fresh weights (*FW*), in the first and second cycles in both trials (Tables 3 and 4). The only exception for the temperature × ASD duration interaction was in the second crop cycle of Trial 2 carried out in the peat soil and in the sandy-loam soil for the tested temperatures and incubation periods (Table 3). The interactions of carbon source × ASD duration and C-source × temperature affected *DI* and *FW* in both soils and trials at the end of the first crop cycle (Supplementary Tables S1 and S2). The three-way interaction between these factors influenced ($P < 0.001$) *DI* and *FW* in the first and second cycles in both trials and soils (Table 3).

The infested non-treated pots without anaerobic conditions (INT-Standard control) showed very high incidence of lettuce basal rot. In the first cycle, 82-90% of the plants were affected in the peat soil kept for 3 or 6 weeks at 21°C or 26°C, with a slight reduction in DI at the end of Trial 2 when peat soil was kept at 31°C for 3 or 6 weeks (49-51% of affected plants) (Tables 5A and 5B). In Trial 1, the *DI* for plants grown in the peat soil in the first crop cycle in the INT-Anaerobic control at 21°C for 6 weeks was reduced ($P < 0.05$) by 28%, and at 26°C by 42%, compared to INT-Standard control. No differences were observed between the infested untreated control, under standard and anaerobic conditions in Trial 2, for either of the tested soils and temperature conditions (Table 5B). The control treatment based on TM reduced the mean *DI* to a range of 63 to 83% in the peat soil (5A and 5B), with a consistent effect also in the second crop cycle.

ASD based-BCp provided 60-69% disease reduction efficacy when incubated for 3 weeks at 21°C or 26°C, without any effect of the extension of the treatment for 6 weeks in Trial 1 at the first crop cycle. A

Table 3. Statistical significance values for the factors ASD duration (0, 3 or 6 weeks), temperature (21, 26 or 31°C), or carbon sources, for lettuce basal rot incidence (% affected plants) and lettuce fresh weights, after trial cycles I and II.

Trial	Fixed factor	Cycle I				Cycle II			
		Sign. % affected plants		Sign. Fresh weight		Sign. % affected plants		Sign. Fresh weight	
		Peat	Sandy-loam	Peat	Sandy-loam	Peat	Sandy-loam	Peat	Sandy-loam
1									
	Carbon source	<0.001	<0.001	<0.001	<0.001	<0.001	<0.001	<0.001	<0.001
	Temperature × ASD duration	<0.001	0.006	<0.001	<0.001	0.0816	<0.001	0.103	<0.001
	Carbon source × ASD duration	<0.001	<0.001	<0.001	<0.001	<0.001	<0.001	<0.001	<0.001
	Carbon source × Temperature	<0.001	<0.001	<0.001	<0.001	<0.001	<0.001	<0.001	<0.001
	Carbon source × Temperature × ASD duration	<0.001	<0.001	<0.001	<0.001	0.0032	<0.001	<0.001	<0.001
2	Carbon source	<0.001	<0.001	<0.001	<0.001	<0.001	<0,001	<0.001	<0,001
	Temperature × ASD duration	<0.001	0.015	<0.001	<0.001	<0.001	0.0163	<0.001	0,416
	Carbon source × ASD duration	<0.001	<0.001	<0.001	<0.001	0.001	<0.001	<0.001	<0.001
	Carbon source × Temperature	<0.001	<0.001	<0.001	<0.001	0.001	<0.001	<0.001	<0.001
	Carbon source × Temperature × ASD duration	<0.001	<0.001	<0.001	<0.001	<0.001	<0,001	<0.001	0.031

Table 4. Interaction between ASD duration (weeks) and temperature (°C) in the peat or sandy-loam soils artificially infested with *Rhizoctonia solani,* for Trials 1 and 2. The data are expressed as A) mean % of lettuce plants with basal rot at the end of the I and II crop cycles B), and mean fresh weights (g pot^{-1}) at the end of the I and II crop cycles. All data represent results from trials 1and 2.

ASD duration (weeks) × temperature (°C)	Peat soil				Sandy-loam soil			
	Mean % affected lettuce plants		Mean plant fresh weight (g pot^{-1})		Mean % affected lettuce plants		Mean plant fresh weight (g pot^{-1})	
	Cycle I	Cycle II	Cycle I	Cycle II	Cycle I	Cycle II	Cycle I	Cycle II
Trial 1								
3 weeks at 21°C	54.4 ±8.2 c[a]	50.0 ±6.6 c	95.7 ±24.3 bc	60.4 ±11.0 a	38.8 ±5.7 a	24.8 ±3.2 a	49.9 ±7.4 b	190.4 ±9.8 a
3 weeks at 26°C	50.2 ±7.4 b	39.7 ±5.7 ab	67.7 ±14.8 c	68.7 ±10.0 a	39.5 ±6.3 a	37.0 ±3.5 bc	52.8 ±8.6 b	131.7 ±8.9 c
6 weeks at 21°C	44.4 ±6.9 b	43.4 ±6.3 bc	117.5 ±20.0 ab	74.1 ±14.1 a	47.8 ±6.8 b	29.8 ±3.4 ab	44.9 ±8.0 b	161.4 ±7.5 b
6 weeks at 26°C	33.4 ±5.7 a	33.8 ±5.2 a	140.7 ±25.5 a	58.6 ±6.7 a	43.6 ±7.0 ab	41.7 ±4.3 c	65.4 ±10.8 a	151.7 ±9.2 bc
Trial 2								
3 weeks at 21°C	40.4 ±3.9 b	39.4 ±3.7 b	90.4 ±33.9 b	127.6 ±19.7 c	18.7 ±1.9 a	20.8 ±2.0 a	77.1 ±4.3 a	13.4 ±6.2 a
3 weeks at 31°C	14.6 ±2.0 a	18.9 ±2.3 a	74.0 ±24.2 b	150.7 ±20.2 c	18.5 ±2.2 a	20.3 ±2.1 a	68.0 ±7.4 ab	12.7 ±5.8 a
6 weeks at 21°C	34.0 ±4.2 b	27.0 ±3.2 b	114.6 ±18.0 a	356.5 ±26.5 a	21.1 ±2.3 ab	21.9 ±2.3 ab	60.3 ±6.1 b	10.2 ±4.6 a
6 weeks at 31°C	21.5 ±3.4 a	11.5 ±2.4 a	119.5 ±23.4 a	251.7 ±25.3 b	22.5 ±2.8 b	24.0 ±2.9 b	79.9 ±8.3 a	16.0 ±7.5 a

[a] Means in each column accompanied by the same letter are not significantly different for Tukey test ($P \leq 0.05$) for cycle I and cycle II in each trial. Standard errors are also indicated.

Table 5A. Mean percentages of lettuce plants affected by basal rot after application of different ASD soil treatments, carried out for 3 or 6 weeks, and at 21 or 26 °C in peat artificially infested with *Rhizoctonia solani*, at the end of the first and second crop cycles (Trial 1).

Carbon source[a], dosage	ASD	Treatment duration (weeks)	Cycle I				Cycle II			
			21°C	E%[c]	26°C	E%	21°C	E%	26°C	E%
Comp, 15 t ha^{-1}	+	3	90.0±0.0 d[b]	**0.0**	76.5±4.9 ef	**6.4**	49.3±0.8 b-d[a]	**45.2**	33.9±1.5 bc	**52.1**
BCp, 15 t ha^{-1}	+	3	28.3±1.0 b	**68.6**	32.3±4.7 bc	**60.5**	54.8±11.8 b-d	**39.1**	45.0±3.1 c	**36.4**
WR, 15 t ha^{-1}	+	3	85.4±4.6 d	**5.1**	71.2±3.5 d-f	**12.9**	56.4±5.0 b-d	**37.3**	40.6±4.5 bc	**42.7**
TM, 2 g m^{-2}	-	3	22.6±1.7 b	**74.9**	15.7±1.6 ab	**80.8**	30.4±4.2 b	**66.2**	29.6±5.9 bc	**58.2**
INT-Anaerobic control	+	3	90.0±0.0 d	**0.0**	53.1±2.8 d-e	**35.0**	72.0±6.1 de	**20.0**	66.1±8.4 de	**6.6**
INT-Standard control	-	3	90.0±0.0 d	**0.0**	81.7±8.3 f	**0.0**	90.0±0.0 e	**0.0**	70.8±2.3 e	**0.0**
NINT-Anaerobic control	+	3	0.0±0.0 a	**100.0**	0.0±0.0 a	**100.0**	0.0±0.0 a	**100.0**	0.0±0.0 a	**100.0**
NINT-Standard control	-	3	0.0±0.0 a	**100.0**	0.0±0.0 a	**100.0**	0.0±0.0 a	**100.0**	0.0±0.0 a	**100.0**
Comp, 15 t ha^{-1}	+	6	61.8±1.7 c	**28.8**	27.1±3.2 bc	**67.0**	42.0±5.2 b	**43.1**	30.7±6.7 bc	**54.5**
BCp, 15 t ha^{-1}	+	6	30.5±3.4 b	**64.9**	33.4±5.2 bc	**59.4**	38.0±6.4 bc	**48.5**	44.2±5.8 c	**34.4**
WR, 15 t ha^{-1}	+	6	56.0±7.9 c	**35.5**	46.6±4.6 cd	**43.3**	42.7±4.6 bc	**42.1**	37.7±1.9 bc	**44.1**
TM, 2 g m^{-2}	-	6	15.6±5.9 ab	**82.0**	19.5±1.1 ab	**76.3**	31.5±2.1 b	**57.3**	23.6±1.9 b	**65.0**
INT-Anaerobic control	+	6	62.2±6.3 c	**28.3**	47.9±2.0 cd	**41.7**	71.3±6.7 de	**3.4**	48.0±4.3 cd	**28.8**
INT-Standard control	-	6	86.8±3.2 d	**0.0**	82.2±4.7 f	**0.0**	73.8±6.4 de	**0.0**	67.4±1.7 de	**0.0**
NINT-Anaerobic control	+	6	0.0±0.0 a	**100.0**	0.0±0.0 a	**100.0**	0.0±0.0 a	**100.0**	0.0±0.0 a	**100.0**
NINT-Standard control	-	6	0.0±0.0 a	**100.0**	0.0±0.0 a	**100.0**	0.0±0.0 a	**100.0**	0.0±0.0 a	**100.0**

[a] Comp: Compost; BCp: *Brassica carinata* pellet with anaerobic conditions; WR: *Diplotaxis* green manure; TM: Tolclofos methyl; INT-Anaerobic control: Inoculated untreated control with anaerobic conditions; INT-Standard control: Inoculated untreated control without anaerobic conditions; NINT-Anaerobic control: Non-inoculated untreated control with anaerobic conditions; NINT-Standard control: Non-inoculated untreated control without anaerobic conditions.

[b] Means in each column accompanied by the same letter are not significantly different ($P \leq 0.05$), according to Tukey's test. Standard errors are also indicated.

[c] E%: Disease reduction compared to the INT-Standard controls carried out for 3 or 6 weeks.

Table 5B. Mean percentages of lettuce plants affected by basal rot after application of different ASD soil treatments, carried out for 3 or 6 weeks, and at 21 or 31°C in peat artificially infested with *Rhizoctonia solani*, at the end of the first and second crop cycles (Trial 2).

Carbon source[a], dosage	ASD	Treatment duration (weeks)	Cycle I						Cycle II					
			21°C		E%[c]	26°C		E%	21°C		E%	26°C		E%
Comp, 15 t ha^{-1}	+	3	86.8±3.2	cd[b]	**3.6**	39.0±4.4	c-e	**21.1**	38.5±0.7	c-g	**27.5**	67.0±8.4	b-e	**25.6**
BCp, 15 t ha^{-1}	+	3	45.3±2.0	ab	**49.7**	23.71±1.1	b-e	**52.0**	36.14±7.9	c-g	**32.0**	63.1±15.5	b-e	**29.9**
WR, 15 t ha^{-1}	+	3	80.1±6.3	b-d	**11.0**	38.2±5.1	c-e	**22.7**	40.6±4.5	d-g	**23.5**	42.8±4.2	a-c	**52.4**
WR, 30 t ha^{-1}	+	3	84.3±5.7	b-d	**6.3**	30.11±0.5	b-e	**39.1**	43.6±3.8	d-g	**17.9**	59.2±15.2	a-d	**34.2**
TM, 2 gm^{-2}	-	3	19.7±4.2	a	**78.1**	14.6±5.4	a-c	**70.4**	13.4±21.0	a-c	**74.8**	0.0±0.0	a	**100.0**
BCp, 15 t ha^{-1}- No anaerobic control	-	3	90.0±0.0	d	**0.0**	38.8±6.1	c-e	**21.5**	42.8±2.2	d-g	**19.4**	67.5±13.9	b-e	**25.0**
INT- Anaerobic control	+	3	90.0±0.0	d	**0.0**	47.9±1.7	de	**3.0**	54.7±3.6	g	**0.0**	82.5±7.5	de	**8.3**
INT- Standard control	-	3	90.0±0.0	d	**0.0**	49.4±1.9	de	**0.0**	53.1±2.6	fg	**0.0**	90.0±0.0	e	**0.0**
NINT- Anaerobic control	+	3	0.0±0.0	a	**100.0**	0.0±0.0	a	**100.0**	0.0±0.0	a	**100.0**	0.0±0.0	a	**100.0**
Comp, 15 t ha^{-1}	+	6	57.3±±4.7	b	**28.1**	40.6±2.8	c-e	**20.1**	28.2±1.8	c-e	**31.6**	31.6±0.9	a-c	**48.2**
BCp, 15 t ha^{-1}	+	6	53.8±2.9	b	**32.5**	10.7±7.1	ab	**78.9**	3.2±3.2	ab	**92.2**	33.9±1.5	a-c	**44.4**
WR, 15 t ha^{-1}	+	6	71.4±6.9	b-d	**10.4**	8.3±8.3	a	**83.7**	21.3±2.9	a-e	**48.3**	28.9±5.4	a-c	**52.6**
WR, 30 t ha^{-1}	+	6	64.1±10.5	bc	**19.6**	11.4±6.6	ab	**77.6**	16.8±2.4	a-c	**59.2**	30.3±8.6	a-c	**50.3**
TM, 2 gm^{-2}	-	6	21.3±2.2	a	**73.3**	17.9±6.3	a-e	**64.8**	8.6±3.0	ab	**79.1**	24.4±5.2	ab	**60.0**
BCp, 15 t ha^{-1}- No anaerobic control	-	6	69.3±14.2	b-d	**13.0**	36.1±2.8	c-e	**28.9**	29.5±3.9	c-e	**28.4**	68.9±10.6	c-e	**-13.0**
INT- Anaerobic control	+	6	70.58.9	b-d	**11.5**	39.3±2.4	de	**22.6**	32.1±4.4	c-f	**22.1**	63.1±13.3	b-e	**-3.4**
INT- Standard control	-	6	79.76.0	b-d	**0.0**	50.8±1.7	e	**0.0**	41.2±2.4	d-g	**0.0**	61.0±2.4	b-e	**0.0**
NINT- Anaerobic control	+	6	0.00.0	a	**100.0**	0.0±0.0	a	**100.0**	0.0±0.0	a	**100.0**	0.0±0.0	a	**100.0**

[a] Comp: Compost; BCp: *Brassica carinata* pellet with or without anaerobic conditions; WR: *Diplotaxis* green manure; TM: Tolclofos methyl; INT-Anaerobic control: Inoculated untreated control with anaerobiotic conditions; INT-Standard control: Inoculated untreated control without anaerobic conditions; NINT-Anaerobic control: Non inoculated untreated control with anaerobic conditions.

[b] Means in each column accompanied by a common letter are not significantly different ($P \leq 0.05$), according to Tukey's test. Standard errors are also reported.

[c] E%: Disease reduction compared to the INT-Standard controls carried out for 3 or 6 weeks.

slight reduction in ASD based-BCp efficacy occurred at the end of the second cycle carried out in the same soil (34–39% efficacy) (Table 5A). The same trend was found in the Trial 2 when ASD based-BCp was applied for 3 weeks at 21°C or 31°C (50–51% efficacy), with an increase in efficacy to 79% when incubated at 31°C for 6 weeks at the end of the first cycle. A positive effect of 6 weeks of ASD based-BCp also occurred in the second crop cycle (Table 5B). BCp applied at 15 t ha^{-1} without anaerobic conditions and tested in Trial 2, provided no statistically significant advantages when applied to the infested peat soil for any of the tested conditions (Tables 5B).

WR used as green manure and mixed with the peat soil was not effective against basal rot when applied for 3 weeks at any of the tested temperatures in Trials 1 and 2 at the end of the first cycle (Tables 5A and 5B) at both the tested dosages. This treatment applied for 6 weeks at 26°C reduced ($P < 0.05$) the disease by 43%, and at 31°C by 78–84%, compared to the INT-Standard control, without any effect of the dosage used.

The greatest efficacy of ASD based-Comp was observed in Trial 1 at 26°C for 6 weeks of incubation (67% efficacy), while the same carbon source did not provide any effect compared to the INT-Standard control in all the tested conditions at the first crop cycle in both trials (Tables 5A and 5B). ASD based-Comp gave increased efficacy against basal rot in the second crop cycle (32 to 54% efficacy), without any significant effects of temperature or duration of the treatment (Tables 5A and 5B).

At the end of the first cycle, the plants grown in the treated peat had generally reduced *FW* at 21°C and 26°C, and only the ASD based-Comp treatment applied for 6 weeks at 26°C improved ($P < 0.05$) the mean plant fresh weights, compared to the inoculated and untreated standard control (Table 6A). The lettuce plants grown in the same peat soil, previously treated with Comp and WR as C-sources for 3 or 6 weeks during the second crop cycle, at both temperatures, generally had greater

Table 6A. Mean fresh weight (g pot^{-1}) of lettuce plants after application of different ASD soil treatments, carried out for 3 or 6 weeks, and at 21 or 26 °C in peat artificially infested with *Rhizoctonia solani*, at the end of the first and second crop cycles (Trial 1).

Carbon source[a], dosage	ASD	Treatment duration (weeks)	Cycle I				Cycle II			
			21°C		26°C		21°C		26°C	
Comp, 15 t ha^{-1}	+	3	2.0±0.0	e[b]	18.0±7.6	c	197.3±5.3	a	166.1±25.2	a
BCp, 15 t ha^{-1}	+	3	70.0±3.7	cd	93.3±12.4	bc	76.4±19.6	b-d	94.6±15.1	b-d
WR, 15 t ha^{-1}	+	3	2.7±2.0	e	9.6±3.9	c	78.9±14.3	b-d	43.4±4.6	ef
TM, 2 gm^{-2}	-	3	67.4±9.2	cd	84.1±2.5	c	40.5±0.8	cd	35.3±2.0	f
INT- Anaerobic control	+	3	2.2±0.0	e	16.4±4.0	c	16.3±5.5	cd	29.3±13.0	f
INT- Standard control	-	3	2.6±0.0	e	2.4±0.0	c	3.0±2.0	d	17.0±4.5	f
NINT- Anaerobic control	+	3	387.6±25.6	a	232.8±27.3	ab	14.0±1.6	cd	33.0±5.1	f
NINT- Standard control	-	3	238.1±19.3	b	153.3±24.3	ab	80.1±8.2	b-d	131.3±8.2	ab
Comp, 15 t ha^{-1}	+	6	93.21±1.8	c	356.2±111.4	a	201.7±14.1	a	108.9±6.1	b
BCp, 15 t ha^{-1}	+	6	52.21±1.4	c-e	143.6±17.8	bc	163.2±59.7	ab	35.9±2.6	f
WR, 15 t ha^{-1}	+	6	96.22±3.9	cd	87.8±14.1	bc	93.7±13.6	b-d	105.4±8.6	b
TM, 2 gm^{-2}	-	6	98.7±24.7	cd	87.4±14.4	bc	42.3±3.7	cd	58.1±11.7	c-f
INT- Anaerobic control	+	6	27.1±8.4	de	42.4±14.2	c	16.7±6.4	cd	46.5±6.8	d-f
INT- Standard control	-	6	1.8±1.0	e	8.1±5.3	c	17.0±11.6	cd	11.7±1.3	f
NINT- Anaerobic control	+	6	210.8±7.4	b	254.3±48.4	ab	13.9±2.7	cd	15.8±2.0	f
NINT- Standard control	-	6	360.419.7	a	246.1±31.5	ab	44.3±4.4	cd	86.3±2.4	b-e

[a] Comp: Compost; BCp: *Brassica carinata* pellet with anaerobic conditions; WR: *Diplotaxis* green manure; TM: Tolclofos methyl; INT-Anaerobic control: Inoculated untreated control with anaerobic conditions; INT-Standard control: Inoculated untreated control without anaerobic conditions; NINT-Anaerobic control: Non-inoculated untreated control with anaerobic conditions; NINT-Standard control: Non-inoculated untreated control without anaerobic conditions.

[b] Means in each column accompanied by the same letter are not significantly different ($P \leq 0.05$), according to Tukey's test. Standard errors are also indicated.

fresh weights than during cycle I. The greatest mean fresh weights reached in the second crop cycle were recorded from the BCp and WR (at 15 t ha^{-1}) carbon sources at 31°C for 6 weeks incubation (Table 6B).

The infested non-treated pots without anaerobiosis (INT-Standard control) had 69% to 79% of basal rot affected plants in the sandy-loam soil at the end of the first crop cycle in Trial 1 (Table 7A), and there was a slight reduction in disease incidence at the end of Trail 2 (32–44% of affected plants) (Table 7B). The control treatment based on TM reduced the incidence of affected plants to a range of 74 to 90% in the sandy-loam soil (Tables 7A and 7B). BCp applied under anaerobic conditions in the sandy-loam soil at 21°C, provided reduced disease (52% in Trial 1 and 72% in Trial 2) when carried out for 3 weeks, compared to INT-Standard control. The same carbon source, applied under anaerobic conditions generally gave more consistent disease reduction when applied at 26°C for both 3 and 6 weeks (52–63% efficacy), and complete disease control was provided by this treatment when it was applied for 6 weeks at 31°C (Table 7B). The efficacy of the ASD based-BCp was generally improved in the second crop cycle (Tables 7A and 7B). The BCp treatment applied without any anaerobic conditions in the sandy-loam soil and tested in Trial 2, reduced basal rot incidence, compared to the INT–Standard control, by 71 % at 31°C for 6 weeks and by 44% at 21°C for 3 weeks (Table 7B). The ASD treatment with WR as green manure applied to the sandy-loam soil at 21°C for 3 weeks generally partially reduced the percentage of affected plants (32–37% efficacy) and resulted in a greater efficacy (from 46 to 59%) at 31°C (Table 7B), with no significant difference between the two dosages in Trial 2. The efficacy of the ASD treatment with WR generally increased in the second crop cycle for all the tested conditions (Tables 7A and 7B). Inconsistent results were observed when the compost was mixed into the sandy-loam soil, with the greatest disease reduction (38–41% efficacy) at 21°C for 3 weeks of incubation (Tables 7A and 7B). Efficacy of the ASD treatment with compost was generally increased in the second crop cycle, compared to the first, with the greatest disease reduction in the sandy-loam soil previously treated for 3 weeks at 21°C (53% efficacy in Trial 1 and 66% efficacy in Trial 2).

Mean fresh weights of the lettuce plants grown in the ASD treated sandy-loam soil at the end of the first crop

Table 6B. Mean fresh weight (g pot^{-1}) of lettuce plants after application of different ASD soil treatments, carried out for 3 or 6 weeks, and at 21 or 31 °C in peat artificially infested with *Rhizoctonia solani*, at the end of the first and second crop cycles (Trial 2).

Carbon source[a], dosage	ASD	Treatment Duration (Weeks)	Cycle I				Cycle II			
			21°C		31°C		21°C		31°C	
Comp, 15 t ha^{-1}	+	3	10.5±0.5	b[b]	111.9±11.6	de	63.4±14.5	c-f	208.0±4.6	c-g
BCp, 15 t ha^{-1}	+	3	36.5±0.0	b	246.5±81.7	a-d	32.7±10.1	d-f	162.0±71.0	d-g
WR, 15 t ha^{-1}	+	3	13.0±12.6	b	287.4±74.8	a-d	41.3±13.1	d-f	198.0±8.3	c-g
WR, 30 t ha^{-1}	+	3	11.0±1.0	b	79.6±6.1	e	141.6±7.0	a-d	281.5±10.4	b-f
TM, 2 gm^{-2}	-	3	102.2±28.1	a	373.65±0.1	a-c	192.4±15.0	ab	305.4±107.4	b-e
BCp, 15 t ha-1- No anaerobic control	-	3	10.3±0.3	b	97.4±31.1	de	97.9±9.2	b-f	47.5±4.8	fg
INT- Anaerobic control	+	3	10.0±0.0	b	69.6±23.7	e	13.8±1.9	f	42.7±24.7	g
INT- Standard control	-	3	12.3±12.3	b	73.2±13.1	e	4.0±0.0	f	47.4±25.0	fg
NINT- Anaerobic control	+	3	117.4±24.0	a	233.7±13.9	b-e	206.21±2.1	a	301±31.8	b-e
Comp, 15 t ha^{-1}	+	6	28.4±10.6	b	99.9±14.5	de	132.0±3.8	a-e	172.5±25.0	c-g
BCp, 15 t ha^{-1}	+	6	13.1±1.8	b	419.0±39.5	ab	195.2±7.5	ab	657.1±45.4	a
WR, 15 t ha^{-1}	+	6	15.6±6.5	b	460.3±31.8	ab	124.81±1.9	b-e	405.4±98.7	bc
WR, 30 t ha^{-1}	+	6	33.9±17.5	b	186.5±50.6	c-e	165.5±25.0	a-c	497.4±52.6	ab
TM, 2 gm^{-2}	-	6	96.4±20.0	a	376±55.6	a-c	99.1±9.1	b-f	334.5±31.7	b-d
BCp, 15 t ha^{-1}- No anaerobic control	-	6	16.9±4.0	b	113.5±5.4	de	12.5±3.4	f	294.2±42.6	b-e
INT- Anaerobic control	+	6	15.7±9.5	b	101.3±7.8	de	25.0±8.7	ef	73.8±8.6	e-g
INT- Standard control	-	6	29.2±4.0	b	70.51±7.7	e	23.0±3.0	ef	89.5±18.9	e-g
NINT- Anaerobic control	+	6	152.9±14.1	a	221±13.5	c-e	132.7±10.1	b-e	239.3±20.4	c-g

[a] Comp: Compost; BCp: *Brassica carinata* pellet with or without anaerobic conditions; WR: *Diplotaxis* green manure; TM: Tolclofos methyl; INT-Anaerobic control: Inoculated untreated control with anaerobiotic conditions; INT-Standard control: Inoculated untreated control without anaerobic conditions; NINT-Anaerobic control: Non inoculated untreated control with anaerobic conditions.

[b] Means in each column accompanied by a common letter are not significantly different ($P \leq 0.05$), according to Tukey's test. Standard errors are also reported.

cycle were very low for all the treatments (Tables 8A and 8B). Moreover, there was a significant reduction in the mean lettuce fresh weights in the non-infested control (NINT-Anaerobic control) incubated for 6 weeks. By the end of the second crop cycle, lettuce plants generally had significantly greater fresh weights than observed after the first cycle. The greatest mean fresh weight was at 21°C using WR at 15 t ha^{-1} for 3 weeks and BCp for 6 weeks (Table 8A). The lettuce plants of the second crop cycle grown in the same sandy-loam soil, previously treated at 31°C for 6 weeks using WR at both the tested dosages and BCp, generally had significantly greater mean fresh weights than the non-inoculated control plants under anaerobic conditions (Table 8B).

DISCUSSION

ASD has been proposed in several reports as a possible solution for soil disinfestation to control several plant pathogens, on different crops, using a variety of C-sources, under controlled conditions and in field experiments (Momma *et al*., 2006; Katase *et al*., 2009; Butler *et al*., 2012 a, b; Runia *et al*., 2012; 2014; Rosskopf *et al*., 2015; Strauss and Kluepfel, 2015; Hewavitharana and Mazzola, 2016; Shrestha *et al*., 2016; Shennan *et al*., 2014; 2018). Since this methodology requires further testing before practical implementation, considerable efforts have aimed to improve ASD efficacy with emphasis on the optimizing factors such as carbon sources (Butler *et al*., 2012a; b; 2014b; Hewavitharana *et al*., 2014; Shrestha *et al*., 2016; Rodríguez-Molina *et al*., 2016; Serrano-Pérez *et al*., 2017), duration of the incubation periods, and soil temperatures (Hewavitharana *et al*., 2015; Shrestha *et al*., 2016; Shennan *et al*., 2014; 2018) for developing standard treatments against specific soilborne pathogens. For example, Runia *et al*., (2012; 2014) set up a controlled laboratory system to simulate ASD treatments in mesocosms to study biotic and abiotic changes over time against *Verticillium dahliae* and *Globodera pallida*. A similar approach has also been used for other pathosystems, including *Phytophthora nicotianae*-pepper (Serrano-Pérez *et al*., 2017) and *Verticillium dahliae*-strawberry (Shennan *et al*., 2018).

Table 7A. Mean percentages of lettuce plants affected by basal rot after application of different ASD soil treatments, carried out for 3 or 6 weeks, and at 21 or 26 °C in sandy-loam artificially infested with *Rhizoctonia solani*, at the end of the first and second crop cycles (Trial 1).

Carbon source[a], dosage	ASD	Treatment Duration (Weeks)	Cycle I						Cycle II					
			21°C		E%[c]	26°C		E%	21°C		E%	26°C		E%
Comp, 15 t ha^{-1}	+	3	45.0±1.2	cd[b]	**41.2**	47.3±4.4	de	**34.5**	19.9±3.6	bc	**66.0**	35.36±3.3	b-d	**27.8**
BCp, 15 t ha^{-1}	+	3	37.0±1.9	c	**51.6**	27.1±3.2	b-d	**62.5**	33.2±1.3	cd	**43.3**	42.86±3.6	c-e	**55.5**
WR, 15 t ha^{-1}	+	3	48.6±2.2	c-e	**36.5**	58.3±6.4	ef	**19.3**	27.8±3.7	bc	**52.6**	52.74±5.2	de	**46.3**
TM, 2 gm^{-2}	-	3	15.7±1.6	b	**79.5**	16.8±2.4	a-c	**76.7**	16.8±2.4	b	**71.3**	20.41±7.5	a-c	**74.0**
INT- Anaerobic control	+	3	67.4±1.7	fg	**11.9**	59.4±2.9	ef	**17.7**	46.5±3.9	d-f	**20.6**	56.18±2.7	de	**19.9**
INT- Standard control	-	3	76.5±4.9	g	**0.0**	72.2±6.4	f	**0.0**	58.6±2.9	f	**0.0**	54.68±3.0	de	**0.0**
NINT- Anaerobic control	+	3	0.0±0.0	a	**100.0**	0.0±0.0	a	**100.0**	0.0±0.0	a	**100.0**	4.61±4.6	a	**100.0**
NINT- Standard control	-	3	0.0±0.0	a	**100.0**	0.0±0.0	a	**100**	0.0±0.0	a	**100.0**	0.0±0.0	a	**100.0**
Comp, 15 t ha^{-1}	+	6	57.9±3.6	d-f	**16.1**	42.1±4.1	de	**46.6**	34.6±2.8	cd	**41.8**	38.23±4.0	b-d	**17.6**
BCp, 15 t ha^{-1}	+	6	49.4±3.9	c-e	**28.4**	36.6±5.0	cd	**53.6**	35.1±5.4	c-e	**41.0**	52.6±11.2	de	**100.0**
WR, 15 t ha^{-1}	+	6	60.3±3.1	ef	**12.6**	78.8±6.7	f	**0.1**	34.7±0.9	c-e	**41.7**	56.73±5.14	de	**49.9**
TM, 2 gm^{-2}	-	6	7.8±4.7	ab	**88.7**	7.8±4.7	ab	**90.1**	15.7±1.6	ab	**73.6**	17.89±6.3	ab	**84.6**
INT- Anaerobic control	+	6	58.2±4.5	d-f	**15.7**	61.4±4.3	ef	**22.2**	50.9±6.9	ef	**14.5**	57.97±4.0	de	**14.0**
INT- Standard control	-	6	69.0±3.6	fg	**0.0**	78.9±3.9	f	**0.0**	59.5±3.4	f	**0.0**	64.7±2.9	e	**0.0**
NINT- Anaerobic control	+	6	0.0±0.0	a	**100.0**	0.0±0.0	a	**100.0**	0.0±0.0	a	**100.0**	0.0±0.0	a	**100.0**
NINT- Standard control	-	6	0.0±0.0	a	**100.0**	0.0±0.0	a	**100.0**	0.0±0.0	a	**100.0**	0.0±0.0	a	**100.0**

[a] Comp: Compost; BCp: *Brassica carinata* pellet with anaerobic conditions; WR: *Diplotaxis* green manure; TM: Tolclofos methyl; INT-Anaerobic control: Inoculated untreated control with anaerobic conditions; INT-Standard control: Inoculated untreated control without anaerobic conditions; NINT-Anaerobic control: Non-inoculated untreated control with anaerobic conditions; NINT-Standard control: Non-inoculated untreated control without anaerobic conditions.

[b] Means in each column accompanied by the same letter are not significantly different ($P \leq 0.05$), according to Tukey's test. Standard errors are also indicated.

[c] E%: Disease reduction compared to the INT-Standard controls carried out for 3 or 6 weeks.

In the present study, effects of ASD using *Brassicaceae* species, either as wild rocket green manure or *Brassica carinata* dry pellets, and compost as C-sources, were evaluated on the lettuce–*R. solani* pathosystem, considering effects on basal rot incidence and on lettuce productivity (fresh weights) in ASD treatments simulated in growth chambers. Our aim was to test the different ASD C-sources at one dosage equivalent to 15 t ha^{-1}, with the only exception being the double dosage tested for WR green manure. The commercial dosage of 3 t ha^{-1} suggested for *B. carinata* pellets for biofumigation treatment was not considered. Our study was also carried out in two soil types, a sandy-loam alkaline soil and an acidic peat soil, at three temperatures (21, 26 or 31°C), and with two treatment durations (3 or 6 weeks). Impacts of these treatments on lettuce grown in the treated and untreated soil was also assessed over two consecutive crop cycles carried out in greenhouse.

Carbon sources, temperatures, incubation periods and their interactions affected the efficacy of the ASD treatments. Differences in efficacy depended on the soil type. *Rhizoctonia* basal rot was reduced at the higher temperatures of 26°C or 31°C for 3 or 6 weeks in the peat soil, with resulting increased plant fresh weights, while generally in the sandy-loam soil, the greatest disease control was achieved with only 3 weeks of incubation, at all temperatures tested. In contrast, several studies have shown the impacts of temperature and ASD duration on pathogen survival, disease control and host yields in several pathosystems. Ebihara and Uematsu (2014) showed that *Fusarium oxysporum* f. sp. *fragariae*, *Phytophthora cactorum* and *Verticillium dahliae*, under anaerobic conditions, survived longer at 10°C, and were eradicated more rapidly at 40°C. Soil temperatures less than 30°C may be a critical factor in the effectiveness of ASD for reducing Fusarium wilt of strawberry (Muramoto *et al*., 2015; Shrestha *et al*., 2016).

Under the experimental conditions tested in the present study, different effects of the applied C-sources were observed. The impacts of *Brassica* crops and *Brassicaceae* seed meal have been shown to be effective biomasses for ASD treatments to control soil-borne diseases caused by *Fusarium* spp., *Rhizoctonia* spp., *Pythium* spp., and *Verticillium* spp. (Blok *et al*., 2000; Messiha *et*

Table 7B. Mean percentages of lettuce plants affected by basal rot after application of different ASD soil treatments, carried out for 3 or 6 weeks, and at 21 or 31 °C in sandy-loam artificially infested with *Rhizoctonia solani*, at the end of the first and second crop cycles (Trial 2).

Carbon source[a], dosage	ASD	Treatment duration (weeks)	Cycle I				Cycle II			
			21°C	E%[c]	31°C	E%	21°C	E%	31°C	E%
Comp, 15 t ha^{-1}	+	3	24.1±8.1 b-d[b]	**38.2**	32.0±4.3 c-e	**27.8**	15.4±2.5 a-c	**52.3**	32.0±4.3 e-g	**22.7**
BCp, 15 t ha^{-1}	+	3	11.1±3.9 ab	**71.5**	19.7±4.2 b-d	**55.5**	11.1±3.9 a-c	**65.6**	9.0±3.1 a-c	**78.2**
WR, 15 t ha^{-1}	+	3	26.4±2.5 b-d	**32.3**	23.8±1.0 b-d	**46.3**	21.8±4.3 b-e	**32.5**	22.8±0.0 c-f	**44.9**
WR, 30 t ha^{-1}	+	3	24.0±4.2 b-d	**38.5**	18.1±2.0 bc	**59.1**	19.5±1.1 be	**39.6**	15.7±1.6 a-d	**62.1**
TM, 2 gm^{-2}	-	3	15.4±2.5 a-c	**60.5**	11.5±7.8 ab	**74.0**	9.7±3.2 ab	**70.0**	11.5±7.8 a-c	**72.2**
BCp, 15 t ha-1- No anaerobic control	-	3	21.8±4.3 b-d	**44.1**	30.6±3.0 c-e	**30.9**	26.4±2.5 c-f	**18.3**	9.7±3.2 a-c	**76.6**
INT- Anaerobic control	+	3	32.1±3.7 cd	**17.7**	35.5±0.8 de	**19.9**	32.1±3.7 ef	**0.6**	30.6±3.0 d-g	**26.1**
INT- Standard control	-	3	39.0±4.7 d	**0.0**	44.3±2.5 e	**0.0**	32.3±2.3 ef	**0.0**	41.4±1.4 f	**0.0**
NINT- Anaerobic control	+	3	0.0±0.0 a	**100.0**	0.0±0.0 a	**100.0**	0.0±0.0 a	**100.0**	0.0±0.0 a	**100.0**
Comp, 15 t ha^{-1}	+	6	32.3±2.3 cd	**1.5**	34.7±2.0 ce	**17.6**	31.5±2.1 ef	**19.2**	35.5±0.8 e-g	**15.7**
BCp, 15 t ha^{-1}	+	6	17.6±8.2 a-c	**46.3**	0.0±0.0 a	**100.0**	11.1±3.9 a-c	**72.5**	0.0±0.0 a	**100.0**
WR, 15 t ha^{-1}	+	6	15.7±1.6 a-c	**52.1**	21.1±3.4 b-d	**49.9**	15.7±1.6 a-d	**59.7**	20.2±2.9 b-e	**52.0**
WR, 30 t ha^{-1}	+	6	17.7±3.2 a-c	**46.0**	30.1±4.7 ce	**28.5**	17.7±3.2 b-e	**54.6**	16.5±2.7 a-d	**60.8**
TM, 2 gm^{-2}	-	6	11.1±3.9 ab	**66.2**	6.5±3.7 ab	**84.6**	11.1±3.9 a-c	**71.5**	20.5±2.1 b-e	**51.3**
BCp, 15 t ha-1- No anaerobic control	-	6	28.9±2.1 b-d	**13.1**	12.2±4.7 ab	**71.0**	32.8±4.6 ef	**15.9**	27.3±2.6 c-f	**35.2**
INT- Anaerobic control	+	6	31.5±2.1 b-d	**4.0**	36.2±2.2 de	**14.0**	31.5±2.1 ef	**19.2**	36.2±3.0 fg	**14.0**
INT- Standard control	-	6	32.8±4.6 cd	**0.0**	42.1±3.2 e	**0.0**	39±4.7 f	**0.0**	42.1±3.2 g	**0.0**
NINT- Anaerobic control	+	6	0.0±0.0 a	**100.0**	0.0±0.0 a	**100.0**	0.0±0.0 a	**100.0**	0.0±0.0 a	**100.0**

[a] Comp: Compost; BCp: *Brassica carinata* pellet with or without anaerobic conditions; WR: *Diplotaxis* green manure; TM: Tolclofos methyl; INT-Anaerobic control: Inoculated untreated control with anaerobiotic conditions; INT-Standard control: Inoculated untreated control without anaerobic conditions; NINT-Anaerobic control: Non inoculated untreated control with anaerobic conditions.

[b] Means in each column accompanied by a common letter are not significantly different ($P \leq 0.05$), according to Tukey's test. Standard errors are also reported.

[c] E%: Disease reduction compared to the INT-Standard controls carried out for 3 or 6 weeks.

al., 2007; Postma *et al*., 2014; Hewavitharan and Mazzola, 2016; Mowlick *et al*., 2012; 2013; Shennan *et al*., 2014; 2018). In the present study, *Brassicaceae* seed meal without anaerobic condition reduced basal rot of lettuce but to a lesser extent than in the ASD treatments, which generally provided more consistent disease control for all the tested temperatures in both soils (between a range of 52 to 72% disease reduction). However, the tested rate of application was five times greater than that suggested for the 'Biofence' product (3 t ha^{-1}) for biofumigation treatment. The economic value of such a high rate application should be evaluated. However, Butler *et al*., (2014 b) suggested that C source rates greater than 4 mg g^{-1} of soil were required when soil temperatures during ASD treatments were low (15-25°C). Serrano-Pérez *et al*. (2017) confirmed that ASD under early spring conditions in Spain, using several C sources at 4 mg g^{-1} of soil, was effective to control *P. nicotianae* disease in pepper. Nevertheless, in the present study effects on disease reduction and lettuce fresh weights were not observed at the greatest WR green manure amount of 30 t ha^{-1}. The efficacy of ASD based-WR was generally greatest at the highest incubation temperature in the peat soil and at the lowest temperature of 21°C in sandy loam soil. MaCarty *et al*. (2014) showed that an ASD treatment based on a mixture of *Sinapis alba* and *Eruca sativa,* affected survival of *R. solani* at approx. 20°C, under accumulated anaerobic conditions of approx. 20,000 mVh. The accumulated soil anaerobic condition achieved in the present study during different treatments only partially explain the ASD efficacy. For instance, the greatest basal rot control was obtained from the *Brassicaceae* seed meal applied for 6 weeks in the sandy-loam soil at 31°C, and this treatment resulted in 88,954 mVh. Almost the same value of cumulative mVh, achieved at 21°C, was only partially effective in the control of *Rhizoctonia* basal rot (28-46% disease reduction), compared to the untreated controls. These were severely affected at the end of the first cultivation cycle. Also, the greatest efficacy of ASD using

Table 8A. Mean fresh weight (g pot^{-1}) of lettuce plants after application of different ASD soil treatments, carried out for 3 or 6 weeks, and at 21 or 26 °C in sandy-loam artificially infested with *Rhizoctonia solani*, at the end of the first and second crop cycles (Trial 1).

Carbon source[a], dosage	ASD	Treatment duration (weeks)	Cycle I				Cycle II			
			21°C		26°C		21°C		26°C	
Comp, 15 t ha^{-1}	+	3	47.8±1.7	de[b]	20.8±1.9	ef	194.9±6.6	bc[a]	166.1±34.4	a-c
BCp, 15 t ha^{-1}	+	3	18.1±0.3	ef	74.1±9.7	b-d	109.9±9.0	de	110.7±20.5	a-d
WR, 15 t ha^{-1}	+	3	16.0±1.5	ef	7.4±1.3	f	303.5±5.4	a	67.4±19.4	d
TM, 2 gm^{-2}	-	3	67.2±6.6	cd	110.4±5.4	a-c	206.1±6.2	bc	167.2±29.2	a-c
INT- Anaerobic control	+	3	24.1±1.6	ef	9.9±1.4	f	170.9±18.5	b-d	74.5±15.9	cd
INT- Standard control	-	3	13.3±2.8	f	7.9±4.3	f	78.8±9.7	e	68.2±12.4	cd
NINT- Anaerobic control	+	3	117.5±12.4	ab	123.6±22.1	a-c	158.3±12.6	b-e	194.8±27.3	a-c
NINT- Standard control	-	3	105.2±2.3	ab	88.2±3.9	cd	300.8±15.6	a	204.9±38.5	ab
Comp, 15 t ha^{-1}	+	6	14.7±2.5	f	13.8±0.6	f	170.2±27.1	b-d	151.5±16.6	a-c
BCp, 15 t ha^{-1}	+	6	5.6±0.9	f	84.9±18.2	cd	236.2±24.3	ab	94.7±32.5	b-c
WR, 15 t ha^{-1}	+	6	25.4±6.9	ef	4.8±2.8	f	136.2±19.0	c-e	83.8±23.6	b-d
TM, 2 gm^{-2}	-	6	87.9±10.5	a-c	155±11.7	a	152.2±14.3	c-e	203.6±24.9	ab
INT- Anaerobic control	+	6	2.5±1.1	f	18.5±2.2	f	88.2±19.6	e	101.8±27.3	a-d
INT- Standard control	-	6	17.6±9.5	ef	5.4±2.3	f	97.5±4.5	de	57.2±17.0	d
NINT- Anaerobic control	+	6	85.7±4.5	bc	137.8±6.8	ab	210.6±22.3	bc	168.5±12.9	a-c
NINT- Standard control	-	6	119.9±12.1	a	103.6±6.6	bc	200.1±13.2	bc	223.5±26.0	a

[a] Comp: Compost; BCp: *Brassica carinata* pellet with anaerobic conditions; WR: *Diplotaxis* green manure; TM: Tolclofos methyl; INT-Anaerobic control: Inoculated untreated control with anaerobic conditions; INT-Standard control: Inoculated untreated control without anaerobic conditions; NINT-Anaerobic control: Non-inoculated untreated control with anaerobic conditions; NINT-Standard control: Non-inoculated untreated control without anaerobic conditions.

[b] Means in each column accompanied by the same letter are not significantly different ($P \leq 0.05$), according to Tukey's test. Standard errors are also indicated.

compost observed in the peat soil at 26°C for 6 weeks of incubation (67% efficacy) resulted in 46,495 mVh, while, at the higher cumulative value of 95,550 mVh, achieved using compost as C- source at 31°C, control of the disease was partial (20% disease reduction). Results from the present study are generally in agreement with those of Shennan *et al*. (2014; 2018), who provided evidence that accumulated soil anaerobic conditions of 50,000 mV h^{-1} at 25°C, achieved using wheat bran in a sandy clay loam soil, was crucial for control *Verticillium dahliae* in strawberry plants, but the same anaerobic condition did not provide efficient inactivation of the pathogen at 15°C.

ASD efficacy is modulated by a complex mechanism, and since a low soil oxygen levels are prerequisites for pathogen inactivation (Runia *et al*., 2014) for some pathogens such as *R. solani*, efficacy is closely related to the carbon source. This is possibly due to different volatile profiles resulting from ASD treated soil, and to microbiological changes (MaCarty *et al*., 2014; Hewavitharana *et al*., 2014; 2015). Several studies have also reported that inoculum inactivation in soil under different temperature and accumulated soil anaerobic conditions during ASD is pathogen specific. Mowlick *et al*., (2012; 2013) showed that the incubation temperature influenced the suppression of *F. oxysporum* f. sp. *spinaciae* to a great extent by stimulating the multiplication of the anaerobic bacteria related to the purely anaerobic clostridial groups in *Brassica*, oat and wheat bran ASD-treatments. The diversity in the clostridial groups was generally greatest in the *Brassica* and wheat bran ASD samples at 30°C, and the diversity was greatly reduced at 20°C in the *Brassica*-treated soil.

The present study has shown that ASD based on *Brassicaceae* and compost as C-sources applied in a sandy-loam soil, had impacts on the control of *R. solani* on lettuce, even at lower temperatures than those required for soil solarisation or biosolarisation (Gamliel, 2000), with a general improvement in disease control in the second crop cycle. For instance, the ASD based on compost was partially effective in reducing basal rot of lettuce at the end of the first crop cycle in both soils, while the greatest disease reductions of 53% and 66% were observed in the second crop cycle in the sandy-loam soil previously treated for 3 weeks at 21°C. The benefits of long-term compost treatments on differ-

Table 8B. Mean fresh weight (g pot^{-1}) of lettuce plants after application of different ASD soil treatments, carried out for 3 or 6 weeks, and at 21 or 31 °C in sandy-loam artificially infested with *Rhizoctonia solani*, at the end of the first and second crop cycles (Trial 2).

Carbon source[a], dosage	ASD	Treatment duration (weeks)	Cycle I				Cycle II			
			21°C		31°C		21°C		31°C	
Comp, 15 t ha^{-1}	+	3	23.7±2.5	cd[b]	28.1±4.3	d-f	71.8±7.4	a-d	26.9±7.7	fg
BCp, 15 t ha^{-1}	+	3	77.9±3.9	b	37.9±4.7	cd	94.7±9.0	ab	149.5±18.2	a
WR, 15 t ha^{-1}	+	3	25.9±8.1	cd	26.3±1.0	d-f	77.9±6.4	a-c	56.0±5.0	d-f
WR, 30 t ha^{-1}	+	3	26.0±4.2	cd	31.9±2.0	ce	89.0±5.8	a-c	74.0±5.6	c-e
TM, 2 gm^{-2}	-	3	38.2±2.3	c	43.6±3.7	c	64.1±12.4	a-e	64.3±20.1	c-f
BCp, 15 t ha^{-1}- No anaerobic control	-	3	34.6±2.5	cd	30.4±4.2	ce	96.1±23.2	ab	77.8±8.1	b-e
INT- Anaerobic control	+	3	17.9±3.7	cd	19.4±3.0	d-f	60.1±5.9	a-e	36.3±4.1	d-f
INT- No anaerobic control	-	3	17.7±2.3	cd	15.3±2.0	ef	48.1±12.8	b-e	23.6±3.2	g
NINT- Anaerobic control	+	3	116.3±8.3	a	109.8±5.6	b	92.2±8.4	ab	127.1±7.1	ab
Comp, 15 t ha^{-1}	+	6	28.5±3.9	cd	15.7±2.5	ef	51.7±5.0	b-e	39.2±3.5	d-f
BCp, 15 t ha^{-1}	+	6	67.3±3.6	b	50.0±0.0	c	83.4±8.7	a-c	150.4±12.9	a
WR, 15 t ha^{-1}	+	6	34.4±1.6	cd	28.9±3.4	d-f	56.1±6.2	b-e	76.5±9.5	c-e
WR, 30 t ha^{-1}	+	6	22.3±3.2	cd	19.9±4.7	d-f	99.3±2.1	ab	109.0±9.0	a-c
TM, 2 gm^{-2}	-	6	39.0±3.9	c	34.5±0.8	cd	36.5±8.2	c-e	77.1±9.3	b-e
BCp, 15 t ha^{-1}- No anaerobic control	-	6	32.4±8.2	cd	38.5±7.8	cd	111.6±22.1	a	49.4±5.6	d-f
INT- Anaerobic control	+	6	18.5±2.1	cd	13.8±2.2	e-f	22.8±1.6	de	35.8±11.7	d-f
INT- No anaerobic control	-	6	13.5±2.9	d	8.0±3.2	f	14.3±3.6	e	49.0±4.4	d-f
NINT- Anaerobic control	+	6	85.3±6.7	b	141.5±6.1	a	69.0±3.2	a-d	158.4±7.5	a

[a] Comp: Compost; BCp: *Brassica carinata* pellet with or without anaerobic conditions; WR: *Diplotaxis* green manure; TM: Tolclofos methyl; INT-Anaerobic control: Inoculated untreated control with anaerobiotic conditions; INT-Standard control: Inoculated untreated control without anaerobic conditions; NINT-Anaerobic control: Non inoculated untreated control with anaerobic conditions.

[b] Means in each column accompanied by a common letter are not significantly different ($P \leq 0.05$), according to Tukey's test. Standard errors are also reported.

ent pathosystems are well known (Abawi and Widmer, 2000; Chellemi, 2002; Gamliel, 2000; Lazarovits and Subbarao, 2010). However, a wide range of results have been achieved when compost has been used as organic amendments, including decreases and increases in soil-borne disease incidence and severity (Hoitink and Fahy, 1986; Abbasi *et al*., 2002; Noble and Coventry, 2005; Bonanomi *et al*., 2007; Pugliese *et al*., 2011; 2015). Compost suppressiveness against *Rhizoctonia solani* in particular is known to be limited (Termorshuizen *et al*., 2006; Pugliese *et al*., 2015), and the use of composted manure for ASD has also been less effective than other carbon sources for controlling this pathogen (Hewavitharana and Mazzola, 2016).

Generally, the variation in efficacy of individual treatment combinations was limited in the second crop cycle, with positive effect on lettuce yields. However, the infection of plants by *Rhizoctonia solani* was generally less in the second crop cycle than in the first, and all the tested C-sources applied to both soils provided greater disease control in the second crop cycle, which resulted in increased lettuce yields.

Although it is well known that ASD treatments may have effects on soil fertility, by influencing different soil properties (MaCarty *et al*., 2014; Butler *et al*., 2014b; Di Gioia *et al*., 2017), they may also have negative effects on crop yields, due to low amounts of available N when large amounts of labile C are applied (Whitmore, 1996), or to phytotoxicity. Phytotoxic effects of ASD treatments could explain the low lettuce fresh weights measured after the first cycle, which may not only be attributable to differences in efficacy of the tested ASD treatments. High-N amendments in soils can lead to the production of ammonia, which is toxic to a wide range of pathogens and nematodes (Conn *et al*., 2005; López-Robles *et al*., 2013; Mazzola *et al*., 2018), but also may have negative effects on plant development (Barker *et al*., 1970). Readily decomposable amendments, under anaerobic conditions, can also favour the production of toxic organic acids which have been linked to the control of fungal, nematode, insect, and weed pests (Okazaki and Nose, 1986; Conn *et al*., 2005; Momma *et al*., 2006; Hestmark *et al*., 2019). The possible phytotoxicity to lettuce from organic acid accumulation or salts during ASD treatments should be considered.

In the present study small increases in soil pH of 0.2 to 0.4 units was observed when *B. carinata* pellets were used. Increased suppressiveness of Rhizoctonia damping-off of sugar beet in a near neutral to alkaline soil, compared to acid soil, from use of dried peanut plant residues, has been reported, due to increased activity of specific antagonistic soil microorganisms (Watanabe *et al*., 2011). Similar disease suppression effects have been obtained by amending soils with composts rich in cellulolytic and oligotrophic actinomycete antagonists (Tuitert *et al*., 1998; Kasuya *et al*., 2006; Ros *et al*., 2006). Changes in the soil microbiome, induced by an ASD treatment in a carbon source dependent manner (Hewavitharan and Mazzola, 2016), can be persistent, and may result in long-term pathogen re-infestation (Goud *et al*., 2004). Improved disease suppression and yields were observed for the ASD treatment-based compost in the second crop cycle, which is similar to other reports (Ros *et al*., 2006; Hestmark *et al*., 2019). Nevertheless, the increased lettuce fresh weights observed after ASD treatment in the second crop cycle may also be explained in part by improved nutritional status of the plants, as was observed by Butler *et al*., (2014 b) and Di Gioia *et al*., (2017).

No chemical or non-chemical methods used alone exhibit the same efficacy as some soil fumigants used in the past (Katan, 2017), so disease reduction offered by ASD studied here is promising. The potential of ASD for controlling *R. solani* incidence in lettuce merits further investigation, so that it can be adapted to different local conditions. The significant but only partial efficacy of ASD when *Brassica carinata* was applied as C-source does not justify the adoption of such treatment in the practice, but this approach integrated with other disease management methods could be worthwhile (Butler *et al*., 2012 a). For sustainable agriculture, the use of compost or *Diplotaxis* green manure as other C-sources possible for evaluation of other green wastes. ASD based on *Diplotaxis* could be useful for managing crop residues in horticultural systems for ready-to-eat salad crops, where stringent quality requirements must be satisfied and crop damage thresholds of 5% make the products unmarketable.

ACKNOWLEDGEMENTS

This study received funding from the European Union's Horizon 2020 research and innovation programme EUCLID EU-CHINA Lever for IPM Demonstration, Grant agreement no. 633999. The authors thank Stefano Demarchi for technical support and Marguerite Jones for English language revision and Prof. Jaacov Katan and the anonymous referees for their valuable suggestions.

CONFLICT OF INTEREST

Massimo Pugliese declares he has a financial interest (shareholder) in AgriNewTech, the company that provided the compost tested in this research.

LITERATURE CITED

Abawi G. S., Widmer T. L., 2000. Impact of soil health management practices on soilborne pathogens, nematodes and root diseases of vegetable crops. *Applied Soil Ecology* 15: 37–47.

Abbasi P.A., Al-Dhmani J., Sahin F., Hoitink H.A.J. Miller S.A., 2002. Effect of compost amendments on disease severity and yield of tomato in conventional and organic production systems. *Plant Disease* 86:156–161.

Barker A.V., Maynard D.N., Mioduchowska B., Buch A., 1970. Ammonium and salt inhibition of some physiological processes associated with seed germination. *Physiol. Plant* 23: 898–907.

Barrière V., Lecompte F., Nicot F.C., Maisonneuve B., Tchamitchian M., Lescourret F., 2014. Lettuce cropping with less pesticides. *Agronomy for Sustainable Agriculture. A review* 34 : 175–198.

Blancard D., Lot H., Maisonneuve B., 2003. Maladies des salades: identifier, connaître et maîtriser. INRA, Paris.

Blok W.J., Lamers J.G., Termorshuizen A.J., Bollen G.J., 2000. Control of soilborne plant pathogens by incorporating fresh organic amendments followed by tarping. *Phytopathology* 90: 253–259.

Bonanomi G., Antignani V., Pane C., Scala F., 2007. Suppression of soilborne fungal diseases with organic amendments. *Journal of Plant Pathology* 89: 311–324.

Butler D. M., Kokalis-Burelle N., Muramoto J., Shennan C., McCollum T. G., Rosskopf E. N. 2012a. Impact of anaerobic soil disinfestation combined with soil solarization on plant parasitic nematodes and introduced inoculum of soilborne plant pathogens in raised-bed vegetable production. *Crop Protection* 39: 33–40.

Butler D. M., Rosskopf E. N., Kokalis-Burelle N., Albano J. P., Muramoto J., … Shennan C., 2012b. Exploring warm season cover crops as carbon sources for anaerobic soil disinfestation (ASD). *Plant and Soil* 355: 149–165.

Butler D.M., Ownley B.H., Dee M.E., Inwood S.E., McCarty D.G., Rosskopf E.N., 2014a. Low carbon Amendment rates during anaerobic soil disinfestation (ASD) at moderate soil temperatures do not decrease viability of *Sclerotinia sclerotiorum* sclerotia or Fusarium root rot of common bean. *Acta Horticulturae* 1044: 19–28.

Butler D.M., Kokalis-Burelle N., Albano J.P., McCollum T.G., Muramoto J., … Rosskopf E.N., 2014b. Anaerobic soil disinfestation (ASD) combined with soil solarization as a methyl bromide alternative: vegetable crop performance and soil nutrient dynamics. *Plant Soil* 378: 365–381.

Chellemi D., 2002. Nonchemical management of soilborne pests in fresh market vegetable production systems. *Phytopathology 92*:1367–1372.

Conn K.L., Tenuta M., Lazarovits G., 2005. Liquid swin e manure can kill *Verticillium dahliae* microsclerotia in soil by volatile fatty acid, nitrous acid, and ammonia toxicity. *Phytopathology 95*: 28–35.

Di Gioia F., Ozores-Hamptona M., Zhaob X., Thomasc J., Wilsonc P., Rosskopf E., 2017. Anaerobic soil disinfestation impact on soil nutrients dynamics and nitrous oxide emissions in fresh-market tomato. *Agriculture, Ecosystems and Environment* 240: 194–205.

Ebihara Y., Uematsu S., 2014. Survival of strawberry-pathogenic fungi *Fusarium oxysporum* f. sp. fragariae, *Phytophthora cactorum* and *Verticillium dahliae* under anaerobic conditions. *Journal General Plant Pathology 8*0: 50–58.

Fiedler S., Vepraskas M.J., Richardson J.L., 2007. Soil Redox Potential: Importance, Field Measurements, and Observations. *Advances in Agronomy* 94:1-54.

Gamliel A., 2000. Soil amendments: a non chemical approach to the management of soilborne pests. *Acta Horticulturae* 532: 39–47.

Garibaldi A., Gilardi G., Gullino M.L., 2014. Critical aspects in disease management as a consequence of the evolution of soil-borne pathogens. *Acta Horticulturae* 1044: 43–52.

Goud J.K.C., Termorshuizen A.J., Blok W.J., Van Bruggen A.H.C., 2004. Long-term effect of biological soil disinfestation on Verticillium wilt. *Plant Disease* 88: 688–694.

Gullino M.L., Gilardi G., Garibaldi A., 2019. Ready-to-eat salad crops: the plant pathogen's heaven. *Plant Disease* 103:2153–2170.

Hestmark K.V., Fernández-Bayo J.D., Harrold D.R., Randall T.E., Achmon Y., Vander Gheynst J.S., 2019. Compost induces the accumulation of biopesticidal organic acids during soil biosolarization. *Resources Conservation Recyclcling* 143: 27–35.

Hewavitharana S. S., Mazzola M., 2016. Carbon source-dependent effects of anaerobic soil disinfestation on soil microbiome and suppression of *Rhizoctonia solani* AG-5 and *Pratylenchus penetrans*. *Phytopathology* 106: 1015–1028.

Hewavitharana S.S., Ruddell D., Mazzola M., 2014. Carbon source-dependent antifungal and nematicidal volatiles derived during anaerobic soil disinfestation. *European Journal of Plant Pathology* 140: 39–52.

Hewavitharana S. S., Shennan C., Muramoto J., Mazzola M., 2015. Anaerobic soil disinfestation disease control performance in strawberry as influenced by environmental variables. *Phytopathology* 105: S4.59.

Hoitink H.A.J., Fahy P.C., 1986. Basis for the control of soilborne plant pathogens with composts. *Annual Review of Phytopathology* 24: 93–114.

Huang X., Liu L., Wen T., Zhang J., Wang F., Cai F., 2016. Changes in the soil microbial community after reductive soil disinfestation and cucumber seedling cultivation. *Applied Microbiology Biotechnol0gy* 100: 5581–5593.

Kasuya M., Olivier A.R., Ota Y., Tojo M., Honjo H., Fukui R., 2006. Induction of soil suppressiveness against *Rhizoctonia* solani by incorporation of dried plant residues into soil. *Phytopathology* 96: 1372–1379.

Katan J., 2017. Diseases caused by soilborne pathogens: biology, management and challenges. *Journal of Plant Pathology* 99: 305–315

Katase M, Kubo C, Ushio S, Ootsuka E, Takeuchi T, Mizukubo T., 2009. Nematicidal activity of volatile fatty acids generated from wheat bran in reductive soil disinfestation. *Japanese Journal of Nematology* 39: 53–62.

Lamers J.G., Runia W.T., Molendijk L.P.G., Bleeker P.O., 2010. Perspectives of anaerobic soil disinfestation. *Acta Horticulturae* 883: 277–283.

Lazarovits G., Subbarao K., 2010. Challenges in controlling Verticillium wilt by the use of non chemical methods. In: *Recent developments in Management of Plant Diseases, Plant Pathology in the 21stCentury* (Gisi U., Chet I., Gullino M.L. Eds.), Springer, Dordrecht, NL, 247–264.

López-Robles J., Olalla C., Rad C., Díez-Rojo M.A., López-Pérez J.A., … Rodríguez-Kábana R., 2013. The use of liquid swine manure for the control of potato cyst nematode through soil disinfestation in laboratory conditions. *Crop Protection* 49: 1-7.

Mazzola M., Brown J., Izzo A.D., Cohen M.F., 2007. Mechanism of action and efficacy of seed meal-induced pathogen suppression differ in a *Brassicaceae* species and time-dependent manner. *Phytopathology* 97: 454–460.

Mazzola M., Granatstein D.M., Elfving D.C., Mullinix K., 2001. Suppression of specific apple root by *Brassica napus* seed meal amendment regardless of glucosinolate content. *Phytopathology* 91: 673–679.

Mazzola M., Hewavitharana S., 2014. Carbon source-dependent volatile production and ASD efficacy for suppression of apple root pathogens and parasites. *Acta Horticulturae* 1044: 208–214.

Mazzola M., Manici L.M., 2012. Apple replant disease: role of microbial ecology in cause and control. *Annual Review of Phytopathology* 50: 45–65.

Mazzola M., Muramoto J., Shennan C., 2018. Anaerobic disinfestation induced changes to the soil microbiome, disease incidence and strawberry fruit yields in California field trials. *Applied Soil Ecology* 127: 74–86.

McCarty D. G., Inwood S. E. E, Ownley B. H., Sams C. E., Wszelaki A. L., Butler, D. M., 2014. Field evaluation of carbon sources for anaerobic soil disinfestation in tomato and bell pepper production in tennessee. *HortScience* 49: 272–280.

Messiha N.A.S., van Diepeningen A.D., Wenneker M., van Beuningen A.R., Janse J.D., …Blok W.J., 2007. Biological Soil Disinfestation (BSD), a new control method for potato brown rot, caused by *Ralstonia solanacearum* race 3 biovar 2. *European Journal of Plant Pathology* 117: 403–415.

Momma N., Yamamoto K., Simandi P., Shishido M., 2006. Role of organic acids in the mechanisms of biological soil disinfestation (BSD) *Journal General Plant Pathology* 72: 247–252.

Momma N., Momma M., Kobara Y., 2010. Biological soil disinfestation using ethanol: Effect on *Fusarium oxysporum* f. sp. *lycopersici* and soil microorganisms. *Journal of General Plant Pathology* 76: 336–344.

Momma N., Kobara Y., Uematsu S., Kita N., Shinmura A., 2013. Development of biological soil disinfestations in Japan. *Applied Microbiology Biotechnology* 97: 3801–3809.

Mowlick S., Takehara T., Kaku N., Ueki K., Ueki A., 2012. Proliferation of diversified clostridial species during biological soil disinfestation incorporated with plant biomass under various conditions. *Applied Microbiology Biotechnology* 97: 8365–8379.

Mowlick S., Yasukawa H., Inoue T., Takehara T., Kaku N., ..., Ueki A., 2013. Suppression of spinach wilt disease by biological soil disinfestation incorporated with *Brassica juncea* plants in association with changes in soil bacterial communities. *Crop Protection* 54: 185–193.

Muramoto J., Shennan C., Zavatta M., Yoyama L., Hewavitharana S.S., Mazzola M., 2015. Controlling Fusarium wilt of strawberries by anaerobic soil disinfestation. Pages 16.1-4. Proc. Annu. Int. Res. Conf. Methyl Bromide Altern. Emiss. Reduct. MBAO, San Diego, CA.

Noble R., Coventry R., 2005. Suppression of soil-borne plant diseases with composts: a review. *Biocontrol Science and Technology* 15: 3-20.

Okazaki H., Nose K., 1986. Acetic acid and N-butyric acid as causal agents of fungicidal activity of glucose-amended flooded soil. *Ann Phytopathol Soc Jpn* 52: 384–393.

Postma J., Schilder M.T., Stevens L.H., 2014. Potential of Organic Amendments to Enhance Soil Suppressiveness against *Rhizoctonia solani* Disease in Different Soils and Crops. *Acta Horticolturae* 1044:127–132.

Pugliese M., Liu B.P., Gullino M.L., Garibaldi A., 2011. Microbial enrichment of compost with biological control agents to enhance suppressiveness to soil-borne diseases. *Journal of Plant Disease and Protection* 118: 45–50.

Pugliese M., Gilardi G., Garibaldi A., Gullino M. L., 2015. Organic Amendments and Soil Suppressiveness: Results with Vegetable and Ornamental Crops. In: *Organic Amendments and Soil Suppressiveness in Plant Disease Management* (Meghvansi M. K. and Varma A. eds.), Soil Biology 46, Springer, ISBN 978-3-319–23074-0, 495–509.

Rabenhorst M.C., Castenson K.L., 2005. Temperature effects on iron reduction in a hydric soil. *Soil Science* 170: 734–742.

Rodríguez-Molina M.C., Serrano-Pérez P., Palo C., 2016. Effect of biofumigation with brassica pellets combined with *Brassicaceae* cover crops and plastic cover on the survival and infectivity of inoculum of *Phytophthora nicotianae* Breda de Haan. *Pest Managagement Science* 72: 1295–1301.

Ros M., Klammer S., Knapp B., Aichberger K., Insam H., 2006. Long-term effects of compost amendment of soil on functional and structural diversity and microbial activity. *Soil Use Manage* 22: 209–218.

Rosskopf E.N., Serrano-Pérez P., Hong J., Shrestha U., Rodríguez-Molina M.C., … Butler D., 2015. Anaerobic soil disinfestation and soilborne pest management. *Soil Biology* 46: 277–305.

Runia W.T., Molendijk L.P.G., Ludeking D.J.W., Schomaker C.H., 2012. Improvement of anaerobic soil disinfestation. *Comm. Appl. Biol. Science* 77: 753–762.

Runia W.T., Thoden T.C., Molendijk L.P.G., van den Berg W., Termorshuizen A.J., …, Meints H., 2014. Unravelling the mechanism of pathogen inactivation during anaerobic soil disinfestation. *Acta Horticulturae* 1044: 177–193.

Serrano-Pérez P., Rosskopf E., De Santiago A., Rodríguez-Molina M.C., 2017. Anaerobic soil disinfestation reduces survival and infectivity of *Phytophthora nicotianae* chlamydospores in pepper. *Scientia Horticolturae* 215: 38–48

Shennan C., Muramoto J., Koike S., Bolda M., Daugovish O., 2010. Optimizing anaerobic soil disinfestation for non-fumigated strawberry production in California. *HortScience* 45: S270.

Shennan C., Muramoto J., Lamers J., Mazzola M., Rosskopf E.N., …, Kobara Y., 2014. Anaerobic soil disinfestation for soil borne disease control in strawberry and vegetable systems: current knowledge and future directions. *Acta Horticulturae* 1044: 157–165.

Shennan C., Muramoto J., Koike S., Baird G., Fennimore S., …Mazzola M., 2018. Anaerobic soil disinfestation is an alternative to soil fumigation for control of some soilborne pathogens in strawberry production. *Plant Pathology* 67: 51–66.

Shinmura A., 2004. Principle and effect of soil sterilization methods by reducing the redox potential of soil. *PSJ Soilborne Disease Workshop Report* 22: 2-12.

Shrestha U., Auge R., Butler D., 2016. A meta-analysis of the impact of anaerobic soildisinfestation on pest suppression and yield of horticultural crops. *Frontiers Plant Science* 7: doi.org/10.3389/fpls.2016.01254.

Sneh B., Jabaji-Hare S., Neate S., Dijs G., 1996. Rhizoctonia Species: Taxonomy, Molecular Biology, Ecology, Pathology and Disease Control. Dordrecht, Netherlands, Kluwer Academic, San Francisco.

Strauss S. L., Kluepfel D.A., 2015. Anaerobic soil disinfestation: A chemical-independent approach to preplant control of plant pathogens. *Journal of Integrative Agriculture* 14: 2309–2318.

Tamietti G., Garibaldi A., 1987. Effectiveness of soil solarization against Rhizoctonia solani in northern Italy. Proc CEC/IOBC Group Meeting on Integrated Pest Management in Protected Vegetable Crops, 27–29 May 1987. Cabrils, Spain, pp 193–197.

Termorshuizen A. J., van Rijn E., van der Gaag D. J., Alabouvette C., Chen Y., …, Zmora-Nahum S., 2006. Suppressiveness of 18 composts against 7 pathosystems: Variability in pathogen response. *Soil Biology & Biochemistry* 38: 2461–2477.

Tuitert G., Szczech M., Bollen G.J., 1998. Suppression of *Rhizoctonia solani* in potting mixtures amended with compost made from organic household waste. *Phytopathology* 88:764–773.

Watanabe K., Matsui M., Honjo H., Becker J.O., Fuk R., 2011. Effects of soil pH on Rhizoctonia damping-off of sugar beet and disease suppression induced by soil amendment with crop residues. *Plant Soil* 347: 255–268.

Whitmore A.P., 1996. Modelling the release and loss of nitrogen after vegetable crops. *Net Journal Agricultural Science* 44: 73–86.

Yossen V., Zumelza G., Gasoni L., Kobayashi K., 2008. Effect of soil reductive sterilization on Fusarium wilt in greenhouse carnation in Cordoba, Argentina. *Australasian Plant Pathology* 37: 520–522.

Phytopathologia Mediterranea
The international journal of the
Mediterranean Phytopathological Union

Firenze University Press
www.fupress.com/pm

Research Paper

Improved DNA extraction and quantitative real-time PCR for genotyping *Erysiphe necator* and detecting the DMI fungicide resistance marker A495T, using single ascocarps

Alexandra PINTYE[1,*], Márk Z. NÉMETH[1], Orsolya MOLNÁR[1], Áron N. HORVÁTH[1], Zsolt SPITZMÜLLER[2], Nikoletta SZALÓKI[2], Károly PÁL[2], Kálmán Z. VÁCZY[2], Gábor M. KOVÁCS[1,3]

[1] *Centre for Agricultural Research, Martonvásár, Hungary*
[2] *Food and Wine Research Institute, Eszterházy Károly University, Eger, Hungary*
[3] *Eötvös Loránd University, Institute of Biology, Department of Plant Anatomy, Budapest, Hungary*
*Corresponding author: pintye.alexandra@agrar.mta.hu

Summary. DNA extraction from minute fungal samples is challenging in all genetic studies. Identification of genetic groups and population biology mostly rely on the laborious production of single conidium isolates or on field samples, including infected plant materials. This paper reports a simple and cost-effective protocol for DNA extraction from individual chasmothecia of *Erysiphe necator* for subsequent applications. It is a less laborious alternative for genotyping purposes than production and analysis of single conidium isolates or analysis of infected plant material from the field. Using the protocols described here for 186 *E. necator* samples tested, genetic groups A and B were assigned. Based on *CYP51* sequences, all the samples belonged to group B, while *TUB2* sequences exhibited SNPs also diagnostic for group A. Additionally, a quantitative real-time PCR detection method of single nucleotide polymorphism in the *CYP51* gene associated with DMI fungicide resistance was applied. The A495T marker, associated with DMI resistance, and here reported for the first time from Hungary, was detected by quantitative real-time PCR assays and direct sequencing of *CYP51*. The methods developed in this study can be applied as routine tests to monitor powdery mildew populations for fungicide resistance and other genetic characteristics.

Keywords. Y136F, azole fungicide sensitivity, *CYP51* gene, chasmothecium.

OPEN ACCESS

Citation: A. Pintye, M.Z. Németh, O. Molnár, Á.N. Horváth, Z. Spitzmüller, N. Szalóki, K. Pál, K.Z. Váczy, G.M. Kovács (2020) Improved DNA extraction and quantitative real-time PCR for genotyping *Erysiphe necator* and detecting the DMI fungicide resistance marker A495T, using single ascocarps. *Phytopathologia Mediterranea* 59(1): 97-106. doi: 10.14601/Phyto-11098

Accepted: February 6, 2020

Published: April 30, 2020

Data Availability Statement: All relevant data are within the paper and its Supporting Information files.

Competing Interests: The Author(s) declare(s) no conflict of interest.

Editor: Philippe Nicot, Plant Pathology Research Unit INRA, Avignon, France.

INTRODUCTION

Powdery mildews (PMs) are frequent diseases of many angiosperm hosts, and are caused by obligate biotrophic fungi in the Erysiphales (Glawe, 2008). These fungi are potential models in a wide range of studies, such as those that describe how coinfections are formed (Susi and Laine, 2017) or that explain disease dynamics (Jousimo *et al.*, 2014; Marçais *et al.*, 2017), pathogen host

range expansions (Vági *et al.*, 2007; Beenken, 2017), host-pathogen co-evolution (Takamatsu *et al.*, 2013) or genome evolution (Frantzeskakis *et al.*, 2019). With very small uncultivable fungi, it is important to use the smallest discrete unit for DNA extraction, which can be identified based on morphology and is large enough to obtain sufficient genomic DNA for molecular genetic analyses. In this way, data can be obtained at the level of individuals, and the possibilities of contamination with other fungi (Sundberg *et al.*, 2018), or cross-contamination with another colony possibly belonging to a different genetic line of the same species, may be reduced.

Grapevine powdery mildew (GPM), caused by *Erysiphe necator*, is one of the most economically significant diseases of grape production (Gadoury *et al.*, 2012). In GPM, molecular characterizations are usually based on mycelium collected directly from the field (e.g. Frenkel *et al.*, 2012) or from single conidium isolates, i.e., GPM colonies each produced by a single conidium on the surface of a surface-sterilized leaf in laboratory conditions (e.g. Brewer and Milgroom, 2010).

Direct PCR methods without DNA purification have been successfully used to identify genetic groups in *E. necator* (Miazzi *et al.*, 2008), or to detect the pathogen in grapevine buds (Gindro *et al.*, 2014). Miazzi *et al.* (2008) obtained the best results with 4-10 conidia picked up from individual leaves using sterile eyelashes, and added directly to PCR mixtures. Gindro *et al.* (2014) used 10- and 100-fold diluted powdery mildew-infected plant samples crushed in polyvinylpolypyrrolidone, and added directly to PCR mixtures before amplification (Gindro *et al.*, 2014). Furthermore, PCRs and quantitative real-time PCRs (qPCRs) with DNA samples originating from individual conidia were also successful for two other powdery mildew species (Matsuda *et al.*, 2005).

Conidia are very small discrete units, and to obtain enough DNA for downstream applications, single conidium isolates should be produced, which is laborious and time consuming. It takes at least 1 month to obtain a clearly monoconidial GPM colony (Rallos and Baudoin, 2016). Ascocarps (chasmothecia) can be considered the smallest discrete unit of a powdery mildew fungus in nature that can still be easily handled, yet are large enough to contain sufficient DNA for multilocus analyses and qPCR.

Chasmothecia of *E. necator* are usually produced in large numbers at the end of the grapevine growing season (Gadoury and Pearson, 1988; Cortesi *et al.*, 1997). Young chasmothecia are hyaline spherical bodies that turn yellow, then brown during maturation. They finally become black with characteristic appendages, and are filled with asci containing ascospores (Gadoury and Pearson, 1988). Chasmothecia have been used for DNA extraction in molecular studies of other PMs (Hirata and Takamatsu, 1996), but not commonly for studies of GPM. Mougou *et al.* (2008) found that ten chasmothecia, collected directly from the surfaces of the host plant leaves, is the minimum number required for amplification of the nrDNA ITS region. However, to our knowledge, individual chasmothecia have not been extensively used for such purposes.

Two distinct genetic groups, A and B, have been described in *E. necator* using single conidium isolates (e.g. Brewer and Milgroom, 2010) or field samples (e.g. Frenkel *et al.*, 2012). The differentiation between these genetic groups is based on different molecular markers, such as sequences of the β-tubulin (*TUB2*) (Amrani and Corio-Costet, 2006) and the eburicol 14α-demethylase (*CYP51*) genes (Délye *et al.*, 1999), as well as sequences of the nrDNA internal transcribed spacer (ITS) region (Délye *et al.*, 1999) and intergenic spacer (IGS) region (Brewer and Milgroom, 2010).

Detection of fungicide resistance, in addition to population genetic studies, is an important task for characterisation of GPM. Demethylation inhibitor (DMI) fungicides inhibit CYP51, a key enzyme of the fungal sterol biosynthetic pathway. This enzyme catalyzes the biosynthesis of ergosterol, which is an important membrane component of fungi (Parker *et al.*, 2014). Because of their site-specific modes of action, the intensive use of DMIs may lead to the spread of the fungicide resistance in GPM populations (Frenkel *et al.*, 2015). A marker for DMI resistance is an A to T nucleotide substitution in position 495 (A495T) in the *CYP51* gene (Délye *et al.*, 1999). This results in amino acid substitution at position 136 (Y136F) and correlates with high levels of azole resistance (Frenkel *et al.*, 2015). Until recently, single conidium isolates (e.g. Miazzi and Hajjeh, 2011; Frenkel *et al.*, 2015) or field samples (Montarry *et al.*, 2009; Dufour *et al.*, 2011), but not chasmothecia, were used to detect marker A495T.

This paper describes a study which aimed to develop a protocol for DNA extraction from individual PM chasmothecia, to provide evidence that the samples are suitable for downstream applications. Here, we also present the application and evaluation of a qPCR assay for the detection the DMI fungicide resistance marker A495T in DNA extracts from individual *E. necator* chasmothecia.

MATERIALS AND METHODS

DNA extraction from individual chasmothecia

Powdery mildew-infected grapevine leaves were examined in the laboratory under a stereo microscope (Zeiss Stemi 2000C), to isolate chasmothecia. Single

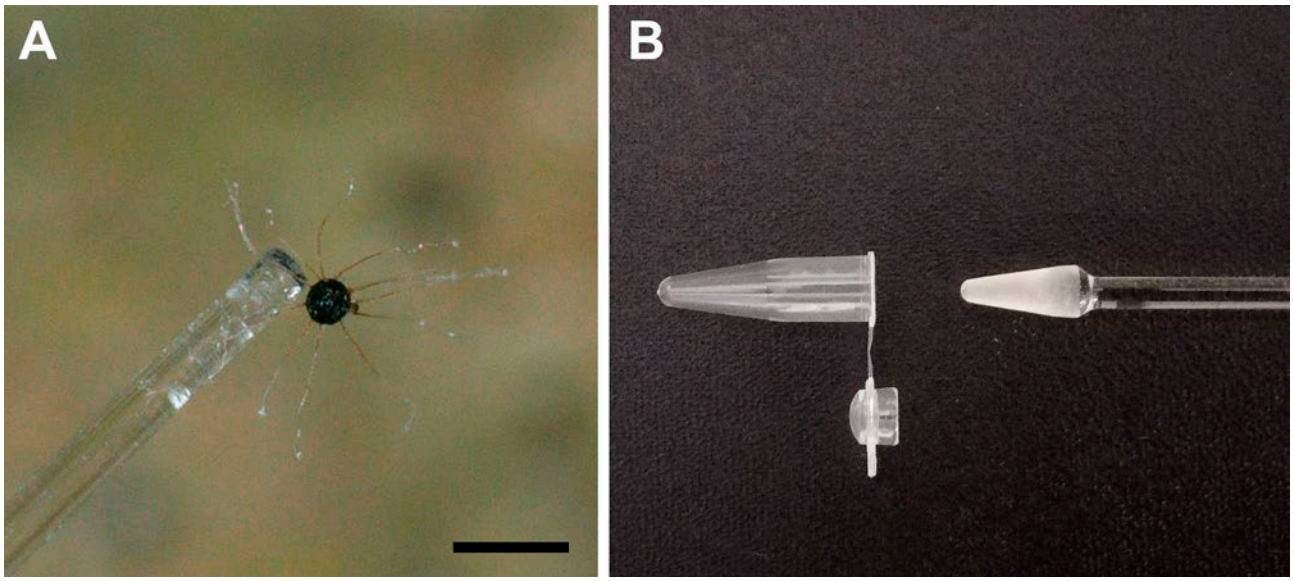

Figure 1. First steps of sample preparation. A: individual *Erysiphe necator* chasmothecium attached to the tip of a glass needle. Bar = 250 µm. B: plastic PCR tube (left) and conical glass micropestle (right).

immature (yellow, orange or brown) and mature (dark brown or black) chasmothecia were separated from the mycelium (without any visible hyphal fragments), using sterile glass needles (Figure 1A), and each placed in a 0.2 mL capacity PCR tube containing 20 µL of extraction medium. The following extraction media were tested: (a) Tris-EDTA (TE) buffer (pH 8; Lonza); (b) 1 M NaOH (Sigma-Aldrich) solution; (c) nuclease-free water (Thermo Fisher Scientific); or (d) dilution buffer of the Phire Plant Direct PCR Kit (Thermo Fisher Scientific). With each extraction medium, DNA was extracted from 15 chasmothecia as a preliminary experiment. To crush single chasmothecia in the extraction medium in PCR tubes, the following tools were tested; micropestles with either spherical or conical ends (Figure 1B), specifically manufactured for this purpose (Ranyák Üvegtechnika Anno 1967) or carved pipette tips. These tools were selected to fit into the PCR tubes. After disrupting individual chasmothecia under observation with a stereo microscope, the suspensions were vortexed for 1 min, centrifuged at 3000 × *g* for 1 min, and incubated at 97°C for 7 min. DNA samples obtained in this way were stored at -20°C. The most suitable extraction medium was selected based on the results of the PCR amplifications (see below).

DNA amplification and sequencing

Four loci were amplified in this study: ITS, IGS, and the *TUB2* and *CYP51* genes. The following primers were used in the amplifications: for ITS, ITSEnF/ITSEnR; for IGS, IGSEn1/NS1R; *TUB2*, Bt2c/Bt2d (Brewer and Milgroom, 2010); and for *EnCYP51*, EnCYP89F/EnCYP856R (Frenkel *et al.*, 2015).

For PCR optimization, three ready-to-use PCR master mix solutions were evaluated. These were Red Taq 2× DNA Polymerase Master Mix (VWR), DreamTaq Green PCR Master Mix (2X) (Thermo Fisher Scientific) or Phusion Green Hot Start II High-Fidelity PCR Master Mix (Thermo Fisher Scientific), which are hereafter referred to as, respectively, *Red Taq*, *DreamTaq* and *Phusion*.

All PCRs were performed in 20 µL final volumes. Reaction components included 1 µL of 10 µM forward and reverse primers (Sigma-Aldrich), 1 µL DNA template and 10 µL *Red Taq, DreamTaq* or *Phusion*. With the *Phusion* master mix solution, a range of target volumes (0.1 to 4 µL) was tested.

Samples previously resulting in successful amplifications were used as positive control samples, and nucleic acid-free water was used as the target in negative control reactions. To determine the optimal target DNA dilutions for the reactions, a series of dilutions was tested, i.e., 50-, 200-, 500-, 1000- and 2000-fold. This test was conducted twice with ten DNA samples for all loci described above using *Phusion*.

Amplification conditions for PCR with *Red Taq* and *DreamTaq* constituted an initial denaturation step for 5 min at 94°C, followed by 35 cycles of 45 s at 94°C, 45 s at 55°C for ITS, at 56°C for IGS and *TUB2* and at 57°C for *CYP51* primers, and 60 s at 72°C, with a final extension

step of 10 min at 72°C. For *Phusion* cycling, times and temperatures were as follows: 2 min at 98°C, followed by 36 cycles of 5 s at 98°C, 5 s at 60°C and 15 s at 72°C, and a final extension step of 5 min at 72°C, for all loci. PCR products were separated on 1.5% agarose gel containing GelRed (Biotium) in 0.5× TBE buffer, and were visualized under UV light.

Randomly selected PCR amplicons from ITS and IGS and all *TUB2* and *CYP51* products were sent for Sanger sequencing to a service laboratory (LGC Genomics GmbH). All PCR products were sequenced in both directions with the same primers used for amplifications. Electrophoregrams were processed and individually inspected using the Staden Program Package (Staden *et al.*, 2000). The SNP positions connected to the A and B genetic groups and the fungicide resistance marker A495T were checked based on Brewer and Milgroom (2010) and Délye *et al.* (1999). The following GenBank accessions were used as references: GQ255475 (*TUB2*), GQ255473 (ITS), GQ255476 (IGS; Brewer and Milgroom, 2010) and U83840 (*CYP51*; Délye *et al.*, 1997). Representative sequences, obtained in the present study were deposited in GenBank under accession numbers MT023360, MT023361 (ITS); MT023362, MT023363 (IGS); MT023364, MT023365 (*TUB2*) and MT023366, MT023367 (*CYP51*).

Molecular cloning of a fragment of CYP51

An approx. 1.8 kb fragment of the *E. necator CYP51* gene was amplified with primers EnCYP89F and EnCYP1752R (Frenkel *et al.*, 2015). In these amplifications *Phusion* was used as described above, with the elongation step in the PCR program set to 40 s. A single chasmothecium DNA extract of a sample was used as target, which harboured the A495T mutation. The product was purified from 1% agarose gel with a GenElute Gel Extraction Kit (Sigma-Aldrich), ligated into the plasmid pJET1.2/blunt using a CloneJET PCR Cloning Kit (Thermo Fisher Scientific), and transformed into One Shot TOP10 Chemically Competent *Escherichia coli* cells (Thermo Fisher Scientific). One clone was selected randomly from the positive clones, which was propagated and used for plasmid extraction with a GenElute Plasmid Miniprep Kit (Sigma-Aldrich). A whole insert sequence was obtained by sequencing with pJET1.2 forward and reverse sequencing primers. The molecular weight of the plasmid was calculated based on the obtained sequence; the concentration of the extracts was measured with a Nanodrop 2000c spectrophotometer. The copy number of plasmids present in the extracts was calculated as described by Whelan *et al.* (2003). A stock of 10^8 *CYP51* containing plasmids μL^{-1} was prepared by diluting in TE buffer, and was aliquoted and stored at -20°C.

Real-time PCR assay

To use qPCR for detection of A495T, the protocol described by Dufour *et al.* (2011) was modified. The allele specific reverse primer and qEN primer pair were the same as outlined in Dufour *et al.* (2011). The forward primer used along with the allele-specific primer was substituted to primer L502 (Rallos and Baudoin, 2016), resulting in slightly greater amplification efficiency (see below). Reactions were performed in a Bio-Rad CFX96 Touch C1000 qPCR machine in 10 µL final volumes, with 5 µL of iTaq Universal SYBR Green Supermix (Bio-Rad), primers (for final concentrations, see below) and 1 µL target. The reaction conditions were as follows: initial denaturation at 95°C for 5 min, followed by 40 cycles of 10 s at 95°C, 10 s at 58°C and 20 s at 72°C. Specificity of the qPCR amplifications was checked by registering a melt curve after cycling. Plasmid DNA extract was used as the target in the control reactions and single chasmothecium DNA extracts were used for allele-specific detection of A495T and for measurements. Negative controls (samples without target DNA) were always included. Each sample was assayed in triplicate, cycle threshold (Cq) data were averaged from the triplicates, and the averages were used in the subsequent data analyses.

A dilution series from 10^6 copies μL^{-1} to 10 copies μL^{-1} of the control plasmid DNA extract was prepared in TE buffer by serially diluting the extract 10 times in each step. This dilution series was used to assess the efficiency of primer pairs in the adapted qPCR method. Preparation of the dilution series and efficiency measurements were carried out at least three times in independent experiments for each of the three primer pairs (qEN forward and reverse; qEN136R forward and reverse; L502 paired with qEN136R reverse).

The optimal concentrations for L502 and qEN136R reverse used in allele-specific reactions were determined by the matrix method, in which 50 nM, 100 nM, 200 nM, 400 nM, 600 nM or 800 nM final concentrations of both primers were tested in all combinations. Plasmid extract diluted to 10^5 copies μL^{-1} was used as a target in these tests, and each test was repeated once. The qEN forward and reverse primers were used in a final concentration of 500 nM each, as indicated by Dufour *et al.* (2011).

To measure qPCR efficiency with *E. necator* DNA extracts, three single chasmothecium DNA extracts of samples harbouring the A495T were diluted 10-, 20- or

50-fold in TE buffer. These, along with the undiluted extract, were amplified with the qPCR method described above, and efficiencies were calculated from the Cq data obtained.

Determination of qPCR cut-off for detection of A495T SNP

A total of 186 single chasmothecium DNA samples were analyzed with the qPCR method described above. The known diagnoses of A495T presence, determined earlier with the direct sequencing method and coded as a binary variable, were paired to the corresponding Cq values. The dataset was used for determination of the qPCR cycle threshold cut-off following the epidemiologic approach (Caraguel *et al.*, 2011). Determination of the cut-off was achieved by conducting a receiver operating characteristic (ROC) plot analysis with the MedCalc for Windows software, version 12.2.1.0 (MedCalc Software; Stephan *et al.*, 2003). The prevalence of A495T among the analyzed samples (25.3%) was assumed to reflect the overall prevalence of the mutation in the sample populations. All other options were used as defaults in the software. The cycle threshold corresponding to the greatest Youden index (J) was selected, because using this Cq as a cut-off minimizes the probability of overall misclassification (Caraguel *et al.*, 2011) and represents a balance between sensitivity and specificity (Nutz *et al.*, 2011). The calculated cut-off was used for discrimination of positive and negative samples (i.e., diagnosis) based on Cq values. Samples having Cq values equal to or less than the cut-off were considered positive (Nutz *et al.*, 2011).

False positive and false negative rates (Kralik and Ricchi, 2017) of the tested qPCR method were calculated based on MedCalc output data.

In 20 samples where incongruences between the results of genotyping by direct sequencing and qPCR analyses were found (see below), the relative amounts of mutant allele present in the samples were quantified using the comparative Ct ($2^{-\Delta\Delta Ct}$) method (Livak and Schmittgen, 2001). Plasmid DNA was used as an internal reference; this contained the A495T allele in a 1:1 ratio relative to the whole amount of *CYP51* DNA, which was reflected by the qEN amplifications.

RESULTS

DNA extractions and PCR amplifications

During the preliminary experiments, DNA was extracted from 15 *E. necator* chasmothecia, with each extraction medium and crushing tool. Because the carved pipette tips and spherical end glass micropestles were not effective for disrupting the chasmothecia, only the conical end glass micropestles were used further. Based on poor PCR amplifications, 90% of the DNA extraction did not result in extracts suitable for PCR amplification when NaOH or water were used as extraction media. However, DNA extractions were successful with 14 of 15 samples when TE buffer or the Phire Plant Direct kit buffer were applied, as reflected by PCR amplifications. For further work, TE buffer was selected, based on durability and the usability of the DNA extracts in molecular work.

All the target loci (ITS, IGS, *TUB2* and *CYP51*) were successfully amplified with all three master mix solutions tested from individual chasmothecium DNA extracts using TE buffer during the extraction protocol. However, the PCR performances of *Phusion* were more consistent with those of other master mixes (Supplementary Figure S1). Because of the low error rate of this high-fidelity enzyme, it was selected for all other comparisons and assessments.

To test the optimal target volume, different target amounts (0.1 to 4 µL) and a series of diluted DNA samples were used as templates for PCR amplifications using *Phusion*. The optimal target volume for *TUB2* was 1 µL from the undiluted DNA extract and 1 µL for the other loci from genomic DNA diluted as described below. Using this target volume, the optimal dilution was 50-fold for ITS and IGS, and 10-fold for *CYP51*. The greatest dilutions resulting in visible PCR amplicons were 2000-fold for ITS and IGS, and 100-fold for *CYP51*. PCRs targeting the *TUB2* locus using diluted DNA did not result in visible amplicons.

DNA was extracted from a total of 190 chasmothecia with TE buffer (including preliminary experiments), and sequences were obtained from 98% of all the samples after successful PCR amplifications.

No prominent differences were observed in PCR amplifications between DNA extracts from mature and immature chasmothecia, for the different master mix solutions, target volumes or dilution assays.

Sequence analysis of ITS, IGS, TUB2 *and* CYP51

All directly sequenced PCR products obtained from individual chasmothecia showed 99% similarity or were identical to the respective reference sequences. Based on *TUB2*, both A and B genotypes were detected in our samples, according to nucleotide site 79 in the referenced GenBank accession (GQ255475). All of the samples belonged to group B, according to two SNP posi-

tions (nucleotide sites 110 and 575 in the coding region of GeneBank accession U83840) in the *CYP51* sequences. Similarly, based on one SNP in ITS (nucleotide site 48 in GQ255473) and one in IGS (nucleotide site 108 in the GQ255476), all the samples belonged to group B.

The mutant allele bearing the A495T point mutation in *CYP51*, which confers DMI-resistance in *E. necator*, was detected from approximately one third of the DNA extracts originating from chasmothecia. This is the first report describing the mutant allele in GPM in Hungary.

Overlapping peaks at three polymorphic positions were found in one fifth of the samples during examination of electrophoregrams. Double peaks were present at position 79 and 368 in *TUB2* and 495 in *CYP51*. Thymine (T) or cytosine (C) at position 79 in *TUB2* is characteristic for groups A and B. In *CYP51*, the overlapping adenine (A) and thymine (T) peaks were present at the nucleotide position corresponding to the A495T mutation (Supplementary Figure S2).

Optimized qPCR protocol for detection of A495T

Regression curves resulting from qPCR efficiency tests using plasmid controls fit with correlation coefficients $R^2 \geq 0.96$. Measured amplification efficiencies were (mean ± standard deviation) 94 ± 2% for the qEN primer pair and 87 ± 1% for the L502-qEN136R reverse primer pair. Primer qEN136R reverse paired with qEN136R forward resulted in lesser amplification efficiencies (79 ± 7%) and less conclusive measurements than L502-qEN136R reverse. Therefore, for allele specific reactions, L502 was used with qEN136R reverse during this study. Primer concentration assay showed that the best combination with the greatest reaction efficiency and low Cq, relative to other combinations, was found at a final concentration of 400 nM for L502 and 600 nM for qEN136R reverse primer.

In the qPCR efficiency tests using single-chasmothecium DNA extracts, 90 ± 1% efficiency was measured for qEN amplifications. Allele-specific amplifications reached an efficiency of 93 ± 8%. All curves fit with regression coefficients $R^2 \geq 0.974$ (Supplementary Figure S3). Based on reaction coefficients, all the tested dilutions were considered to fit in the log-linear range of the applied qPCR method.

Detection of the A495T marker with qPCR

In the ROC analysis that used samples with known diagnoses based on direct sequencing, the resulting Cq cut-off value with the greatest Youden index was 31.3 (Supplementary Figure S4). The applied method has 4% false negative and 12% false positive rates using this Cq cut-off (Supplementary Figure S4). Twenty samples (10.8%) of the 186 tested were differently genotyped by qPCR than by direct sequencing. Seventeen of these samples were positive in qPCR (harbouring the A495T mutation) but were genotyped as wild-type by direct sequencing. Based on qPCR mea-surements, the ratio of the mutant allele was 20 ± 13% (mean ± standard deviation) in these samples.

The electrophoregrams showed that 39 samples contained double peaks at position 495 of *CYP51*. All but three of these samples were positive in qPCR for the presence of the A495T mutation exhibiting the presence of the specific allele involved in DMI resistance.

DISCUSSION

This paper describes an improved DNA extraction and qPCR protocol for genotyping *E. necator* samples, and for identifying the A495T mutation in this pathogen, which is involved in DMI fungicide resistance. This study demonstrates that only a single chasmothecium of starting material is sufficient, and that a crude DNA extract can be used to obtain nucleotide sequences and perform qPCR.

In powdery mildew research, molecular protocols without any purification steps, or with only a minor DNA purification step, such as direct PCR methods, have occasionally been used (Hirata and Takamatsu, 1996; Matsuda *et al.*, 2005; Miazzi *et al.*, 2008; Gindro *et al.*, 2014). Conidia and chasmothecia have been used in these protocols with different amounts of starting material. Miazzi *et al.* (2008) harvested 10 to 20 conidia from infected samples. Matsuda *et al.* (2005) picked only individual conidia from each powdery mildew colony, using a glass needle and a manipulator and transferred these directly to the PCR mixture. With these protocols, multiplex PCR amplifications are possible, but there is no remaining target DNA for further assessment. Gindro *et al.* (2014) extracted DNA from grapevine buds infected with *E. necator*, diluted the extracts and used them directly for PCR. The detection limit with this method, as for earlier reports (Matsuda *et al.*, 2005; Falacy *et al.*, 2007), was one conidium per microliter (Gindro *et al.*, 2014). Obtaining DNA from individual conidia for downstream applications, like qPCR and LAMP (Thiessen *et al.*, 2016), is also possible, but for this it is necessary to use either a DNA extraction kit (Thiessen *et al.*, 2016) or Chelex 100 reagent (Thiessen *et al.*, 2018). To obtain more DNA, with less purification steps, extract-

ing from larger structures (such as chasmothecia), can be a solution. Based on our findings, only one chasmothecium is enough to obtain sufficient DNA for multiple PCR amplifications. In contrast to earlier protocols using 20 (Hirata and Takamatsu, 1996) or ten (Mougou *et al.*, 2008) chasmothecia, we were able to amplify and sequence four loci and perform qPCR from only 20 µL DNA extracts of individual chasmothecia.

During DNA extraction from one chasmothecium, different extracting media were tested. Sodium hydroxide can be used for DNA extraction from plant material, with the reasoning that the alkaline pH suppresses nucleases and does not affect the subsequent PCR amplifications (Wang *et al.*, 1993). However, our results showed that water and NaOH were of reduced extraction efficiency. TE buffer and Phire Plant Direct PCR kit buffer were superior as extraction media, demonstrated by the high success rate of PCR amplifications using these solutions. For further extractions, TE buffer was selected because the shelf life of the DNA extract was prolonged compared with other extraction media (Yagi *et al.*, 1996). DNA extractions from mature and immature chasmothecia gave equal success rates of PCR amplifications (98%), which demonstrates that this method can be implemented for small structures, such as yellow, immature ascocarps.

The method described here enabled genotyping of *E. necator* from individual chasmothecia, using multilocus sequencing to determine if each sampled belonged to genetic group A or B of the pathogen. Based on direct sequencing of *TUB2*, group A was detected several times. In contrast, all of our samples belonged to group B based on *CYP51* sequences, without any polymorphism in two marker nucleotide positions, which have been shown to be diverse in other samples (Délye *et al.*, 1999). Amrani and Corio-Costet (2006) and Araya *et al.* (2014) found no contradiction between the results obtained based on genotyping of *TUB2* and *CYP51*; that is, all the markers were congruent and assigned to one genetic group. Further work is needed to study the linkages between the loci used for the description of groups A and B.

Délye and Corio-Costet (1998) and Délye *et al.* (1997; 1999) stated that group A only reproduces clonally. However, samplings from some populations have suggested that sexual reproduction may be possible (Miazzi *et al.*, 2003; Cortesi *et al.*, 2004). Mating type assays revealed that group A can produce chasmothecia and viable ascospores in laboratory conditions (Miazzi *et al.*, 2003; Cortesi *et al.*, 2004). We detected markers of group A in chasmothecia, which indicates that sexual reproduction is also possible in field conditions. Moreover, co-occurrence of groups A and B was detected in DNA extracts from individual chasmothecia, indicating that mating between these two groups happens in vineyards. This phenomenon was demonstrated in *in vitro* experiments (Miazzi *et al.*, 2008), but has not been reported from field samples. If only anamorph structures are examined, it is not possible to determine if any of the genotypes reproduces sexually. Extended sampling of many chasmothecia and application of the genotyping method described here would address this question. Using only individual conidia or mixtures of chasmothecia for DNA extraction may hide the presence of group A, described previously as only clonal, if it were present at low ratios. This also emphasizes the importance using individual chasmothecia for DNA extractions. Double peaks were present in about a fifth of the electropherograms obtained in the present study, indicating the presence of a mixture of different genotypes in some DNA extracts from individual chasmothecia (Lesemann *et al.*, 2006; Kovács *et al.*, 2011). Possible explanations could be sexual processes between two colonies harbouring two different genotypes (for *TUB2* and *CYP51*), or increased copy number (for *CYP51*) under pressure from DMI fungicide applications (Jones *et al.*, 2014; Rallos and Baudoin, 2016). For DNA extractions, we only sampled chasmothecia, and despite great care was taken, it cannot be ruled out that in some cases mycelium around each chasmothecium was also sampled. This may have resulted in mixed genotypes in the DNA extracts, which were not present in the chasmothecia.

The qPCR and DNA extraction protocol described here is suitable for high-throughput genotyping of *E. necator* samples to determine the presence of the A495T mutation. The method is more rapid and cost-effective for this purpose than genotyping based on direct sequencing. From our samples, 20 were differentially diagnosed by qPCR and direct sequencing, and most (17) were diagnosed positive for the mutation only by qPCR. This implies that the method used for reference (e.g. direct sequencing) has less sensitivity than the developed qPCR-based diagnostic method (Kralik and Ricchi, 2017). Consequently, we conducted quantification of the resistant allele in these samples. The samples genotyped as resistant based on qPCR had a low ratio of the mutant allele (20 ± 13%), and these were identified as harbouring the wild-type allele only by direct sequencing. The protocol involving PCR followed by direct sequencing is possibly not sensitive enough for accurate characterization if the targeted allele is present at low ratios.

For cut-offs differentiating positive and negative samples based on measured Cq values, we selected that with the greatest Youden index. This method sets the cut-off so that the assay has the least probability of misclassifi-

cation (Caraguel *et al*., 2011), when the calculated cut-off of Cq = 31.3 is used for diagnostics. However, the cut-off can be set to prioritize other characteristics of the assay, for example, to minimize the probability of false-negatives or false-positives. The most suitable selection should be based on the purpose of each diagnostic test (Caraguel *et al*., 2011).

An individual chasmothecium can be a discrete unit for gaining an adequate amount of DNA, and for providing information on inter- and intra-specific variation, species complexes and population biology. Conidia are also discrete units. However, to obtain enough DNA for downstream processes (e.g., multilocus analyses), labour intensive methods (e.g. Thiessen *et al*., 2016) or time consuming production of single conidial colonies, is currently necessary (Erickson and Wilcox, 1997; Miazzi *et al*., 2008). In contrast to single conidia, chasmothecia can be collected from herbarium material (e.g. pressed leaves) without any visible hyphal fragments from the adjacent colonies.

We have developed a rapid DNA extraction method for very small fungal samples to obtain DNA for downstream sequencing and qPCR purposes. As fruiting bodies are morphologically and taxonomically identifiable units, and are large enough to genotype fungal samples, this method may be applicable to any chasmothecia-producing powdery mildew species, as well as for fruiting bodies of other plant colonizing fungi. The qPCR protocol presented here for detection of the SNP linked to DMI fungicide resistance can be implemented in plant disease diagnostics.

ACKNOWLEDGEMENTS

This research was supported by the Széchenyi 2020 Programme, the European Regional Development Fund and the Hungarian Government (GINOP-2.3.2-15-2016-00061), and partly supported by ELTE Institutional Excellence Program by the National Research, Development and Innovation Office (NKFIH-1157-8/2019-DT). K.Z. Váczy's contribution was supported by a János Bolyai Research Scholarship from the Hungarian Academy of Sciences. M.Z. Németh was supported by the ÚNKP-19-3 New National Excellence Program of the Ministry for Innovation and Technology.

LITERATURE CITED

Amrani L., Corio-Costet M.F., 2006. A single nucleotide polymorphism in the β-tubulin gene distinguishing two genotypes of *Erysiphe necator* expressing different symptoms on grapevine. *Plant Pathology* 55: 505–512.

Araya C., Rosales I., Mendez M.A., Delmotte F., 2014. Identification and geographic distribution of genetic groups of *Erysiphe necator* in Chilean vineyards. *Vitis* 53: 163–165.

Beenken L., 2017. First records of the powdery mildews *Erysiphe platani* and *E. alphitoides* on *Ailanthus altissima* reveal host jumps independent of host phylogeny. *Mycological Progress* 16: 135–143.

Brewer M.T., Milgroom M.G., 2010. Phylogeography and population structure of the grape powdery mildew fungus, *Erysiphe necator*, from diverse *Vitis* species. *BMC Evolutionary Biology* 10: 268.

Caraguel C.G., Stryhn H., Gagné N., Dohoo I.R., Hammell K.L., 2011. Selection of a cutoff value for real-time polymerase chain reaction results to fit a diagnostic purpose: analytical and epidemiologic approaches. *Journal of Veterinary Diagnostic Investigation* 23: 2–15.

Cortesi P., Ottaviani M.-P., Milgroom M.G., 2004. Spatial and genetic analysis of a flag shoot subpopulation of *Erysiphe necator* in Italy. *Phytopathology* 94: 544-550.

Cortesi P., Bisiach M., Ricciolini M.,Gadoury D.M., 1997. Cleistothecia of *Uncinula necator*—an additional source of inoculum in Italian vineyards. *Plant Disease* 81: 922–926.

Délye C., Corio-Costet M.-F., 1998. Origin of primary infections of grape by *Uncinula necator*: RAPD analysis discriminates two biotypes. *Mycological Research* 102: 283–288.

Délye C., Laigret F., Corio-Costet M.-F., 1997. A mutation in the 14 alpha-demethylase gene of *Uncinula necator* that correlates with resistance to a sterol biosynthesis inhibitor. *Applied and Environmental Microbiology* 63: 2966–2970.

Délye C., Ronchi V., Laigret F., Corio-Costet M.-F., 1999. Nested allele-specific PCR primers distinguish genetic groups of *Uncinula necator*. *Applied and Environmental Microbiology* 65: 3950–3954.

Dufour M.C., Fontaine S., Montarry J.,Corio-Costet M.-F., 2011. Assessment of fungicide resistance and pathogen diversity in *Erysiphe necator* using quantitative real-time PCR assays. *Pest Management Science* 67: 60-69.

Erickson E.O.,Wilcox W.F., 1997. Distributions of sensitivities to three sterol demethylation inhibitor fungicides among populations of *Uncinula necator* sensitive and resistant to triadimefon. *Phytopathology* 87: 784–791.

Falacy J.S., Grove G.G., Mahaffee W.F., Galloway H., Glawe D.A., Larsen R.C.,Vandemark G.J., 2007.

Detection of *Erysiphe necator* in air samples using the polymerase chain reaction and species-specific primers. *Phytopathology* 97: 1290–1297.

Frantzeskakis L., Németh M.Z., Barsoum M., Kusch S., Kiss L., Takamatsu S., Panstruga R., 2019. The Parauncinula polyspora Draft Genome Provides Insights into Patterns of Gene Erosion and Genome Expansion in Powdery Mildew Fungi. *mBio* 10: e01692–01619.

Frenkel O., Cadle-Davidson L., Wilcox W.F., Milgroom M.G., 2015. Mechanisms of resistance to an azole fungicide in the grapevine powdery mildew fungus, *Erysiphe necator*. *Phytopathology* 105: 370–377.

Frenkel O., Portillo I., Brewer M., Peros J.-P., Cadle-Davidson L., Milgroom M., 2012. Development of microsatellite markers from the transcriptome of *Erysiphe necator* for analysing population structure in North America and Europe. *Plant Pathology* 61: 106–119.

Gadoury D.M., Pearson R.C., 1988. Initiation, development, dispersal and survival of cleistothecia of *Uncinula necator* in New York vineyards. *Phytopathology* 78: 1413–1421.

Gadoury D.M., Cadle-Davidson L., Wilcox W.F., Dry I.B., Seem R.C., Milgroom M.G., 2012. Grapevine powdery mildew (*Erysiphe necator*): a fascinating system for the study of the biology, ecology and epidemiology of an obligate biotroph. *Molecular Plant Pathology* 13: 1–16.

Gindro K., Lecoultre N., Molino L., de Joffrey J.-P., Schnee S., … Dubuis P.-H., 2014. Development of rapid direct PCR assays to identify downy and powdery mildew and grey mould in *Vitis vinifera* tissues. *OENO One* 48: 261–268.

Glawe D.A., 2008. The powdery mildews: a review of the world's most familiar (yet poorly known) plant pathogens. *Annual Review of Phytopathology* 46: 27–51.

Hirata T., Takamatsu S., 1996. Nucleotide sequence diversity of rDNA internal transcribed spacers extracted from conidia and cleistothecia of several powdery mildew fungi. *Mycoscience* 37: 283–288.

Jones L., Riaz S., Morales-Cruz A., Amrine K.C., McGuire B., … Cantu D., 2014. Adaptive genomic structural variation in the grape powdery mildew pathogen, *Erysiphe necator*. *BMC Genomics* 15: 1081.

Jousimo J., Tack A.J., Ovaskainen O., Mononen T., Susi H., Tollenaere C., Laine A.-L., 2014. Ecological and evolutionary effects of fragmentation on infectious disease dynamics. *Science* 344: 1289–1293.

Kovács G.M., Jankovics T., Kiss L., 2011. Variation in the nrDNA ITS sequences of some powdery mildew species: do routine molecular identification procedures hide valuable information? *European Journal of Plant Pathology* 131: 135.

Kralik P., Ricchi M., 2017. A basic guide to real time PCR in microbial diagnostics: definitions, parameters, and everything. *Frontiers in Microbiology* 8: 108.

Lesemann S., Schimpke S., Dunemann F., Deising H., 2006. Mitochondrial heteroplasmy for the cytochrome b gene controls the level of strobilurin resistance in the apple powdery mildew fungus *Podosphaera leucotricha* (Ell. & Ev.) ES Salmon. *Journal of Plant Diseases and Protection* 113: 259–266.

Livak K.J., Schmittgen T.D., 2001. Analysis of relative gene expression data using real-time quantitative PCR and the 2− ΔΔCT method. *Methods* 25: 402–408.

Marçais B., Piou D., Dezette D., Desprez-Loustau M.-L., 2017. Can oak powdery mildew severity be explained by indirect effects of climate on the composition of the Erysiphe pathogenic complex? *Phytopathology* 107: 570–579.

Matsuda Y., Sameshima T., Moriura N., Inoue K., Nonomura T., … Toyoda H., 2005. Identification of individual powdery mildew fungi infecting leaves and direct detection of gene expression by single conidium polymerase chain reaction. *Phytopathology* 95: 1137–1143.

Miazzi M., Hajjeh H., 2011. Differential sensitivity to triadimenol of *Erysiphe necator* isolates belonging to different genetic groups. *Journal of Plant Pathology*: 729–735.

Miazzi M., Hajjeh H., Faretra F., 2003. Observations on the population biology of the grape powdery mildew fungus *Uncinula necator*. *Journal of Plant Pathology*: 123–129.

Miazzi M., Hajjeh H., Faretra F., 2008. Occurence and Distribution of Two Distinct Genetic Groups In Populations of *Erysiphe necator* Schw. in Southern Italy. *Journal of Plant Pathology*: 563–573.

Montarry J., Cartolaro P., Richard-Cervera S., Delmotte F., 2009. Spatio-temporal distribution of *Erysiphe necator* genetic groups and their relationship with disease levels in vineyards. *European Journal of Plant Pathology* 123: 61–70.

Montarry J., Cartolaro P., Delmotte F., Jolivet J., Willocquet L., 2008. Genetic structure and aggressiveness of *Erysiphe necator* populations during grapevine powdery mildew epidemics. *Applied and Environmental Microbiology* 74: 6327–6332.

Mougou A., Dutech C., Desprez-Loustau M.L., 2008. New insights into the identity and origin of the causal agent of oak powdery mildew in Europe. *Forest Pathology* 38: 275–287.

Nutz S., Döll K., Karlovsky P., 2011. Determination of the LOQ in real-time PCR by receiver operating characteristic curve analysis: application to qPCR assays for Fusarium verticillioides and F. proliferatum. *Analytical and Bioanalytical Chemistry* 401: 717–726.

Parker J.E., Warrilow A.G., Price C.L., Mullins J.G., Kelly D.E., Kelly S.L., 2014. Resistance to antifungals that target CYP51. *Journal of Chemical Biology* 7: 143–161.

Rallos L.E.E., Baudoin A.B., 2016. Co-occurrence of two allelic variants of CYP51 in *Erysiphe necator* and their correlation with over-expression for DMI resistance. *PloS One* 11: e0148025.

Staden R., Beal K.F., Bonfield J.K. 2000. The staden package, 1998. Pages 115-130 in: *Bioinformatics methods and protocols*. Springer.

Stephan C., Wesseling S., Schink T., Jung K., 2003. Comparison of eight computer programs for receiver-operating characteristic analysis. *Clinical Chemistry* 49: 433–439.

Sundberg H., Ekman S., Kruys Å., 2018. A crush on small fungi: An efficient and quick method for obtaining DNA from minute ascomycetes. *Methods in Ecology and Evolution* 9: 148–158.

Susi H., Laine A.L., 2017. Host resistance and pathogen aggressiveness are key determinants of coinfection in the wild. *Evolution* 71: 2110–2119.

Takamatsu S., Matsuda S., Grigaliunaite B., 2013. Comprehensive phylogenetic analysis of the genus *Golovinomyces* (Ascomycota: Erysiphales) reveals close evolutionary relationships with its host plants. *Mycologia* 105: 1135–1152.

Thiessen L., Keune J., Neill T., Turechek W., Grove G., Mahaffee W., 2016. Development of a grower-conducted inoculum detection assay for management of grape powdery mildew. *Plant Pathology* 65: 238–249.

Thiessen L.D., Neill T.M., Mahaffee W.F., 2018. Development of a quantitative loop-mediated isothermal amplification assay for the field detection of *Erysiphe necator*. *PeerJ* 6: e4639.

Vági P., Kovacs G.M., Kiss L., 2007. Host range expansion in a powdery mildew fungus (*Golovinomyces* sp.) infecting *Arabidopsis thaliana*: *Torenia fournieri* as a new host. *European Journal of Plant Pathology* 117: 89–93.

Wang H., Qi M., Cutler A.J., 1993. A simple method of preparing plant samples for PCR. *Nucleic Acids Research* 21: 4153.

Whelan J.A., Russell N.B., Whelan M.A., 2003. A method for the absolute quantification of cDNA using real-time PCR. *Journal of Immunological Methods* 278: 261–269.

Yagi N., Satonaka K., Horio M., Shimogaki H., Tokuda Y., Maeda S., 1996. The role of DNase and EDTA on DNA degradation in formaldehyde fixed tissues. *Biotechnic & Histochemistry* 71: 123–129.

Phytopathologia Mediterranea
The international journal of the
Mediterranean Phytopathological Union

Firenze University Press
www.fupress.com/pm

Research Paper

Characterization of mycotoxigenic *Alternaria* species isolated from the Tunisian halophyte *Cakile maritima*

Arbia CHALBI[1,2,3], Besma SGHAIER-HAMMAMI[1,*], Giuseppe MECA[4], Juan Manuel QUILES[4], Chedly ABDELLY[1], Carmela MARANGI[5], Antonio F. LOGRIECO[3], Antonio MORETTI[3], Mario MASIELLO[3]

[1] *Laboratoire des Plantes Extrêmophiles, Centre de Biotechnologie de Borj-Cédria, BP 901, Hammam-Lif 2050, Tunisia*
[2] *Faculty of Sciences of Tunis, University Campus 2092, University of Tunis El Manar, Tunis, Tunisia*
[3] *Institute of Sciences of Food Production, Research National Council (ISPA-CNR), Via G. Amendola 122/O, 70126, Bari, Italy*
[4] *Laboratory of Food Toxicology, Department of Preventive Medicine, Nutrition and Food Science Area, Faculty of Pharmacy, University of Valencia Avenida Vicent Andres Estelles s/n, 46100 Burjassot, Valencia, Spain*
[5] *Institute for Applied Mathematics "M. Picone", Via G. Amendola 122/D, 70126, Bari, Italy*
* Corresponding author: sghaierhammamibesma@gmail.com

Summary. *Cakile maritima* is a typical halophyte of the Mediterranean coasts. In addition to its ecological and industrial properties, *C. maritima* has antiscorbutic, diuretic and purgative roles in folk remedies. This plant is infected by different fungal species, mainly belonging to *Alternaria* genus. Two-hundred *Alternaria* strains were collected from four different pedo-climatic areas in Tunisia, from *C. maritima* fresh plant tissues showing symptoms of *Alternaria* infection. Phylogenetic analyses of 79 representative *Alternaria* strains, were carried out using multi-locus gene sequencing. All the strains clustered in the *Alternaria* Section: 47 strains had high homology with *A. alternata* reference strain, 13 grouped with *A. arborescens* reference strain, 12 grouped with *A. mali* reference strain, and seven strains were not well defined with *A. mali* as their closest species. *In vitro* production of tenuazonic acid (TA), alternariol (AOH), alternariol-monomethyl ether (AME), and altenuene (ALT) was evaluated. Approx. 68% of strains simultaneously produced AOH, AME and TA. Only two *A. alternata* and one *A. mali* strains were ALT producing. Pathogenicity tests on leaves of *C. maritima* were carried out with 41 representative strains. *Alternaria arborescens* showed the greatest pathogenicity compared to *A. alternata* and *A. mali*, although no statistically significant differences in pathogenicity were observed. This is the first study on Tunisian populations of *Alternaria* species isolated from the extremophile *C. maritima*.

Keywords. *Alternaria* section, *Alternaria arborescens*, *Alternaria mali*, *Alternaria* mycotoxins.

OPEN ACCESS

Citation: A. Chalbi, B. Sghaier-Hammami, G. Meca, J.M. Quiles, C. Abdelly, C. Marangi, A.F. Logrieco, A. Moretti, M. Masiello (2020) Characterization of mycotoxigenic *Alternaria* species isolated from the Tunisian halophyte *Cakile maritima*. *Phytopathologia Mediterranea* 59(1): 107-118. doi: 10.14601/Phyto-10720

Accepted: February 7, 2020

Published: April 30, 2020

Data Availability Statement: All relevant data are within the paper and its Supporting Information files.

Competing Interests: The Author(s) declare(s) no conflict of interest.

Editor: Laura Mugnai, Università di Firenze, Italy.

Key contributions. Four clades of *Alternaria* species were identified from the halophyte plant *Cakile maritima*.

Alternaria alternata was the most abundant (60%) and especially in stems and leaves.

A new genetic entity among the *Alternaria* strains studied needs to be further characterized. The majority of *Alternaria* strains (74%) produced the AME mycotoxin.

AME and AOH were the most frequently produced mycotoxins by all the *Alternaria* strains.

Alternaria arborescens strains were the most pathogenic.

INTRODUCTION

Cakile maritima (sea rocket) is an extremophile C3 halophyte (Brassicaceae) which is widely distributed on sandy coasts (Clausing *et al.*, 2000; Kadereit *et al.*, 2005). This plant, together with *Xanthium italicum* and *Eryngium maritimum*, is typical coastal vegetation of several regions including the Black Sea coasts, the Mediterranean basin, the Atlantic coasts of North Africa and Europe, and the North Sea and Baltic Sea coasts (Clausing *et al.*, 2000). These plants grow a few meters from shorelines, and are useful barriers defending coastal ecosystems. Sea rocket is an annual succulent plant, growing in geographical areas characterized by high salinity and low soil fertility (Barbour *et al.*, 1970). It is tolerant to abiotic stress conditions such as high salinity, water stress and high temperature, which are all the characteristics of halophyte plants (Debez *et al.*, 2012). *Cakile maritima* is a good candidate model plant for understanding botanical biochemical and physiological mechanisms.

In Tunisia, *C. maritima*, in addition to its role in ecosystem coastal preservation, is also considered an edible plant, used traditionally as a green vegetable for human and animal consumption. Dried root powder is also mixed with cereal flour to make bread (Zarrouk *et al.*, 2003; Debez *et al.*, 2004). The whole plant, harvested at flowering for its high content of iron, ascorbic acid and iodine, is traditionally used in antiscorbutic, diuretic and purgative folk remedies (Kubiak-Martens *et al.*, 1999).

Spontaneous plants of *C. maritima* are colonized by fungi causing necrotic lesions on above-ground parts. Among fungal species, *Alternaria brassicicola* (Schwein.) Wiltshire (1947) has been often associated to *C. maritima* infections (Thrall *et al.*, 2000), so several studies have been carried out to evaluate this host-pathogen interaction (Thrall *et al.*, 2000; 2002; 2005; Oliver *et al.*, 2001; Bock *et al.*, 2005; Linde *et al.*, 2010).

Alternaria is ubiquitous and abundant in the atmosphere and in soil, seeds, and agricultural commodities. This genus includes plant pathogenic and saprophytic species that may affect crops in the field or can cause harvest and postharvest decay of plant products (Logrieco *et al.*, 2009; Patriarca, 2016; Somma *et al.*, 2019). *Alternaria* spores have been related to human infections, such as rhinosinusitis, asthma, cutaneous and subcutaneous infections, and oculomycosis (Pastor and Gaurro, 2008; Canova *et al.*, 2013; Hattab *et al.*, 2019). Mycotoxins are major food contaminants affecting global food security, especially in low and middle-income countries (Moretti *et al.*, 2019). Several studies have confirmed the toxic effects of *Alternaria* metabolites for animals and humans, but these toxins are not regulated by legislation, and acceptable levels in food are not determined. *Alternaria* mycotoxins are arousing interest worldwide, and the European Food Safety Authority (EFSA) has provided scientific opinion on the risks for animal and public health related to the presence of *Alternaria* toxins in food and feed (Arcella *et al.*, 2016).

Among the secondary metabolites produced by *Alternaria* species, there are both phytotoxins, that can play an important role in the plant pathogenesis processes, and mycotoxins, that can be harmful to humans and animals (Logrieco *et al.*, 2009). Therefore, since *C. maritima* is used in traditional food, consumption of *Alternaria* toxin-contaminated plants can represent a serious toxicological risk for consumers (Wang *et al.*, 1996; Ostry, 2008; Logrieco *et al.*, 2009; Lou *et al.*, 2013).

The dibenzopyrone derivatives alternariol (AOH), alternariolmonomethyl ether (AME) and altenuene (ALT), and the tetramic acid derivative tenuazoic acid (TA), are among the most important mycotoxins produced by *Alternaria* species. Alternariol and AME are usually found in combination, and have teratogenic and fetotoxic effects (Fehr *et al.*, 2009). Genotoxic activity on human colon cancer cell lines has also been observed (Wang *et al.*, 1996; Ostry, 2008; Fehr *et al.*, 2009; Bensassi *et al.*, 2012). A recent study also reported that AOH was an androgen agonist in *in vitro* assay (Stypula-Trebas *et al.*, 2017).

Tenuazonic acid is a well-known mycotoxin and phytotoxin, produced primarily by *A. alternata* (Fr.) Keissl. (1912) and by other phytopathogenic *Alternaria* species, including *A. japonica* Yoshii (1941), detected on wheat in Tunisia (Bensassi *et al.*, 2009), *A. longipes* (Ellis & Everh.) E.W. Mason (1928), *A. radicina* Meier, Drechsler & E.D. Eddy (1922), and *A. tenuissima* (Kunze) Wilt-

shire (1933). In central and southern Africa, TA has been associated with human hematologic disorder known as "onalay", a thrombocytopenia (Steyn and Rabie, 1976). The presence of these mycotoxins in wheat has also been related to elevated levels of human esophageal cancer in China (Liu *et al*., 1992).

Morphological identification of *Alternaria* species is often difficult due to interspecific similarities and intraspecific polymorphisms (Simmons, 1990; Simmons and Roberts, 1993; Roberts *et al*., 2000; Pryor and Michailides, 2002; Serdani *et al*., 2002; Belisario *et al*., 2004; Hong *et al*., 2006). The high sensitivity of *Alternaria* to environmental factors may lead to ambiguities if taxonomy is based only on phenotype (Andrew *et al*., 2009). "Polyphasic" approaches using morphological, molecular and chemical techniques could therefore be useful for characterization of *Alternaria* species (Andersen *et al*., 2008; Brun *et al*., 2013).

Although several studies have focused on the occurrence of *Alternaria* species and *Alternaria* metabolites in food commodities, little knowledge is available on the *Alternaria* species living on extremophile plants. Santiago *et al.* (2018) suggested that *Alternaria* species that colonize extremophile plant environments show great adaptation to survival under extreme conditions, such as high temperature, low water and nutrient availability, osmotic stress, desiccation, and exposure to high levels of UV radiation, so these fungi are interesting examples of fungal diversity.

Based on this lack of knowledge, the aims of the present study were: i) to isolate and estimate the distribution of *Alternaria* species on *C. maritima* growing in different bioclimatic conditions, in Tunisia; ii) to identify *Alternaria* at species level using a polyphasic approach; iii) to analyze the profile of the main mycotoxins produced by the species isolated from *C. maritima*; and iv) to test their pathogenicity on *C. maritima* leaves.

MATERIAL AND METHODS

Origin of the samples

Leaves, stems and seeds of spontaneous *C. maritima* plants, showing typical symptoms of *Alternaria* infections, were collected arbitrarily in Tunisia. Approximately 20 plants were collected per province, and five portions of each plant were used for fungal isolation. A total of 100 *C. maritima* samples were collected per province. Four provinces, from the north to the south of Tunisia and with two pedo-climatic conditions, were considered: Rades and Raouad, characterized by temperate winters and annual rainfall of 200–700 mm (semi-arid regions), and Sfax and Djerba, characterized by temperate winters and annual rainfall of 100–200 mm (arid regions).

Fungus isolation and growth conditions

After surface-disinfestation with 2% sodium hypochlorite solution for 2 min and two washings with sterilized distilled water for 1 min, symptomatic plant tissues were cut into small pieces (5 mm diam.) with a sterilized scalpel and dried on a sterile filter paper in a laminar flow cabinet. Single tissue pieces were then transferred into Petri dishes containing Potato Dextrose Agar (PDA) amended with 0.10 g L^{-1} streptomycin sulphate salt and 0.05 g L^{-1} neomycin. The dishes were incubated at 25 ± 1°C for 7 d under an alternating light/darkness cycle of 12 h photoperiod. From the 100 samples selected per province, 50 isolates were kept as monoconidium and homogeneous cultures. Two hundred *Alternaria* strains were collected from the four sample sites.

Morphological characterization

Following procedures of Simmons (2007), *Alternaria* strains were grown on PDA and on Potato Carrot Agar (PCA) to characterize their morphological traits. After 7 d of incubation at 25 ± 1°C, under an alternating light/darkness cycle of 12 h photoperiod, conidium dimensions, colour, septation, conidiophore branching, and dimensions of catenulate conidia were determined using a light microscope (×40 magnification).

Molecular characterization and phylogenetic analysis of Alternaria *strains*

Based on morphological traits, 79 representative strains were selected for phylogenetic and chemical analyses. Thirty-eight *Alternaria* strains were from the semi-arid region (Rades: 21 and Raouad: 17) and 41 were from the arid region (Djerba: 19 and Sfax: 22).

Mycelium of 3-d-old colonies, grown on sterilized cellophane disks overlaid on PDA plates, was collected by scraping and then frozen. Genomic DNA was extracted and purified from powdered lyophilized mycelia (each sample, 10–15 mg) using the Wizard Magnetic DNA Purification System for Food kit (Promega Corporation), according to the manufacture's protocol. Quantity and integrity of DNA were checked at Thermo-Scientific Nanodrop (LabX, Midland, Ontario, Canada), and by comparison with a standard 1 kb DNA Ladder (Fermentas GmbH) on 0.8% agarose gel, after electrophoretic separation.

For each *Alternaria* strain, the informative target genes, allergen alt-a1 (*alt-a1*), glyceraldeyde-3-phosphate dehydrogenase (*gpd*) and translation elongation factor 1-α (*tef*), were amplified, respectively, with the following primer pairs: gpd1/gpd2 (Berbee *et al*., 1999), alt-for/alt-rev (Hong *et al*., 2005), and Alt-tef1/Alt-tef2 (Somma *et al*., 2019), and were sequenced for phylogeny analyses.

The Polymerase Chain Reaction mixture (15 µL), contained 15 ng of DNA template, 0.45 µL of each primer (10 mM), 0.3 µL of dNTPs (10mM) and 0.075 µL of Hot Master Taq DNA Polymerase (1 U μL^{-1}; 5 Prime). The three fragment genes were amplified using the PCR conditions of Ramires *et al.* (2018). All PCR products were visualized under UV light after electrophoretic separation in 1× TAE buffer on 1.5% agarose gel**.**

Each PCR product was purified with the enzymatic mixture Exo/FastAP (Exonuclease I, FastAP thermosensitive alkaline phosphatase, Thermo Scientific) and then sequenced using the Big Dye Terminator Cycle Sequencing Ready Reaction Kit (Applied Biosystems), according to the manufacture's recommendations. Both strands were purified by filtration through Sephadex G-50 (5%) (Sigma-Aldrich) and sequenced in an "ABI PRISM 3730 Genetic Analyzer" (Applied Biosystems). The FASTA sequences were obtained with BioNumerics software (Applied Maths). Phylogenetic trees of single and combined genes, following a multi-locus sequence approach, were generated using the Maximum Likelihood statistical method and bootstrap analyses (1000 replicates, removing gaps) with MEGA5 (Tamura *et al*., 2011).

Phylogeny analysis was carried out considering the gene sequences of the following reference strains: *A. alternata* E.G.S.34.016, *A. tenuissima* E.G.S.34.015, *A. arborescens* E.G.S.39.128, *A. infectoria* ex type E.G.S.27.193, *A. brassicicola* ATCC96836, *A. capsici* BMP0180, *A. carthami* BMP1963, *A. citriarbusti* BMP2343, *A. crassa* BMP0172, *A. fragariae* BMP3062, *A. gaisen* BMP2338, *A. limoniasperae* BMP2335, *A. longipes* BMP0313, *A. macrospora* BMP1949, *A. mali* BMP3064, *A. solani* BMP0185, *A. tagetica* BMP0179, *A. tangelonis* BMP2327, *A. tomatophila* BMP2032, and *A. turkisafria* BMP3436. The gene sequences of these reference strains were downloaded from the National Center for Biotechnology Information (NCBI) and "Alternaria Genomes Database" (AGD). *Alternaria infectoria* ex type E.G.S.27.193 was used as the outgroup in phylogenetic analyses.

Mycotoxin extraction and chemical profile analyses

Chemical analyses of the 79 *Alternaria* strains were carried out to evaluate their capabilities to produce AOH, AME, ALT and TA. Following the methods of Li, *et al.* (2001), all the strains were inoculated onto sterilized rice grain and grown for 21 d at 25 ± 1°C in darkness. The cultures were then dried and powdered before mycotoxin extraction.

Mycotoxin analyses were based on the methods of Rubert *et al.* (2012), with modifications. The samples were each finely ground with an Oster Classic grinder (220–240V, 50/60 Hz, 600W). Five grams of each homogenized sample were weighed in a 50 mL capacity plastic tube, and 25 mL of methanol was added. The extraction was carried out using an Ultra Ika T18 basic Ultra-turrax for 3 min. The extract was centrifuged at 4000 rpm for 5 min at 5°C. The supernatant (1 mL) was filtered through a 13 mm × 0.22 µm nylon filter, and diluted before injection into high performance liquid chromatography associated with a diode array detector (LC-DAD). All the extractions were carried out in triplicate.

Alternariol, AME, ALT, and TA were determined using a Merk HPLC with a diode array detector (LC-DAD) L-7455 (Merk), at 256 nm, and Hitachi Software Model D-7000 version 4.0 was used for data analysis. A Gemini C18 column (Phenomenex) 4.6 × 150 mm and 3 µm particle size was used as the stationary phase. The mobile phase consisted of two eluents, eluent A (water with 50 µL L^{-1} trifluoroacetic acid), and eluent B (acetonitrile with 50 µL L^{-1} trifluoroacetic acid). A gradient programme with a constant flow rate of 1 mL min^{-1} was used, starting with 90% A and 10% B, reaching 50% B after 15 min and 100% B after 20 min which was maintained for 1 min. The gradient was then returned to 10% B for 1 min and allowed to equilibrate for 3 min before the next analysis (Myresiotis *et al*., 2015). The limit of detection (LOD) for this method was 0.01 mg L^{-1} and the limit of quantification (LOQ) was 0.1 mg L^{-1}. The data of mycotoxin production were statistically processed using the Prism 5 software (La Jolla; www.graphpad.com).

Pathogenicity tests

A set of 41 representative strains, belonging to all phylogenetic groups previously characterized (Figure 2), were tested for pathogenicity on *C. maritima* leaves. Twenty-four strains of the *A. alternata* group, eight of the *A. arborescens* group, five of the *A. mali* group, and four strains of unknown identity were tested. Seeds were sown into plastic pots (diam, 29 cm; height, 23 cm), filled with inert sand, which were then watered each day with distilled water until germination. The pots were maintained in a greenhouse under controlled conditions

of 16 h light/8 h dark cycles, 25 ± 1°C and 60% relative humidity. Resulting seedlings were irrigated each day for 2 weeks with the nutrient solution (Hewitt, 1996). 1966). At 6 weeks after sowing, leaves of the plants were cut and placed on glass slides in Petri dishes (one slide per dish) containing a moist filter paper. The leaves were then inoculated with *Alternaria* conidium suspension (10^8 conidia mL^{-1}). Control plants were grown in similar condition without fungal inoculation. Separate leaves (six replicates per inoculation treatment) were inoculated. A 10 µL droplet of conidium suspension (10^8 conidia mL^{-1}; 0.05% Tween 20) was placed in the centre of each leaf. Controls were inoculated by a droplet of sterile distilled water 0.05% Tween 20 solution. The Petri dishes containing leaves were then incubated under laboratory conditions (25 ± 3°C; 12h light/12 h dark photoperiod). Disease progress was evaluated at 7 d post-inoculation (dpi) (Taheri, 2019).

After the incubation period, lesion appearance and external and internal lesion diameters were assessed. The degree of pathogenicity of each inoculated strain was assessed by calculating the diameter of the lesion. Statistical analyses of data were performed using the statistical package Statistix8. A one-way ANOVA was used to test the hypothesis of *Alternaria* species differentiation with respect to the lesion diameter, and means were compared at $P < 0.05$.

RESULTS

Host symptoms and morphological characterization of Alternaria *strains infecting* Cakile maritima

Symptomatic plants of *C. maritima* were sampled from two different pedo-climatic conditions (arid and semi-arid). All collected samples (stems, leaves and seeds) showed blight symptoms typical of *Alternaria* infections (Figure 1). Infected plant tissues had necrotic flecks surrounded by chlorotic halos which coalesced into nearly circular or irregularly shaped lesions.

Conidium lengths of *Alternaria* strains ranged from 6 to 29 µm (greatest average = 17.45 µm). Conidium widths ranged from 3 to 10 µm (greatest average = 5.52 µm) (Supplementary Table S1). The numbers of transverse septa varied from 4 to 11 and longitudinal septa varied from 1 to 3. Different margin types, (smooth and rough surfaces) were observed and the colour of margins varied from brown to dark brown or blackish brown. Different forms of conidia were also observed, including ellipsoidal to long ellipsoidal, subspherical, base conical, rounded or obtuse, and apex rounded.

Based on morphological traits, all the strains were identified has *A. alternata*, *A. arborescens* E.G. Simmons or *A. tenuissima*. However, variations in culture characteristics such as margin types and colony colours were observed.

Figure 1. Symptoms of *Alternaria* infections on *Cakile maritima*. Whole plant (a), stem (b), seed (c)and leaves (d).

Molecular and phylogenetic analyses of Alternaria *strains*

Seventy-nine *Alternaria* strains were identified by sequencing informative fragments of the *alt-a1*, *gpd* and *tef* genes. All PCR reactions gave amplicons of the expected sizes of approx. 620 nucleotides for *alt-a1*, 510 for *gpd* and 590 for *tef*.

For sequence alignment of the *gpd* gene, a fragment of about 470 nucleotides was analyzed; however, in the *A. brassicicola* (ATCC96836) sequence, beginning at position 104 of the fragment considered, a short deletion of 27 nucleotides was observed. For *tef* and *alt-a1* sequence alignments, common fragments of about 490 nt (*tef*) and 460 nt (*alt-a1*) were considered. The *tef* gene showed low variability with few polymorphic sites, whereas the *alt-a1* gene showed greater variability among *Alternaria* species.

To further determine the identity of the strains, phylogenetic analysis of the concatenated sequences of the three fragments was carried out. The phylogenetic tree, obtained with Mega5 software using the Maximum Likelihood method, allowed definition of four well-separated clades, corresponding to Section *Alternaria*, Section *Porri*, Section *Brassicicola*, and Section *Infectoriae*, as determined using reference strains (Figure 2). The resolution of all the clades was supported by high bootstrap values. *Alternaria brassicicola* ATCC 96836 and *A. infectoria* E.G.S.27.193 did not cluster with any *Alternaria* strains isolated from *C. maritima*. In the Section *Porri*, only reference strains were clustered together (Figure 2). All *Alternaria* strains clustered in Section *Alternaria*. Forty-seven strains showed homology close to 100% with *A. alternata* E.G.S. 34.016, *A. tenuissima* E.G.S.34.015, *A. limoniasperae* BMP2335, *A. turkisafria* BMP3436 (Figure 2).

A well-supported group clustered 13 field strains with *A. arborescens* E.G.S.39.128.. However, *A. arborescens* was not detected in Raouad region. There was high variability in this group (Figure 2). In *Alternaria* Section, a sub-clade grouped together 12 *Alternaria* strains showing 100% homology with *A. mali* BMP3064 and *A. citriarbusti* BMP2343*A*, and seven *Alternaria* strains (ITEM17797, ITEM17798, ITEM17799, ITEM17800, ITEM17801, ITEM17803, ITEM17809), showing 100% of homology among them, all of which were collected in Sfax region.

Based on these data, four phylogenetic *Alternaria* groups can be discriminated. The *A. alternata* group was the most frequent (60% of strains), followed by *A. arborescens* (16%), and *A. mali* (15%). Seven strains (9%), phylogenetically closely-related to *A. mali*, were not identified at species level (Figure 2).

Mycotoxin production profiles of Alternaria *strains*

Data of mycotoxin production are summarized in Table 1 and in Supplementary Table S2. Altenuene was produced by two *A. alternata* strains (39.2 mg kg^{-1} by ITEM17789 and 43.1 mg kg^{-1} by ITEM17855) and one *A. mali* strain (77.3 mg kg^{-1} by ITEM17788). The amounts of AME, AOH and TA were very variable. These were: for AOH, from 4.4 mg kg^{-1} (*A. alternata* ITEM17782) to 1,856.8 mg kg^{-1} (*A. alternata* ITEM17791); for AME, from 53.4 mg kg^{-1} (*A. alternata* ITEM17848 to 9,149.4 mg kg^{-1} (*A. mali* ITEM17835); and for TA, from 344.4 mg kg^{-1} (*A. mali* ITEM17849) to 19,837.3 mg kg^{-1} (*A. alternata* ITEM17808). Between the four clades of *Alternaria* species, qualitative and quantitative differences in mycotoxin production were examined. However, close correlation between phylogenetic clade and mycotoxin production was not detected.

Alternariol mono-methyl ether was produced by 63 of the 79 strains, (production ranges in parentheses): 38 of 47 *A. alternata* strains (53.4 to 8,766.6 mg kg^{-1}); seven of 13 *A. arborescens* strains (61.8 to 1,848.7 mg kg^{-1}); ten of 12 *A. mali* strains (54.0 to 9,149.4 mg kg^{-1}); and all seven *Alternaria* spp. strains (213 to 1,661.7 mg kg^{-1}). Alternariol was produced by 70 of the 79 stains: 42 of 47 *A. alternata* strains (4.4 to 1,856.8 mg kg^{-1}); nine 13 *A. arborescens* strains (9.8 to 514.4 mg kg^{-1}); all 12 *A. mali* strains (10.8 to 1,671.7 mg kg^{-1}); and all seven *Alternaria* spp. strains (40.9 to 179.6 mg kg^{-1}). Tenuazonic acid was produced by 64 of the 79 stains: 36 of 47 *A. alternata* strains (787.4 to 19,837.6 mg kg^{-1}); eight of 13 *A. arborescens* strains (953 to 6,202mg kg^{-1}); 11 of 12 *A. mali* strains (344.4 to 6,692.3 mg kg^{-1}); and all 7 *Alternaria* spp. strains (1.941.6 to 8904.1mg kg^{-1}.

Pathogenicity tests

Symptoms of tissue browning followed by necrosis were observed at 3 and 7 d after inoculation. Necrosis with yellowing occurred at 3 dpi which became more intense at 7 dpi. The control plants did not show disease symptoms (Figure 3).

According to the phylogenetic strain identification, the 24 selected *A. alternata* strains produced a mean lesion diameter of 0.79 cm; the *A. arborescens* strains produced lesions of 0.86 cm mean diameter; the *A. mali* strains gave mean lesion diameter of 0.62 cm; and the *Alternaria* spp. strains produced lesions of 0.88 cm mean diameter. The statistical analyses did not show significant differences in pathogenicity among the different strains used in the tests. Only *A. alternata* and *A. mali* strains gave slight significant differences in mean lesion

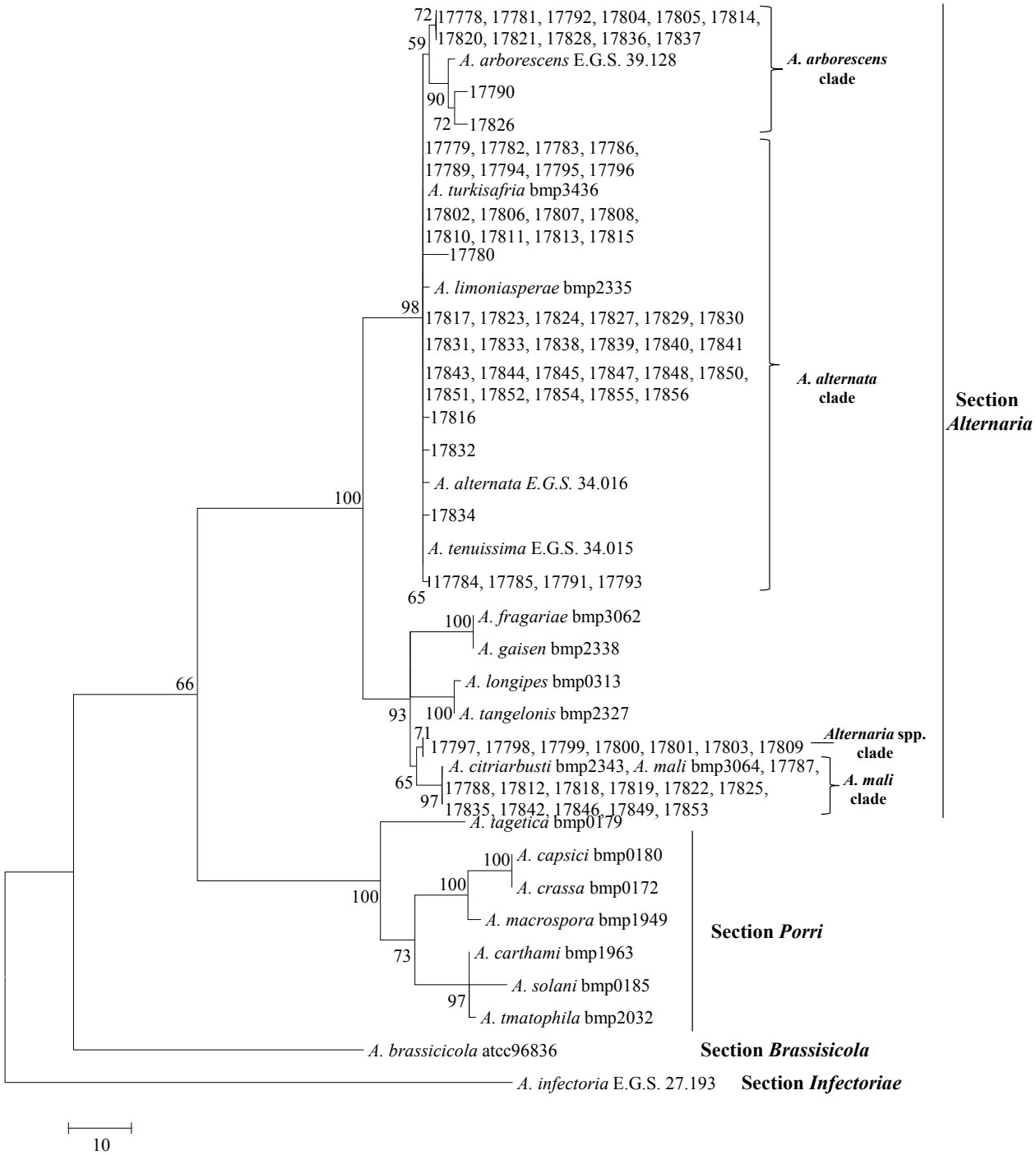

Figure 2. Phylogenetic tree generated by the Maximum Likelihood method (bootstrap 1,000 replicates) of combined *alt-a1*, *gpd*, and *tef* gene sequences from 79 *Alternaria* strains isolated from *Cakile maritima* in Tunisia. *Alternaria infectoria* E.G.S.27.193 was used as outgroup in tree.

sizes (Supplementary Table S3). A one-way ANOVA was performed using the lesion diameters as a factor to test the pathogenicity of the different species. The significance level was set at $\alpha = 0.05$, and the strains were considered as replicates of the species. The probability ($P = 0.0846$) indicated that the species did not exhibit

Table 1. Mycotoxin production and mycotoxin incidence for different phylogenetic *Alternaria* clades. Proportions of strains, and mean amounts of four mycotoxins, are indicated of each clade

Clade		Mean amount of mycotoxin produced (mg kg^{-1})[a]			
		AOH	AME	TA	ALT
A. alternata	No. of positive/total strains	41/47	38/47	36/47	2/47
	Frequency (%)	87.2	80.8	76.6	4.2
	Mean Value	198.6	1632.0	3767.5	41.1
	Min Value	4.4	53.4	787.4	39.2
	Max Value	1856.8	8766.6	19837.6	43.1
A. arborescens	No. of positive/total strains	9/13	7/13	8/13	0/47
	Frequency (%)	69.2	53.8	61.5	0
	Mean Value	130.6	814.2	2993.5	-
	Min Value	9.8	61.8	953.0	-
	Max Value	514.4	1848.7	6202.0	-
A. mali	No. of positive/total strains	12/12	10/12	11/12	1/12
	Frequency (%)	100	83.3	91.7	8.3
	Mean Value	331.8	2108.7	4223.2	-
	Min Value	10.8	54.0	344.4	-
	Max Value	1671.7	9149.4	6692.3	-
Alternaria spp.	No.r of positive/total strains	7/7	7/7	7/7	0/7
	Frequency (%)	100	100	100	-
	Mean Value	119.6	975.4	4631.5	-
	Min Value	40.9	213.0	1941.6	-
	Max Value	179.6	1661.7	8904.1	-

[a] AOH, Alternariol; AME, Alternariol methyl ether; TA, Tenuazonic Acid; ALT, Altenuene.

a statistically significant difference in mean lesion sizes. However, the distributions of lesion diameters for *A. mali* was separated from those for the other species, as indicated by the box plots in Figure 4. To assess this difference a multiple comparison test was carried out. This was a pairwise comparison of the groups (species) using with different comparison procedures (Least Significative Difference; Bonferroni, Scheffe, Dunn and Sidak; or Fisher's least significant differences method). Only the Least Significative Difference method detected a statistically significant difference between *A. mali* and the other species. For the other comparison methods, the difference between the species were not statistically significant.

DISCUSSION

This study has characterized *Alternaria* species occurring on the halophyte *C. maritima* from different bioclimatic areas in Tunisia. *Alternaria* species are major contaminants and pathogens of a wide range of crops, causing economic losses for producers, and health risks for consumers due to the accumulation of toxic metabolites (Da Cruz Cabrala *et al.*, 2016).

Morphological characterization of the representative strains *Alternaria* examined in this study has shown high variability in conidium size, shape, dimensions and septation, confirming that the species identification based on morphological characters is unreliable. Furthermore, there was no correlation between specific morphological traits of the different strains and their bioclimatic region origins. There was also no correlation with the different plant tissues from which the strains were isolated. Similar results were observed by Chethana *et al.* (2018), who found different morphological traits of *Alternaria* strains isolated from onion did not depend from their geographical or plant tissue origins. To perform a more discriminating identification at species level, a representative set of the *Alternaria* strains was investigated by using a polyphasic approach, based also on molecular and chemical characterization.

All the representative strains were phylogenetically identified in Section *Alternaria* (Lawrence *et al.*, 2013),

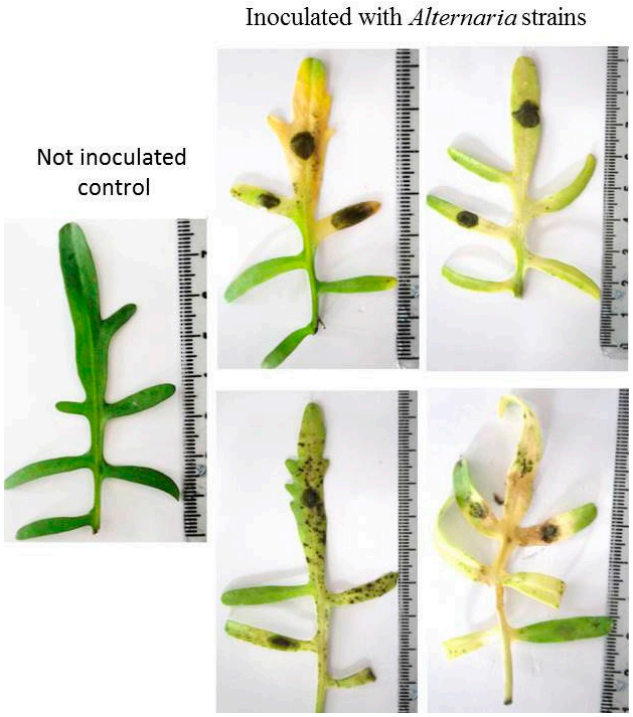

Figure 3. Symptoms resulting on *Cakile maritima* leaves 7 d after inoculation with *Alternaria* strains *A. alternata* (ITEM17830; two upper photographs) or *A. mali* (ITEM17842; lower photographs).

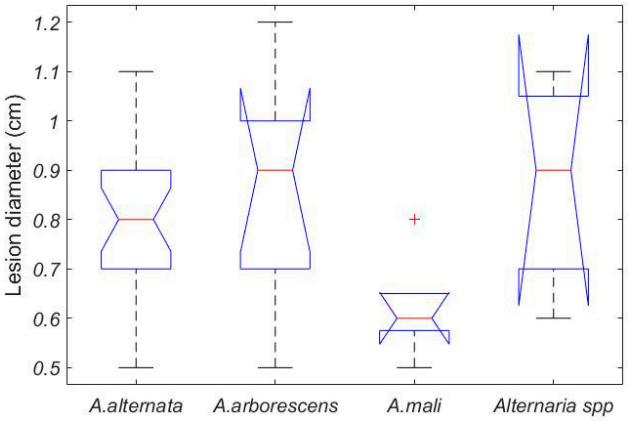

Figure 4. Boxplots (median (red), upper and lower 25th and 75th percentiles, 95% confidence intervals) of lesion diameters produced on inoculated *Cakile maritima* plants by different *Alternaria* species. The large overlap for *A. alternata, A. arborescens, Alternaria* spp. is obvious.

which includes the most important mycotoxigenic *Alternaria* species, and has *A. alternata* as the type species (Woudemberg *et al.*, 2015). The three genes (*gpd*, *tef*, *alta1*) used for multi-locus sequence analyses were selected for their informative responses in *Alternaria*, as suggested by Somma *et al.* (2019). All the strains grouped into four phylogenetic clades: 13 strains were identified as *A. arborescens*, although they showed a great variability; the largest clade included 47 strains, with a high level of homology, and was identified as *A. Alternaria*; 12 strains were identified as *A. mali*; and seven strains were grouped in a clade closely related to, but different from, *A. mali*. These seven strains were not assigned to any species. The different identified *Alternaria* species could not be related to particular plant tissues and/or bioclimatic conditions. *Alternaria alternata* and *A. mali* strains colonize all types of *C. maritima* tissues, and were isolated from the two climatic regions. The exception was all the strains of the unidentified clade, (*Alternaria* spp.; Figure 2), which were isolated only from the seeds of *C. maritima* plants collected in the arid region of Sfax. Also, the *A. arborescens* strains were not detected in the semi-arid region of Raouad. Similar results were reported by Bensassi *et al.* (2009; 2011), who identified *A. alternata* as the most frequent *Alternaria* species occurring on wheat growing in all regions of Tunisia sampled, which were characterized by different environmental conditions. Schiro *et al.* (2018) also showed that conidium production of several *Alternaria* spp. on wheat plants was not correlated with specific microclimatic conditions and was uniform in the field in all regions sampled.

Several authors (Andersen *et al.*, 2008; Brun *et al.*, 2013; Somma *et al.*, 2019), have shown that accurate identification of *Alternaria* spp. requires the polyphasic approach, using morphology, phylogeny, and mycotoxin profiling. *Cakile maritima* is also often used for human and animal consumption. The parts of the plants used for nutrition could become potential natural sources of *Alternaria* mycotoxins, if contaminated by *Alternaria* species. However, since there is still little knowledge of the natural *Alternaria* mycotoxin contamination in these plants, more investigations are required before conclusions can be drawn on the health risks associated to *C. maritima* consumption. Capability to produce mycotoxins by representative strains of the *Alternaria* population isolated in this study has showed that most (90%) of the strains, produced at least one of four assessed mycotoxins, sometimes at very high levels (Supplementary Table S1). This indicated the potential mycotoxicological risk of *Alternaria* strains isolated from these plants. Only three strains produced ALT, while production AME and AOH by the strains analyzed was proven strictly correlated (Supplementary Table S2). This confirms previous reports (Bensassi *et al.*, 2011; Ramires *et al.*, 2018). *Alternaria* mycotoxins have been frequently reported as natural contaminants

of agri-food crops (Puntscher *et al*., 2018), and their production under natural conditions has been associated to several factors such as plant species and host cultivar, environmental conditions, cultivation techniques, plant growth stage, time of harvesting, and crop rotation (Lauren and Fadwa, 2008). The dominance of mycotoxigenic *Alternaria* species on *C. maritima*, reported here for the first time, suggests that this plant can potentially be a risk for human and animal health, if contaminated parts of plants are consumed. In addition, *C. maritima* could be a source of inoculum of *Alternaria* species, if the plants grow in the proximity of other important food plants such as wheat.

The pathogenicity tests showed that the levels of aggressiveness of different *Alternaria* strains from *C. maritima* leaves were different among species, with the pathogenicity of *A. mali* being less than for the other species.

The phylogenetic study indicated the occurrence of a set of strains closely-related to *A. mali*, that could represent a new phylogenetic species. This shows that *C. maritima* could be a source of *Alternaria* genetic diversity to be further investigated. This study also confirms that it is still important to provide genetically well-defined reference isolates for taxonomic investigations of *Alternaria*. These should be accurately validated by a standardized common approach in research dealing with *Alternaria* taxonomy (Somma *et al*., 2019).

CONCLUSION

These results reported here show that the Tunisian halophyte *C. maritima* can be commonly infected by mycotoxigenic *Alternaria* species. Morphological, molecular and mycotoxin analyses confirmed variability within *Alternaria* species of Tunisian origin from different climates. However, no clear links between species with host or geographic origins could be established. This research has shown that *C. maritima* can be a source of *Alternaria* genetic diversity to be further investigated, to provide new information on the taxonomy of the genus.

ACKNOWLEDGMENTS

This work was supported by a grant from the Tunisian Ministry of Higher Education, Scientific Research and Technology (LR15CBBC02) and by H2020-E.U.3.2-678781-MycoKey-Integrated and innovative key actions for mycotoxin management in the food end feed chain. Dr. Besma Sghaier-Hammami was supported by a project "Programme d'encouragement des jeunes chercheurs (19PEJC07-17)".

LITERATURE CITED

Andersen B., Dongo A., Pryor B.M., 2008. Secondary metabolite profiling of *Alternaria dauci*, *A.porri*, *A.solani* and *A. tomatophila***.** *Mycological Research* 112: 241–250.

Andrew M., Peever T.L., Pryor B.M., 2009. An expanded multilocus phylogeny does not resolve morphological species within the small-spored *Alternaria* species complex. *Mycologia* 101: 95–109.

Arcella D., Eskola M., Gómez Ruiz J.A., 2016. Dietary exposure assessment to *Alternaria* toxins in the European population. *EFSA Journal* 4654: 14.

Barbour M., 1970. Seedling Ecology of *Cakile maritima* along the California Coast. *The Journal of the Torrey Botanical Society* 97: 280–289.

Belisario A., Maccaroni M., Coramusi A., Corazza L., Figuli P., Pryor B.M., 2004. First report of *Alternaria* species groups involved in disease complexes of hazelnut and walnut fruit. *Plant Disease* 88: 404.

Bensassi F., Zid M., Rhouma A., Bacha H., Hajlaoui M.R., 2009. First report of *Alternaria* species associated with black point of wheat in Tunisia. *Annals of Microbiology* 59: 465–467.

Bensassi F., Chennaoui M., Bacha H., Hajlaoui M.R., 2011. Survey of the mycobiota of freshly harvested wheat grains in the main production areas of Tunisia. *African Journal of Food Science* 5: 292–298.

Bensassi F., Gallerne C., El Dein O.S., Hajlaoui M.R., Bacha H., Lemaire C., 2012. Cell death induced by the Alternaria mycotoxin Alternariol. *Toxicology In Vitro* 26: 915–923.

Berbee M.L., Pirseyedi M., Hubbard S., 1999. *Cochliobolus* phylogenetics and the origin of known, highly virulent pathogens, inferred from ITS and glyceraldehyde-3-phosphate dehydrogenase gene sequences. *Mycologia* 91: 964–977.

Bock C.H., Thrall P.H., Burdon J.J., 2005. Genetic structure of populations of *Alternaria brassicicola* suggests the occurrence of sexual recombination. *Mycological Research* 109: 227–236.

Brun S., Madrid H., Gerrits Van Den Ende B., Andersen B., Marinach-Patrice C., Mazier D., 2013. Multilocus phylogeny and MALDI-TOF analysis of the plant pathogenic species *Alternaria dauci* and relatives. *Fungal Biology* 117: 32–40.

Canova C., Heinrich J., Anto J.M., Leynaert B., Smith M., … Jarvis D., 2013. The influence of sensitisation to

pollens and moulds on seasonal variations in asthma attacks. *European Respiratory Journal* 42: 935–945.

Chethana B.S., Ganeshan G., Rao A.S., Bellishree K., 2018. Morphological and Molecular Characterization of *Alternaria* Isolates Causing Purple Blotch Disease of Onion. *International Journal of Current Microbiology and Applied Sciences* 7: 3478–3493.

Clausing G., Vickers K., Kadereit J.W., 2000. Historical biogeography in a linear system: genetic variation of Sea Rocket (*Cakile maritima*) and Sea Holly (*Eryngiummaritimum*) along European coasts. *Molecular Ecology* 9: 1823–1833.

Da Cruz Cabrala L., Terminiello L., Pinto V.F., Fog K., Patriarca N.A., 2016. Natural occurrence of mycotoxins and toxigenic capacity of *Alternaria* strains from mouldy peppers. *International Journal of Food Microbiology* 7: 155–160.

Debez A., Ben Hamed K., Grignon C., Abdelly C., 2004. Salinity effects on germination, growth, and seed production of the halophyte *Cakile maritima*. *Plant Soil* 262: 179–189.

Debez A., Braun H.P., Pich A., Taamalli W., Koyro H.W., Abdelly C., Huchzermeyer B., 2012. Proteomic and physiological responses of the halophyte *Cakile maritima* to moderate salinity at the germinative and vegetative stages. *Journal of Proteomics* 75: 5667–5694.

Fehr M., Pahlke G., Fritz J., Christensen M.O., Boege F., Altemoller M., Podlech J., Marko D., 2009. Alternariol acts as a topoisomerase poison, preferentially affecting the IIa isoform. *Molecular Nutrition & Food Research* 53: 441–451.

Hattab Z., Lasfar N.B., Abid M., Bellazreg F., Fathallah A., … Letaief A., 2019. *Alternaria alternata* infection causing rhinosinusitis and orbital involvement in an immunocompetent patient. *New Microbes and New Infections* 100561: 2052–2975.

Hewitt E.J., 1966. Sand and water culture methods used in the study of plant nutrition. 2nd Ed., East Malling: Commonwealth Agricultural Bureaux.

Hong S.G., Cramer R.A., Lawrence C.B., Pryor B.M., 2005. Alt a1 allergen homologs from *Alternaria* and related taxa: Analysis of phylogenetic content and secondary structure. *Fungal Genetics and Biology* 42: 119–129.

Hong S.G., Maccaroni M., Figuli P.J., Pryor B.M., Belisario A., 2006. Polyphasic classification of *Alternaria* isolated from hazelnut and walnut fruit in Europe. *Mycological Research* 110: 1290–1300.

Kadereit J.W., Arafeh R., Somogyl G., Westberg E., 2005. Terrestrial growth and marine dispersal? Comparative phylogeography of five coastal plant species at a European scale. *Taxon* 54: 861–876.

Kubiak-Martens L., 1999. The plant food component of the diet at the late Mesolithic (Ertebølle) settlement at TybrindVig, Denmark. *Veg. Hist. Archaeobot* 8: 117–127.

Lauren J., Fadwa T., 2008 Factors Affecting Mycotoxin Production in Fruits. In: *Mycotoxins in Fruits and Vegetables* (R. Barkai-Golan, N. Paster, ed.), Academic Press, 75–104.

Lawrence D.P., Gannibal P.B., Peever T.L., Pryor B.M., 2013. The sections of *Alternaria*: Formalizing species-group concepts. *Mycologia* 105: 530–546.

Li N., Toyazaki T., Yoshizawa J., 2001. Production of Alternaria mycotoxins by *Alternaria alternata* isolated from weather-damaged wheat. *Journal of Food Protection* 64: 567–571.

Linde C.C., Liles J.A., Thrall P.H., 2010. Expansion of Genetic Diversity in Randomly Mating Founder Populations of *Alternaria brassicicola* Infecting *Cakile maritima* in Australia. *Applied Environmental Microbiology* 76: 1946–1954.

Liu G.T., Qian Y.Z., Zhang P., Dong W.H, Qi Y.M., Guo H.T., 1992. Etiological role of *Alternaria alternata* in human esophageal cancer. *Chinese Medical Journal* 105: 394–400.

Logrieco A., Moretti A., Solfrizzo M., 2009. *Alternaria* toxins and plant diseases: An overview of origin, occurrence and risks. *World Mycotoxin Journal* 2: 129–140.

Lou J., Fu L., Peng Y., Zhou L., 2013. Metabolites from *Alternaria* Fungi and Their Bioactivities. *Molecules* 18: 5891–5935.

Moretti A., Pascale M., Logrieco A.F., 2019. Mycotoxin risks under a climate change scenario in Europe. *Trends in Food Science &Technology* 84: 38–40.

Myresiotis C.K., Testempasis S., Vryzas Z., Karaoglanidis G.S., Mourkidou P.E., 2015. Determination of mycotoxins in pomegranate fruits and juices using a QuEChERS-based method. *Food Chemistry* 182: 81–88.

Oliver E.J., Thrall P.H., Burdon J.J., Ash J.E., 2001. Vertical disease transmission in the *Cakile-Alternaria* host-pathogen interaction. *Australian Journal of Botany* 49: 561–569.

Ostry V., 2008. Alternaria mycotoxins: An overview of chemical characterization, producers, toxicity, analysis and occurrence in foodstuffs. *World Mycotoxin Journal* 1: 175–188.

Pastor F.J., Gaurro J., 2008. *Alternaria* infections: laboratory diagnosis and relevant clinical features. *Clinical Microbiology and Infection* 14: 737–746.

Patriarca A., 2016. *Alternaria* in food products. *Current Opinion in Food Science* 11: 1–9.

Pryor B.M., Michailides T., 2002. Morphological, Pathogenic, and Molecular Characterization of *Alternaria* Isolates Associated with *Alternaria* Late Blight of Pistachio. *Phytologia* 92: 406–416.

Puntscher H., Kütt M.L., Skrinjar P., Mikula H., Podlech J., … Warth B., 2018. Tracking emerging mycotoxins in food: development of an LC-MS/MS method for free and modified *Alternaria* toxins. *Analytical and Bioanalytical Chemistry* 410: 4481–4494.

Ramires F.A., Masiello M., Somma S., Villani A., Susca A., … Moretti A., 2018. Phylogeny and Mycotoxin Characterization of *Alternaria* Species Isolated from Wheat Grown in Tuscany, Italy. *Toxins* 10: 472.

Roberts R.G., Reymond S.T., Andersen B., 2000. RAPD fragment pattern analysis and morpholigcal segregation of small-spored *Alternaria* species and species groups. *Mycological Research* 104: 151–160.

Rubert J., Dzuman Z., Vaclavikova M., Zachariasova M., Soler C., Hajslova J., 2012. Analysis of mycotoxins in barley using ultra high liquid chromatography high resolution mass spectrometry: Comparison of efficiency and efficacy of different extraction procedures. *Talanta* 99: 712–719.

Santiago I.F., Goncalves V.N., Gomez-Silva B., Galetovic A., Rosa L.H., 2018. Fungal diversity in the Atacama Desert. *Antonie Van Leeuwenhoek* 111: 1345–1360.

Schiro G., Müller T., Verch G., Sommerfeld T., Mauch T., … Müller M.E.H., 2018. The distribution of mycotoxins in a heterogeneous wheat field in relation to microclimate, fungal and bacterial abundance. *Journal of Applied Microbiology* 126: 177–190.

Serdani M., Kang J.C., Andersen B., Crous P.W., 2002. Characterization of *Alternaria* species-group associated with core rot of apples in South-Africa. *Mycological Research* 106: 561–569.

Simmons E.G., 1990. *Alternaria* themes and variations (17–53). *Mycotaxon* 37: 79–119.

Simmons E.G., 2007. *Alternaria*: An Identification Manual, 6th ed.; CBS Fungal Biodiversity Centre: Utrecht, The Netherlands, 775 pp.

Simmons E.G., Roberts R., 1993. *Alternaria* themes and variations (73). *Mycotaxon* 48: 109–140.

Somma S., Amatulli M.T., Masiello M., Moretti A., Logrieco A.F., 2019. *Alternaria* species associated to wheat black point identified through a multilocus sequence approach. *International Journal of Food Microbiology* 293: 34–43.

Steyn P.S., Rabie C.J., 1976. Characterization of magnesium and calcium tenuazonate from *Phoma sorghina*. *Phytochemistry* 15: 1977–1979.

Stypuła-Trębas S., Minta M., Radko L., Jedziniak P., Posyniak A., 2017. Nonsteroidal mycotoxin alternariol is a full androgen agonist in the yeast reporter androgen bioassay. *Environmental Toxicology and Pharmacology* 55: 208–211.

Taheri P., 2019. Disease resistance and virulence screen in *Solanum tuberosum–Alternaria tenuissima* interaction: the role of pathogenicity factors. *Euphytica* 215: 15.

Tamura K., Peterson D., Peterson N., Stecher G., Nei M., Kumar S., 2011. MEGA5: Molecular Evolutionary Genetics Analysis Using Maximum Likelihood, Evolutionary Distance, and Maximum Parsimony Methods. *Molecular Biology and Evolution* 28: 2731–2739.

Thrall P.H., Andrew Y.G., Burdon J.J., 2000. An analysis of mating structure in populations of the annual sea rocket, *Cakile maritima* (Brassicaceae). *Australian Journal of Botany* 48: 731–738.

Thrall P.H., Burdon J.J., Bock C.H.,2002. Short-term epidemic dynamics in the *Cakile maritima – Alternaria brassicicola* host-pathogen association. *Journal of Ecology* 89: 723–735.

Thrall P.H., Barrett L.G., Burdon J.J., Alexander H.M., 2005. Variation in pathogen aggressiveness within a metapopulation of the *Cakile maritima–Alternaria brassicicola* host-pathogen association. *Plant Pathology* 4: 265–274.

Wang W., Jones C., Ciacci-Zanella J., Holt T., Gilchrist D.G., Dickman M.B., 1996. Fumonisins and *Alternaria alternata* lycopersici toxins: Sphinganine analog mycotoxins induce apoptosis in monkey kidney cells. *Proceedings of the National Academy of Sciences* 93: 3461–3465.

Woudenberg J.H.C., Seidl M.F., Groenewald J.Z., De Vries M., Stielow J.B., … Crous P.W., 2015. Alternaria section Alternaria: Species, formaespeciales or pathotypes? *Studies in Mycology* 82: 1–21.

Zarrouk M., Elalmi H., Youssef N.B., Sleimi N., Smaoui A., … Abdelly C., 2003. Lipid composition of local halophytes seeds: *Cakile maritima*, *Zygophyllum album* and *Crithmummaritimum*. In: *Crash crop halophytes: recent studies* (Lieth H, Mochtchenko M eds). Springer, Berlin, 121–126.

Phytopathologia Mediterranea
The international journal of the
Mediterranean Phytopathological Union

Firenze University Press
www.fupress.com/pm

Research Paper

Microscope observations of Botryosphaeriaceae spp. in the presence of grapevine wood

José Abraham OBRADOR-SÁNCHEZ[1], Rufina HERNANDEZ-MARTÍNEZ[2,*]

[1] *Departamento de parasitología, Universidad Autónoma Agraria Antonio Narro Unidad Laguna (UAAAN-UL), Torreón, Coahuila, México, 27059*
[2] *Departamento de Microbiología, Centro de Investigación Científica y de Educación Superior de Ensenada (CICESE), Ensenada, Baja California, México, 22860*
*Corresponding author: ruhernan@cicese.mx

Summary. Grapevine trunk diseases (GTD) are important threats to long-term longevity, productivity, and profitability in all grape production systems. Botryosphaeria dieback is caused by at least 32 Botryosphaeriaceae fungi. The main symptoms of this disease on grapevines are wedge-shaped cankers in the trunks, general decline and eventually death of affected plants. Pathogens from this family have broad host ranges and varying virulence. This study aimed to compare, and gain some insight into how, *Lasiodiplodia gilanensis*, *Diplodia seriata,* and *D. corticola* colonize grapevine tissues. *In vitro* studies using pycnidiospores as inoculum, showed that the presence of grapevine wood affected spore germination, hyphal growth and branching, and biomass production, especially in *L. gilanensis*. *In planta,* microscopy revealed the use of xylem vessels as the preferred sites of pathogen entry, and differences in growth and hyphal branching among species. *Lasiodiplodia gilanensis* produced cellulases at the beginning of the pathogen/host interaction to degrade plant tissues and invade parenchymal tissue, while *D. seriata* and *D. corticola* grew endophytically in the first stages of grapevine colonization.

Keywords. Grapevine trunk disease fungi, Botryosphaeria dieback, plant-pathogen interaction.

OPEN ACCESS

Citation: J.A. Obrador-Sánchez, R. Hernandez-Martínez (2020) Microscope observations of Botryosphaeriaceae spp. in the presence of grapevine wood. *Phytopathologia Mediterranea* 59(1): 119-129. doi: 10.14601/Phyto-11040

Accepted: February 10, 2020

Published: April 30, 2020

Data Availability Statement: All relevant data are within the paper and its Supporting Information files.

Competing Interests: The Author(s) declare(s) no conflict of interest.

Editor: Hanns Kassmeyer.

INTRODUCTION

Grapevine trunk diseases (GTDs) are a significant challenge for grape production; they threaten grapevine longevity, productivity, and profitability in all grape production systems. To date, there are no effective control methods available for these diseases. GTDs are a group of complex diseases, including Petri disease, Black foot, Esca complex, Eutypa dieback, and Botryosphaeria dieback (Gramaje *et al*., 2018; Mondello *et al*., 2018). The causal agents are fungi, which diminish grape yields, causing gradual deterioration that eventually can lead to the death of grapevines (Siebert, 2001; Gubler *et al*., 2005; Bertsch *et al*., 2013).

The principal point of entry of GTD fungi to host plants is through mechanical damage, pruning wounds, and natural openings (Gubler *et al*.,

2005). Fungi colonize the xylem vessels of plant tissues causing reduction of the flow of nutrients, release of toxins, and degradation of xylem vessel cell walls by release of hydrolytic enzymes. These slowly kill affected vines (Valtaud *et al*., 2009). Plants react to the infections, producing biochemical barriers as accumulations of tyloses and gummosis, causing blockage of the xylem vessels that limit the fungal invasion (Fontaine *et al*., 2016).

From 2000, the role of Botryosphaeriaceae in the GTD black dead arm has been increasingly recognized (Phillips, 2002), and later the disease was renamed as Botryosphaeria dieback (Úrbez-Torres, 2011). To date, at least 30 different species of fungi have been associated with Botryosphaeria dieback, belonging to the genera *Botryosphaeria, Diplodia, Dothiorella, Lasiodiplodia, Neofusicoccum, Neoscytalidium, Phaeobotryosphaeria,* and *Spencermartinsia* (Úrbez-Torres, 2011; Billones-Baaijens *et al*., 2015; Yang *et al.,* 2017). Disease symptoms include wedge-shaped perennial cankers in grapevine trunks, dead arms, sprout decay, bud necrosis, and death of grafts (Úrbez-Torres, 2011).

Botryosphaeriaceae have cosmopolitan distribution (Úrbez-Torres, 2011), although it has been suggested that some genera are more common in different climates, for example, *Diplodia* in temperate regions (Burgess and Wingfield, 2002) and *Lasiodiplodia* in tropical and sub-tropical regions (Mohali *et al*., 2005; Burgess *et al*., 2006). These fungi colonize weak and stressed plants, for example, after drought, hail, wind, or frost (Smith *et al*., 1994; Denman *et al.,* 2000).

The Botryosphaeriaceae have life cycles divided into a sexual phase (teleomorph), which rarely occurs in nature, and an asexual phase (anamorph). Asexual reproduction is through the formation of multilocular ascomata with multilayer walls, which together form in pycnidia (Denman *et al*., 2000). Humidity and rain promote the release of the pycnidiospores which are dispersed mainly by wind (Epstein *et al*., 2008).

In Mexico, five species of Botryosphaeriaceae have been reported, including *Lasiodiplodia theobromae*, *Diplodia seriata, D. corticola, Neofusicoccum vitifusiforme,* and *N. australe* (Úrbez-Torres *et al*., 2008; Candolfi-Arballo *et al*., 2010). Pathogenicity tests showed *L. theobromae* was more virulent than *D. seriata* or *D. corticola*, with *D. corticola* acting as a weak pathogen of *Vitis vinifera* (Úrbez-Torres *et al*., 2009; Varela *et al*., 2011).

Little is known of how Botryosphaeriaceae penetrate and invade host tissues. *Lasiodiplodia theobromae* is also highly aggressive in rubber tree (*Hevea brasiliensis)* (Encinas, 1997), Caribbean pine (*Pinus caribaea)* (Cedeño *et al*., 1996), and cashew *(Anacardium occidentale)* (Muniz *et al*., 2011). In naturally and experimentally infected tissues of Caribbean pine, *L. theobromae* invades all the tissues of sapwood but grows more abundantly in the rays; hyphae invade transversely and longitudinally, degrading the xylem cell walls, quickly invading the vessels, intercellular spaces, and parenchyma (Cedeño *et al*., 1996). On fresh wood of rubber (*H. brasiliensis*) and aspen (*Populus tremula*), after 2 to 3 d, the fungus has fast and abundant growth, with ray and axial parenchyma, and vessels, being the preferred pathways of colonization (Encinas and Daniel, 1997). In 2-month-old cashew plants, *L. theobromae* hyphae are located within the xylem vessels, with extensive development in the secondary xylem tissues (Muniz *et al*., 2011). Differently than in grapevine, *D. corticola* is one of the most aggressive fungal pathogens of *Quercus*, and uses stomata as the host entry points. Strains of this pathogen differ in virulence, inducing different symptoms in infected plants (Félix *et al*., 2017). In peach (*Prunus persica), D. seriata* invades xylem tissues of the superficial xylem layers of the xylem, phloem, meristematic tissues, and parenchyma, causing necrosis (Biggs and Britton, 1988). Conidia of *Neofusicoccum luteum* inoculated onto green tissues were unable to germinate without wounding (Amponsah *et al*., 2012). In apple (*Malus domestica*), *Botryosphaeria dothidea* entered host twigs at the lenticels and grew intercellularly in the exocarps (Guan *et al*., 2015).

Understanding the biology and mechanisms of infection of the Botryosphaeriaceae in grapevine could help with the implementation of disease management methods, which are not able to limit GTDs. In the present study, several microscopy techniques were used to analyze and compare the infection mechanisms of *L. gilaniensis, D. seriata,* and *D. corticola*. Since these fungi are, respectively, of high, intermediate, and low virulence to grapevine (*Vitis vinifera*), the main aim was to study their colonization behaviour during infection of this host.

MATERIALS AND METHODS

Strains used in this study

Diplodia corticola SASII2-3 and *D. seriata* BY06-3 were isolated from grapevines growing in the county of Ensenada, Baja California, Mexico, and these isolates are held in the laboratory of plant pathology of the Center for Scientific Research and Higher Education of Ensenada (CICESE) (Candolfi-Arballo, 2010). *Lasiodiplodia gilaniensis* UCD256Ma, previously isolated and classified as *L. theobromae* (Úrbez-Torres *et al*., 2006), was provided by Dr Douglas W. Gubler from the University of California, Davis. Isolates were identified based on their morphological characteristics and by comparing their ITS

and EF1α with those deposited in the GenBank of the NCBI. All the isolates were grown on potato dextrose agar (PDA; BD Difco™), and were preserved at -80°C in a solution of water and 20% glycerol.

Induction of pycnidia and inoculum preparation

To induce formation of pycnidia, *L. gilaniensis* and *D. seriata* were incubated in Petri plates containing water agar (WA) at 15 g L^{-1}, which was supplemented with 15 μg mL^{-1} chloramphenicol to inhibit bacterial growth. Four to six autoclaved wood toothpicks were placed on the top of the culture medium in each plate, and the plates were kept at 28°C for 3 weeks with a daily photoperiod of 12 h light and 12 h darkness. This procedure gives few pycnidia in *D. corticola*, for pycnidium induction in this fungus, autoclaved vine wood sticks (approx. 3 cm long and 1 cm diam.) were placed on the agar and plates were kept in the above conditions for 4 weeks. Pycnidia were collected with the aid of a dissecting needle. Pycnidiospores were released from pycnidia using a previously sterilized pestle and mortar. Conidia were recovered from the pycnida remains by washing with sterile distilled water and passing twice through Miracloth (475855, EMD Millipore). The final concentration of pycnidiospore suspensions was adjusted to 40 μL^{-1} after counting using a Neubauer chamber.

Evaluation of growth rates of Botryosphaeriaceae in the presence of grapevine wood

Growth rates were each evaluated using 10 μL of pycnidiospore solution of each strain (obtained as above) that were placed at one side of a 9 cm diam. Petri dish, either containing Vogel's Minimum Medium (VMM) or VMM supplemented with grapevine wood (VMM-W). VMM-W was prepared using fresh wood obtained from grapevine plants (approx. 1-y-old). This was washed in sterile purified water, ground in an Osterizer 541® blender, and then sterilized together with VMM medium. The pycniospore-inoculated dishes were placed at 28°C for 72 h. Growth of the fungi was evaluated by measuring the longest hyphae from the inoculation point in each dish.

Comparison of biomass production among Botryosphaeriaceae in the presence of grapevine wood

To evaluate the variation in the biomass production of the three Botryosphaeriaceae in presence of grapevine wood, circles (80 mm diam.) were obtained from a dialysis membrane (Spectrapor membrane tubing, Spectrum Medical Industries, Inc.). The membrane circles were weighed, boiled for 1 h to eliminate salts, and then autoclaved while immersed in distilled water. Once sterilized, they were each placed in the centre of a Petri dish containing either VMM or VMM-W media. Pycnidiospore suspensions (10 μL each) were then individually inoculated on the top of the membrane, and the membrane-containing plates were incubated at 28°C for 60 h. The membranes were then removed from the plates, and the fresh weight of mycelium was determined for each treatment.

Comparison of germination percent and branching in the presence of grapevine wood

Pycnidiospores of Botryosphaeriaceae are released usually in cirri; in *L. gilanensis* and *D. corticola* at the beginning, the pycnidiospores are one-celled and hyaline, but later they become two-celled and pigmented (Úrbez-Torres, 2011). In *D. seriata,* pycnidiospores are initially hyaline but soon became brown before they are released from the pycnidia (Phillips *et al*., 2007). To evaluate the variation in germination of pycnidiospores and the hyphal branches produced for the three Botryosphaeriaceae, the percent of germination and the branching rate were evaluated using the pycnidiospore suspension of each isolate (obtained as above). Ten μL of suspension were placed into each 9 cm diam. Petri dish containing VMM or VMM-W and spread over the medium surface with a glass rod. Plates were incubated at 28°C and observed using an inverted microscope (Zeiss Axiovert) at 2, 4, 6, 8, 12 and 24 h after inoculation, to determine the germination rate, and at 2, 4, 6, and 8 h, to estimate the number of branches produced from each pycnidiospore. For *L. gilaniensis* and *D. corticola*, 60 pycnidiospores were evaluated, half of which were pigmented and half hyaline. For *D. seriata,* 30 pycnidiospores were assessed, since this species only produced pigmented pycnidiospores. The pycnidiospores were each considered as germinated when they presented a hypha of at least half the pycnidiospore length.

Plant inoculation assays to evaluate wood colonization by Botryosphaeriaceae

One-year-old plants of *Vitis vinifera* 'Cabernet Sauvignon', maintained in a greenhouse with temperatures from 15 to 28 °C, were inoculated with spore suspensions, using five plants for each of the tested fungi. Fresh wounds were made by cutting the top of the woody plant stems. After 30 min to avoid exudate

from the plants, 30 µL of the pycnidiospore suspension of each isolate was placed on the wound surface. After 12, 24, and 48 hours post-inoculation, a sample of wood (approx. 1 cm length) from each inoculation site was collected and processed for epifluorescence microscopy and scanning electron microscopy (SEM) observations (see below). For epifluorescence, samples were fixed in FAA solution (90 mL of 50% ethanol, 5 mL of 40% formaldehyde solution, and 5 mL of glacial acetic acid). For SEM, samples were fixed in Karnovsky's reagent (3% glutaraldehyde and 2% formaldehyde in 0.1M phosphate buffer, pH 7.4). Treated samples were kept in the respective fixatives for 24 h at 4°C.

Epifluorescence microscopy and SEM observations of host colonization

Fixed samples in FAA were stained with the solutions of Calcofluor White stain (Fluka) at 1:1 with 10 % KOH (w/v) and Calcofluor White M2R (Exc/Ems 355/433 nm, Cyanamid) at 1 % (v/v) in 15% KOH (w/v). Each sample was covered with 10 µL of Calcofluor White for 2 min, the excess was then removed, and 10 µL of Calcofluor White M2R was added. After 30 s, the stained samples were observed in an inverted microscope (Zeiss Axiovert) under UV light (340 nm) using a DAPI filter.

For observation with SEM, samples previously fixed with Karnovsky's reagent were washed three times (15 min each) with phosphate buffer (0.2 M, pH 7.2). They were then postfixed under a fume extraction hood with 4% osmium tetraoxide, and incubated for 2 h at 4°C. After another three 15 min washes in the phosphate buffer, samples were dried for 1 week in a desiccator containing silica beads. Dehydrated samples were covered with gold (Ted Pella, 99.99%) using a sputter coater, and were kept in a desiccator until SEM (JEOL JSM-35c) observation.

For epifluorescence and SE microscopy, observations were made in the wound areas of the samples, in longitudinal and transverse stem incisions.

Statistical analyses

Fungus growth, germination, and branching experiments were carried out in triplicate, and data were processed using multiple variance analysis (ANOVA) as a parametric test and by Kruskal-Wallis assessment as a nonparametric analysis. For the isolate biomass data, a T-test analysis was performed. Data were processed using STATISTICA™ software (Hill and Lewicki, 2012).

RESULTS

Effects of grapevine wood on growth and biomass production of L. gilaniensis*,* D. seriata *and* D. corticola

In general, more growth of the three fungi was observed in the presence of grapevine wood (VMM-W) than in VMM. *Lasiodiplodia gilaniensis* reached average colony diameter 6.51 ± 0.15 cm in VMM-W and 5.59 ± 0.13 cm in VMM, with no statistical differences among the treatments. *Diplodia seriata* average colony diameter was 5.58 ± 0.39 cm in VMM-W and 3.67 ± 0.3 cm in VMM; and for *D. corticola,* 3.33 ± 0.3 cm in VMM-W and 1.22 ± 0.09 cm VMM. For both *Diplodia* spp., there were significant differences ($P < 0.05$) among treatments (Figure 1).

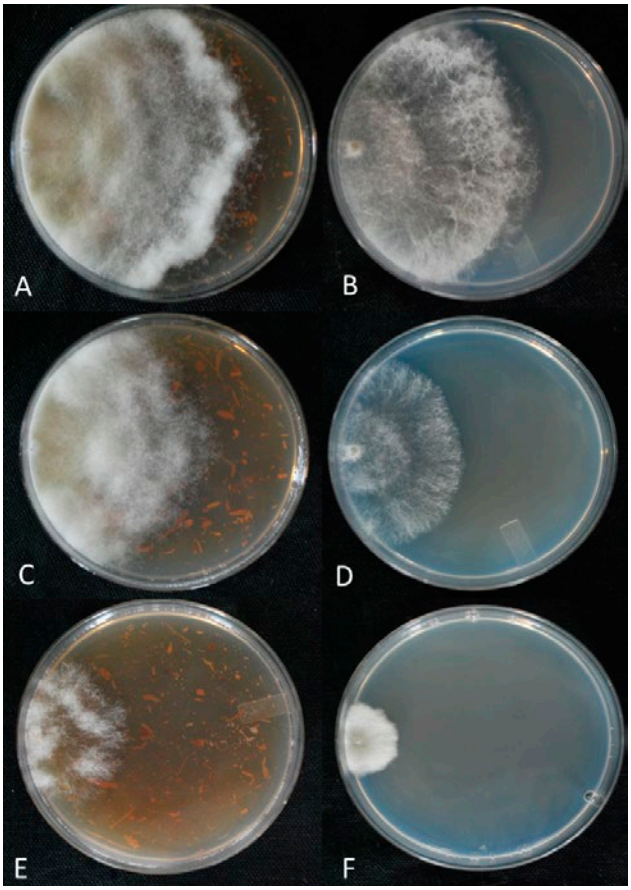

Figure 1. Mean colony diameters for three fungi on Vogel's Minimum Medium with (VMM-W) (A, C, and E) or without (VMM) (B, D, and F) ground grapevine wood. The fungi were *Lasiodiplodia gilaniensis* (A and B), *Diplodia seriata* (C and D), and *D. corticola* (E and F). The fungi were grown for 72 h at 28°C.Visible effects were observed, mainly in *D. corticola* and *D. seriata*.

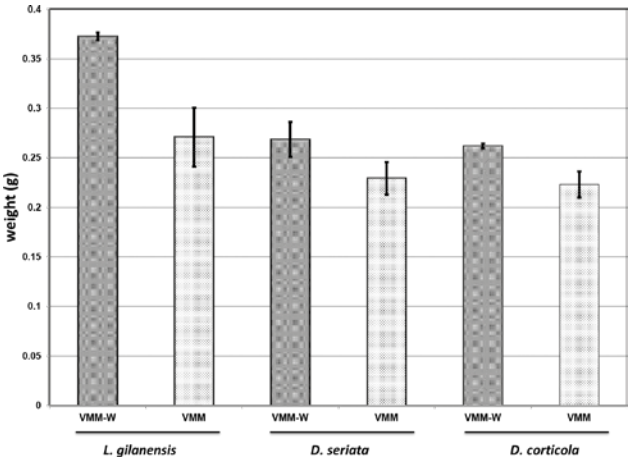

Figure 2. Mean weight of biomass of *Lasiodiplodia gilaniensis*, *Diplodia seriata* or *D. corticola* grown on Vogel's Minimum Medium in the presence (VMM-W) or the absence (VMM) of grapevine wood. There was a strong effect for the presence of grapevine wood for *L. gilaniensis*.

Lasiodiplodia gilaniensis produced the greatest biomass (average weight = 0.372 ± 0.004 g on VMM-W and 0.271 ± 0.029 g on VMM, while for *D. seriata,* the average biomass weight was 0.268 ± 0.018 g on VMM-W and 0.229 ± 0.016 g on VMM. *Diplodia corticola* produced the least biomass in both treatments, with an average weight of 0.262 ± 0.002 g on VMM-W and 0.223 ± 0.013 g on VMM. There were no significant differences ($P > 0.05$) between *D. corticola* and *D. seriata* for both treatments, or with *L. gilaniensis* in the absence of ground grapevine wood in the medium (Figure 2).

Effects of grapevine wood on germination and hyphal branching from pycnidiospores of Botryosphaeriaceae

The presence of wood in the growth medium influenced germination of pycnidiospores. In general, pycnidiospores germinated more rapidly and in greater proportions in the presence of grapevine wood (Figure 3). Two h after inoculation, 70% of *L. gilaniensis* pigmented pycnidiospores germinated on VMM-W (43% on VMM), and reached 90% germination at 4 h in the wood-amended media and 73% on VMM. Six h after inoculation, there were no statistically significant differences observed between the two media (96% on VMM-W and 93% in VMM), because most spores in VMM-W had germinated already at 4 h. Similarly, hyaline pycnidiospores germinated more rapidly and in greater proportions on VMM-W, but germination was less for these pycnidiospores than for pigmented ones (Figure 3A).

In *D. seriata,* germination commenced later (4 h after inoculation) than for the other two fungi, always resulting greater germination in the presence of grapevine wood. However, significant differences were found only at 4 h (53% for VMM-W and 6% for VMM) (Figure 3B).

In *D. corticola*, 60% of pigmented pycnidiospores germinated on VMM-W after 2 h, while there was no germination after the same period on VMM. After 8 h, 90% germination was recorded on the wood-amended media, compared with 46% on VMM. Similarly, hyaline pycnidiospores germinated more rapidly and in greater proportions on VMM-W, but always at less proportions than pigmented pycnidiospores (Figure 3C).

Lasiodiplodia gilaniensis exhibited the greatest hyphal branching on VMM-W (ten branches after 8 h), while *D. seriata* had one branch and *D. corticola* two

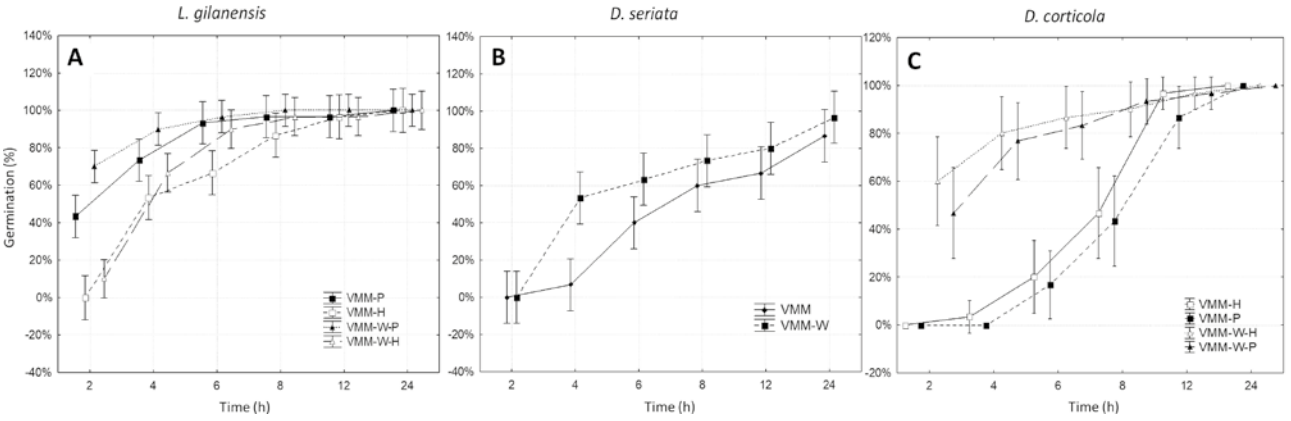

Figure 3. Mean germination proportions for pigmented (P) and hyaline (H) pycnidiospores of *Lasiodiplodia gilaniensis* (A), *Diplodia corticola* (B), and *D. seriata* (C), grown in Vogel's Minimum Medium (VMM) or VMM supplemented with grapevine wood (VMM-W). The presence of grapevine wood in the medium mostly affected germination of *D. corticola*.

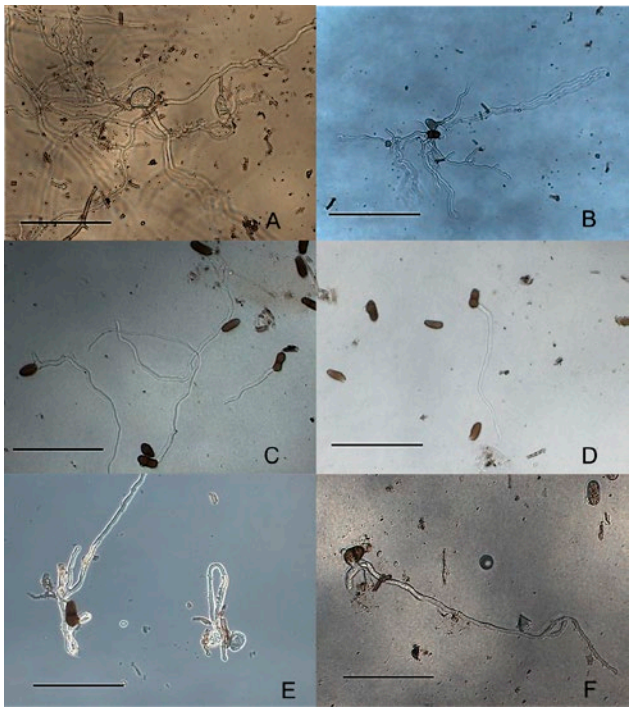

Figure 4. Hyphal branches observed in the fungi *Lasiodiplodia gilaniensis* (A and B), *Diplodia seriata,* (C and D) and *D. corticola* (E and F), after 8 h growth on Vogel's Minimum Medium supplemented with (A, C, and E) or without grapevine wood (B, D, and F). Increased numbers of hyphal branches were observed in the media containing wood. Bars = 50 µm.

branches after the same period) (Figure 4). The presence of grapevine wood in the media did not affect the branching in *L. gilaniensis*, but there were differences among hyaline and pigmented pycnidiospores, with a greater number of branches observed in pigmented than hyaline pycnidiospores (Figure 5A). In *D. seriata,* the presence of wood stimulated hyphal branching, although with no statistical significance (Figure 5B). In *D. corticola,* the number of hyphal branches was greater in the treatments with wood for both hyaline and pigmented pycnidiospores (Figure 5C).

Colonization of grapevine woody tissues by three Botryospaeriaceae *pathogens*

Microscope observations showed no germinated pycnidiospores of *L. gilaniensis, D. seriata* or *D. corticola* in grapevine wood 12 h after inoculation (Figures 6A, 6D, and 6G). In contrast, after 24 h, germination was abundant observed (Figures 6B, 6E, and 6H), especially in *L. gilaniensis*. None of the fungi formed appressoria.

At 24 h after inoculation, all the pycnidiospores of *L. gilaniensis* had germinated. Germ tubes emerged from the central parts of the spores, and the resulting hyphal branches showed directional growth to xylem vessels, tracheids, and phloem. The xylem vessels were the most frequent site of pathogen entry (Figure 6B). In SEM, the entrance through xylem vessels and tracheids was more evident, as was collapse of some spores (Figures 7A, 7B).

Also at 24 h after inoculation, most of the pycnidiospores of *D. seriata* had germinated, developing two to three branches with linear growth of the hyphae until finding openings to penetrate host tissues (Figure 6E). Similar to *L. gilaniensis*, germination hyphae came out from the central parts of the pycnidiospore towards xylem vessels and tracheids, with the xylem vessels being the most common host entry sites (Figure 6E). In SEM,

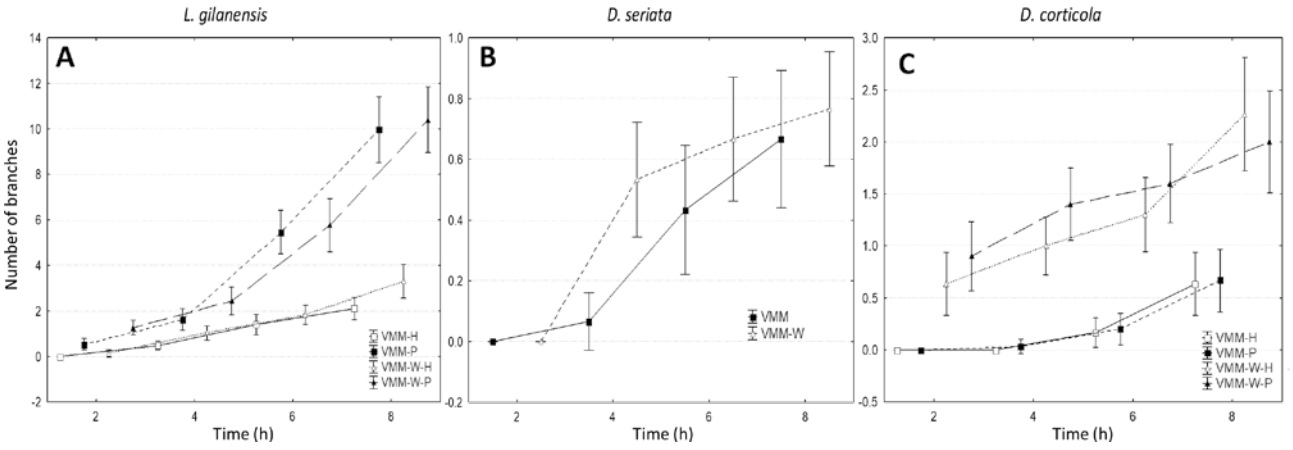

Figure 5. Mean numbers of hyphal branches produced by pigmented (P) or hyaline (H) pycnidiospores of *Lasiodiplodia gilaniensis* (A), *Diplodia seriata* (B), or *D. corticola* (C), in the absence (VMM) or presence of grapevine wood (VMM-W) in the growth medium. The presence of grapevine wood affected the branching of *D. corticola*.

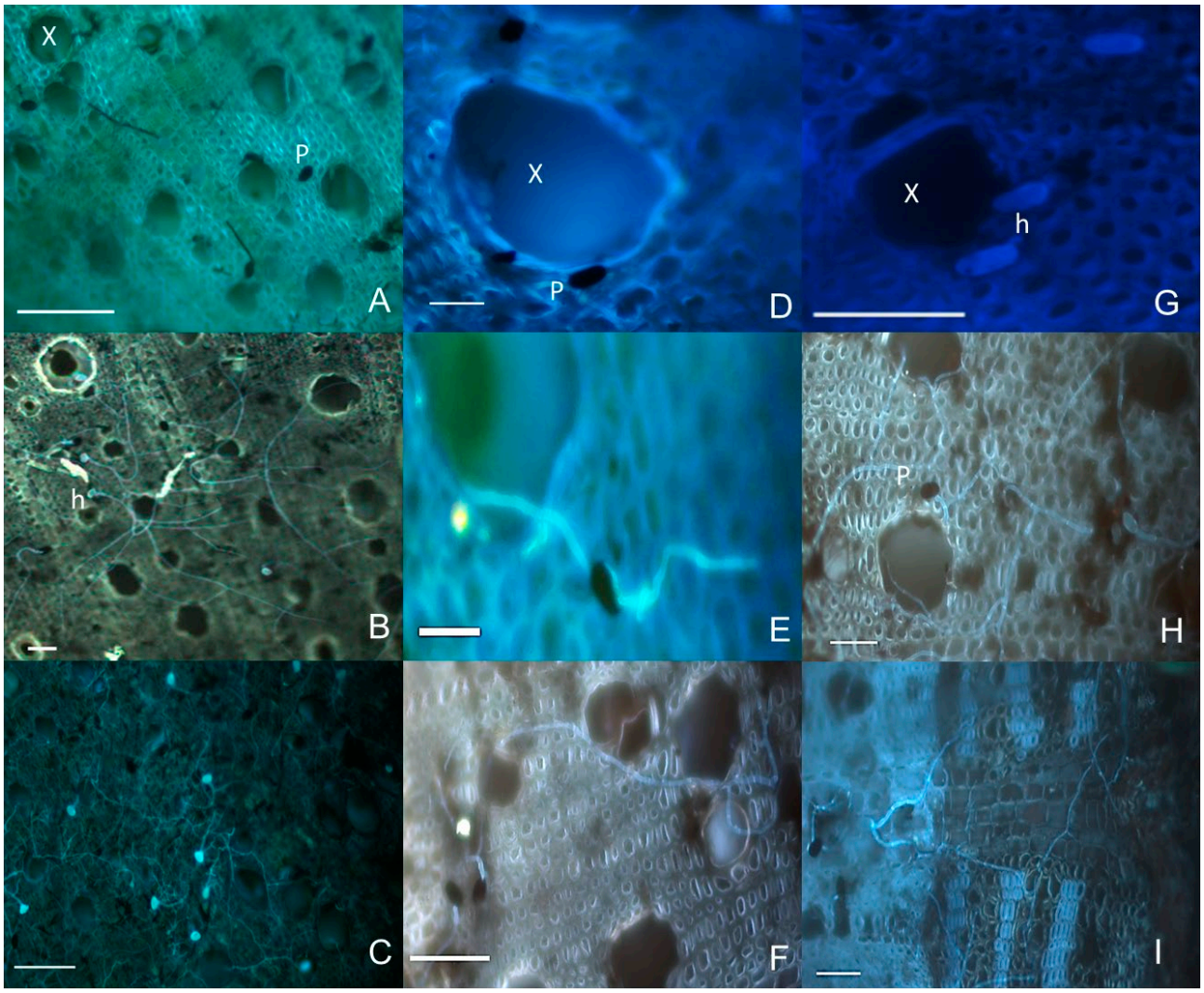

Figure 6. Transverse sections of grapevine stems inoculated with pycnidiospores of *Lasiodiplodia gilanensis* (A, B and C), *Diplodia seriata* (D, E, and F) or *D. corticola* (G, H and I), observed under epifluorescence microscopy at 12 h (A, D and G), 24 h (B, E and H) or 48 h (C, F and I) after inoculation with these fungi. Greater hyphal branching and colonization was observed in stems inoculated with *L. gilanensis.* X) xylem vessel; h) hyaline pycnidiospores; p) pigmented pycnidiospores. Bars = 50 µm.

D. seriata grew in and out of the xylem vessels, and in some cases, hyphae and conidia were distorted (Figures 7C and 7D).

In contrast, fewer pycnidiospores of *D. corticola* germinated and showed few ramifications and septa at 24 h (Figures 6H). As in the other species, hyphae came out from the central parts of the spores and entered the host xylem vessels, tracheids, and phloem, with the xylem vessels being the most common site of entry (Figures 6H, 7E, 7F). In pycnidiospores close or inside the xylem vessels, several mycelium branches were observed (Figures 7E and 7F).

At 48 h after inoculation for the grapevines inoculated with *L. gilaniensis,* extensive mycelium growth was observed invading the host wood, as highly branched hyphae of different diameters. These entered through xylem vessels, tracheids, and phloem (Figure 6C). In longitudinal stem sections, the fungus colonized the xylem vessels, degrading and thickening the cell walls of the pits, and moved to the adjacent tissue (Figures 8A, 8B). More hyphae were observed entering the xylem vessels and tracheids than the phloem tissues. In transverse stem sections, *L. gilaniensis* was growing on medullary and radial parenchymal tissues, but growth was mainly observed in the secondary xylem. In the xylem vessels, formation of tyloses was evident but without obvious tissue damage (Figures 9A, 9B).

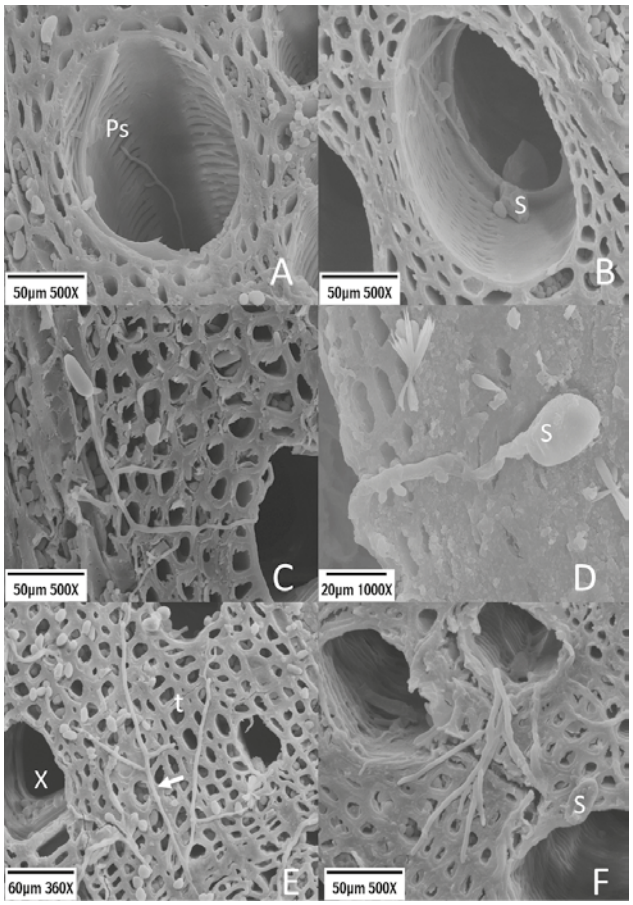

Figure 7. SEM of cross-sections of grapevine stems inoculated with spores of *Lasiodiplodia gilaniensis* (A and B), *Diplodia seriata* (C and D) or *D. corticola* (E and F), at 24 h after inoculation. A, hyphae entering the pits to colonize adjacent tissue. B, spores and hyphae growing in and out of a xylem vessel. C and D, hyphae entering the xylem vessels and tracheids. E, hyphae entering tracheids. F, germinated spore with hyphae entering and branching in and out of a xylem vessel. X) xylem vessel; t) tracheids; S) spore; Ps) pits.

The germinated spores of *D. seriata* also developed four to six branches, moving towards of the phloem and xylem vessels (Figures 6F, 9D). The formation of tyloses was also observed (Figure 9C). In longitudinal stem sections, *D. seriata* colonized the xylem vessels and the medullar and radial parenchymal tissues, without showing symptoms of degradation of the tissues but using the pits as anchorage sites and possibly for the colonization of the adjacent cells (Figure 8B).

Also at 48 h after inoculation with *D. corticola,* most pycnidiospores were germinated, and hyphae were entering the xylem vessels (Figure 6I). In longitudinal sections, hyphae were colonizing the xylem vessels; however, no degradation of the xylem walls or colonization of the adjacent tissues was observed (Figure 8C). Mycelium

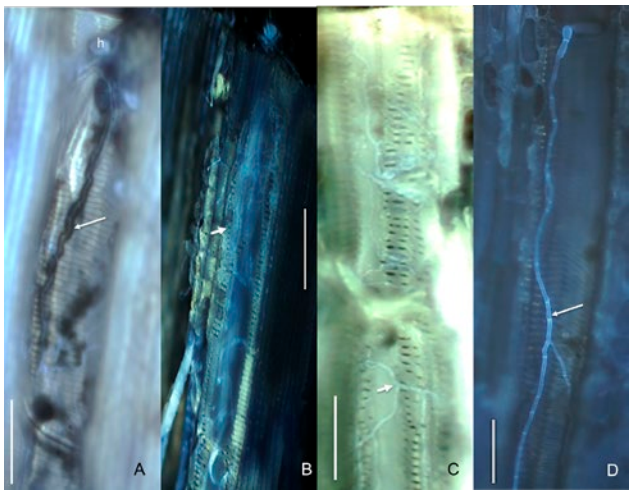

Figure 8. Longitudinal sections of grapevine stems inoculated with pycnidiospores of *Lasiodiplodia gilaniensis* (A and B), *Diplodia seriata* (C) or *D. corticola* (D), observed using epifluorescence microscopy 48 h after inoculation. In *L. gilaniensis*, degradation of the cell wall of a vessel (A) and colonization of the xylem vessels (B) were observed. C, Hyphal branches inside the trachea colonizing a vessel and using pits as anchorage sites. D, Hyphal branches growing along the trachea. X) xylem vessel; h) hyaline pycnidiospores, arrow) hypha. Bars = 50 µm.

was growing on medullary and radial parenchymal tissues of the vessels, and the hyphal branches were using the pits as anchoring sites, possibly for colonization of adjacent tissues (Figures 9E and 9F).

DISCUSSION

The initial state for the establishment of some fungi in host plants is germination of spores, and the substrate to which the spore attaches regulates germ tube directional growth, branching, and appressorium formation (Nicholson and Epstein, 1991). The purpose of the present investigation was to determine the influence of grapevine wood upon these infection stages in three Botryosphaeriaceae species.

Pathogen growth rates were affected by the presence of grapevine wood, especially in *D. seriata* and *D. corticola*. For *L. gilanensis,* this effect was less, possibly due to rapid growth, since the most rapid growth was observed in *L. gilanensis*, followed by *D. seriata*, which had medium growth, and *D. corticola* with the least. Pathogenicity tests in grapevine have shown that *Lasiodiplodia* spp. are highly virulent pathogens, causing pronounced tissue damage in comparison with other species of the Botryosphaeriaceae (Úrbez-Torres and Gubler, 2009; Candolfi-Arballo *et al.*, 2010). This obser-

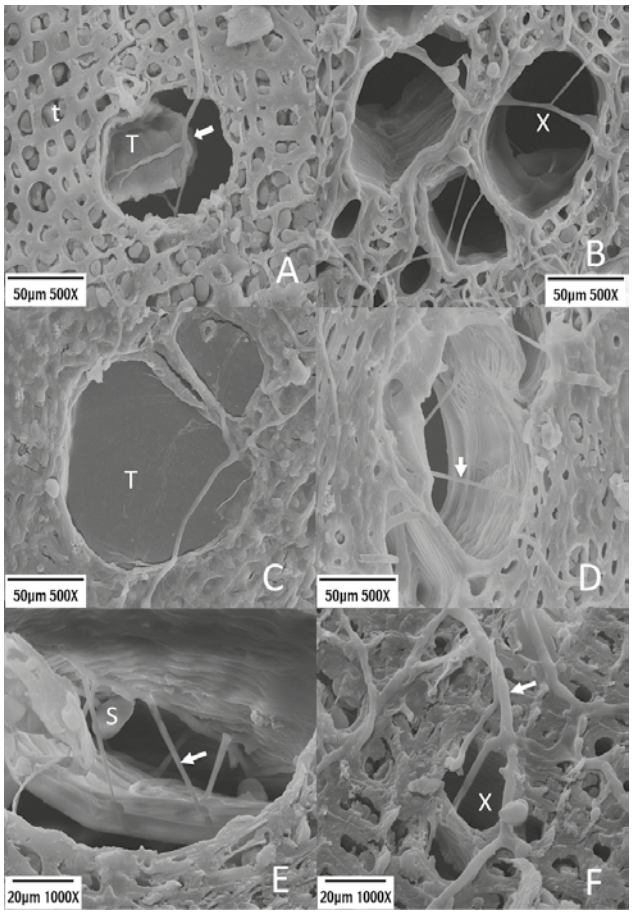

Figure 9. SEM cross-sections of grapevine stems inoculated with pycnidiospores of *Lasiodiplodia gilaniensis* (A and B), *Diplodia seriata* (C and D) or *D. corticola* (E and F), at 48 h after inoculation. A, tylosis formation in a xylem vessel, and hyphae entering the vessel. B, hyphae entering a xylem vessel. A large amount of mycelium is present. C, hyphal entrance blocked by a tylosis. D, hyphae entering xylem vessels, using pits as anchoring sites for colonization of the xylem vessel cell walls (arrow). E, pycnidiospore inside a trachea, colonizing a xylem vessel and using the pits as anchor sites. The cell wall is not damaged. D, hyphae entering a xylem vessel. Arrows indicate hyphae. X) xylem vessel; T) tyloses; t) tracheids; S) pycnidiospore.

vation is similar to that for the present study, where *L. gilaniensis* had more rapid growth on grapevine stems that the two *Diplodia* spp. This rapid growth is likely to assist rapid colonization of grapevine by *L. gilaniensis*.

The presence of wood also increased the germination of spores, especially in pigmented pycnidiospores of *L. gilanensis*, which had the highest percentage of germination in the shortest time. Differently, in previous work, hyaline spores of *L. theobromae* had a higher percentage of germination than pigmented spores, and a faster germination rate in PDA, a nutritionally rich media (Úrbez-Torres *et al*., 2010). Here, minimal media was used; thus, the observed differences probably are due to the isolate and the composition of the culture medium (Arauz and Sutton, 1989).

Pycnidiospores germinated more rapidly in culture media compared with *in planta*. *In vitro,* after a period of 12 h in the presence of grinded grapevine wood, up to 80% of the spores of the three species had germinated. Similarly, up to 90% of spores of *B. dothidea* germinated at 4 h in PDA at 25°C (Úrbez-Torres *et al*., 2010); while in apple after 9 h at 25°C these spores had not completely germinated (Kim *et al.,* 1999). Since autoclaving wood increases soluble sugars (Hulme and Shields, 1970), the media supplemented with grapevine wood probably enhanced spore germination, while *in planta*, the lack of appropriate conditions for germination, such as temperature, water availability and the presence of nutrients transferred from the host into the water, may have slowed the spore germination (Barkai-Golan, 2001).

Formation of appressoria in Botryosphaeriaceae has been previously observed only in *B. dothidea* growing in apple fruit (Kim *et al*., 1999). Similarly, none of the three pathogens studied here formed appressoria. Instead, after germination, the hyphae entered the closest traqueid or xylem vessels.

Greater biomass was produced in the three fungal species in the presence of grapevine wood than without, especially in *L. gilanensis*. Also in this fungus, when growing *in planta,* hyphae were surrounded by dark haloes, and the invasion of parenchyma cells was observed. Since calcofluor binds to chitin and cellulose (Harrington and Hageage, 2003), the halo indicates the production of cellulases and the degradation of cell walls of xylem vessels. For the isolate of *L. gilanensis* used here (formerly named *L. theobromae*), several plant cell wall-degrading enzymes involved in cellulose and hemicellulose degradation have been found to be up-regulated in response to grapevine wood (Paolinelli-Alfonso *et al*., 2016). This fungus may therefore be using the cell wall components for growth from the beginning of the fungus-plant interaction. In contrast, tissue degradation was not observed in *D. seriata* or *D. corticola*. This supports the likelihood that both these species can penetrate and survive in plants without causing damage, while having the capacity to become pathogens. However, both of these *Diplodia* spp. are less pathogenic to grapevine than *L. theobromae* (Taylor *et al*., 2005; Candolfi-Arballo *et al*., 2010; Úrbez-Torres, 2011).

There was a marked tendency for the three species to use xylem vessels as a preferential site of entry to grapevine stems, with tracheids as a secondary entrance point, and phloem very rarely. These observations are consistent with those for other members of Botryosphaeriaceae,

such as *Neofusicoccum australe*, *N. luteum*, *N. parvum,* and *D. mutila* infecting grapevine (Amponsah *et al*., 2012); *L. theobromae* infecting *Pinus caribaea* (Cedeño *et al*., 1996), *Populus tremula*, *Hevea brasiliensis* (Encinas and Daniel, 1997) and *Anacardium occidentale* (Muniz *et al*., 2011); and for *Diplodia seriata* and *B. dothidea* in *Prunus persica* (Biggs and Britton, 1988).

SEM observations confirmed the tracheae (vessel elements) were a preferred site for grapevine wood colonization in all three pathogen species evaluated. The three Botryosphaeriaceae interacted differently with parenchyma tissue, where degradation and invasion were detected during *L. gilanensis* colonization, while no colonization by *D. seriata* and *D. corticola* was observed. This agrees with the behaviour of *D. seriata* observed in peach, where xylem vessel colonization occurred 7 d after inoculation, while the colonization of parenchymal tissue occurred after 28 d (Biggs and Britton,1988). The present study also confirmed that *L. gilaniensis* rapidly colonizes grapevine tissues.

The formation of tyloses in response to the colonization by the three fungi agrees with observations of *L. theobromae* (Al-Saadoon, 2012). SEM also indicated the ability of *L. gilaniensis* to use the xylem pits to colonize adjacent tissues, but this was not observed in *D. seriata* or *D. corticola*. The same behaviour was reported for *Neofusicoccum luteum* which is another highly virulent pathogen of grapevine, and colonizes cashew (Muniz *et al*., 2011), and grapevine (Amposah *et al*., 2012; (Úrbez-Torres, 2011). The ability of these species to use xylem pits may confer ability to efficiently colonize hosts and increase virulence.

This is the first study to compare effects of grapevine wood on germination kinetics and colonization of three botryosphaeriaceous fungi, indicating that their behaviour *in planta* correlates with their relative levels of pathogenicity.

ACKNOWLEDGEMENTS

José Abraham Obrador-Sánchez received a masters scholarship from CONACYT (No. 231117). The authors thank Douglas Gubler (UCDavis), Jorge Cáceres, Yanet Guerrero and Luis Carlos Gradilla (CICESE) for helping with isolates, protocols or equipment, and Arturo Estolano Cobian for critical review of the manuscript of this paper.

LITERATURE CITED

Al-Saadoon A.H., 2012. Histopathology of grapevine inoculated with *Lasiodiplodia theobromae*. *Basrah Journal of Agricultural Sciences* 25: 1–12.

Amponsah N.T., Jones E.E., Ridgway H.J., Jaspers M.V., 2012. Microscopy of some interactions between Botryosphaeriaceae species and grapevine tissues. *Australasian Plant Pathology* 41: 665–673.

Arauz L.F., Sutton T.B., 1989. Influence of temperature and moisture on germination of ascospores and conidia of *Botryosphaeria obtusa*. *Phytopathology* 79: 667–674.

Barkai-Golan R., 2001. *Postharvest Diseases of Fruits and Vegetables: Development and Control*. 1st ed. Elsevier, Amsterdam, NL, 442 pp.

Bertsch C., Ramírez-Suero M., Magnin-Robert M., Larignon P., Chong J., … Fontaine F., 2013. Grapevine trunk diseases: complex and still poorly understood. *Plant Pathology* 62: 243–265.

Biggs A.R., Britton K.O., 1988. Presymptom histopathology of peach trees inoculated with *Botryosphaeria obtusa* and *B. dothidea*. *Phytopathology* 78: 1109–1118.

Billones-Baaijens R., Jaspers M., Allard A., Hong Y., Ridgway H., Jones E., 2015. Management of Botryosphaeriaceae species infection in grapevine propagation materials. *Phytopathologia Mediterranea* 54: 355–367.

Burgess T.I., Barber P.A., Mohali S., Pegg G., De Beer W., Wingfield M.J., 2006. Three new *Lasiodiplodia* spp. from the tropics, recognized based on DNA sequence comparisons and morphology. *Mycologia* 98: 423–435.

Burgess T.I., Wingfield M.J., 2002. Quarantine is important in restricting the spread of exotic seed-borne tree pathogens in the southern hemisphere. *International Foresty Review* 4: 56–65.

Candolfi-Arballo O., Valenzuela-Solano C., Gubler W.D., Hernández-Martínez R., 2010. Botryosphaeriaceae species associated with grapevine decline in Mexico. *Phytopathologia Mediterranea* 49: 105–106.

Cedeño L., Mohali S., Palacios-Prü E., 1996. Ultrastructure of *Lasiodiplodia theobromae* causal agent of caribbean pine blue stain in Venezuela. *Interciencia* 21: 264–271.

Denman S., Crous P.W., Taylor J.E., Kang J.C., Pascoe I., Wingfield M.J., 2000. An overview of the taxonomic history of Botryosphaeria, and a re-evaluation of its anamorphs based on morphology and ITS rDNA phylogeny. *Studies in Mycology* 45: 129–140.

Encinas O., Daniel G., 1997. Degradation of the gelatinous layer in aspen and rubberwood by the blue stain fungus *Lasiodiplodia theobromae*. *IAWA Journal* 18: 107–115.

Epstein L., Sukhwinder K.S., Vandergheynst J., 2008. Botryosphaeria-related dieback and control investigated in noncoastal California grapevines. *California Agriculture* 62: 161–166.

Félix C., Pinto G., Amaral J., Fernandes I., Alves A., Esteves A.C., 2017. Strain-related pathogenicity in *Diplodia corticola*. *Forest Pathology* 47: e12366.

Fontaine F., Pinto C., Vallet J., Clément C., Gomes A.C., Spagnolo A., 2016. The effects of grapevine trunk diseases (GTDs) on vine physiology. *European Journal of Plant Pathology* 144: 707–721.

Gramaje D., Úrbez-Torres J.R., Sosnowski M.R., 2018. Managing grapevine trunk diseases with respect to etiology and epidemiology: current strategies and future prospects. *Plant Disease* 102: 12–39.

Guan Y., Chang R., Liu G., Wang Y., Wu T., … Zhang X., 2015. Role of lenticels and microcracks on susceptibility of apple fruit to *Botryosphaeria dothidea*. *European Journal of Plant Pathology* 143: 317–330.

Gubler W. D., Rolshausen P.E., Trouillase F.P., Urbez J. R., Voegel, T., 2005. Grapevine trunk diseases in California. *Practical Winery and Vineyard* 1-9.

Harrington B.J., Hageage J.G. Jr. 2003. Calcofluor white: a review of its uses and applications in clinical mycology and parasitology. *Laboratory medicine* 34: 361–367.

Hill T., Lewicki P., 2012. *(Electronic Version): StatSoft, Inc.* Available at: http://www.statsoft.com/textbook/. Tulsa, OK: StatSoft.

Hulme M.A., Shields J.K., 1970. Biological control of decay fungi in wood by competition for non-structural carbohydrates. *Nature* 227: 300–301.

Kim K.W., Park E.W., Ahn K.K., 1999. Pre-penetration behavior of *Botryosphaeria dothidea* on apple fruits. *The Plant Pathology Journal* 15: 223–227.

Mohali S., Burgess T.I., Wingfield M.J., 2005. Diversity and host association of the tropical tree endophyte *Lasiodiplodia theobromae* revealed using simple sequence repeat markers. *Forest Pathology* 35: 385–396.

Mondello V., Songy A., Battiston E., Pinto C., Coppin C., Trotel-Aziz, P., … Fontaine F., 2018. Grapevine trunk diseases: a review of fifteen years of trials for their control with chemicals and biocontrol agents. *Plant Disease* 102: 1189–1217.

Muniz C.R., Freire F.C.O., Viana F.M.P., Cardoso J.E., Cooke P., … Guedes M.I., 2011. Colonization of cashew plants by *Lasiodiplodia theobromae*: Microscopical features. *Micron* 42: 419–428.

Nicholson R.L., Epstein L., 1991. Adhesion of fungi to the plant surface: prerequisite for pathogenesis. In: *The Fungal Spore and Disease Initiation in Plants and Animals* (G.T. Cole, H.C. Hoch, ed). Plenum Press, NY, USA, 3–23.

Paolinelli-Alfonso M., Villalobos-Escobedo J.M., Rolshausen P., Herrera-Estrella A., Galindo-Sánchez C., … Hernandez-Martinez, R. (2016). Global transcriptional analysis suggests *Lasiodiplodia theobromae* pathogenicity factors involved in modulation of grapevine defensive response. *BMC Genomics* 17: 615.

Phillips A.J., Crous, P.W., Alves A., 2007. *Diplodia seriata*, the anamorph of "*Botryosphaeria*" *obtusa*. *Fungal Diversity* 25: 141–155.

Phillips A., 2002. Botryosphaeria species associated with diseases of grapevines in Portugal. *Phytopathologia Mediterranea* 41: 3–18.

Siebert J.B., 2001. *Eutypa*: the economic toll on vineyards. *Wines & Vines* 50: 56.

Smith H., Kemp G. H.J., Wingfield M.J., 1994. Canker and die-back of *Eucalyptus* in South Africa caused by *Botryosphaeria dothidea*. *Plant Pathology* 43: 1031–1034.

Taylor A., Hardy G.S.J., Wood P., Burgess T. 2005. Identification and pathogenicity of Botryosphaeria species associated with grapevine decline in Western Australia. *Australasian Plant Pathology* 34(2): 187–195.

Úrbez-Torres J.R., 2011. The status of Botriosphaeriaceae species infecting grapevines. *Phytopathologia Mediterranea* 50: S5-S45.

Úrbez-Torres J.R., Gubler W.D., 2009. Pathogenicity of Botryosphaeriaceae species isolated from grapevine cankers in California. *Plant Disease* 93: 584–592.

Úrbez-Torres J.R., Leavitt G.M., Guerrero J.C., Guevara J., Gubler W.D., 2008. Identification and pathogenicity of *Lasiodiplodia theobromae* and *Diplodia seriata*, the causal agents of bot canker disease of grapevines in Mexico. *Plant Disease* 92: 519–529.

Úrbez-Torres J.R., Leavitt G.M., Voegel T.M., Gubler W.D., 2006. Identification and distribution of Botryosphaeria spp. associated with grapevine cankers in California. *Plant Disea*se 90: 1490–1503.

Úrbez-Torrez J.R., Bruez E., Hurtado J., Gubler W.D., 2010. Effect of temperature on conidial germination of Botryosphaeriaceae species infecting grapevines. *Plant Disease* 94: 1476–1484.

Valtaud C., Larignon P., Roblin G., Fleurat-Lessard P., 2009. Developmental and ultrastructural features of *Phaeomoniella chlamydospora* and *Phaeoacremonium aleophilum* in relation to xylem degradation in esca disease of the grapevine. *Journal of Plant Pathology* 91: 37–51.

Varela C.P., Fernández V.R., Casal O.A., Vázquez J.M., 2011. First report of cankers and dieback caused by *Neofusicoccum mediterraneum* and *Diplodia corticola* on grapevine in Spain. *Plant Disease* 95: 1315.

Yang T., Groenewald J.Z., Cheewangkoon R., Jami F., Abdollahzadeh J., … Crous P.C., 2017. Families, genera, and species of Botryosphaeriales. *Fungal Biology* 121: 322–346.

Phytopathologia Mediterranea
The international journal of the
Mediterranean Phytopathological Union

Firenze University Press
www.fupress.com/pm

Research Paper

Alternaria brown spot on new clones of sweet orange and lemon in Italy

Dalia AIELLO[1,*], Vladimiro GUARNACCIA[2,3], Antonino AZZARO[1], Giancarlo POLIZZI[1]

[1] *Dipartimento di Agricoltura, Alimentazione e Ambiente, sez. Patologia vegetale, University of Catania, Via S. Sofia 100, 95123 Catania, Italy*
[2] *DiSAFA, University of Torino, Largo Paolo Braccini, 2, 10095 Grugliasco, TO, Italy*
[3] *Centre for Innovation in the Agro-Environmental Sector, AGROINNOVA, University of Torino, Largo Braccini 2, 10095 Grugliasco (TO), Italy*
*Corresponding author: dalia.aiello@unict.it

Summary. Since 2013 an Alternaria disease has been observed in Italy on new clones of sweet orange and lemon, during pre-harvest stages. Isolations were made from diseased leaves and fruit collected from these hosts and from other known *Alternaria* hosts (*Citrus* x *clementina*, *Citrus reticulata* 'Mandalate' and *Citrus sinensis* 'Valencia'). The typical small-conidium *Alternaria* species was consistently isolated from symptomatic tissues. One hundred and sixty-two *Alternaria* isolates were recovered from 15 citrus orchards in Catania, Syracuse and Palermo provinces, and 148 of these were used for multigene phylogenetic analyses based on the glyceraldehyde-3-phosphate dehydrogenase (*GAPDH*) and translation elongation factor 1-α (*EF-1α*) genes. Most of the characterized isolates (97.3%) belonged to the *A. alternata* clade, and the remainder were *A. arborescens*. Pathogenicity tests of 49 isolates of *A. alternata* and one of *A. arborescens* were performed on young detached leaves and on detached immature fruit of orange, lemon, calamondin, and rangpur lime. Toxicity of culture filtrates of representative isolates on detached leaves was also evaluated. In addition, pathogenicity tests were carried out on immature fruit *in planta* under controlled environment conditions. Most of the isolates (72%, including *A. alternata* and *A. arborescens*) were pathogenic on all inoculated citrus species and caused brown spot symptoms identical to those induced on tangerine. This study demonstrates the ability of *A. alternata* to cause damage in the field on new and popular clones of sweet orange and lemon. The hypothesis is supported that secondary metabolites, in addition to the ACT-toxin or ACR-toxin, could play roles in *Alternaria* spp. pathogenicity to citrus hosts.

Keywords. Multigene analysis, pathogenicity, disease symptoms.

OPEN ACCESS

Citation: D. Aiello, V. Guarnaccia, A. Azzaro, G. Polizzi (2020) Alternaria brown spot on new clones of sweet orange and lemon in Italy. *Phytopathologia Mediterranea* 59(1): 131-145. doi: 10.14601/Phyto-10769

Accepted: February 13, 2020

Published: April 30, 2020

Data Availability Statement: All relevant data are within the paper and its Supporting Information files.

Competing Interests: The Author(s) declare(s) no conflict of interest.

Editor: Juan A. Navas-Cortes, Spanish National Research Council (CSIC), Cordoba, Spain.

INTRODUCTION

Alternaria species cause four diseases of citrus, including Alternaria brown spot of tangerine (*Citrus reticulata* Blanco) and their hybrids, Alternaria leaf spot of rough lemon (*C. jambhiri* Lush.) and rangpur lime (*C. limonia* Osbeck), Alternaria black rot of many citrus cultivars, and Mancha

foliar of Mexican lime (*C. aurantifolia* Swingle) (Timmer *et al*., 2003; Peever *et al*., 2004). Black rot of citrus is considered distinct from Alternaria brown spot, and is a significant postharvest disease that may appear in the field prior to harvest on navel oranges (*Citrus sinensis* L. Osbeck) and in storage on lemons, tangerines and their hybrids (Peever *et al*., 2004, 2005). Brown spot is caused by *Alternaria alternata* in all citrus producing countries. The pathogen attacks young leaves, twigs and fruit causing brown to black lesions surrounded by yellow haloes. Under appropriate environmental conditions, severe infections may cause leaf and fruit drop and significant losses of yield and marketable fruit (Peever *et al*., 2002; Akimitsu *et al*., 2003; Timmer *et al*., 2003). Alternaria brown spot is a serious disease in humid areas, and highly susceptible cultivars cannot be grown in some regions. In semiarid areas this disease can also be a significant problem (Akitimitsu *et al*., 2003).

Two distinct pathotypes of *A. alternata* associated with citrus species have been described based on differences in host specificity and toxin production (Kohmoto *et al*., 1993; Peever *et al*., 1999; Ohtani *et al*., 2009). The tangerine pathotype is specific to tangerines, tangelos (*C. reticulata* × *C. paradisi*), tangors (*C. reticulata* × *C. sinensis*) and hybrids, and produces a host-selective ACT-toxin. The rough lemon pathotype is specific to this host and rangpur lime, and produces a host specific ACR-toxin. On some citrus species the disease was reproduced only by artificial inoculation or by the toxin assay (Kohmoto *et al*., 1979; Solel and Kimchi, 1997; Elena, 2006).

Despite the well-known role of ACTs as pathogenicity factors, Garganese *et al*. (2016) have shown the ability of 20 selected isolates collected in Spain and Italy to cause brown spot of tangerine on freshly detached citrus fruit and leaves (*C. reticulata* cv. Fortune) in the absence of ACTT1/ACTT2 expression.

During a survey conducted in December 2013 in an orchard located in Catania province (Sicily, southern Italy), symptoms resembling Alternaria brown spot were detected on sweet orange clone 'Tarocco Sciara' and lemon (*Citrus* × *limon* (L.) Burm. f.) clone 'Femminello Siracusano 2KR'. Severe brown spot symptoms were observed on leaves and fruit, similar to those caused by *A. alternata* (Polizzi and Azzaro, 2015). During the period from 2014 to 2019 the disease was much more widespread and was observed in different orchards in Catania, Syracuse and Palermo provinces. The symptoms were observed in the spring and summer on different cultivars and clones of sweet orange, lemon, bitter orange, mandarin, clementine, mandalate and 'Carrizo' citrange trees. Small brown necrotic leaf spots of various sizes appeared on leaves, with sometimes extension of necrosis into the leaf veins. Lesions were often surrounded by yellow halos. On immature fruit, slightly depressed brown to black lesions surrounded by yellow halo areas were the first symptoms. Summer infections in many cases caused leaf drop and considerable yield losses (up to 40%). Sometimes, the typical anthracnose symptoms on leaves and fruit associated with brown spot were also observed (Aiello *et al*., 2015; Piccirillo *et al*., 2018). Premature colouration and development of light brown to blackish discolouration of the rind at or near the stylar end of fruit were also observed.

After the discovery of severe symptoms on citrus species in orchards, the research reported here aimed to: i) determine the identity of the pathogens causing the infections; ii) evaluate pathogenicity of these organisms on different citrus hosts; and iii) determine the toxicity of culture filtrates from selected pathogen isolates.

MATERIALS AND METHODS

Fungus isolates

During surveys conducted from 2014 to 2019, infected leaves and fruit were collected from different citrus species with Alternaria disease symptoms (Figure 1).

Isolations were performed by disinfesting at least 1,200 fragments of symptomatic tissues (each approx. 5 mm^2) with 1% NaOCl for 1 min, rinsed in sterile distilled water (SDW), then placed on potato dextrose agar (PDA, Oxoid) amended with streptomycin sulphate (Sigma) at 100 mg/L, and then incubated at 25±1°C in the dark. After 7 d, single conidia were selected from resulting colonies and transferred into PDA plates. For long-term storage, each plate was covered with six pieces of sterilized filter paper (1 cm^2), which was then inoculated and incubated for 7 d in the dark. Colonized filter paper was gently removed and placed into sterile envelopes, which were dried overnight in a laminar flow hood (Peever *et al*., 2002). All envelopes were stored at -20°C.

DNA extraction, amplification and sequencing

Fungus isolates were grown on malt extract agar (MEA) for 7 d at room temperature (20°C). Resulting mycelium of each isolate was harvested with a sterile scalpel, and the genomic DNA was extracted using the Wizard® Genomic DNA Purification Kit (Promega Corporation), according to the manufacturer's protocol. The internal transcribed spacer of ribosomal DNA (rDNA-ITS) region was targeted for PCR amplification and sequencing. Two genomic regions, translation elongation

factor 1-α (*EF-1α*) and glyceraldehyde-3-phosphate dehydrogenase (*GAPDH*), were selected due to their highly informative combined to distinguish *A. alternata* from all the other *Alternaria* species of the section *Alternaria* (Woudenberg *et al*., 2015). The primers used for these regions were: ITS5 and ITS4 for ITS (White *et al*., 1990), EF1-728F and EF1-986R for *EF-1α* (Carbone and Kohn, 1999) and GPD1 and GPD2 for *GAPDH*. The PCR amplifications were performed on a GeneAmp PCR System 9700 (Applied Biosystems). The PCR mixtures for ITS, *GAPDH* and *EF-1α* contained 1 µL of genomic DNA, 2 µM $MgCl_2$, 40 µM of each dNTP, 0.2 µM of each primer and 0.5 Unit GoTaq® Flexi DNA polymerase (Promega), in a total volume of 12.5 µL. The PCR conditions were: initial denaturation at 94°C for 5 min; 35 cycles amplification at 94°C for 30 s; annealing at 48°C (ITS) or 52°C (*EF-1α*) for 50 sec, and extension at 72°C for 2 min; and a final extension at 72°C for 7 min. Following PCR amplification, the amplicons were visualized on a 1% agarose gel stained with GelRed™ (Biotium) and viewed under ultra-violet light. The sizes of resulting amplicons were determined against a HyperLadder 1 kb molecular marker (Bioline). The amplicons were sequenced in both directions using the same primers used for amplification and a BigDye® Terminator Cycle Sequencing Kit v. 3.1 (Applied Biosystems Life Technologies), following the protocol provided by the manufacturer. DNA sequencing amplicons were purified through Sephadex G-50 Superfine columns (Sigma Aldrich) in 96-well MultiScreen HV plates (Millipore). Purified sequence reactions were analysed on an Applied Biosystems 3730 × l DNA Analyzer (Life Technologies). The DNA sequences generated were analysed and consensus sequences were determined using Seqman (DNA Star Inc.). All sequences were manually corrected, and arrangement of nucleotides in ambiguous positions was corrected using comparisons of the sequences generated from both the forward and reverse primers. Novel sequences were lodged in GenBank (Table 1). The sequences of *EF-1α* and *GAPDH* genes of 148 *Alternaria* isolates from citrus in Sicily and 25 representative strains of *Alternaria* sect. *Alternaria* (Wounderberg *et al*., 2015) obtained from GenBank (http://www.ncbi.nlm.nih.gov) were subsequently aligned using the Muscle algorithm in MEGA V.6 (Tamura *et al*., 2013). Phylogenetic analyses were performed in MEGA V.6 using both Neighbour-Joining (NJ) (Saitou and Nei, 1987) and Maximum Likelihood (ML). The phylogenetic trees were calculated, first singularly for each locus to verify the genealogical concordance phylogenetic species recognition (GCPSR), and subsequently in a concatenated tree. For the phylogenetic analysis, the evolutionary history was inferred by using the Maximum Likelihood method based on the Tamura 3-parameter model (Tamura, 1992). An initial tree(s) for the heuristic search was obtained automatically by applying Neighbor-Join and BioNJ algorithms to a matrix of pairwise distances estimated using the Maximum Composite Likelihood (MCL) approach, and selecting the topology with the superior log likelihood value. A discrete Gamma distribution was used to model evolutionary rate differences among sites [five categories (+G, parameter =0.1625)]. All positions containing gaps and missing data were eliminated.

Pathogenicity test on detached leaves

To evaluate the pathogenicity of *Alternaria* isolates on citrus species, 50 isolates collected in this study were selected and inoculated on detached 10- to 15-day-old leaves. The plants used for tests were grown under controlled environment conditions in a growth chamber, and included calamondin, rangpur lime, sweet orange ('Moro', 'Valencia', 'Tarocco Nucellare', 'Tarocco Sciara') and lemon ('Femminello Siracusano 2KR'). Calamondin is susceptible to the tangerine pathotype of *A. alternata* but resistant to the rough lemon pathotype, and rangpur lime is sensitive to the rough lemon pathotype but not to the tangerine pathotype (Kohmoto *et al*., 1991; 1993; Timmer *et al*., 2003; Ohtani *et al*., 2009). One isolate of profile I and one of profile II of tangerine pathotype of *A. alternata* (Vega and Dewdney, 2014) were also included.

Each isolate was grown on V8 agar in Petri plates to induce the production of conidia (Vega *et al*., 2012). After 7–10 d, conidium suspensions from each isolate were prepared by adding SDW to the plates and gently rubbing the mycelia with a sterile loop and filtering the suspension through a triple layer of cheesecloth. Conidium suspensions (1×10^5 conidia mL^{-1}, adjusted using a microscope slide haemocytometer) were each sprayed on the adaxial side of three leaves of each citrus species. SDW was sprayed on young leaves as negative controls. Inoculated leaves were placed on sterile aluminium trays, placed into plastic bags covered with plastic film, and then incubated at 25±1°C in the dark. After 48-72 h, development of necrotic spots on the leaves was evaluated. If at least two of the three leaves showed these symptoms, the pathogenicity reaction was considered positive (Table 2). The experiment was conducted twice.

Pathogenicity test on detached fruit

The pathogenicity of eight representative isolates (AA2, AA19, AA22, AA27, AA37, AA66, AA144 and AA145), from different groups determined with patho-

Table 1. Isolates from citrus used in this study, and their GenBank accession numbers.

Strain number[1]	Host, cultivar, clone	Symptom	Location	GenBank accession number[2]		
				ITS	*GAPDH*	*EF-1α*
AA 1	*Citrus reticulata* 'Nova'	Leaf spot	Italy (Sicily, Catania province)	KX056429	KX019989	KX064063
AA 2	*Citrus reticulata* 'Nova'	Leaf spot	Italy (Sicily, Catania province)	KX056422	KX020143	KX064201
AA 3	*Citrus reticulata* 'Nova'	Leaf spot	Italy (Sicily, Catania province)	KX056423	KX020002	KX064064
AA 4	*Citrus reticulata* 'Nova'	Leaf spot	Italy (Sicily, Catania province)	KX056424	KX019990	-
AA 5	*Citrus reticulata* 'Nova'	Leaf spot	Italy (Sicily, Catania province)	KX056421	KX020134	KX064065
AA 6	*Citrus reticulata* 'Nova'	Leaf spot	Italy (Sicily, Catania province)	KX056318	KX020144	KX064202
AA 7	*Citrus reticulata* 'Nova'	Leaf spot	Italy (Sicily, Catania province)	KX056340	KX020065	KX064066
AA 8	*Citrus reticulata* 'Nova'	Leaf spot	Italy (Sicily, Catania province)	KX056408	KX019991	KX064067
AA 9	*Citrus reticulata* 'Nova'	Leaf spot	Italy (Sicily, Catania province)	KX056319	KX019992	KX064068
AA 10	*Citrus reticulata* 'Nova'	Leaf spot	Italy (Sicily, Catania province)	KX056404	KX020145	KX064203
AA 11	*Citrus reticulata* 'Nova'	Leaf spot	Italy (Sicily, Catania province)	KX056405	KX020006	KX064069
AA 12	*Citrus reticulata* 'Nova'	Leaf spot	Italy (Sicily, Catania province)	KX056320	KX019993	KX064070
AA 13	*Citrus reticulata* 'Nova'	Leaf spot	Italy (Sicily, Catania province)	KX056403	KX020007	KX064071
AA 14	*Citrus sinensis* 'Tarocco Sciara'	Fruit spot	Italy (Sicily, Catania province)	KX056321	KX020008	KX064072
AA 15	*Citrus reticulata* 'Nova'	Leaf spot	Italy (Sicily, Catania province)	KX056402	KX020110	KX064073
AA 16	*Citrus sinensis* 'Tarocco Sciara'	Leaf spot	Italy (Sicily, Catania province)	KX056322	KX020124	KX064074
AA 17	*Citrus sinensis* 'Tarocco Sciara'	Leaf spot	Italy (Sicily, Catania province)	KX056401	KX019994	KX064075
AA 18	*Citrus sinensis* 'Tarocco Sciara'	Leaf spot	Italy (Sicily, Catania province)	KX056323	KX020009	KX064076
AA 19	*Citrus sinensis* 'Tarocco Sciara'	Fruit spot	Italy (Sicily, Catania province)	KX056400	KX020111	KX064213
AA 20	*Citrus sinensis* 'Tarocco Sciara'	Fruit spot	Italy (Sicily, Catania province)	KX056324	KX020120	KX064204
AA 22	*Citrus sinensis* 'Tarocco Sciara'	Fruit spot	Italy (Sicily, Catania province)	KX056399	KX020044	KX064205
AA 23	*Citrus sinensis* 'Tarocco Sciara'	Fruit spot	Italy (Sicily, Catania province)	KX056325	KX020112	KX064077
AA 24	*Citrus sinensis* 'Tarocco Nucellare'	Fruit spot	Italy (Sicily, Catania province)	KX056398	KX020010	KX064078
AA 25	*Citrus sinensis* 'Tarocco Sciara'	Fruit spot	Italy (Sicily, Catania province)	KX056326	KX020051	KX064079
AA 26	*Citrus sinensis* 'Tarocco Sciara'	Fruit spot	Italy (Sicily, Catania province)	KX056397	KX020102	KX064080
AA 27	*Citrus sinensis* 'Navelina'	Fruit spot	Italy (Sicily, Catania province)	KX056327	KX020129	KX064081
AA 28	*Citrus sinensis* 'Tarocco Sciara'	Fruit spot	Italy (Sicily, Catania province)	KX056396	KX020103	KX064206
AA 30	*Citrus sinensis* 'Tarocco Sciara'	Fruit spot	Italy (Sicily, Catania province)	KX056328	KX020011	KX064082
AA 31	*Citrus sinensis* 'Tarocco Sciara'	Fruit spot	Italy (Sicily, Catania province)	KX056395	KX020041	KX064083
AA 32	*Citrus sinensis* 'Tarocco Sciara'	Fruit spot	Italy (Sicily, Catania province)	KX056329	KX020052	KX064084
AA 33	*Citrus sinensis* 'Tarocco Sciara'	Fruit spot	Italy (Sicily, Catania province)	KX056434	KX020088	KX064085
AA 34	*Citrus sinensis* 'Tarocco Sciara'	Fruit spot	Italy (Sicily, Catania province)	KX056394	KX020012	KX064086
AA 35	*Citrus sinensis* 'Tarocco Sciara'	Fruit spot	Italy (Sicily, Catania province)	KX056330	KX019995	KX064214
AA 36	*Citrus sinensis* 'Tarocco Nucellare'	Fruit spot	Italy (Sicily, Catania province)	KX056341	KX020074	KX064087
AA 37	*Citrus sinensis* 'Tarocco Nucellare'	Fruit spot	Italy (Sicily, Catania province)	KX056342	KX020118	KX064088
AA 38	*Citrus sinensis* 'Tarocco Nucellare'	Fruit spot	Italy (Sicily, Catania province)	KX056393	KX019996	KX064089
AA 39	*Citrus sinensis* 'Tarocco Nucellare'	Fruit spot	Italy (Sicily, Catania province)	KX056343	KX020119	KX064090
AA 40	*Citrus sinensis* 'Tarocco Nucellare'	Fruit spot	Italy (Sicily, Catania province)	KX056331	KX020013	KX064091
AA 41	*Citrus sinensis* 'Tarocco Nucellare'	Fruit spot	Italy (Sicily, Catania province)	KX056392	KX020132	KX064092
AA 42	*Citrus sinensis* 'Tarocco Nucellare'	Fruit spot	Italy (Sicily, Catania province)	KX056332	KX020014	KX064093
AA 43	*Citrus sinensis* 'Tarocco Nucellare'	Fruit spot	Italy (Sicily, Catania province)	KX056391	KX020121	KX064094
AA 44	*Citrus sinensis* 'Tarocco Nucellare'	Fruit spot	Italy (Sicily, Catania province)	KX056333	KX020045	KX064095
AA 45	*Citrus sinensis* 'Tarocco Nucellare'	Fruit spot	Italy (Sicily, Catania province)	KX056390	KX020046	KX064195
AA 46	*Citrus sinensis* 'Tarocco Nucellare'	Fruit spot	Italy (Sicily, Catania province)	KX056334	KX020047	KX064096
AA 47	*Citrus sinensis* 'Tarocco Nucellare'	Fruit spot	Italy (Sicily, Catania province)	KX056389	KX019997	KX064097
AA 48	*Citrus sinensis* 'Tarocco Nucellare'	Fruit spot	Italy (Sicily, Catania province)	KX056335	KX020048	KX064209
AA 50	*Citrus sinensis* 'Navelina'	Fruit spot	Italy (Sicily, Catania province)	KX056388	KX020015	KX064098

(Continued)

Table 1. (Continued).

Strain number[1]	Host, cultivar, clone	Symptom	Location	GenBank accession number[2]		
				ITS	*GAPDH*	*EF-1α*
AA 51	*Citrus sinensis* 'Navelina'	Fruit spot	Italy (Sicily, Catania province)	KX056336	KX020016	KX064099
AA 52	*Citrus sinensis* 'Navelina'	Fruit spot	Italy (Sicily, Catania province)	KX056387	KX020073	KX064100
AA 53	*Citrus sinensis* 'Navelina'	Fruit spot	Italy (Sicily, Catania province)	KX056278	KX020142	KX064210
AA 54	*Citrus sinensis* 'Navelina'	Fruit spot	Italy (Sicily, Catania province)	KX056344	KX020096	KX064211
AA 55	*Citrus sinensis* 'Navelina'	Fruit spot	Italy (Sicily, Catania province)	KX056406	KX020054	KX064101
AA 56	*Citrus sinensis* 'Navelina'	Fruit spot	Italy (Sicily, Catania province)	KX056279	KX020081	-
AA 57	*Citrus sinensis* 'Navelina'	Fruit spot	Italy (Sicily, Catania province)	KX056345	KX020109	KX064102
AA 58	*Citrus sinensis* 'Navelina'	Fruit spot	Italy (Sicily, Catania province)	KX056280	KX020106	KX064103
AA 59	*Citrus sinensis* 'Navelina'	Fruit spot	Italy (Sicily, Catania province)	KX056281	KX020125	-
AA 60	*Citrus sinensis* 'Navelina'	Fruit spot	Italy (Sicily, Catania province)	KX056282	KX020122	KX064104
AA 61	*Citrus sinensis* 'Navelina'	Fruit spot	Italy (Sicily, Catania province)	KX056346	KX020101	KX064105
AA 62	*Citrus limon* 'Femminello Siracusano 2KR'	Fruit spot	Italy (Sicily, Syracuse province)	KX056337	KX020017	KX064106
AA 63	*Citrus limon* 'Femminello Siracusano 2KR'	Fruit spot	Italy (Sicily, Syracuse province)	KX056386	KX019998	KX064107
AA 64	*Citrus limon* 'Femminello Siracusano 2KR'	Fruit spot	Italy (Sicily, Syracuse province)	KX056338	KX020130	KX064108
AA 65	*Citrus limon* 'Femminello Siracusano 2KR'	Fruit spot	Italy (Sicily, Syracuse province)	KX056385	KX019999	KX064109
AA 66	*Citrus limon* 'Femminello Siracusano 2KR'	Fruit spot	Italy (Sicily, Syracuse province)	KX056339	KX020138	KX064196
AA 67	*Citrus limon* 'Femminello Siracusano 2KR'	Fruit spot	Italy (Sicily, Syracuse province)	KX056283	KX020082	KX064110
AA 68	*Citrus limon* 'Femminello Siracusano 2KR'	Fruit spot	Italy (Sicily, Syracuse province)	KX056284	KX020003	KX064111
AA 69	*Citrus limon* 'Femminello Siracusano 2KR'	Fruit spot	Italy (Sicily, Syracuse province)	KX056285	KX020053	KX064112
AA 70	*Citrus limon* 'Femminello Siracusano 2KR'	Fruit spot	Italy (Sicily, Syracuse province)	KX056286	KX020083	KX064113
AA 71	*Citrus sinensis* 'Tarocco Sciara'	Leaf spot	Italy (Sicily, Catania province)	KX056287	KX020049	KX064215
AA 72	*Citrus sinensis* 'Tarocco Sciara'	Leaf spot	Italy (Sicily, Catania province)	KX056288	KX020084	KX064216
AA 73	*Citrus sinensis* 'Tarocco Sciara'	Leaf spot	Italy (Sicily, Catania province)	KX056407	KX020018	KX064114
AA 74	*Citrus sinensis* 'Tarocco Sciara'	Fruit spot	Italy (Sicily, Catania province)	KX056289	KX020104	KX064197
AA 75	*Citrus sinensis* 'Tarocco Sciara'	Fruit spot	Italy (Sicily, Catania province)	KX056290	KX020085	KX064115
AA 76	*Citrus sinensis* 'Tarocco Sciara'	Fruit spot	Italy (Sicily, Catania province)	KX056291	KX020126	KX064116
AA 77	*Citrus limon* 'Femminello Siracusano 2KR'	Twig lesion	Italy (Sicily, Syracuse province)	KX056420	KX020137	KX064117
AA 78	*Citrus limon* 'Femminello Siracusano 2KR'	Twig lesion	Italy (Sicily, Syracuse province)	KX056292	KX020019	KX064118
AA 79	*Citrus limon* 'Femminello Siracusano 2KR'	Leaf spot	Italy (Sicily, Syracuse province)	KX056293	KX020086	KX064119
AA 80	*Citrus limon* 'Femminello Siracusano 2KR'	Leaf spot	Italy (Sicily, Syracuse province)	KX056294	KX020123	-
AA 81	*Citrus limon* 'Femminello Siracusano 2KR'	Leaf spot	Italy (Sicily, Syracuse province)	KX056295	KX020100	KX064120
AA 82	*Citrus limon* 'Femminello Siracusano 2KR'	Leaf spot	Italy (Sicily, Syracuse province)	KX056296	KX020055	KX064121
AA 83	*Citrus limon* 'Femminello Siracusano 2KR'	Fruit spot	Italy (Sicily, Syracuse province)	KX056347	KX020114	KX064122
AA 84	*Citrus limon* 'Femminello Siracusano 2KR'	Fruit spot	Italy (Sicily, Syracuse province)	KX056433	KX020078	KX064123
AA 85	*Citrus limon* 'Femminello Siracusano 2KR'	Fruit spot	Italy (Sicily, Syracuse province)	KX056348	KX020066	KX064200
AA 86	*Citrus limon* 'Femminello Siracusano 2KR'	Fruit spot	Italy (Sicily, Syracuse province)	KX056349	KX020089	KX064124
AA 87	*Citrus limon* 'Femminello Siracusano 2KR'	Fruit spot	Italy (Sicily, Syracuse province)	KX056350	KX020067	KX064125
AA 88	*Citrus sinensis* 'Valencia'	Leaf spot	Italy (Sicily, Catania province)	KX056351	KX020090	KX064126
AA 89	*Citrus sinensis* 'Valencia'	Leaf spot	Italy (Sicily, Catania province)	KX056352	KX020115	KX064127
AA 90	*Citrus sinensis* 'Valencia'	Fruit spot	Italy (Sicily, Catania province)	KX056297	KX020099	KX064128
AA 91	*Citrus sinensis* 'Valencia'	Fruit spot	Italy (Sicily, Catania province)	KX056298	KX020056	KX064129
AA 92	*Citrus sinensis* 'Tarocco Nucellare'	Leaf spot	Italy (Sicily, Catania province)	KX056299	KX020076	KX064130
AA 93	*Citrus sinensis* 'Tarocco Nucellare'	Leaf spot	Italy (Sicily, Catania province)	KX056300	KX020057	KX064198
AA 94	*Citrus sinensis* 'Tarocco Nucellare'	Leaf spot	Italy (Sicily, Catania province)	KX056425	KX020004	KX064131
AA 95	*Citrus sinensis* 'Tarocco Nucellare'	Leaf spot	Italy (Sicily, Catania province)	KX056426	KX020058	KX064132
AA 96	*Citrus sinensis* 'Tarocco Nucellare'	Leaf spot	Italy (Sicily, Catania province)	KX056427	KX020020	KX064133
AA 97	*Citrus limon* 'Femminello Siracusano 2KR'	Fruit spot	Italy (Sicily, Syracuse province)	KX056428	KX020059	KX064134

(Continued)

Table 1. (Continued).

Strain number[1]	Host, cultivar, clone	Symptom	Location	GenBank accession number[2]		
				ITS	*GAPDH*	*EF-1α*
AA 98	*Citrus limon* 'Femminello Siracusano 2KR'	Fruit spot	Italy (Sicily, Syracuse province)	KX056430	KX020131	KX064135
AA 99	*Citrus sinesis* × *Poncirus trifoliata* 'Carrizo'	Leaf spot	Italy (Sicily, Catania province)	KX056432	KX020105	KX064136
AA 100	*Citrus sinensis* × *Poncirus trifoliata* 'Carrizo'	Leaf spot	Italy (Sicily, Catania province)	KX056431	KX020021	KX064137
AA 101	*Citrus sinensis* × *Poncirus trifoliata* 'Carrizo'	Leaf spot	Italy (Sicily, Catania province)	KX056303	KX020022	KX064138
AA 102	*Citrus* × *clementina*	Fruit spot	Italy (Sicily, Palermo province)	KX056353	KX020116	KX064139
AA 103	*Citrus* × *clementina*	Fruit spot	Italy (Sicily, Palermo province)	KX056384	KX020001	KX064140
AA 104	*Citrus* × *clementina*	Fruit spot	Italy (Sicily, Palermo province)	KX056354	KX020068	KX064141
AA 105	*Citrus* × *clementina*	Fruit spot	Italy (Sicily, Palermo province)	KX056383	KX020079	KX064142
AA 106	*Citrus* × *clementina*	Fruit spot	Italy (Sicily, Palermo province)	KX056355	KX020075	KX064143
AA 107	*Citrus* × *clementina*	Fruit spot	Italy (Sicily, Palermo province)	KX056304	KX020060	KX064144
AA 108	*Citrus reticulata* 'Nova'	Fruit spot	Italy (Sicily, Catania province)	KX056382	KX020139	KX064145
AA 109	*Citrus reticulata* 'Nova'	Fruit spot	Italy (Sicily, Catania province)	KX056356	KX020127	KX064146
AA 110	*Citrus reticulata* 'Nova'	Fruit spot	Italy (Sicily, Catania province)	KX056381	KX020097	KX064147
AA 111	*Citrus aurantium*	Leaf spot	Italy (Sicily, Catania province)	KX056305	KX020061	KX064148
AA 112	*Citrus sinensis* × *Poncirus trifoliata* 'Carrizo'	Twig lesion	Italy (Sicily, Catania province)	KX056357	KX020095	KX064149
AA 113	*Citrus sinensis* × *Poncirus trifoliata* 'Carrizo'	Twig lesion	Italy (Sicily, Catania province)	KX056306	KX020133	KX064150
AA 114	*Citrus sinensis* × *Poncirus trifoliata* 'Carrizo'	Twig lesion	Italy (Sicily, Catania province)	KX056316	KX020023	KX064151
AA 115	*Citrus sinensis* 'Valencia'	Fruit spot	Italy (Sicily, Catania province)	KX056317	KX020024	KX064199
AA 116	*Citrus sinensis* 'Valencia'	Fruit spot	Italy (Sicily, Catania province)	KX056380	KX020117	KX064152
AA 117	*Citrus aurantium*	Fruit spot	Italy (Sicily, Catania province)	-	-	-
AA 118	*Citrus aurantium*	Fruit spot	Italy (Sicily, Catania province)	KX056358	KX020038	KX064153
AA 119	*Citrus aurantium*	Fruit spot	Italy (Sicily, Catania province)	KX056301	KX020025	KX064154
AA 120	*Citrus sinensis* 'Moro'	Fruit spot	Italy (Sicily, Catania province)	KX056302	KX020107	KX064155
AA 121	*Citrus sinensis* 'Moro'	Fruit spot	Italy (Sicily, Catania province)	KX056379	KX020091	KX064156
AA 122	*Citrus sinensis* 'Moro'	Fruit spot	Italy (Sicily, Catania province)	KX056359	KX020128	KX064157
AA 123	*Citrus sinensis* 'Moro'	Fruit spot	Italy (Sicily, Catania province)	KX056378	KX020080	KX064158
AA 124	*Citrus sinensis* 'Moro'	Fruit spot	Italy (Sicily, Catania province)	KX056315	KX020062	KX064159
AA 125	*Citrus sinensis* 'Valencia'	Fruit spot	Italy (Sicily, Catania province)	KX056360	KX020098	KX064160
AA 126	*Citrus sinensis* 'Valencia'	Fruit spot	Italy (Sicily, Catania province)	KX056377	KX020092	KX064161
AA 127	*Citrus sinensis* × *Poncirus trifoliata* 'Carrizo'	Leaf spot	Italy (Sicily, Catania province)	KX056307	KX020026	KX064162
AA 128	*Citrus limon* 'Femminello Siracusano 2KR'	Fruit spot	Italy (Sicily, Syracuse province)	KX056409	KX020027	KX064163
AA 129	*Citrus limon* 'Femminello Siracusano 2KR'	Fruit spot	Italy (Sicily, Syracuse province)	KX056314	KX020087	KX064164
AA 130	*Citrus limon* 'Femminello Siracusano 2KR'	Fruit spot	Italy (Sicily, Syracuse province)	KX056419	KX020028	KX064165
AA 131	*Citrus limon* 'Femminello Siracusano 2KR'	Fruit spot	Italy (Sicily, Syracuse province)	KX056410	KX020136	-
AA 132	*Citrus reticulata* 'Ciaculli'	Fruit spot	Italy (Sicily, Catania province)	KX056418	KX020029	KX064166
AA 133	*Citrus reticulata* 'Ciaculli'	Fruit spot	Italy (Sicily, Catania province)	KX056308	KX020030	KX064167
AA 134	*Citrus reticulata* 'Ciaculli'	Fruit spot	Italy (Sicily, Catania province)	KX056313	KX020031	KX064168
AA 135	*Citrus reticulata* 'Ciaculli'	Fruit spot	Italy (Sicily, Catania province)	KX056309	KX020032	KX064169
AA 136	*Citrus reticulata* 'Ciaculli'	Fruit spot	Italy (Sicily, Catania province)	KX056411	KX020033	KX064170
AA 137	*Citrus reticulata* 'Ciaculli'	Fruit spot	Italy (Sicily, Catania province)	KX056312	KX020063	KX064171
AA 138	*Citrus reticulata* 'Mandalate'	Fruit spot	Italy (Sicily, Catania province)	KX056310	KX020141	KX064172
AA 139	*Citrus reticulata* 'Mandalate'	Fruit spot	Italy (Sicily, Catania province)	KX056417	KX020034	KX064173
AA 140	*Citrus reticulata* 'Mandalate'	Fruit spot	Italy (Sicily, Catania province)	KX056311	KX020042	KX064174
AA 141	*Citrus reticulata* 'Mandalate'	Fruit spot	Italy (Sicily, Catania province)	KX056412	KX020146	KX064207
AA 142	*Citrus reticulata* 'Mandalate'	Fruit spot	Italy (Sicily, Catania province)	KX056416	KX020035	KX064175
AA 143	*Citrus reticulata* 'Mandalate'	Fruit spot	Italy (Sicily, Catania province)	KX056361	KX020093	KX064208
AA 144	*Citrus reticulata* 'Mandalate'	Fruit spot	Italy (Sicily, Catania province)	KX056413	KX020108	KX064176

(Continued)

Table 1. (Continued).

Strain number[1]	Host, cultivar, clone	Symptom	Location	GenBank accession number[2]		
				ITS	*GAPDH*	*EF-1α*
AA 145	*Citrus reticulata* 'Mandalate'	Fruit spot	Italy (Sicily, Catania province)	KX056376	KX020069	KX064177
AA 146	*Citrus reticulata* 'Mandalate'	Fruit spot	Italy (Sicily, Catania province)	-	KX020036	KX064178
AA 147	*Citrus sinensis* 'Tarocco Scire'	Fruit spot	Italy (Sicily, Catania province)	KX056362	KX020077	KX064179
AA 148	*Citrus sinensis* 'Tarocco Scire'	Fruit spot	Italy (Sicily, Catania province)	KX056375	KX020005	KX064180
AA 149	*Citrus sinensis* 'Tarocco Scire'	Fruit spot	Italy (Sicily, Catania province)	-	KX020000	KX064181
AA 150	*Citrus sinensis* 'Tarocco Scire'	Fruit spot	Italy (Sicily, Catania province)	KX056363	KX020050	KX064182
AA 151	*Citrus sinensis* 'Tarocco Scire'	Fruit spot	Italy (Sicily, Catania province)	KX056374	KX020070	KX064183
AA 152	*Citrus sinensis* 'Tarocco Scire'	Fruit spot	Italy (Sicily, Catania province)	KX056364	-	KX064184
AA 153	*Citrus sinensis* 'Tarocco Scire'	Fruit spot	Italy (Sicily, Catania province)	KX056373	KX020039	KX064185
AA 154	*Citrus sinensis* 'Tarocco Scire'	Fruit spot	Italy (Sicily, Catania province)	-	KX020043	KX064186
AA 155	*Citrus sinensis* 'Tarocco Scire'	Fruit spot	Italy (Sicily, Catania province)	KX056365	KX020135	KX064187
AA 156	*Citrus sinensis* 'Tarocco Scire'	Fruit spot	Italy (Sicily, Catania province)	KX056372	KX020071	KX064188
AA 157	*Citrus limon*	Fruit spot	Italy (Sicily, Catania province)	KX056415	KX020064	KX064189
AA 158	*Citrus sinensis* 'Tarocco Scire'	Leaf spot	Italy (Sicily, Catania province)	KX056414	KX020037	KX064190
AA 159	*Citrus sinensis* 'Tarocco Scire'	Leaf spot	Italy (Sicily, Catania province)	KX056366	-	-
AA 160	*Citrus sinensis* 'Tarocco Scire'	Leaf spot	Italy (Sicily, Catania province)	KX056371	KX020094	KX064191
AA 163	*Citrus limon*	Fruit spot	Italy (Sicily, Catania province)	KX056367	KX020113	KX064212
AA 164	*Citrus limon*	Fruit spot	Italy (Sicily, Catania province)	KX056370	KX020140	KX064192
AA 165	*Citrus limon*	Fruit spot	Italy (Sicily, Catania province)	KX056368	KX020040	KX064193
AA 166	*Citrus limon*	Fruit spot	Italy (Sicily, Catania province)	KX056369	KX020072	KX064194
AA 167	*Citrus limon*	Fruit spot	Italy (Sicily, Catania province)	-	-	-

[1] AA: Cultures stored at the University of Catania, Italy.
[2] ITS: internal transcribed spacer region, *EF-1α*: translation elongation factor 1-α, *GAPDH:* glyceraldehyde-3-phosphate dehydrogenase.

Table 2. Pathogenicity of *Alternaria* isolates on detached leaves and immature fruit.

Isolate	Citrus host			
	Calamondin	Sweet orange	Rangpur Lime	Lemon
GROUP A				
AA1, AA3-11, AA15, AA17-AA24, AA26-31, AA36-38, AA40-41, AA48, AA55, AA57-58, AA62, AA74, AA80, AA86	+	+	+	+
GROUP B				
AA2	-	+	+	+
GROUP C				
AA12-14, AA16, AA25, AA32, AA39, AA52, AA59, AA70, AA144, AA145	+	+	-	+
GROUP D				
AA66	+	-	-	-

The isolates AA2, AA19, AA22, AA27, AA37, AA66, AA144, AA145 were inoculated on immature fruit.
+ positive reaction (necrotic spots) on leaves and fruit in two inoculation experiments.
– negative reaction on leaves and fruit in two inoculation experiments.

genicity tests on detached leaves, was tested on immature fruit of calamondin, rangpur lime, 'Femminello Siracusano 2KR' lemon and 'Tarocco Sciara' sweet orange. Each fruit was punctured (four punctures per fruit) with a sterile needle, and was then inoculated with 10 µL of a conidium suspension. Ten fruit from each host were inoculated, and ten fruit were inoculated without needle punctures. The inoculated fruit were placed into

plastic bags, covered with plastic films and incubated at 25 ± 1°C in the dark. Negative controls were wounded fruit with 10 µL of SDW applied to each wound. Symptom development was evaluated after 4, 7 and 10 d. The experiment was conducted twice.

Pathogenicity test on fruit in planta

The pathogenicity of eight representative isolates (AA2, AA19, AA22, AA27, AA37, AA66, AA144 and AA145) from different groups was also tested *in planta* on fruit of calamondin, rangpur lime, 'Femminello Siracusano 2KR' lemon, 'Tarocco Sciara' sweet orange. Each fruit was punctured with a sterile needle and was inoculated with 10 µL of conidium suspension (four punctures per fruit). Ten fruit on each host were inoculated, and ten fruit were inoculated without needle punctures. Inoculated fruit were covered with plastic bags and incubated at 25 ± 1°C and 95% relative humidity (RH) in a 12 h fluorescent light/12 h dark regime in a growth chamber. Negative controls were fruit treated with SDW. Symptom development was observed after 4, 7 and 10 d. The experiments were conducted twice.

Toxins in culture filtrates

Toxicity of culture filtrates of the eight representative isolates (AA2, AA19, AA22, AA27, AA37, AA66, AA144 and AA145) was determined using a leaf necrosis assay (Kohmoto *et al*., 1993; Masunaka *et al*., 2000). Culture filtrates of profile I and II of tangerine pathotype were also assessed. The citrus species and clones used for pathogenicity tests on immature fruit (see above) were used. The isolates were grown on V8-juice agar plates. Small pieces of mycelium were inoculated into modified Richard's solution (Kohmoto *et al*., 1993), and incubated for 3 weeks at 25°C under cool-white fluorescent light. Each culture was then filtered through four layers gauze to retain the mycelium. Supernatant of these culture filtrates was harvested by centrifugation at 1,500 g for 5 min (Kohmoto *et al*., 1993; Masunaka *et al*., 2000). Host leaves were washed and disinfested for 1 min in 1.5 % NaOCl, rinsed twice in SDW, and then each punctured with a sterile needle on the lower surface (four punctures per leaf). Each leaf puncture was then treated with a 10 µL droplet of culture filtrate. The leaves were incubated in a moist chamber in the dark at 25°C to encourage transpiration. When toxin was present, dark necroses developed around the points of filtrate treatment. The experiment was conducted twice.

RESULTS

Fungus isolates

From symptomatic tissues, typical small conidium *Alternaria* species were consistently isolated. Occasionally, typical *Colletotrichum* spp. colonies were recovered in association with *Alternaria* species. One hundred sixty-two *Alternaria* isolates were collected from brown spot lesions from plants in 15 citrus orchards (Table 1). Disease incidence was from 5 to 100% of the trees in each orchard, depending on host species. The symptoms appeared on leaves and fruit of different cultivars and clones of sweet orange ('Moro', 'Valencia', 'Navelina', 'Tarocco Sciara', 'Tarocco Scirè', 'Tarocco Gallo', 'Tarocco Nucellare'), 'Femminello Siracusano 2KR' lemon, bitter orange (*Citrus aurantium* L.), 'Nova' mandarin, clementine (*Citrus clementina* Hort. ex Tan.), mandalate (*Citrus reticulata* × *Citrus deliciosa*) and 'Carrizo' citrange (*Citrus sinensis* Osbeck × *Poncirus trifoliata* Raf.) (Figure 1).

DNA extraction, amplification and sequencing

In total, 173 fungus isolates were included in the phylogenetic analysis. Of these, 148 were collected from citrus in Sicily and 25 were representative strains of *Alternaria* species (Wounderberg *et al*., 2015), the sequences of which were obtained from GenBank (http://www.ncbi.nlm.nih.gov). Four of the 148 strains collected from *Citrus* spp. clustered within the *A. arborescens* species complex, and the remaining strains clustered with *A. alternata*. The tree is drawn to scale, with branch lengths measured in the number of substitutions per site. The tree with the highest log likelihood (-1624.2743) is shown (Figure 4). The analysis involved 173 nucleotide sequences. The final dataset consisted of 767 bases totally, represented by 530 from *GAPDH* and 237 from *EF-1α* locus.

Pathogenicity tests on detached leaves

All of the isolates inoculated gave positive pathogenicity reactions (Table 2). Typical brown spot lesions were observed 3-4 d after inoculation (Figure 2). Profile I and profile II isolates from tangelo 'Minneola' and tangor 'Murcott', known to be pathogenic to these hosts but not to rangpur lime (Peever *et al*., 1999; Vega and Dewdney, 2014), were also pathogenic to all inoculated cultivars and clones of sweet orange and lemon. Twelve isolates (group C) of 50 inoculated (24%) were pathogenic and showed the same behaviour of profile I and II of the *A. alternata* pathotype. Thirty-five isolates

Figure 1. Natural symptoms observed on fruit of (a) mandarin 'Nova'; (b) and (c), lemon 'Femminello 2KR'; (d) 'Tarocco Sciara'; and (e) 'Tarocco Gallo' sweet orange. (f), (g) and (h) show symptoms caused by artificial inoculation with *Alternaria alternata* on fruit of lemon, and (i) on sweet orange *in planta*.

of *A. alternata* and one isolate of *A. arborescens* (group A) of 50 isolates (72%) were pathogenic to all citrus species inoculated. One isolate of *A. alternata* (AA2) (group B) was pathogenic to all species, but not to calamondin, showing typical behaviour of the rough lemon pathotype. One isolate of *A. alternata* (AA66) (group D) was pathogenic only to calamondin. The negative controls remained symptomless. Re-isolation of the pathogens from symptomatic leaves confirmed the etiology of infection, fulfilling Koch's postulates. Very similar results were obtained in both experiments.

Pathogenicity tests on detached fruit

The isolates which were pathogenic on detached leaves were also pathogenic on immature fruit. Four

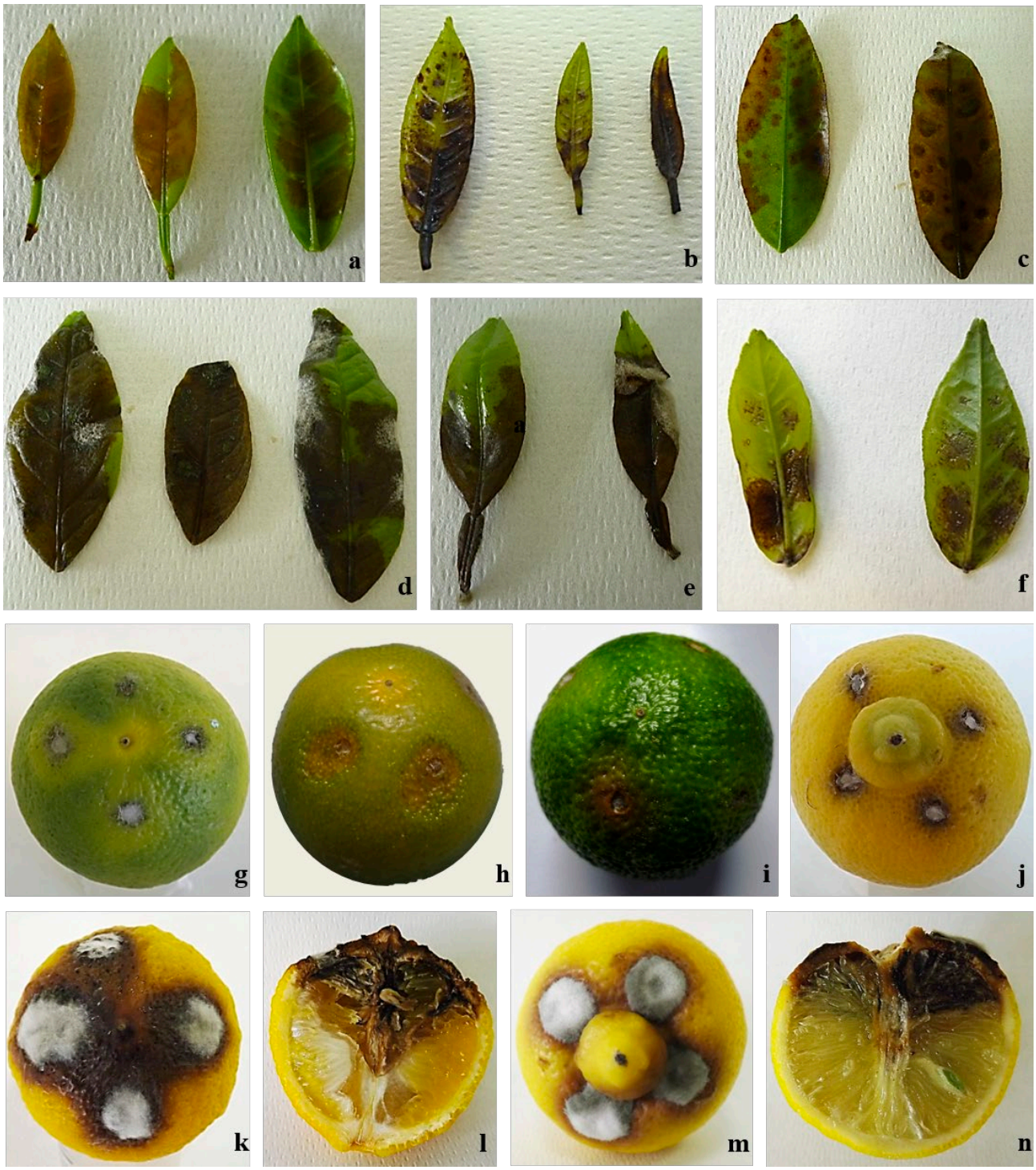

Figure 2. Symptoms caused by artificial inoculation of *Alternaria alternata* on detached leaves of calamondin (a), rangpur lime (b), lemon 'Femminello 2KR' (c), 'Moro' sweet orange (d), 'Valencia' sweet orange (e), or 'Tarocco Sciara' sweet orange (f); or on detached immature fruit of 'Tarocco Sciara' sweet orange (g); calamondin (h), rangpur lime (i), or lemon (j). Symptoms after 10 d on fruit of rangpur lime (k, l), lemon (m, n). Sporulation of *Alternaria alternata* on rangpur lime (k) and lemon (m).

Figure 3. Toxicity of culture filtrates of *Alternaria alternata* on leaves of 'Tarocco Sciara' sweet orange (a), calamondin (b), rangpur lime (c), or lemon 'Femminello 2KR' (d).

d after inoculation, all fruit had started to show brown spots with small diameters. Seven days after inoculation, brown spots of 1 cm diam., covered by *Alternaria* mycelium, were observed on these fruit. The inoculated fruit were each cut in half at 10 d after inoculation, and those inoculated with isolates AA37, AA27 and AA22 had black rot symptoms (Figure 2). When inoculated without needle punctures, the isolates were not pathogenic on orange, lemon or rangpur lime, but were pathogenic to calamondin. Control fruit remained symptomless. Re-isolation of the pathogens from symptomatic fruit confirmed the etiology of infections, fulfilling Koch's postulates. Very similar results were obtained in both experiments.

Pathogenicity tests on fruit in planta

The isolates which were pathogenic on detached fruit were also pathogenic on fruit *in planta* when they were inoculated with needle punctures, confirming the results obtained on detached fruit. Small brown lesions were observed 4 d after pathogen inoculation. After 7 d, lesions varied from small specks to large pockmarks on all inoculated fruit. In some cases, the fruit rinds responded to infections by forming barriers of corky tissues that erupted from the fruit surfaces. These corky tissue sometimes falls out, forming craters or pockmarks on the fruit surfaces after 10 d (Figure 1). When inoculated without wounds, the isolates were not pathogenic on orange, lemon or rangpur lime but were pathogenic on calamondin. Control fruit remained symptomless. Re-isolation of the pathogens from symptomatic fruit confirmed the etiology of infections, fulfilling Koch's postulates. Very similar results were obtained in both experiments.

Toxicity of culture filtrates

Toxin assays on leaves revealed complete correlation between pathogenicity reactions and responses to toxins. Culture filtrates from group A isolates caused dark necroses on all host species 3 d after treatment (Figure 3). The isolates of group C caused symptoms on calamondin, sweet orange and lemon leaves identical to symptoms caused by profile I and II of the tangerine pathotype, but caused no visible effects on rangpur lime. In contrast, isolate AA2 (group B) produced symptoms on all the treated host species, but did not affect calamondin, while isolate AA66 (group D) showed symptoms only on calamondin. Similar results were obtained in both experiments.

DISCUSSION

In this study, brown spot symptoms were widely detected pre-harvest on sweet orange ('Tarocco Nucellare', 'Tarocco Sciara', 'Tarocco Scirè', 'Tarocco Gallo', 'Navelina', 'Moro') and lemon ('Femminello Siracusano 2KR') in Sicily (southern Italy). One hundred sixty-two *Alternaria* isolates were collected from symptomatic citrus species, and from other well-known Alternaria brown spot-susceptible citrus species from 2014 in Catania, Syracuse and Palermo provinces.

Alternaria is a cosmopolitan genus that consists of different saprophytic and pathogenic species. *Alternaria* was divided into 26 sections by Woudenberg *et al.* (2013). *Alternaria* sect. *Alternaria* contains most of the small-conidium *Alternaria* species with concatenated conidia, including important plant, human and postharvest pathogens. Species within sect. *Alternaria* have been mostly described based on morphology and/or host-specificity, and genetic variation among them is minimal. Based on genome and transcriptome comparisons and molecular phylogeny, *Alternaria* sect. *Alternaria* consists of only 11 phylogenetic species and one species complex. Thirty-five morphospecies, which cannot be distinguished based on multi-gene phylogeny, have been synonymized under *A. alternata* (Woudenberg *et al.*, 2015). In the present study, we compared isolates of *Alternaria* with the isolates used by Wounderberg *et al.* (2015). Of 148 isolates used in phylogenetic analyses, four clustered in the *A. arborescens* species complex (AASC), while the majority of the isolates did not form clear phylogenetic clades and were grouped in *A. alternata*. *Alternaria arborescens* was reported in Italy from citrus by Garganese *et al.* (2016).

Lemon and sweet orange are reported to be resistant to Alternaria brown spot in field conditions. However,

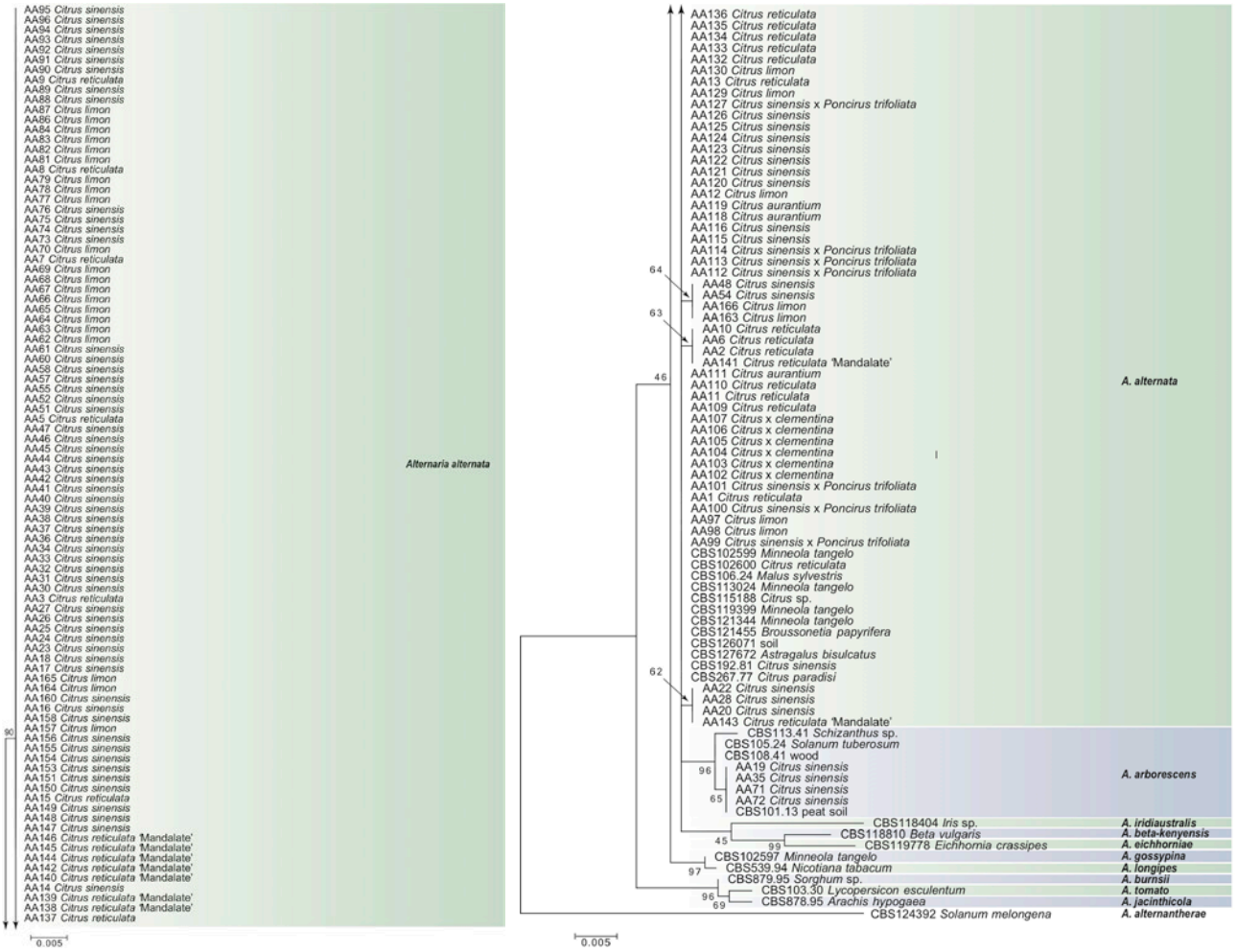

Figure 4. Multilocus glyceraldehyde-3-phosphate dehydrogenase (*GAPDH*) and translation elongation factor 1-α (*EF-1α*) phylogenetic tree developed using the maximum likelihood (ML) method. The tree with the greatest obtained log likelihood (-1624.2743) is shown.

after artificial inoculation, some symptoms were induced in 'Valencia', 'Shamouti' and 'Washington Navel' sweet orange as well as in 'Volkameriano' lemon (Kohmoto *et al*., 1979; Solel and Kimchi, 1997), and on 'Moro' sweet orange in Greece (Elena, 2006) after inoculating *A. alternata* tangerine pathotype obtained from 'Minneola' tangelo.

Pathogenicity of *A. alternata* is controlled by the production of host-selective toxins (HSTs). HSTs can be defined as groups of chemically diverse and complex metabolites produced by plant pathogenic isolates of certain fungi during germination of spores on plant surfaces, which play important roles in host specificity and isolate virulence (Nishimura and Kohmoto, 1983; Gardner *et al*., 1986; Walton, 1996). ACR-toxin is an HST produced by the *A. alternata* rough lemon pathotype, and cultivars of rough lemon and rangpur lime are known to be sensitive to this toxin (Kohmoto *et al*., 1979, 1991; Gardner *et al*., 1985; Akimutsu *et al*., 2003). Tangerine, mandarin and grapefruit are completely insensitive to ACR-toxin. ACT-toxin is an HST produced by the *A. alternata* tangerine pathotype, and this toxin affects only this host and hybrids (Kohomoto *et al*., 1993; Timmer *et al*., 2000). The exclusive roles of ACTs as pathogenic factors have, however, been questioned by Garganese *et al*. (2016). They demonstrated the ability of 20 selected *Alternaria* isolates to cause brown spot of tangerine, even in the absence of ACTT1/ACTT2 expression. They also concluded that mycotoxin effects could be equivalent to phytotoxin effects in disease outcomes, so that in the absence of phytotoxins, some level of virulence may also be evident.

In the present study, artificial inoculations on detached leaves revealed that 24% of the isolates tested

were pathogenic to calamondin, lemon and sweet orange but not to rangpur lime, showing behaviour of profile I and II of *A. alternata* and indicating that these isolates belong to the tangerine pathotype of *A. alternata*. Only one isolate (AA2) was pathogenic to all host species, calamondin excluded, indicating that this isolate belong to the rough lemon pathotype, whereas the isolate AA66 caused symptoms only on calamondin. Instead, 72% of our isolates (group A), including the *A. arborescens* isolate, were pathogenic to all the citrus species inoculated, and did not show any host specificity. This questions the unique role of phytotoxins as pathogenic factors. Nonpathogenic *Alternaria* isolates were not recognized among those tested, confirming that the presence of these on brown spot lesions occurs at low frequencies (Peever *et al*., 1999).

Toxicity tests of culture filtrates revealed close relationship between pathogenicity reactions and responses to toxins. The symptoms caused by the culture filtrates of the profile I and II tangerine pathotype on sweet orange and lemon were the same as symptoms produced from culture filtrates of group C. No symptoms were observed on rangpur lime. In contrast, the isolate AA2 (group B) produced necrosis on all host species treated, except calamondin. The isolate AA66 (group D) produced symptoms only on calamondin, whereas the culture filtrates from group A caused necrosis on all host species treated.

On the basis of the data presented here, we hypothesise that the isolates belonging to group A (72% of those inoculated) produce two HSTs, ACT-toxin of the tangerine pathotype and ACR-toxin of the rough lemon pathotype. The presence of dual host specificity and toxin production is not common in populations of *A. alternata* on citrus. Masunaka *et al*. (2005) reported only one isolate that produced both toxins among hundreds of isolates examined in Florida. *Alternaria* species have no known sexual cycle in nature, and the populations of *A. alternata* on citrus are clonal. Therefore, the ability to produce both toxins is acquired when a dispensable chromosome carrying the gene cluster controlling biosynthesis of one HST is transferred horizontally and rearranged in another isolate of the fungus carrying gene for biosynthesis of the other HST (Masunaka *et al*., 2005). Instead, the hypothesis that other toxins may have played roles in pathogenicity of selected isolates is more plausible, as reported by da Garganese *et al*. (2016). However, this needs to be confirmed by specific assays.

Our data demonstrate that most of *A. alternata* isolates and one of *A. arborescens* were pathogenic on detached leaves, detached fruit, and *in planta*, producing symptoms similar to those observed in the field. The artificial inoculation experiments with different host species gave symptoms the same as those observed in orchards on tangerine and their hybrids. Occasionally, fruit inoculated with isolates AA37, AA27 and AA22 developed symptoms similar to black rot. Black rot is a significant citrus postharvest problem that may appear in the field prior to harvest. This disease occurs most commonly on sweet orange in the field, and on tangerines and their hybrids and lemon in storage, and affects all citrus under the appropriate conditions (Brown and Eckert, 2000). Most small-conidium species of *Alternaria* have been reported as capable of causing black rot when inoculated into wounded citrus fruit. These fungi include saprophytic isolates, epiphytes and the tangerine and rough lemon pathotypes (Peever *et al*., 2005).

Management of Alternaria brown spot includes the use of cultural practices such as disease-free nursery stock, wide tree spacing in orchards, reduction of nitrogen fertilization, and fungicide applications (Timmer and Peever, 1997; Dewdney, 2016). Chemical management is the main strategy to control disease on citrus. Quinone-outside inhibitors (QoIs) have been widely used in Florida over the last decade, but are classified as high risk for development of fungicide resistance. Currently in Italy, mancozeb and pyraclostrobin are the only fungicides approved in integrated citrus production, but chemical control strategies must be developed for the different orchard areas.

In conclusion, this study has demonstrated the high pre-harvest incidence of Alternaria disease on the common and widespread new clones of sweet orange and lemon in Sicily. These infections could be promoted by favourable local environmental conditions.

ACKNOWLEDGMENTS

This research was partially funded by the CBS-KNAW, Fungal Biodiversity Centre (CBS), Utrecht, the Netherlands, and the Agricultural, Food and Environment department, University of Catania, Italy. The first author thanks all the staff at the CBS for their guidance and technical support during training at Westerdijk Fungal Biodiversity Institute, Utrecht. The authors also thank M. Dewdney, University of Florida, for providing isolates of profile I and II of the tangerine pathotype.

LITERATURE CITED

Aiello D., Carrieri R., Guarnaccia V., Vitale A., Lahoz E., Polizzi, G., 2015. Characterization and pathogenicity

of *Colletotrichum gloeosporioides* and *C. karstii* causing preharvest disease on *Citrus sinensis* in Italy. *Journal of Phytopathology* 163(3): 168–177.

Akimitsu K., Peever T.L., Timmer, L.W., 2003. Molecular, ecological and evolutionary approaches to understanding Alternaria diseases of citrus. *Molecular Plant Pathology* 4: 435–436.

Brown G.E., Eckert J.W., 2000. Alternaria rot. In: *Compendium of Citrus Diseases* (L.W. Timmer, S.M. Garnsey, J.H. Graham ed.). The American Phytopathological Society, St. Paul, MN, 37.

Carbone I., Kohn, L.M., 1999. A method for designing primer sets for speciation studies in filamentous ascomycetes. *Mycologia* 91: 553–556.

Dewdney M.M., 2016. Alternaria brown spot. In: Florida Citrus Pest Management Guide. Univ. Florida. https://edis.ifas.ufl.edu/pdffiles/CG/CG02100.pdf.

Elena K., 2006. Alternaria brown spot of Minneola in Greece; evaluation of citrus species susceptibility. *European Journal of Plant Pathology* 115: 259–262.

Gardner J.M., Kono Y., 1986. Chandler. Bioassay and host-selectivity of *Alternaria citri* toxins affecting rough lemon and mandarins. *Physiological and Molecular Plant Pathology* 29: 293–304.

Gardner J.M., Kono Y., Tatum J.H., Suzuki Y., Takeuchi S., 1985. Structure of major component of ACRL toxins, host-specific phytotoxic compound produced by *Alternaria citri*. *Agricultural and Biological Chemistry* 49: 1235–1238.

Garganese F., Schena L., Siciliano I., Prigigallo M.I., Spadaro D., De Grassi A., Ippolito A., Sanzani S.M., 2016. Characterization of Citrus-Associated Alternaria Species in Mediterranean Areas. *PlosOne* 16: e0163255.

Kohmoto K., Scheffer R.P., Whiteside J.O., 1979. Host-selective toxins from *Alternaria citri*. *Phytopathology* 69: 667–671.

Kohmoto K., Akimitsu K., Otani H., 1991. Correlation of resistance and susceptibility of citrus to *Alternaria alternata* with sensitivity to host specific toxins. *Phytopathology* 81: 719–722.

Kohmoto K., Itoh Y., Shimomura N., Kondoh Y., Otani H., ... Nakatsuka S., 1993. Isolation and biological activities of two host-specific toxins from the tangerine pathotype of *Alternaria alternata*. *Phytopathology* 83: 495–450.

Masunaka A., Tanaka A., Tsuge T., Peever T.L., Timmer L.W., … Akimitsu K., 2000. Distribution and characterization of AKT homologs in the tangerine pathotype of *Alternaria alternata*. *Phytopathology* 90: 762–768.

Masanuka, A., Ohtani, K., Peever, T. L., Timmer, L. W., Tsuge, T., … Akimitsu K., 2005. An isolate of *Alternaria alternata* that is pathogenic to both tangerines and rough lemon and produces two host-selective toxins, ACT- and ACR-toxins. *Phytopathology* 95: 241–247.

Nishimura S., Kohmoto K., 1983. Host-specific toxins and chemical structures from Alternaria species. *Annual Review of Phytopathology* 21: 87–116.

Ohtani K., Fukumoto T., Nishimura S., Miyamoto Y., Gomi K., Akimitsu K., 2009. Alternaria Pathosystems for Study of Citrus Diseases. *Tree and Forestry Science and Biotechnology* 3: 108–115.

Peever T.L., Canihos Y., Olsen L., Ibañez A., Liu Y.C., Timmer L.W., 1999. Population genetic structure and host specificity of *Alternaria* spp. causing brown spot of Minneola tangelo and rough lemon in Florida. *Phytopathology* 89: 851–860.

Peever T.L., Ibañez A., Akimitsu K., Timmer L.W., 2002. Worldwide phylogeography of the citrus brown spot pathogen, *Alternaria alternata*. *Phytopathology* 92: 794–802.

Peever T.L., Su G., Carpenter-Boggs L., Timmer L.W., 2004. Molecular systematics of citrus-associated *Alternaria* species. *Mycologia* 96: 119–134.

Peever T.L., Carpenter-Boggs L.W., Timmer L.W., Carris L.M., Bhatia A., 2005. Citrus Black rot is caused by phylogenetically distinct lineages of *Alternaria alternata*. *Phytopathology* 95: 512–518.

Piccirillo G., Carrieri R., Polizzi G., Azzaro A., Lahoz E., … Vitale A., 2018. *In vitro* and *in vivo* activity of QoI fungicides against *Colletotrichum gloeosporioides* causing fruit anthracnose in *Citrus sinensis*. *Scientia Horticulturae* 236: 90–95.

Polizzi G., Azzaro A., 2015. Maculatura bruna degli agrumi su limone e arancio Tarocco. *Informatore agrario* 1: 2–4.

Saitou N., Nei M., 1987. The neighbor-joining method-a new method for reconstructing phylogenetic trees. *Molecular Biology Evolution* 4: 406–425.

Solel Z., Kimchi M., 1997. Susceptibility and resistance of citrus genotypes to *Alternaria alternata* pv. *citri*. *Journal of Phytopathology* 145: 389–391.

Tamura K., 1992. Estimation of the number of nucleotide substitutions when there are strong transition-transversion and G + C-content biases. *Molecular Biology Evolution* 9: 678-687.

Tamura K., Stecher G., Peterson D., Filipski A., Kumar S., 2013. MEGA6: molecular evolutionary genetics analysis version 6.0. *Molecular Biology Evolution* 30: 2725–2729.

Timmer L.W., Peever T.L., 1997. Managing Alternaria brown spot. *Citrus Industry* 78: 24–25.

Timmer L.W., Solel Z., Orozco-Santos M., 2000. Alternaria brown spot of mandarins. In: *Compendium of*

Citrus Diseases (L.W. Timmer, S.M. Garnsey, J.H. Graham ed.), APS Press, Inc., St. Paul, MN, USA, 19–21.

Timmer L.W., Peever T.L., Solel Z., Akimitsu K., 2003. Alternaria diseases of citrus-novel pathosystems. *Phytopathologia Mediterranea* 42: 99–112.

Vega B., Dewdney M.M., 2014. Distribution of QoI resistance in populations of tangerine-infecting *Alternaria alternata* in Florida. *Plant Disease* 98: 67–76.

Vega B., Liberti D., Harmon P.F., Dewdney M.M., 2012. A rapid resazurin-based microtiter assay to evaluate QoI sensitivity for *Alternaria alternata* isolates and their molecular characterization. *Plant Disease* 96: 1262–1270.

Walton J.D., 1996. Host-selective toxins: Agents of compatibility. *Plant Cell* 8: 1723–1733.

White T.J., Bruns T.D., Lee S.B., Taylor J.W. 1990. Amplification and direct sequencing of fungal ribosomal RNA genes for phylogenetics. In: PCR protocols: a guide to methods and applications (M.A. Innis, D.H. Gelfand, J.J. Sninsky, T.J. White (ed). Academic Press, New York, 315–322.

Woudenberg J.H.C., Groenewald J.Z., Binder M., Crous P.W., 2013. *Alternaria* redefined. *Studies in Mycology* 75: 171–212.

Woundernberg J.H.C., Seidl M.F., Groenewald J.Z., De Vries M., Stielow J.B., … Crous P.W., 2015. *Alternaria* section *Alternaria*: Species, *formae speciales* or pathotypes? *Studies in Mycology* 82: 1–21.

Phytopathologia Mediterranea
The international journal of the
Mediterranean Phytopathological Union

Firenze University Press
www.fupress.com/pm

Research Paper

Molecular and pathogenic characterization of *Cochliobolus* anamorphs associated with common root rot of wheat in Azerbaijan

Göksel ÖZER[1,*], Mustafa IMREN[1], Mehtap ALKAN[1], Timothy C. PAULITZ[2], Harun BAYRAKTAR[3], Gülsüm PALACIOĞLU[3], Ibrahim MEHDIYEV[4], Hafiz MUMINJANOV[5], Abdelfattah A. DABABAT[6,*]

[1] *Department of Plant Protection, Faculty of Agriculture and Natural Sciences, Bolu Abant Izzet Baysal University, Bolu, 14030, Turkey*
[2] *United States Department of Agriculture, Agricultural Research Service, Wheat Health, Genetics and Quality Research Unit, Washington State University, Pullman, WA 99164-6430, USA*
[3] *Department of Plant Protection, Faculty of Agriculture, Ankara University, Ankara, 06110, Turkey*
[4] *Plant Health and Phytosanitary Control Sector of the Shaki Regional Division, Food Safety Agency of the Republic of Azerbaijan, Azerbaijan*
[5] *Food and Agriculture Organization of the United Nations, Plant Production and Protection Officer, Ankara, Turkey*
[6] *International Maize and Wheat Improvement Center (CIMMYT) P.O. Box. 39 Emek, Ankara, Turkey*
*Corresponding authors: gokozer@gmail.com, a.dababat@cgiar.org

Summary. Genetic variation among the Azerbaijani isolates of anamorphs of *Cochliobolus* spp., the causal agents of common root rot of wheat, was evaluated using pathogenicity assessments, sequence analyses of the internal transcribed spacer (ITS) region and glyceraldehyde-3-phosphate dehydrogenase (GPDH) gene, as well as inter-simple sequence repeat (ISSR) and inter-primer binding site (iPBS) markers. Twenty-eight isolates used in this study were obtained from diseased wheat plants in cereal growing regions of Azerbaijan in 2017. *Bipolaris sorokiniana*, *Curvularia spicifera*, and *Curvularia inaequalis* were identified. *Bipolaris sorokiniana* isolates were the most virulent on wheat seedlings, followed by isolates of *C. spicifera* and *C. inaequalis*. Phylogenetic analyses of a combined dataset of the ITS and GPDH regions grouped the isolates into three clusters, each of which contained isolates of one species. The dendrogram derived from the unweighted pair-grouped method by arithmetic average (UPGMA) cluster analyses based on the data of ISSR and iPBS markers divided the isolates into three clusters in concordance to their taxonomic grouping at species level, but without correlation to their geographic origins. Population structure of isolates was estimated based on Bayesian modelling, and this showed three populations (K = 3) supporting the separation of isolates in the dendrogram with the greatest mean value of Ln likelihood (-893,8). Utilization of the markers either separately or together produced a high level of polymorphism at interspecies level, which allowed for the separation of species. Although both marker systems had similar discrimination power to reveal genetic differences among the species, ISSR markers were more informative for eliciting intraspecies polymorphisms within *B. sorokiniana* and *C. spicifera* isolates.

OPEN ACCESS

Citation: G. Özer, M. Imren, M. Alkan, T.C. Paulitz, H. Bayraktar, G. Palacioğlu, I. Mehdiyev, H. Muminjanov, A.A. Dababat (2020) Molecular and pathogenic characterization of *Cochliobolus* anamorphs associated with common root rot of wheat in Azerbaijan. *Phytopathologia Mediterranea* 59(1): 147-158. doi: 10.14601/Phyto-10772

Accepted: February 18, 2020

Published: April 30, 2020

Data Availability Statement: All relevant data are within the paper and its Supporting Information files.

Competing Interests: The Author(s) declare(s) no conflict of interest.

Editor: Diego Rubiales, Institute for Sustainable Agriculture, (CSIC), Cordoba, Spain.

This is the first study on genetic diversity and population structure of anamorphic stages of *Cochliobolus* associated with common root rot of wheat using iPBS markers.

Keywords. ISSR, iPBS, phylogeny, aggressiveness.

INTRODUCTION

The species of *Cochliobolus* Drechsler are important pathogens associated with cereals. Their anamorphs are classified into *Bipolaris* and *Curvularia* genera based on morphological characteristics (Sivanesan, 1987). *Bipolaris sorokiniana* (Sacc. in Sorokin) Shoemaker [teleomorph: *Cochliobolus sativus* (S. Ito and Kuribayashi) Drechsler ex Dastur] is the most common species among *Cochliobolus* anamorphs, causing common root rot, spot blotch, seed black point, seedling blight, and head blight on wheat (Bakonyi *et al*., 1997). Common root rot (CRR) of wheat is a well-known and serious disease, which causes dark discolouration on lower leaf sheaths, crowns, subcrown internodes, and roots. CRR is responsible for annual yield losses of 6% in wheat production (Ledingham *et al*., 1973). Similar but less severe symptoms on cereals are also caused by different species of *Bipolaris* and *Curvularia*, including *B. bicolor*, *C. spicifera*, *C. inaequalis* (Gonzalez and Trevathan, 2000; Bach *et al*., 2003; Morejon *et al*., 2006; Safaee *et al*., 2008).

Using host genotypes/cultivars with natural genetic resistance and breeding new resistant cultivars to *Bipolaris* spp. and *Curvularia* spp. are likely to be the most economically and environmentally sound strategies for management of CRR. Differences both in host response and in pathogen virulence have been determined in previous studies to evaluate aggressiveness of CRR pathogens under controlled or field conditions on barley and wheat (Wildermuth *et al*., 1992; Valjavec-Gratian and Steffenson, 1997; Duveiller and Garcia, 2000; Gonzalez and Trevathan, 2000; Arabi and Jawhar, 2007, 2017). Accurate identification of isolates and analyses of the genetic and pathogenicity variabilities within pathogen populations provides key information to determine control strategies and breeding programmes. Due to their similarities, species identified as *Bipolaris* spp., *Curvularia* spp., and other anamorphs of *Cochliobolus* based on morphological characteristics pose difficulties (Sivanesan, 1987; Manamgoda *et al*., 2014, 2015). To overcome these, molecular analyses based on the internal transcribed spacer of ribosomal DNA (ITS), translation elongation factor 1-α (EF1-α), large subunit (LSU) ribosomal RNA and the glyceraldehyde 3-phosphate dehydrogenase (GPDH) locus have been successfully used for the identification of different species in these genera (Berbee *et al*., 1999; Manamgoda *et al*., 2012, 2014, 2015; Marin-Felix *et al*., 2017). Molecular marker techniques such as random amplified polymorphic DNAs (RAPD), retrotransposon microsatellite amplified polymorphism (REMAP) and amplified fragment length polymorphism (AFLP), have been most frequently and successfully utilized to reveal genetic variation among *B. sorokiniana* populations in Australia, the Czech Republic, Syria, Brazil, Poland, and the United States of America (Zhong and Steffenson, 2001; Müller *et al*., 2005; Arabi and Jawhar, 2007; Knight *et al*., 2010; Baturo-Ciesniewska, 2011; Ghazvini and Tekauz, 2012).

The inter-simple sequence repeat (ISSR) technique allows DNA amplification between identical SSR regions with a primer complementary to a target microsatellite region in PCR (Bornet and Branchard, 2001). The inter-primer binding site (iPBS) amplification technique is a universal method for DNA fingerprinting based on the universal presence of a tRNA complement as a reverse transcriptase PBS in long terminal repeats (LTR) retrotransposons (Kalendar *et al*., 2010). To date, both of these DNA marker techniques have been used in the analyses of population structures and differentiating fungal plant pathogens at intra- and interspecies levels (Özer *et al*., 2016; Altınok *et al*., 2018; Özer and Bayraktar, 2018; Skipars *et al*., 2018).

The present study was carried out to identify and characterize isolates of *Bipolaris* spp. and *Curvularia* spp. associated with crown and root rot of wheat in Azerbaijan, using sequence analysis of ITS and GPDH loci and pathogenicity tests. ISSR and iPBS molecular markers were also employed to assess genetic diversity within the isolates at intra- and interspecies levels.

MATERIAL AND METHODS

Fungus isolates

Samples of diseased plants were taken from 76 winter wheat fields located in the main wheat-growing regions of Azerbaijan, at the crop maturity stage and at harvesting time during June and July of 2017. Each sample consisted of at least 20 plants selected randomly from each field. Crown, root, sub-crown internodes, and

leaf sheaths of plants showing symptoms of CRR were washed thoroughly with running tap water to remove soil and organic particles for 3–5 min. Small sections from symptomatic tissues were surface-disinfested with 1% sodium hypochlorite solution for 1 min, rinsed with sterile distilled water, then dried between sterile tissue papers in a laminar flow cabinet. The tissue segments were then placed in 9 cm diam. Petri dishes containing 1/4 strength potato dextrose agar (PDA; Merck) supplemented with 100 mg L^{-1} streptomycin sulphate and 25 mg L^{-1} of chloramphenicol. After three-day-incubation at 22°C in constant darkness, the culture plates were examined under a dissecting microscope, and single conidia of 28 isolates similar to *Bipolaris* and *Curvularia* were picked off and transferred to Petri plates containing full strength PDA (Table 1). The plates were incubated under fluorescent lighting (12 h d^{-1}) at 22°C for 5 d. Morphological characteristics of the fungi were examined using a microscope (model DM1000, Leica Microsystems), and 30 conidia per isolate were measured at 400× magnification using the Leica LAS EZ software.

Pathogenicity assessments

The isolates were grown in 9 cm Petri dishes containing PDA and incubated at 22°C in the dark for 10 d to allow sporulation. For assessing pathogenicity, sterilized nursery soil was inoculated with a conidial suspension of each isolate to obtain an inoculum density of 250

Table 1. Isolates, their identities, locations, mean conidium dimensions, mean disease severity scores, and GenBank accession numbers related to sequences of their ITS and GPDH regions.

Isolate	Species	Location	Conidium length and width (µm)	Mean disease severity score[a]	GenBank accession numbers	
					(ITS)	(GPDH)
Co 01	*B. sorokiniana*	Qobustan	74.1 × 23.2	3.39 (ABCD)	MG661716	MH844812
Co 02	*B. sorokiniana*	İsmayıllı	75.8 × 22.2	2.85 (F)	MG654486	MK024315
Co 03	*B. sorokiniana*	İsmayıllı	79.4 × 23.0	3.36 (ABCDE)	MK022342	MH844813
Co 04	*B. sorokiniana*	İsmayıllı	84.7 × 20.6	2.88 (F)	MK022343	MH844814
Co 05	*B. sorokiniana*	İsmayıllı	81.7 × 18.9	3.05 (DEF)	MG654432	MH844815
Co 06	*B. sorokiniana*	Oğuz	71.1 × 18.9	3.53 (AB)	MG661717	MH844816
Co 07	*B. sorokiniana*	Oğuz	72.8 × 21.4	3.15 (BCDEF)	MK022344	MH844817
Co 08	*B. sorokiniana*	Oğuz	72.3 × 21.9	2.88 (F)	MK022345	MH844818
Co 09	*B. sorokiniana*	Şeki	71.3 × 21.2	3.48 (ABC)	MK022346	MK024316
Co 10	*B. sorokiniana*	Şeki	67.0 × 20.9	2.98 (EF)	MG661715	MK024317
Co 11	*B. sorokiniana*	Şeki	73.4 × 23.3	3.54 (AB)	MK022347	MK024318
Co 12	*B. sorokiniana*	Şeki	74.2 × 19.8	3.52 (ABC)	MG654433	MK024319
Co 13	*B. sorokiniana*	Şeki	73.0 × 21.9	3.33 (ABCDE)	MG654488	MK024320
Co 14	*B. sorokiniana*	Şeki	72.7 × 19.2	3.33 (ABCDE)	MG654487	MK024321
Co 15	*B. sorokiniana*	Ağdaş	83.0 × 20.9	3.44 (ABCD)	MG654434	MK024322
Co 16	*B. sorokiniana*	Kürdemir	73.0 × 18.9	2.97 (EF)	MK022348	MK024323
Co 17	*B. sorokiniana*	Kürdemir	81.2 × 18.9	3.60 (A)	MK022349	MH844819
Co 18	*B. sorokiniana*	Kürdemir	79.7 × 22.4	3.24 (ABCDEF)	MK022350	MH844820
Co 19	*B. sorokiniana*	Kürdemir	81.8 × 20.9	3.12 (CDEF)	MK022351	MH844821
Co 20	*C. spicifera*	Oğuz	27.4 × 9.7	2.01 (GHI)	MK022352	MH809683
Co 21	*C. spicifera*	Şeki	29.0 × 9.3	2.19 (GH)	MG654489	MH809678
Co 22	*C. spicifera*	Şeki	25.8 × 11.2	2.10 (GH)	MK022353	MH809679
Co 23	*C. spicifera*	Şeki	28.7 × 9.7	2.34 (G)	MK022354	MH809680
Co 24	*C. spicifera*	Şeki	30.2 × 9.5	2.31 (G)	MG661718	MH809681
Co 25	*C. spicifera*	Kürdemir	31.8 × 9.1	2.30 (G)	MK022355	MH809682
Co 26	*C. inaequalis*	Şeki	34.4 × 12.9	1.58 (J)	MG654437	MH844810
Co 27	*C. inaequalis*	Ağdaş	31.9 × 11.6	1.62 (IJ)	MK022356	MH844811
Co 28	*C. inaequalis*	Ağdaş	34.8 × 11.9	1.80 (HIJ)	MG654438	MK049127

[a]Means for each isolate within this column sharing the same letter are not significantly different ($P = 0.05$) according to the least significant difference test. LSD value for cultivar Seri-82 was 0.405.

conidia g^{-1} (Duczek *et al*., 1985). Seeds of wheat cultivar Seri-82 were sown (10 seeds per pot) into plastic pots (15 cm height, 9 cm diam.) filled with the inoculated soil. Sterilized soil was used as non-inoculated controls. Four replicates (ten seeds per replicate) were used for the experiment, which was repeated once. Resulting plants were maintained in a growth chamber with a 12 h photoperiod at 24°C for 7 weeks. Common root rot symptoms were assessed using the sub-crown internode index system (Ledingham *et al*., 1973); where 1 = no discolouration (clean), 2 = slight discolouration, 3 = extended linear lesions not surrounding the circumference (moderate), and 4 = discolouration of at least 50% and surrounding the circumference of the sub-crown internode (severe). Disease severity scores were analysed with analysis of variance, followed by Fisher's least significant difference test (LSD) at $P = 0.05$ using the Statistical Analysis System (SAS Version 9.0; SAS Institute Inc.).

DNA extraction from isolates

A modified version of the CTAB-based method, as described in the DArT protocol (http://www.diversityarrays.com), was used to extract genomic DNA from isolates. Approx. 100 mg of mycelia and conidia of each isolate were harvested by gently scraping the surface of respective cultures and was transferred into a 1.5 mL microfuge tube. Preheated (65°C) extraction–lysis buffer (750 µL; 125 mM Tris-HCl pH 8.0, 25 mM EDTA pH 8.0, 2% CTAB, 2% PVP-40, 0.8 M NaCl, 0.5% sodium disulfite, and 1% sarcosyl) was added to each tube. The sample was then uniformly homogenized by a micropestle and then incubated at 65°C for 60 min, shaken every 15 min. 750 µL of chloroform/isoamyl alcohol (24:1 v/v) was then added, mixed gently for 10 min and then centrifuged at 12,000 g for 15 min at 4°C. The supernatant was transferred to a clean centrifuge tube and 0.6 volume of isopropanol added to precipitate DNA. After centrifugation at 12,000 g for 5 min at room temperature, the supernatant was discarded. The pellet was washed with 70% ethanol (v/v) and then dried at room temperature. DNA was dissolved in 200 µL of sterile ultra-pure water. The concentration of DNA in each extraction sample was measured by spectrophotometer (DS-11 FX series, Denovix Inc.) and adjusted to 50 ng μL^{-1} for PCR assays.

ITS and GPDH amplification and sequencing

PCR amplifications were carried out in an Arktik Thermal Cycler (Thermo Scientific). PCR reactions were conducted in a 50 µL reaction mixture containing 5 µL of 10× PCR reaction buffer, 0.4 µM of each primer, 50 ng template DNA, 0.2 mM of each dNTPs, and 1.25 unit *Taq* DNA Polymerase (New England BioLabs). To amplify the ITS loci of genomic DNA, the primers ITS1 (5'-TCC GTA GGT GAA CCT GCG G-3') and ITS4 (5'-TCC TCC GCT TAT TGA TAT GC-3') (White *et al*., 1990) were used. To amplify the GPDH loci, the gpd1 (5'-CAA CGG CTT CGG TCG CAT TG-3') and gpd2 (5'-GCC AAG CAG TTG GTT GTG-3') primers were used (Berbee *et al*., 1999). The amplification protocol consisted of a 3 min initial denaturation step at 94°C and a 10 min final extension at 72°C, followed by 35 cycles for 30 s at 94°C, 30 s at 52°C, and 1 min at 72°C for the ITS, and with 1 min at 94°C, 1 min at 52°C and 45s at 72°C for the GPDH gene amplification. The amplified DNA fragments were purified with the Wizard SV Gel and PCR Clean-Up System (Promega) according to the manufacturer instructions and were subjected to bidirectional direct sequencing by a commercial company (Macrogen Inc.).

Genetic diversity evaluations using iPBS and ISSR markers

To evaluate genetic diversity among the isolates, genomic DNA was subjected to PCR amplification of 83 iPBS primers designed by Kalendar *et al*. (2010) and 20 ISSR markers including dinucleotide or trinucleotide repeats. Annealing temperatures for iPBS markers were performed as recommended, and ISSR markers were optimized depending on G+C contents of the primers. Five isolates with different morphological structures were screened with ISSR + iPBS markers to assess the ability of the markers to produce polymorphic and clear banding profiles. Five of ISSR markers and six of iPBS markers (Table 2) were selected to screen intra- and interspecific polymorphisms among all isolates. ISSR-PCR amplifications were carried out in a 25 µL reaction mixture containing 2.5 µL of 10× PCR reaction buffer, 0.24 µM of each primer, 50 ng template DNA, 200 µm of each dNTPs, and 0.8 unit *Taq* DNA Polymerase (New England BioLabs). The amplification was performed as follows: 3 min at 94°C, followed by 35 cycles of 30 s at 94°C, 30 s at an annealing temperature (between 52-54°C depending upon primers), and 2 min at 72°C, ending with one cycle of 10 min at 72°C. iPBS amplifications were conducted with Dream *Taq* DNA polymerase (Thermo Scientific) and *Pfu* DNA polymerase (Thermo Scientific) according to the protocols of Kalendar *et al*. (2010). Amplification products were subjected to electrophoresis in 1.4% (w/v) agarose gel over 1.5 h, and were visualized

Table 2. ISSR and iPBS markers used in this study and their characteristics.

Primers	Primer sequences (5'–3')[a]	T (°C)	GC (%)	TB[b]	PB[b]	PPB (%)[b]	PIC[b]	RP[b]
ISSR-SD2	ACACACACACACACACACRY	54	50	23	22	95.65	0.28	8.86
ISSR-SD3	GAGAGAGAGAGAGAGAGARY	54	50	21	21	100.00	0.27	7.93
ISSR-HR7	GAGAGAGAGAGAGAGAYT	52	47.2	16	16	100.00	0.32	4.36
ISSR-HR10	ACACACACACACACACYT	52	47.2	10	10	100.00	0.36	9.14
ISSR-HR13	BHBGAGAGAGAGAGAGA	52	51	21	21	100.00	0.29	8.50
Total				91	90			
	Average per primer			18.20	18.00	99.13	0.31	7.76
iPBS2395	TCCCCAGCGGAGTCGCCA	53	72.2	25	25	100.00	0.31	10.07
iPBS2077	CTCACGATGCCA	55	58.3	17	16	94.12	0.28	6.21
iPBS2219	GAACTTATGCCGATACCA	53	44.4	14	14	100.00	0.26	4.64
iPBS2393	TACGGTACGCCA	51	58.3	13	13	100.00	0.38	6.86
iPBS2389	ACATCCTTCCCA	50	50	13	13	100.00	0.31	5.50
iPBS2277	GGCGATGATACCA	52	53.8	13	13	100.00	0.29	5.07
Total				95	94			
	Average per primer			15.83	15.67	99.08	0.30	7.08

[a] Y, Pyrimidine; R, Purine; B, C, G or T and H, A, C, or T.
[b] T (°C) annealing temperature; TB, total band; PB, polymorphic band; PPB (%), percentage polymorphic band (%); PIC, polymorphism information content; RP, resolving power..

using a G:Box F3 Gel Documentation System (Syngene) after ethidium bromide staining.

Data analyses

The sequences were aligned with the ClustalW multiple sequence alignment method (Thompson *et al*., 1994). Phylogenetic analyses of the isolates, and reference isolates of *B. sorokiniana*, *C. spicifera*, and *C. inaequalis* available in the GenBank database, were performed with MEGA X software (Kumar *et al*., 2018) for combined datasets of the ITS region and GPDH gene. The neighbour-joining tree was constructed using the Tamura and Nei (1993) model, with 1,000 bootstrap replicates. The sequence of *Pyrenophora tritici-repentis* strain 200899 was included as an outgroup to root the phylogenetic tree.

All bands obtained by ISSR and iPBS analyses were scored as present (1) or absent (0) at positions to construct a binary data matrix. Each primer-sample combination was repeated in at least two different PCR amplifications, and only reproducible bands were evaluated. To evaluate the suitability of ISSR and iPBS markers to analyse genetic profiles of the isolates, the performance of the markers was measured using the polymorphic information content (PIC; Rolden-Ruiz *et al*., 2000) and resolving power (RP; Prevost and Wilkinson, 1999).

The data matrixes produced from each marker system were converted into a genetic similarity matrix, individually and in combination, using Jaccard's similarity coefficient with the NTSYS-pc numerical taxonomy package, version 2.02 (Rohlf, 2000). The unweighted pair-grouped method by arithmetic average (UPGMA) cluster analyses were used to construct a dendrogram. For each of the dendrograms obtained from the ISSR, iPBS and ISSR + iPBS combination data, a cophenetic matrix was generated. To check the goodness of fit of ISSR and iPBS markers, the Mantel significance test was used to calculate the correlation between the similarity coefficients matrix and the dendrogram, and compare each pair of the similarity matrices, using the MxComp Module of NTSYS 2.02 (Rohlf, 2000).

Polymorphisms among and within populations were analysed with Nei's gene diversity, Shannon's information index, degree of genetic differentiation and estimation of the amount of gene flow between populations, calculated using the Popgene statistical software ver. 1.32 (Yeh *et al*., 1999). All isolates belonging to one species were considered as one population. Further, evaluation of population genetic structure with data matrix was performed using the software Structure 2.3.4 with the Bayesian model-based clustering program (Pritchard *et al*., 2000). Structure Harvester (Earl and Vonholdt, 2012) was used to evaluate the level of genetic stratification for collating results generated by the program STRUCTURE.

RESULTS

Fungus isolates and pathogenicity assessments

A total of 106 *Cochliobolus* anamorph isolates were obtained from symptomatic wheat samples collected from 76 fields in the winter wheat growing regions of Azerbaijan in 2017. Species identification based on morphological and molecular tools showed that 96 isolates (from 19 fields) were *B. sorokiniana*, 14 isolates from six fields were *C. spicifera*, and six isolates were *C. inaequalis*. *Bipolaris sorokiniana* isolates were the most prevalent (19 of 28; 68%), followed by *C. spicifera* (six of 28; 21%) and *C. inaequalis* (3 of 28; 11%). One isolate from each of these species in the same field was selected for further studies.

The isolates were identified as *B. sorokiniana*, *C. spicifera*, and *C. inaequalis*. Mean conidium length and width dimensions (30 measurements) for these species were: *B. sorokiniana*, 76.1 (±7.2) µm × 21 (±2.4) µm; *C. spicifera,* 28.8 (±3) µm × 9.8 (±1) µm; and *C. inaequalis* 33.7 (±3.6) µm × 13.4 (±1.9) µm (Table 1).

All isolates of *B. sorokiniana* caused typical symptoms on wheat seedlings, including necrosis and discolouration of plant crowns and seminal roots, seedling blight and stunted seedlings. Discolouration of crowns and seminal roots was observed on the seedlings inoculated with *C. spicifera* isolates, but these symptoms were less severe than those induced by isolates of *B. sorokiniana*. Isolates of *C. inaequalis* caused slight discolouration of some crowns and seminal roots of the inoculated wheat seedlings. Mean disease severity scores ranged from 1.58 to 3.60 for all isolates, and differences (P = 0.05) were detected in aggressiveness among the isolates (Table 1). The mean disease severity scores were 3.2 for *B. sorokiniana* isolates, 2.2 for *C. spicifera* isolates and 1.7 observed for *C. inaequalis* isolates. No disease symptoms developed on control wheat seedlings.

Sequence alignment and phylogenetic analyses

PCR amplification of the ITS region of rDNA and GPDH region for all isolates produced DNA fragments ranging in size from 557-591 bp for the ITS region and 530-594 bp for the GPDH region. BLASTn queries based on the ITS and GPDH regions indicated that the sequences of all isolates were 99–100% identical to those of the species in the GenBank database. All obtained sequences were deposited in GenBank with the accession numbers listed in Table 1. Phylogenetic analyses based on a combined dataset of the ITS and GPDH sequences of isolates obtained from this study and reference sequences of the species available in the GenBank indicated that the isolates belonging to the different species were clearly separated from each other, and from *Pyrenophora tritici-repentis* strain 200899, with a bootstrap support of 100% (Figure 1).

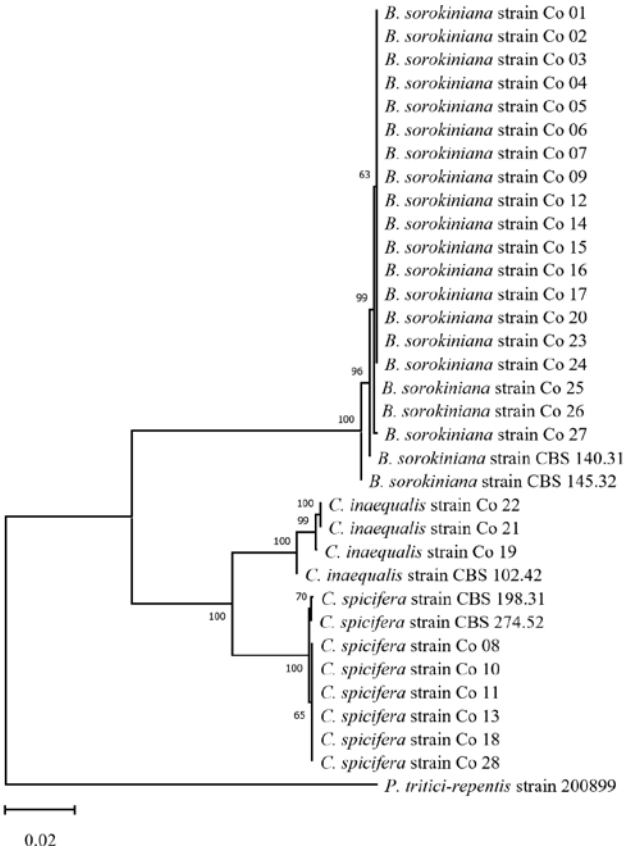

Figure 1. The neighbour-joining tree generated using Tamura and Nei (1993) for analyses of combined datasets of the ITS and GPDH sequences of 28 isolates from the present study, and for reference isolates. The phylogenetic tree was rooted with the *Pyrenophora tritici-repentis* reference strain. The percentage of replicate trees in which the associated taxa clustered together in the bootstrap test (1,000 replicates) are shown next to each branch.

iPBS and ISSR-PCR analyses

In total, 186 loci were obtained from PCR amplifications with five ISSR and six iPBS markers for 28 isolates. Both marker systems generated very distinct fragments, providing considerable variability between the isolates belonging to the different fungal species (Figure 2). A total of 91 fragments identified from ISSR-PCR were scored, out of which 90 (99%) were polymorphic (Table 2). Ninety-five reproducible fragments from iPBS PCR were scored, out of which 94 (99%) were polymorphic.

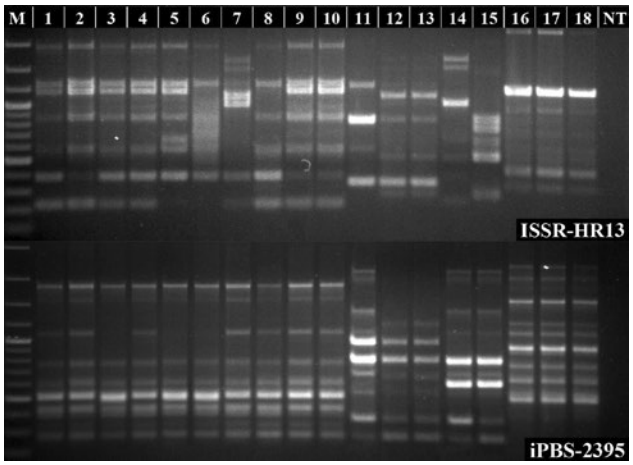

Figure 2. The representative of reproducible gel profiles with ISSR-HR13 and iPBS2395 primers. Lanes 1-10, *Bipolaris sorokiniana*; lanes 11-15, *Curvularia spicifera*; lanes 16-18, *Curvularia inaequalis*. Lane M is the DNA marker GeneRuler 100 bp plus (Thermo Scientific).

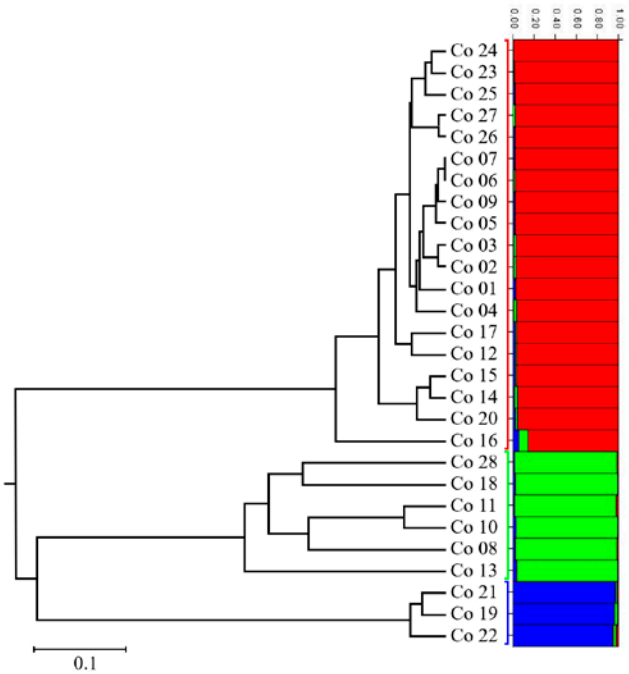

Figure 3. UPGMA tree based on the ISSR and iPBS combined marker data for 28 isolates, and STRUCTURE bar plots for individual assignment results for K = 3.

The number of amplified fragments with ISSR primers ranged from 10 (ISSR-HR7) to 23 (ISSR-SD2), giving a ratio of 18.2 bands per primer, while with iPBS primers ranged from 13 (iPBS2393; iPBS2389 and iPBS2277) to 25 (iPBS2395) with 15.83 fragments per primer.

PIC and RP indices were calculated for the two marker systems and are presented in Table 2. The greatest PIC index of 0.36 (ISSR-HR10) and the least PIC index 0.27 (ISSR-SD3), with an average PIC per primer of 0.31, were obtained from ISSR primers. For iPBS primers, PIC indices ranged from 0.26 (iPBS2219) to 0.38 (iPBS2393), with an average of 0.30. The means of RP indices, a parameter for the discriminatory potential of the primers, were 7.76 for ISSR primers and 7.08 for iPBS primers. Primer iPBS2395 produced the greatest RP value (10.07), while the ISSR-HR7 primer yielded the least RP index of 4.36.

The isolates on dendrograms from UPGMA cluster analyses of ISSR + iPBS combination data (Figure 3) grouped into three major clusters, which comprised the isolates of each particular species based on genetic similarity. Geographical-based clustering for the isolates did not occur in the phylogenetic tree. The cophenetic correlation values were 0.995 for ISSR data, 0.968 for iPBS data and 0.998 for ISSR + iPBS combination data. The correlation value between cophenetic matrix values obtained from these analyses was $r = 0.967$, suggesting very close similarity between ISSR and iPBS dendrograms.

The values of the genetic parameters were calculated with each dataset from ISSR, iPBS and ISSR + iPBS, including observed number of alleles (N_a), effective number of alleles (N_e), Nei's gene diversity (h) and Shannon's information index (I), to provide a detailed assessment of the distribution of genetic variation among populations that shared close similarities (Table 3). The value of h among the species was determined from the ISSR markers (0.30), which was similar to values detected by the iPBS and ISSR + iPBS data. The average values of G_{st} and N_m were 0.52 and 0.46 for ISSR, 0.67 and 0.25 for iPBS, and 0.60 and 0.34 for ISSR + iPBS. The value of genetic variation among the populations (G_{st}) was greater in iPBS (0.67) than ISSR (0.52), but the estimate

Table 3. Summary of genetic diversity indices analysed in populations of isolates.

Marker		Genetic diversity index[a]					
		N_a	N_e	h	I	G_{st}	N_m
ISSR	Mean	1.99	1.48	0.30	0.46	0.52	0.46
	St. Dev	0.10	0.30	0.14	0.17		
iPBS	Mean	1.99	1.48	0.30	0.47	0.67	0.25
	St. Dev	0.10	0.25	0.12	0.15		
iPBS + ISSR	Mean	1.99	1.48	0.30	0.47	0.60	0.34
	St. Dev	0.10	0.28	0.13	0.16		

[a] N_a, observed number of alleles; N_e, effective number of alleles; h, Nei's (1973) gene diversity; I, Shannon's Information index; G_{st}, degree of genetic differentiation; N_m, estimate of gene flow.

Table 4. Genetic variation values for three fungal species, from ISSR and iPBS markers.

Species	NI[a]	Marker	Value[a]				
			TB	PB	PPB (%)	h	I
Bipolaris sorokiniana	19	ISSR	47	30	63.83	0.147	0.240
		iPBS	37	2	5.40	0.015	0.024
Curvularia spicifera	6	ISSR	47	37	78.72	0.316	0.462
		iPBS	40	15	37.50	0.151	0.221
Curvularia inaequalis	3	ISSR	25	2	8.00	0.035	0.050
		iPBS	35	4	11.43	0.050	0.073

[a] NI, number of isolates; TB, total band; PB, polymorphic band; PPB (%), percentage polymorphic band; h, Nei's (1973) gene diversity; I, Shannon's Information index.

of gene flow among the populations (N_m) was more in ISSR (0.46) than iPBS (0.25). To reveal the genetic variability within populations, the ISSR markers provided a greater percentage of polymorphic bands, *h*, and *I* value, than those of the iPBS markers for *B. sorokiniana* and *C. spicifera*. In comparison, relatively high values of these genetic diversity parameters were obtained for *C. inaequalis* with the iPBS marker system (Table 4).

Analyses by STRUCTURE indicated that the isolates distinctly clustered according to their respective taxonomic groups, and the 28 isolates were in three clusters (Figure 3). The result of the harvester structure analyses showed that the best dataset number for the three populations was K = 3, providing the greatest mean value (-893,8) of Ln likelihood for the data.

DISCUSSION

Species of *Bipolaris* and *Curvularia*, which are the anamorphs of *Cochliobolus* species, are important plant pathogens of Poaceae host plants. Disease symptoms caused by these pathogens include leaf spots, blight, root rot, and crown rots (Sivanesan, 1987; Berbee *et al*., 1999; Manamgoda *et al*., 2014). The present study focused on isolates of *Bipolaris* and *Curvularia* species obtained from wheat afflicted with root and crown rot in Azerbaijan.

Twenty-eight isolates from diseased wheat plants were separated into three groups using morphological and molecular characterization methods. These were *B. sorokiniana* (19 isolates), *C. spicifera* (six isolates) and *C. inaequalis* (three isolates), as presented in Table 1. This is the first report of *C. spicifera* and *C. inaequalis* causing root and crown rot on wheat in Azerbaijan. *Bipolaris sorokiniana* was the predominant species occurring on crown and root tissues of wheat and was detected in 25% of the fields surveyed. This confirms previous observations, that this fungus has been the most frequently isolated from crown and root tissues of winter wheat (Fedel-Moen and Harris, 1987; Chen *et al*., 1996).

Comparison of the conidium sizes of the three species examined in this study was consistent with results from previous studies conducted by Sivanesan (1987), Koo *et al*. (2003), and Morejon *et al*. (2006). The conidium characteristics were useful criteria for the discrimination of *B. sorokiniana* isolates from other isolates, but could not be used for the differentiation between *C. spicifera* and *C. inaequalis* due to their morphological similarities. Previous studies have recommended using molecular tools to distinguish these species, due to inadequate differentiation using morphological characters (Berbee *et al*., 1999; Marin-Felix *et al*., 2017). The multi-sequence analyses of ITS and GPDH sequences have been suggested to identify and differentiate the species in *Bipolaris* and *Curvularia* (Manamgoda *et al*., 2012, 2014, 2015). The phylogenetic tree constructed in the present study, based on the ITS and GPDH gene of isolates, distinctly separated all the isolates into three clusters according to their taxonomic groups.

Pathogenicity tests demonstrated that all the isolates (all three species) were pathogenic to wheat but at a different level of pathogenicity. The study conducted by Ghazvini and Tekauz (2007) also reported no host specificity amongst similar fungi. However, pathogenicity comparisons, among these species showed that the *B. sorokiniana* isolates produced more severe symptoms on wheat seedlings than *C. spicifera* or *C. inaequalis* isolates. Similarly, Gonzalez and Trevathan (2000) showed that isolates of *C. spicifera* were virulent on wheat, causing discolouration of the seedling crowns and seminal roots, but these symptoms were less severe than those produced by *B. sorokiniana* isolates. Following identification and the pathogenicity test, *B. sorokiniana* was here shown to be the most aggressive of the three species associated with wheat, as well as the most widespread in Azerbaijan. This species has been reported as the most common fungus associated with root and crown rot of wheat in Turkey, the North China Plain, and Canada (Ledingham *et al*., 1973; Tunali *et al*., 2008; Xu *et al*., 2018). Statistically significant differences in virulence of the isolates belonging to each species were found in the present study. These could be explained by genetic differences between the isolates. Ghazvini and Tekauz (2012) found a close association between genetic diversity and virulence of *B. sorokiniana* on barley.

The possibility of genetic polymorphism among isolates was investigated with iPBS and ISSR markers. iPBS

markers have been successfully used to evaluate genetic diversity in fungi since this was discovered in 2010 by Kalendar *et al.* (Özer *et al.*, 2016; Özer and Bayraktar, 2018; Wu *et al.*, 2019; Ates *et al.*, 2019). Similarly, ISSR markers have been more extensively used for the analyses of different fungal populations (Bayraktar and Dolar, 2009; Altınok *et al.*, 2018). iPBS markers have not previously been employed for studying genetic diversity in these genera. In the present study, each of the UPGMA cluster analyses from the genetic dissimilarity matrices derived from ISSR, iPBS and combined ISSR + iPBS data provided clear differentiation among three anamorph species of *Cochliobolus* (Figure 3). The harvester structure analyses showed that the best dataset number for the three populations was K = 3, at which population of 28 individuals was divided into three clusters similar to the dendrogram. No apparent relationship, however, was obtained between the clustering and geographic origins of the isolates. This result is similar to those of Arabi and Jawhar (2014) and Knight *et al.* (2010). Although marker systems iPBS, based on retrotransposons, and ISSR, based on microsatellite repeat regions, differ in the nature of the respective evolutionary mechanisms underlying changes and distribution in the genome of the fungi, the highly significant correlation coefficient (r = 0.967) was determined between the co-phenetic matrices based on the genetic distance for ISSR and iPBS data. The high cophenetic correlation values indicate that both molecular markers were powerful tools for analysing interspecific variability among the isolates. The values of percentage polymorphic bands, polymorphism information content, and resolving power in these molecular marker systems were almost similar, which was in accordance with similar studies on *Lens* species (Baloch *et al.*, 2015). In all the isolates, the G_{st} and N_m values were, respectively, 0.67 and 0.25 for iPBS markers and 0.52 and 0.46 for ISSR markers. This showed that the majority of genetic variation obtained from these marker systems, especially the iPBS markers, resulted from differences among the species, not within the species.

To evaluate genetic variability among *B. sorokiniana* isolates from Azerbaijan, ISSR markers provided greater resolution, and were marginally more informative, than the iPBS marker system, with the values of 63.83, 0.147 and 0.24, respectively, for percentage polymorphic bands, *h* and *I* analyses. The mean of polymorphic bands (PB) produced by ISSR markers was 6.0 with the nineteen *B. sorokiniana* isolates, while Yadav *et al.* (2013) found 3.4 PB per RAPD marker with Indian isolates, and an average of 6.1 PB was produced by AFLP markers with Australian isolates (Mann *et al.*, 2014) and 11.9 PB with the isolates obtained from seven countries including the United States of America, Canada, Brazil, Poland, China, Uruguay, and Japan (Zhong and Steffenson, 2001). Similarly, the ISSR markers provided more detailed information to investigate polymorphisms among the isolates of *C. spicifera*, while iPBS markers were slightly better for isolates of *C. inaequalis*.

In the present study, high levels of interspecific variation among *Bipolaris* and *Curvularia* isolates was detected by the pathogenicity tests, sequencing of ITS and GPDH regions, and the ISSR and iPBS marker systems. These results confirmed that the sequencing of the ITS and GPDH regions could provide useful information for the identification and discrimination of the species used in this research. Comparisons of the information with marker systems revealed that ISSR markers showed highly informative markers for investigating genetic polymorphisms among the pathogen populations causing root rot disease on wheat. This study presented, for the first time, molecular data for *Cochliobolus* anamorphs of associated with common root rot of wheat using iPBS markers. The high polymorphism rate at the interspecies level, derived using ISSR and iPBS markers either separately or together, provided valuable information for species identification, and for elucidating evolutionary relationships among the pathogen species without any sequence data.

ACKNOWLEDGEMENTS

The authors thank the Food and Agriculture Organization of the United Nations, CIMMYT and Research and Development Unit (BAP) of Bolu Abant Izzet Baysal University (Project no: 2018.10.06.1392) for funding this study. The tremendous efforts are appreciated of Mr. Vugar Bashirov (National Project Management Consultant, FAO, Azerbaijan) during the project period. Colleagues are also thanked for their support during the project, especially Mr. Agil Gasimov, Mr. Jamal Guliyev, Mr. Taleh Shamiyev, Ms. Gular Ahmadova, and Ms. Sabina Khalilova. Colleagues in the survey regions provided invaluable support, particularly Mr. Talat Mehdiyev, Mr. Movsum Huseinov, Mr. Nazim Bakhshaliev, Mr. Asadov Akif, Mr. Javanshir Talai, Ms. Konul Aslanova, and Mr. Atabay Jahangirov.

LITERATURE CITED

Altinok H.H., Can C., Altinok M.A., 2018. Characterization of *Fusarium oxysporum* f. sp. *melongenae* isolates from Turkey with ISSR markers and DNA sequence

analyses. *European Journal of Plant Pathology* 150: 609–621.

Arabi M.I.E., Jawhar M., 2007. Molecular and pathogenic variation identified among isolates of *Cochliobolus sativus*. *Australasian Plant Pathology* 36: 17–21.

Arabi M.I.E., Jawhar M., 2014. Cultural and genetic evaluation of *Cochliobolus sativus* during successive passages through susceptible barley. *Advances in Horticultural Science* 28: 119–122

Ates D., Altinok H.H., Ozkuru E., Ferik F., Erdogmus S., Can C., Tanyolac M.B., 2019. Population structure and linkage disequilibrium in a large collection of *Fusarium oxysporum* strains analysed through iPBS markers. *Journal of Phytopathology* 167: 576–590.

Bach E.E., Barros B.C., Kimati H., 2003. Induced resistance against *Bipolaris bicolor*, *Bipolaris sorokiniana* and *Drechslera tritici-repentis* in wheat leaves by xanthan gum and heat-inactivated conidial suspension. *Journal of Phytopathology* 151: 411–418.

Bakonyi J., Aponyi I., Fischl G., 1997. Diseases caused by *Bipolaris sorokiniana* and *Drechslera tritici repentis* in Hungary. In: *Helminthosporium Blights of Wheat: Spot Blotch and Tan Spot* (E. Duveiller, H.J. Dubin, J. Reeves, A. McNab, eds.) CIMMYT, DF, Mexico, 80–85.

Baloch F.S., Derya M., Andeden E.E., Alsaleh A., Cömertpay G., Kilian B., Özkan H., 2015. Inter-primer binding site retrotransposon and inter-simple sequence repeat diversity among wild *Lens* species. *Biochemical Systematics and Ecology* 58: 162–168.

Baturo-Ciesniewska A., 2011. Genetic variability and pathogenicity among Polish isolates of *Bipolaris sorokiniana* from spring barley. *Journal of Plant Pathology* 93: 291–302.

Bayraktar H., Dolar F.S., 2009. Genetic diversity of wilt and root rot pathogens of chickpea, as assessed by RAPD and ISSR. *Turkish Journal of Agriculture and Forestry* 33: 1-10.

Berbee M.L., Pirseyedi M., Hubbard S., 1999. *Cochliobolus* phylogenetics and the origin of known, highly virulent pathogens, inferred from ITS and glyceraldehyde-3-phosphate dehydrogenase gene sequences. *Mycologia* 91: 964–977.

Bornet B., Branchard M., 2001. Nonanchored inter simple sequence repeat ISSR markers: reproducible and specific tools for genome fingerprinting. *Plant Molecular Biology Reporter* 19: 209–215.

Chen C., Collins D. J., Morgan-Jones G., 1996. Fungi associated with root rot of winter wheat in Alabama. *Journal of Phytopathology* 144: 193–196.

Duczek L.J., Verma P.R., Spurr D.T., 1985. Effect of inoculum density of *Cochliobolus sativus* on common root rot of wheat and barley. *Canadian Journal of Plant Pathology* 7: 382–386.

Duveiller E., Garcia Altamirano I., 2000. Pathogenicity of *Bipolaris sorokiniana* isolates from wheat roots, leaves and grains in Mexico. *Plant Pathology* 49: 235–242.

Earl D.A., Vonholdt B.M., 2012. Structure Harvester: a website and program for visualizing Structure output and implementing the Evanno method. *Conservation Genetics Resources* 4: 359–361.

Fedel-Moen R., Harris J.R., 1987. Stratified distribution of *Fusarium* and *Bipolaris* on wheat and barley with dryland root rot in South Australia. *Plant Pathology* 36: 447–454.

Ghazvini H., Tekauz A., 2007. Virulence diversity in the population of *Bipolaris sorokiniana*. *Plant Disease* 91: 814–821.

Ghazvini H., Tekauz A., 2012. Molecular diversity in the barley pathogen *Bipolaris sorokiniana* (*Cochliobolus sativus*). *Australasian Plant Pathology* 41: 283–293.

Gonzalez M.S., Trevathan L.E., 2000. Identity and pathogenicity of fungi associated with root and crown rot of soft red winter wheat grown on the upper coastal plain land resource area of Mississippi. *Journal of Phytopathology* 148: 77–85.

Kalendar, R. Antonius, K. Smýkal, P. Schulman, A.H. 2010. iPBS: a universal method for DNA fingerprinting and retrotransposon isolation. *Theoretical and Applied Genetics* 121: 1419–1430.

Knight N.L., Platz G.J., Lehmensiek A., Sutherland M.W., 2010. An investigation of genetic variation among Australian isolates of *Bipolaris sorokiniana* from different cereal tissues and comparison of their abilities to cause spot blotch on barley. *Australasian Plant Pathology* 39: 207–216.

Koo H.M., Lee S.H., Jung I.M., Chun S.C., 2003. A seedborne fungus *Bipolaris spicifera* detected from imported grass seeds. *The Plant Pathology Journal* 19: 133–137.

Kumar S., Stecher G., Li, M., Knyaz C., Tamura K., 2018. MEGA X: molecular evolutionary genetics analyses across computing platforms. *Molecular Biology and Evolution* 35: 1547–1549.

Ledingham R.J., Atkinson T.G., Horricks J.S., Mills, J.T., Piening L.J., Tinline R.D., 1973. Wheat losses due to common root rot in the prairie provinces of Canada, 1969–71. *Canadian Plant Disease Survey* 53: 113–122.

Manamgoda D.S., Cai L., McKenzie E.H.C., Crous P.W., Madrid H., … Hyde K.D., 2012. A phylogenetic and taxonomic re-evaluation of the *Bipolaris - Cochliobolus - Curvularia* Complex. *Fungal Diversity* 56: 131–144.

Manamgoda D.S., Rossman A.Y., Castlebury L.A., Crous P.W., Madrid H., Chukeatirote E., Hyde K.D., 2014. The genus *Bipolaris*. *Studies in Mycology* 79: 221–288.

Manamgoda D.S., Rossman A.Y., Castlebury L.A., Chukeatirote E., Hyde K.D., 2015. A taxonomic and phylogenetic re-appraisal of the genus *Curvularia* Pleosporaceae: human and plant pathogens. *Phytotaxa* 212: 175–198.

Mann M.B., Minotto E., Feltrin T., Milagre L.P., Spadari C., Van Der Sand S.T., 2014 Genetic diversity among monoconidial and polyconidial isolates of *Bipolaris sorokiniana*. *Current Microbiology* 69: 874–879.

Marin-Felix Y., Senwanna C., Cheewangkoon R., Crous P.W., 2017. New species and records of *Bipolaris* and *Curvularia* from Thailand. *Mycosphere* 8: 1556–1574.

Morejon K.R., Moraes M.H.D., Bach E.E., 2006. Identification of *Bipolaris bicolor* and *Bipolaris sorokiniana* on wheat seeds *Triticum aestivum* L. in Brazil. *Brazilian Journal of Microbiology* 37: 247–250.

Müller M.V.G., Germani J.C., Van Der Sand S.T., 2005. The use of RAPD to characterize *Bipolaris sorokiniana* isolates. *Genetics and Molecular Research* 4: 642–652.

Nei M., 1973. Analysis of Gene Diversity in Subdivided Populations. *PNAS* 70: 3321–3323;

Özer G., Bayraktar H., Baloch F.S., 2016. iPBS retrotransposons 'A Universal Retrotransposons' now in molecular phylogeny of fungal pathogens. *Biochemical Systematics and Ecology* 68: 142–147.

Özer G., Bayraktar H., 2018. Genetic diversity of *Fusarium oxysporum* f. sp. *cumini* isolates analyzed by vegetative compatibility, sequences analyses of the rDNA IGS region and iPBS retrotransposon markers. *Journal of Plant Pathology* 100: 225–232.

Pritchard J.K., Stephens M., Rosenberg N.A., Donnelly P., 2000. Association mapping in structured populations. *The American Journal of Human Genetics* 67: 170–181.

Prevost A., Wilkinson M.J., 1999. A new system of comparing PCR primers applied to ISSR fingerprinting of potato cultivars. *Theoretical and Applied Genetics* 98: 107–112.

Rohlf F.J., 2000. NTSYS-pc, numerical taxonomy and multivariate analyses system, vol v. 2.1. Exceter Software, New York.

Roldàn-Ruiz I., Dendauw J., Van Bockstaele E., Depicker A., De Loose M.A.F.L.P., 2000. AFLP markers reveal high polymorphic rates in ryegrasses *Lolium* spp. *Molecular Breeding* 6: 125–134.

Safaee D., Okhovat S.M., Hedjaroude G.H., Younesi H., 2008. Diagnosis of *Bipolaris* form species involving root and crown rot of wheat, their distribution and disease severity in Kermanshah Province. *Journal of Science and Technology of Agriculture and Natural Resources* 12: 207–214.

Sivanesan A., 1987. Graminicolous species of *Bipolaris, Curvularia, Drechslera, Exserohilum* and their teleomorphs. CAB International, Wallingford, UK, 261pp.

Šķipars V., Siaredzich M., Belevich V., Bruņeviča N., Brūna L., Ruņģis D.E., 2018. Genetic differentiation of *Phoma* sp. isolates using retrotransposon-based iPBS assays. *Environmental and Experimental Biology* 16: 307–314.

Tamura K., Nei M., 1993. Estimation of the number of nucleotide substitutions in the control region of mitochondrial DNA in humans and chimpanzees. *Molecular Biology and Evolution* 10: 512–526.

Thompson J.D., Higgins D.G., Gibson T.J., 1994. CLUSTAL W: improving the sensitivity of progressive multiple sequence alignment through sequence weighting, position-specific gap penalties and weight matrix choice. *Nucleic Acids Research* 22: 4673–4680.

Tunali B., Nicol J.M., Hodson D., Uckun Z., Büyük O., Erdurmuş D., Bağci S.A., 2008 Root and crown rot fungi associated with spring, facultative, and winter wheat in Turkey. *Plant Disease* 92: 1299–1306.

Valjavec-Gratian M., Steffenson B.J., 1997. Genetics of virulence in *Cochliobolus sativus* and resistance in barley. *Phytopathology* 87: 1140–1143.

White T.J., Bruns T., Lee S.J.W.T., Taylor J.L., 1990. Amplification and direct sequencing of fungal ribosomal RNA genes for phylogenetics. *PCR protocols: a guide to methods and applications* 18: 315–322.

Wildermuth G.B., Tinline R.D., McNamara R.B., 1992. Assessment of yield loss caused by common root rot in wheat cultivars in Queensland. *Australian Journal of Agricultural Research* 43: 43–58.

Wu J., Xie X., Shi Y., Chai A., Wang Q., Li B., 2019. Analysis of pathogenic and genetic variability of *Corynespora cassiicola* based on iPBS retrotransposons. *Canadian Journal of Plant Pathology* 41: 76–86.

Xu F., Yang G., Wang J., Song Y., Liu L., Zhao K., Han Z., 2018. Spatial distribution of root and crown rot fungi associated with winter wheat in the North China Plain and its relationship with climate variables. *Frontiers in Microbiology* 9: 1054.

Yadav B., Singh R., Kumar A., 2013. Genetic variability and relationship analyses of *Bipolaris sorokiniana* isolates causing spot blotch disease in wheat using random amplified polymorphic DNA RAPD markers. *African Journal of Biotechnology* 12: 2526–2531.

Yeh F.C., Yang R.C., Boyle T., 1999. POPGENE version1. 32, Microsoft window-base software for population genetic analyses: a quick user's guide. University of

Alberta. Center for International Forestry Research, Alberta, Canada.
Zhong S., Steffenson B.J., 2001. Virulence and molecular diversity in *Cochliobolus sativus*. *Phytopathology* 91: 469–476.

Phytopathologia Mediterranea
The international journal of the
Mediterranean Phytopathological Union

Firenze University Press
www.fupress.com/pm

Research Paper

A non-pathogenic strain of *Fusarium oxysporum* and grape marc compost control Verticillium wilt of olive

Antonio MULERO-APARICIO*, Antonio TRAPERO, Francisco Javier LÓPEZ-ESCUDERO

Departamento de Agronomía, ETSIAM, Universidad de Córdoba, Campus de Rabanales, Edif. C4, 14071 Córdoba, Spain
*Corresponding author: z32muapa@uco.es

Summary. Verticillium wilt of olive (VWO), caused by the widespread soil-borne fungus *Verticillium dahliae* Kleb., is currently the most serious disease affecting olive trees (*Olea europaea* L.) in all production areas. An integrated management strategy using eco-friendly approaches such as genetic resistance and biological control is considered the most advisable approach for controlling the disease in commercial olive orchards. This study evaluated a non-pathogenic strain of *F. oxysporum* (FO12) and the grape marc compost CGR03 for reducing inoculum density of *V. dahliae* and the disease progress in two olive cultivars with different VWO resistance levels. The experiment was conducted under semi-controlled conditions, using a naturally infested soil with two inoculum densities of *V. dahliae*. The biocontrol treatments (FO12 and CGR03) were previously selected out of 220 natural products as two of the most effective treatments against the pathogen. FO12 and CGR03 treatments significantly reduced pathogen inoculum density in comparison with that of the control (P = 0.05), with minimum microsclerotium amounts of 0.13 g^{-1} for FO12 and 0.53 g^{-1} for CGR03, during the experimental period. CGR03 reduced the progression of the disease compared with that in the control (P = 0.05), and FO12 achieved complete control of VWO, since no plants treated with this biological control strain developed VWO symptoms. This study highlights the effectiveness of these biocontrol treatments, and the potential use of eco-friendly approaches for control of VWO.

Keywords. Biocontrol agents, *Olea europaea*, organic amendment, microsclerotia, *Verticillium dahliae*.

OPEN ACCESS

Citation: A. Mulero-Aparicio, A. Trapero, F.J. López-Escudero (2020) A non-pathogenic strain of *Fusarium oxysporum* and grape marc compost control Verticillium wilt of olive. *Phytopathologia Mediterranea* 59(1): 159-167. doi: 10.14601/Phyto-11106

Accepted: February 19,2020

Published: April 30, 2020

Data Availability Statement: All relevant data are within the paper and its Supporting Information files.

Competing Interests: The Author(s) declare(s) no conflict of interest.

Editor: Epaminondas Paplomatas, Agricultural University of Athens, Greece.

ABBREVIATIONS:

ANOVA: Analysis of variance; BCAs: Biological control agents; DAP: Days after planting; HID: High inoculum density; ID: Inoculum density; LID: Low inoculum density; LSD: Least significant difference; MS: Microsclerotia; MSPA: Modified sodium polypectate agar medium; PDA: Potato dextrose agar; RAUDPC: Relative area under the disease progress curve; RAUIPC: Relative area under the inoculum progress curve; VWO: Verticillium wilt of olive.

INTRODUCTION

The widespread soil-borne fungus *Verticillium dahliae* Kleb. is known to cause vascular diseases in several crops with agronomic value (Pegg and Brady, 2002). Verticillium wilt of olive (VWO) is the most serious disease caused by this pathogen affecting olive trees (*Olea europaea* L.) in all olive-producing areas, causing significant economic losses and plant death (López-Escudero and Mercado Blanco, 2011). In the infested olive groves of the Guadalquivir valley (Andalusia, Spain), this disease has reached an average incidence of 20% (López-Escudero *et al*., 2010).

Since there is no efficient control of VWO when control measures are individually applied, an integrated management strategy is the most advisable approach to reducing the disease in commercial olive crops (López-Escudero and Mercado Blanco, 2011). Within this strategy, and due to current environmental concerns, eco-friendly approaches such as cultural practices, genetic resistance and biological control have acquired increased relevance. The genetic resistance levels of olive cultivars against VWO have been assessed in previous studies. López-Escudero *et al*. (2004) reported that cv. 'Picual' and 'Arbequina' are highly susceptible to the defoliating pathotype of *V. dahliae* when they are artificially inoculated by root dipping. Additionally, the relationship between inoculum density (ID) of *V. dahliae* in infested soils and the resistance among olive cultivars was confirmed in several studies. López-Escudero and Blanco-López (2007) reported that 'Picual' was extremely susceptible to *V. dahliae* when planted in soils with low ID, while 'Arbequina' was moderately resistant under the same conditions (Trapero *et al*., 2013b). This relationship was confirmed in a study carried out in commercial olive orchards (Roca *et al*., 2015).

Although there are numerous studies related to the biological control of *V. dahliae*, few have addressed the use of biocontrol treatments against VWO. The use of *Pseudomonas* spp. (Mercado-Blanco *et al*., 2004; Triki *et al*., 2012; Gómez-Lama *et al*., 2017) and *Trichoderma* spp. (Lima *et al*., 2007; Jiménez-Díaz *et al*., 2009) have been reported as promising biological control agents (BCAs) against VWO. Preliminary studies on the use of organic amendments against VWO have been conducted (Vitullo *et al*., 2013). An extensive screening was conducted to evaluate the effectiveness of 220 natural compounds, including microorganisms (Lozano-Tovar *et al*., 2013; Varo *et al*., 2016), organic amendments (Varo-Suárez *et al*., 2018) and plant extracts (Varo *et al*., 2017), against *V. dahliae*, in *in vitro* and *in planta* experiments under controlled conditions. The most effective treatments were evaluated under field conditions (Mulero-Aparicio *et al*., 2020), as the only study that has evaluated biological control treatments against VWO in natural conditions. From these two studies, a non-pathogenic strain of *Fusarium oxysporum*, designated FO12, and a grape marc compost, labelled CGR03, were selected as two of the most effective treatments against the pathogen. However, further studies evaluating these products under semi-controlled and different field conditions are essential for demonstrating their effectiveness against VWO.

Knowledge of the interactions between different disease management strategies, such as genetic resistance or biological control, used for integrated control of VWO is important for achieving efficient control of the disease. However, the combined effects of these two strategies remains unknown. The main objective of the present study was to evaluate the effect of two biological treatments, the non-pathogenic strain of *F. oxysporum* FO12 and the grape marc compost CGR03, on the progression of ID of *V. dahliae*, and on the development of VWO, using two olive cultivars with different levels of genetic resistance to the disease.

MATERIALS AND METHODS

Plant material

One-year-old rooted olive plants of cv. 'Picual' and 'Arbequina' (respectively susceptible and moderately susceptible to VWO) (Trapero *et al*., 2013a) were used for the experiment. These plants were obtained from a commercial nursery producing plants that were certified free of *V. dahliae* and other olive pathogens. At planting time, the plants were 1 y old and 1.0 to 1.1 m high, each with a single trunk and three or four secondary branches.

Naturally infested soil and inoculum density estimation

The soil used in this study was collected from a commercial field previously cultivated with cotton over the last 50 years, located in Villanueva de la Reina (UTM coordinates X: 38.012845; Y: 3.909219) in Jaen Province (Andalusia, southern Spain).

To estimate the ID of *V. dahliae* in this soil, five soil sub-samples of ≈500 g were collected from the upper 30 cm of soil, using a cylindrical soil auger. Sub-samples were mixed, air-dried at room temperature, and sieved (0.8 mm mesh) to remove large particles. Inoculum density of *V. dahliae* in the soil was estimated by wet sieving (Huisman and Ashworth, 1974) onto modified sodium polypectate agar medium (MSPA) (Butterfield and DeVay,

1977). Three samples (25 g each) of the naturally infested soil were suspended in 100 ml of distilled water, shaken at 270 rpm for 30 min at room temperature and filtered through 150 and 35 µm sieves. The residue retained on the 35 µm sieve was recovered in 100 ml of distilled water. Part of this suspension was then plated across ten plates of MSPA (1 ml/plate), and the plates were incubated for 14 d at 24 ± 2°C in the dark. Soil residues were removed from the agar surfaces under running tap water, and colonies of *V. dahliae* were counted using a stereomicroscope (Nikon SMZ-2T). The ID in soil was estimated from the number of *V. dahliae* colonies counted per sample and was expressed as microsclerotia (MS) per gram of soil (MS g^{-1}) (López-Escudero and Blanco-López, 2005).

Biocontrol treatments

Two biocontrol treatments were evaluated in this study. The grape marc compost CGR03 and the non-pathogenic strain of *Fusarium oxysporum* FO12 were selected due to their suppressive effects on VWO demonstrated in previous *in vitro* and *in vivo* experiments (Varo *et al*., 2016; Varo-Suárez *et al*., 2018; Mulero-Aparicio *et al*., 2019a).

Grape marc compost CGR03

The organic amendment CGR03 was provided by the agri-food cooperative "Cooperativa San Acacio", Montemayor, Córdoba (southern Spain). To produce the compost, grape marc wastes consisting of grape skins, seeds and stems of the grapevine cv. 'Pedro Ximénez' from the wine industry were used as feedstock. Grape marc is collected annually from August to September and composted in insulated bins each of 15 m^3 for 8 months. When the compost temperature fell below 60°C at a depth of 50 cm, the compost was turned to promote aeration and homogeneity and to renew the composting process. Compost was collected for use when the temperature permanently fell below 40°C (maturation/recolonization phase). The pH of the compost was 6.9, determined in 1:5 (v:v) compost/water extract. Before use, the compost was proven to be mature and stable by measuring its temperature (30-35°C for mature compost) to avoid phytotoxicity (Mehta *et al*., 2014; Varo-Suárez *et al*., 2018).

Non-pathogenic strain of Fusarium oxysporum

The non-pathogenic *F. oxysporum* strain FO12, from to the fungal collection of the Department of Agronomy, University of Córdoba (Spain), was used as a BCA. The isolate was prepared from a single-spore stock culture maintained on potato dextrose agar (PDA; Difco® Laboratories) slants at 4°C. Seven-d-old cultures of *F. oxysporum* incubated on PDA at 25°C under a 12-h photoperiod of fluorescent light were used as the inoculum source. To prepare the inoculum suspension of FO12 needed for the treatment, a 2 L Erlenmeyer flask containing 1 L of potato dextrose broth (PDB; Difco® Laboratories) was inoculated with a conidium suspension from a 7 d PDA-mycelium culture of the BCA. The conidium concentration of the inoculated PDB flask was adjusted to 2×10^5 conidia mL^{-1} (assessed by haemocytometer) and incubated at 25°C on an orbital shaker (Grant bio PSU-20i, Grant Instruments) at 90 rpm for 7 d. After incubation, the FO12 inoculum was adjusted to 10^6 conidia mL^{-1} prior to application.

Semi-controlled conditions and experimental design

The experiment was conducted under semi-controlled conditions in a set of microplots located at the 'Campus de Rabanales' at the University of Córdoba (UCO, Córdoba Province, Andalusia region, southern Spain. UTM coordinates X: 37.919056; Y: -4.724306) from March 2015 to January 2017. The setup consisted of a line of 18 cement and brick containers (microplots) built on the ground. Each container was of 1 m^3 capacity and was open at the bottom, and the line of containers was oriented north to south and protected from rain and excessive sun by a metal rooftop structure. This microplot system has been used previously in epidemiological studies of VWO (López-Escudero and Blanco-López, 2007; Pérez-Rodriguez *et al*., 2015).

The ID of *V. dahliae* in the original naturally infested soil (above) and used in this experiment was estimated at 168 MS g^{-1}. To study the influence of the initial ID of *V. dahliae* on the effectiveness of the two biocontrol treatments, the soil was diluted to obtain two different IDs. The original naturally infested soil was mixed with *V. dahliae*-free sand at two rates: 1:2 and 1:10 (v:v; infested soil:sand). Both mixtures were separately homogenized by mixing using a motor hoe (Zeppelin® 111 7HP) at the experimental site. The initial ID of the two mixtures was determined (as above) to be 83.6 MS g^{-1} for the high inoculum density (HID) mixture and 23.6 MS g^{-1} for low inoculum density (LID) mixture.

Each microplot was filled with 800 kg of the required soil mixture (bulk density = 1,300 kg m^3), and eight olive plants were planted in each microplot, four of each of the two cultivars. A total of 18 microplots were used in this experiment, which was carried out in a split-split-

plot design with three blocks, each block composed of six microplots, two levels of ID (HID and LID) as the main plot, three treatments (FO12, CGR03 or water treated control) as the subplot and two olive cvs. ('Arbequina' or 'Picual') as the sub-subplot, with a total of 144 olive plants (72 of each cultivar).

Plant establishment and treatment application

Olive plants were transplanted in March 2015, and microplots were treated with the grape marc compost (CGR03) or with the non-pathogenic strain of *F. oxysporum* (FO12). To prevent damage to the roots of the olive plants, CGR03 was incorporated into the soil just before planting as an organic amendment, by tillage (to 30 cm depth) with a manual hoe at a rate of 20% (v:v) (i.e., 60 L/microplot). Subsequently, microplots treated with CGR03 were planted and watered with 30 L of tap water. The treatment with FO12 was applied just after planting by watering each microplot with 30 L of the inoculum suspension (10^6 conidia mL^{-1}). Microplots treated with 30 L of tap water were used as the experimental controls. Treatments were applied twice a year at the beginning of each spring and autumn season, until the end of the experiment in January 2017. The subsequent treatments with CGR03 were applied at less than the initial dose (i.e., 30 L/microplot) by superficial tillage to prevent damage to the plants. The microplots were irrigated each week during spring, summer and autumn and biweekly during the winter season, according to Pérez-Rodríguez *et al*. (2015).

Assessment of inoculum density progress

The ID of *V. dahliae* in the soil of each microplot was periodically quantified to evaluate the ID progression over time in each treatment. A total of nine soil samples were collected during the experiment. Initially, soil samples were collected at 15, 30 and 60 d after planting (DAP). From 60 d until the end of the experiment, samples were collected at the beginning of each season, which corresponded to 100, 180, 250, 390, 470 or 570 DAP. At each sampling time, four soil sub-samples (100 g) per microplot were collected, using a cylindrical (3.5 cm × 22 cm) auger at a soil depth of 20 to 30 cm. The sub-samples from each microplot were mixed to obtain a homogenous sample, which was then processed to estimate the ID using the wet sieving method described above. The randomized area under the inoculum progress curve (RAUIPC) for each treatment was calculated by the trapezoidal integration method (Campbell and Madden, 1990) from all ID values obtained from the nine soil sampling times.

Disease assessments

The first symptoms of VWO were observed 4 months after planting, in July 2015. The plants in the experiment were surveyed each week for wilt symptoms, from disease onset until the end of the experiment in January 2017. Disease severity was estimated using a 0 to 16 rating scale, according to the proportions of plant tissue affected by chlorosis, necrosis or defoliation. The scale estimated the percentage of affected tissue using four main categories (≤ 25, 26–50, 51–75, or 76–100%), with four ratings per category. Each scale value represented the number of sixteenths of affected plant area. The scale values (X) were linearly related to the percentage of affected tissue (Y) using the equation $Y = 6.25X - 3.125$ (Varo-Suárez *et al*., 2018). At the end of the disease assessments, the relative area under the disease progress curves (RAUDPC) were calculated from the disease severity values, using the trapezoidal integration method (Campbell and Madden, 1990). In addition, plant infection by *V. dahliae* was confirmed by isolating the fungus from the affected shoots of diseased plants, as described by Varo-Suárez *et al*. (2018).

Data analyses

Analyses of variance (ANOVA) were carried out for the disease parameters (final disease severity and RAUDPC) and of the inoculum progress data (final ID and RAUIPC). Values of these parameters met the assumptions of normality and homogeneity of variances for these analyses. Final disease severity and RAUDPC data were analysed according to a split-split-plot experimental design, with the initial IDs as the main plots, treatments as the subplots and the cultivars as the sub-subplot factors. The data of final ID and RAUIPC were arranged in a split-plot design with the initial ID levels as the main plots and treatments as the subplots. When the ANOVA showed statistically significant differences among treatments, values were compared using Fisher's protected least significant difference (LSD) at $P = 0.05$. All statistical analyses were carried out using Statistix 10 (Analytical Software, 2013).

RESULTS

The ID progress of *V. dahliae* in naturally infested soils after the application of CGR03 and FO12 is repre-

sented in Figure 1. The effectiveness of CGR03 in reducing the ID of *V. dahliae* was observed at the first sampling time (15 DAP) for both initial inoculum densities (HID and LID). At this time, in the case of a high initial pathogen ID (HID), CGR03 reduced (P = 0.0006) the ID in comparison with that in the control and from the FO12 treatment, with an ID of 2.3 MS g^{-1}. A more pronounced effect from CGR03 compared with that from FO12 was observed at the first stages of the experiment (Figure 1a). On the other hand, FO12 gave a significant reduction in ID at 100 DAP (P = 0.0059) compared with the control, with a concentration of 23.9 MS g^{-1} (Figure 1a). Fluctuations in the ID of *V. dahliae* during the sampling period were observed for all treatments tested, reaching minimum values of 39.2 for the control (15 DAP), 0.8 from CGR03 (470 DAP), and 0.53 MS g^{-1} (470 DAP) from FO12. At the last sampling (570 DAP), differences (P < 0.0001) were found among treatments, with CGR03 resulting in the greatest reduction in ID, with a final ID of 1.9 MS g^{-1}.

When the initial ID was low (LID), both biocontrol treatments reduced (P = 0.0005) the ID of *V. dahliae* in comparison with that in the control at 15 DAP, with IDs of 13.6 MS g^{-1} for the control, 3.4 MS g^{-1} from the FO12 treatment, and 0.5 MS g^{-1} from CGR03 (Figure 1b). The ID of *V. dahliae* in soil treated with each of the biocontrol products remained less (P = 0.0003) than that in the control until the end of the experiment, reaching final IDs of 17.2 MS g^{-1} for the control, 3.6 MS g^{-1} from FO12, and 1.2 MS g^{-1} from CGR03. The CGR03 treatment also gave a greater reduction in the viable inocula of *V. dahliae* in this case (Figure 1b). In LID soil, fluctuations in ID during the experiment occurred from all the treatments, with minimum ID values of 13.6 MS g^{-1} for the control (15 DAP), 0.53 MS g^{-1} from CGR03 (15 DAP) and 0.13 MS g^{-1} from FO12 (470 DAP) (Figure 1b).

The initial ID had no effect on RAUIPC (P = 0.9224), but statistically significant differences were found between treatments (HID, P = 0.0004 and LID, P < 0.0001). In both cases (HID and LID), CGR03 was the most effective treatment for reducing the ID, giving significantly lower values of RAUIPC than those from FO12 and the control (respectively, 7.6 and 7.4% for HID and LID; Figure 2a and b).

VWO symptoms were first observed in control plants 17 weeks after planting (Figure 3a). A delay of symptom onset was observed in plants treated with CGR03. For microplots containing LID of *V. dahliae*, VWO were first observed in the control and CGR03-treated plants 7 months after planting (Figure 3b). Reisolations from shoots of diseased plants confirmed their infection by *V. dahliae*. There were no significant differences between the two initial pathogen ID levels and final disease severity (P = 0.4557) or RAUDPC (P = 0.1993). Similarly, no significant differences in final disease severity were

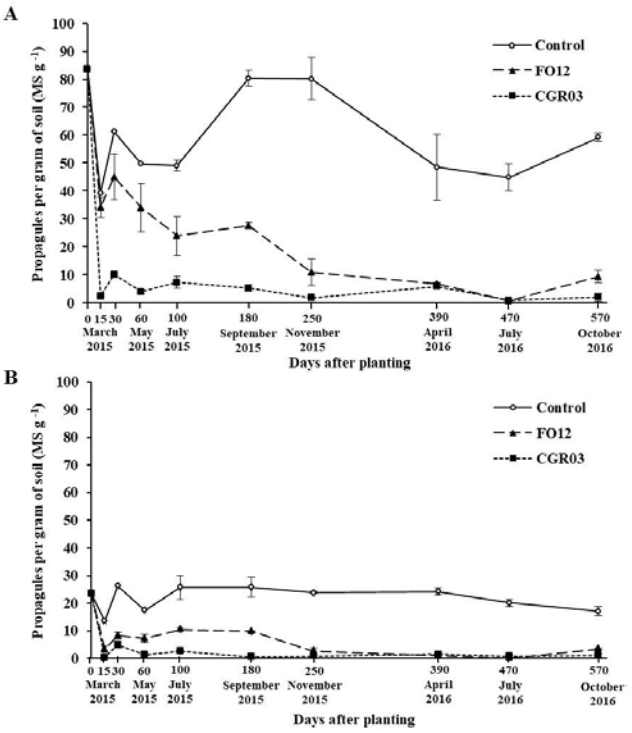

Figure 1. Progress of inoculum density (ID) of *Verticillium dahliae* at nine sampling times (from 15 to 570 days after planting), in naturally infested soils with a) high inoculum density (HID) or b) low inoculum density (LID), after treatment with FO12 or CGR03. For each sampling time, the means of three soil samples per treatment are shown, and the bars are standard errors of the means.

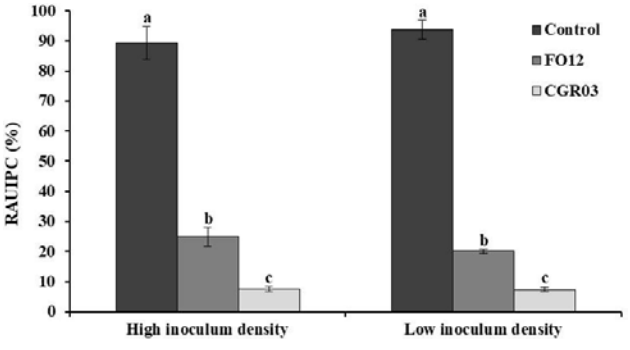

Figure 2. Mean relative area under inoculum progress curves (RAUIPC, %) in naturally infested soils with high *Verticillium dahliae* inoculum density (HID) or inoculum density (LID) for each treatment at 570 d after planting. For each treatment, the histogram is the mean of three replications. Different letters indicate statistically significant differences (P = 0.050, according to Fisher´s protected LSD test, and the bars are the standard errors of the means.

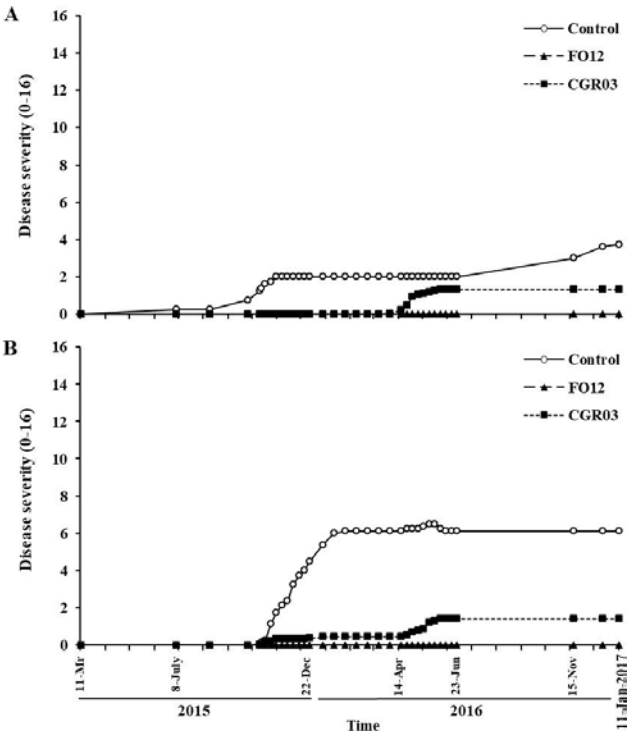

Figure 3. Progress of Verticillium wilt severity of in olive plants grown in naturally infested soils with a) high inoculum density (HID) and b) low inoculum density (LID) of *Verticillium dahliae* during 2 years under semi-controlled conditions, after treatment with the non-pathogenic *Fusarium oxysporum* strain FO12 and the grape marc compost CGR03. Disease severity was estimated based on a 0-16 scale (0 = no lesions, 16 = 94-100% of canopy with symptoms). Each datum is the mean of 24 plants.

found between cv. 'Picual' and 'Arbequina' (P = 0.2632), or RAUDPC (P = 0.5483). Data for each disease parameter (severity and RAUDPC) for both cultivars were grouped for statistical analyses (Table 1) and significant differences between treatments were observed. The plants grown in the microplots treated with CGR03 or FO12 showed had reduced disease severity (P = 0.0190) and RAUDPC (P = 0.0054) compared with those of the control (Table 1). The treatment with FO12 achieved complete control of the disease, as no plants treated with this BCA showed VWO symptoms (Table 1).

DISCUSSION

Verticillium wilt of olive is the most important disease affecting olive groves in Mediterranean countries. To date, there is no effective control measure for this disease when the control is individually applied. In this study, the non-pathogenic *F. oxysporum* strain FO12 and the suppressive grape marc compost CGR03 have been evaluated for effectiveness in controlling this major disease, under semi-controlled conditions. These biocontrol products were selected from previous studies since they were the most effective at suppressing *V. dahliae* growth *in vitro* and *in planta* (Varo *et al*., 2016; Varo-Suárez *et al*., 2018; Mulero-Aparicio *et al*., 2019a), and under field conditions (Mulero-Aparicio *et al*., 2020). This study is a final step indicating the potential of these treatments before their evaluation under different scenarios of natural infections or field conditions, where olive producers urgently require feasible control strategies.

Results obtained in this study agree with those reported by Varo-Suárez *et al*. (2018) and Mulero-Aparicio *et al*. (2019a), where CGR03 and FO12 were two of the most effective products for reducing the ID of *V. dahliae* in two different soils in an *in vitro* experiment. Similarly, these results agree with those of Mulero-Aparicio *et al*. (2020), where these treatments reduced ID of the pathogen in natural conditions. Results from the present study also indicate that the CGR03 treatment, compared with FO12, achieved a greater reduction in ID during the first stages of the experiment when the initial ID was greatest (HID). However, when the initial ID was least, both biocontrol treatments showed similar efficacy for ID reduction at the first sampling (15 DAP). In addition, the

Table 1. Disease-related parameters for olive plants grown in naturally infested soil by *Verticillium dahliae* during along 2 years under semi-controlled conditions, after treatments with the non-pathogenic strain of *Fusarium oxysporum* FO12 and the grape marc compost CGR03.

Initial ID[a]	Treatment	Disease severity (%)[b]	RAUDPC (%)[c]
High inoculum density (HID, 83.6 MS g^{-1})	Control	23.0 ± 15.2 a	16.1 ± 11.8 a
	CGR03	8.1 ± 5.2 b	5.0 ± 3.2 b
	FO12	0.0 ± 0.0 c	0.0 ± 0.0 c
Low inoculum density (LID, 23.6 MS g^{-1})	Control	37.1 ± 15.1 a	36.2 ± 14.5 a
	CGR03	8.6 ± 5.2 b	6.2 ± 3.9 b
	FO12	0.0 ± 0.0 c	0.0 ± 0.0 c

[a] Initial inoculum density (ID) of *V. dahliae* in the two soil mixtures used in the experiment.
[b] Final disease severity (%) ± standard error 22 months after planting based on a 0-16 rating scale (0 = no lesions, 16 = 94-100% of canopy with symptoms).
[c] Relative area under the disease progression curve (RAUDPC, %) ± standard error developed over the assessment period (22 months).
[b, c] In each column, data represent the mean of 24 replicated plants per treatment. Mean values followed by the same letter do not differ significantly according to Fisher's protected LSD test at P = 0.05.

minimum values of ID reached during the assessment period were similar for the CGR03 and FO12 treatments. This confirms the effectiveness of these two biological treatments for reducing viable inoculum of *V. dahliae* in naturally infested soils, regardless of the initial ID of the pathogen. Nevertheless, neither of the two biocontrol treatments tested in this study eliminated inoculum of *V. dahliae* from the soil, and the pathogen was detected at all sampling times. Fluctuations in *V. dahliae* ID during the sampling period were observed. The increases in ID observed in July 2015 and July 2016 in the HID control microplots were similar to the results of López-Escudero and Blanco-López (2001). They attributed these ID changes in July probable decreases in the superficial soil microbiota due to the high temperatures at that time of year. This change in microbiota could lead to high *V. dahliae* ID due probably to low microbial competition against the pathogen in the natural soil, or in the MSPA Petri dishes used for the assessment.

The similar levels of resistance to VWO of 'Picual' and 'Arbequina' observed in this study have been reported. Previous studies under controlled conditions reported that resistance of 'Arbequina' was overcome when plants were artificially inoculated by root dipping with a large amount of the pathogen (10^6 conidia mL^{-1}), with this cultivar showing the same level of resistance to VWO as the susceptible 'Picual' (López-Escudero *et al*., 2004). Nevertheless, in field studies carried out in naturally infested soils with ID levels ranging from 5 to 21 MS g^{-1}, 'Arbequina' had greater resistance to VWO than 'Picual' (Trapero *et al*., 2013b). Similarly, an earlier study conducted under semi-controlled conditions in brick containers and using a naturally infested soil with moderate *V. dahliae* inoculum densities (9.8 MS g^{-1}) confirmed the greater VMO resistance of 'Arbequina' compared to 'Picual' (Pérez-Rodríguez *et al*., 2015). In the present study, with much greater initial pathogen IDs (83.6 and 23.6 MS g^{-1})), both cultivars may have shown similar resistance to VWO due to the high inoculum pressure of the pathogen at the beginning of the experiment which overcame the genetic resistance of 'Arbequina'.

Plants treated with FO12 did not develop VWO symptoms over the experimental period. These results agree with those of Varo *et al*. (2016) and Mulero-Aparicio *et al*. (2019a), in which this *F. oxysporum* strain gave complete control of VWO in experiments conducted under controlled conditions. In studies evaluating the suppressive effects of organic amendments against *V. dahliae,* reductions of inoculum were correlated with reductions of disease progress in 80% of the cases (Bonanomi *et al*., 2007). In the present study, treatment with CGR03 reduced disease development in comparison with that in the control, but complete prevention of VWO was not achieved This was probably due to the presence of remaining inoculum to infect the plants. This is similar to the results of López-Escudero *et al*. (2007), who reported an initial ID of 0.04 MS g^{-1} was enough to infect olive plants of the susceptible 'Picual' and cause development of the disease.

Understanding the mechanisms of action of organic amendments in their effects against fungal diseases has become a challenge for researchers, due to their biological and chemical complexity. Organic compost based on cotton wastes reduced severity of Verticillium wilt of eggplant by triggering induced systemic resistance in host plants (Markakis *et al*., 2016). Furthermore, studies evaluating different olive mill waste composts showed that their suppressive effects against *V. dahliae* were due to biotic and abiotic factors (Papasotiriou *et al*., 2013). The mechanisms involved in the suppressive effects of the grape marc compost CGR03 remain unknown. Further research evaluating the roles of biotic and abiotic factors is required to improve the efficacy of this organic amendment against VWO.

Although FO12 was not the most efficient treatment for reducing ID of *V. dahliae*, its capability to (i) colonize the host plant rhizosphere, (ii) produce volatile organic compounds with antifungal effects, and (iii) produce chlamydospores that remain attached within host root systems (Mulero-Aparicio *et al*., 2019b). These could all play roles in its antagonistic effects against the pathogen by competing in the rhizosphere for infection sites, thus preventing the infection of olive roots by *V. dahliae* and achieving effective control of VWO. These traits have been previously observed in other non-pathogenic strains of *F. oxysporum* used as BCAs in herbaceous crops (Fravel *et al.,* 2003). For instance, the non-pathogenic *F. oxysporum* strain F2 competed with *V. dahliae* for nutrients and space on root surfaces of eggplants (Pantelides *et al*., 2009). Similarly, the widely studied non-pathogenic *F. oxysporum* strain Fo47 has been reported to use different modes of action against *V. dahliae*, including induction of systemic resistance and competition for infection points on pepper plants (Veloso *et al.,* 2016).

The effectiveness of these biocontrol products against *V. dahliae* shown in the present study confirms the consistency of these treatments, since they were previously reported as effective biocontrol treatments against *V. dahliae* in studies conducted under controlled conditions (Varo *et al*., 2016; Varo-Suárez *et al*., 2018; Mulero-Aparicio *et al*., 2019a) and in the field (Mulero-Aparicio *et al*., 2020). Consistency is considered one of the most important traits for biocontrol products (Deketelaere *et*

al., 2017), since they are often known for their contradictory results between laboratory, semi-controlled and field conditions. Further research on the modes and times of application is needed to evaluate the efficacy and consistency of these products under different commercial field conditions, as well as further research on the mechanisms responsible for the suppressive effects of these agents and products.

In conclusion, the present study highlights the effectiveness of these two biocontrol treatments for reducing *V. dahliae* ID and progress of VWO under semi-controlled conditions. This study also expands knowledge about the use of biocontrol strategies as an eco-friendly approach to effective control of VWO, within an integrated disease management strategy. Although further research is needed to study the interactions of different biocontrol treatments with olive cultivars with different resistance levels in field conditions, the results obtained here indicate potential for applying these biocontrol treatments in *V. dahliae*-infested commercial fields, both before planting and during cultivation, to reduce initial pathogen inoculum pressure. This strategy, in combination with the use of moderately resistant olive cultivars, could be effective for the control of VWO.

ACKNOWLEDGEMENTS

This research was funded by the Spanish Ministry of Science, Innovation and Universities (MICINN; project AGL2016-76240-R), and co-financed by the European Union FEDER Funds. A.M.A. is the holder of a 'Formación de Profesorado Universitario' (FPU) fellowship from the Spanish Ministry of Education, Culture and Sports (MECD).

The authors declare that they have no conflicts of interest.

LITERATURE CITED

Analytical Software, 2013. Statistix10. User's manual. Tallahassee, FL.

Bonanomi G., Antignani V., Pane C., Scala F., 2007. Suppression of soilborne fungal diseases with organic amendments. *Journal of Plant Pathology* 89: 311–324.

Butterfield E.J., DeVay J.E., 1977. Reassessment of soil assays for *Verticillium dahliae*. *Phytopathology* 67: 1073–1078.

Campbell C.L., Madden L.V., 1990. Introduction to plant disease epidemiology. John Wiley and Sons Ltd, New York, NY, USA.

Deketelaere S., Tyvaert L., França S.C., Höfte M., 2017. Desirable traits of a good biocontrol agent against Verticillium wilt. *Frontiers in Microbiology* 8: 1186.

Fravel D.R., Olivain C., Alabouvette C., 2003. *Fusarium oxysporum* and its biocontrol. *New Phytologist* 157: 493–502.

Gómez-Lama C., Sesmero R., Valverde-Corredor A., López-Escudero F.J., Mercado-Blanco J., 2017. A split-root system to assess biocontrol effectiveness and defense-related genetic responses in aboveground tissues during the tripartite interaction *Verticillium dahliae*-olive-*Pseudomonas fluorescens* PICF7 in roots. *Plant and Soil* 417: 433–452.

Huisman O.C., Ashworth Jr L.J., 1974. Quantitative assessment of *Verticillium albo-atrum* in field soils: procedural and substrate improvements. *Phytopathology* 64: 1043–1044.

Jiménez-Díaz R.M., Trapero-Casas J.L., Boned J., Landa B., Navas-Cortés J.A., 2009. Uso de Bioten para la protección biológica de plantones de olivo contra la Verticilosis causada por el patotipo defoliante de *Verticillium dahliae*. *Boletín de Sanidad Vegetal Plagas* 36: 595–615.

Lima G., De Curtis F., D´Onghia A.M., Nigro F., 2007. Comparison between real-time PCR and semi-selective medium in monitoring *Verticillium dahliae* microsclerotia in the olive rhizosphere and suppression of the pathogen by compost. *IOBC/WPRS Bulletin* 30: 221–224.

López-Escudero F.J., Blanco-López M.A., 2001. Effect of a single or double soil solarization to control Verticillium wilt in established olive orchards in Spain. *Plant Disease* 85: 489–496.

López-Escudero F.J., del Río C., Caballero J.M., Blanco-López M.A., 2004. Evaluation of olive cultivars for resistance to *Verticillium dahliae*. *European Journal of Plant Pathology* 110: 79–85.

López-Escudero F.J., Blanco-López M.A., 2005. Isolation and morphologic characterization of microsclerotia of *Verticillium dahliae* isolates from soil. *Biotechnology* 4: 296–304.

López-Escudero F.J., Blanco-López M. A., 2007. Relationship between the inoculum density of *Verticillium dahliae* and the progress of Verticillium wilt of olive. *Plant Disease* 91: 1372–1378.

López-Escudero F.J., Roca J.M., Mercado-Blanco J., Valverde-Corredor A., Blanco-López M.A., 2010. Verticillium wilt of olive in the Guadalquivir Valley (southern Spain): relations with some agronomical factors and spread of *Verticillium dahliae*. *Phytopathologia Mediterranea* 49: 370–380.

López-Escudero F.J., Mercado-Blanco J., 2011. Verticillium wilt of olive: A case study to implement an

integrated strategy to control a soil-borne pathogen. *Plant and Soil* 344: 1–50.

Lozano-Tovar M.D., Ortiz-Urquiza A., Garrido-Jurado I., Trapero-Casas A., Quesada-Moraga E., 2013. Assessment of entomopathogenic fungi and their extracts against a soil-dwelling pest and soil-borne pathogens of olive. *Biological Control* 67: 409–420.

Markakis E.A., Fountoulakis M.S., Daskalakis G.C., Kokkinis M., Ligoxigakis E.K., 2016. The suppressive effect of compost amendments on *Fusarium oxysporum* f. sp. *radicis-cucumerinum* in cucumber and *Verticillium dahliae* in eggplant. *Crop Protection* 79: 70–79.

Mehta C.M., Palni U., Franke-Whittle I.H., Sharma A.K., 2014. Compost: its role, mechanism and impact on reducing soil-borne plant diseases. *Waste Management* 34: 607–622.

Mercado-Blanco J., Rodríguez-Jurado D., Hervás A., Jiménez-Díaz R.M., 2004. Suppression of Verticillium wilt in olive planting stocks by root-associated fluorescent *Pseudomonas* spp. *Biological Control* 30: 474–486.

Mulero-Aparicio A., Agustí-Brisach C., Varo A., López-Escudero F.J., Trapero A., 2019a. A non-pathogenic strain of *Fusarium oxysporum* as a potential biocontrol agent against Verticillium wilt of olive. *Biological Control* 139. https://doi.org/10.1016/j.biocontrol.2019.104045.

Mulero-Aparicio A., Cernava T., Turrà D., Schaefer A., Di Pietro A., López-Escudero F.J., Trapero A., Berg G., 2019b. The role of volatile organic compounds and rhizosphere competence in mode of action of the non-pathogenic *Fusarium oxysporum* FO12 towards Verticillium wilt. *Frontiers in Microbiology* 10:1808.

Mulero-Aparicio A., Varo A., Agustí-Brisach C., López-Escudero F.J., Trapero A., 2020. Biological control of Verticillium wilt of olive in the field. *Crop Protection* 128. https://doi.org/10.1016/j.cropro.2019.104993.

Papasotiriou F.G., Varypatakis K.G., Christofi N., Tjamos S.E., Paplomatas E.J., 2013. Olive mill wastes: a source of resistance for plants against *Verticillium dahliae* and a reservoir of biocontrol agents. *Biological Control* 67: 51–60.

Pantelides I.S., Tjamos S.E., Striglis I.A., Chatzipavlidis I., Paplomatas E.J., 2009. Mode of action of a non-pathogenic *Fusarium oxysporum* strain against *Verticillium dahliae* using Real Time QPCR analysis and biomarker transformation. *Biological Control* 50: 30–36.

Pegg G.F., Brady B.L., 2002. Verticillium wilts. CAB International, Wallingford.

Pérez-Rodríguez M., Alcántara E., Amaro M., Serrano N., Lorite I.J., … López-Escudero F.J., 2015. The Influence of irrigation frequency on the onset and development of Verticillium wilt of olive. *Plant Disease* 99: 488–495.

Roca L.F., Moral J., Trapero C., Blanco-López M.A., López-Escudero F.J., 2015. Effect of inoculum density on Verticillium wilt incidence in commercial olive orchards. *Journal of Phytopathology* 164: 61–64.

Trapero C., Díez C.M., Rallo L., Barranco D., López-Escudero F.J., 2013a. Effective inoculation methods to screen for resistance to Verticillium wilt in olive. *Scientia Horticulturae* 162: 252–259.

Trapero C., Serrano N., Arquero O., Del Río C., Trapero A., López-Escudero F.J., 2013b. Field resistance to Verticillium wilt in selected olive cultivars grown in two naturally infested soils. *Plant Disease* 97: 668–674.

Triki M.A., Hadj-Taieb S.K., Mellouli I.H., Rhouma A., Gdoura R., Hassairi A., 2012. Identification and screening of bacterial isolates from Saharan weeds for *Verticillium dahliae* control. *Journal of Plant Pathology* 94: 305–311.

Varo A., Raya-Ortega M.C., Trapero A., 2016. Selection and evaluation of microorganisms for biocontrol of *Verticillium dahliae* in olive. *Journal of Applied Microbiology* 121: 767–777.

Varo A., Mulero-Aparicio A., Adem M., Roca L.F., Raya-Ortega M.C., … Trapero A., 2017. Screening water extracts and essential oils from Mediterranean plants against *Verticillium dahliae* in olive. *Crop Protection* 92: 168–175.

Varo-Suárez A., Raya-Ortega M.C., Agustí-Brisach C., García-Ortíz-Civantos C., Fernández-Hernández A., … Trapero A., 2018. Evaluation of organic amendments from agro-industry waste for the control of Verticillium wilt of olive. *Plant Pathology* 67: 860–870.

Veloso J., Alabouvette C., Olivain C., Flores V., Pastor V., García T., Díaz J., 2016. Modes of action of the protective strain Fo47 in controlling Verticillium wilt of pepper. *Plant Pathology* 65: 997–1007.

Vitullo D., Altieri R., Esposito A., Nigro F., Ferrara M., Alfano G., Ranalli G., De Cicco V., Lima G., 2013. Suppressive biomasses and antagonist bacteria for an eco-compatible control of *Verticillium dahliae* on nursery-grown olive plants. *International Journal of Environmental Science and Technology* 10: 209–220.

Phytopathologia Mediterranea
The international journal of the
Mediterranean Phytopathological Union

Firenze University Press
www.fupress.com/pm

Research Paper

Synergy between endophytic *Bacillus amyloliquefaciens* GGA and arbuscular mycorrhizal fungi induces plant defense responses against white rot of garlic and improves host plant growth

Younes M. RASHAD[1,*], Mohamed A. ABBAS[2], Hoda M. SOLIMAN[2], Ghada G. ABDEL-FATTAH[2], Gamal M. ABDEL-FATTAH[2]

[1] *Plant Protection and Biomolecular Diagnosis Department, Arid Lands Cultivation Research Institute, City of Scientific Research and Technological Applications, New Borg El-Arab, Egypt*
[2] *Botany Department, Faculty of Science, Mansoura University, El-Mansoura, Egypt*
*Corresponding author: younesrashad@yahoo.com

Summary. White rot, caused by *Sclerotium cepivorum*, is a serious and economically important disease of garlic, which leads to losses in the garlic production in most of the tropical, subtropical and temperate areas. Biocontrol potential of an endophytic *Bacillus amyloliquefaciens* GGA and/or arbuscular mycorrhizal fungi (AMF) against this disease was investigated. The *B. amyloliquefaciens* GGA exhibited antagonistic activity against *S. cepivorum in vitro*. Scanning electron microscopy revealed alterations in the morphology of the pathogen in response to the exposure to the bacterial metabolites. Results from a pot experiment demonstrated that application of the dual treatment of the *B. amyloliquefaciens* GGA and AMF reduced disease incidence and severity more than the single treatments, and led to the greatest increases in total phenol content, activities of the defense-related enzymes phenylalanine ammonia-lyase, polyphenoloxidase and peroxidase, and transcriptional expression levels of the defensin and chitinase genes. Growth and yield parameters of garlic plants were enhanced after this treatment. This study showed good efficacy on the tested biocontrol agents for control white rot of garlic plants grown in pots. Future research should evaluate these biocontrol strategies under field conditions.

Keywords. *Allium sativum*, chitinase, defensin, electron microscopy, real-time PCR, *Sclerotium cepivorum*.

OPEN ACCESS

Citation: Y.M. Rashad, M.A. Abbas, H.M. Soliman, G.G. Abdel-Fattah, G.M. Abdel-Fattah (2020) Synergy between endophytic *Bacillus amyloliquefaciens* GGA and arbuscular mycorrhizal fungi induces plant defense responses against white rot of garlic and improves host plant growth. *Phytopathologia Mediterranea* 59(1): 169-186. doi: 10.14601/Phyto-11019

Accepted: March 2, 2020

Published: April 30, 2020

Data Availability Statement: All relevant data are within the paper and its Supporting Information files.

Competing Interests: The Author(s) declare(s) no conflict of interest.

Editor: Jesus Murillo, Public University of Navarre, Spain.

INTRODUCTION

Garlic (*Allium sativum* L.), has been widely used since ancient times for multiple cooking and therapeutic purposes (Bayan *et al.*, 2014). In Egypt, this plant is one of the most important vegetable crops for local consumption and export, and Egypt is the sixth most important garlic-producing country. The

area of garlic cultivation in Egypt in 2018 was 12,782 ha, with total production of 286,213 tons (FAOSTAT, 2019).

White rot, caused by the soil-borne fungus *Sclerotium cepivorum* Berk, is one of the most destructive diseases of garlic, and other members of the *Allium* genus. This pathogen affects crop yields leading to yield losses up to 100% (Siyoum and Yesuf, 2013). The pathogen can produce microconidia and overwintering sclerotia. The sclerotia can remain viable in the soil for many years, and can be transmitted to non-infested fields by poor sanitation practices (Amin *et al*., 2014). Fungicides such as tebuconazole, iprodione, and dicloran are available and widely used against white rot, but these may have adverse effects on environments, human and animal health, and remain in soils for long periods (Yang *et al*., 2011).

Biological control using microbial antagonists may provide an effective, eco-friendly, and safe alternative approach to control of garlic white rot. Among promising biocontrol agents, endophytes have received increasing interest. These organisms are defined as symbionts (bacteria or fungi) that asymptomatically inhabit plant tissues for a period of their life cycles (Clay *et al*., 2016; Strobel, 2018). During these relationships, complex plant-endophyte interactions differentially occur according to the type of endophyte, host plant and environmental conditions (De Silva *et al*., 2019). Biocontrol activity of many endophytic bacteria, including *Bacillus* spp., *Burkholderia* spp., *Enterobacter* spp., *Pseudomonas* spp., and *Serratia* spp., has been studied against different plant pathogens (Hong and Park, 2016; de Almeida Lopes *et al*., 2018). Hazarika *et al*., (2019) reported *B. subtilis* SCB-1 as the most potent antagonist among seven endophytic bacteria which were isolated from sugarcane and screened for the antifungal potential against *Alternaria* sp., *Cochliobolus* sp., *Curvularia* sp., *Fusarium* sp., and *Saccharicola* sp. Their antagonistic activity was attributed to production of the antifungal lipopeptide surfactin. In general, the probable biocontrol mechanisms utilized by endophytic bacteria include direct mechanisms such as antibiosis and competition, and/or indirect mechanisms through triggering plant defense responses against invading pathogens. In addition, they may promote plant growth through phytostimulation and/or biofertilization (Santos *et al*., 2018).

Arbuscular mycorrhizal fungi (AMF), are obligate endophytes which can form mutualistic relationships with most terrestrial plants (Spatafora *et al*., 2016). Biocontrol activity of AMF against various plant diseases has been widely reported (Abdel-Fattah *et al*., 2011; El-Sharkawy *et al*., 2018; Aseel *et al*., 2019). Mustafa *et al*. (2017) reported a 78% reduction in the severity of powdery mildew of wheat plants when the plants were colonized with the *Funneliformis mosseae* under controlled conditions. AMF can also enhance plant tolerance to salinity and drought, and improve plant growth and nutrient uptake (Asrar *et al*., 2014).

The present study aimed to: 1) assess the *in vitro* antifungal activity of an endophytic *B. amyloliquefaciens* strain against *S. cepivorum,* the white rot pathogen of garlic; 2) evaluate the biocontrol potential of application of *B. amyloliquefaciens* and/or AMF on the diseased garlic plants under natural conditions; and 3) investigate probable effects of their application on molecular and biochemical host defense responses, and on growth of garlic plants.

MATERIALS AND METHODS

Microorganisms used in this study

A highly pathogenic isolate of *S. cepivorum* (S6) from a garlic plant showing white rot symptoms, was obtained from the Plant Pathology Research Institute, Egypt. Inoculum was prepared by growing this isolate in 500 mL capacity flasks containing sterilized medium composed of sand: sorghum grains (2:1, v/v) for 15 d at 20°C.

In a preliminary trial, nine isolates of endophytic bacteria were obtained from healthy garlic plants, and these were screened for their antifungal activity. A promising isolate with highly antagonistic activity was selected, identified using the 16S rRNA gene as *B. amyloliquefaciens* GGA (NCBI GenBank accession no. MN592674.1), and used in this study. Inoculum of this strain was prepared by culturing in 500 mL capacity flasks containing sterilized nutrient broth at 37°C for 2 d. The bacterial resulting inoculum was adjusted to 2×10^5 CFU mL^{-1}.

The AMF inoculum used in this study was provided by Prof. Gamal M. Ouf, Botany Department, Mansoura University, Egypt. This was a mixture of AMF species (in equal proportions), of *Funneliformis mosseae* (T.H. Nicolson & Gerd.) C. Walker & A. Schüßler, *Glomus monosporum* Gerd. & Trappe, *Acaulospora laevis* Gerd. & Trappe, and *Rhizoglomus clarum* (T.H. Nicolson & N.C. Schenck) Sieverd., G.A. Silva & Oehl. Spores of these AMF were propagated under Sudan grass in sterilized soil for 6 months (83% colonization index).

Assessment of the antagonistic in vitro *activity of the endophytic* B. amyloliquefaciens *GGA*

The antifungal activity of *B. amyloliquefaciens* GGA was assessed against *S. cepivorum* S6, using the dual cul-

ture plate technique. A 5 mm diam. disc, taken from 7 d culture of *S. cepivorum* S6 was placed 1 cm from the edge of each potato dextrose agar (PDA) plate, and a loop of *B. amyloliquefaciens* GGA was streaked 1 cm from the opposite edge of the plate. PDA plates each inoculated only with the fungal disc served as experimental controls. The test was performed in triplicate. The plates were incubated at 20°C and the inward linear growth of the pathogen was measured after 4, 8, and 12 d. The test was ended when fungal growth completely covered the control plates. Fungal growth inhibition was calculated using the following equation:

$$\text{Growth Inhibition (\%)} = \frac{R1 - R2}{R1} \times 100$$

where R1= inward linear growth in the control plate, and R2= inward linear growth in the dual culture plate.

Scanning electron microscopy (SEM)

From a dual culture plate, a PDA block (1 cm^2) of mycelial growth at the edge of the growth inhibition zone was transferred and processed for SEM observation, using the tissue processor (Leica Biosystems, Inc.). Sample fixation using osmium oxide, and dehydration by ethanol and acetone were performed before the sample was dried using a critical point drier (EMS 850), and coated with gold using a sputter coater (EMS 550), as described by Hayat (2000). The sample was then examined using a scanning electron microscope (JEOL JSM-6510LV).

Pot experiment

Pots (25 cm diam.) were each filled with 2.5 kg of autoclaved soil (2:1 clay: sand, v/v). The soil physicochemical properties were: pH, 7.8; electrical conductivity, 170 $\mu S.cm^{-1}$; organic matter, 2.11%; available phosphorus, 6.14 $\mu g\ g^{-1}$; and total nitrogen, 0.58%. Three healthy garlic cloves (cv. Sids 40) were surface sterilized using sodium hypochlorite solution (0.05%) for 3 min, rinsed with sterile water, and then planted into each pot. Ten grams of AMF inoculum (≅50 spores and infected roots pieces g^{-1} soil) was added as a seed bed under each garlic clove at the time of planting. Non-mycorrhizal cloves each received equal amount of autoclaved soil to produce the same nutrients without mycorrhizal propagules. The bacterial inoculum was applied by adding 5 mL (2×10^5 CFU mL^{-1}) onto each garlic clove at the planting time. After 4 weeks from the AMF inoculations, soil infestation was achieved by mixing *S.cepivorum* inoculum with the upper layer of the soil in each pot at the rate of 2% (w/w). The fungicide tebuconazole (50% WP) was used as a positive experimental control, and was applied as a clove dressing at the recommended dose (3mL L^{-1} cloves). Pots treated with tap water were used as negative experimental controls. All pots were arranged in a factorial design (split-split plot ($3 \times 6 \times 2$). Three levels of time (30, 60 or 90 d post-inoculation (dpi) with *S. cepivorum*), six treatments (C, F, P, B, B+P and F+P; see below) and two levels of mycorrhizal status (M or NM, see below) were applied. Twelve pots were used as replicates for each treatment. All the pots were kept under natural outdoor conditions (day temperature 25°C, night temperature 20°C, 16 h light period) and watered when necessary.

The treatments applied are summarized as follows:
CNM = untreated control;
CM = treated with AMF;
FNM = treated with tebuconazole fungicide;
FM = treated with tebuconazole and AMF;
PNM = inoculated with *S. cepivorum*;
PM = inoculated with *S. cepivorum* and treated with AMF;
FPNM = inoculated with *S. cepivorum*, and treated with tebuconazole;
FPM = inoculated with *S. cepivorum,* and treated with tebuconazole and AMF;
BNM = treated with the endophytic bacteria;
BM = treated with the endophytic bacteria and AMF;
PBNM = inoculated with *S. cepivorum*, and treated with the endophytic bacteria, and
PBM = inoculated with *S. cepivorum*, and treated with the endophytic bacteria and AMF.

Disease assessments

Four garlic plants from each treatment were assessed for white rot incidence (DI) and severity (DS) at 30, 60, or 90 dpi. DI was calculated using the following equation:

$$\text{DI (\%)} = \frac{\text{Number of infected plants}}{\text{Total number of inoculated plants}} \times 100$$

The garlic bulbs were visually assessed for white rot severity (DS) using a five point severity scale; where 1 = healthy bulb, 2 = 1–10% bulb rot, 3 = 11–25% bulb rot, 4 = 26–50% bulb rot, and 5 > 50% bulb rot (Entwistle, 1990). DS was then calculated using the following equation:

$$DS\ (\%) = \frac{\Sigma(ab)}{5N} \times 100$$

where a = number of diseased plants having the same disease score, b = the disease score, N = total number of assessed plants and 5 = the highest disease score.

Evaluation of the plant growth and yield parameters

Four plants from each treatment were carefully uprooted at 30, 60, or 90 dpi, and were washed under running water to remove soil particles. The plants were then evaluated for shoot and root lengths and dry weights, and number of leaves per plant. Yield parameters (fresh and dry weights of bulbs, bulb and clove diameters, clove length, and number of cloves per bulb) were also assessed at each harvest time. Dry weights were calculated after oven drying of samples at 80°C for 48 h until constant weight.

Estimation of mycorrhizal colonization

Mycorrhizal colonization was estimated in four garlic plants from each treatment at 30, 60, or 90 dpi. Garlic roots were cut into 1 cm pieces and then stained with trypan blue (Phillips and Hayman, 1970). Forty stained root pieces from each treatment were examined using a light microscope (Carl Zeiss) at ×400 magnification, and the colonization level was estimated according to Trouvelot *et al*. (1986) using the mycocalc program (https://www2.dijon.inra.fr/mychintec/Mycocalc-prg/download.html).

Analyses of biochemical parameters in garlic plants

Estimation of the photosynthetic pigments

The photosynthetic pigment contents (chlorophyll *a*, chlorophyll *b*, carotenoids) were estimated (Harborne, 1984) in four leaves of each garlic plant (0.5 g of fresh leaves) for each treatment at 30, 60, or 90 dpi.

Estimation of nutrients content

For each treatment, nutrient contents (N, P, K, Ca, and Mg) were estimated in leaves (0.5g of dry leaves) from four garlic plants at 30, 60, or 90 dpi. Total nitrogen content was determined by the Kjeldahl method (Sadasivam and Manickam 1992). Total phosphorus content was determined as described by Jackson (1958). Total potassium was estimated using a flame photometer (Corning 400), according to Peterburgski (1968). Total magnesium (Mg) and calcium (Ca) were determined using an atomic absorption spectrometer (ZEEnit 700P, Analytik Jena) and the method of Allen (1989).

Estimation of total phenol content

Total phenol content was estimated in four garlic roots (0.5 g of fresh roots) from each treatmentat 30, 60, or 90 dpi, using Folin-Ciocalteu reagent according to the method of Malik and Singh (1980).

Assay of the defense-related enzymes activities

Activities of three plant defense-related enzymes were assessed in four garlic roots (0.5 g of fresh roots) from each treatment at 30, 60, or 90 dpi. Assessments of enzymes activities were carried out as follows: phenylalanine ammonia-lyase (PAL) according to Beaudoin-Eagan and Thorpe (1985), polyphenoloxidase (PPO) according to Galeazzi *et al*. (1981), and peroxidase (POD) according to Maxwell and Bateman (1967).

Quantitative Real-Time PCR (qRT-PCR)

Garlic roots from each treatment were subjected to qRT-PCR at 30 dpi using a TOPreal™ qPCR 2X PreMIX SYBR Green (Enzynomics). The reaction program was performed using a real-time PCR system (Rotor-Gene Q, Qiagen) as follows: one cycle (15 min, 95°C), and 45 cycles (10 sec at 95°C, 15 sec at 60°C, 30 sec at 72 °C). Primers of the chitinase A gene (F, 5'-GCCCATGGAAGGAATCAGTTATGCGCAAAT-3', R, 5'-GCGGATCCCAACGCACTGCAACCGATTAT-3'), and defensin gene (F, 5'-CCAAATGCCTCGTCATCT-3', and R, 5'-ATTAGAGTCAAGCTCAAAAGG-3') were used. The reference gene used in this reaction was β-actine (F, 5'-GTGGGCCGCTCTAGGCACCAA-3', and R, 5'-CTCTTTGATGTCACGCACGATTTC-3') (Saleha, 2010). The data obtained were analyzed using the comparative method (Ct) (Schmittgen and Livak, 2008).

Statistical analyses

All results were analyzed using analysis of variance (ANOVA) and the statistical analysis software CoStat (version 6.4). Comparisons among means were made using the least significant difference (LSD) or Duncan's multiple range test (Duncan 1955).

RESULTS

Dual culture test

Means of *S. cepivorum* S6 growth inhibition achieved for the *B. amyloliquefaciens* GGA are presented in Table 1. Results obtained indicated that the bacterium exhibited strong antagonistic activity against *S. cepivorum* with a mean of 63.8% inhibition after 12 d compared to the control plates. The dual culture test is illustrated in Figure 1, showing the inhibition zone between the two microorganisms.

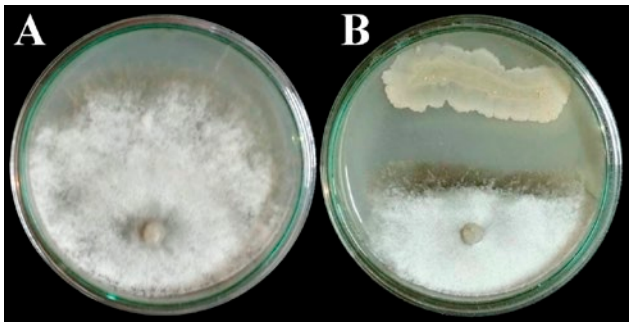

Figure 1. *In vitro* antifungal activity of *Bacillus amyloliquefaciens* GGA against *Sclerotium cepivorum* S6 (8-d old cultures). A, a PDA plate of *S. cepivorum* S6; B, a dual culture plate of *S. cepivorum* S6 and *B. amyloliquefaciens* GGA.

Electron microscopy

The antagonistic effects of *B. amyloliquefaciens* GGA on the morphology of the fungal structures of *S. cepivorum* S6 were examined using SEM to confirm the results of the dual culture test. SEM observations of the fungus from a control plate showed normal spherical sclerotia with intact rough-surfaced external rind layers (Figure 2A), small globose to subglobose rough-walled microconidia on mycelium emerging from the sclerotia (Figure 2B), and typical well-developed branched aerial hyphae (Figure 2C). SEM observations of the fungus from the dual culture plate showed alterations in the morphology of the fungal structures as a response to the exposure to the bacterial metabolites. These included wrinkled sclerotia with depressions in their surfaces and ruptured rinds (Figure 2D), distorted and shrunken microconidia (Figure 2E), and twisted, curled and collapsed hyphae (Figure 2F).

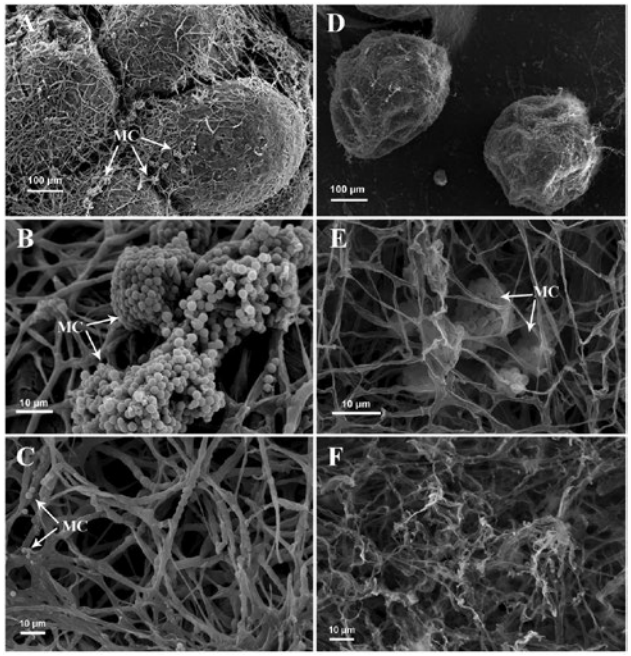

Figure 2. Scanning electron micrographs showing the antifungal effects of *Bacillus amyloliquefaciens* GGA on the morphology of *Sclerotium cepivorum* S6 in the dual culture test. A, normal spherical sclerotia with intact, rough-surfaced external rind layers; B, small globose to subglobose rough-walled microconidia on mycelium emerging from sclerotic; C, typical well-developed branched aerial hyphae; D, wrinkled sclerotia with depressions on their surfaces and ruptured rinds; E, distorted and shrunken microconidia; and F, twisted, curled and collapsed hyphae. MC = microconidia.

Pot experiment

Disease assessments

Mean DS and DI(%) of white rot on garlic plants in response to the tested treatments are illustrated in Figure 3. These results showed that DS and DI increased with increasing the age of the infected garlic plants, compared with the untreated plants. However, the disease severity and incidence in the non-mycorrhizal infected plants were significantly greater than those of the mycorrhizal infected plants at the three harvests. Inoculated plants treated with *B. amyloliquefaciens*

Table 1. Dual culture test between *Sclerotium cepivorum* S6 and *Bacillus amyloliquefaciens* GGA.

Treatment	Mean inward linear growth* (cm) after		
	4 d	8 d	12 d
S. cepivorum S6	3.9	6.8	8.0
S. cepivorum S6 + *B. amyloliquefaciens* GGA	2.2	2.6	2.9

* Each value is the mean of three replicates.

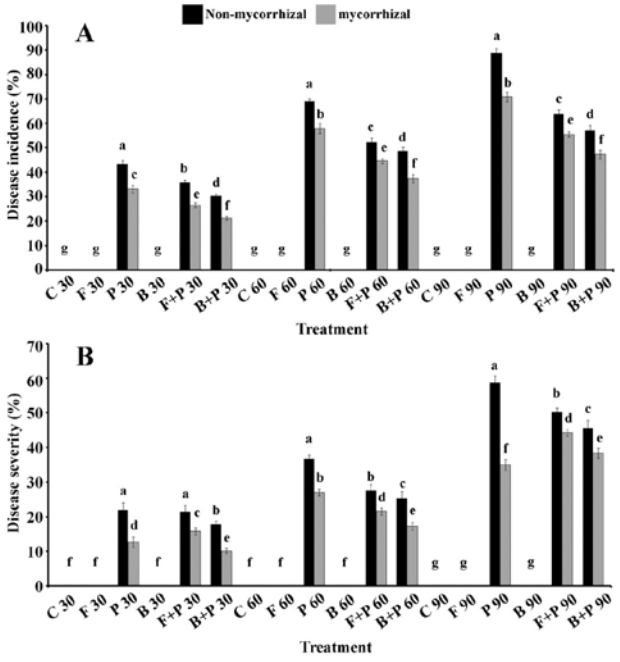

Figure 3. Mean disease incidence (A) and severity (B) of garlic plants in response to the tested treatments. C = untreated control, F = treated with tebuconazole, P = inoculated with *Sclerotium cepivorum*, B = inoculated with *Bacillus amyloliquefaciens* GGA, F+P = treated with tebuconazole and inoculated, and B+P = inoculated with S. cepivorum and treated with the bacteria, at three plant growth stages (30, 60, or 90 days post inoculation). At each growth stage, columns accompanied by the same letter are not significantly different (P=0.05) according to Duncan's multiple range test.

GGA showed disease severity and incidence that were less than the untreated-infected plants. However, garlic plants treated with AMF and *B. amyloliquefaciens* GGA had the greatest reductions in DS and DI, when compared with those for the plants treated with tebuconazole, or from the untreated-infected treatments.

Evaluation of the growth parameters

Effects of application of AMF and/or *B. amyloliquefaciens* GGA treatments on means of the garlic plant growth parameters are presented in Table 2. In general, all evaluated growth parameters increased with the increasing time after inoculations. All the assessed growth parameters were significantly reduced in the plants affected by white rot, compared with the untreated control plants. However, most of these parameters were significantly increased in plants inoculated with AMF compared with the non-mycorrhizal plants at the three harvests, regardless whether the plants were inoculated with *S. cepivorum* or not. In addition, inoculation with *B. amyloliquefaciens* GGA most of the assessed plant growth parameters at the three growth stages, in the healthy and pathogen inoculated plants, when compared with the untreated control plants. However, the combined treatment (AMF plus *B. amyloliquefaciens* GGA) gave the greatest plant growth parameters compared with the other treatments.

Garlic plant yield parameters

Results obtained from the pot experiment for the plant yield parameters in response to application of AMF and/or *B. amyloliquefaciens* GGA are presented in Table 3 and illustrated in Figure 4. The yield parameters were reduced as a result of *S. cepivorum* inoculation compared to the un-inoculated plants. However, these parameters were greater mycorrhizal plants than in the non-mycorrhizal plants. Application of *B. amyloliquefaciens* GGA increased all the assessed yield parameters in the healthy and pathogen inoculated plants compared with the untreated controls. However, the dual treatment of AMF and *B. amyloliquefaciens* GGA gave the greatest mean plant parameters compared with the other treatments.

Estimations of mycorrhizal colonization

Data of mycorrhizal colonization of garlic roots are summarized in Table 4. Amounts of root mycorrhizal colonization increased with increasing plant age for all the treatments, regardless of whether the plants were inoculated with *S. cepivorum* S6 or not. Mycorrhizal colonization was reduced in garlic roots infected with *S. cepivorum* S6, compared with the other treatments. In addition, application of the tebuconazole for plants inoculated with AMF led to reductions in mycorrhizal colonization levels, particularly at 60 and 90 dpi. In contrast, levels of mycorrhizal colonization showed pronounced increases where the AMF-inoculated garlic plants were also treated with *B. amyloliquefaciens* GGA at all the plant harvests. No mycorrhizal colonization was observed in garlic roots not inoculated with AMF.

Biochemical changes in garlic plants in response to the applied treatments

Photosynthetic pigments in garlic plants

Amounts of the photosynthetic pigments (chlorophyll *a*, chlorophyll *b* and carotenoids) in garlic leaves in response to the different treatments are summarized

Table 2. Mean garlic plant growth parameters (± standard error) for plants inoculated with *Sclerotium cepivorum* and treated with AMF and/or *Bacillus amyloliquefaciens* GGA.

Days post pathogen inoculation	Treatment[a]	Mycorrizal status[b]	Shoot dry wt. (g)	Root dry wt. (g)	Shoot height (cm)	Root length (cm)	Number of leaves
30	C	NM	0.81 ± 0.05	0.29 ± 0.003	15.6 ± 0.21	6.80 ± 0.06	5.0 ± 0.0
		M	1.18 ± 0.06	0.56 ± 0.006	22.2 ± 0.23	10.3 ± 0.09	5.7 ± 0.3
	F	NM	0.80 ± 0.07	0.27 ± 0.014	14.6 ± 0.22	6.50 ± 0.06	5.0 ± 0.0
		M	1.15 ± 0.08	0.55 ± 0.003	21.7 ± 0.15	10.1 ± 0.06	5.7 ± 0.3
	P	NM	0.38 ± 0.01	0.11 ± 0.004	10.7 ± 0.12	5.23 ± 0.01	4.0 ± 0
		M	0.67 ± 0.07	0.25 ± 0.002	16.3 ± 0.29	8.94 ± 0.05	5.3 ±0.3
	B	NM	1.15 ± 0.08	0.42 ± 0.002	18.6 ± 0.17	9.18 ± 0.01	6.0 ± 0.0
		M	1.78 ± 0.14	0.65 ± 0.002	26.6 ± 0.12	13.6 ± 0.12	7.0 ± 0.0
	F+P	NM	0.71 ± 0.03	0.19 ± 0.001	12.5 ± 0.06	7.02 ± 0.04	5.0 ± 0.0
		M	0.93 ± 0.02	0.32 ± 0.004	15.7 ± 0.12	9.79 ± 0.05	5.7 ± 0.3
	P+B	NM	1.04 ± 0.03	0.29 ± 0.002	15.1 ± 0.09	8.15 ± 0.01	5.0 ± 0.0
		M	1.38 ± 0.02	0.51 ± 0.001	20.8 ± 0.03	11.2 ± 0.09	7.0 ± 0.0
60	C	NM	1.94 ± 0.03	0.59 ± 0.002	22.8 ± 0.06	10.4 ± 0.15	6.3 ± 0.3
		M	2.91 ± 0.04	0.80 ± 0.004	30.7 ± 0.09	16.6 ± 0.12	7.3 ± 0.3
	F	NM	1.85 ± 0.07	0.58 ± 0.001	21.4 ± 0.21	10.1 ± 0.06	6.0 ± 0.0
		M	2.64 ± 0.23	0.79 ± 0.002	29.7 ± 0.12	16.3 ± 0.25	6.7 ± 0.3
	P	NM	1.10 ± 0.07	0.30 ± 0.001	16.8 ± 0.09	8.17 ± 0.09	5.0 ± 0.0
		M	1.99 ± 0.09	0.50 ± 0.002	22.4 ± 0.21	11.6 ± 0.17	6.3 ± 0.3
	B	NM	3.13 ± 0.04	0.73 ± 0.002	29.4 ± 0.06	17.4 ± 0.24	8.0 ± 0.0
		M	3.95 ± 0.02	0.95 ± 0.003	40.3 ± 0.12	24.6 ± 0.09	8.3 ± 0.3
	F+P	NM	1.81 ± 0.01	0.38 ± 0.002	18.7 ± 0.12	9.70 ± 0.15	6.7 ± 0.7
		M	2.07 ± 0.02	0.61 ± 0.002	25.5 ± 0.19	12.6 ± 0.15	8.3 ± 0.3
	P+B	NM	2.37 ± 0.09	0.61 ± 0.002	28.6 ± 0.18	15.4 ± 0.27	6.6 ± 0.3
		M	3.09 ± 0.01	0.75 ± 0.002	38.8 ± 0.09	23.3 ± 0.25	7.0 ± 0.0
90	C	NM	3.02 ± 0.09	0.91 ± 0.001	33.4 ± 0.22	20.6 ± 0.15	9.0 ± 0.0
		M	4.44 ± 0.03	1.14 ± 0.017	42.7 ± 0.09	29.7 ± 0.09	9.7 ± 0.3
	F	NM	3.05 ± 0.08	0.89 ± 0.002	32.6 ± 0.09	20.1 ± 0.06	8.3 ± 0.3
		M	4.22 ± 0.07	1.10 ± 0.009	40.9 ± 0.14	28.3 ± 0.24	9.3 ± 0.3
	P	NM	1.83 ± 0.04	0.59 ± 0.002	24.8 ± 0.09	17.4 ± 0.03	7.7 ± 0.3
		M	3.45 ± 0.23	0.88 ± 0.004	32.2 ± 0.15	26.7 ± 0.12	8.7 ± 0.3
	B	NM	4.15 ± 0.04	1.07 ± 0.012	40.7 ± 0.09	35.5 ± 0.17	11.0 ± 0.0
		M	4.95 ± 0.09	1.52 ± 0.038	56.7 ± 0.19	48.4 ± 0.47	13.0 ± 0.0
	F+P	NM	2.73 ± 0.09	0.71 ± 0.003	30.3 ± 0.18	18.2 ± 0.06	8.3 ± 0.3
		M	3.89 ± 0.12	0.99 ± 0.001	36.6 ± 0.15	27.6 ± 0.18	9.0 ± 0.0
	P+B	NM	3.67 ± 0.14	0.95 ± 0.001	35.5 ± 0.18	33.7 ± 0.41	10.0 ± 0.0
		M	4.13 ± 0.04	1.21 ± 0.020	50.4 ± 0.19	51.3 ± 0.68	12.0 ± 0.0
LSD (P<0.05)			0.379	0.025	0.431	1.464	0.717
Treatment			**	**	**	**	*
Harvest			**	***	**	***	*
Harvest × Treatment			**	**	**	**	*
Mycorrhiza			***	***	***	***	**
Mycorrhiza × Treatment			**	**	**	**	*
Mycorrhiza × Harvest			***	***	**	***	*
Mycorrhiza × Harvest × Treatment			**	**	**	**	*

[a] C, untreated control; F, fungicide; P, inoculated with *S. cepivorum*; B, treated with bacteria; F+P, inoculated with *S. cepivorum* and treated with fungicide; P+B, inoculated with *S. cepivorm* and treated with bacteria.
[b] NM, non-mycorrhizal; M, mycorrhizal.
* Significant at P<0.05, ** significant at P<0.01, and *** significant at P<0.001.

Table 3. Mean garlic plant yield parameters (± standard error) for plants treated with AMF and/or *Bacillus amyloliquefaciens* GGA as bio-control agents against *Sclerotium cepivorum*.

Treatment[a]	Mycorrhizal status[b]	Fresh wt. of bulb (g)	Dry wt. of bulb (g)	Bulb diameter (cm)	No. of cloves per bulb	Clove length (cm)	Clove diameter (cm)
C	NM	19.8 ± 0.09	5.74 ± 0.29	3.30 ± 0.19	13.7 ± 0.33	2.60 ± 0.03	1.80 ± 0.04
	M	23.1 ± 0.10	8.59 ± 0.14	4.18 ± 0.04	16.7 ± 0.33	3.55 ± 0.04	2.08 ± 0.04
F	NM	19.1 ± 0.20	5.62 ± 0.26	3.07 ± 0.02	12.3 ± 0.33	2.47 ± 0.02	1.68 ± 0.05
	M	23.2 ± 0.3	8.21 ± 0.13	4.05 ± 0.03	16.3 ± 0.33	3.22 ± 0.02	2.04 ± 0.03
P	NM	12.7 ± 0.45	4.13 ± 0.05	2.05 ± 0.03	10.3 ± 0.33	1.37 ± 0.07	1.08 ± 0.06
	M	17.7 ± 0.92	6.49 ± 0.22	3.07 ± 0.02	13.3 ± 0.33	2.40 ± 0.01	1.85 ± 0.12
B	NM	24.8 ± 0.26	10.1 ± 0.11	5.20 ± 0.03	21.3 ± 0.33	4.12 ± 0.01	2.36 ± 0.04
	M	35.6 ± 0.46	14.1 ± 0.07	6.19 ± 0.04	26.3 ± 0.88	5.02 ± 0.01	2.98 ± 0.07
F+P	NM	14.5 ± 0.53	4.26 ± 0.06	3.06 ± 0.02	11.3 ± 0.33	2.14 ± 0.02	1.37 ± 0.08
	M	19.4 ± 0.44	5.37 ± 0.14	3.88 ± 0.06	14.3 ± 0.33	2.76 ± 0.04	1.87 ± 0.10
P+B	NM	21.9 ± 0.37	7.69 ± 0.17	4.44 ± 0.07	15.3 ± 0.33	3.79 ± 0.04	2.09 ± 0.17
	M	28.0 ± 0.55	10.3 ± 0.15	5.95 ± 0.05	19.3 ± 0.33	4.42 ± 0.04	2.59 ± 0.06
LSD (P<0.05)		4.06	1.78	0.69	2.53	0.54	0.35
Treatment		***	***	***	**	***	***
Mycorrhiza		***	***	***	**	***	***
Mycorrhiza × Treatment		***	***	**	**	**	**

[a] C, untreated control; F, fungicide; P, inoculated with *S. cepivorum*; B, treated with bacteria; F+P, inoculated with *S. cepivorum* and treated with fungicide; P+B, inoculated with *S. cepivorm* and treated with bacteria.
[b] NM, non-mycorrhizal; M, mycorrhizal.
** Significant at P<0.01, and *** significant at P<0.001.

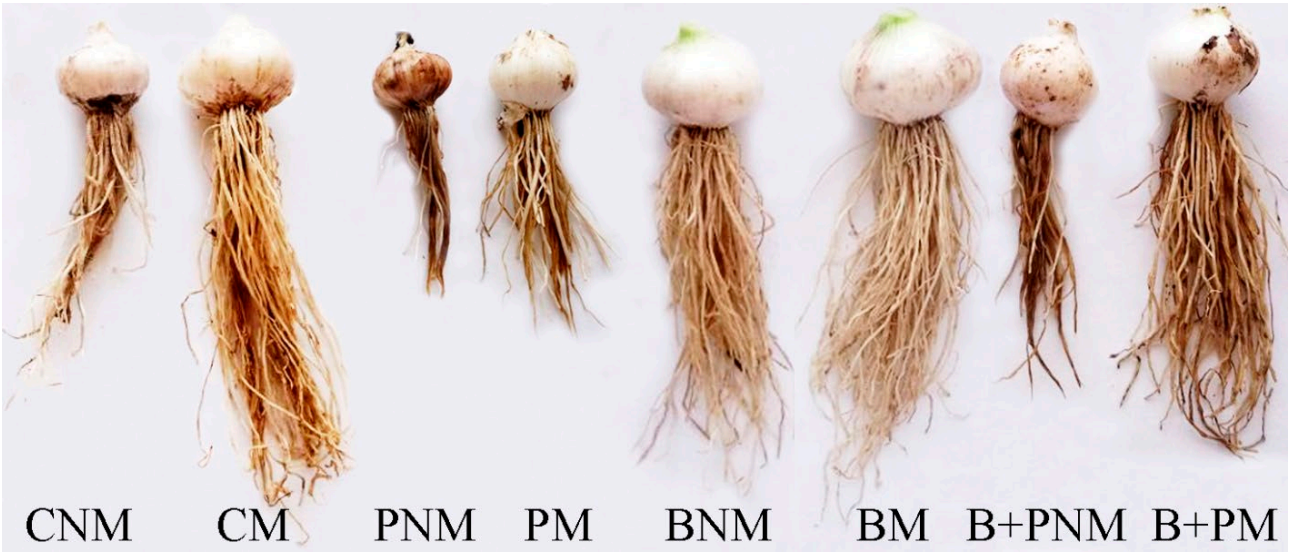

Figure 4. Photograph showing effects of different treatments on resulting bulbs of garlic plants. The treatments were: CNM = untreated control, CM = treated with AMF, PNM = inoculated with *Sclerotium cepivorum*, PM = inoculated with *S. cepivorum* and treated with AMF, BNM = treated with *Bacillus amyloliquefaciens* GGA, BM = treated with *B. amyloliquefaciens* GGA and AMF, PBNM = inoculated with *S. cepivorum* and treated with *B. amyloliquefaciens* GGA, and PBM = inoculated with *S. cepivorum* and treated with *B. amyloliquefaciens* GGA and AMF.

in Table 5. For all the treatments, amounts of these pigments increased from 30 to 60 dpi at which they reached the maximum values then decreased at 90 dpi. Infection of garlic plants with *S. cepivorum* led to decreases in the amounts of pigments compared with the untreated garlic plants. The pigment quantities in the mycorrhizal

Table 4. Mean proportions (± standard error) of mycorrhizal colonization in garlic plant roots at intervals after different treatments were applied.

Days after pathogen inoculation	Treatment [a]	Mycorrhizal status [b]	F (%)[c]	I (%)[c]	A (%)[c]
30	C	NM	0.0	0.0	0.0
		M	81.6 ± 0.76	37.5 ± 0.91	13.8 ± 0.61
	F	NM	0.0	0.0	0.0
		M	81.0 ± 0.35	36.8 ± 0.63	13.3 ± 0.23
	P	NM	0.0	0.0	0.0
		M	59.4 ± 0.8	19.4 ± 0.3	7.2 ± 0.37
	B	NM	0.0	0.0	0.0
		M	83.8 ± 1.65	46.1 ± 0.92	23.0 ± 0.83
	F+P	NM	0.0	0.0	0.0
		M	74.6 ± 0.43	25.77 ± 0.61	10.1 ± 0.28
	P+B	NM	0.0	0.0	0.0
		M	81.7 ± 0.55	41.46 ± 0.28	21.1 ± 0.52
60	C	NM	0.0	0.0	0.0
		M	94.1 ± 0.89	65.1 ± 0.84	37.8 ± 0.71
	F	NM	0.0	0.0	0.0
		M	91.6 ± 0.61	62.1 ± 0.67	35.3 ± 1.13
	P	NM	0.0	0	0
		M	76.6 ± 0.53	33.6 ± 0.51	25.6 ± 0.61
	B	NM	0.0	0.0	0.0
		M	100	71.3 ± 0.54	58.5 ± 0.73
	F+P	NM	0.0	0.0	0.0
		M	84.8 ± 0.09	48.6 ± 0.73	31.0 ± 0.35
	P+B	NM	0.0	0.0	0.0
		M	97.8 ± 0.32	75.8 ± 1.18	48.4 ± 0.64
90	C	NM	0.0	0.0	0.0
		M	100	73.0 ± 1.53	57.1 ± 0.91
	F	NM	0.0	0.0	0.0
		M	95.6 ± 0.74	54.2 ± 0.78	55.1 ± 0.22
	P	NM	0.0	0.0	0.0
		M	83.1 ± 0.94	86.7 ± 0.63	39.6 ± 0.66
	B	NM	0.0	0.0	0.0
		M	100	83 ± 2.08	64.0 ± 1.24
	F+P	NM	0.0	0.0	0.0
		M	90.66 ± 0.55	65.4 ± 0.87	49.5 ± 2.68
	P+B	NM	0.0	0.0	0.0
		M	100	79.9 ± 0.42	61.5 ± 0.69
LSD (P<0.05)			1.27	1.56	1.85
Treatment			***	***	***
Harvest			***	***	***
Harvest × Treatment			***	***	***
Mycorrhiza			***	***	***
Mycorrhiza × Treatment			***	***	***
Mycorrhiza × Harvest			***	***	***
Mycorrhiza × Harvest × Treatment			***	***	***

[a] C, untreated control; F, fungicide; P, inoculated with *Sclerotium cepivorum*; B, treated with bacteria; F+P, inoculated with *S. cepivorum* and treated with fungicide; P+B, inoculated with *S. cepivorm* and treated with bacteria.
[b] NM, non-mycorrhizal; M, mycorrhizal.
[c] F, frequency of root colonization; I, intensity of cortical colonization; A, frequency of arbuscules.
*** Significant at P<0.001.

Table 5. Mean concentrations (μg g^{-1} fresh weight, ± standard error) of photosynthetic pigments in garlic plants at intervals after different *Sclerotium cepivorum* inoculation and microbial treatments were applied.

Days after pathogen inoculation	Treatment[a]	Mycorrhizal status[b]	Chlorophyll *a*	Chlorophyll *b*	Carotenoids
30	C	NM	590 ± 2.89	392 ± 1.45	301 ± 1.86
		M	614 ± 2.33	413 ± 3.18	387 ± 1.13
	F	NM	540 ± 2.91	394 ± 2.61	315 ± 2.82
		M	664 ± 2.08	443 ± 1.63	402 ± 3.75
	P	NM	441 ± 4.41	315 ± 2.84	241 ± 4.42
		M	541 ± 2.07	385 ± 2.72	318 ± 4.29
	B	NM	690 ± 4.62	422 ± 1.53	397 ± 2.17
		M	796 ± 1.86	483 ± 2.08	431 ± 3.35
	F+P	NM	517 ± 6.51	354 ± 2.33	285 ± 2.56
		M	594 ± 2.32	412 ± 1.45	326 ± 2.92
	P+B	NM	630 ± 2.83	398 ± 1.52	341 ± 2.09
		M	715 ± 2.89	426 ± 1.67	411 ± 2.64
60	C	NM	609 ± 1.58	441 ± 1.86	320 ± 2.86
		M	870 ± 2.64	615 ± 2.33	421 ± 2.09
	F	NM	598 ± 4.16	439 ± 3.48	420 ± 2.81
		M	824 ± 3.63	601 ± 1.86	491 ± 2.12
	P	NM	515 ± 1.47	389 ± 0.77	311 ± 2.09
		M	621 ± 2.09	430 ± 3.21	401 ± 1.85
	B	NM	715 ± 2.33	588 ± 0.88	425 ± 2.86
		M	820 ± 2.89	718 ± 1.15	590 ± 2.62
	F+P	NM	547 ± 1.81	399 ± 0.75	335 ± 2.88
		M	667 ± 1.45	518 ± 1.67	430 ± 2.90
	P+B	NM	687 ± 2.09	440 ± 2.89	403 ± 3.51
		M	737 ± 4.31	509 ± 3.78	464 ± 2.33
90	C	NM	479 ± 3.19	399 ± 3.17	365 ± 3.84
		M	595 ± 2.83	435 ± 2.88	434 ± 2.09
	F	NM	465 ± 2.88	389 ± 3.18	415 ± 2.88
		M	590 ± 2.37	404 ± 1.45	442 ± 3.71
	P	NM	375 ± 2.84	295 ± 0.88	211 ± 2.09
		M	441 ± 1.86	333 ± 1.86	292 ± 3.15
	B	NM	502 ± 3.18	422 ± 2.12	310 ± 2.89
		M	617 ± 2.84	482 ± 2.52	371 ± 3.53
	F+P	NM	365 ± 1.29	306 ± 1.67	296 ± 3.51
		M	500 ± 1.82	371 ± 3.84	381 ± 3.28
	P+B	NM	471 ± 2.14	315 ± 2.89	289 ± 1.88
		M	541 ± 2.08	429 ± 3.78	339 ± 3.19
LSD (P<0.05)			9.94	7.68	8.93
Treatment			*	**	**
Harvest			**	*	**
Harvest × Treatment			*	*	**
Mycorrhiza			**	**	**
Mycorrhiza × Treatment			*	**	*
Mycorrhiza × Harvest			**	*	**
Mycorrhiza × Harvest × Treatment			**	**	*

[a] C, untreated control; F, fungicide; P, inoculated with *S. cepivorum*; B, treated with bacteria; F+P, inoculated with *S. cepivorum* and treated with fungicide; P+B, inoculated with *S. cepivorm* and treated with bacteria.
[b] NM, non-mycorrhizal; M, mycorrhizal.
* Significant at P<0.05, and ** significant at P<0.01.

Table 6. Mean amounts (mg g^{-1} dry weight, ± standard error) of mineral nutrients in garlic plant leaves contents at intervals after different *Sclerotium cepivorum* inoculation and microbial treatments were applied.

Days after pathogen inoculation	Treatment[a]	Mycorrhizal status[b]	N	P	K	Ca	Mg
30	C	NM	12.4 ± 0.21	0.95 ± 0.021	10.9 ± 0.32	5.93 ± 0.10	0.55 ± 0.01
		M	15.5 ± 0.42	1.18 ± 0.038	13.2 ± 0.41	6.86 ± 0.12	0.81 ± 0.02
	F	NM	12.1 ± 0.23	0.94 ± 0.014	10.8 ± 0.42	5.73 ± 0.12	0.51 ± 0.01
		M	14.7 ± 0.23	1.24 ± 0.012	12.9 ± 0.64	6.54 ± 0.20	0.80 ± 0.02
	P	NM	8.80 ± 0.27	0.78 ± 0.023	8.74 ± 0.52	3.98 ± 0.10	0.22 ± 0.01
		M	10.7 ± 0.51	0.82 ± 0.002	9.37 ± 0.74	4.61 ± 0.11	0.38 ± 0.01
	B	NM	17.8 ± 0.33	1.03 ± 0.002	14.1 ± 0.67	8.53 ± 0.17	0.82 ± 0.01
		M	23.2 ± 0.26	2.40 ± 0.032	17.5 ± 0.52	10.3 ± 0.10	0.95 ± 0.02
	F+P	NM	10.3 ± 0.13	0.80 ± 0.009	9.14 ± 0.36	5.22 ± 0.14	0.42 ± 0.01
		M	12.6 ± 0.12	0.89 ± 0.004	10.9 ± 0.35	5.94 ± 0.17	0.54 ± 0.01
	P+B	NM	15.7 ± 0.55	0.97 ± 0.012	12.2 ± 0.29	7.64 ± 0.14	0.76 ± 0.01
		M	20.7 ± 0.65	1.89 ± 0.003	16.1 ± 0.51	9.06 ± 0.11	0.84 ± 0.01
60	C	NM	15.6 ± 0.13	1.53 ± 0.007	15.4 ± 0.72	8.63 ± 0.05	0.96 ± 0.01
		M	19.7 ± 0.37	1.84 ± 0.004	19.2 ± 0.63	10.2 ± 0.17	1.14 ± 0.02
	F	NM	14.8 ± 0.25	1.51 ± 0.011	15.2 ± 0.64	8.36 ± 0.16	0.92 ± 0.01
		M	18.7 ± 0.46	1.83 ± 0.004	18.9 ± 0.42	10.0 ± 0.15	1.07 ± 0.01
	P	NM	8.70 ± 0.71	0.99± 0.008	10.5 ± 0.45	5.12 ± 0.19	0.45 ± 0.01
		M	11.4 ± 0.53	1.34 ± 0.006	12.8 ± 0.73	5.92 ± 0.07	0.74 ± 0.01
	B	NM	21.5 ± 0.55	1.89 ± 0.002	18.9 ± 0.56	11.9 ± 0.14	1.16 ± 0.05
		M	30.3 ± 0.34	2.66 ± 0.003	23.4 ± 0.37	13.3 ± 0.01	1.69 ± 0.11
	F+P	NM	12.5 ± 0.48	1.43 ± 0.002	13.2 ± 0.46	7.81 ± 0.11	0.77 ± 0.01
		M	15.8 ± 0.33	1.64 ± 0.015	16.3 ± 0.69	8.25 ± 0.41	0.87 ± 0.02
	P+B	NM	20.7 ± 0.65	1.79 ± 0.006	17.1 ± 0.38	10.1 ± 0.11	1.11 ± 0.05
		M	22.3 ± 0.43	2.23 ± 0.008	21.1 ± 0.31	12.2 ± 0.09	1.57 ± 0.01
90	C	NM	14.5 ± 0.43	1.41 ± 0.007	14.3 ± 0.29	7.12 ± 0.12	0.84 ± 0.01
		M	16.8 ± 0.52	1.58 ± 0.017	15.4 ± 0.47	8.01 ± 0.26	0.98 ± 0.01
	F	NM	14.1 ± 0.36	1.40 ± 0.002	14.1 ± 0.32	7.02 ± 0.06	0.81 ± 0.01
		M	16.3 ± 0.53	1.53 ± 0.009	14.9 ± 0.44	7.88 ± 0.07	0.92 ± 0.02
	P	NM	8.36 ± 0.47	0.82 ± 0.002	9.19 ± 0.59	4.78 ± 0.03	0.37 ± 0.03
		M	10.2 ± 0.34	0.96 ± 0.006	10.3 ± 0.32	5.22 ± 0.06	0.53 ± 0.01
	B	NM	20.4 ± 0.52	1.53 ± 0.010	17.6 ± 0.69	10.0 ± 0.08	1.10 ± 0.03
		M	24.9 ± 0.69	1.99 ± 0.008	20.1 ± 0.22	11.9 ± 0.07	1.51 ± 0.02
	F+P	NM	11.1 ± 0.52	0.97 ± 0.003	11.6 ± 0.41	6.7 ± 0.06	0.67 ± 0.02
		M	12.9 ± 0.55	1.11 ± 0.009	13.9 ± 0.55	7.06 ± 0.10	0.76 ± 0.02
	P+B	NM	17.6 ± 0.49	1.43 ± 0.003	15.8 ± 0.67	9.4 ± 0.07	1.01 ± 0.02
		M	20.9 ± 0.34	1.77 ± 0.007	18.9 ± 0.39	10.5 ± 0.11	1.33 ± 0.06
LSD (P<0.05)			1.327	0.221	2.36	1.135	0.179
Treatment			**	**	*	**	**
Harvest			**	***	**	**	**
Harvest × Treatment			**	**	*	**	**
Mycorrhiza			***	**	**	***	**
Mycorrhiza × Treatment			***	***	**	**	**
Mycorrhiza × Harvest			**	***	**	***	**
Mycorrhiza × Harvest × Treatment			**	**	**	**	**

[a] C, untreated control; F, fungicide; P, inoculated with *S. cepivorum*; B, treated with bacteria; F+P, inoculated with *S. cepivorum* and treated with fungicide; P+B, inoculated with *S. cepivorm* and treated with bacteria.
[b] NM, non-mycorrhizal; M, mycorrhizal.
* Significant at P<0.05, ** significant at P<0.01, and *** significant at P<0.001.

plants were greater than those of the non-mycorrhizal plants, at all three stages of garlic growth, whether the plants were pathogen-inoculated or not, so mycorrhizal colonization of the inoculated plants reduced the negative effects of the pathogen, compared with the non-mycorrhizal plants. In contrast, treating the garlic plants with *B. amyloliquefaciens* GGA led to increases of all photosynthetic pigments at the three plant growth stages in the inoculated non-inoculated plants. Application of AMF and *B. amyloliquefaciens* GGA in combination increased photosynthetic pigment contents at the three plant growth stages, compared with the untreated control plants.

Mineral nutrients in garlic plants

Amounts of mineral nutrients in leaves of garlic plants receiving the different treatments are summarized in Table 6. Inoculation with *S. cepivorum* led to reductions in all amounts of assessed elements, compared with the untreated control plants. Nutrient contents in the mycorrhizal-infected plants were greater than those for non-mycorrhizal *S. cepivorum* inoculated plants at the three harvests, when compared to control plants. Application of *B. amyloliquefaciens* GGA increased all leaf nutrient contents, whether inoculated or not, when compared with the untreated control treatment. The highest nutrient contents were measured for the uninfected garlic plants treated with AMF and *B. amyloliquefaciens* GGA, when compared with the untreated plants.

Total phenol contents and activities of defense-related enzymes in garlic plants

Effects of applications of AMF and/or *B. amyloliquefaciens* GGA on the total phenol content and activities of defense-related enzymes of garlic plants infected with white rot disease are summarized in Table 7. Inoculation with *S. cepivorum* led to significant increases in the total phenol content and activities of defense-related enzymes of mycorrhizal and non-mycorrhizal plants, compared with untreated control plants. The increases in the mycorrhizal plants were greater than in the non-mycorrhizal plants at all harvests. The maximum values of total phenol contents and enzyme activities occurred after 60 days and decreased after 90 days from inoculation with the pathogen.

In addition, garlic plants (whether *S. cepivorum*-inoculated or not) which were treated with *B. amyloliquefaciens* GGA had greater amounts of phenol and greater enzyme activities compared with the corresponding untreated plants. The greatest amounts total phenol and enzyme activity were for the pathogen inoculated plants treated with the combined treatment of AMF and *B. amyloliquefaciens* GGA, when compared with the control plants, particularly at 60 dpi.

Transcript levels of the defense-related enzymes (qRT-PCR)

The transcript levels of the defensin gene in garlic plants was quantified using qRT-PCR in response to the different applied treatments (Figure 5A). There were significant inductions of defensin expression from all the treatments, at both harvests, compared to the control treatment. The induction effect was greatest at 30 dpi than at 60 dpi. For the two harvests, *S. cepivorum* inoculated plants treated with AMF and *B. amyloliquefaciens* GGA had the greatest gene expression (13.2-fold increase at 30 dpi, and 9.5-fold at 60 dpi).

Expression of the chitinase gene (Figure 5B) was also affected by varying degrees. Expression at 30 dpi was greater than at 60 dpi. Plants inoculated with *S. cepivorum* and treated with AMF and *B. amyloliquefaciens* GGA gave the greatest gene expression levels (8.9-fold increase at 30 dpi), compared with the untreated control treatment. At 60 dpi, greatest chitinase gene expression was recorded for the non-pathogen inoculated plants treated with AMF and *B. amyloliquefaciens* GGA, compared with the untreated control plants.

DISCUSSION

White rot, caused by *S. cepivorum*, is a serious disease of garlic leading to considerable yield losses. This study investigated the synergistic interactions between endophytic microorganisms (AMF and *B. amyloliquefaciens* GGA) and their effects on biochemical and molecular plant defense-responses against white rot, as well as effects on garlic plant growth.

Results obtained from the dual culture tests showed potent *in vitro* antagonistic activity of *B. amyloliquefaciens* GGA against *S. cepivorum*, which was confirmed by SEM observations of *S. cepivorum* mycelium, sclerotia, and microconidia. Fungitoxic activity of *B. amyloliquefaciens* has been studied by many researchers against a wide range of soil-borne fungi (Li *et al*., 2016; Lee *et al*., 2017). Several antifungal metabolites have been reported to be produced by *B. amyloliquefaciens*, including lipopeptides (e.g. bacillomycin, fengycin, and surfactin), volatile compounds, hydrolytic enzymes, and siderophores such as bacillibactin (Yuan *et al*., 2012; Hanif *et al*., 2019). However, their production may be

Table 7. Mean amounts (± standard error) of the defense-related enzymes phenylalanine ammonia-lyase (PAL), polyphenoloxidase (PPO) and peroxidase (POD), and total phenol in garlic plants receiving different treatments of *Sclerotium cepivorum* inoculation or AMF and/or *B. amyloliquefaciens* GGA.

Days after pathogen inoculation	Treatment[a]	Mycorrizal status[b]	PAL (μmol *t*-cinnamic acid h^{-1} g^{-1} f wt)	PPO (Δ A_{420} min^{-1} g^{-1} f wt)	POD (Δ A_{470} min^{-1} g^{-1} f wt)	Total phenol (μg g^{-1} f wt)
30	C	NM	200.7 ± 2.18	4.50 ± 0.05	25.3 ± 0.58	185.0 ± 2.88
		M	236.7 ± 9.28	5.36 ± 0.03	39.9 ± 0.07	394.3 ± 5.46
	F	NM	197.7 ± 5.04	4.43 ± 0.05	25.1 ± 0.46	184.3 ± 1.86
		M	235.3 ± 9.94	5.31 ± 0.04	39.9 ± 0.10	385.3 ± 6.49
	P	NM	394.0 ± 3.05	5.88 ± 0.03	59.3 ± 0.62	410.0 ± 2.88
		M	422.0 ± 3.07	6.36 ± 0.02	66.3 ± 0.25	590.7 ± 3.84
	B	NM	415.3 ± 1.45	6.01 ± 0.02	66.2 ± 0.61	339.7 ± 3.17
		M	541.7 ± 7.26	6.81 ± 0.08	73.1 ± 0.98	544.6 ± 5.82
	F+P	NM	382.0 ± 3.06	4.41 ± 0.05	24.1 ± 0.08	393.0 ± 2.52
		M	421.3 ± 8.99	5.24 ± 0.02	37.9 ± 1.08	540.3 ± 4.84
	P+B	NM	436.0 ± 5.19	6.10 ± 0.03	61.7 ± 0.98	355.0 ± 2.88
		M	551.7 ± 9.89	6.98 ± 0.17	74.3 ± 0.88	630.0 ± 9.58
60	C	NM	361.7 ± 9.28	6.88 ± 0.06	30.7 ± 0.31	200.7 ± 6.69
		M	504.3 ± 7.82	7.19 ± 0.06	41.1 ± 0.48	413.0 ± 6.11
	F	NM	363.3 ± 9.16	6.89 ± 0.04	30.3 ± 0.23	199.6 ± 2.73
		M	500.7 ± 2.13	7.30 ± 0.08	40.4 ± 0.26	407.3 ± 4.18
	P	NM	509.3 ± 2.97	7.10 ± 0.05	72.1 ± 1.02	463.3 ± 9.93
		M	652.7 ± 8.29	8.95 ± 0.03	80.9 ± 0.38	661.7 ± 8.98
	B	NM	657.7 ± 7.33	8.12 ± 0.06	70.3 ± 0.14	397.3 ± 8.12
		M	794.7 ± 8.86	9.08 ± 0.03	77.8 ± 1.40	596.0 ± 6.24
	F+P	NM	412.7 ± 3.81	5.14 ± 0.02	30.2 ± 0.15	448.3 ± 9.08
		M	560.3 ± 3.85	6.11 ± 0.02	47.5 ± 1.11	565.7 ± 8.39
	P+B	NM	689.0 ± 7.09	8.72 ± 0.05	72.5 ± 0.44	410.3 ± 5.48
		M	908.0 ± 8.51	9.78 ± 0.24	83.1 ± 0.78	717.7 ± 8.76
90	C	NM	173.7 ± 4.19	3.50 ± 0.05	21.6 ± 0.54	146.0 ± 7.21
		M	225.0 ± 5.73	4.23 ± 0.09	31.5 ± 0.77	305.6 ± 4.08
	F	NM	172.7 ± 3.92	3.45 ± 0.04	21.1 ± 0.69	149.6 ± 7.96
		M	209.7 ± 2.40	4.11 ± 0.06	30.9 ± 0.57	304.7 ± 2.60
	P	NM	355.7 ± 5.81	4.85 ± 0.04	30.7 ± 0.66	296.0 ± 4.93
		M	401.7 ± 8.81	5.11 ± 0.02	55.7 ± 0.18	520.0 ± 5.77
	B	NM	374.0 ± 9.18	5.05 ± 0.03	59.5 ± 0.31	323.3 ± 9.89
		M	447.3 ± 6.88	5.83 ± 0.12	65.8 ± 0.12	524.3 ± 7.89
	F+P	NM	371.7 ± 3.89	4.09 ± 0.06	22.2 ± 0.42	311.7 ± 4.41
		M	367.0 ± 6.81	4.67 ± 0.07	32.8 ± 0.23	508.7 ± 3.18
	P+B	NM	406.3 ± 5.24	5.74 ± 0.09	58.8 ± 0.92	333.0 ± 7.23
		M	519.3 ± 7.38	6.02 ± 0.07	66.7 ± 0.46	545.7 ± 5.21
LSD (P<0.05)			34.33	0.212	12.24	21.62
Treatment			**	**	*	**
Harvest			**	*	**	*
Harvest × Treatment			*	*	**	*
Mycorrhiza			***	***	***	***
Mycorrhiza × Treatment			**	**	*	**
Mycorrhiza × Harvest			**	*	**	*
Mycorrhiza × Harvest × Treatment			**	**	**	**

[a] C, untreated control; F, fungicide; P, inoculated with *S. cepivorum*; B, treated with bacteria; F+P, inoculated with *S. cepivorum* and treated with fungicide; P+B, inoculated with *S. cepivorm* and treated with bacteria.
[b]NM, non-mycorrhizal; M, mycorrhizal.
* Significant at P<0.05, ** significant at P<0.01, and *** significant at P<0.001.

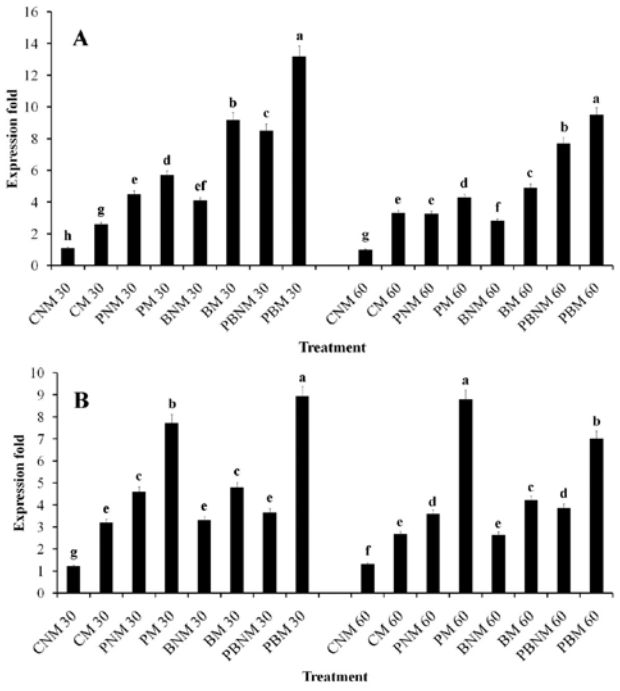

Figure 5. Mean relative transcription expression levels of the defensin gene (A) and chitinase gene (B) in garlic plants after different treatments of *Sclerotium cepivorum* inoculation or AMF and or *B. amyloliquefaciens* GGA at 30 or 60 dpi. CNM = untreated control, CM = treated with AMF, PNM = inoculated with *S. cepivorum*, PM = inoculated with *S. cepivorum* and treated with AMF, BNM = treated with *B. amyloliquefaciens* GGA, BM = treated with *B. amyloliquefaciens* GGA and AMF, PBNM = inoculated with *S. cepivorum* and treated with *B. amyloliquefaciens* GGA, and PBM = inoculated with *S. cepivorum* and treated with *B. amyloliquefaciens* GGA and AMF. Each value represents the mean of three biological replicates, each analyzed in triplicate. Error bars are standard errors. At each growth stage 30 or 60 dpi), means accompanied by the same letter(s) are not significantly different ($P<0.05$), Duncan's multiple range test.

induced in a species-specific manner, so that production may vary in type or quantity depending on the particular fungal pathogen (Li *et al*., 2014). The probable mechanisms of action of these metabolites include interference with cell membrane components, particularly sterol and phospholipid molecules, altering their structure and affecting membrane permeability (Sur *et al*., 2018). In addition, inhibition of fungal DNA biosynthesis and cell lysis were also reported to cause cell death (Tao *et al*., 2011; Liu *et al*., 2011).

Results from the pot experiment demonstrated that single inoculation of *B. amyloliquefaciens* GGA or AMF reduced severity and incidence of white rot on garlic plants. Dual inoculation with both of these organisms gave the greatest disease reductions. This result is similar to that of Haggag and Abdel-latif (2001), who reported a synergistic effect of the combined treatment of *G. mosseae* and *B. subtilis* against the root rot pathogens *F. solani* and *Macrophomina phaseolina* on geranium plants.

Biocontrol activity of AMF, alone or in combination with other biocontrol agents, has been extensively studied against different fungal diseases of many plant species (Abdel-Fattah *et al*., 2011; El-Sharkawy *et al*., 2018; Rashad *et al*., 2020). Berdeni *et al*. (2018) found that resistance of apple trees (*Malus pumila*) was induced against canker caused by *Neonectria ditissima*, when plants were inoculated with AMF. Various defense-related mechanisms have been reported to be induced in host plants in response to the colonization with AMF. These include physical, biochemical and molecular changes. Lignification of host cell walls is one of the main induced defense-related responses against phytopathogenic fungi. Cell wall lignification acts as a physical barrier which restricts pathogen spread within host tissues, and diffusion of pathogen-produced toxins into plant cells. Lignification also obstructs passage of water and nutrients from cells to invading pathogens (Miedes *et al*., 2014). Rashad *et al*. (2020) reported the triggering effect of sunflower colonization by *Rhizophagus irregularis* on transcriptional expression of lignification-related genes. Cell wall thickening of bean roots against the Rhizoctonia root rot pathogen as a result to AMF colonization was also observed by Abdel-Fattah *et al*. (2011). Triggering of host cells for production of some fungitoxic phenolic compounds as a result of AMF colonization has also been reported. This mechanism was confirmed by the results obtained in the present study, where high total phenol contents were recorded in the infected garlic plants inoculated with AMF. El-Sharkawy *et al*. (2018) found that mycorrhizal stem rust-infected wheat plants inoculated with AMF had greater amounts of phenolic compounds than the non-mycorrhizal plants. AMF colonization also leads to elicitation of flavonoids and chlorogenic acid-related genes in tomato and sunflower against invading pathogens (Aseel *et al*., 2019; Rashad *et al*., 2020). Phenolic compounds are antimicrobial substances which are defensively produced by infected plants from adjacent cells encircling pathogen infections, in order to restrict pathogen growth into healthy cells. This is known as localized acquired resistance (Ewané *et al*., 2012). Induction of some defense-related enzymes and accumulation of phytoalexins was also reported for AMF colonization (Song *et al*., 2011). Biochemical data from the present study revealed induction of the defense-related enzymes PAL, PPO, and POD. In addition, triggering of the transcriptional expression levels of defensin and chitinase genes was also observed in the

mycorrhizal garlic plants compared to the non-mycorrhizal plants, suggesting that induction of host systemic resistance is likely to be another defense mechanism induced by AMF.

Results from the present work demonstrated the biocontrol activity of *B. amyloliquefaciens* GGA against white rot of garlic. This result is similar to that of Zouari *et al*. (2016), who reported the biocontrol potential of endophytic *B. amyloliquefaciens* CEIZ-11 against damping-off of tomato, caused by *Pythium aphanidermatum*. Different biocontrol mechanisms were reported to be involved for *B. amyloliquefaciens* against many fungal pathogens, including production of fungitoxic secondary metabolites such as lipopeptides, volatile compounds, hydrolytic enzymes, and siderophores (Cawoy *et al*., 2015). Induction of plant systemic resistance against invading pathogens has also been reported as a biocontrol mechanism of *B. amyloliquefaciens*. Li *et al*. (2015) reported that cucurbit seedlings treated with *B. amyloliquefaciens* LJ02 or culture filtrates of the bacterium reduced the infection by *Sphaerotheca fuliginea*, and triggered biosynthesis of the defense-related enzymes superoxide dismutase, peroxidase, polyphenol oxidase and phenylalanine ammonia-lyase. Salicylic acid production and the transcriptional expression of the pathogenesis-related gene *PR-1* were also elevated, indicating that salicylic acid-mediated defense responses were induced. Similar to these results, the present study revealed considerable increases in the activities of defense-related enzymes (PAL, PPO, and POD), as well as up-regulation of the transcriptional expression of the defense-related genes defensin and chitinase, as responses to treating of garlic plants with *B. amyloliquefaciens* GGA and/or AMF. This indicates that induction of the host systemic resistance contributed the biocontrol behavior of both the tested biocontrol agents against the garlic white rot pathogen. In addition, competition with the pathogen for nutrients may play a part in the biocontrol activity (Ntushelo *et al*., 2019).

On the other hand, data from the pot experiment in this study showed that treating of garlic plants with endophytic *B. amyloliquefaciens* GGA and/or AMF improved the plant growth and enhanced the yield. One of the most beneficial effects of colonization by mycorrhizal fungi on the host plant is the elevation in the uptake of macro- and micronutrients from the soil via the extraradical mycelium network of AMF, specifically of phosphate (Ingraffia *et al*., 2019) which lead to increased biomass accumulation. Enhancing of the photosynthetic pigments in the host leaves and improving the plant water supply from the soil (Zhang *et al*., 2018) were also reported in the mycorrhizal plants, which promote the plant growth and yield (Begum *et al*., 2019). Promoting effect of *B. amyloliquefaciens* on different crop plants was reported in previous studies. In this regard, Kim *et al*. (2017) found that treating of Chinese cabbage, radish, tomato, and mustard plants with *B. amyloliquefaciens* H-2-5 led to enhancement of their growth. Production of the phytohormones gibberellins (GA4, GA8, GA9, GA19, and GA20) and phosphate solubilization ability were the used mechanisms. Production of indole-3-acetic acid has been also reported to contribute to their plant-growth-promoting effect (Shao *et al*., 2015). These mechanisms seem to contributed to the plant growth promoting potential of *B. amyloliquefaciens* GGA on garlic plants.

In conclusion, the present study demonstrated the biocontrol activity of AMF and/or the endophytic *B. amyloliquefaciens* GGA against the white rot of garlic. However, the synergistic effect of application of AMF and the endophytic *B. amyloliquefaciens* GGA as a dual biocontrol treatment was also confirmed. Both of them played important roles in triggering the garlic resistance to the infection with *S. cepivorum* through improving plant nutrition, growth, stimulating photosynthetic pigments, accumulation of some antimicrobial substances (phenolic compounds and defense-related enzymes), and activation of some defense-related genes. For upcoming work, we suggest studying application of these biocontrol agents under open field conditions to evaluate their efficacy, survival, and microbial interactions with the soil microbiome.

ACKNOWLEDGEMENTS

The authors are grateful to Prof. Zakaria A. Baka (Damietta University, Egypt) for his assistance in SEM investigations. This research did not receive any specific grant from public, commercial, or not-for-profit funding agencies.

LITERATURE CITED

Abdel-Fattah G.M., El-Haddad S.A., Hafez E.E., Rashad Y.M., 2011. Induction of Defense Responses in Common Bean Plants by Arbuscular Mycorrhizal Fungi. *Microbiological Research* 166(4): 268–281.

Allen S.E., 1989. *Chemical Analysis of Ecological Materials*. 2nd ed. Blackwell Scientific Publications, Oxfordand London, UK.

Amin M., Tadele S., Selvaraj T., 2014. White rot (*Sclerotium cepivorum*-Berk)- an aggressive pest of onion

and garlic in Ethiopia: an overview. *Journal of Agricultural Biotechnology and Sustainable Development* 6(1): 6-15.

Aseel D.G., Rashad Y.M., Hammad S.M., 2019. Arbuscular Mycorrhizal Fungi Trigger Transcriptional Expression of Flavonoids and Chlorogenic Acid Biosynthetic Pathways Genes in Tomato against *Tomato Mosaic Virus*. *Scientific Reports* 9: 9692.

Asrar A.A., Abdel-Fattah G.M., Elhindi K.M., Abdel-Salam E.M., 2014. The impact of arbuscular mychorrhizal fungi in improving growth, flower yield and tolerance of kalanchoe (*Kalanchoe blossfeldiana* Poelin) plants grown in NaCl-stress conditions. *Journal of Food, Agriculture and Environment* 12(1): 105–112.

Bayan L., Koulivand P.H., Gorji A., 2014. Garlic: a review of potential therapeutic effects. *Avicenna Journal of Phytomedicine* 4(1): 1–14.

Beaudoin-Eagan L.D., Thorpe T.A., 1985. Tyrosine and phenylalanine ammonia lyase activities during shoot inhibition in tobacco callus cultures. *Plant Physiology* 78: 438–441.

Begum N., Qin C., Ahanger M.A., Raza S., Khan M.I., … Zhang L., 2019. Role of arbuscular mycorrhizal fungi in plant growth regulation: implications in abiotic stress tolerance. *Frontiers in Plant Science* 10: 1068.

Berdeni D., Cotton T.E.A., Daniell T.J., Bidartondo M.I., Cameron D.D., Evans K.L., 2018. The effects of arbuscular mycorrhizal fungal colonisation on nutrient status, growth, productivity, and canker resistance of apple (*Malus pumila*). *Frontiers in Microbiology* 9, 1461.

Cawoy H., Debois D., Franzil L., De Pauw E., Thonart P., Ongena M., 2015. Lipopeptides as main ingredients for inhibition of fungal phytopathogens by *Bacillus subtilis/amyloliquefaciens*. *Microbial Biotechnology* 8: 281–295.

Clay K., Shearin Z.R.C., Bourke K.A., Bickford W.A., Kowalski K.P., 2016. Diversity of fungal endophytes in nonnative *Phragmites australis* in the Great Lakes. *Biological Invasions* 18: 2703e2716.

de Almeida Lopes K.B., Carpentieri-Pipolo V., Fira D., Balatti P.A., López S.M.Y., … Degrassi G., 2018. Screening of bacterial endophytes as potential biocontrol agents against soybean diseases. *Journal of Applied Microbiology* 125(5): 1466–1481.

De Silva N.I., Brooks S., Lumyong S., Hyde K.D., 2019. Use of endophytes as biocontrol agents. *Fungal Biology Reviews* 33(2): 133–148.

Duncan D.B., 1955. Multiple range and multiple F test. *Biometrics* 11: 1-24.

El-Sharkawy H.H., Rashad Y.M., Ibrahim S.A., 2018. Biocontrol of Stem Rust Disease of Wheat using Arbuscular Mycorrhizal Fungi and *Trichoderma* spp. *Physiological and Molecular Plant Pathology* 103: 84–91.

Entwistle A.R., 1990. *Allium* white rot and its control. *Soil Use and Management* 6(4): 201–208.

Ewané C.A., Lepoivre P., de Bellaire L.L., Lassois L., 2012. Involvement of phenolic compounds in the susceptibility of bananas to crown rot, a review. *Biotechnology, Agronomy, Society and Environment* 16(3): 393–404.

FAOSTAT © FAO, Statistics Division, http://www.fao.org/faostat/en/#data/QC (2019).

Galeazzi M.A.M., Sgarbieri V.C., Constantinides S.M., 1981. Isolation, purification and physicochemical characterization of polyphenoloxidases (PPO) from a dwarf variety of banana (*Musa cavendishii*, L). *Journal of Food Science* 46: 150–155.

Haggag W.M., Abdel-latif F.M., 2001. Interaction between vasicular arbuscular mycorrhizae and antagonistic biocontrol micro-organisms on controlling root-rot disease incidence of geranium plants. *Journal of Biological Sciences* 1: 1147–1153.

Hanif A., Zhang F., Li P., Li C., Xu Y., … Gao X., 2019. Fengycin Produced by *Bacillus amyloliquefaciens* FZB42 Inhibits *Fusarium graminearum* Growth and Mycotoxins Biosynthesis. *Toxins* 11: 295.

Harborne J.B., 1984. *Phytochemical Methods: A guide modern techniques of plant analysis*. Chapman and Hall press, London, UK.

Hayat M.A., 2000. *Principles and techniques of electron microscopy: Biological applications*. 4th ed. Cambridge University Press, Cambridge, UK, 543 pp.

Hazarika D.J., Goswami G., Gautom T., Parveen A., Das P., … Boro R.C., 2019. Lipopeptide mediated biocontrol activity of endophytic *Bacillus subtilis* against fungal phytopathogens. *BMC microbiology* 19(1): 71.

Hong C.E., Park J.M., 2016. Endophytic bacteria as biocontrol agents against plant pathogens: current state-of-the-art. *Plant Biotechnology Reports* 10(6): 353–357.

Ingraffia R., Amato G., Frenda A.S., Giambalvo D., 2019. Impacts of arbuscular mycorrhizal fungi on nutrient uptake, N_2 fixation, N transfer, and growth in a wheat/faba bean intercropping system. *PLoS ONE* 14(3): e0213672.

Jackson M.L., 1958. *Soil chemical analysis*. Prentice-Hall. Englewood Cliffs, N.J. 498 pp.

Kim M.J., Radhakrishnan R., Kang S.M., You Y.H., Jeong E.J., … Lee I.J., 2017. Plant growth promoting effect of *Bacillus amyloliquefaciens* H-2-5 on crop plants and influence on physiological changes in soybean under soil salinity. *Physiology and molecular biology of plants* 23(3): 571–580.

Lee T., Park D., Kim K., Lim S.M., Yu N.H., … Kim J.C., 2017. Characterization of *Bacillus amyloliquefaciens* DA12 Showing Potent Antifungal Activity against Mycotoxigenic *Fusarium* Species. *Plant Pathology Journal* 33(5): 499–507.

Li B., Li Q., Xu Z., Zhang N., Shen Q., Zhang R., 2014. Responses of beneficial *Bacillus amyloliquefaciens* SQR9 to different soilborne fungal pathogens through the alteration of antifungal compounds production. *Frontiers in Microbiology* 5: 636.

Li Y., Gu Y., Li J., Xu M., Wei Q., Wang Y., 2015. Biocontrol agent *Bacillus amyloliquefaciens* LJ02 induces systemic resistance against cucurbits powdery mildew. *Frontiers in Microbiology* 6: 883.

Li X., Zhang Y., Wei Z., Guan Z., Cai Y., Liao X., 2016. Antifungal activity of isolated *Bacillus amyloliquefaciens* SYBC H47 for the biocontrol of peach gummosis. *PLoS One* 11(9): e0162125.

Liu J., Zhou T., He D., Li X.-z., Wu H., … Gao X., 2011. Functions of lipopeptides bacillomycin D and fengycin in antagonism of *Bacillus amyloliquefaciens* C06 towards *Monilinia fructicola*. *Journal of Molecular Microbiology and Biotechnology* 20: 43–52.

Malik C.P., Singh M.B., 1980. *Estimation of total phenols, Plant Enzymology and Histo-Enzymology*. Kalyani Publishers, New Delhi, India, 286 pp.

Maxwell D.P., Bateman D.F., 1967. Changes in the activities of some oxidases in extracts of Rhizoctonia-infected bean hypocotyls in relation to lesion maturation. *Phytopathology* 57: 132–136.

Miedes E., Vanholme R., Boerjan W., Molina A., 2014. The role of the secondary cell wall in plant resistance to pathogens. *Frontiers in Plant Science* 5: 358.

Mustafa G., Khong N.G., Tisserant B., Randoux B., Fontaine J., … Sahraoui A.L., 2017. Defence mechanisms associated with mycorrhiza-induced resistance in wheat against powdery mildew. *Functional Plant Biology* 44: 443–454.

Ntushelo, K., Ledwaba L.K., Rauwane M.E., Adebo O.A., Njobeh P.B., 2019. The mode of action of *Bacillus* species against *Fusarium graminearum*, tools for investigation, and future prospects. *Toxins* 11: 606.

Peterburgski A.V., 1968. *Handbook of Agronomic Chemistry*. Kolop Publishing House, Moscow, Russia.

Phillips J.M., Hayman D.S., 1970. Improved procedures for clearing roots and staining parasitic and vesicular-arbuscular mycorrhizal fungi for rapid assessment of colonization. *Transactions of the British Mycological Society* 55: 158–161.

Rashad Y.M., Aseel D.G., Hammad S.M., ElKelish A.A., 2020. *Rhizophagus irregularis* and *Rhizoctonia solani* differentially elicit systemic transcriptional expression of polyphenol biosynthetic pathways genes in sunflower. *Biomolecules* 10(3): 379.

Sadasivam S. Manickam A., 1992. Estimation of nitrogen by Micro-Kjeldahl. In: *Biochemical Methods for Agricultural Sciences*. Wiley Eastern Limited, New Delhi, India, 34–37 pp.

Saleha Y.M., 2010. Gene expression and histopathology alterations during rat mammary carcinogenesis induced by 7,12-dimethylbenz[a]anthracene and the protective role of Neem (*Azadirachta indica*) leaf extract. *Journal of American Science* 6: 9.

Santos M.L., Berlitz D.L., Wiest S.L.F., Schünemann R., Knaak N., Fiuza L.M., 2018. Benefits associated with the interaction of endophytic bacteria and plants. *Brazilian Archives of Biology and Technology* 61: e18160431.

Schmittgen T.D. Livak K.J., 2008. Analyzing real-time PCR data by the comparative C_T method. *Nature Protocols* 3: 1101–1108.

Shao J., Li S., Zhang N., Cui X., Zhou X., … Zhang R., 2015. Analysis and cloning of the synthetic pathway of the phytohormone indole-3-acetic acid in the plant-beneficial *Bacillus amyloliquefaciens* SQR9. *Microbial Cell Factories* 14: 130.

Siyoum Z. Yesuf M., 2013. Searching and evaluating of cost effective management options of garlic white rot (*Sclerotium cepivorum* Berk) in Tigray, Northern Ethiopia. *Journal of Plant Pathology and Microbiology* 4:189.

Song F., Song G., Dong A., Kong X., 2011. Regulatory mechanisms of host plant defense responses to arbuscular mycorrhiza. *Acta Ecologica Sinica* 31(6): 322–327.

Spatafora J.W., Chang Y., Benny G.L., Lazarus K., Smith M.E., … Stajich J.E., 2016. A phylum-level phylogenetic classification of zygomycete fungi based on genome-scale data. *Mycologia*108(5): 1028–1046.

Strobel G., 2018. The Emergence of Endophytic Microbes and Their Biological Promise. *Journal of Fungi* 4(2): E57.

Sur S., Romo T.D., Grossfield A., 2018. Selectivity and mechanism of fengycin, an antimicrobial lipopeptide, from molecular dynamics. *The Journal of Physical Chemistry B* 122(8): 2219–2226.

Tao Y., Bie X.M., Lv F.X., Zhao H.Z. Lu Z.X., 2011. Antifungal activity and mechanism of fengycin in the presence and absence of commercial surfactin against *Rhizopus stolonifer*. *The Journal of Microbiology* 49: 146–150.

Trouvelot A., Kough J.L., Gianinazzi-Pearson V., 1986. Mesure du taux de mycorhization VA d'un système

radiculaire recherche de methods d'estimation ayant une signification fonctionnelle. In: *Physiological and Genetical Aspects of Mycorrhizae* (V. Gianinazzi-Pearson, S. Gianinazzi, ed.) INRA Publ, Paris, France, 217–221.

Yang C., Hamel C., Vujanovic V., Gan Y., 2011. Fungicide: Modes of Action and Possible Impact on Nontarget Microorganisms *International Scholarly Research Notices: Ecology* 2011: 130289.

Yuan J., Raza W., Shen Q., Huang Q., 2012. Antifungal activity of *Bacillus amyloliquefaciens* NJN-6 volatile compounds against *Fusarium oxysporum* f. sp. *cubense*. *Applied and Environmental Microbiology* 78: 5942–5944.

Zhang F., Zou Y.-N., Wu Q.-S., 2018. Quantitative estimation of water uptake by mycorrhizal extraradical hyphae in citrus under drought stress. *Scientia Horticulturae* 229: 132–136.

Zouari I., Jlaiel L., Tounsi S., Trigui M., 2016. Biocontrol activity of the endophytic *Bacillus amyloliquefaciens* strain CEIZ-11 against *Pythium aphanidermatum* and purification of its bioactive compounds. *Biological Control* 100: 54–62.

Phytopathologia Mediterranea
The international journal of the
Mediterranean Phytopathological Union

Firenze University Press
www.fupress.com/pm

Research Paper

Impacts of previous crops on inoculum of *Fusarium culmorum* in soil, and development of foot and root rot of durum wheat in Tunisia

Eya KHEMIR[1,2,*], Samira CHEKALI[3], Antonio MORETTI[4], Mohamed Salah GHARBI[1], Mohamed Bechir ALLAGUI[1], Samia GARGOURI[1]

[1] *National Agronomic Institute of Research of Tunisia, University of Carthage, Tunis, Tunisia*
[2] *National Agronomic Institute of Tunisia, University of Carthage, Tunis, Tunisia*
[3] *Regional Pole of Agricultural Research and Development of North-West, Kef, Tunisia*
[4] *Institute of Sciences of Food Production, Research National Council (ISPA-CNR), Bari, Italy*
*Corresponding author: eya-khemir@hotmail.fr

Summary. Fusarium foot and root rot (FFRR) of cereals, caused by *Fusarium culmorum* and other *Fusarium* spp., is one of the most important soil- and residue-borne diseases in Tunisia. Management of the disease relies primarily on cultural practices such as crop rotation. Impacts of previous crops on the population of *F. culmorum* in the soil, and the incidence and severity of FFRR in durum wheat, were evaluated under Tunisian farming systems. A field trial showed that break crops of faba bean and fenugreek reduced the amount of *F. culmorum* DNA in soil, by 58% (faba bean) and 65% (fenugreek), and decreased numbers of *F. culmorum* propagules per g of soil by 83% (faba bean) and 85% (fenugreek). Farm demonstration trials also showed that faba bean and vetch used as previous crops reduced *F. culmorum* inoculum in the soil. Non-cereal crops also reduced the incidence of *F. culmorum* present in durum wheat roots and stem bases. The greatest grain yields and thousand kernel weights were recorded when faba bean and vetch were used as previous crops, but were less where durum wheat was previously grown. There were strong correlations between inoculum level of *F. culmorum* in the soil and incidence of FFRR in the following year. Results obtained in the field trial were supported by those collected from three demonstration farm trials during two cropping seasons. This study demonstrated for the first time in Tunisia and the Mediterranean region that break crops are effective for reducing *F. culmorum* inoculum in the soil and decreasing the pathogen in wheat roots and stem bases. Inoculum levels in soil can predict the expression of the disease in the following year in Tunisian farming conditions. These results are likely to be useful for developing and implementing guidelines for the management of FFRR of durum wheat.

Keywords. Faba bean, fenugreek, legumes, rotation, vetch.

OPEN ACCESS

Citation: E. Khemir, S. Chekali, A. Moretti, M.S. Gharbi, M.B. Allagui, S. Gargouri (2020) Impacts of previous crops on inoculum of *Fusarium culmorum* in soil, and development of foot and root rot of durum wheat in Tunisia. *Phytopathologia Mediterranea* 59(1): 187-201. doi: 10.14601/Phyto-10827

Accepted: March 5, 2020

Published: April 30, 2020

Data Availability Statement: All relevant data are within the paper and its Supporting Information files.

Competing Interests: The Author(s) declare(s) no conflict of interest.

Editor: Andy Tekauz, Cereal Research Centre, Winnipeg, MB, Canada.

INTRODUCTION

In Tunisia, cereals and their by-products are the main sources of dietary calories, and are the common base of all diets and the historical base of the

Mediterranean diet. The average *per capita* consumption of cereals in Tunisia is 184 kg per year (Slama *et al*., 2005; ONAGRI, 2016). Cereals are grown on approx. 1 million hectares of the agricultural land, with the number of the farmers involved estimated to be approx. 250,000. About 63% of farmers are smallholders, each with land areas of less than 10 ha (Bachta, 2011; Anonymous 2, 2018). Fusarium foot and root rot (FFRR) has been recognized as one of the most important diseases of cereals in Tunisia since the 1970s (Ghodbane *et al*., 1974), and this disease is responsible for significant economic losses, especially in arid and semi-arid regions (Van Wyk *et al*., 1987; Bateman, 1993; Hollaway *et al*., 2013). Yield losses of up to 26% in durum wheat and 18% in barley have been recorded (Chekali *et al*., 2013).

FFRR is caused by a complex of fungal pathogens. The two most reported are *Fusarium pseudograminearum* (O'Donnell & Aoki) (syn. *F. graminearum* group 1, *Giberella coronicola*) and *F. culmorum* (W. G. Sm.). *F. pseudograminearum* is the dominant species in several countries, including Australia (Burgess *et al*., 1975; Akinsanmi *et al*., 2004; Smiley *et al*., 2005), United States of America (Cook, 1980; Smiley and Patterson, 1996; Smiley *et al*., 2005) and New Zealand (Cromey *et al*., 2006), while *F. culmorum* is the dominant pathogen in Tunisia and the Mediterranean region (Cassini, 1981; Balmas,1994; Rossi *et al*., 1995; Mergoum *et al*., 2000; Gargouri *et al*., 2001).

FFRR is difficult to manage since *F. culmorum* can survive as hyphae in stubble residues of cereals (Cook, 1968; Bateman and Murray, 2001; Burgess, 2011; Khemir *et al*., 2018) and other grasses (Wallwork *et al*., 2004), and has the ability to persist as chlamydospores in soil (Sitton and Cook, 1981). This survival ability has major implications for designing strategies for effective disease management. Control of FFRR relies on agronomic management strategies, since in-crop fungicides are largely inefficient, and host resistance is limited (Burgess *et al*., 2001; Pereyra and Dill-Macky, 2004; Wisniewska and Kowalczyk, 2005).

The market situation in Tunisia has influenced the diversity of crops that are grown, where continuous wheat cropping and short crop rotations have become popular during the last 30 years. These cropping systems promote the increase of soil-borne diseases and resulting yield losses. In addition, durum wheat, which is highly susceptible to FFRR (Burgess *et al*., 2001), is the dominant crop, representing approx. 60 % of the cereal growing area (Slama *et al*., 2005; Gharbi and Felah, 2013). In the context of climate change, this disease could become more important, especially as the Mediterranean region has been qualified as a "hot spot for climate change" (Giorgi, 2006; Vicente-Serrano, 2006; Anonymous 1, 2019). It is important, therefore, to consider the best cultural practices for FFRR control. Crop rotations with non-hosts such as legumes has been reported to efficiently control the disease in many countries including the United Kingdom (Bateman and Kwasana, 1999; Bateman and Murray, 2001), Australia (Felton *et al*., 1998; Kirkegaard *et al*., 2004; Evans *et al*., 2010) and South Africa (Lamprecht *et al*., 2006).

Very little research has been conducted in the Mediterranean basin, including Tunisia (Chekali *et al*., 2016), to evaluate the impacts of break crops on development of FFRR. Fenugreek, an annual legume that grows well in Mediterranean climates (Duke *et al*., 1981), and which has demonstrated strong insecticidal, nematicidal and antifungal activity (Pemonge *et al*., 1997; Zia *et al*., 2001; Evidente *et al*., 2007; Haouala *et al*., 2008; Omezzine *et al*., 2014), has not been evaluated for reducing *F. culmorum* levels in soil, and its impacts on the disease. Very few studies have focused on monitoring *F. culmorum* soil inoculum under different cropping systems (McKenzie and Taylor, 1983; Evans et *al*., 2010).

The present study aimed to assess: i) the potential benefits of previous crops for reducing *F. culmorum* populations in the soil; ii) the impacts of previous crops on the incidence and severity of FFRR on stems and roots of durum wheat; and iii) the relationships between preplanting inoculum of *F. culmorum* and FFRR disease expression and grain yields.

MATERIALS AND METHODS

Site characteristics and cultural practices

To understand the effect of previous crops on populations of *F. culmorum* in the soil and incidence of FFRR in durum wheat, a field trial and three demonstration trials were established during the cropping seasons 2012/13, 2013/14 and 2014/15, in Northwest Tunisia.

Field trial

The field trial was carried out in a farm field located at Bou Salem (N36 53.012 E9 31.251). The area has a typical Mediterranean climate (Köppen, 1936), with hot summers and cold, wet winters. The monthly rainfall during the three cropping seasons at Bou Salem is summarized in Table 1, where the 10-yr annual average rainfall is approx. 500 mm.

The trial was established in 2012/13 as a randomized complete block design (RCBD) with three crop-

Table 1. Monthly rainfall (mm) recorded during the 2012/2013, 2013/14 and 2014/15 cropping seasons at Bou Salem, Tunisia.

Cropping season	Sep.	Oct.	Nov.	Dec.	Jan.	Feb.	Mar.	Apr.	May.	Jun.	Jul.	Aug.	Total
2012/13	62	67	22	27	50	64	22	28	4	0	10	31	387
2013/14	14	45	118	44	81	23	82	24	47	4	0	0	482
2014/15	1	36	33	103	118	128	79	2	18	1	0	21	540
10 years means (2006/2015)	35	58	50	61	73	60	69	46	29	8	1	9	499

Source: National Institute of Meteorology.

Table 2. Monthly rainfall (mm) recorded during the 2012/2013, 2013/14 and 2014/15 cropping seasons at Fernana, Tunisia.

Cropping season	Sep.	Oct.	Nov.	Dec.	Jan.	Feb.	Mar.	Apr.	May.	Jun.	Jul.	Aug.	Total
2012/13	89	106	22	138	149	221	25	28	23	0	0	1	802
2013/14	23	18	298	82	91	46	109	70	32	9	4	2	784
2014/15	45	95	35	138	115	120	65	40	40	7	2	1	703
15 years means (2001/2015)	31	78	81	126	128	120	82	83	32	12	3	5	781

Source: National Institute of Meteorology.

ping sequences and four replications. An area of 7,500 m^2 was divided into four blocks. Each block was subdivided into three plots (each of 12 × 50 m) which were sown with durum wheat (*Triticum durum*) var. 'Karim', faba bean (*Vicia faba*) var. 'Bachar' or fenugreek (*Trigonella foenum-graecum*) var 'Rihana'. The impacts of previous crops were assessed during the two following cropping seasons of 2013/14 and 2014/15. Durum wheat was sown at the recommended rate of 150 kg ha^{-1}; faba bean was sown at 140 kg ha^{-1} and fenugreek at 35 kg ha^{-1}. All these crops were seeded in early to mid-November of each year. Diammonium phosphate (P) (150 kg ha^{-1}) was applied with seed (Zadoks growth stage (ZGS) 1; Zadoks *et al*. 1974), and ammonium nitrate fertilizer (N) (150 kg ha^{-1}) was applied at tillering (ZGS 21) and at stem elongation (ZGS 32). For uniform suppression of grass weeds in the faba bean and fenugreek plots, clethodim (Select super®) was applied at 1 L ha^{-1} post-emergence of grass weeds from the 3-leaf stage of the crop plants.

Demonstration trials

Demonstration trials were established in three farmer's fields (36°37'29.28'N, 8°42'04.56'E; 36°36'47.56'N, 8°34'39.42'E and 36°37'01.10'N. 8°40'35.90'E) at Fernana. This region is also characterized by hot summers and cold, wet winter, but with greater annual rainfall than at the field trial site. The monthly rainfall during the three cropping seasons is summarized in Table 2, and the 15 y average rainfall was approx.780 mm at this location.

In 2012/13, an area of 3,000 m^2 at each farm was divided into three plots, which were each sown with faba bean (*Vicia faba*) var. 'Bachar', durum wheat (*Triticum durum*) var. 'Karim' or a local variety of vetch (*Vicia sativa*). The plots were 10 m wide and 100 m long. The effects of previous crops were evaluated during the two subsequent cropping seasons (2013/14 and 2014/15). These trials were direct seeded (without tillage) to retain uniform and high inoculum levels of *F. culmorum* at the beginning of the study. The three previous crops were applied according to common farmer practices. Durum wheat was seeded at 150 kg ha^{-1}, faba bean at 130 kg ha^{-1} and vetch at 100 kg ha^{-1}. Diammonium phosphate (P) (150 kg ha^{-1}) was applied with seed (Zadoks growth stage (ZGS) 1; Zadoks *et al*. 1974), and ammonium nitrate fertilizer (N) (150 kg ha^{-1}) was applied at tillering (ZGS 21) and at stem elongation (ZGS 32).

To control annual grass weeds, glyphosate (3 L ha^{-1}) was applied prior to sowing of durum wheat and mésosulfuron-méthyl (Mesomax®) + iodosulfuron + méfenpyr (Amilcar®) (1 L ha^{-1}) was applied in January 2014 and in January 2015. The faba bean plots received simazine (1.5 L ha^{-1}) and clethodim (Select Super ®) (1 L ha^{-1}) at post-emergence of the grassy weeds.

Fusarium culmorum *inoculum density*

Soil sampling

Soil samples were collected in July 2013, following the crop sequence treatments from the 12 plots of

the field trial at Bou Salem, and the three plots from each of the demonstration trials at Fernana. One hundred soil cores, including any plant residus, were taken within each plot to a depth of 100 mm, using a 15-mm diam. Accucore corer (Spurr Soil Probes), and were then bulked to provide a single sample for each plot. The samples were air-dried for several days. Dry soil (500 g) for each plot was sent to the South Australian Research and Development Institute (SARDI), Adelaide, Australia, for assays of *F. culmorum* DNA ('Predicta® B' Soil Testing Service). The remaining soil from each plot was used for soil dilution plating (below).

Soil dilution plating

This was carried out to estimate populations of *F. culmorum* (Cook, 1980), following the procedure of Snyder and Nash (1968), with modifications as described by Bateman and Coskun (1995), Bateman *et al*., (1998) and Bateman and Murray (2001). Briefly, 10 g of soil from each plot were added to 100 mL of 0.1 % water agar and mixed thoroughly for 30 sec. Further dilution series were made using 1 mL aliquots from the starting suspension. An aliquot of 1 mL of the final dilution (1/100, based on premilary tests) was transferred to each of five Petri dishes containing Peptone-PCNB agar medium. This medium contained 15 g Difco peptone, 20g agar, 1 g KH_2PO_4, 0.5g $MgSO_4\,7H_2O$, 1 g pentachloronitrobenzene (PCNB), 100 mg L^{-1} streptomycin sulfate and 80 mg L^{-1} neomycin. Aliquots were dispersed by circular agitation of the Petri dishes (Steinkellner and Langer, 2004). The Petri dishes were incubated at 20°C for 5–7 d with a 16 h light/8 h dark regime. *Fusarium culmorum* was identified morphologically according to Leslie and Summerell (2006).

To confirm fungal identifications, some colonies were transferred to ¼ strength potato dextrose agar (PDA) and then to carnation leaf agar (CLA). Amounts of *F. culmorum* in the soil samples were expressed as the numbers of colony forming units per gram of air-dried soil (CFU g^{-1} soil).

CFU g^{-1} was calculated using the formula:

$$\text{CFU g}^{-1} = \frac{\text{Number of colonies} \times \text{dilution factor}}{\text{Volume of culture plate}}$$

With dilution factor = 10^2, and volume of culture plate = 1 mL.

Quantitative real-time polymerase chain reaction (qPCR)

The amount of *F. culmorum* DNA present in soil from each plot was evaluated, after applying the crop sequence treatments (July 2013). Soil samples were submitted to the SARDI Root Disease Testing Service. This includes a suite of tests for the quantification of *F. culmorum* DNA in soil. QPCR assays using rDNA (TaqMan) probe sequences specific to *F. culmorum* were made for the total pathogen DNA extracted from the soil. Levels of *F. culmorum* DNA in soil can be related to disease risk in the following crop year (Hogg *et al*., 2007). Extraction protocols and analyses of DNA from soil were done according to Ophel-Keller *et al*. (2008). Inoculum concentrations of DNA per gram of soil were expressed in pictograms.

Pathogen isolation and disease incidence

During the 2013/14 and 2014/15 seasons, 50 plants of durum wheat were collected randomly along a W-shaped transcript, from each of the 12 plots of the field trial, and from the nine plots of the three demonstration trials, at the durum wheat anthesis stage (ZGS 85). The incidence of FFRR was calculated as the frequency of isolation of *F. culmorum*, separately from roots or stem bases.

Stem base sections and root sections (2–3 mm length) were surface-sterilized with 70% ethanol for 15 s, followed by 3% sodium hypochlorite for 1min, and then rinsed three times with distilled water, and were then air-dried on sterile filter paper. Five sections from each sample were then plated onto ¼ strength PDA containing 20 mL L^{-1} streptomycin sulfate (100 mg L^{-1}) and 12 mL L^{-1} neomycin sulfate (80 mg L^{-1}) in Petri dishes. The plates were incubated up to 7 days at 25°C in a 12 h light/12 h dark regime. Hyphae of *Fusarium* spp. were subsequently transferred onto CLA to promote conidium production. *Fusarium culmorum* was identified using morphological criteria, according to Leslie and Summerell (2006).

Disease severity

FFRR disease severity was assessed only during the 2014/15 cropping season in the three farm demonstration trials, at the durum wheat anthesis stage (ZGS 85). Severity of *F. culmorum* was evaluated by measuring surface of stem bases showing browning. Fifty durum wheat plants were randomly removed from each plot and scored using a scale 0 to 3, where: 0 = no browning (no visible symptoms); 1 = 0.1 to 1.9 cm extent of browning; 2 = 2 to 3.9 cm of browning; and 3 = > 4 cm browning.

Ratings were converted to severity indices using the following formula:

$$\text{Severity index} = \frac{((0) \times (n0) + (1) \times (n1) + (2) \times (n2) + (3) \times (n3))}{N}$$

Where: N = number of evaluated plants; n_0 = number of plants in class 0; n_1 = number of plants in class 1; n_2 = number of plants in class 2; and n_3 = number of plants in class 3.

Yield parameters

Grain yields of durum wheat, subjected to different crop rotations, were assessed from the three demonstration trials in the 2013/14 and 2014/15 cropping seasons. The yields (kg ha^{-1}) were based on harvesting all of the grain from each plot.

Statistical analyses

Field trial

The trial was arranged in a randomized complete block design (RCBD) with four replicates. All data were subjected to analysis of variance (ANOVA) using 'SPSS Statistics version 20' software published by 'IBM Crop 2011'. The year and previous crop were considered as main factors. Means comparisons were performed using the Student's LSD test (at $P = 0.05$ or $P = 0.01$).

Regression analyses used Pearson's correlation test, to identify possible associations between the incidence of *F. culmorum* isolated from stem bases and roots (2013/14 cropping season data) and the amounts of *F. culmorum* in the soil (DNA and CFU) left after each treatment, measured at plant maturity in July 2013.

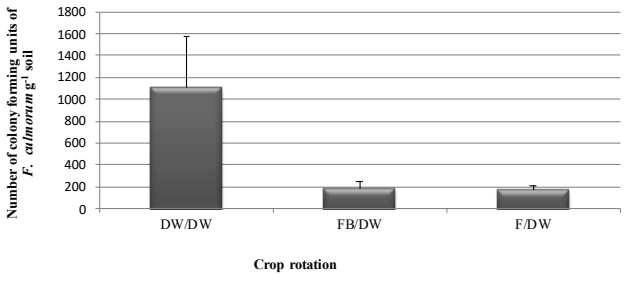

Figure 1. Mean numbers of colony forming units of *Fusarium culmorum* g^{-1} of soil, estimated by dilution plating, sampled from the experimental trial at Bou Salem, Tunisia, after different crop rotations. Error bars are 2 × standard deviations. DW = durum wheat, FB = faba bean, F = fenugreek.

Demonstration trials

Regression analyses were carried out (as above), to identify possible correlations between *F. culmorum* DNA content in soil (determined by qPCR), the number of CFU of *F. culmorum* per gram of soil (determined by soil dilution plating) and the incidence of *F. culmorum* isolations from stem bases and roots of durum wheat (2013/14 cropping season data). In addition, regression analysis was used to identify possible association between FFRR expression and grain yields from subsequent durum wheat crops.

RESULTS

Fusarium culmorum *inoculum in the soil*

Soil dilution plating and morphological identification revealed several *Fusarium* species from the soil samples. These included *F. acuminatum*, *F. avenaceum*, *F. culmorum*, *F. compactum*, *F. equiseti*, *F. oxysporum* and *F. solani*. However, *F. culmorum* was by far the dominant pathogenic species in the samples. The DNA analyses conducted for detection of the two recognized pathogenic species, *F. culmorum* and *F. pseudograminearum*, showed the presence of only *F. culmorum* in the samples.

Field trial

Soil dilution plating revealed the presence of *F. culmorum* in all 12 plots of the field trial at Bou Salem. ANOVA of data from the trial revealed that the number of CFU of *F. culmorum* in the upper 10 cm soil layer was significantly ($P = 0.002$) affected by the different break crops. Faba bean and fenugreek used as previous crops, *vs.* durum wheat monoculture, reduced the number of *F. culmorum* propagules in soil by 83% for faba bean and 85% for fenugreek (Figure 1). The number of propagules ranged from 133 to 1,733 CFU g-1 of soil, with a mean of 1100 for durum wheat, 183 for faba bean and 166 for fenugreek. DNA analyses confirmed the presence of *F. culmorum* in soil from the 12 plots of the field trial. The amounts of DNA of the pathogen were significantly ($P = 0.004$) different among previous crop treatments, ranging from 27 to 212 pg DNA g^{-1} of soil. Overall, the amounts of *F. culmorum* DNA in the soil were decreased by 58% following faba bean and by 65 %, following fenugreek. The greatest amounts of *F. culmorum* DNA occurred in the treatment where durum wheat was cultivated in monoculture, and here was no statistically

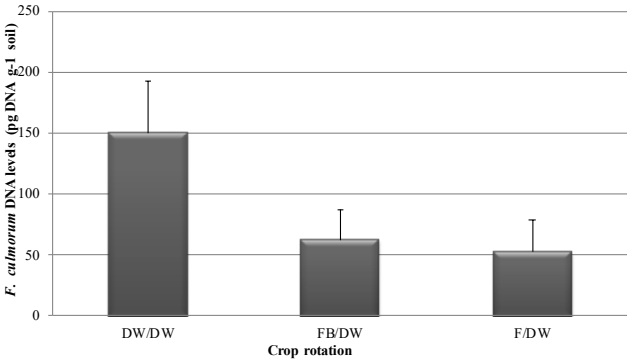

Figure 2. Amounts of *Fusarium culmorum* DNA in soil (pg DNA $^{-1}$g of soil) 1 year after different crop rotations from the experimental field trial at Bou Salem, Tunisia. Error bars are 2 × standard deviations. DW: durum wheat, FB = faba bean, F = fenugreek.

significant difference in DNA amounts between the two legume treatments (Figure 2).

Soil dilution plating and qPCR both showed greater amounts of *F. culmorum* in soil following a previous durum wheat crop, compared to previous faba bean or fenugreek crops. Pearson's correlation test showed that *F. culmorum* DNA concentration (pg DNA g^{-1} soil) was correlated (r = 0.92; $P < 0.001$) with the number of propagules of this fungus (CFU g^{-1} soil) detected in the soil 1 year after treatment.

Demonstration trials

Based on soil dilution plating, propagules of *F. culmorum* in the soil were more abundant after wheat (average of 866 propagules g^{-1} of soil) compared to vetch (358 propagules g^{-1} of soil) or faba bean (289 propagules g^{-1} of soil) (Table 3). Thus, faba bean and vetch, used as previous crops, reduced the number of *F. culmorum* propagules in soil by 66 % after faba bean and 58 % after vetch, compared to durum wheat monoculture. In addition, the results indicated that *F. culmorum* propagules were less abundant after faba bean as a previous crop compared to vetch.

The DNA analyses showed greater amounts of *F. culmorum* DNA in soil from Farm 1 and 2 compared to Farm 3 (Table 3). Based on real-time qPCR, the amount of DNA of *F. culmorum* was less following a legume compared to wheat at Farms 1 and 2. However, at Farm 3, where the DNA amounts were low in all cases, there were no differences in *F. culmorum* DNA between the different previous crops. Based on the SARDI risk assessment protocol, DNA amounts for all plots at Farm 3 were classified as leading to low risk of subsequent crop damage.

Overall, for the 12 plots of the field trial and the six plots of the demonstration trials at Farms 1 and 2, legumes used as previous crops reduced the inoculum of *F. culmorum*, as detected by qPCR and by soil dilution plating.

Disease assessments

A total of 4,200 stems and roots were examined to determine the impacts of crop sequence on soil-borne diseases of cereals in the field and demonstration trials. Visual assessments revealed evidence of take-all, eyespot and FFRR. Only the results for previous crop effects on FFRR development are presented here.

Field trial

Incidence of infection by *F. culmorum* in durum wheat was greater in durum wheat stem bases than in roots. Statistical analyses showed that there was a difference ($P = 0.047$) between the two growing seasons (2013/14 and 2014/15) for incidence of *F. culmorum* recovered from durum wheat stem bases. No significant difference was detected in the incidence of *F. culmorum* recovered from wheat roots during these two cropping seasons (Figure 3).

ANOVA of data from the field trial revealed that there was a highly significant ($P < 0.001$) effect of previous crop on the incidence of FFRR infection of stem bases and roots of durum wheat. Fenugreek or faba

Table 3. Number of colony forming units (CFU g^{-1} of soil), levels of DNA (pg DNA g^{-1} soil) of *Fusarium culmorum* 1 year after treatment at three demonstration trial sites, and risk of resultant crop losses (Predicta® B test).

Previous crop rotation	Site 1			Site 2			Site 3		
	CFU g^{-1}	pg DNA g^{-1}	Risk	CFU g^{-1}	pg DNA g^{-1}	Risk	CFU g^{-1}	pg DNA g^{-1}	Risk
Durum wheat/durum wheat	1071	104	medium	928	328	high	600	14	low
Durum wheat/vetch	142	41	low	500	150	medium	433	44	low
Durum wheat/faba bean	0	14	low	500	163	medium	366	50	low

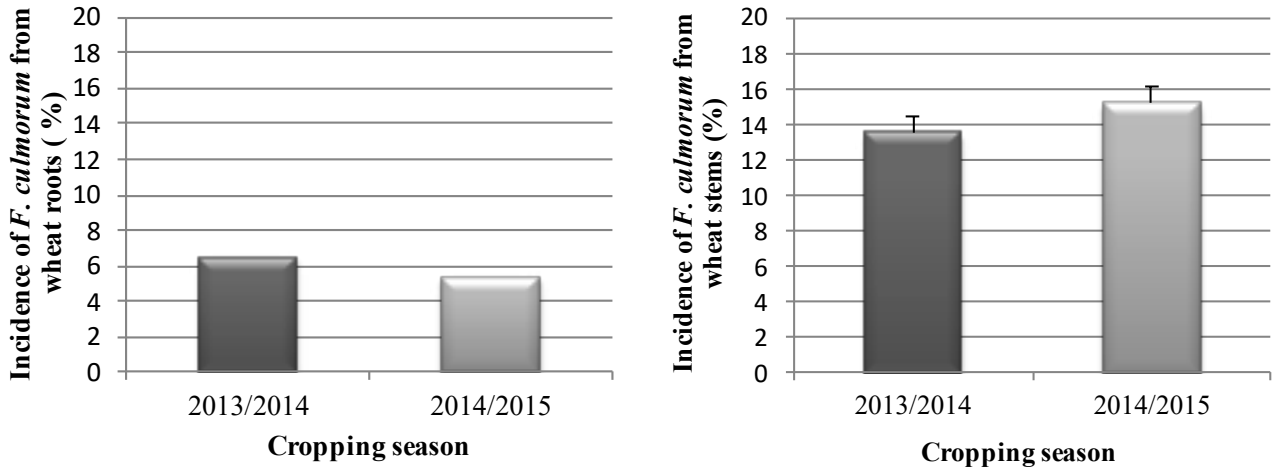

Figure 3. Mean incidence of *Fusarium culmorum* isolations from durum wheat roots (A) and stem bases (B) during two cropping seasons, at the Bou Salem,Tunisia, field trial. Error bars are 2 × standard deviations.

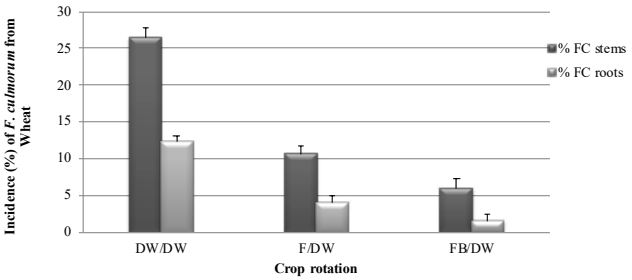

Figure 4. Mean incidence of *Fusarium culmorum* infection on wheat stem bases and roots as affected by different previous crops (DW = durum wheat; F = fenugreek; FB = faba bean), at the Bou Salem, Tunisia, field trial in the 2013/14 and 2014/15 cropping seasons. Error bars are 2 × standard deviations.

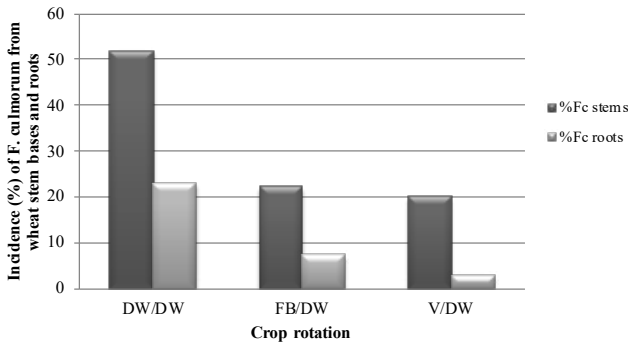

Figure 5. Mean incidence of *Fusarium culmorum* (Fc) from durum wheat stem bases and roots from three demonstration trials, after previous crops of durum wheat faba bean and vetch.

bean used as the previous crop decreased the incidence of *F. culmorum* affected durum wheat roots more than 3× for fenugreek and 9× for faba bean, compared to durum wheat. Similarly, fenugreek and faba bean decreased the incidence of *F. culmorum* in durum wheat stem bases, by more than 3× for fenugreek and 5× for faba bean. Data analyses showed that the incidence of infection by *F. culmorum* on durum wheat stem bases and roots was least ($P < 0.001$) when faba bean was the previous crop (Figure 4).

Demonstration trials

Data from the three demonstration trials showed that the presence of *F. culmorum* in durum wheat roots and stem bases when they were sampled during the 2013/14 and 2014/15 cropping seasons. Assessments of development of FFRR showed that stem bases were much more likely to be infected by *F. culmorum* than roots. Faba bean and vetch, used as previous crops, resulted in a less isolation incidence of *F. culmorum* than for durum wheat monoculture. Compared to durum wheat, the mean reduction in *F. culmorum* incidence after faba bean was 59% in stem bases and 68% in roots, and after vetch was 62% in stem bases and 87% in roots (Figure 5).

FFRR severity was evaluated only in spring 2015 (2014/15 cropping season). Compared to durum wheat monocropping, vetch used as the previous crop reduced disease severity by 80% and faba bean as the previous crop reduced severity by 50 % (Figure 6).

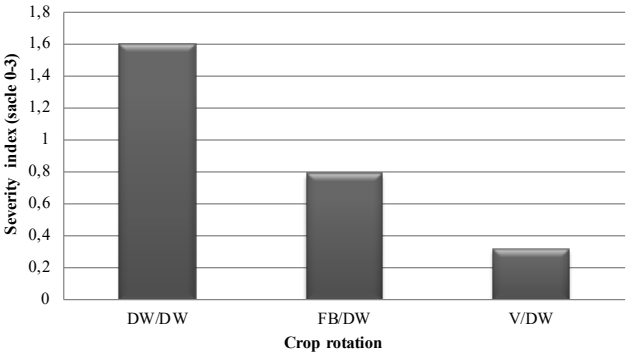

Figure 6. Mean durum wheat foot and root rot severity indices for wheat grown after durum wheat (DW), faba bean (FB) or vetch (V) at the Fernana demonstration trials during the 2014/2015 cropping season.

Relationships between Fusarium culmorum inoculum density in soil and development of FFRR

Field trial

According to Pearson's correlation test, the amounts of *F. culmorum* DNA detected in soil samples 1 year after treatment were positively correlated with the incidence of *F. culmorum*, durum wheat roots (R^2 = 0.56, P = 0.005) and in stem bases (R^2 = 0.80, P = 0.001) for wheat grown in the following year (Figure 7).

The association between pre-planting inoculum concentrations, indicated by *F. culmorum* CFU g^{-1} of soil, and disease expression, indicated by incidence of *F. culmorum* in wheat roots, was significantly positive (R^2 = 0.58, P = 0.004) (Figure 7A). This was also true for this relationship in stem bases (R^2 = 0.83, P = 0.000) (Figure 7B).

Demonstration trials

Inoculum levels of *F. culmorum* detected in the soil after each treatment, as determined by soil dilution plating, were positively correlated with incidence of *F. culmorum* in wheat roots (R^2 = 0.66) and stem bases R^2 = 0.64 (Figure 8, A and B). In addition, a positive relationship was observed between the amounts of *F. culmorum* DNA and the incidence of *F. culmorum* in wheat roots (R^2 = 0.65) and stem bases (R^2 = 0.7) after each treatment (Figure 8, A and B).

Grain yields

The greatest durum wheat grain yield (3,833 kg ha^{-1}) was recorded when vetch was the previous crop, followed by faba bean (3,583 kg ha^{-1}) and durum wheat (3,239 kg ha^{-1}) (Figure 9). Regression analyses showed a negative correlation between grain yields (kg ha^{-1}) and *F. culmorum* incidence on durum wheat stem bases (Figure 10) (r = -0.74), and grain yields FFRR severity indices (r = - 0.56) (Figure 11).

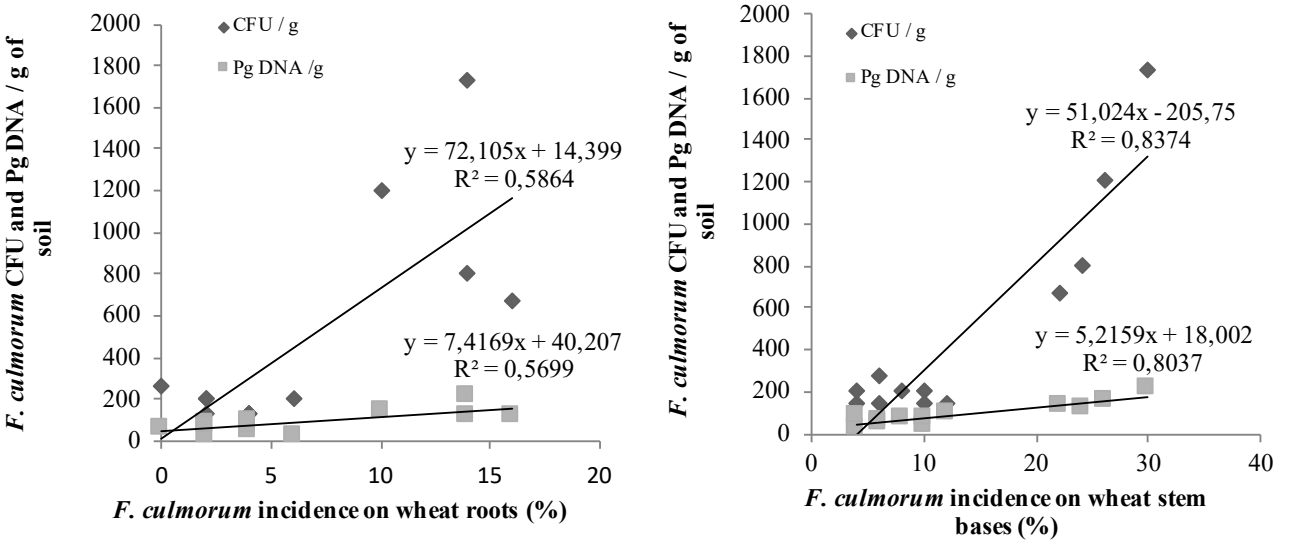

Figure 7. Correlations (Pearson's correlation test) between *Fusarium culmorum* on wheat roots (A) and stem bases (B) and amounts of *F. culmorum* inoculum left in the soil after 1 year at the Bou Salem experimental trial, as analyzed by soil dilution plating and quantitative real-time polymerase chain reaction (qPCR).

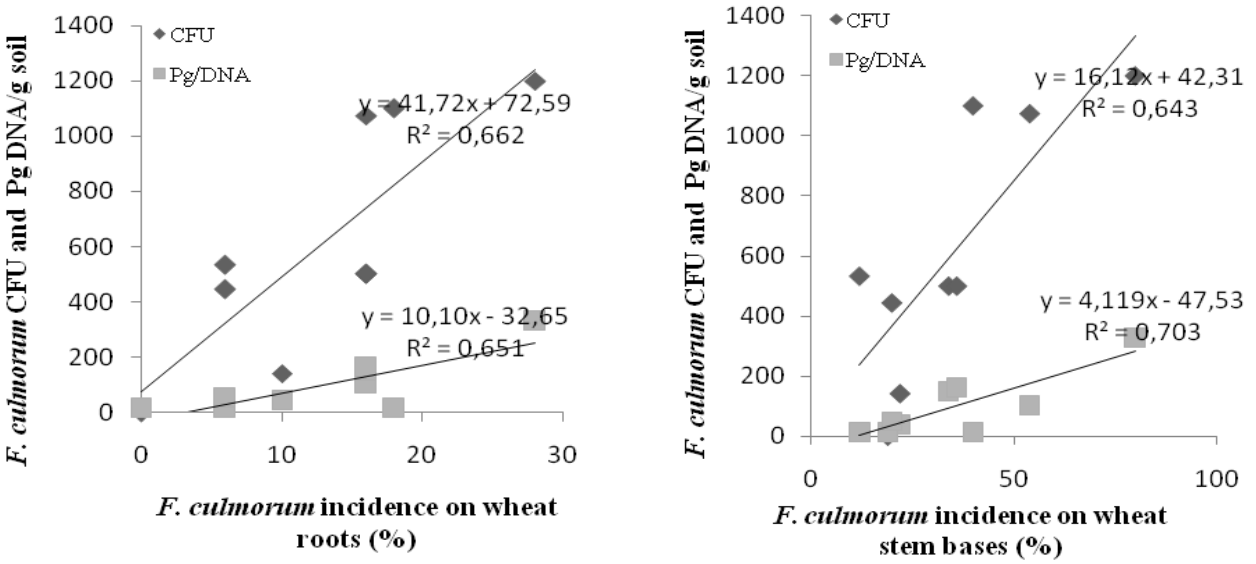

Figure 8. Correlations between *Fusarium culmorum* incidence (%) on wheat roots (A) and stem bases (B) and inoculum levels of *F. culmorum* left in the soil after 1 year, for three demonstration trials at Fernana, Tunisia.

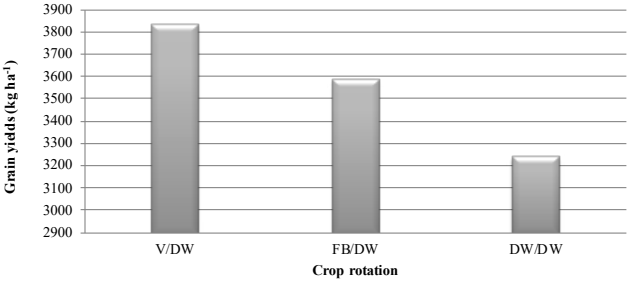

Figure 9. Mean grain yields (kg ha^{-1}) of durum wheat harvested after different rotation crops (DW = durum wheat, FB = faba bean, V = vetch), from three demonstration trials at Fernana, Tunisia, during the two cropping seasons 2013/14 and 2014/15.

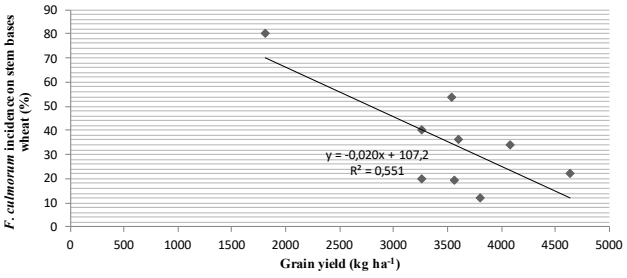

Figure 10. Correlation between *Fusarium culmorum* incidence (%) on wheat stem bases and grain yields (kg ha^{-1}) of durum wheat harvested from three demonstration trials at Fernana, Tunisia.

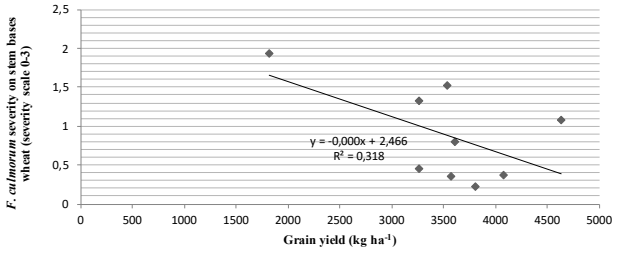

Figure 11. Correlation between disease severity index (scale 0-3) and grain yield (kg ha^{-1}) of durum wheat harvested from three demonstration trials at Fernana, Tunisia.

DISCUSSION

In this study effects of previous crops on inoculum levels of *F. culmorum* in soil, development of FFRR, and yield parameters of durum wheat were evaluated in Tunisian farming conditions. Data were collected from an experimental trial, and from demonstration trials established in three farmer's fields.

Inoculum levels of *F. culmorum* in the soil were quantified using two methods, soil dilution plating and qPCR. Both methods showed the dominance of *F. culmorum* in the upper 10 cm soil layers of the trial sites. *Fusarium pseudograminearum*, which has been isolated in other studies from Tunisia (Gargouri *et al*., 2001, 2007; Chekali *et al*., 2016), was not detected in the present study. However, this is not surprising since it has been demonstrated that *F. pseudograminearum* is restricted to arid zones in Tunisia (Gargouri *et al*., 2001), whereas in more humid regions, such as Fernana and Bou Salem where this study was conducted, *F. culmorum* is the dominant species. These observations have also been confirmed in other regions of the world, including

the Pacific Northwest of United States of America, and in Australia (Backhouse *et al*., 2004; Poole *et al*., 2012).

The results presented here demonstrated that break crops, including faba bean, vetch and fenugreek, reduced the number of propagules of *F. culmorum* in the soil. These data are confirming previous results which showed that populations of *F. culmorum* in the soil are affected by the previous crops (Snyder and Nash, 1968; McKenzie and Taylor, 1983). Steinkellner and Langer (2004) also demonstrated that the number of *Fusarium* CFU in soil was affected by previous crops.

Overall, the results from soil dilution plating were confirmed by qPCR, except for those from Farm 3 in the demonstration trials. At this farm, the amounts of *F. culmorum* DNA detected were very low, and this may have affected the qPCR analyses. The correlations observed between the two techniques suggest that both are effective for quantifying inoculum levels of *F. culmorum* in field soil. To our knowledge, this is the first report examining correlations between soil dilution and qPCR data for *F. culmorum* and durum wheat. In addition, this study was the first to measure the levels of *F. culmorum* inoculum in Tunisian soils, and may have been the first to make these assessments in the Mediterranean region.

The amount of *F. culmorum* DNA in the soil was generally reduced when legumes were used as previous crops before durum wheat. This is consistent with the results of Evans *et al*. (2010) in south-east Australia, who demonstrated that DNA of *F. culmorum* in soil was much less after field pea (115 pg DNA g^{-1}) and greater after durum wheat (974 pg DNA g^{-1}) or barley (1,196 pg DNA g^{-1}).

The numbers of propagules of *F. culmorum* detected in the present study (0 to 1,974 CFU g^{-1} of soil) was low compared to other studies. In Austria, Steinkllner and Langer, (2004) reported that inoculum of *F. culmorum* and *F. pseudograminearum* in the upper 10 cm layer, ranged between 0 to 8,750 CFU g^{-1}. Similarly, the amounts of *F. culmorum* DNA recorded in the present study were less than those found in Australia (Evans *et al*., 2010; Halloway *et al*., 2013).

Development of soil-borne diseases depends on the concentration of the inoculum in the soil (Cook, 1981). Cook (1968) demonstrated that 100 propagules of *F. culmorum* per gram of soil were sufficient to cause damage even when host plants are not under stress. In addition, McKay *et al*. (2008) suggested guidelines that related DNA amounts of *F. culmorum* in the soil before sowing to the risk of FFRR and yield losses in bread and durum wheat. They indicated that pre-planting DNA soil amounts less than 100 pg of fungal DNA g^{-1} of soil for bread wheat and less than 25 pg for durum wheat, would lead to minimal risk of yield losses due to crown rot caused by *Fusarium* spp.

The low amounts of *F. culmorum* inoculum in the soil may be explained by several factors. Differences in climatic conditions (Doohan *et al*., 2003; Xu *et al*., 2018), tillage methods (Steinkellner and Langer, 2004) and various cultural practices (Klem *et al*., 2007; Muller *et al*., 2010; Blandino *et al*., 2012; Chekali *et al*., 2016; Hemissi *et al*., 2018) are known to affect *Fusarium* populations in the soil. However, the low levels of inoculum observed in the present study were likely related to soil tillage. Low- or no-till are not common practices in Tunisia. Even in the demonstration trials reported here, direct seeding was applied for the first time. Steinkellner and Langer, (2004) found that the total number of CFU of *Fusarium* spp. was affected by tillage treatment. This agrees with previous studies by Toledo-Souza *et al*. (2008), who demonstrated that *Fusarium* inoculum was greater in a no-tillage system than a conventional one. Paulitz (2006) also showed that FFRR can cause significant damage when no-tillage practices and stubble retention are used. Recently, in Tunisia, Khemir *et al*. (2018) showed that stubble residue retention on soil surfaces increased *F. culmorum* inoculum levels in plant residues. The impact of no-tillage was also previously reported by Evans *et al*. (2010), who demonstrated that tillage reduced inoculum levels in soil by burying and promoting rapid degradation of infested plant residues. Furthermore, type and quantity of crop residues left on the soil surface, influence microorganisms and microbial processes in soil (Kandeler *et al*., 1999). Yi *et al*. (2002) showed that decomposition of crop residues was associated with a decline in CFU of *Fusarium* species.

The present study showed that frequency of isolation of *F. culmorum* from wheat roots and stem bases was affected by the previous crop in both trials, and was reduced by up to 70%. However, the results showed that in general the incidence of the pathogen was greater in stem bases than in roots. Knudsen *et al*. (1995) reported that FFRR was a consequence of initial stem base infections, while Beccari *et al*. (2011) and Covarelli *et al*. (2012) found that the stem bases of durum wheat were more heavily infected by *F. culmorum* compared to the roots. Knight and Sutherland (2013; 2017) reported that *F. culmorum* caused minor necrosis of the primary roots of cereals (durum wheat, bread wheat and barley), but caused serious cortical rot in leaf sheath tissues. These results emphasize the importance of crop residues left on the soil at the level of plant crowns for infection by the *Fusarium* species and the development of FFRR.

The use of break crops, including faba bean, fenugreek and vetch, decreased the incidence and sever-

ity of FFRR and increased grain yield in the subsequent durum wheat crop. These results are consistent with previous studies (Felton *et al*., 1998; Montanari *et al*., 2006; Zhou and Everts, 2007; Evans *et al*., 2010; Chekali *et al*., 2016). Other studies also demonstrated that preceding crops are key factors increasing the risk of *Fusarium* diseases on cereals (Klem *et al*., 2007; Muller *et al*., 2010; Blandino *et al*., 2012; Chekali *et al*., 2016). Rotations with chickpea (Felton *et al*., 1998; Chekali *et al*., 2016), faba bean (Kirkegaard *et al*., 2004), pea (Smiley *et al*., 1996; Evans *et al*., 2010) or lentil (Chekali *et al*., 2016) have been reported to reduce the incidence of FFRR. Chekali *et al*. (2016), showed, in northwest of Tunisia, that faba bean and chickpea used as previous crops could contribute to decreased incidence of infection of roots and stem bases of durum wheat by *F. culmorum*, and increase grain yields compared to durum wheat as a previous crop.

Rasmussen *et al*. (2002) hypothesized that this reduction in *F. culmorum* could be due to the non-host character of legumes, or to their high cellulose contents which increases microbial activity in the soil and leads to decrease of *Fusarium* spp. survival. In contrast, a high level of infection of wheat by *F. culmorum* has been reported when monoculture is practiced (Blecharczyk *et al*., 2006; Kurowsk et Adamiak, 2007; Kraska et Mielniczuk, 2012). In the present study, the Mediterranean forage legume fenugreek was reduced soil inoculum levels of *F. culmorum* by more than 60%, and decreased *F. culmorum* incidence on durum wheat stem bases, compared inoculum and disease incidence in durum wheat monoculture. These results confirm the antifungal activity of fenugreek. Omezzine *et al*. (2014) assessed *in vitro* antifungal activity of aqueous extracts from *T. foenum-graecum*, *against F. oxysporum f.* sp. *radicis-lycopersici and F. oxysporum f.* sp. *lycopersici*, and reported the antifungal and allelopathic potential of extracts from aerial parts of a Tunisian fenugreek cultivar. Other studies have also reported similar activities (Devasena and Menon, 2003; Oddepally and Guruprasad, 2015; Dharajiya *et al*., 2016; Sudan *et al*., 2020). Here, we have demonstrated, for the first time in Tunisia, the beneficial effects of fenugreek as a previous crop to decrease *F. culmorum* populations in soil and the development of FFRR in durum wheat.

Our results showed positive correlation between *F. culmorum* inoculum concentrations in the soil prior to sowing and subsequent FFRR expression. A negative correlation was also observed between FRRR expression and durum wheat grain yield. These results are similar to those of Smiley *et al*. (2005), Hollaway *et al*. (2013) and Chekali *et al*. (2016). Hollaway *et al*. (2013) suggested that pre-planting amounts of *F. culmorum* inoculum and expression of FFRR were positively correlated. Given that control options for FFRR are limited, this information would be valuable for grain producers, to prevent the yield losses caused by these diseases. In Australia, a DNA-based soil testing service (the 'PreDicta® B' system) was developed in 1997, to improve assessment of risks from root diseases and assist grain producers in planning cropping programmes (Ophel-Keller *et al*., 2008). Previous applications of this system have been mainly utilized in Australia and the United States (Paulitz *et al*., 2010; Bithell *et al*., 2012). This analysis tool is currently not available in Tunisia or in other Mediterranean countries. Our results encourage the use of systematic surveys across years and regions to document *Fusarium* inoculum levels in soil and FFRR occurrence and severity, and grain yield of durum wheat. This will assist development of a predictive model useful to farmers in Tunisia and the wider Mediterranean region.

In this study, the demonstration trials which involved farmers may impact on extension workers and other grain production stakeholders, to promote adoption of crop rotation as a tool for reducing soil-borne diseases of wheat in Tunisian cropping systems. Further studies would be useful to develop and implement a predictive model based on *Fusarium* inoculum levels in soil, to assess the risks and estimate the potential yield losses resulting from FFRR. This could be achieved by adjusting cropping sequences and other cultural practices to maximize yields. Our results could be useful for the Mediterranean basin, where FFRR is an endemic disease wherever wheat is cultivated.

ACKNOWLEDGEMENTS

This research was supported by the Ministry of Higher Education and Scientific Research of Tunisia, and was part of the CANA project CSE-2011-025 (Adapting conservation agriculture for rapid adoption by smallholder farmers in North Africa) financed by the Australian Centre for International Agricultural Research (ACIAR) and managed by the International Centre for Agricultural Research in the Dry Areas (ICARDA). We thank the farmers who collaborated with the researchers in this project.

LITERATURE CITED

Akinsanmi O.A., Mitter V., Simpfendorfer S., Backhouse D., Chakraborty S., 2004. Identity and pathogenic-

ity of *Fusarium* spp. isolated from wheat fields in Queensland and northern New South Wales. *Australian Journal of Agricultural Research* 55: 97–107.

Anonymous 1, 2019. Middle East and North Africa (MENA) is the most water-stressed region on earth. ICARDA. Available at: https://www.icarda.org/media/news/middle-east-and-north-africa-mena-most-water-stressed-region-earth.

Anonymous 2, 2018. Tunisie : Plus de 1 million d'hectares de superficies ensemencées en céréales. WEBMANAGERCENTER. Available at https://www.webmanagercenter.com/2018/03/08/417049/tunisie-les-superficies.

Bachta M. S., 2011. La céréaliculture en Tunisie une politique de régulation à repenser. *Les notes d'analyse du CIHEAM* 64: 1-19.

Backhouse D., Burgess L.W., 2002. Climatic analysis of the distribution of *Fusarium graminearum*, *F. pseudograminearum* and *F. culmorum* on cereals in Australia. *Australasian Plant Pathology* 31: 321–327.

Backhouse D., Abubakar A.A., Burgess L.W., Dennis J.I., Hollaway G.J., … Henry F.J., 2004. Survey of *Fusarium* species associated with crown rot of wheat and barley in eastern Australia. *Australian Plant Pathology* 33: 255–261.

Balmas V., 1994. Root rot of wheat in Italy caused by *Fusarium graminearum* Group 1. *Plant Disease* 78: 317.

Bankina B., Bimsteine G., Paulvoska L., Paura L., 2019. Effects of soil tillage and crop rotation on the development of wheat stem base diseases. *Canadian Journal of Plant Pathology* 41: 1-27.

Bateman G. L., 1993. Development of disease symptoms and fungal pathogens on shoot bases in continuous winter wheat. *Plant Pathology* 42: 595–608.

Bateman G. L., Coskun H., 1995. Populations of *Fusarium* spp. in soil growing continuous winter wheat, and effects of long-term application of fertilizers and of straw incorporation. *Mycological Research* 99: 1391–1394.

Batteman G.L., Kwasana H., 1999. Effects of number of winter wheat crops grown successively on fungal communits on wheat roots. *Applied Soil Ecology* 13: 271–282.

Bateman G.L., Murray G., 2001. Seasonal variation in population of *Fusarium* species in wheat-field soil. *Applied Soil Ecology* 18: 117–128.

Bateman G.L., Murray G., Gutteridge R.J., Coskun H., 1998. Effects of method of straw disposal and depth of cultivation on populations of *Fusarium* spp. in soil and on brown foot rot in continuous winter wheat. *Annals of Applied Biology* 132: 35–47.

Beccari G., Covoralli L., Nicholson P., 2011. Infection processes and soft wheat response to root rot and crown rot caused by *Fusarium culmorum*. *Plant Pathology* 60: 671–684.

Bithell S.L., McKay A., Butler R.C., Herdina, Hartley D., Cromey M.G., 2012. Predicting take-all severity in second-year wheat using soil DNA concentrations of *Gaeumannomycesgraminis* var. *tritici* determined with qPCR. *Plant Disease* 96: 443–451.

Blandino M., Haidukowski M., Pascale M., Plizzari L., Scudellari D., Reyeneri A., 2012. Integrated strategies for the control of *Fusarium* head blight and deoxynivalenol contamination in winter wheat. *Field Crops Research* 133: 139–149.

Blecharczyk A., Sierpowski J., Sawinska Z., 2006. Impact of tillage systems on diseases in continuous cropping of winter wheat. *Progress Plant Protection* 46: 677–680.

Burgess L.W., 2011. Foot, crown, and root rots of cereals - insidious diseases of global importance: A Tunisian perspective. 2011. *Tunisian Journal of Plant Protection*, 6 (Guest Editorial).

Burgess L.W., Wearing A.H., Toussoun T.A., 1975. Surveys of Fusaria associated with crown rot of wheat in eastern Australia. *Australian Journal* of *Agricultural Research* 26: 791–799.

Burgess L.W., Backhouse D., Summerell B.A., Swan L.J., 2001. Crown rot of wheat. Pages: 271–294. In: *Fusarium.* Paul E. Nelson Memorial Symposium. (B.A. Summerell, J.F. Leslie, D. Backhouse, W.L. Bryden, and L.W. Burgess, eds.) APS press, The American Phytopathological Society, St. Paul, Minnesota, USA.

Cassini R., 1981. *Fusarium* diseases of wheat and corn in Western Europe. Pages 56–63 in*: Fusarium*: Diseases, Biology, and Taxonomy. (P.E. Nelson, T.A. Toussoun, and R.J. Cook, eds). The Pennsylvania State University Press, University Park, PA, USA.

Chekali S., Gargouri S., Berraies S., Gharbi M.S., Nicol J.M., Nasraoui B., 2013. Impact of *Fusarium* foot and root rot on yield of cereals in Tunisia. *Tunisian Journal of Plant Protection* 8: 75–86.

Chekali S., Gargouri S., Rezgui M., Paulitz T. and Nasraoui B., 2016. Impact of previous crops on *Fusarium* foot and root rot, and on yields of durum wheat in North West Tunisia. *Phytopathologia Mediterranea* 55: 253–261

Cook R.J., 1968. *Fusarium* root and foot rot of cereals in the Pacific Northwest. *Phytopathology* 58: 127–131.

Cook R.J., 1980. *Fusarium* foot rot and its control in the Pacific Northwest. *Plant Disease* 64: 1061–1066.

Cook R.J., 1981. *Fusarium* diseases of wheat and other small grains in North America. Pages: 39–52 In:

Fusarium. Diseases, Biology and Taxonomy. (P.E. Nelson, T.A. Toussoun, and R.J. Cook, eds). Editions of Pennsylvania State University Press, University Park, PA, USA.

Covarelli L., Beccari G., Steed A., Nicholson P., 2012. Colonization of soft wheat following infection of the stem base by *Fusarium culmorum* and translocation of deoxynivalenol to the head. *Plant Pathology* 61: 1121–1129.

Cromey M.G., Parkes R.A., Fraser P.M., 2006. Factors associated with stem base and root diseases of New Zealand wheat and barley crops. *Australian Plant Pathology* 35: 391–400.

Devasena T., Menon V.P., 2003. Fenugreek affects the activity of beta-glucuronidase and mucinase in the colon. *Phytotherapy Research* 17: 1088–1091.

Dharajiya D., Jasani H., Khatrani T., Kapuria M., Pachchigar K., Patel P., 2016. Evaluation of antibacterial and antifungal activity of fenugreek (*Trigonella foenum-graecum*) extracts. *International Journal of Pharmacy and Pharmaceutical Sciences* 8: 212–217.

Doohan F.M., Brennan J., Cooke B.M., 2003. Influence of climatic factors on *Fusarium* species pathogenic to cereals. *European Journal of Plant Pathology* 109: 755–768.

Duke J.A., Reed C.F., Weder P., 1981. *Trigonella foenum graecum* L. In: Handbook of legumes of world economic importance (J.A. Duke, ed.) New York: Plenum Press.

Evans M.L., Hollaway G. J., Dennis J. I., Correll R., Wallwork H., 2010. Crop sequence as tool for managing populations of *Fusarium pseudograminearum* and *Fusarium culmorum* in south-eastern Australia. *Australasian Plant Pathology* 39: 376–382.

Evidente A., Monoca F.A., Andolfi A., Rubiales D., Motta A., 2007. Trioxazonane, a monosubstituted trioxazonane from *Trigonella foenum-graecum* root exudates, inhibits *Orobranche crenata* seed germination. *Phytochemistry* 68: 2487–2492.

Felton W.L., Marcellos H., Alston C., Martin R. J., Backhouse D., … Herridge D.F., 1998. Chickpea in wheat-based cropping systems and crown rot in the following crop. *Australian Journal of Agricultural Research* 49: 401–408.

Gargouri S., Hajlaoui M.R., Guermech A., Marrakchi M., 2001. Identification des espèces fongiques associées à la pourriture du pied du blé et étude de leur répartition selon les étages bioclimatiques en Tunisie. *Bulletin OEPP/EPPO Bull* 31: 499–503.

Gargouri S., Kammoun L., Guermech A., Hajlaoui M.R., 2007. Evaluation de l'incidence, de la sévérité et des pertes de rendement dues à la pourriture du pied du blé en Tunisie. *Annales de l'INRAT* 80: 7-20.

Gharbi M.S., El Felah M., 2013. Les céréales en Tunisie : plus d'un siècle de recherche variétale. *Annales de l'INRAT* 86 : 45–68.

Ghodbane A., Mahjoub M., Djerbi M., Mlaik A., Sharen A.L., 1974. Etude des pertes causées par les pathogènes du blé, *Septoria tritici* et *Fusarium* spp. *Rapport annuel du ministère de l'agriculture. Office des Céréales, Tunisie* 106.

Giorgi F., 2006. Climate change hot-spots'; geophysical Resources Letters, 33: 707–715. GTZ. 2007. Adaptation to climate change: development of a national strategy for agriculture, ecosystems and water resources in Tunisia 2005 to December 2007. 3p

Haouala R., Hawala S., El-Ayeb A., Khanfir R., Boughanmi N., 2008. Aqueous and organic extracts of *Trigonella foenum-graecum* L. inhibit the mycelia growth of fungi. *Journal of Environmental Sciences* (China) 20: 1453–1457.

Hemissi I., Gargouri S., Hlel D., Hachana A., Abdi N., Sifi, B., 2018. Impact of nitrogen fertilization on *Fusarium* foot and root rot and yield of durum wheat. *Tunisian Journal of Plant Protection* 13: 31–38.

Hogg A.C., Johnston R.H., Dyer A.T., 2007. Applying real time quantitative PCR to *Fusarium* crown rot of wheat. *Plant Disease* 91: 1021–1028.

Hollaway G., Evans M., Wallwork H., Dyson C., McKay A., 2013. Yield loss in cereals, caused by *Fusarium culmorum* and *F. pseudograminearum*, is related to fungal DNA in soil prior to planting, rainfall and cereal type. *Plant Dis*ease 97: 977–982. Available at https://doi.org/10.1094/PDIS-09–12-0867-RE.

Kandeler E., Tscherko D., Spiegel H., 1999. Long-term monitoring of microbial biomass, N mineralization and enzyme activities of a Chernozem under different tillage management. *Biology Fertility Soils* 28: 343–351.

Khemir E., Chekali S., Souissi A., Gharbi M.S., 2018. Survival of *Fusarium culmorum*, causal agent of foot and root rot of cereals, on wheat, barley and oat residues in Tunisia. *Annales de L'INRAT* 91: 162–172.

Kirkegaard J.A., Simpfendorfer S., Holland J., Bambach R., Moore K.J., Rebetzke G.J., 2004. Effect of previous crops on crown rot and yield of durum and bread wheat in northern NSW. *Australian Journal of Agricultural Research* 55: 321–334.

Klem K., Vanova M., Hajslova J., Lancova K., Sehnalova M., 2007. A neutral network model for prediction of deoxynivalenol content in wheat grain based on weather data and preceding crop. *Plant Soil Environment* 53: 421–429.

Knight N.L., Sutherland M.W., 2013. Histopathological assessment of wheat seedling tissues infected by

Fusarium pseudograminearum. *Plant Pathology* 62: 679–687.

Knight N.L., Sutherland M.W., 2017. Assessment of *Fusarium pseudograminearum* and *F. culmorum* Biomass in seedlings of potential host cereal species. *Plant Disease* 101: 2116–2122.

Knudsen I.M.B., Hockenhull J., Jensen D.F., 1995. Biocontrol of seedling diseases of barley and wheat caused by *Fusarium culmorum* and *Bipolaris sorokiniana*: effects of selected fungal antagonists on growth and yield components. *Plant Pathology* 44: 467–477.

Köppen W., 1936. The geographic climate system. In: Handbuch der Klimatologie (W. Köppen, R. Geiger, ed.), Gebrüder Borntraeger, Berlin, 1-44 (in German).

Kurowski T., Adamiak E., 2007. Occurrence of stem base diseases of four cereal species grown in long-term monocultures. *Polish Journal Natural Sciences* 22: 574–583.

Kraska P., Mielniczuk E., 2012. The occurrence of fungi on the stem base and roots of spring wheat (*Triticum aestivum* L.) grown in monoculture depending on tillage systems and catch crops. *Acta Agrobotanica* 65: 79–90.

Lamprecht S.C., Marasas W.F.O., Hardy M.B., Calitz, F.J., 2006. Effect of crop rotation on crown rot and the incidence of *Fusarium pseudograminearum*in wheat in the Western Cape, South Africa. *Australian Plant Pathology* 35: 419–426.

Leslie J.F., Summerell B.A., 2006. The *Fusarium* Laboratory Manual. Blackwell Publishing, 388 pp.

McKay A., Roget D., Hannam R., Ophel Keller K., 2008. Root Disease Risk Management Resource Manual. PIRSA Publishing: Adelaide.

McKenzie F., Taylor G.S., 1983. *Fusarium* populations in British soils relative to different cropping practices. *Transactions of the British Mycological Society* 80: 409–413.

Mergoum M., Braun H.J., Nicol J., Bagci A., Ekiz H., … Keser M., 2000. Screening wheat for root rot disease in WANA region. Page 186. In: Abstracts of the 6th International Wheat Conference, 4–9 June, 2000, Budapest, Hungary.

Montanari A., Innocenti G., Toderi G., 2006. Effects of cultural management on the foot and root disease complex of durum wheat. *Plant Pathology* 88: 149–156.

Muller M.E.H., Brenning A., Verch G., Koszinski S., Sommer M., 2010. Multifactorial spatial analysis of mycotoxin contamination of winter wheat at the field and landscape scale. *Agriculture, Ecosystems & Environment* 139: 245–254.

Oddepally R., Guruprasad L., 2015. Isolation, purification, and characterization of a stable defensin-like antifungal peptide from *Trigonella foenum-graecum* (fenugreek) seeds. *Biochemistry* (*Moscow*) 80: 332–342.

Omezzine F., Daami-Remadi M., Ladhari A., Haouala R., 2014. Variation in phytochemical content and antifungal activity of *Trigonella foenum-graecum* L. with plant developmental stage and ploidy level. *South African Journal of Botany* 92: 120–125

ONAGRI, 2016: Observatoire Nationale de l'Agriculture, Annuaire statistique 2016. 190 pp. (in French).

Ophel-Keller K., Mckay A., Hartely D., Herdina P., Curran J., 2008. Development of a routine DNA-based testing service for soil borne diseases in Australia. *Australian Plant Pathology* 37: 243–253.

Paulitz T.C., 2006. Low input no-till cereal production in the Pacific Northwest of the U.S.: The challenges of root diseases. *European Journal of Plant Pathol*ogy 115: 271–281.

Paulitz T.C., Schroeder K. L., Schillinger W. F., 2010. Soil borne pathogens of cereals in an irrigated cropping system: effects of tillage, residue management, and crop rotation. *Plant Disease* 94: 61–68.

Pemonge J., Pascual-Villalobos M.J., Regnault-Roger C., 1997. Effects of material and extracts of *Trigonella foenum-graecum* L. against the stored product pests *Triboleum castaneum* (Herbst) (Coleoptera: Tenebrionidae) and *Acanthoscelides obtectus* (Say) (Coleoptera: Bruchidae). *Journal of Stored Products Research* 33: 209–217

Pereyra S.A., Dill-Macky R., 2004. Survival and inoculum production of *Gibberella zeae* in wheat residue. *Plant Disease* 88: 724–730.

Poole G.J., Smiley R.W., Paulitz T.C., Walker C.A., Carter A.H., …, Garland-Campbell K., 2012. Identification of quantitative trait loci (QTL) for resistance to *Fusarium* crown rot (*Fusarium pseudograminearum*) in multiple assay environments in the Pacific Northwestern US. *Theoretical and Applied Genet*ics 125: 91–107.

Rasmussen P.H., Knudsen I.M.B., Elmholt S., Jensen D.F., 2002. Relationship between soil cellulotytic activity and suppression of seeding blight of barley in arable soils. *Applied Soil Ecology* 19: 91–96.

Rossi V., Cervi C., Chiusa G., Languasco L., 1995. Fungi associated with foot rots on winter wheat in northwest Italy. *Journal of Phytopathology* 143: 115–119.

Sitton J.W., Cook R.J., 1981. Comparative morphology and survival of chlamydospores of *Fusarium roseum* '*Culmorum*' and '*Graminearum*'. *Phytopathology* 71: 85–90.

Slama A., Ben Salem M., Ben Naceur M., Zid E., 2005. Les céréales en Tunisie: Production, effet de la sécheresse et mécanismes de résistance. *Sècheresse* 16: 225–229 (in French).

Smiley R.W., Gourlie J.A., Easly G.S., Patterson L.M., Whittaker R.G., 2005. Crop damage estimates for crown rot of wheat and barley in the Pacific Northwest. *Plant Disease* 89: 595–604.

Smiley R.W., Patterson L.M., 1996. Pathogenic fungi associated with *Fusarium* foot rot of winter wheat in the semiarid Pacific Northwest. *Plant Disease* 80: 944–949.

Smiley R.W., Patterson L.M., Shelton C.W., 1996. Fungicide seed treatments influence emergence of winter wheat in cold soil. *Journal of Production Agriculture* 9: 559–563.

Snyder W.C., Nash, S.M., 1968. Relative incidence of *Fusarium* pathogens of cereals in rotation plots at Rothamsted. *Transactions of the British Mycological Society* 51: 417–425.

Steinkellner S., Langer I., 2004. Impact of tillage on the incidence of *Fusarium* spp.in soil. *Plant and Soil* 267: 13–22.

Sudan P., Goswami M., Singh J., 2020. Antifungal potential of fenugreek seeds (*Trigonella foenum-graecum*) crude extracts against *Microsporum gypseum*. *International Journal of Research in Pharmaceutical Sciences* 11: 646–649.

Toledo-Souza E.D., Silveira P.M., Lobo J.M., Café Filho A.C., 2008. Soil Density and Soil Pathogens Survival. *Pesquisa Agropecuária Brasileira* 43: 971–978.

Van Wyk P.S., Los O., Rheeder J.P., Marasas W.F.O., 1987. *Fusarium* species associated with crown rot of wheat in the Humansdrop District, Cape Province. *Phytophylactica* 19: 343–344.

Vicente-Serrano S.M., 2006. Spatial and temporal analysis of droughts in the Iberian Peninsula (1910–2000). *Hydrological Sciences Journal* 51: 83–97.

Wallwork H., Butt M., Cheong J.P.E., Williams K.J., 2004. Resistance to crown rot in wheat identified through an improved method for screening adult plants. *Australian Plant Pathology* 33: 1–7.

Wisniewska H., Kowalczyk K., 2005. Resistance of cultivars and breeding lines of spring wheat to *Fusarium culmorum* and powdery mildew. *Journal of Applied Genetics* 46: 35–40.

Xu F., Yang G., Wang J., Song Y., Liu L., Zhao K., Li Y., Han Z., 2018. Spatial distribution of root and crown rot fungi associated with winter wheat in the north China plain and its relationship with climate variables. *Frontiers in Microbiology* 9: 1054.

Yi C., Kaul H.-P., Kübler E., Aufhammer W., 2002. Populations of *Fusarium graminearum* on crop residues as affected by incorporation depth, nitrogen and fungicide application. J*ournal of Plant Diseases and Protection* 109: 252–263.

Zadoks J.C., Chang T.T., Konzak C.F., 1974. A decimal code for the growth stages of cereals. *Weed Research* 14: 415–421.

Zhou W.G., Everts K.L., 2007. Effects of host resistance and inoculum density on the suppression of *Fusarium* wilt of watermelon induced by hairy vetch. *Plant Disease* 1: 92–96.

Zia T., Siddiqui I.A., Nazrul-Hasnain., 2001. Nematicidal activity of *Trigonella foenum-graecum* L. *Phytotherapy Research* 15: 538–540.

Phytopathologia Mediterranea
The international journal of the
Mediterranean Phytopathological Union

Firenze University Press
www.fupress.com/pm

Short Notes

Detection of viruses in olive cultivars in Greece, using a rapid and effective RNA extraction method, for certification of virus-tested propagation material

Matthaios M. MATHIOUDAKIS[1,*], Maria SAPONARI[2], Beata HASIÓW-JAROSZEWSKA[3], Toufic ELBEAINO[4], Georgios KOUBOURIS[5,*]

[1] *Institute of Olive Tree, Subtropical Crops and Viticulture, Plant Pathology Laboratory, Karamanlis Ave. 167, Gr-73134, Chania*
[2] *Consiglio Nazionale delle Ricerche-Istituto per la Protezione Sostenibile delle Piante (CNR-IPSP), Sede Secondaria di Bari, 70126, Bari, Italy*
[3] *Institute of Plant Protection-National Research Institute, Department of Virology and Bacteriology, ul. Wł. Węgorka 20, 60-318, Poznań, Poland*
[4] *Istituto Agronomico Mediterraneo di Bari, Via Ceglie 9, Valenzano, 70010, Bari, Italy*
[5] *Institute of Olive Tree, Subtropical Crops and Viticulture, Laboratory for Olive Cultivation, Karamanlis Ave. 167, Gr-73134, Chania*
*Corresponding authors: mathioudakis@nagref-cha.gr, koubouris@nagref-cha.gr

Summary. Although Greece is the world's third largest olive production country, information about the presence of olive viruses is limited. A survey for the presence of virus infections in the ten most important Greek cultivars was conducted in a germplasm collection olive grove located in Chania, Crete. Samples were RT-PCR assayed for the presence of *Arabis mosaic virus* (ArMV), *Cherry leafroll virus* (CLRV), *Strawberry latent ring spot virus* (SLRSV), and *Olive leaf yellowing-associated virus* (OLYaV), amplifying part of the capsid protein (ArMV), the 3′UTR (CLSRV, SLRSV) or the HSP70h (OLYaV) gene. Total RNAs were purified using the Trizol method, yielding good quality and purity, thereby confirming application of the method as a rapid economic extraction protocol for detection of olive viruses. SLRSV was the most predominant virus, with an infection rate of 55%, followed by CLRV and OLYaV in 5% of the tested samples. ArMV was detected only in one sample. Mixed virus infections were also commonly detected. The DNA amplicons of the obtained viruses from the infected samples were sequenced. The partial sequences of ArMV, CLRV and SLRSV from olives, which are reported for the first time, showed 74-100% nucleotide similarity with available homologous sequences from other crops, whereas OLYaV isolates showed high sequence variability of 25%. The phylogenetic analysis based on olive-OLYaV HSP70h partial-nucleotide sequences grouped the olive isolate sequences according to the geographical origins of the host germplasm collection. This is the first official report of the occurrence of olive viruses in Greece, emphasizing the need to implement a certification programme for production and distribution of high-quality (virus-free) olive propagation material, in Greece and more generally in the Mediterranean basin.

Keywords. Olive viruses, RT-PCR, olive RNA extraction protocol, virus-tested propagation material.

OPEN ACCESS

Citation: M.M. Mathioudakis, M. Saponari, B. Hasiów-Jaroszewska, T. Elbeaino, G. Koubouris (2020) Detection of viruses in olive cultivars in Greece, using a rapid and effective RNA extraction method, for certification of virus-tested propagation material. *Phytopathologia Mediterranea* 59(1): 203-211. doi: 10.14601/Phyto-11033

Accepted: December 2, 2019

Published: April 30, 2020

Data Availability Statement: All relevant data are within the paper and its Supporting Information files.

Competing Interests: The Author(s) declare(s) no conflict of interest.

Editor: Nihal Buzkan, Kahramanmaraş Sütçü Imam University, Turkey.

INTRODUCTION

Olive (*Olea europaea* L.) is one of the most important fruit tree crops in Greece, with total area of olive orchards of 830,000 ha, and total world annual production >250,000 t (IOC, 2018). There are over one hundred olive cultivars grown in Greece (Linos *et al.,* 2014), with 'Koroneiki' and 'Kalamon' being the most predominant (Metzidakis and Koubouris, 2006). Despite the richness of the olive autochthonous varieties cultivated in different parts of the country, which indicates their importance, it is estimated that over 90% of the new plantations employ only the ten most popular cultivars. In an attempt to create new plantations and increase their productivity of superior quality olive oil (monovarietal), the phytosanitary status of the most economically and commercially important olive cultivars was evaluated. This was to create high-quality olive germplasm, from which pre-basic certified propagation material could be produced. This is considered mandatory to enhance national and international olive industry.

Olive is susceptible to several pathogens, caused by fungi, bacteria, viruses and phytoplasmas, which are transmitted and disseminated in host propagation material. Fifteen viruses belonging to seven genera (*Nepovirus*, *Cucumovirus*, *Tobamovirus*, *Alphanecrovirus*, *Oleavirus*, *Necrovirus*, *Marafivirus*), and one unassigned member of the Secoviridae and one of the Closteroviridae families, have been recorded in olive (Martelli, 1999; Felix and Clara, 2002; Cardoso *et al.,* 2004; Al Abdullah *et al.,* 2010; Loconsole *et al.,* 2010). Many of these viruses cause latent infections, and are symptomless and restricted in olive trees; however, some other viruses have wide host ranges and can spread to numerous economically important crops which are virus reservoirs for serious diseases. Research conducted on the olive virus records in Italy, Spain, and Portugal was initiated in 1999 (Martelli, 1999). However, more attention has been recently drawn to the virus sanitary status of olive trees in several countries of the Mediterranean basin.

The recent outbreak of the olive quick decline syndrome, caused by *Xylella fastidiosa* in Italy (Saponari *et al.,* 2013), and the detection of this bacterium in other European countries (France, Spain, Germany), has prompted the necessity for annual surveys and inspections in the olive groves of Greece. This action was taken as a preventive measure to cope with the introduction of *X. fastidiosa* in Greece. However, there are no data regarding the presence of olive-infecting viruses in this country.

This paper reports results of a preliminary investigation into olive-infecting viruses, by testing a plot of an olive germplasm collection and using a rapid and effective RNA extraction protocol. This is the first survey report on the detection of olive viruses in Greece. This survey for the presence of *Arabis mosaic virus* (ArMV; *Nepovirus*), *Cherry leaf roll virus* (CLRV; *Nepovirus*), *Strawberry latent ring spot virus* (SLRSV; Secoviridae), and *Olive leaf yellowing associated virus* (OLYaV; Closteroviridae), according to the EU regulations PM 4/17(2) (EPPO, 2006) for the certification of olive propagation material, was conducted from the ten most widely-grown olive cultivars in Greece. Genetic diversity and phylogenetic relationships between virus isolates were also analyzed and are reported herein.

MATERIALS AND METHODS

Study area, plant material and virus sources

A survey was carried out during March 2018, and a total of 40 trees was collected from a germplasm collection plot located at the Institute of Olive Tree, Subtropical Crops and Viticulture (IOSV) in the region of Chania, Crete, Greece. This collection plot contained young olive trees (4–5 years old) from different accessions of Greek cultivars, which have been analyzed and genetically characterized (SSR) for their identification and authentication.

Table 1 lists the ten most important olive cultivars that were chosen, according to their economic importance throughout Greece. Samples were collected from four different trees of each cultivar. Each labelled sample consisted of four sub-samples of cuttings (each 25-35 cm in length) from 1- to 2-year-old twigs, from all four quadrants of the canopy of each plant (two shoots from each quadrant). No typical virus symptoms were observed in the collected samples, with the exception of light leaf yellowing in samples originating from two different cultivars.

Total RNA aliquots originally extracted from characterized olive material, infected with CLRV and OLYaV, or herbaceous hosts infected with ArMV and SLRSV, were used as positive controls to confirm the reliability of the method used for virus detection.

RNA isolation and evaluation of the method for olive tissues

Phloem and leaf tissues from at least eight shoots per surveyed tree were separately scraped and powdered in liquid nitrogen. Approximately 0.1 g of each sample was subjected to RNA isolation by the Trizol method, using

Table 1. Sampled Greek olive cultivars, and results of the molecular detection of ArMV, CLRV, OLYaV and SLRSV.

Cultivar	No. of tested trees	Detected virus and number of infected trees			
		ArMV	CLRV	OLYaV	SLRSV
Gaidourelia	4	0	1	0	0
Lianolia Kerkiras	4	0	0	0	1
Koroneiki	4	1	0	0	2
Throubolia	4	0	1	0	2
Megaritiki	4	0	0	0	4
Patrini	4	0	0	0	3
Kalamon	4	0	0	0	2
Amfissis	4	0	0	0	3
Chalkidikis	4	0	0	1	3
Mastoidis	4	0	0	1	2
Total	40	1	2	2	22

the TRIzol reagent (Invitrogen, ThermoFisher Scientific) as described in the manufacturer's instructions. Initially, the resulting RNAs from phloem and leaves were compared to each other for quality and quantity, and also with total RNAs extracted using the RNeasy Plant Mini kit (Qiagen) from the same ground tissues. The final RNAs were diluted to a final concentration of 150 ng μL^{-1}.

To evaluate the functionality and the sensitivity of the Trizol method in olive tissues, the following experiments were carried out: i) molecular assays for the partial amplification of the β-tubulin, an endogenous olive gene, and ii) molecular assays to assess the purity of the total RNA from genomic DNA (gDNA) during the extraction procedure.

Detection of olive viruses and olive-specific genes using One-step RT-PCR assays

A previously reported One-Step Reverse Transcription-Polymerase Chain Reaction (RT-PCR) was used for the detection of olive-infecting viruses, which used reliable sets of primers (Supplementary Table S1) that partially amplify the coat protein (CP) gene of ArMV, the 3′UTR of CLRV and SLRSV, and the Heat shock protein 70 homolog (HSP70h) gene of OLYaV (Loconsole *et al.,* 2010). This was applied under the following modifications. Briefly, 2 μL of total RNA was added in the reaction mixture (final volume 25 μL), along with 5× GoTaq Polymerase buffer, 1.5 mM $MgCl_2$, 5 mM DTT, 0.4 mM dNTPs, 0.2 μM of each virus-specific primer pair, 5 U AMV (Promega), 20 U RNase Out (New England BioLabs) and 1.25 U GoTaq Polymerase (Promega). The cDNA synthesis was performed at 48°C for 45 min, followed by denaturation at 95°C for 5 min. The target amplification was carried out under the following cycling scheme: 35 cycles of 94°C for 30 s, 55°C for 45 s (for OLYaV 58°C was used), 72°C for 30 s, with a final extension step at 72°C for 7 min. The PCR conditions were the same for all viruses. Positive and water controls were used in all of the tests.

The same one-step RT-PCR protocol was applied for detection of the β-tubulin gene, using the following modifications: 0.5 mM dNTPs, annealing temperature of 59°C and 0.25 μM of the specific primers (Supplementary Table S1). To confirm the purity of RNA from gDNA, the same reaction was carried out with exclusion of the reverse transcription enzyme.

The amplified products were analyzed by electrophoresis in 1.5% TAE (1×) agarose gel stained with GelRed (Biotium Inc.).

Sequencing, recombination and phylogenetic analyses

The resulting DNA amplicons were purified using the NucleoSpin Gel and PCR Clean-up kit (Macherey-Nagel). The nucleotide sequences from all detected isolates were determined by direct sequencing using both of the virus-specific primers, with the Sanger method (Macrogen Inc.).

For the bioinformatics analyses, the partial olive virus sequences obtained here were aligned, after clipping the primer-binding region with all the known homologous deposited nucleotide viral sequences using Muscle software as implemented in MEGA X (Kumar *et al.,* 2018). Prior to phylogenetic analyses, the occurrence of potential recombination events within virus isolates was analyzed using the RDP, GENECONV, Chimaera, MaxChi, BootScan, SiScan, and 3Seq methods implemented in the RDP version 4 program (Martin *et al.,* 2015) with default settings. Recombination events were considered as significant if four or more of these methods had a $P < 0.05$, in addition to phylogenetic evidence of recombination. Sequence alignments were used for inferring phylogenetic evolutionary relationships and the construction of maximum-likelihood trees in MEGA X. The best nucleotide substitution model was calculated for each set of sequences. The Kimura 2-parameter model (Kimura, 1980) was applied for ArMV, CLRV and SLRSV, and the Tamura 3-parameter model (Tamura, 1992) for OLYaV. Confidence in branch points in the phylogenetic tree was assessed by the bootstrap method with 1,000 pseudo-random replicates (Felsenstein, 1985).

RESULTS AND DISCUSSION

The integrity and quality of the Trizol-total RNAs obtained from olive phloem and leaves was confirmed by electrophoresis, showing a similar pattern as those extracted using another commercial kit. The yield of total RNA was greater for phloem tissues than from the leaves (data not shown), varying from 0.2–0.3 μg μL^{-1} for the RNeasy Plant Mini kit (Qiagen) to 0.4–0.7 μg μL^{-1} for Trizol. The purity (ratio A_{260}/A_{280}) in both cases was in the optimal range. In previous studies, the use of the RNeasy kit has been commonly adopted for olive total RNA isolation, following various laboratory validations and a comparison with silica microchromatography preparations (Loconsole *et al.,* 2010). In the present study, Trizol was successfully used for preparation of the olive total RNA templates, extracted from phloem, for detection of the target viruses. The β-tubulin gene was successfully detected (data not shown), thereby confirming the effectiveness and suitability of the Trizol-purified olive total RNAs for setting amplification reactions. No amplifications occurred when the total RNAs were directly subjected to PCR without a reverse transcription step (data not shown). This indicated that the Trizol-purified RNAs were free from gDNA. The Trizol method could be used as a simple and high-quality olive RNA extraction protocol (within 3 h duration), minimizing costs without the need of additional purification steps.

The one-step RT-PCR reactions generated the expected amplicons for all positive controls. All four viruses investigated were present in the tested Greek olive germplasm plants, with different infection rates. In Greece, occurrence of olive viruses has not been previously investigated. The only previous report of an olive-infecting virus in Greece was for *Olive mild mosaic virus* (Gratsia *et al.,* 2012), which was detected in spinach.

The present study found at least one virus present in 25 out of 40 samples, with an average of 62.5% virus infection (Table 1). This infection level was comparable to those reported from other Mediterranean countries and Syria (51–86%) (Saponari *et al.,* 2002; Al Abdullah *et al.,* 2005; Faggioli *et al.,* 2005; Youssef *et al.,* 2010; Faggioli *et al.,* 2017), but in contrast to Albania, where virus incidence was very low (2%) (Luigi *et al.,* 2009). In Lebanon and Croatia, incidence of these viruses varied from 20 to 31% (Fadel *et al.,* 2005; Luigi *et al.,* 2011; Godena *et al.,* 2016).

SLRSV was the most frequently detected virus, being present in 22 samples (55%), in almost all of the olive Greek cultivars except 'Gaidourelia' (Table 1). The high infection rates of SLRSV in Greece is in contrast to previous reports in other neighboring countries, where incidence of this virus varied from 0.5 to 29.2% (Saponari *et al.,* 2002; Al Abdullah *et al.,* 2005; Fadel *et al.,* 2005; Faggioli *et al.,* 2005; Luigi *et al.,* 2009; El Air *et al.,* 2011; Godena *et al.,* 2016). The high incidence of SLRSV (a nematode-borne virus) in the tested olive plants could indicate the presence of SLRSV in other crops or in olive itself, which have bordered the sampled grove as a reservoir of infection. The transmission of SLRSV by *Xiphinema diversicaudatum* in nature is well known, and this cannot be excluded; however, there is no evidence that this nematode is able to transmit SLRSV from olive to olive or from other crops to olive.

ArMV was detected only in one sample collected from a tree of 'Koroneiki' (designated as ArMV-Gr/Kr), whereas CLRV was detected in single infections on two olive cultivars, 'Throuboulia' and 'Gaidourelia' (designated, respectively, as CLRV-Gr/Tr and CLRV-Gr/Gd). The low infection percentages of ArMV (2.5%) and CLRV (5%), confirmed similar results reported in the Mediterranean basin. For ArMV, the absence of infection in Italy, Croatia, and Tunisia (Faggioli *et al.,* 2005; El Air *et al.,* 2011; Godena *et al.,* 2016), and one report of sporadic infection (0.7%) from Egypt (Youssef *et al.,* 2010), are noteworthy. The only reports available are from Lebanon and Syria that show similar infection rates (0.7–2%) (Al Abdullah *et al.,* 2005; Fadel *et al.,* 2005). The incidence of CLRV, as indicated in other countries, varied from very low (0.5%) in Spain (Bertolini *et al.,* 2001) to higher infection rates such as 12% in Croatia (Godena *et al.,* 2016), 13% in Tunisia (El Air *et al.,* 2011), and 4.9–33.3% in Italy (Saponari *et al.,* 2002; Faggioli *et al.,* 2005).

OLYaV was also detected with low incidence (5%), in two olive cultivars, 'Mastoidis' and 'Chalkidikis' (these virus isolates designated, respectively, as OLYaV-Gr/Ms and OLYaV-Gr/Ck). This was similar to OLYaV incidence found in Albania (2%) (Luigi *et al.,* 2009), but OLYaV infection-rates were greater in Tunisia (49%) (El Air *et al.,* 2011), Italy (21–64%) (Saponari *et al.,* 2002; Albanese *et al.,* 2003; Faggioli *et al.,* 2005), Lebanon (23.6%) (Fadel *et al.,* 2005), Syria (14.5%) (Al Abdullah *et al.,* 2005), and especially in California, where OLYaV is the most prevalent virus (93%) (Al Rwahnih *et al.,* 2011). The low infection rate of OLYaV in Greece could be explained by the possible absence or limited presence of the vector of this virus in the country, which is not known but suspected to be the olive psyllid *Euphylluria olivinae* (Sabanadzovic *et al.,* 1999). Another explanation could be the high genetic variability which is well known in Closteroviridae viruses. This could influence the specificity of the primers used in the detection assays. This is probably limited for OLYaV, as the primers were designed in a conserved HSP70h motif. There have been numerous divergent isolates of OLYaV detected to date, but it can-

not be excluded as a cause of particular reported greater variability compared to other closteroviruses (Essakhi *et al.,* 2006; Al Rwahnih *et al.,* 2011).

The proportions of mixed virus infections was of 8%, in 'Mastoidis' by SLRSV and OLYaV, and in 'Koroneiki' by ArMV and SLRSV. At least one host tree of each cultivar was free from the tested viruses, except for the cultivar 'Megaritiki' (Table 1).

Sequences of PCR-amplicons showed nucleotide homologies with the respective homologous viral sequences in the GenBank, confirming the specificity of the amplicons. No recombination events were detected within the analyzed sequences from each virus. The sequences obtained from ArMV, CLRV and SLRSV represent the first genetic information recovered from olive-infected material.

The comparative sequence analyses undertaken in this study revealed the presence of some unique nucleotide substitutions in the ArMV, OLYaV and SLRSV sequences from olives. The ArMV-Gr/Kr isolate showed two unique nucleotide substitutions, whereas the similarities varied from 74 to 94%. In the case of OLYaV, the sequence was only obtained from one of the RT-PCR amplicons from 'Mastoidis'. Molecular characterization of the Greek OLYaV-Gr/Ms isolate revealed the presence of a unique adenine substitution (position 66) and high molecular diversity with previously reported isolates, as indicated for European and American isolates (Essakhi *et al.,* 2006; Al Rwahnih *et al.,* 2011). The variability levels of the Greek isolate in comparison with isolates from California ranged from 3 to 25%, whereas the nucleotide similarities varied from 75 to 80% compared with Italian isolates. Within the sequence dataset used, there were also three isolates from Greek olive cultivars ('Tragolea', 'Conservolia', 'Gaidourelia') maintained in the germplasm repository of California sharing 75 to 93% nucleotide similarity with the Greek isolate reported here. This HSP70h sequence variability was significantly greater compared with other Closteroviridae viruses, suggesting the need of further studies to elucidate taxonomic relationships within the family.

Sequence analysis of the 22 SRLSV isolates revealed six diverse isolates from the olive cultivars 'Throuboulia', 'Kalamon', 'Amfissis' and 'Chalkidikis' (these virus isolates are designated, respectively, as SLRSV-Gr/Tr, SLRSV-Gr/Km1, SLRSV-Gr/Km2, SLRSV-Gr/Af and SLRSV-Gr/Ck), whereas all the others SRLSV isolates were identical with the sequence of SLRSV-Gr/Tr. A sequences alignment comparison with those available in the database (from mint, cherry, strawberry, black locust, Japanese rose and peach) showed different variability levels up to 24%. The most variable sequences to the olive isolates were those from peach and mint. There was 100% similarity between the SLRSV from black locust (*Robinia pseudoacacia*) in Poland and the SLRSV-Gr/Ck isolate, demonstrating the significant role of possible reservoir hosts in the virus dissemination. Six unique nucleotide substitutions were present only in olive isolates, with the exception of the isolate from black locust. Between the Greek isolates, the divergency ranged from 1 to 17%, with the SLRSV-Gr/Af and SLRSV-Gr/Km1 isolates being the most variable showing, respectively, 26 and 14 unique nucleotide substitutions. The high sequence divergency values of olive isolates are in accordance with the results of Dullemans *et al.* (2019). In previous studies the primer pair used for the detection of SLRSV was reported to target part of the CP gene (Faggioli *et al.,* 2002) instead of the 3′UTR, probably due to the limited knowledge of the virus genome organization.

The CLRV Greek isolates (CLRV-Gr/Tr and CLRV/Gr/Gd) were 100% similar, and multiple nucleotide alignments with the available CRLV sequences from pome and stone fruits, woody and herbaceous hosts, revealed that the Greek isolates had two unique nucleotide substitutions. The olive isolates, except the nucleotide variations, exhibited a motif of eight nucleotide deletions (positions 127 to 134), which was also present in CLRV isolates from birch and walnut, but not from *Chenopodium quinoa* and stone fruit hosts. The variability at nucleotide levels ranged from 2 to 13%, depending on the host, with the lowest values detected with isolates from birch and walnut.

All of the sequences determined in this study were deposited in the EMBL-EBI database under the accession numbers LR593885, MK936232 to MK936236 and MN706529 to MN706532.

Phylogenetic analyses were also carried out to investigate evolutionary relationships among the virus isolates. In the case of ArMV and CLRV, there were no available sequences; consequently, these analyses only confirmed the clustering of olive isolates with those from different hosts. All the viruses grouped within the virus-specific tree with ArMV-Gr/Kr isolate being more closely related to those sequenced from narcissus and lily, whereas the most distantly-related isolate was from butterbur (Figure 1A). The CLRV olive isolates were grouped in a separate clade of a sub-cluster with closely related isolates from walnut and birch (Figure 1B). For SLRSV, all the six diverse olive isolates grouped together but in a separate cluster from the other isolates of different host origins, with the exception of an isolate from black locust which was grouped in a sub-cluster together with SLRSV-Gr/Tr and SLRSV-Gr/Ck isolates (Figure 1C). The olive SLRSV-

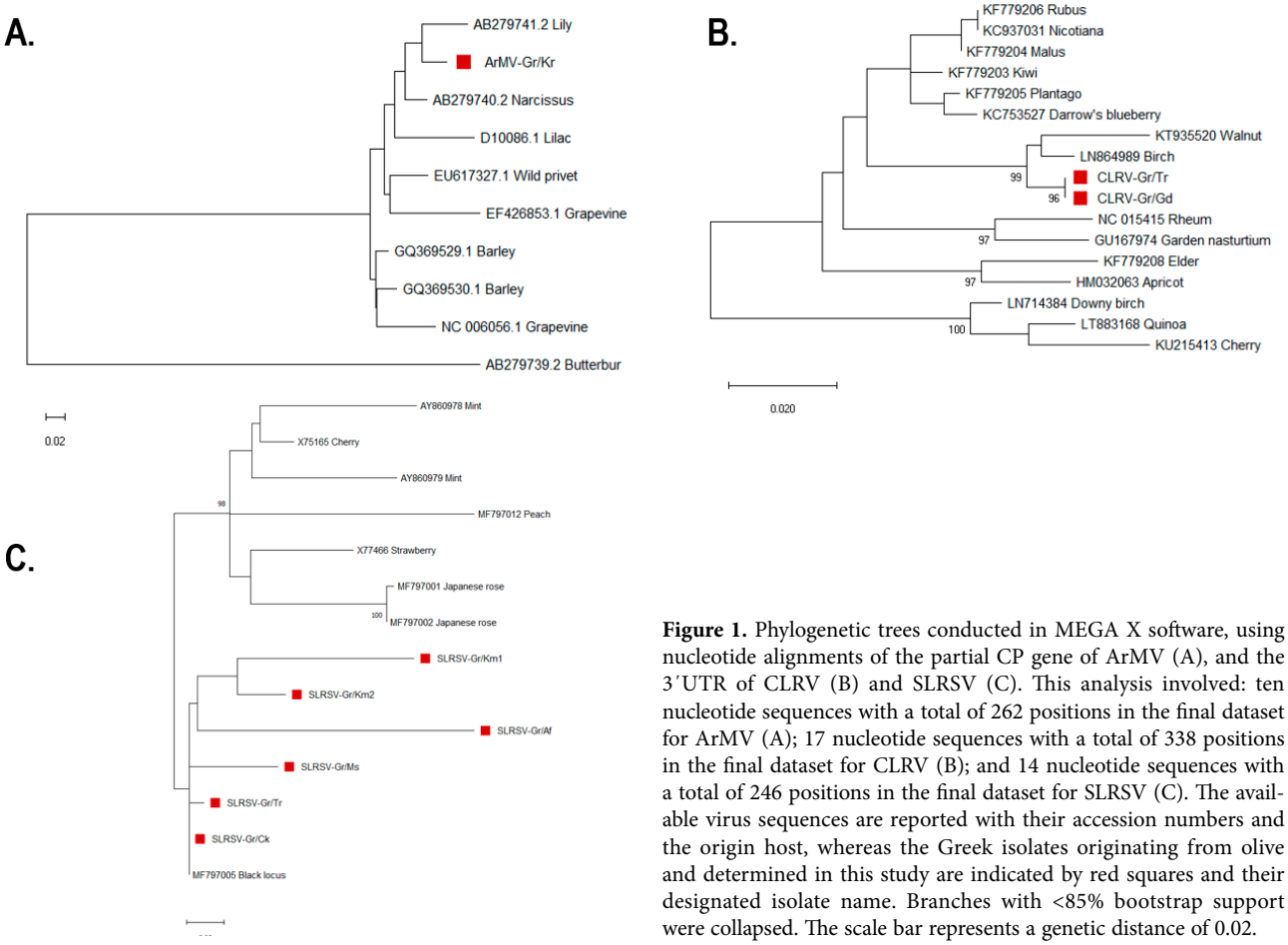

Figure 1. Phylogenetic trees conducted in MEGA X software, using nucleotide alignments of the partial CP gene of ArMV (A), and the 3′UTR of CLRV (B) and SLRSV (C). This analysis involved: ten nucleotide sequences with a total of 262 positions in the final dataset for ArMV (A); 17 nucleotide sequences with a total of 338 positions in the final dataset for CLRV (B); and 14 nucleotide sequences with a total of 246 positions in the final dataset for SLRSV (C). The available virus sequences are reported with their accession numbers and the origin host, whereas the Greek isolates originating from olive and determined in this study are indicated by red squares and their designated isolate name. Branches with <85% bootstrap support were collapsed. The scale bar represents a genetic distance of 0.02.

Gr/Af isolate, which was the most diverse, was alone in a separate clade, and the diverse peach isolate was grouped alone in a separate clade. These recently identified variable isolates from black locust, Japanese pear and peach were used for a new classification of the unassigned SLRSV by Dullemans *et al.* (2019). According to that study, a new taxonomic position is proposed for SLRSV as a member of the new genus *Stalarivirus*. Based on phylogenetic analyses of the CP full-genome, SLRSV-A, SLRSV-B and the *Lychnis mottle virus* are suggested as three distinct species of *Stalarivirus* (Dullemans *et al.*, 2019). In the present study, although the sequences used for inferring evolutionary relationships were from the 3′UTR of SLRSV, it is clear that the olive virus isolates are grouped with the SLRSV-A isolates, with an exception of the diverse peach isolate which is suggested as an isolate of SLRSV-B (Figure 1C).

Since the host range of OLYaV is limited to olive, the available homologous sequences in the database were from that host. In total, 56 OLYaV isolates from Italy and the United States of America were used to further characterize the evolutionary relationships of the Greek isolate with other OLYaV isolates. The results clearly showed two main different clusters with the first divided into two sub-clusters, A and B. The isolates clustering in groups A and C separated according to geographical origin of the germplasm collection. The Greek isolate clustered with the Californian isolates (Figure 2). The smaller sub-cluster group B contained two separate clades by sequences from the same geographical origin of the germplasm collection, with insertion of two isolates of different origin in each group. Previous phylogenetic studies on OLYaV comparable sequences were conducted using either isolates coming from Italian (Bari) or North American (California) olive tree collections. These studies demonstrated the existence of either three cluster groups of isolates from the Italian collection (Essakhi *et al.,* 2006) or six groups from isolates obtained from the Californian collection (Al Rwahnih *et al.,* 2011). Although each of these collections contained olive cultivars originating from different countries, the study of Essakhi et al. (2006) suggested a clustering of

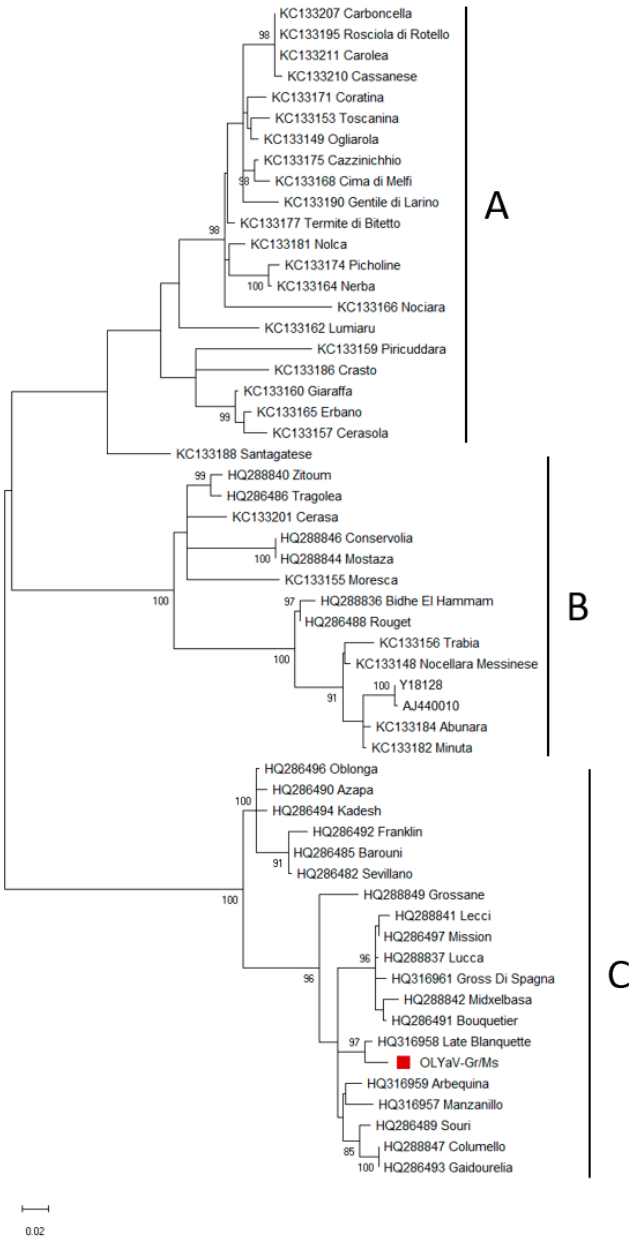

Figure 2. Evolutionary analyses conducted by MEGA X using nucleotide sequences of the OLYaV HSP70h gene. The analysis involved 56 nucleotide sequences. There was a total of 353 positions in the final dataset. The available OLYaV sequences originating from Italian and American germplasm collections (cultivars from different countries) are reported with their accession numbers and cultivar name, whereas the Greek isolate determined in this study is indicated by a red square and its designated name. Branches with <85% bootstrap support were collapsed. The scale bar represents a genetic distance of 0.02.

isolates based on the country of origin (except for the third group, which was geographically heterogeneous). This is in conflict with the second study, in which none of the clusters showed country of origin homogeneity (Al Rwahnih *et al.*, 2011). These studies cannot give clear interpretations of whether the relationships between isolates are geographically-dependent, as OLYaV isolates were not initially detected in their country of origin. Although the origin of the trees was from different countries, they were all maintained as part of an olive-tree germplasm collection, so the possibility of virus infection and dissemination after plantation establishment cannot be excluded for some viruses. In the present study we combined most of these previously reported sequences, and the results showed clear demarcation of the isolates based on the collections (Italian vs. American) into two clusters. Clusters A and C consisted of isolates from the Italian or North American collections, whereas the smaller sub-cluster B was mixed, but again the isolates from the different collections were grouped together in individual clades (Figure 2). The Greek OLYaV/Gr-Ms isolate was more closely related in terms of evolution with isolates from the North American collection, indicating a prominent role of exchange of infected host material in virus dissemination.

Although the present study should be subsequently upscaled to an extensive, country-wide sampling, to elucidate the virus infection status of olive trees in Greece, it has provided fundamental knowledge on the application of a rapid and economic RNA isolation protocol to facilitate virus detection techniques. The study has also made the first record of some olive viruses at unexpectedly high incidence proportions, in one of the leading olive producing countries. Olive virus sequences from olive hosts are also reported for first time. These results illustrate the urgent need to implement certification schemes for the production of virus-tested olive propagation material and prevention of virus dissemination. Phytosanitary controls are also of great importance for local cultivars in order to maintain their PDO recognition. A novel result from this study was the identification of sixteen virus-tested olive accessions from nine out of ten cultivars tested. Further research in large-scale surveys in this olive germplasm, in the National Germplasm Repository of Greece and in commercial olive groves will determine virus infection status for more Greek cultivars, which could represent potential candidates of a pre-basic mother plantation. This could supply increasing international demand for certified olive propagation material.

ACKNOWLEDGMENTS

The authors thank the mLingua Worldwide Translation Center for the English editing review of this paper. Part of this research has been financed by Greek nation-

al funds through the Action 'Establishment of a National Research Network in the Olive Value Chain', code 2018ΣΕ01300000 of GSRT.

LITERATURE CITED

Al Abdullah A., Elbeaino T., Saponari M., Hallakand M., 2005. Preliminary evaluation of the status of olive-infecting viruses in Syria. *Bulletin OEPP/EPPO Bulletin* 35: 249–252.

Al Abdullah A., Minafra A., Elbeaino T., Saponari M., De Stradis A., Savino V., Martelli G.P., 2010. Complete nucleotide sequence of *Olive latent virus 3*, representing a new genome structure in the genus *Marafivirus*. *Virus Research* 152: 10–17.

Al Rwahnih M., Guo Y., Daubert S., Golino D., Rowhani A., 2011. Characterization of latent viral infection of olive trees in the national clonal germplasm repository in California. *Journal of Plant Pathology* 93: 227–231.

Albanese G., Faggioli F., Ferretti L., Sciarroni R., La Rosa R., Barba M., 2003. Sanitary status evaluation of olive cultivars in Calabria and Sicily. *Journal of Plant Pathology* 85: 304.

Banilas G., Karampelias M., Makariti I., Kourti A., Hatzopoulos P., 2010. The olive DGAT2 gene is developmentally regulated and shares overlapping but distinct expression patterns with DGAT1. *Journal of Experimental Botany* 62: 521–532.

Bertolini E., Olmos A., Martinez M.C., Gorris M.T., Cambra M., 2001. Single-step multiplex RT-PCR for simultaneous and colorimetric detection of six RNA viruses in olive trees. *Journal of Virological Methods* 96: 33–41.

Cardoso J.M.S., Felix M.R., Oliveira S., Clara M.I.E., 2004. A *Tobacco necrosis virus D* isolate from *Olea europea* L.: viral characterization and coat protein sequence analysis. *Archives of Virology* 149: 1129–1138.

Dullemans A.M., Botermans M., de Kock M.J.D., de Krom C.E., van der Lee T.A.J., …, van der Vlugt R.A.A., 2020. Creation of a new genus in the family *Secoviridae* substantiated by sequence variation of newly identified *Strawberry latent ringspot virus* isolates. *Archives of Virology* 165: 21–31.

El Air M., Mahfoudi N., Digiaro M., Najjar A., Elbeaino T., 2011. Detection of olive-infecting viruses in Tunisia. *Journal of Phytopathology* 159: 283–286.

EPPO Standards PM 4 / 17 (2), 2006. Schemes for the production of healthy plants for planting. Pathogen-tested olive trees and rootstocks. *Bulletin OEPP / EPPO Bulletin* 36: 77–83.

Essakhi S., Elbeaino T., Digiaro M., Saponari M., Martelli G.P., 2006. Nucleotide sequence variations in the HSP70 gene of *Olive leaf yellowing-associated virus*. *Journal of Plant Pathology* 88: 285–291.

Fadel C., Digiaro M., Choueiri E., Elbeaino T., Saponari M., Savino V., Martelli G.P., 2005. On the presence and distribution of olive viruses in Lebanon. *Bulletin OEPP/EPPO Bulletin* 35: 33–36.

Faggioli F., Ferretti L., Albanese G., Sciarroni R., Pasquini G., Lumia V., Barba M., 2005. Distribution of olive tree viruses in Italy as revealed by one-step RT-PCR. *Journal of Plant Pathology* 87: 45–51.

Faggioli F., Ferretti L., Pasquini G., Barba M., 2002. Detection of *Strawberry latent ring spot virus* in leaves of olive trees in Italy using a one-step RT-PCR. *Journal of Phytopathology* 150: 636–639.

Faggioli F., Roschetti A., Luigi M., Leo G., Albanese G., 2017. Sanitary Selection of Olive (*Olea europaea* L.) Cultivars for Worldwide Distribution. *Asian Journal of Plant Pathology* 11: 28–34.

Felix M.R., Clara M.I.E., 2002. Two necrovirus isolates with properties of *Olive latent virus 1* and *Tobacco necrosis virus* from olive in Portugal. *Acta Horticulturae* 586: 725–728.

Felsenstein S., 1985. Confidence limits on phylogenies: an approach using the bootstrap. *Evolution* 39: 783–791.

Godena S., Faggioli F., Luigi M., Saponari M., Loconsole G., …, Đermić E., 2016. Incidence of viruses on autochthonous and introduced olive varieties in Croatian Istria detected by three diagnostic techniques. *Journal of Plant Pathology* 98: 657–660.

Gratsia M.E., Kyriakopoulou P.E., Voloudakis A.E., Fasseas C., Tzanetakis I.E., 2012. First report of *Olive mild mosaic* virus and *Sowbane mosaic virus* in spinach in Greece. *Plant Disease* 96: 123.

IOC, 2018. International Olive Council: World olive oil figures. http://www.internationaloliveoil.org/estaticos/view/131-world-olive-oil-figures

Kimura M., 1980. A simple method for estimating evolutionary rate of base substitutions through comparative studies of nucleotide sequences. *Journal of Molecular Evolution* 16: 111–120.

Kumar S., Stecher G., Li M., Knyaz C., Tamura K., 2018. MEGA X: Molecular Evolutionary Genetics Analysis across computing platforms. *Molecular Biology and Evolution* 35: 1547–1549.

Linos A., Nikoloudakis N., Katsiotis A., Hagidimitriou M., 2014. Genetic structure of the Greek olive germplasm revealed by RAPD, ISSR and SSR markers. *Scientia Horticulturae* 175: 33–43.

Loconsole G., Saponari M., Faggioli F., Albanese G., …, Savino V., 2010. Inter-laboratory validation of PCR-

based protocol for detection of olive viruses. *Bulletin OEPP/EPPO Bulletin* 40: 423–428.

Luigi M., Manglli A., Thomaj F., Buonaurio R., Barba M., Faggioli F., 2009. Phytosanitary evaluation of olive germplasm in Albania. *Phytopathologia Mediterranea* 48: 2 80–284.

Luigi M., Godena S., Đermić E., Barba M., Faggioli F., 2011. Detection of viruses in olive trees in Croatian Istria. *Phytopathologia Mediterranea* 50: 150–153.

Martelli G.P., 1999. Infectious diseases and certification of olive: an overview. *Bulletin OEPP/EPPO Bulletin* 29: 127–133.

Martin D.P., Murrell B., Golden M., Khoosal A., Muhire B., 2015. RDP4: detection and analysis of recombination patterns in virus genomes. *Virus Evolution* 1: 1–5.

Metzidakis I.T., Koubouris G.C., 2006. Olive cultivation and industry in Greece. Proceedings of the Second International Seminar "Biotechnology and Quality of Olive Tree Products around the Mediterranean Basin", 5-10 November 2006, Marsala-Mazara del Vallo, Italy. p. 133–140.

Sabanadzovic S., Abou-Ghanem N., La Notte P., Savino V., Scarito G., Martelli G.P., 1999. Partial molecular characterization and RT-PCR detection of a putative closterovirus associated with leaf yellowing. *Journal of Plant Pathology* 81: 37–45.

Saponari M., Alkowni R., Grieco F., Driouech N., Hassan M., Di Terlizzi B., 2002. Detection of Olive-infecting virus in the Mediterranean basin. *Acta Horticulturae* 586: 787–790.

Saponari M., Boscia D., Nigro F., Martelli G.P., 2013. Identification of DNA sequences related to *Xylella fastidiosa* in oleander, almond and olive trees exhibiting leaf scorch symptoms in Apulia (Southern Italy). *Journal of Plant Pathology* 95: 668.

Tamura K., 1992. Estimation of the number of nucleotide substitutions when there are strong transition-transversion and G + C-content biases. *Molecular Biology and Evolution* 9: 678–687.

Werner R., Mühlbach H.P., Büttner C., 1997. Detection of *Cherry leaf roll nepovirus* (CLRV) in birch, beech and petunia by immunocapture reverse transcription-PCR using a conserved primer pair. *European Journal of Forest Pathology* 27: 309–318.

Youssef S.A., Moawed S.M., El-Sayed M., Shalaby A.A., 2010. Detection of olive viruses in Egypt by one-step RT-PCR. *Julius-Kuhn-Archiv* 427: 51–55.

Phytopathologia Mediterranea
The international journal of the
Mediterranean Phytopathological Union

Firenze University Press
www.fupress.com/pm

New or Unusual Disease Reports

Identification of *Neofusicoccum parvum* causing canker and twig blight on *Ficus carica* in Italy

Dalia AIELLO[1,*], Giorgio GUSELLA[1], Alberto FIORENZA[1], Vladimiro GUARNACCIA[2,3], Giancarlo POLIZZI[1]

[1] *Dipartimento di Agricoltura, Alimentazione e Ambiente, sezione Patologia Vegetale, University of Catania, Via S. Sofia 100, 95123 Catania, Italy*
[2] *DiSAFA, University of Torino, Largo Paolo Braccini, 2, 10095 Grugliasco, TO, Italy*
[3] *Centre for Innovation in the Agro-Environmental Sector, AGROINNOVA, University of Torino, Largo Braccini 2, 10095 Grugliasco (TO), Italy*
*Corresponding author: dalia.aiello@unict.it

Summary. During June 2018, several symptomatic fig (*Ficus carica*) cuttings, showing twig blight, subcortical discolouration and apical dieback were collected from a nursery in Catania province, Sicily (Italy). Isolations from diseased tissue consistently showed the presence of the same fungal colony. Morphology of the fungal isolates together with sequence data of the nuclear rDNA internal transcriber spacer (ITS) region, translation elongation factor 1-alpha (*tef*1) gene and partial beta-tubulin (*tub2*) gene of representatives isolates revealed the presence of the fungus *Neofusicoccum parvum*. Pathogenicity tests were conducted by inoculating fig cuttings with mycelial plugs. After 10 days, the inoculated plants developed cankers similar to those observed in the greenhouse and after 26 days all inoculated plants were dead. To the best of our knowledge, this is the first report worldwide of *N. parvum* causing disease on this host.

Keywords. Fig cuttings, pathogenicity, molecular analysis, Botryosphaeriaceae.

OPEN ACCESS

Citation: D. Aiello, G. Gusella, A. Fiorenza, V. Guarnaccia, G. Polizzi (2020) Identification of *Neofusicoccum parvum* causing Canker and Twig Blight on *Ficus carica* in Italy. *Phytopathologia Mediterranea* 59(1): 213-218. doi: 10.14601/Phyto-10798

Accepted: November 22, 2019

Published: April 30, 2020

Data Availability Statement: All relevant data are within the paper and its Supporting Information files.

Competing Interests: The Author(s) declare(s) no conflict of interest.

Editor: Alan J.L. Phillips.

INTRODUCTION

Fig (*Ficus carica L.*) is one of the most cultivated crop of the Mediterranean basin Countries. Several diseased caused by bacteria, viruses, oomycetes and fungi are reported for this crop throughout the world (Ferguson *et al.*, 1990).

In the last years, there has been increased interest in "edible landscapes" and some woody ornamental plant genera or species are selected for attractive garden plants that also have edible fruit. Small edible ornamental figs obtained from cutting are produced in Sicily both for aesthetic value as well as consumption. During June 2018, examination of 1,500 fig cuttings in an ornamental nursery in Catania province, Sicily (Italy), revealed that up to 20% of the plants showed canker and twig blight during the rooting step of the propagation process. Therefore, the aim of this study was to identify the causal agent of canker and twig blight on fig in Sicily, Italy.

MATERIAL AND METHODS

Isolation and morphological characterization of the pathogen

Twenty symptomatic fig cuttings, showing canker and twig blight were collected from a greenhouse in Catania province, Sicily (Italy) during the rooting step of the propagation process. Small sections of diseased woody tissue were surface disinfected for 1 min in 1.5% sodium hypochlorite, rinsed in sterile water, placed on potato dextrose agar (3.9% PDA, Oxoid) amended with 100 mg/liter of streptomycin sulfate (Sigma-Aldrich) to prevent bacterial growth, and then incubated at 25 ± 1°C for three–four days. A total of 12 morphologically similar isolates were obtained from single conidium or hyphal tip of pure cultures on PDA at 25 ± 1°C. For the morphological characterization of the pathogen, the isolates were transferred on PDA and technical agar (TA, 1.2% agar, Oxoid) with sterilized pine needles deposited onto the surface, and then incubated in a growth chamber at 25 ± 1°C with a 12 h photoperiod. Size and shape of conidia were recorded from colonies grown on TA with sterilized pine needles after 3 weeks.

Pathogenicity tests

Pathogenicity tests were conducted on eighteen potted, healthy, 1-month-old cuttings of fig, with the same number for the control. A piece of bark was removed with a 6 mm diam. cork borer and 6-mm-diameter mycelial plugs taken from a 7-day-old culture of isolate Di3AFC1 (CBS 145622) were applied to two separate wounds on each twig. The wounds were covered with Parafilm® (Pechney Plastic Packaging Inc., Chicago, USA) to prevent desiccation. Controls consisted of sterile PDA plugs applied to wounds. All replicates were kept in a growth chamber with a 12 h photoperiod at 25 ± 1°C. The presence and length of the resulting lesions was recorded 10, 14 and 26 days after inoculation.

Molecular identification

Genomic DNA was extracted from isolates Di3AFC1, Di3AFC2 and Di3AFC3 (CBS 145622, CBS 145623 and CBS 145624) using the Wizard Genomic DNA Purification Kit (Promega Corporation, WI, USA). The internal transcriber spacer region (ITS) of the nuclear ribosomal RNA operon was amplified with primers ITS5 and ITS4 (White *et al.,* 1990), the primers EF1-728F and EF1-986R (Carbone and Kohn, 1999) were used to amplify part of the translation elongation factor 1alpha gene (*tef1*) while the primer set Bt-2a and Bt-2b (Glass and Donaldson 1995) were used for the partial beta-tubulin (*tub2*) gene. The PCR products were sequenced in both directions by Macrogen Inc. (South Korea). The DNA sequences generated were analysed and consensus sequences were computed using the program Geneious v. 11.1.5.

Phylogenetic analysis

The sequences obtained in this study were blasted against the NCBIs GenBank nucleotide database to determine the closest relatives to be included in the phylogenetic analysis. Blast analisys indicated that all the isolates belonged to the genus *Neofusicoccum*. Sequence alignments of the different gene regions, including sequences generated in this study and sequences downloaded from GenBank, were initially performed using the MAFFT v. 7 online server (http://mafft.cbrc.jp/alignment/server/index. html) (Katoh and Standley, 2013), and then manually adjusted in MEGA v. 7 (Kumar *et al*., 2016). To establish the identity of fungal isolates, phylogenetic analyses were conducted using individual locus (data not shown) as well as concatenated analyses of three loci (ITS, *tef1* and *tub2*). Additional reference sequences were selected based on recent studies on *Neofusicoccum* genus (Yang *et al*., 2017). Phylogenetic analyses were based on Maximum Parsimony (MP) for all the individual loci and on both MP and Bayesian Inference (BI) for the combined multilocus analyses. For BI, the best evolutionary model for each partition was selected based on MrModeltest v. 2.3 (Nylander 2004) and incorporated into the analyses. MrBayes v. 3.2.5 (Ronquist *et al*., 2012) was used to generate phylogenetic trees under optimal criteria per partition. The Markov Chain Monte Carlo (MCMC) analysis used four chains and started from a random tree topology. The heating parameter was set to 0.2 and trees were sampled every 1 000 generations. Analyses stopped once the average standard deviation of split frequencies was below 0.01. The MP analysis was done using PAUP (Swofford, 2003). Phylogenetic relationships were estimated by heuristic searches with 100 random addition sequences. Tree bisection- reconnection was used, with the branch swapping option set on 'best trees' only with all characters weighted equally and alignment gaps treated as fifth state. Tree length (TL), consistency index (CI), retention index (RI) and rescaled consistence index (RC) were calculated for parsimony and the bootstrap analyses (Hillis & Bull 1993) were based on 1 000 replicates. Sequences generated in this study were deposited in GenBank (Table 1).

Table 1. Collection details and GenBank accession numbers of isolates included in this study.

Species	Culture no.[1]	Host	Country	GenBank no.[2]		
				ITS	*tef1*	*tub2*
Diplodia seriata	CBS 110875	*Vitis vinifera*	South Africa	AY343456	KX464592	KX464827
Neofusicoccum arbuti	CBS 116131^T	*Arbutus menziesii*	USA: Washington	AY819720	KF531792	KF531793
N. australe	CBS 139662^T	*Acacia* sp.	Australia	AY339262	AY339270	AY339254
	CBS 121115	*Prunus persica*	South Africa	EF445355	EF445386	KX464948
N. batangarum	CBS 124924^T	*Terminalia catappa*	Cameroon	FJ900607	FJ900653	FJ900634
N. cryptoaustrale	CBS 122813^T	*Eucalyptus* sp.	South Africa	FJ752742	FJ752713	FJ752756
N. kwambonambiense	CBS 102.17^T	*Carya illinoensis*	USA: Florida	KX464169	KX464686	KX464964
N. luteum	CBS 562.92^T	*Actinidia deliciosa*	New Zealand	KX464170	KX464690	KX464968
N. mangiferae	CBS 118532	*Mangifera indica*	Australia	AY615186	DQ093220	AY615173
N. mediterraneum	CBS 121718^T	*Eucalyptus* sp.	Greece	GU251176	GU251308	-
N. parvum	CBS 123650	*Syzygium cordatum*	South Africa	KX464182	KX464708	KX464994
	CMW 9081^T	*Populus nigra*	New Zealand	AY236943	AY236888	AY236917
	Di3AFC1	*Ficus carica*	Italy	*MN611179*	*MN623346*	*MN623343*
	Di3AFC2	*Ficus carica*	Italy	*MN611180*	*MN623347*	*MN623344*
	Di3AFC3	*Ficus carica*	Italy	*MN611181*	*MN623348*	*MN623345*
N. pistaciarum	CBS 113083^T	*Pistacia vera*	USA: California	KX464186	KX464712	KX464998
N. protearum	CBS 114176	*Leucadendron laureolum*	South Africa	AF452539	KX464720	KX465006
N. stellenboschiana	CBS 110864^T	*Vitis vinifera*	South Africa	AY343407	AY343348	KX465047
	CBS 121116	*Prunus armeniaca*	South Africa	EF445356	EF445387	KX465049
N. terminaliae	CBS 125264	*Terminalia sericea*	South Africa	GQ471804	GQ471782	KX465053
N. vitifusiforme	CBS 110887^T	*Vitis vinifera*	South Africa	AY343383	AY343343	KX465061

[1] CBS: Westerdijk Fungal Biodiversity Institute, Utrecht; CMW: Tree Pathology Co-operative Program, Forestry and Agricultural Biotechnology Institute, University of Pretoria, South Africa; Di3A: Dipartimento di Agricoltura Alimentazione e Ambiente. Ex-type and ex-epitype cultures are indicated with ^{T}.

[2] ITS: internal transcribed spacers 1 and 2 together with 5.8S nrDNA; tef1: translation elongation factor 1-alpha; tub2: partial beta-tubulin gene. Sequences generated in this study are indicated in italics.

RESULTS AND DISCUSSION

Symptomatic plants showed cankers, shoot blight and subcortical discolouration (Figure 1a, b). One type of colony was consistently obtained from these symptomatic tissues. A total of 12 fungal isolates were established from single conidium or hyphal tip cultures on PDA. The isolates developed abundant, aerial mycelium that became grey after 2–3 days and then black with age. On pine needles the isolates formed black, globose pycnidia after 3 weeks. Conidia were hyaline, non-septate, ellipsoid, thin walled and measured 14–20 × 4.5–7 µm. After 10 days from inoculation cankers, characterized by discolouration and necrotic internal tissue, developed at both inoculation points with an average lesion length of 14.5 cm. Pycnidia developed above and near each lesion. Infection also resulted in shoot blight and apical dieback of the inoculated plants. After 14 days, 44% of the inoculated plants were dead and after 26 days, all the inoculated plants had died (Figure 1c, d, e). These symptoms on the inoculated plants were identical to those observed in diseased fig cuttings in the greenhouse. All the control plants, inoculated only with agar plugs, did not develop any symptoms. Some of the diseased tested plants were used to re-isolate the fungus in order to fulfill the Koch's postulates. These results confirm that the isolated fungus was the causal agent of the disease.

The three MP trees derived from the single gene sequence alignments (ITS, *tef1* and *tub2*) produced topologically similar trees. The combined phylogeny of *Neofusicoccum* species consisted of 21 sequences, including the outgroup sequences of *Diplodia seriata* (culture CBS 110875). A total of 1 262 characters (ITS: 1–507, *tef1*: 514–821, *tub2*: 828–1262) were included in the phylogenetic analysis. The results showed 114 characters were parsimony-informative, 185 were variable and parsimony-uninformative and 951 characters were constant. A maximum of 1 000 equally most parsimonious trees were saved (Tree length = 438, CI = 0.811, RI = 0.842 and RC = 0.682). Bootstrap support values from the parsimony analysis are plotted on the Bayes-

Figure 1. Natural symptoms of disease (a, b) and disease symptoms reproduced from artificial inoculation of fig cuttings (c–e). a, shoot blight; b, internal discolouration; c, shoot blight and apical dieback 26 days after pathogen inoculation; d, dark pycnidia above the inoculation point; e, internal lesion and discolouration under the inoculation point after 10 days on artificially inoculated fig cuttings.

ian phylogenies in Figure 2. For the Bayesian analyses, MrModeltest suggested that all partitions should be analysed with dirichlet state frequency distributions. The following models were recommended by MrModeltest and used: K80+I+G for ITS, HKY+G for *tef1* and *tub2*. In the Bayesian analysis, the ITS partition had 74 unique site patterns, the *tef1* partition had 118 unique site patterns and the *tub2* partition had 62 unique site patterns, and the analysis ran for 1100000 generations, resulting in 2022 trees of which 1320 trees were used to calculate the posterior probabilities.

In the combined analyses, the three representative isolates clustered with one reference strain and the ex-type strain of *N. parvum* (CMW9081). The individual alignments and trees of the single loci used in the analyses were compared with respect to their performance in species recognition. According with morphological and molecular analyses, the isolates were identified as *Neofusicoccum parvum* (Pennycook & Samuels) Crous, Slippers & A.J.L. Phillips.

Fungi belonging to the Botryosphaeriaceae family are reported worldwide as pathogens of several *Ficus* species (Al-Bedak, 2018; Mohali *et al*., 2017; El-Atta and Aref, 2013). The cultivated fig (*F. carica*), is reported to be attacked by different species in the Botryosphaeriaceae, including *Lasiodiplodia theobromae* (Pat.) Griffon & Maubl. (Çeliker and Michailides, 2012) and *Neoscytalidium dimidiatum* (Penz.) Crous & Slippers (Elshafie and Ba-Omar, 2002; Ray *et al*., 2010). Until now, *N. parvum* has been reported only on the ornamental *Ficus microcarpa* L. in association with other Botryosphaeriaceae species causing branch canker and dieback (Mayorquin *et al*., 2012).

Neofusicoccum parvum, characterized by the proven ability to induce disease, has a very wide geographical and host distribution (Sakalidis *et al.,* 2013), and in Italy was already reported to cause several diseases on different woody hosts, like olive (Carlucci *et al.,* 2013), mango (Ismail *et al.,* 2013), avocado (Guarnaccia *et al.,* 2016;), loquat (Giambra *et al.,* 2016), pomegranate (Riccioni *et al.,* 2017) grapevine (Mondello *et al.,* 2013; Carlucci *et al.,* 2015) and *Rhaphiolepis indica* (Gusella *et al*., 2020). Since *N. parvum* has been reported on the genus *Ficus*, although on a different species (Mayorquin *et al*., 2012), it is no surprise to find it on another species of the same genus. Nevertheless, we need to point out that in this

case *N. parvum* was found causing serious disease on an important crop for the southern regions of in Italy, and for several other countries of the Mediterranean Basin, like Turkey, Morocco, Egypt and Algeria. In addition, we need to highlight that this report refers to the propagation process of fig cuttings that represents a crucial step to avoid severe infections before the commercialization of this species in Italy and abroad. The recovery of this fungus from fig cuttings confirms its high diffusion in Italy and the high risk for other susceptible crops. To the best of our knowledge, this is the first report worldwide of the fungus *N. parvum* attacking *F. carica*.

ACKNOWLEDGEMENTS

This research was supported by Research Project 2016–2018 "Monitoraggio, caratterizzazione e controllo sostenibile di microrganismi e artropodi di interesse agrario" WP2 - 5A722192134.

LITERATURE CITED

Al-Bedak O.A., Mohamed R.A., Seddek N.H., 2018. First detection of *Neoscytalidium dimidiatum* associated

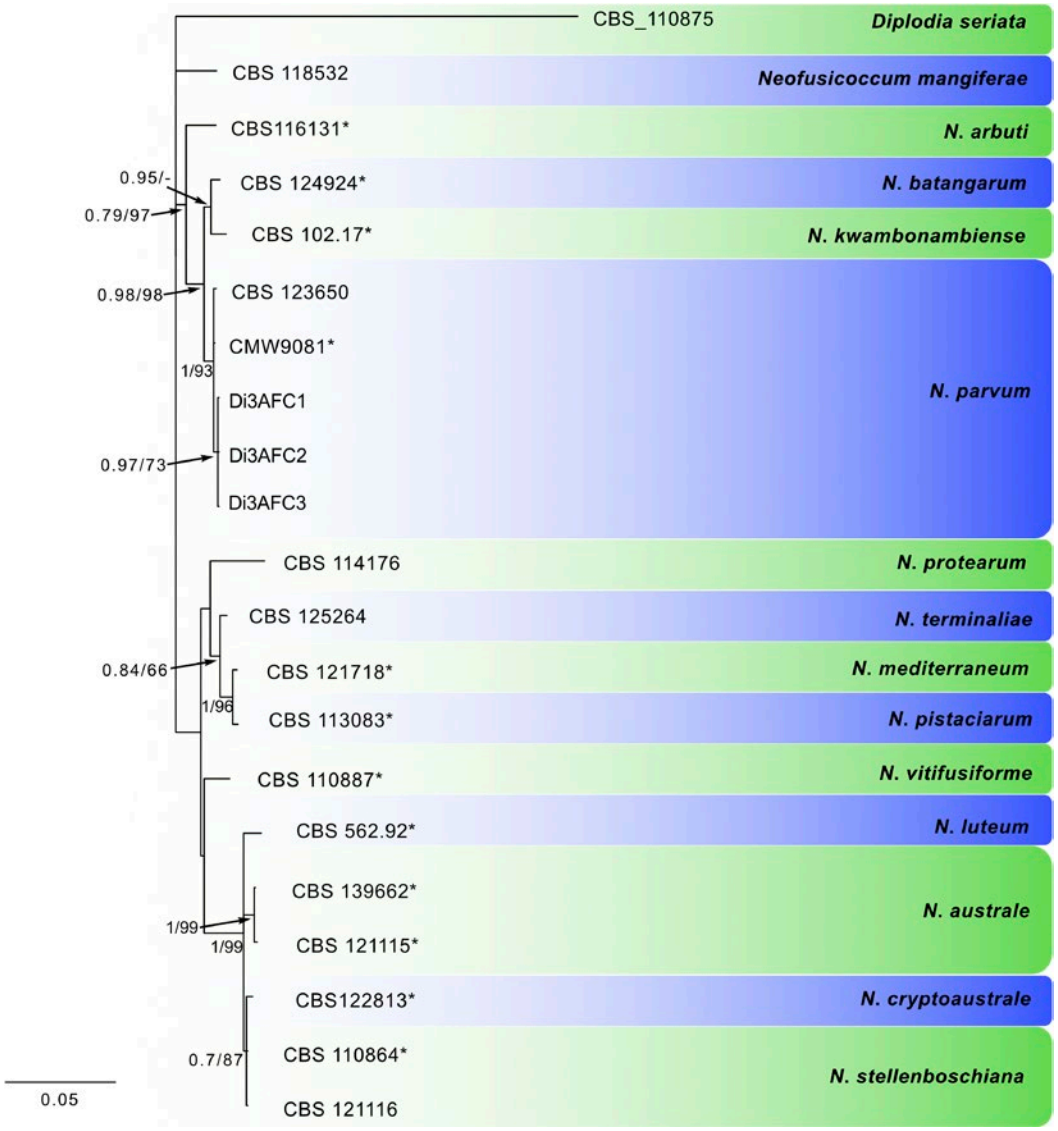

Figure 2. Consensus phylogram of 1320 trees resulting from a Bayesian analysis of the combined ITS, *tef1* and *tub2* sequences. Bootstrap support values and Bayesian posterior probability values are indicated at the nodes. *Neofusicoccum* species are listed next to the strain numbers. *indicates ex-type strains. The tree was rooted to *Diplodia seriata* (CBS 110875).

with canker disease in Egyptian *Ficus* trees. *Forest Pathology* 48: e12411.

Carbone I., Kohn L.M., 1999. A method for designing primer sets for speciation studies in filamentous ascomycetes. *Mycologia* 91: 553–556.

Carlucci A., Cibelli F., Lops F., Raimondo M.L., 2015. Characterization of Botryosphaeriaceae species as causal agents of trunk diseases on grapevines. *Plant Disease* 99: 1678–1688.

Carlucci A., Raimondo M.L., Cibelli F., Phillips A.J., Lops F., 2013. *Pleurostomophora richardsiae, Neofusicoccum parvum* and *Phaeoacremonium aleophilum* associated with a decline of olives in southern Italy. *Phytopathologia Mediterranea* 52: 517–527.

Çeliker N.M., Michailides T.J., 2012. First report of *Lasiodiplodia theobromae* causing canker and shoot blight of fig in Turkey. *New Disease Reports* 25: 12.

El-Atta H.A., Aref I.M., 2013. Pathogenic mortality of *Ficus* spp. *International Journal of Plant, Animal and Environmental Sciences* 3: 204–210.

Elshafie A.E., Ba-Omar T., 2002. First report of *Albizia lebbeck* dieback caused by *Scytalidium dimidiatum* in Oman. *Mycopathologia* 154: 37–40.

Ferguson L., Michailides T.J., Shorey H.H., 1990. The California fig industry. *Horticultural Reviews* 12: 409–490.

Giambra S., Piazza G., Alves A., Mondello V., Berbegal M., Burruano S., 2016. Botryosphaeriaceae species associated with diseased loquat trees in Italy and description of *Diplodia rosacearum* sp. nov. *Mycosphere* 7: 978–989.

Guarnaccia V., Vitale A., Cirvilleri G., Aiello D., Susca A., Polizzi G., 2016. Characterization and pathogenicity of fungal species associated with branch cankers and stem-end rot of avocado in Italy. *European Journal of Plant Pathology* 146: 963–976.

Gusella G., Aiello D., Polizzi G., 2020. First report of leaf and twig blight of Indian hawthorn (*Rhaphiolepis indica*) caused by *Neofusicoccum parvum* in Italy. *Journal of Plant Pathology* 102: 275.

Hillis D.M., Bull J.J., 1993. An empirical test of bootstrapping as a method for assessing confidence in phylogenetic analysis. *Systematic Biology* 42: 182–192.

Ismail A.M., Cirvilleri G., Lombard L., Crous P.W., Groenewald J.Z., Polizzi G., 2013. Characterization of *Neofusicoccum* species causing mango dieback in Italy. *Journal of Plant Pathology* 95: 549–557.

Katoh K., Standley D.M., 2013. MAFFT Multiple sequence alignment software version 7: improvements in performance and usability. *Molecular Biology and Evolution* 30: 772–780.

Kumar S., Stecher G., Tamura K., 2016. MEGA 7: molecular evolutionary genetics analysis version 7.0 for bigger datasets. *Molecular Biology and Evolution* 33: 1870–1874.

Mayorquin J.S., Eskalen A., Downer A.J., Hodel D.R., Liu A., 2012. First report of multiple species of the Botryosphaeriaceae causing bot canker disease of Indian laurel-leaf fig in California. *Plant Disease* 96: 459.

Mohali S.R., Castro-Medina F., Úrbez-Torres J.R., Gubler W.D., 2017. First report of *Lasiodiplodia theobromae* and *L. venezuelensis* associated with blue stain on *Ficus insipida* wood from the Natural Forest of Venezuela. *Forest Pathology* 47: e12355.

Mondello V., Lo Piccolo S., Conigliaro G., Alfonzo A., Torta L., Burruano S., 2013. First report of *Neofusicoccum vitifusiforme* and presence of other Botryosphaeriaceae species associated with Botryosphaeria dieback of grapevine in Sicily (Italy). *Phytopathologia Mediterranea* 52: 388–396.

Nylander J.A.A., 2004. *MrModeltest* v. 2. Programme distributed by the author. Uppsala: Evolutionary Biology Centre, Uppsala University.

Ray J.D., Burgess T., Lanoiselet V.M., 2010. First record of *Neoscytalidium dimidiatum* and *N. novaehollandiae* on *Mangifera indica* and *N. dimidiatum* on *Ficus carica* in Australia. *Australasian Plant Disease Notes* 5: 48–50.

Riccioni L., Valente M.T., Giambattista G.D., 2017. First report of *Neofusicoccum parvum* causing shoot blight and plant decay on pomegranate in Tarquinia, Italy. *Journal of Plant Pathology* 99: 294.

Ronquist F., Teslenko M., van der Mark P., Ayres D.L., … Huelsenbeck J.P., 2012. MrBayes 3.2: efficient Bayesian phylogenetic inference and model choice across a large model space. *Systematic Biology* 61, 539–542.

Sakalidis M.L., Slippers B., Wingfield B.D., Hardy G.S.J., Burgess T.I., 2013. The challenge of understanding the origin, pathways and extent of fungal invasions: global populations of the *Neofusicoccum parvum-N. ribis* species complex. *Diversity and Distributions* 19: 873–883.

Swofford D.L., 2003. *PAUP*: phylogenetic analysis using parsimony (*and other methods), v. 4.0b10.* Sunderland, MA: Sinauer Associates.

White T.J., Bruns T., Lee S. J.W.T., Taylor J.L., 1990. Amplification and direct sequencing of fungal ribosomal RNA genes for phylogenetics. In: *PCR Protocols: a Guide to Methods and Applications* (M.A. Innis, D.H. Gelfand, J.J. Sninsky, T.J. White, ed.), Academic Press, New York, USA, pp 315–321.

Yang T., Groenewald J.Z., Cheewangkoon, R., Jami, F., Abdollahzadeh, J., Lombard, L., Crous, P.W., 2017. Families, genera, and species of Botryosphaeriales. *Fungal Biology* 121, 322–346.

Finito di stampare da
Logo s.r.l. – Borgoricco (PD) – Italia

Mediterranean Phytopathological Union

Founded by Antonio Ciccarone

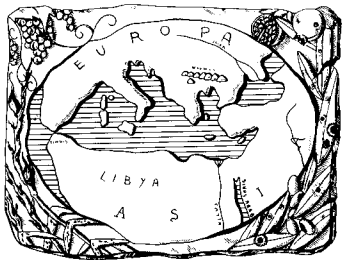

The Mediterranean Phytopathological Union (MPU) is a non-profit society open to organizations and individuals involved in plant pathology with a specific interest in the aspects related to the Mediterranean area considered as an ecological region. The MPU was created with the aim of stimulating contacts among plant pathologists and facilitating the spread of information, news and scientific material on plant diseases occurring in the area. MPU also intends to facilitate and promote studies and research on diseases of Mediterranean crops and their control.
The MPU is affiliated to the International Society for Plant Pathology.

MPU Governing Board

Affiliated Societies

Arab Society for Plant Protection (ASPP), http://www.asplantprotection.org/
French Society for Phytopathology (FSP), http://www.sfp-asso.org/
Hellenic Phytopathological Society (HPS), http://efe.aua.gr/
Israeli Phytopathological Society (IPS), http://www.phytopathology.org.il/
Italian Phytopathological Society (SIPAV), http://www.sipav.org/
Portuguese Phytopathological Society (PPS), http://www.spfitopatologia.org/
Spanish Society for Plant Pathology (SEF), http://www.sef.es/sef/

2020 MPU Membership Dues

Institutional MPU Membership: : € 200.00 (college and university departments, libraries and other facilities or organizations). Beside the open-access on-line version of *Phytopathologia Mediterranea*, the print version can be received with a € 50 contribution to mail charges (total € 250,00 to receive the print version). Researchers belonging to an Institution which is a member of the Union are entitled to publish with a reduced page contribution, as the Individual Regular members.
Individual Regular MPU Membership*: € 50.00 (free access to the open-access on-line version of Phytopathologia Mediterranea and can get the print version with a contribution to mail charges of € 50 (total € 100,00 to receive the print version).

*Students can join the MPU as a Student member on the recommendation of a Regular member. Student MPU members are entitled to a 50% reduction of the membership dues (proof of student status must be provided).

Payment information and online membership renewal and subscription at www.mpunion.com

For subscriptions and other information visit the MPU web site:
www.mpunion.com
or contact us at: Phone +39 39 055 2755861/862 – E-mail: phymed@unifi.it

Phytopathologia Mediterranea

Volume 59, April, 2020

Contents

Direttore responsabile: Giuseppe Surico • Autorizzazione del Tribunale di Firenze n. 4923 del 5-1-2000 • *Printed by* Logo S.r.l. - Padova, Maggio 2020
€ 70,00